

**UNIVERSITY OF GLASGOW**

**DEPARTMENT OF CIVIL ENGINEERING**

**DISCHARGE ASSESSMENT IN STRAIGHT AND  
MEANDERING COMPOUND CHANNELS**

**JAMES BINNING WARK B. Eng**

**July 1993**

**Volume 1**

**A thesis submitted in fulfilment of the regulations governing the award of the  
degree of Doctor of Philosophy**

**© James B. Wark 1993**

ProQuest Number: 13818426

All rights reserved

INFORMATION TO ALL USERS

The quality of this reproduction is dependent upon the quality of the copy submitted.

In the unlikely event that the author did not send a complete manuscript and there are missing pages, these will be noted. Also, if material had to be removed, a note will indicate the deletion.



ProQuest 13818426

Published by ProQuest LLC (2018). Copyright of the Dissertation is held by the Author.

All rights reserved.

This work is protected against unauthorized copying under Title 17, United States Code  
Microform Edition © ProQuest LLC.

ProQuest LLC.  
789 East Eisenhower Parkway  
P.O. Box 1346  
Ann Arbor, MI 48106 – 1346

Thesis  
9616  
copy 1  
Vol 1

GLASGOW  
UNIVERSITY  
LIBRARY

## ABSTRACT

The conveyance capacity of compound channels is investigated. Initially the case of straight compound channels is examined and a novel approach to calculating the lateral distribution of flow across channel widths is derived and verified against a wide range of laboratory and field data. Secondly a similar exercise for the case of meandering compound channels is carried out. A new procedure for calculating the discharge capacity of meandering two stage channels is derived and verified against the available data. Thus the work presented in this thesis is specifically directed towards providing improved methods of estimating the overall conveyance capacity of compound channels.

In the past a considerable amount of work has been carried out in to the behaviour of compound channels. Much of this work has concentrated on particular aspects of the hydraulics of compound channels. Recent work has stressed the practical importance of compound channels to river engineers. The general approach followed in deriving these new methods is as follows.

The mathematical formulation of river flows is examined. The 3-D turbulence equations are depth integrated to obtain the shallow water equations. A novel approach to the approximation to both bed friction and lateral shear stress terms was followed. The relationship between the shallow water equation and the 1-D St Venant equations is explored. This review of the mathematical aspects of river and floodplain flows provides the physical and theoretical basis of much of the following work on compound channels.

A literature search is presented into flow mechanisms in straight compound channels. The important flow mechanisms are identified and possible techniques of accounting for their effects on the conveyance capacity of straight compound channels are identified. A simplification of the 2-D shallow water equations results in the technique called the Lateral Distribution Method (LDM). A suitable finite difference technique was applied to the basic differential equation and combined with the most promising lateral eddy viscosity model, based on bed shear stresses.

The available laboratory and field data<sup>a, b, c</sup> used to investigate the performance of the LDM and the range of non-dimensional eddy viscosities. The LDM is compared with methods developed by other authors.

A literature search into flow mechanisms in meandering compound channels is presented. The important flow mechanisms are identified and strategies for accounting for the effects on the conveyance capacities of meandering channels are identified. A semi-empirical analysis of the best laboratory data available is carried out and improved methods of discharge estimation for meandering channels are derived. These new methods were verified against independent laboratory and field data.

Strategies for future research are presented. These should concentrate on the collection of reliable field data to confirm findings based on laboratory data and the development of sophisticated numerical models, which may then be used to extend the detailed understanding of the complex mechanisms present during compound channel flows.

In summary the author has derived and developed an improved version of the lateral distribution model for discharge estimation in straight compound channels. This model is shown to be superior in many respects to existing models. Laboratory and field data are used to investigate the behaviour of possible lateral viscosity models and the use of a single value of non-dimensional eddy viscosity is found to be adequate in a wide range of situations. The author has also derived two new models for discharge estimation in meandering compound channels. These models are verified against the available laboratory and field data and are shown to be superior to the existing methods.

For convenience this thesis is presented in two volumes. Volume 1 contains the main text of the thesis and volume 2 contains the tables, figures and appendices referred to in volume 1.

## ACKNOWLEDGEMENTS

The author is grateful for the help, encouragement, guidance and patience which he received from his two supervisors, Dr D A Ervine of the University of Glasgow and Dr P G Samuels of HR Wallingford. The work presented in this thesis could not have been carried out without their support.

Many other colleagues at The University of Glasgow and HR Wallingford are also owed a debt of gratitude. The author would like to thank Dr W J Withers, Dr Y R Fares, Mary Johnstone, Judith Slade, Phil Hollinrake, David Ramsbottom and Dr Nigel Walmsley from whom he has learned much about Engineering, Hydraulics and Computing. The author is grateful to the illustrators in the graphics department at HR Wallingford, who prepared many of the sketches and figures presented here.

The author is grateful for the financial support extended by the Science and Engineering Research Council and HR Wallingford Ltd. in the form of a CASE post-graduate studentship. The opportunity to gain experience of academic and industrial research is greatly appreciated. Much of the work presented in this thesis was refined and extended by the author after he moved to HR Wallingford in 1990. Some of the work on straight compound channels was carried out with funding from the Ministry of Agriculture Fisheries and Food (MAFF) under their strategic research commissions. Some of this material has appeared in Wark et al (1991). The work on the values of non-dimensional eddy viscosity for the SERC FCF presented in section 4.4.1 and 4.4.2 was carried out under the supervision of P Ackers and was summarized by Ackers (1991) and Wark et al (1991).

The work presented in chapters 5 and 6 resulted largely from a collaborative research project funded by the National Rivers Authority for England and Wales. The author is indebted to his collaborator: Professor C S James of The University of Witwatersrand, Johannesburg, South Africa. The project involved analyzing the data collected during Phase B of the FCF research programme and required close collaboration with Professor James over a nine month period. Some of the material included in chapters 5 and 6 is based on analysis carried out by Professor James and is presented here for completeness. In particular the following sections are the sole work of Professor James: 5.6, 5.7, 6.4.2, 6.4.3 and 6.4.5. Reports submitted, from HR Wallingford, to the NRA during the project include EX 2485, EX 2548 and EX 2606. A much more detailed report was

also submitted to MAFF at the end of the project, James and Wark (1992).

The author is extremely grateful to Professor James for his help and encouragement and fully acknowledges his contribution to the work presented in this thesis.

The academics and research assistants who carried out the Phase B investigation on the SERC FCF also gave invaluable assistance in collating the available data and providing the author with some results of their own analysis. The assistance of the following is gratefully acknowledged: Prof B B Willetts and Dr R Hardwick (The University of Aberdeen); Prof R H J Sellin and Dr R Greenhill (The University of Bristol); Dr D A Ervine and Dr M L Lorena (The University of Glasgow) and Dr D W Knight (The University of Birmingham).

The author would like to acknowledge the support and encouragement which he received from his father and family. This thesis would never have been completed without this support.

## CONTENTS VOLUME 1

	Page
ABSTRACT	C.1
ACKNOWLEDGEMENTS	C.3
CONTENTS	C.5
NOTATION	C.10
LIST OF TABLES	C.15
LIST OF FIGURES	C.17
1. INTRODUCTION	1.1
2. THE EQUATIONS OF RIVER AND FLOODPLAIN FLOW	2.1
2.1 Introduction	2.1
2.2 The basic equations of fluid flow	2.2
2.2.1 Introduction	2.2
2.2.2 The 3-D flow equations	2.2
2.2.3 The body force vector	2.3
2.2.4 The internal stress tensor	2.4
2.2.5 Incompressible fluid	2.6
2.2.6 The effects of turbulence	2.6
2.3 Derivation of the 2-D flow equations	2.9
2.3.1 Initial assumptions	2.9
2.3.2 The 2-D continuity equation	2.10
2.3.3 The 2-D dynamic equations	2.10
2.4 Modelling the boundary shear terms	2.15
2.4.1 The boundary stresses	2.15
2.4.2 The local coordinate system	2.16
2.4.3 Approximating the boundary stresses	2.18
2.4.4 The wind stresses	2.19
2.4.5 The bed stresses	2.19
2.4.6 Summary of 2-D equations	2.22
2.5 Derivation of the St Venant equations	2.23
2.5.1 Initial assumptions	2.23
2.5.2 The 1-D continuity equation	2.24
2.5.3 The 1-D dynamic equation	2.24
2.5.4 Summary of 1-D equations	2.26

2.6	Summary and Conclusions	2.26
3.	<b>FLOW MECHANISMS IN STRAIGHT COMPOUND CHANNELS</b>	3.1
3.1	Introduction	3.1
3.2	Compound channels and the important mechanisms	3.1
3.2.1	Definition of a compound channel	3.1
3.2.2	Research into flows in straight compound channels	3.4
3.3	Summary of flow mechanisms in straight compound channels	3.31
3.4	Methods for conveyance estimation available in the literature	3.33
3.5	A new approach to the lateral distribution equation	3.39
3.6	Conclusions	3.42
4.	<b>DISCHARGE ESTIMATION IN STRAIGHT COMPOUND CHANNELS</b>	4.1
4.1	Introduction	4.1
4.2	Summary of data	4.1
4.2.1	Laboratory data	4.1
4.2.2	Field data	4.4
4.3	Comparison between analytic and numerical solutions for the LDM	4.7
4.4	Application of LDM to SERC FCF Phase A data	4.8
4.4.1	Investigation of NEV values	4.9
4.4.2	Discharge estimation with fixed NEV values	4.10
4.4.3	Calculated distributions of velocity and discharge	4.12
4.4.4	Conclusions	4.14
4.5	Application of LDM to Laboratory and field data	4.14
4.5.1	Laboratory data	4.14
4.5.2	Field data	4.15
4.6	Comparison of different methods of calculating discharge	4.20
4.6.1	The methods	4.20
4.6.2	SERC FCF Phase A	4.21
4.6.3	Myers' data	4.23
4.6.4	Lambert's data	4.24
4.6.5	Field data	4.25

4.6.6	Comparison with backwater calculations	4.30
4.7	Summary and Conclusions	4.31
5	<b>FLOW MECHANISMS IN MEANDERING CHANNELS</b>	5.1
5.1	Introduction	5.1
5.2	Laboratory investigations into meandering flow	5.1
5.2.1	Phase B SERC FCF	5.2
5.2.2	Aberdeen	5.7
5.2.3	US Army Vicksburg	5.8
5.2.4	Toebe and Sooky	5.10
5.2.5	Smith	5.11
5.2.6	James and Brown	5.12
5.2.7	Kiely	5.13
5.2.8	Stein and Rouve	5.14
5.3	General comments	5.15
5.4	Bed friction	5.17
5.5	Summary	5.19
5.6	Inbank meandering flow	5.20
5.6.1	Background	5.20
5.6.2	Energy loss in channel bends	5.22
5.6.3	Methods of evaluating non-friction losses	5.23
5.6.4	Data sets	5.23
5.6.5	Results and conclusions	5.24
5.6.6	Energy loss mechanisms in channel bends	5.28
5.6.7	Stage-discharge prediction methods	5.33
5.7	Application of prediction methods	5.45
5.7.1	The methods	5.45
5.7.2	Data set	5.47
5.7.3	Results and conclusions	5.48
5.8	Summary and conclusions	5.51
6	<b>DISCHARGE ESTIMATION IN MEANDERING COMPOUND CHANNELS</b>	6.1
6.1	Introduction	6.1
6.2	Application of straight channel methods to meandering data	6.1
6.2.1	The methods	6.1
6.2.2	The data set	6.3

6.2.3	Results	6.4
6.3	Procedures for discharge estimation in meandering compound channels	6.5
6.3.1	Important mechanisms	6.5
6.3.2	Methods available in the literature	6.6
6.4	Approach to conveyance estimation	6.10
6.4.1	Introduction	6.10
6.4.2	Formulation zone 1	6.12
6.4.3	Formulation zone 2	6.26
6.4.4	Formulation zones 3 and 4	6.40
6.4.5	Boundary shear stresses	6.41
6.4.6	Summary	6.43
6.5	Verification of the procedure	6.45
6.5.1	Background	6.45
6.5.2	Methods	6.45
6.5.3	Application to laboratory data	6.46
6.5.4	Application to straight laboratory data	6.54
6.5.5	Application to field data	6.55
6.6	Summary and conclusions	6.58
7	RECOMMENDATIONS FOR FUTURE RESEARCH	7.1
7.1	Introduction	7.1
7.2	Straight compound channels	7.1
7.2.1	Background	7.1
7.2.2	Laboratory studies	7.2
7.2.3	Further development of discharge estimation techniques	7.3
7.3	Meandering compound channels	7.4
7.3.1	Stage-discharge prediction for inbank flows	7.4
7.3.2	Laboratory studies	7.5
7.4	Field data collection	7.7
7.4.1	Strategy for field data collection	7.8
7.4.2	Suitable sites	7.9
7.4.3	Hydraulic data	7.10
7.5	Computational modelling	7.11
7.5.1	Turbulence modelling	7.11
7.5.2	One dimensional modelling	7.11
8.	CONCLUSIONS	8.1
9.	REFERENCES	R.1

## NOTATION

$a, b, c$	constants
$a_{ij}, b_{ij}$	$i, j$ /th elements of arbitrary tensors
$A$	3x3 matrix defined in chapter 3
$A$	cross-sectional area
$A$	unsubscripted, cross-sectional area of main channel
$A^{-1}$	the inverse matrix of $A$
$b$	the elevation of the channel bed
$B$	ratio of an arbitrary sloping area to its horizontal projection
$B$	top width of main channel
$c$	coefficient in equation for zone 1 adjustment factor
$C, D$	constants
$C$	Chezy bed friction parameter
$C_{sl}$	length coefficient for expansion and contraction losses, zone 2
$C_{ssc}$	side slope coefficient for contraction loss, zone 2
$C_{sse}$	side slope coefficient for expansion loss, zone 2
$C_{wd}$	shape coefficient for expansion and contraction losses, zone 2
$C_{ij}$	the $i, j$ /th element of the 2-D convection tensor
$\underline{C}$	the 2 - D convection tensor
$ds, D_s$	element of area with arbitrary orientation
$ds_m, D_{sm}$	the projection of $ds$ onto a plane with normal vector lying along the $m$ coordinate direction
$dF_i$	the $i$ /th component of the force vector which acts on an arbitrary sloping surface
$\underline{dF}$	the force vector which acts on an arbitrary sloping surface
$D$	the local depth of flow
$D_{50}$	median size of bed material
$e_{ij}$	the $i, j$ /th component of the rate of strain tensor
$\underline{E}$	the rate of strain tensor
$f$	Darcy-Weisbach friction factor due to bed friction only
$f_i$	Darcy-Weisbach friction factor due to channel bends
$f_i$	the $i$ /th component of the body force vector
$f'$	Total Darcy-Weisbach friction factor due to bed friction and bends ( $f + f_i$ )
$f'$	ratio of flood plain and main channel Darcy-Weisbach friction factors
$f_{*R}$	parameter in Ranga Ragu's resistance law
$F_r$	Froude number
$F_1$	factor for non-friction losses in zone 2 associated with main channel geometry
$F_2$	factor for additional non-friction losses in zone 2 associated with main channel sinuosity
$\underline{F}$	the body force vector
$g$	the gravitational acceleration

$h$	the elevation of the free water surface
$h$	hydraulic depth of main channel, = $A/B$
$h_L$	head loss through a bend
$\hat{i}_r$	the unit vector in the $r$ /th coordinate direction
$\hat{i}$	the unit vector in the $x$ coordinate direction
$\mathbf{I}$	the unit matrix
$\hat{j}$	the unit vector in the $y$ coordinate direction
$k_S$	Nikuradse's roughness size
$K$	coefficient in equation for zone 1 adjustment factor
$K_e$	factor for expansion and contraction losses in zone 2
$K_c$	contraction coefficient
$K_L$	bend loss coefficient
$\hat{k}$	the unit vector in the $z$ coordinate direction
$l$	length of bend
$l_c$	length of bend required for fully developed secondary currents
$L$	meander wavelength
$L_{co}$	length of straight cross over
$m$	coefficient in equation for zone 1 adjustment factor
$M_i$	the $i$ /th component of a general stress vector which acts on an arbitrary sloping surface
$\underline{M}$	the general stress vector which acts on an arbitrary sloping surface
$\underline{M}_b, \underline{M}_w$	the stress vector above defined for the channel bed and the free water surface respectively
$n$	Manning's friction parameter bed friction only
$n'$	Manning's friction parameter including bend losses
$\underline{n}$	the unit vector
$N$	parameter related to free vortex flow
$P$	the mechanical pressure
$q_i$	the $i$ /th component of the unit flow vector
$\underline{q}$	the unit flow vector
$Q$	discharge
$Q$	zonal discharge
$Q_{calc}$	calculated discharge
$Q_{meas}$	measured discharge
$Q_{bf}$	main channel bankfull discharge
$Q_T$	total discharge
$Q_1'$	adjustment factor for zone 1 discharge
$r_c$	mean radius of curvature
$r_o$	outer radius of curvature
$r_i$	inner radius of curvature
$r_{ij}$	the $i,j$ /th element of the Reynolds' stress tensor
$R$	hydraulic radius
$R_e$	Reynolds number
$\underline{R}$	the Reynolds' stress tensor
$s$	channel sinuosity
$S_i$	the slope of a general surface along the $i$ /th coordinate direction ( $S_x, S_y$ )
$S_o$	flood plain gradient

$S_f$	friction gradient
$S_s$	cotangent of main channel side slope
$S_{sf}$	cotangent of flood plain side slope
$S''$	gradient associated with transverse secondary currents
$S''_{fd}$	gradient associated with fully developed transverse secondary currents
$t$	the time variable
$T$	temperature in degrees centigrade
$T_{ij}$	the i,j/th element of the effective stress tensor
$\underline{\mathbf{T}}$	the effective stress tensor
$u_i$	the i/th component of the 3-D instantaneous velocity vector (u, v, w)
$u_i$	the i/th component of the 3-D temporal mean velocity vector (u, v, w)
$u$	the x component of the 3-D velocity vector
$u_i'$	the i/th component of the 3-D fluctuating velocity vector (u', v', w')
$U_i$	the i/th component of the 2-D depth averaged velocity vector (U, V)
$U$	the x component of the 2-D depth averaged velocity vector
$\underline{\mathbf{U}}$	the 2-D depth averaged velocity vector
$v$	the y component of the 3-D velocity vector
$v_r$	transverse velocity
$v_{rc}$	transverse velocity at the water surface in the centre of the channel
$v_{rcfd}$	fully developed vrc
$V$	the y component of the 2-D depth averaged velocity vector
$V$	flow velocity
$V_*$	shear velocity
$w$	the z component of the 3-D velocity vector
$w_i$	the i/th component of the 2-D wind velocity vector
$W_2$	width of zone 2
$W_T$	width of flood plain
$\underline{\mathbf{W}}$	the 2-D wind velocity vector
$x,y,z$	a set of right handed cartesian coordinate axes
$\bar{x},\bar{y},\bar{z}$	a set of coordinate axes
$y$	flow depth
$y_m$	average flow depth at position along bend where secondary currents become fully developed
$y_2$	flow depth on flood plain at main channel bank
$y$	dimensionless flow depth on flood plain, = $y_2/(A/B)$
$z$	vertical distance
	angle between cross over length of main channel and flood plain centre line
$Z_0$	the elevation of either the channel bed or the free water surface

$\alpha$	an arbitrary angle
$\alpha_{ij}$	the $i,j$ /th velocity distribution factor
$\delta_{ij}$	the kronecker delta
$\Delta$	the local rate of expansion
$\epsilon$	an arbitrary angle
$\Phi$	arbitrary functions describing the vertical variations of components of the velocity vector over the flow depth
$\Phi$	parameter related to bend angle
$\xi$	parameter in Ranga Ragu's resistance law
$\kappa$	von Karman constant
$\rho$	fluid density
$\nu$	kinematic viscosity
$\tau$	shear stress
$\tau_i$	shear stress due to channel curvature
$\tau_s$	shear stress due to friction only
$\mu$	the viscosity of a fluid
$\nu$	the kinematic viscosity of a fluid
$\nu_t$	the kinematic eddy viscosity
$\alpha_{ij}$	the $i,j$ /th element of the internal stress tensor
$\underline{\sigma}$	the internal stress tensor
$\tau_{ij}$	the $i,j$ /th element of the deviatoric stress tensor
$\tau_{bi}$	the $i$ /th component of the shear stress vector acting on the channel bed
$\tau_{wi}$	the $i$ /th component of the shear stress vector acting on the free water surface
$\underline{\tau}$	the deviatoric stress tensor
$\underline{\tau}_b$	the shear stress vector acting on the channel bed
$\underline{\tau}_w$	the shear stress vector acting on the free water surface
$\theta_{fd}$	angle of bend required for fully developed secondary currents
$\theta_m$	mean angle between flood plain centre line and main channel centre line
$\theta_{pl}$	the angle between the coordinate directions $\underline{p}$ and $\underline{\tau}$ known as a direction cosine

Subscripts :

$i,j$	dummy variables which can take the values 1,2 or 3 representing the x,y and z cartesian coordinate directions respectively
1	zone 1
2	zone 2
bf	bankfull
ave	average
calc	predicted value
meas	measured value
m	measured value
p	predicted value

Operators :

$$\frac{\partial}{\partial x_i}$$

the partial derivative operator with respect to  $x_i$ .

Note:

The repeated index convention for tensor notation has been used, see Appendix 1, section 2.

## LIST OF TABLES

Note all tables and figures are included in volume 2

### Chapter 4

- 4.1 Summary of Phase A experiments on SERC FCF
- 4.2 Overbank gauging sites
- 4.3 Overbank gauging sites, channel and floodplain widths
- 4.4 Overbank gauging sites, channel and floodplain depths
- 4.5 Overbank gauging sites, Manning's n values
- 4.6 Mean values of back calculated NEV SERC FCF
- 4.7 Mean values of back calculated NEV inbank SERC FCF
- 4.8 Mean values of back calculated NEV all data SERC FCF
- 4.9 Mean errors with NEV fixed smooth floodplains SERC FCF
- 4.10 Mean errors with NEV fixed rough floodplains SERC FCF
- 4.11 Mean errors NEV fixed inbank SERC FCF
- 4.12 Mean errors NEV fixed all data SERC FCF
- 4.13 Mean errors NEV fixed all inbank data SERC FCF
- 4.14 Mean errors in discharge for various methods SERC FCF
- 4.15 Mean errors in discharge for various methods SERC FCF all data
- 4.16 Mean errors in depth for various methods SERC FCF
- 4.17 Mean errors in depth for various methods SERC FCF all data
- 4.18 Mean errors in discharge Myers lab data
- 4.19 Mean errors in depth Myers lab data
- 4.20 Mean errors in discharge Lambert lab data
- 4.21 Mean errors in depth Lambert lab data
- 4.22 Mean errors in discharge for each overbank gauging site
- 4.23 Mean errors in discharge overbank gauging sites

### Chapter 5

- 5.1 Summary of SERC Phase B tests
- 5.1 (cont) Summary of SERC Phase B tests
- 5.2 Summary of SERC Phase B stage discharge tests
- 5.3 Summary of Aberdeen experiments
- 5.4 Summary of Vicksburg experiments 2ft wide channel
- 5.5 Geometric parameters lab studies meandering channels
- 5.6 Non-dimensional geometric parameters meandering channels
- 5.7 Bend losses for 60<sup>0</sup> meander geometry, trapezoidal cross-section
- 5.8 Non-friction losses for 60<sup>0</sup> meander geometry, natural cross-section
- 5.11 Non-friction losses for 110<sup>0</sup> meander geometry, natural cross-section
- 5.12 Summary of mean errors in bend loss predictions

### Chapter 6

- 6.1 Mean errors straight methods meandering data
- 6.2 Contraction loss coefficients (Rouse, 1950)
- 6.3 Main channel integrated discharges

- 6.4 Variables for defining main channel flow
- 6.5 Adjusted variables for defining main channel flow
- 6.6 Roughness and sinuosity adjustment to  $Q1'$
- 6.7 Roughness and sinuosity adjustment to  $c$
- 6.8 Errors (%) in reproducing  $Q1'$  for high values of  $y'$
- 6.9 Data sets for inner flood plain analysis
- 6.10 Equation parameters for  $y'$  greater than 0.2
- 6.11 Geometric data overbank laboratory studies
- 6.12 Geometric data Sooky's laboratory study
- 6.13 Main channel geometric data
- 6.14 Mean % errors in discharge FCF data
- 6.15 Mean % errors in discharge Aberdeen, Vicksburg and Kiely data
- 6.16 Mean % errors in discharge Sooky data
- 6.17 Mean % errors in discharge all data
- 6.18 Ranking of methods
- 6.19 Mean % errors in stage FCF data
- 6.20 Mean % errors in stage Aberdeen, Vicksburg and kiely data
- 6.21 Mean % errors in stage Sooky data
- 6.22 Mean % errors in stage all data
- 6.23 Sensitivity tests : effect of errors in wave length
- 6.24 Sensitivity tests : effect of errors in channel side slope
- 6.25 Measured zonal discharges, Sooky and Kiely data
- 6.26 Errors (%) in calculated total flows, Sooky and Kiely data
- 6.27 Measured and calculated flow distributions
- 6.28 Reach averaged geometric parameters Roding study
- 6.29 Errors in predicting overbank discharges
- 6.30 Sensitivity tests on the effect of floodplain roughness

## LIST OF FIGURES

### Chapter 1

- 1.1 Simple channel
- 1.2 Compound channel

### Chapter 2

- 2.1 Rotation about y axis
- 2.2 Rotation about  $\bar{x}$  axis
- 2.3 Definitions for a river channel

### Chapter 3

- 3.1 Simple channel
- 3.2 Compound channel
- 3.3 Variation of A, P and R for the River Severn at Montford, after Knight et al (1989)
- 3.4 Variation of Manning's n and friction factor with stage
- 3.4a Surface streamlines for a straight compound channel, after Sellin (1964)
- 3.5 Definition of apparant shear forces for compound channels
- 3.6 James and Brown's correction factor for straight compound channels, after James and Brown (1977)
- 3.7 Definition sketch for Rajaratnum and Ahmadi's channel, after Rajaratnum and Ahmadi (1981)
- 3.8 The vertical distribution of velocity in compound channels, after Rajaratnum and Ahmadi (1981)
- 3.9 Depth averaged velocity in the main channel, after Rajaratnum and Ahmadi (1981)
- 3.10 Depth averaged velocity and bed shear stress on the floodplain, after Rajaratnum and Ahmadi (1981)
- 3.11 Variations in friction parameters for the SERC FCF Phase A data, after Myers and Brennan (1990)
- 3.12 Turbulence data from the SERC FCF, after Knight and Shiono (1990)
- 3.13 Distribution of Reynolds stresses in the horizontal plane, after Knight and Shiono (1990)
- 3.15 Lateral variation of local friction factor for the SERC FCF, after Knight and Shiono (1990)
- 3.16 Lateral variation of depth averaged lateral eddy viscosity, after Knight and Shiono (1990)
- 3.17 Bed shear stress disributions for SERC FCF, after Knight and Shiono (1990)
- 3.18 Example distribution of discharge adjustment factors for SERC FCF, after Ackers 1991.
- 3.19 Secondary current distributions, after Tominaga et al (1989, 1991)
- 3.20 Secondary current distributions, after Shiono and Knight (1989, 1991)
- 3.21 Illustration of secondary currents, after Shiono and Knight (1989)
- 3.22 Shear layer width in a rectangular channel, after Samuels (1988)

- 3.23  $\lambda$  values for FCF derived by Shiono and Knight (1991)
- 3.24 Lateral distribution of convection terms in FCF, after Shiono and Knight (1991)
- 3.25 Cross-section for the River Severn at Montford, after Knight et al (1991)
- 3.26 Calculated lateral distributions of velocity for the Severn at Montford, after Knight et al (1991)
- 3.27 Calculated lateral distributions of velocity and shear stress after Keller and Rodi (1988)
- 3.28 Summary of mechanisms in a straight compound channel, after Knight et al (1983)
- 3.29 Divided channel methods

#### Chapter 4

- 4.1 Layout of the SERC FCF during Phase A, after Knight and Sellin (1989)
- 4.2 Channel cross-sections, SERC FCF Phase A
- 4.2a Compound channel definitions
- 4.3 Myers' laboratory cross-sections
- 4.4 Lambert's laboratory cross-sections
- 4.5 Natural channels cross-sections
- 4.6 Natural channels cross-sections
- 4.7 Cross-sections for the River Penk
- 4.8 Cross-sections for the River Trent
- 4.9 Main channel Manning's n values natural channels
- 4.10 Main channel Manning's n values natural channels
- 4.11 Analytic and numerical solutions (LDM, LDM2) rectangular channel
- 4.12 Analytic and numerical solutions (LDM, LDM2) quadrilateral channel
- 4.13 Computed stage-discharges (LDM) for SERC FCF Phase A smooth data
- 4.14 Computed stage-discharges (LDM) for SERC FCF Phase A smooth data
- 4.15 Computed stage-discharges (LDM) for SERC FCF Phase A rough data
- 4.16 Computed distributions of NEVC for SERC FCF Phase A smooth data
- 4.17 Computed distributions of NEVC for SERC FCF Phase A rough data
- 4.18 Distributions of %error in  $Q_{calc}$  with  $NEV = 0.16$  for SERC FCF Phase A smooth data
- 4.19 Distributions of %error in  $Q_{calc}$  with  $NEV = 0.16$  for SERC FCF Phase A rough data
- 4.20 Calculated depth averaged velocity profiles LDM Series 2 SERC FCF Phase A data
- 4.21 Calculated depth averaged velocity profiles LDM Series 3 SERC FCF Phase A data
- 4.22 Calculated depth average velocity profiles LDM and LDM2 Series 2 SERC FCF Phase A data
- 4.23 Calculated depth average velocity profiles LDM and LDM2 Series 3

#### SERC FCF Phase A data

- 4.24 Calculated unit flow profiles LDM Series 2 SERC FCF Phase A data
- 4.25 Calculated unit flow profiles LDM Series 3 SERC FCF Phase A data
- 4.26 Stage discharge curves for Myers' lab data LDM
- 4.27 Calculated depth averaged velocity profiles LDM Myers' Series A
- 4.28 Calculated depth averaged velocity profiles LDM Myers' Series F
- 4.29 Stage discharge curves for Lambert's lab data LDM
- 4.30 Cross-section and stage discharge curve for Kiely's lab data LDM
- 4.31 Calculated depth averaged velocity profiles LDM Kiely
- 4.32 Stage-discharge curves for field data LDM
- 4.33 Stage-discharge curves for field data LDM
- 4.34 Stage-discharge curves with fixed and variable NEV values LDM, Severn at Montford
- 4.35 Stage-discharge curves LDM and LDM2, Severn at Montford
- 4.36 Velocity profiles fixed and variable NEV, Severn at Montford
- 4.37 Velocity profiles fixed and variable NEV LDM2, Severn at Montford
- 4.38 Velocity profiles River Main section 14
- 4.39 Velocity profiles River Ouse at Skelton
- 4.40 Velocity profiles River Penk at Penkridge
- 4.41 Velocity profiles River Trent at North Muskham, bankfull n values
- 4.42 Velocity profiles River Trent at North Muskham, calibrated n values
- 4.43 Unit flow profiles, fixed NEV, Severn at Montford
- 4.44 Unit flow profiles, variable NEV, Severn at Montford
- 4.45 Unit flow profiles, n constant and variable, Severn at Montford
- 4.46 Depth averaged velocities, n constant and variable, Severn at Montford
- 4.47 Errors in calculated discharges SERC FCF Phase A, Smooth data
- 4.48 Errors in calculated discharges SERC FCF Phase A, Rough data
- 4.49 Errors in calculated depths SERC FCF Phase A, Smooth data
- 4.50 Errors in calculated depths SERC FCF Phase A, Rough data
- 4.51 Mean errors in discharge and depth SERC FCF Phase A
- 4.52 Proportion of flow in main channel, SERC FCF Phase A
- 4.53 Differences in calculated and measured proportions of flow in main channel, SERC FCF Phase A
- 4.54 Mean errors in discharge and depth Myers' lab data
- 4.55 Differences in calculated and measured proportions of flow in main channel, Myers' lab data
- 4.56 Errors in calculated discharges Lambert's lab data
- 4.57 Errors in calculated depths Lambert's lab data
- 4.58 Mean errors in discharge and depth Lambert's lab data
- 4.59 Mean errors in discharge river gauging data
- 4.60 Variation of errors in discharge with stage river gauging data, LDM
- 4.61 Variation of errors in discharge with stage river gauging data, DCM
- 4.62 Variation of errors in discharge with stage river gauging data, SCM
- 4.63 Variation of errors in discharge with stage river gauging data, SCM3, SSGM
- 4.64 Variation of errors in discharge with stage river gauging data, DCM2
- 4.65 Variation of errors in discharge with stage river gauging data, ACKM
- 4.66 Backwater profiles for the River Thames at Wallingford reach 1
- 4.67 Example velocity profiles River Thames at Wallingford

4.68 Backwater profiles for the River Thames at Wallingford reach 2

4.69 Backwater profiles for the River Tees at Low Moor

## Chapter 5

5.1 Detailed plan geometry of FCF 60° meander

5.2 Plan of flume and natural cross-section geometry for 60° meander

5.3 Detailed plan geometry for FCF 110° meander

5.4 Plan of flume and natural cross-section geometry for 110° meander

5.5 Plan geometries of the Aberdeen flume with channel sinuosities of 1.40 and 2.04 (after Willetts 1992)

5.6 Plan geometry of the Aberdeen flume with channel sinuosity of 1.21 (after Willetts 1992)

5.7 Plan and cross-sections for Vicksburg flume (after US Army 1956)

5.8 Plan and cross-sections for Sooky's flume (after Sooky 1964)

5.9 Plan and cross-sections for Kiely's flume (after Kiely 1990)

5.10 Flow processes in a meandering compound channel (after Ervine and Jasem)

5.11 Adjustment to Manning's  $n$  for bend losses: measured and predicted

5.12 Predicted adjustments to  $n$  for bend losses: modified Chang method

## Chapter 6

6.1 Cross-section subdivision for overbank flows Ervine and Ellis method

6.2 Variation of main channel discharge along a meander during overbank flow (FCF Phase B)

6.3 Inbank stage-discharge relationship for 60° trapezoidal channel

6.4 Inbank stage-discharge relationship for 60° natural channel

6.5 Inbank stage-discharge relationship for 110° natural channel

6.6 Variation of dimensionless main channel discharge with flow depth

6.7 Variation of dimensionless main channel discharge with dimensionless flow depth

6.8 Variation of dimensionless main channel discharge with dimensionless flow depth with points adjusted for friction factor ratio

6.9 Additional adjustment to discharge for relative roughness

6.10 Adjustment to  $c$  for relative roughness

6.11 Flow expansion over a downward step

6.12 Flow contraction over an upward step

6.13 Expansion and contraction flow patterns

6.14 Width to depth ratio correction for expansion losses

6.15 Width to depth ratio correction for contraction losses

6.16 Width to depth ratio correction for combined expansion and contraction losses

6.17 Errors for SERC predictions before sinuosity predictions

6.18 Errors for Aberdeen predictions before sinuosity predictions

6.19 Adjustment factor for inner flood plain discharges for SERC Phase B experiments

6.20 Adjustment factor for inner flood plain discharges for Aberdeen experiments

6.21 Adjustment factor for inner flood plain discharges for  $y' > 0.2$ , SERC Phase B data

- 6.22 Adjustment factor for inner flood plain discharges for  $y' > 0.2$ , Aberdeen data
- 6.23 Variation of  $a$  with  $s$
- 6.24 Variation of  $b$  with  $B^2/A$
- 6.25 Comparison of predicted zone 2 adjustment factor with SERC data
- 6.26 Comparison of predicted zone 2 adjustment factor with Aberdeen data
- 6.27 Example of boundary shear stress distribution in a meandering compound channel (after Lorena)
- 6.28 Cross-section subdivision for overbank flows, James and Wark
- 6.29 Errors in predicted discharge and depth BFO
- 6.30 Errors in predicted discharge and depth JW
- 6.31 Errors in predicted discharge and depth JW2
- 6.32 Errors in predicted discharge and depth EE
- 6.33 Errors in predicted discharge and depth GH4
- 6.34 Errors in predicted discharge and depth GH5
- 6.35 Location plan of study area on River Roding at Abridge (after Sellin et al 1990)
- 6.36 Roding at Abridge sample cross-section
- 6.37 Roding at Abridge measured and calculated stage-discharges

# CHAPTER 1

## INTRODUCTION

### River flooding and compound channels

The river engineer is faced with the problem of calculating discharge capacities, in natural and man made channels, on a regular basis. These calculations are required for a variety of purposes such as water supply, drainage, flood alleviation or pollution monitoring schemes. In certain circumstances the traditional methods of discharge estimation are known, or thought, to be inaccurate.

One such case is during overbank flow, when a river has flooded. Figure 1.1 shows a typical simple or compact channel, and Figure 1.2 shows a compound channel. Compound channels are very common, both in natural and man made rivers. During normal periods the flow is restricted to the main channel and only affects the berms or floodplains during unusually high flow conditions. The flood plains of rivers are generally developed by man for residential, industrial or agricultural use. Indeed many of the early civilizations in history were founded along river valleys subject to periodic floods. The regular flooding of the fields enriched the land by depositing minerals and sediments. This natural irrigation and fertilization of the land allowed these societies to support large numbers of inhabitants and to develop sophisticated societies.

While in a rural agricultural area such flooding may be generally beneficial there comes a point where the size and duration of the flood is such that the good effects such as irrigation and fertilization of fields are negated by the destruction of homes and infrastructure and the loss of life. A modern day example is evident in Bangladesh, where a largely rural population rely on the regular inundation of their fields to provide the correct conditions for the rice crop but who are also at risk from larger floods, which regularly kill thousands and destroy crops.

In more developed countries the floodplain is often developed for mainly residential or industrial uses. In these situations the tolerance of flooding is much reduced

compared to agricultural situations, even a comparatively small flood can cause a large economic loss to individuals and the general economy.

The river engineer is involved in predicting the effects of floods and in developing strategies or schemes to mitigate the damage floods inflict on human activities. In order to carry out these roles effectively the engineer requires techniques which allow the conveyance capacity of compound channels to be accurately assessed.

### **Research strategy**

The purpose of the work presented in this thesis is to investigate methods of calculating conveyance, or discharge, capacity of compound channels. There is a general body of opinion that traditional hydraulic techniques are in some way deficient if applied to compound channels. Much of the early literature sets out to prove this and directed later work into describing, measuring and understanding the mechanisms which make this true.

The approaches which have been followed, to various aspects of this topic in this thesis, reflect the perceived need for research, the available information and possible solution techniques. In particular the following questions are addressed:

- 1) What is a compound channel?
- 2) Are there problems in assessing the conveyance capacity of compound channels?
- 3) What research has been carried out into these problems?
- 4) Is there a clear consensus on which are the important mechanisms and parameters, which control the conveyance capacity of compound channels?
- 5) Given the current state of knowledge of flow mechanisms is it possible to develop or construct improved methods or models which the practising engineer may use?

As a preliminary, to addressing these questions seriously, the following chapter

reviews the formulation of the equations which govern the flow of fluid within the river and floodplain environment. The starting point are the 3-D Navier Stokes equations. These equations are generally simplified by following Reynolds' approximations to deal with the small scale turbulent fluctuations. Applying the Boussinesq eddy viscosity approximation and integrating the Reynolds' equations through depth results in the shallow water equations, which describe the flow of fluid in a two dimensional domain with a free surface assuming that the discharges and velocities are uniform in the vertical. Further simplifications are possible by integrating the shallow water equations across a channel and result in the 1-D St Venant equations.

A sound working knowledge of the various possible equations and associated levels of complexity, which may be used to describe river and floodplain flows, is essential to understand both the context and the technical details of research in to compound channels. In general for straight compound channels most approaches are based on providing some procedure for adjusting the discharges calculated by simple 1-D theory. While in the case<sup>of</sup> meandering channels 2 or 3 dimensional theory and analysis is more appealing.

A review of the literature shows that the cases of straight and meandering compound channels are different. There are contrasts in the strength and type of mechanisms which affect the conveyance capacities in these two cases. Consequently this investigation considers straight compound channels (chapters 3 and 4) before progressing to the more difficult case of meandering channels (chapters 5 and 6).

Experimental and theoretical modelling of straight compound channel flows is reviewed. The important mechanisms, which affect the discharge capacity of compound channels, are distinguished and various procedures which account for these mechanisms are identified. A new procedure, based on a simplification of the shallow water equations and a simple turbulence model, which provides the lateral distribution of flow across a channel is identified and developed. An investigation of the behaviour of the LDM against the available laboratory and field data from

straight compound channels is carried out. A comparison between the new method and existing techniques is carried out based on laboratory and field data.

Any study of flows in meandering compound channels is handicapped by the relative sparseness of the available laboratory and field data. Before progressing to devising some model or procedure for calculating the discharge capacity of a meandering channel and floodplain it is necessary to review the data available and summarise the main conclusions and findings from these studies. A secondary requirement is to review the effect of channel meanders on the inbank conveyance capacity of a channel, this is a logical precursor to the more complex situation of overbank flow in meandering compound channels. The important mechanisms which affect the discharge capacity of these channels are identified.

A further literature review is presented covering proposed methods of calculating discharges in meandering compound channels. A promising method is then developed on the basis of the SERC FCF Phase B data and data from the University of Aberdeen. These methods are then tested and verified against laboratory and field data.

The methods identified above are all based on relatively simple conceptual models based on traditional engineering concepts for flows in straight channels. Flow in compound meandering channels is very complex and the development of methods to analyze it accurately will probably follow directions that are highly computational. The development of suitable 3-D models including sophisticated turbulence models is the ultimate goal of much research and the SERC FCF Phase B data is an important data set to use in the validation of such models. A slightly simpler approach would be to develop a 2-D depth integrated model with turbulence terms and this approach is useful in the case of straight compound channels.

The initial intention was to develop a 2-D finite element model based on the shallow water equations and continue the work of Samuels (1985). However the work involved in developing such a complex numerical model was prohibitive and it was

felt that it would be useful to develop a simple hand calculation technique which could provide the engineer with a method of obtaining a reasonable first estimate of the discharge capacity of meandering compound channels. This form of analysis can be seen as an intermediate step towards the development of more sophisticated models.

It was felt that the methods should be developed to be design oriented and expressed in terms of physical parameters which are meaningful in a design context. For example, the dependence of channel capacity on design variables, such as cross-section shape and size, should be fairly explicit and should not be expressed in terms of variables which are easy to apply to simplistic laboratory channels but difficult to apply to natural rivers.

To ensure a degree of generality in the design methods, it was decided to base them on conceptual models of the physical processes involved in dissipating energy and determining flow structure. The SERC data <sup>are</sup> used to quantify these processes, in terms of geometric and fluid state parameters. This involves theoretical and empirical formulations. The relative importance of the individual processes varies with the scale of the physical system, and possibly also with the flow condition. Separation and individual treatment of the processes should account for the effects of these variations on the required predictions (of stage-discharge relationships, for example) better than if these were made in terms of the geometries and fluid state parameters directly. The approach will also have the advantage of being able to include data from different sources and obtained under different conditions, and will allow the methods to be easily modified as new results and analyses become available in the future.

The division of the channel in to four zones as proposed by Ervine and Ellis (1987) was adopted as the most flexible approach. The stage-discharge relationship for a compound meandering channel is predicted by dividing the cross-section into zones and calculating the zonal discharges separately. The division is by a horizontal line at bankfull level and a vertical line on either side of the meander belt.

A comparison of the new methods and existing procedures is carried out. The methods are applied to predict the stage discharge values for a selection of the laboratory data available. In some cases zonal discharges were also measured and these provide a check on the predicted distribution of flows in addition to total discharges.

To summarize, the nature of the work presented in this thesis falls into two main areas:

- 1) The review of earlier experimental and conceptual modelling of flood plain flows.
- 2) The development of useful models for the conveyance capacities of compound channels.

Much of the work presented is based or verified against data from Phases A and B of the SERC FCF work. The Author was not part of the official FCF programme, however the work presented complements the official programme. The main original contributions made are:

- 1) The derivation of the unit flow form of the shallow water equations, including the B factor in the bed friction terms.
- 2) The use of the unit flow version of the lateral distribution equation to obtain flow distributions in straight compound channels. This model is applied to a much wider range of laboratory and field data than previously available.
- 3) The development of a new method for estimating conveyance capacity of meandering compound channels and its verification against the widest available range of laboratory and field data.

## CHAPTER 2

### THE EQUATIONS OF RIVER AND FLOODPLAIN FLOW

#### 2.1 Introduction

As mentioned in the previous chapter there were two main aims behind the work presented in this thesis. The first intention was to develop an understanding of the physical processes which affect the conveyance capacity of compound channels. Following on from this understanding it should then be possible to develop improved models which will accurately predict the important aspects of over-bank flow. In order to fulfil these aims it is necessary to be familiar with the basic physical equations of fluid flow. Our limited understanding of the problems leads us to suppose that any such model will be computer-based. The development of a deterministic computer model which adequately describes a physical phenomenon, such as fluid flow, can be categorised into at least four distinct stages:

- 1) Identification and application of the governing physical laws expressed in appropriate symbolic form - The conceptual model.
- 2) The introduction of simplifications and assumptions to produce a mathematical model which describes the system to the required degree of complexity - The mathematical model.
- 3) Application of the chosen algorithms (numerical techniques) to approximate the solution to the mathematical model - The numerical model.
- 4) Combining the numerical model with prototype data, (topographic, boundary roughness, fluid properties etc.), followed by implementation on the chosen computer system. - The computational model.

Each one of these stages involves the use of explicit or implicit assumptions and simplifications. These will affect the models' range of applicability; the accuracy of the solution it produces, (*if it actually does give a unique solution*), and the cost of using it to solve the original problem.

This chapter describes the first two of the above stages in an attempt to understand the type of processes which may operate and as a first step in developing a computational model of flow in a river channel floodplain

environment. The following section describes the basic equations governing the motion of fluids. Section two deals with integrating these 3-D equations over the flow depth to produce the 2-D equations. And the final section of this chapter is concerned with approximating the boundary shear stress terms which arise from this integration process.

## **2.2 The basic equations of fluid flow**

### **2.2.1 Introduction**

This section forms a preliminary to the following section in which the equations outlined below shall be integrated over the flow depth to produce the so called two dimensional depth integrated or shallow water equations. This approach to the problem of free surface flow in areas which are two dimensional in plan is not new. For example see Leendertse (1967), Kuipers and Vreugdenhil (1973), Falconer (1977), Tong (1983) and Samuels (1985). The main attraction of basing a model on the integrated equations is the reduction in complexity and cost of using the computational model; while still providing a sufficiently detailed description of the flow for many practical purposes.

There are two methods of deriving the 2-D depth integrated, or depth averaged, equations:

- 1) Integration of the equations of three dimensional fluid motion over the flow depth, applying suitable boundary conditions at the channel bed and free water surface.
- 2) The so called 'Engineering' approach of isolating a free body, or control volume. Identifying the forces acting and applying Newtons' laws from first principles. The engineering method is comparatively simple to understand and apply. But some care is required in the resolution of the forces acting on the control volume. The explicit integration approach, although more difficult to carry out, has the advantage of being mathematically more rigorous and is adopted here.

### **2.2.2 The 3-D flow equations**

The basic equations describing the motion of a continuous medium, such as a fluid, are easily derived using Newtons' laws of conservation of mass and momentum (see Batchelor (1967) and Hunter (1983)). Expressed in terms of a

right handed cartesian coordinate system they are as follows: Note : *The equations in this chapter are expressed in standard tensor notation wherever possible - see Appendix A.*

### The continuity equation

$$\frac{\partial \rho}{\partial t} + \frac{\partial \rho u_i}{\partial x_i} = 0 \quad (2.1)$$

### The dynamic equation

$$\frac{\partial \rho u_i}{\partial t} + u_j \frac{\partial \rho u_i}{\partial x_j} - \rho f_i - \frac{\partial \alpha_{ij}}{\partial x_j} = 0 \quad (2.2)$$

Where:

- $f_i$  the  $i$ /th component of the body force vector  $\underline{F}$
- $t$  time variable
- $u_i$  the  $i$ /th component of the velocity vector  $\underline{u}$ .
- $x_i$  the  $i$ /th coordinate direction in the cartesian system.
- $\rho$  the fluid density.
- $\alpha_{ij}$  the  $i,j$ /th component of the internal stress tensor  $\underline{\alpha}$ .

Subscripts :

- $i, j$  dummy variables which can take the values 1, 2 or 3 representing the  $x, y$  and  $z$  cartesian coordinate directions respectively.

Operators :

- $\frac{\partial}{\partial x_i}$  the partial derivative operator with respect to  $x_i$ .

Note: The repeated index summation convention for tensor notation has been used, see Appendix A, Section 2.

The following sections form a brief description of the body force vector, the internal stress tensor and the effects of turbulence. This is felt to be necessary because the following chapter will deal, in some detail, with the problems posed by these terms during the integration process.

### 2.2.3 The body force vector

This term represents the effect of the environment on the bulk matter of the fluid. Typical body forces include gravity and Coriolis accelerations. If we consider a cartesian coordinate system which has the  $z$  axis aligned vertically upwards, (We

shall refer to this set of cartesian axes as the NATURAL coordinate system and any other set of cartesian axes as a LOCAL coordinate system), then the body force vector due to gravity is :  $\underline{F} = (0,0, -g)$

$$\text{ie. } f_i = \begin{cases} 0 & \text{if } i = 1,2 \\ -g & \text{if } i = 3 \end{cases} \quad (2.3)$$

Where

$f_i$  the  $i$ /th component of the body force vector,  $\underline{F}$   
 $g$  the gravitational acceleration.

#### 2.2.4 The internal stress tensor

The internal stress tensor  $\underline{\sigma}$  represents the short range forces exerted on the boundaries of a fluid element. The element  $\sigma_{ij}$  of  $\underline{\sigma}$  is the  $i$ /th component of stress exerted across a plane surface which is normal to the  $j$  coordinate direction, (Batchelor p.10, Hunter chapter 4). It is possible to write  $\underline{\sigma}$  in the matrix notation shown below:

$$\underline{\sigma} = \begin{bmatrix} \sigma_{xx} & \sigma_{xy} & \sigma_{xz} \\ \sigma_{yx} & \sigma_{yy} & \sigma_{yx} \\ \sigma_{zx} & \sigma_{zy} & \sigma_{zz} \end{bmatrix} \quad (2.4)$$

The elements which lie on the leading diagonal, ( $\sigma_{ij}$ ,  $i=j$ ), are the normal stresses acting within the fluid. All the other elements, ( $\sigma_{ij}$ ,  $i \neq j$ ) are the tangential or shear stresses. It is simple to show that  $\underline{\sigma}$  is symmetric, ( $\sigma_{ij} = \sigma_{ji}$ ), and has only six independent components. When considering a moving fluid it is convenient to regard  $\underline{\sigma}$  as the sum of an isotropic part,  $P \underline{I}$ , and a deviatoric part,  $\underline{\tau}$ .

$$\sigma_{ij} = -P \delta_{ij} + \tau_{ij} \quad (2.5)$$

Where:

$P$  is the mechanical pressure defined as  $1/3$  of the trace of  $\underline{\sigma}$   
 $= 1/3 \sigma_{ii} = 1/3 (\sigma_{xx} + \sigma_{yy} + \sigma_{zz})$

$\delta_{ij}$  the kronecker delta, the elements of the unit matrix :  $\underline{I}$

$\underline{\tau}$  the deviatoric stress tensor, by definition  $\tau_{ii} = 0$ . Its components,  $\tau_{ij}$ , are zero in a motionless fluid.

In stationary fluid  $P$  is the actual pressure, since only normal isotropic stresses can exist.

$$\delta_{ij} = \begin{cases} 1 & \text{if } i=j \\ 0 & \text{if } i \neq j \end{cases} \quad (2.6)$$

Substituting equation 2.5 into the dynamic equation, 2.2, gives Stokes' equation:

$$\frac{\partial \rho u_i}{\partial t} + u_j \frac{\partial \rho u_i}{\partial x_j} - \rho f_i + \frac{\partial P}{\partial x_i} - \frac{\partial \tau_{ij}}{\partial x_j} = 0 \quad (2.7)$$

Equation 2.7 is quite general and is applicable to any type of fluid. The main problem arises in estimating the stress terms. The pressure, P, is a function of position within the fluid and, in general, is one of the unknowns which are to be determined. The shear stresses are also unknown but are often assumed to be related to the local rates of strain occurring in the fluid. These assumptions result in the so called constitutive equations of the fluid. It is clear that the simplest constitutive relationship possible is:

$$\tau_{ij} = 0 \quad (2.8)$$

Which reduces 2.7 to 2.9, Euler's equation of motion for an ideal fluid. (An ideal fluid is one in which only normal stresses can exist.)

$$\frac{\partial \rho u_i}{\partial t} + u_j \frac{\partial \rho u_i}{\partial x_j} - \rho f_i + \frac{\partial P}{\partial x_i} = 0 \quad (2.9)$$

However in many fluids the shear stress terms are not known to be negligible in advance and we must make use of a more general assumption. The simplest, non trivial, relationship is applied to the so called Newtonian fluids; in which the deviatoric, (shear), stress terms are assumed to depend on a linear combination of the local velocity gradients thus:

$$\tau_{ij} = 2\mu (e_{ij} - \frac{1}{3} \Delta \delta_{ij}) \quad (2.10)$$

Where :

$e_{ij}$  - the i,j/th component of the rate of strain tensor,  $\underline{E}$ , given by:

$$e_{ij} = \frac{1}{2} \left[ \frac{\partial u_i}{\partial x_j} + \frac{\partial u_j}{\partial x_i} \right] \quad (2.11)$$

$\mu$  the fluid viscosity

$\Delta$  the local rate of expansion =  $e_{ii}$

The introduction of 2.10 into Stokes' equation results in the Navier - Stokes equation of motion:

$$\frac{\partial \rho u_i}{\partial t} + u_j \frac{\partial \rho u_i}{\partial x_j} - \rho f_i + \frac{\partial P}{\partial x_i} - \frac{\partial}{\partial x_j} (2\mu e_{ij} - \frac{2}{3} \mu \Delta \delta_{ij}) = 0 \quad (2.12)$$

### 2.2.5 Incompressible fluid

In the case of a fluid with uniform, fixed density the continuity equation simplifies to:

$$\frac{\partial u_i}{\partial x_i} = 0 \quad (2.13)$$

Equation 2.13 and the assumption of uniform density allow the convective terms in the dynamic equations 2.2, 2.7, 2.9 and 2.12 to be written as:

$$u_j \frac{\partial \rho u_i}{\partial x_j} = \rho \frac{\partial u_i u_j}{\partial x_j} \quad (2.14)$$

Similarly the local rate of expansion,  $\Delta$ , is zero in an incompressible fluid and  $\tau_{ij}$  is given by :

$$\tau_{ij} = \mu \left[ \frac{\partial u_i}{\partial x_j} + \frac{\partial u_j}{\partial x_i} \right] \quad (2.15)$$

or

$$\tau_{ij} = \rho \nu \left[ \frac{\partial u_i}{\partial x_j} + \frac{\partial u_j}{\partial x_i} \right] \quad (2.16)$$

Where  $\nu$  is the kinematic viscosity of the fluid defined as:  $\nu = \mu/\rho$ . Hence the Navier - Stokes equation of motion for a uniformly incompressible Newtonian fluid can be written as:

$$\frac{\partial u_i}{\partial t} + \frac{\partial u_i u_j}{\partial x_j} - f_i + \frac{1}{\rho} \frac{\partial P}{\partial x_i} - \frac{\partial}{\partial x_j} \left[ \nu \left( \frac{\partial u_i}{\partial x_j} + \frac{\partial u_j}{\partial x_i} \right) \right] = 0 \quad (2.17)$$

Equations 2.13 and 2.17 are the basic equations describing the motion of many fluids of practical interest, including water. They are the basis of all the following discussions relating to the mechanics of flow over a river channel/floodplain environment. However they are non-linear and in practical applications invariably give rise to the phenomenon known as turbulence. The following section describes the basic characteristics of turbulence and its consequences in fluid flow.

### 2.2.6 The effects of turbulence

Turbulence is characterised by high frequency, low amplitude fluctuations, in the flow variables and although the above equations do describe turbulent flow, the resolution of the turbulent fluctuations is prohibitive. The normal approach taken is to derive equations describing the bulk (or temporal) mean motion of the fluid. This is the statistical theory of turbulence due to Osborne Reynolds (1895) who introduced the concept of first replacing an instantaneous value with a mean and fluctuating component and then taking an average over time. The time period, of

the averaging, is normally considered to be large in comparison with the periods of the turbulent fluctuations but small relative to the changes taking place in the mean flow.

For a detailed description of this process see Reynolds (1974), chapter 1, or Tong (1985), Appendix A. For our purposes it is sufficient to note the resulting, (so called Reynolds'), equations of incompressible turbulent flow for a fluid with uniform density :

### The continuity equation

$$\frac{\partial u_i}{\partial x_i} = 0 \quad (2.18)$$

### The dynamic equation

$$\frac{\partial u_i}{\partial t} + \frac{\partial u_i u_j}{\partial x_j} - f_i + \frac{1}{\rho} \frac{\partial P}{\partial x_i} - \frac{\partial}{\partial x_j} \left[ \nu \left( \frac{\partial u_i}{\partial x_j} + \frac{\partial u_j}{\partial x_i} \right) \right] - \frac{\partial}{\partial x_j} \left[ \overline{u_i' u_j'} \right] = 0 \quad (2.19)$$

Where :

$u_i'$  the turbulent fluctuations in the instantaneous velocity vector

$u_i$  the mean parts of the instantaneous velocity vector

And the overbar signifies a temporal mean value

It is obvious that 2.19 differs from 2.17 only by an extra deviatoric term.

Indeed the terms  $\overline{(\rho u_i' u_j')}$  are often said to be analogous to the viscous shear stresses, and referred to as Reynolds' stresses. The presence of these Reynolds' stresses greatly complicates matters, because they give more unknown variables than equations in the description of the flow. This is the classical closure problem in modelling turbulent flow. In order to obtain a solution we must make use of some kind of turbulence model, in general these fall into two categories :

- 1) Make some assumption, either arbitrary or empirical, as to the distribution of the Reynolds' stresses in the flow. Mixing length and simple eddy viscosity models are well known examples.
- 2) Introduce extra equations, which describe the distribution of the Reynolds' stresses in the flow field. Examples include the  $k-\epsilon$  model and the algebraic stress model.

The literature provides detailed descriptions of the above models. This chapter is concerned more with giving a brief description of the basic equations of fluid motion, rather than a full discussion of the practicalities of obtaining a solution. It is sufficient to note that models falling in the second of the above categories require large amounts of computer and operator time to set up and calibrate. The resulting models are far more expensive than ones based on simpler semi-empirical assumptions. And in the case of open channel hydraulics can by no means guarantee a better description of the mean flow. (eg. see Tong, 1983). It is felt that one of the simpler methods will prove sufficient in our particular case.

### The Boussinesq eddy viscosity concept

Rather than approach the problem of the Reynolds' stresses directly, it is possible to make use of the eddy viscosity concept. Stated simply the Reynolds' stresses are assumed to be related to the mean flow in the same way as the viscous stresses in a Newtonian fluid:

$$\tau_{ij} = \tau_{ji} = \overline{\rho u_i' u_j'} = \rho \nu_t \left[ \frac{\partial u_i}{\partial x_j} + \frac{\partial u_j}{\partial x_i} \right] \quad (i=1,2,3) \quad (2.20)$$

Where :

- $\tau_{ij}$  the i,j/th component of the Reynolds stress tensor  $\underline{\mathbf{R}}$
- $\nu_t$  the kinematic eddy viscosity.

In practice it is possible to assume that  $\nu_t$  is constant or, more realistically, that it depends on the local flow and turbulence conditions. In which case the purpose of the chosen turbulence model, whether it is simple or complex, is to evaluate the distribution of the eddy viscosity rather than the Reynolds' stresses. In many flows of practical interest, including almost all open channel flows, the viscous stresses are small compared to the Reynolds' stresses and so are negligible. Hence it is possible to express equation 2.19 as :

$$\frac{\partial u_i}{\partial t} + \frac{\partial u_i u_j}{\partial x_j} - f_i + \frac{1}{\rho} \frac{\partial P}{\partial x_i} - \frac{\partial}{\partial x_j} \left[ \nu_t \left( \frac{\partial u_i}{\partial x_j} + \frac{\partial u_j}{\partial x_i} \right) \right] = 0 \quad (2.21)$$

## 2.3 Derivation of the 2-D flow equations

### 2.3.1 Initial assumptions

The following assumptions are usually reasonable when considering flow in a river channel and over its floodplain. (Samuels 1985, p17)

- 1) The flow is turbulent.
- 2) The fluid is uniform and incompressible.
- 3) The spatial variation of atmospheric pressure is negligible.
- 4) The Coriolis accelerations are insignificant.
- 5) The river bed is fixed (ie. it does not change with time).

Of the above assumptions only 4 and 5 cause any loss of generality in the resulting model. The Coriolis accelerations are produced by the rotation of the earth. And can be regarded as a type of body force, which is present only in accelerating frames of reference. In general it is likely that, in the case of floodplain flow, these terms will be small compared to bed friction. However where the rate of flow is low or the depth large, causing bed friction to be less important overall, the Coriolis accelerations may need to be included.

The assumption of a fixed channel bed is widely applied in all areas of hydraulics, even elementary sediment transport problems have been tackled in this way. Of course, intuition and observation imply that it is not strictly true. But, in view of some of the other assumptions and approximations we shall be forced to introduce, it is reasonable to assume that the channel bed has a mean overall shape. And that it will vary around this mean depending on the changing flow characteristics.

Obviously assumptions 1 and 2 above give equations 2.18 and 2.21 as the starting point in deriving the 2-D flow equations. Also required are the boundary conditions on the free water surface and the channel bed. These are obtained by applying the kinematic condition of no relative normal motion, (Batchelor, p60-70), giving :

$$\frac{\partial Z_o}{\partial t} + u \frac{\partial Z_o}{\partial x} + v \frac{\partial Z_o}{\partial y} - w = 0 \quad (2.22)$$

Where  $Z_o$  is the elevation of either the bed or the water surface. Alternatively by assumption 3, equation 2.23, the zero slip law, could be taken as the boundary

condition on the bed. It does not matter which is used since both expressions result in the same final 2-D equations.

$$u_i = 0 \quad (i=1,2,3) \quad (2.23)$$

Note: Equation 2.23 is only true for fluids with finite, non-zero, viscosity.

### 2.3.2 The 2-D continuity equation

Considering the Natural coordinate system, then the 2-D continuity equation is obtained by integration of equation 2.18 over the flow depth :

$$\int_b^h \frac{\partial u_i}{\partial x_i} dz = 0 \quad (2.24)$$

Where:

- h the elevation of the free water surface.
- b the elevation of the channel bed.

Application of Leibnitz's rule to equation 2.24 gives:

$$\frac{\partial}{\partial x} \int_b^h u dz + \frac{\partial}{\partial y} \int_b^h v dz - \left[ u \frac{\partial z}{\partial x} + v \frac{\partial z}{\partial y} - w \right]_b^h = 0 \quad (2.25)$$

Defining the components,  $q_i$ , of the unit flow vector  $\mathbf{q}$  as :

$$\int_b^h u_i dz = q_i \quad (i=1,2) \quad (2.26)$$

And replacing the boundary terms in equation 2.25 with equation 2.22 gives :

$$\frac{\partial h}{\partial t} - \frac{\partial b}{\partial t} + \frac{\partial q_i}{\partial x_i} = 0 \quad (i=1,2) \quad (2.27)$$

Which simplifies to equation 2.28 under assumption 3:

$$\frac{\partial h}{\partial t} + \frac{\partial q_i}{\partial x_i} = 0 \quad (2.28)$$

### 2.3.3 The 2-D dynamic equations

The two horizontal depth integrated dynamic equations are obtained in the same way as equation 2.28. Unfortunately this is not as straightforward as above, due to the more complex nature of the dynamic equation 2.21. The initial difficulty relates to the distribution of pressure with depth. And in order to resolve this problem the z component of the dynamic equation is considered in isolation.

The introduction of assumption 6, vertical accelerations small compared to the effect of gravity, also allows the shear stresses, in this component of the dynamic equation, to be neglected. Hence if gravity is the only body force present then the dynamic equation in the z direction is given by :

$$\frac{1}{\rho} \frac{\partial P}{\partial z} + g = 0 \quad (2.29)$$

Integration of 2.28, combined with the condition that  $P=P_a$  at  $z=h$ , results in the hydrostatic pressure distribution :

$$P = P_a + \rho g (h-z) \quad (2.30)$$

Where  $P_a$  is the atmospheric pressure. The required assumption of small vertical accelerations is a serious limitation in the following derivation. It limits application of the model to situations in which no secondary currents exist. Which is certainly not the case in a natural river channel, where structures such as meander bends, weirs and steep banks can all generate secondary currents. However, the adoption of assumption 6 is the only practical option and so we shall proceed to make use of equation (2.30), bearing in mind the above reservations. It is possible to include the effects of certain types of secondary currents in the model. This can be achieved by systematically adjusting the values of the velocity distribution factors, which are defined below. However, further work is required to identify when it is necessary to introduce this complication, to obtain an accurate picture of the overall flow pattern. If we now consider the x component of the dynamic equation and integrate through depth thus :

$$\int_b^h \left[ \frac{\partial u}{\partial t} + \frac{\partial u^2}{\partial x} + \frac{\partial uv}{\partial y} + \frac{\partial uw}{\partial z} + \frac{1}{\rho} \frac{\partial P}{\partial x} - \frac{1}{\rho} \left[ \frac{\partial r_{xx}}{\partial x} + \frac{\partial r_{xy}}{\partial y} + \frac{\partial r_{xz}}{\partial z} \right] \right] dz = 0 \quad (2.31)$$

Applying Leibnitz's rule to the first four terms in 2.10, recognising that the boundary terms reduce to zero by 2.22, results in the expressions below.

$$\frac{\partial}{\partial t} \int_b^h u \, dz + \frac{\partial}{\partial x} \int_b^h u^2 \, dz + \frac{\partial}{\partial y} \int_b^h uv \, dz \quad (2.32)$$

If we follow Miles and Weare (1973) or Samuels (1985) and consider the vertical variations in velocity to be given by expressions of the form :

$$\begin{aligned} u &= \phi_x U \\ v &= \phi_y V \end{aligned} \quad (2.33)$$

where  $\phi_x$  and  $\phi_y$  are functions of  $z$ , (eg. the well known logarithmic distribution).  $U$  and  $V$  are the  $x$  and  $y$  components of the depth averaged velocity vector  $\underline{U}$ , defined by 2.34.

$$U_i = q_i / D \quad (i=1,2) \quad (2.34)$$

Where  $D$  is the flow depth =  $(h-b)$ . Note: In the general case the functions,  $\phi_i(z)$ , vary in the two plan coordinate directions,  $x$  and  $y$ . It is simple to confirm that:

$$\int \phi_i dz = D \quad (2.35)$$

Defining the components,  $C_{ij}$ , of the 2-D convection tensor  $\underline{c}$ :

$$C_{ij} = C_{ji} = \int_b^h u_i u_j dz \quad (i=1,2) \quad (2.36)$$

And the velocity distribution factors,  $\alpha_{ij}$ , as :

$$\alpha_{ij} = \alpha_{ji} = \frac{1}{D} \left[ \int_b^h \phi_i \phi_j dz \right] \quad (2.37)$$

Then it is possible to write  $\underline{c}$  in matrix notation as :

$$\underline{c} = [C_{ij}] = \frac{1}{D} \begin{bmatrix} \alpha_{xx} q_x^2 & \alpha_{xy} q_x q_y \\ \alpha_{xy} q_x q_y & \alpha_{yy} q_y^2 \end{bmatrix} \quad (2.38)$$

So, for example, from 2.37 and 2.38 the term  $C_{xx}$  is given by :

$$C_{xx} = \int_b^h u^2 dz = \frac{\alpha_{xx} q_x^2}{D} \quad (2.39)$$

Samuels (1985, p25) shows that if the velocity distributions are power laws then the  $\alpha$  factors are identical and lie in the range 1.021 to 1.008. However, he makes use of a power law approximation to the logarithmic law with values of the exponent which give good agreement, between the two, only for relatively smooth channels. The presence of other factors, such as the lateral shear layers observed at channel–floodplain interfaces or secondary currents in channel bends, will also affect both the values and the distribution of  $\alpha$  through the induced non uniformity of the vertical flow profiles. These complications have generally been ignored in practice and the  $\alpha$  factors taken to be unity. This is certainly

reasonable in situations such as flow in river estuaries or tidal currents in very large scale marine environments, (see Miles and Weare, 1973). However it is, at present, not at all clear whether the same is true in the case of floodplain flow, and further research is required on this point.

Some authors consider the vertical variation of velocity as producing terms analogous to the depth integrated Reynolds' stresses (see for example Falconer, 1977 or Kuipers and Vreugdenhil, 1973. However Samuels, 1985 (p.37) shows that in certain circumstances the resulting equations give spurious solutions, which cannot exist in practice. Considering integration of the pressure term :

$$\frac{1}{\rho} \int_b^h \frac{\partial P}{\partial x} dz \quad (2.40)$$

By assumptions 1, 2 and 6 we obtain the expression

$$g \int_b^h \frac{\partial}{\partial x} (h-z) dz \quad (2.41)$$

By applying Leibnitz's rule and evaluating the resulting integral and boundary expressions it is easy to show that equation 2.41 becomes :

$$g \ D \ \frac{\partial h}{\partial x} \quad (2.42)$$

Term 2.42 shows that the net effect of the fluid weight, on its motion, can be considered to operate through the water surface gradients. Turning attention to the Reynolds' stress terms in equation 2.31 and again applying Leibnitz's rule it is possible to show that :

$$\begin{aligned} - \frac{1}{\rho} \int_b^h \left[ \frac{\partial r_{xx}}{\partial x} + \frac{\partial r_{xy}}{\partial y} + \frac{\partial r_{xz}}{\partial z} \right] dz &= \\ - \frac{1}{\rho} \left[ \frac{\partial}{\partial x} \left[ \int_b^h r_{xx} dz \right] + \frac{\partial}{\partial y} \left[ \int_b^h r_{xy} dz \right] \right] & \quad (2.43a) \end{aligned}$$

$$- \frac{1}{\rho} \left[ r_{xx} \frac{\partial h}{\partial x} + r_{xy} \frac{\partial h}{\partial y} - r_{xz} \right]_h \quad (2.43b)$$

$$+ \frac{1}{\rho} \left[ r_{xx} \frac{\partial b}{\partial x} + r_{xy} \frac{\partial b}{\partial y} - r_{xz} \right]_b \quad (2.43c)$$

The boundary terms, 2.43b and 2.43c, are generally referred to as the wind and

bed shear stresses,  $\tau_{wx}$  and  $\tau_{bx}$ , respectively. It can be shown that they are related to the stresses which act on the sloping boundaries, (see the following chapter). The integral expressions in 2.43a can be considered to be the elements,  $\tau_{ij}$ , of the effective stress tensor  $\underline{\tau}$ , where :

$$\tau_{ij} = \tau_{ji} = \int_b^h r_{ij} dz \quad (i=1,2) \quad (2.44)$$

Equation 2.44 may be evaluated by replacing the Reynolds' stresses with 2.15. For example:

$$\tau_{xx} = \int_b^h r_{xx} dz = 2\rho \int_b^h v_t \frac{\partial u}{\partial x} dz \quad (2.45)$$

$$\tau_{xy} = \int_b^h r_{xy} dz = \rho \int_b^h v_t \left[ \frac{\partial u}{\partial y} + \frac{\partial v}{\partial x} \right] dz \quad (2.46)$$

In order to evaluate equations 2.45 and 2.46 some knowledge of the vertical distribution of the eddy viscosity is required. The simplest approach is to assume that  $v_t$  only varies in the horizontal directions ( $x, y$ ) in which case equation 2.45 becomes:

$$2\rho v_t \frac{\partial q_x}{\partial x} - 2\rho v_t \left[ u_h \frac{\partial h}{\partial x} - u_b \frac{\partial b}{\partial x} \right] \quad (2.47)$$

Where the terms of the form

$$\rho v_t \left[ u_h \frac{\partial h}{\partial x} - u_b \frac{\partial b}{\partial x} \right] \quad (2.48)$$

represent boundary shear stresses which act on the vertical projection of the sloping boundaries. Most authors neglect these stresses as small compared to those acting on the horizontal projection and so simplify 2.45 and 2.46 to 2.49, (see for example Tong, 1985).

$$\tau_{ij} = \rho v_t \left[ \frac{\partial q_i}{\partial x_j} + \frac{\partial q_j}{\partial x_i} \right] \quad (i=1,2) \quad (2.49)$$

Attempts have been made to account for the vertical variation in  $v_t$  by use of a general mixing length model (eg. Falconer, 1977). However it is necessary to assume that the velocity gradients in the vertical direction are much larger than those in the two horizontal directions and that the mixing length is given by an expression which is consistent with a logarithmic velocity profile and a linear shear stress distribution. This approach is fundamentally flawed, since this mixing length expression is only strictly applicable to stresses which lie on horizontal planes. In any case the resulting expressions are extremely difficult to

evaluate, the solutions given by Falconer (1979) being rather dubious approximations. It is felt that expression 2.49, although based on the rather arbitrary initial assumption of constant eddy viscosity with depth, will prove accurate enough for most purposes. It is interesting to note the similarity between 2.49 and 2.16 and that the depth integrated effective stresses are directly analogous to the Reynolds' stresses in three dimensional flow.

Assembling the terms resulting from the above integration the x component of the dynamic equation is:

$$\begin{aligned} \frac{\partial q_x}{\partial t} + \frac{\partial}{\partial x} \left[ \alpha_{xx} \frac{q_x^2}{D} \right] + \frac{\partial}{\partial y} \left[ \alpha_{xy} \frac{q_x q_y}{D} \right] + g D \frac{\partial h}{\partial x} \\ - \frac{1}{\rho} (\tau_{wx} - \tau_{bx}) - \frac{1}{\rho} \left[ \frac{\partial T_{xx}}{\partial x} + \frac{\partial T_{xy}}{\partial y} \right] = 0 \end{aligned} \quad (2.50)$$

By symmetry the 2-D dynamic equation can be written in tensor notation as shown.

$$\frac{\partial q_i}{\partial t} + \frac{\partial C_{ij}}{\partial x_j} + g D \frac{\partial h}{\partial x_i} - \frac{1}{\rho} (\tau_{wi} - \tau_{bi}) - \frac{1}{\rho} \frac{\partial T_{ij}}{\partial x_j} = 0 \quad (2.51)$$

Where  $C_{ij}$  and  $T_{ij}$  are defined by equations 2.38 and 2.39 respectively. For completeness the 2-D continuity equation is :

$$\frac{\partial h}{\partial t} + \frac{\partial q_i}{\partial x_i} = 0 \quad (i=1,2) \quad (2.52)$$

The following section considers the bed and wind stress terms and examines the assumptions adopted by previous authors.

## 2.4 Modelling the boundary shear terms

### 2.4.1 The boundary stresses

It was demonstrated in the previous chapter that depth integration of the Reynolds' stresses produces two types of boundary shear terms in the 2-D dynamic equation. The terms which involve the eddy viscosity and the boundary gradients, equation 2.46, are generally neglected, leaving the terms below in the final equation.

$$\tau_{wx} = \left[ r_{xx} \frac{\partial h}{\partial x} + r_{xy} \frac{\partial h}{\partial y} - r_{xz} \right]_h \quad (2.53)$$

$$\tau_{bx} = \left[ r_{xx} \frac{\partial b}{\partial x} + r_{xy} \frac{\partial b}{\partial y} - r_{xz} \right]_b \quad (2.54)$$

Most authors simply assume that these expressions represent stresses acting on the sloping surfaces. In order to show that this assumption is reasonable when the boundaries have small slopes, and to provide a better approximation when they are not, we must define the LOCAL coordinate system.

#### 2.4.2 The local coordinate system

Consider a plane surface which passes through the origin, in the NATURAL coordinate system this plane is defined by :

$$ax + by + cz = 0 \quad (2.55a)$$

or

$$z = -(a/c)x - (b/c)y \quad (2.55b)$$

Defining the slopes of the surface as:

$$S_i = \frac{\partial z}{\partial x_i} \quad (i = 1,2) \quad (2.56)$$

it is apparent that  $s_x = -a/c$  and  $s_y = -b/c$  so equation 2.55b becomes :

$$z = S_x x + S_y y \quad (2.57)$$

From simple geometry it is possible to write the unit normal to the surface,  $\underline{n}$ , as :

$$\underline{n} = 1/B (-S_x, -S_y, 1) \quad (2.58)$$

Where

$$B = (S_x^2 + S_y^2 + 1)^{1/2} \quad (2.59)$$

Our objective is to define a transformation which takes the NATURAL coordinate system,  $x_i$ , to a LOCAL system,  $\tilde{x}_i$ , in which the  $\tilde{i}_3$  coordinate direction lies along the normal to the surface defined by equation 2.57.

Such a transformation can be considered to consist first of a rotation about the y axis, through an angle  $\alpha$ , taking the x axis to the  $\check{x}$  ( $\tilde{x}$ ) axis, which lies in the plane of the surface. And secondly of another rotation about the  $\check{x}$  axis, through an angle  $\epsilon$ , which takes the  $\check{y}$  ( $y$ ) axis to the  $\tilde{y}$  axis and  $\check{z}$  to  $\tilde{z}$  (see Figures 2.1 and 2.2). The first transformation,  $x \rightarrow \check{x}$ , is defined by :

$$\underline{\check{i}} = \underline{i} \cos\alpha - \underline{k} \sin\alpha \quad (2.60)$$

$$\underline{\check{j}} = \underline{j} \quad (2.61)$$

$$\underline{\check{k}} = \underline{i} \sin\alpha + \underline{k} \cos\alpha \quad (2.62)$$

$$\check{x} = x \cos\alpha - z \sin\alpha \quad (2.63)$$

$$\check{y} = y \quad (2.64)$$

$$\check{z} = x \sin\alpha + z \cos\alpha \quad (2.65)$$

and the second one,  $\tilde{x} \rightarrow \bar{x}$ , by :

$$\tilde{\mathbf{i}} = \mathbf{i} \tag{2.66}$$

$$\tilde{\mathbf{j}} = \mathbf{j} \cos\epsilon + \mathbf{k} \sin\epsilon \tag{2.67}$$

$$\tilde{\mathbf{k}} = -\mathbf{j} \sin\epsilon + \mathbf{k} \cos\epsilon \tag{2.68}$$

$$\bar{x} = \tilde{x} \tag{2.69}$$

$$\bar{y} = \tilde{y} \cos\epsilon + \tilde{z} \sin\epsilon \tag{2.70}$$

$$\bar{z} = -\tilde{y} \sin\epsilon + \tilde{z} \cos\epsilon \tag{2.71}$$

Where the angles  $\alpha$  and  $\epsilon$  have the lower and upper limits  $-\pi/2$  and  $\pi/2$  respectively. And the positive sense is given by the right hand rule. To obtain the desired transformation ( $x \rightarrow \bar{x}$ ) substitute 2.60 to 2.65 into 2.66 to 2.71:

$$\tilde{\mathbf{i}} = \mathbf{i} \cos\alpha - \mathbf{k} \sin\alpha \tag{2.72}$$

$$\tilde{\mathbf{j}} = \mathbf{j} \sin\alpha \sin\epsilon + \mathbf{j} \cos\epsilon + \mathbf{k} \cos\alpha \sin\epsilon \tag{2.73}$$

$$\tilde{\mathbf{k}} = \mathbf{j} \sin\alpha \cos\epsilon - \mathbf{j} \sin\epsilon + \mathbf{k} \cos\alpha \cos\epsilon \tag{2.74}$$

$$\bar{x} = x \cos\alpha - z \sin\alpha \tag{2.75}$$

$$\bar{y} = x \sin\alpha \sin\epsilon + y \cos\epsilon + z \sin\epsilon \tag{2.76}$$

$$\bar{z} = x \sin\alpha \cos\epsilon - y \sin\epsilon + z \cos\epsilon \tag{2.77}$$

It is simple to verify that :

$$\tilde{\mathbf{i}}\tilde{\mathbf{j}} = \tilde{\mathbf{i}}\tilde{\mathbf{k}} = \tilde{\mathbf{j}}\tilde{\mathbf{k}} = 0 \tag{2.78}$$

and thus show that  $\tilde{x}$  is a true cartesian coordinate system. It is convenient to express the above transformation in terms of the local surface slopes. Remembering that the unit normal to the surface is given by equation 2.59 and that  $\tilde{\mathbf{k}}$  is by definition also the unit normal, then by comparing 2.74 and 2.59 we obtain :

$$\sin\alpha \cos\epsilon = -S_x/B \tag{2.79}$$

$$\sin\epsilon = S_y/B \tag{2.80}$$

$$\cos\alpha \cos\epsilon = 1/B \tag{2.81}$$

by squaring and adding 2.79 and 2.81, bearing in mind the limits on  $\alpha$  and  $\epsilon$ , it is possible to express  $\cos\epsilon$  in terms of the surface gradients :

$$\cos\epsilon = \frac{1}{B}(1 + S_x^2)^{1/2} \tag{2.82}$$

substituting for  $\cos\epsilon$  in 2.79 and 2.81 gives the results shown :

$$\sin\alpha = -S_x/(1 + S_x^2)^{1/2} \tag{2.83}$$

$$\cos\alpha = 1/(1 + S_x^2)^{1/2} \tag{2.84}$$

Substituting expressions 2.79 → 2.81 for the terms involving the angles  $\alpha$  and  $\epsilon$  in equations 2.75 → 2.77 we obtain the transformation,  $x \rightarrow \bar{x}$ , in terms of the surface

gradients. In matrix notation this is written,  $\tilde{x} = Ax$ , thus :

$$\begin{bmatrix} \tilde{x} \\ \tilde{y} \\ \tilde{z} \end{bmatrix} = \begin{bmatrix} 1/C & 0 & S_x/C \\ -D/BC & C/B & S_y/BC \\ -S_x/B & -S_y/B & 1/B \end{bmatrix} \begin{bmatrix} x \\ y \\ z \end{bmatrix} \quad (2.85)$$

The reverse transformation,  $x = A^{-1}\tilde{x}$ , is given by:

$$\begin{bmatrix} x \\ y \\ z \end{bmatrix} = \begin{bmatrix} 1/C & -D/BC & -S_x/B \\ 0 & C/B & -S_y/B \\ S_x/C & S_y/BC & 1/B \end{bmatrix} \begin{bmatrix} \tilde{x} \\ \tilde{y} \\ \tilde{z} \end{bmatrix} \quad (2.86)$$

Where

$$B = (S_x^2 + S_y^2 + 1)^{1/2} \quad (2.87)$$

$$C = (S_x^2 + 1)^{1/2} \quad (2.88)$$

$$D = S_x S_y \quad (2.89)$$

It is simple to confirm that 2.85 and 2.86 are allowable cartesian transformations by showing that  $AA^{-1} = I$  is true.

### 2.4.3 Approximating the boundary stresses

It is possible to use the tensor transformation laws to express the elements of the Reynolds' stress tensor in terms of the locally defined coordinate system. By substituting into 2.53 and 2.54 it is also possible to express  $\tau_w$  and  $\tau_b$  in terms of stress components which are related to the boundary surface. However the resulting expressions are complex and are no easier to evaluate than 2.53 and 2.54. The stress vector defined by A2-11 represents the stresses acting on a sloping surface and it is much simpler to relate to the  $\tau$ 's. From the definition of the plane boundary surfaces, 3.5, and the resulting coordinate transformation, 2.85, the stresses vector defined by A2-11 has the components :

$$M_x = 1/B (S_x\alpha_{xx} + S_y\alpha_{xy} - \alpha_{xz}) \quad (2.90)$$

$$M_y = 1/B (S_x\alpha_{xy} + S_y\alpha_{yy} - \alpha_{yz}) \quad (2.91)$$

By comparing 2.53 and 2.54 with 2.90 and 2.91 it is clear then that the stresses  $\tau_x$  and  $\tau_y$  can be related to stresses acting on the sloping surfaces by the expressions :

$$\tau_{bi} = B M_{bi} \quad \text{on the channel bed} \quad (2.92)$$

$$\tau_{wi} = B M_{wi} \quad \text{on the water surface} \quad (2.93)$$

Where the surface slopes are small, (ie  $S_x^2, S_y^2 \approx 0$ ), B has a value close to unity and the  $\tau$  terms are a good approximation to the stresses on the sloping surfaces. But when the surface gradients are not small the  $\tau$  terms are greater than the bed

stresses by the factor B, which is considerably larger than unity. B can be thought of as the ratio of the sloping surface area to its horizontal projection and is always greater than one. Thus where the surface slopes are likely to be significant the term :

$$-1/\rho (\tau_{wi} - \tau_{bi}) \quad (2.94)$$

should be replaced with :

$$-1/\rho (B_w M_{wi} - B_b M_{bi}) \quad (2.95)$$

in the dynamic equation. The stress vectors  $\underline{M}_w$  and  $\underline{M}_b$  can be approximated by empirical expressions, (see below). The inclusion of the factor B in the stress terms is new in the general context of 2-D flow modelling, although it has been used in the comparatively simple case of flow in straight, uniform compound channels, (see Shiono and Knight, 1988, or Keller and Rodi, 1988).

#### 2.4.4 The wind stresses

The stresses  $B_w M_{wi}$  are assumed to act on the water surface as the result of air currents blowing across the flow domain. Assumption 6 effectively limits application of the model to situations with small water surface gradients so  $B_w$  can be set to unity.  $\underline{M}_{wi}$  is usually related to the wind velocity vector,  $\underline{w}$ , by empirical expressions of the form :

$$M_{wi} = \text{const. } |\underline{w}| w_i \quad (2.96)$$

See Heaps (1969) or Connor and Brebbia (1976, chapter 7). Expressions of this type assume that  $\underline{M}_w$  and  $\underline{w}$  both act in the same direction. Samuels (1985) states that, in the case of flood plain flow, significant wind stresses will occur only at very high wind velocities and consequently the wind stresses can be neglected. However in situations where the wind stresses are of the same order as the other terms in the dynamic equation they should be included in the model. Examples include modelling tides in coastal regions and circulation in shallow lakes or lagoons, (in these cases the Coriolis accelerations will also be important).

#### 2.4.5 The bed stresses

$$\tau_{bi} = B_b M_{bi} \quad (2.97)$$

The correct representation of the bed stress  $\underline{M}_b$  is complex and depends on both the unit flow vector and the small scale characteristics of the roughness elements which make up the channel bed. Details of the shape, orientation and density of the bed roughness are unlikely to be available in practice. The usual approach is

to assume that  $\underline{M}_b$  acts along the same direction as the unit flow vector,  $\underline{q}$ , and that its magnitude can be estimated by one of the well known friction laws, which were developed for 1-D flow, resulting in expressions of the form :

$$M_{bi} = \frac{\rho f}{8D^2} q_i | \underline{q} | \quad (2.98)$$

Where

$f$  is the Darcy friction factor.

Hence  $\underline{\tau}_b$  has components

$$\tau_{bx} = B \frac{\rho f}{8D^2} q_x (q_x^2 + q_y^2)^{1/2} \quad (2.99a)$$

and

$$\tau_{by} = B \frac{\rho f}{8D^2} q_y (q_x^2 + q_y^2)^{1/2} \quad (2.99b)$$

There are two types of expression commonly used for evaluating  $f$  :

1) Empirical relationships derived from observation of flow in real river channels. The two well known equations of this type are :

a) **Chezy's law**

$$f = 8 g / C^2 \quad (2.100)$$

where  $C$  is Chezy's coefficient and has units  $L^{1/2}T^{-1}$

b) **Manning's equation**

$$f = 8 g n^2 D^{-1/3} \quad (2.101)$$

where  $n$  is Mannings roughness coefficient with units  $L^{-1/3}T$

2) Semi-empirical relationships derived from consideration of the turbulent structure of the flow and the roughness condition of the channel bed.

It is possible to derive two basic equations:

a) **The smooth turbulent law**

$$f = (2 \log_{10} ( f^{1/2} / 2.51 Re ) )^{-2} \quad (2.102)$$

Where  $Re$  is the Reynolds' number of the flow defined as

$$Re = \frac{4|U|D}{\nu} = \frac{4|q|}{\nu} \quad (2.103)$$

b) **The rough turbulent law.**

$$f = (2 \log_{10} (14.8 D / k_s))^2 \quad (2.104)$$

Where  $k_s$  is the Nikuradse roughness size with units of length.

The smooth turbulence law is applicable at relatively low Reynolds' numbers where the friction factor depends only on the flow conditions and not on the roughness of the channel. This type of flow only occurs in situations which are said to be hydraulically smooth and is extremely rare in prototype river channels, although it will occur in small scale models. Where low flow velocities and unnaturally smooth boundaries give smooth turbulent flow.

Rough turbulence, in which the friction factor is determined by the roughness of the channel boundary and not the flow conditions, is the normal type of flow which occurs in prototype channels. Chezy's law and Manning's equation are also valid only in rough turbulent flow. Both types of flow regime can exist in any particular channel as can intermediate flow conditions, for which the friction factor is a function of both Reynolds' number and bed roughness. None of the above expressions give the friction factor for these intermediate conditions. This problem was resolved by Colebrook and White. Who combined equations 2.102 and 2.104 in an empirical way to produce an expression, 2.105, which accurately estimates the friction factor for nearly all flow conditions.

c) **The Colebrook-White equation**

$$f = \left\langle -2 \log_{10} \left\langle \frac{k_s}{14.8 D} + \frac{2.51}{Re f^{1/2}} \right\rangle \right\rangle^{-2} \quad (2.105)$$

The problem with equation 2.105 is that it is not an explicit expression and the unknown,  $f$ , appears on both sides. This makes the finding a solution difficult and iterative techniques must be used. Equation 2.106 is Barr's approximation to the Colebrook-White equation, it is fully explicit and is said to agree with equation 2.105 to within 1% for Reynolds' numbers in excess of  $10^5$ , see Chadwick and Morgett (1986)

$$f = \left\langle -2 \log_{10} \left\langle \frac{k_s}{14.8 D} + \frac{5.12886}{Re^{0.89}} \right\rangle \right\rangle^{-2} \quad (2.106)$$

In general the Colebrook-White equation is best used when modelling flow in model channels. Where the small length scales and relatively smooth boundaries cause Reynolds' numbers to be low and the flow to fall either in the smooth or intermediate turbulent zones. For a fuller discussion of the above see Henderson (1966), Webber (1971) or Chadwick and Morfett (1986).

The equations 2.100 to 2.106 are written for the case of a flow area of unit width and depth D. They are more commonly written for 1-D channels in terms of the hydraulic radius R, where D in the above equations is given by  $D = R$ .

#### 2.4.6 Summary of 2-D equations

The governing equations of 2-D depth integrated flow have been derived. In the absence of body forces, other than gravity, and wind stresses on the the free surface they are :

##### Continuity equation

$$\frac{\partial h}{\partial t} + \frac{\partial q_i}{\partial x_i} = 0 \quad (i=1,2) \quad (2.107)$$

##### Dynamic equation

$$\begin{aligned} \frac{\partial q_i}{\partial t} + \frac{\partial (c_{ij})}{\partial x_j} + gD \frac{\partial h}{\partial x_i} + \frac{Bf}{8D^2} q_i |q_i| \\ - \frac{\partial}{\partial x_j} [ \nu_t [ \frac{\partial q_i}{\partial x_j} + \frac{\partial q_j}{\partial x_i} ] ] = 0 \quad (i=1,2) \end{aligned} \quad (2.108)$$

where  $c_{ij}$  is defined by:

$$c = [C_{ij}] = \frac{1}{D} \left[ \begin{array}{cc} \alpha_{xx} q_x^2, & \alpha_{xy} q_x q_y \\ \alpha_{xy} q_x q_y, & \alpha_{yy} q_y^2 \end{array} \right] \quad (2.109)$$

These equations should adequately describe flow in a river channel-floodplain environment. The introduction of the factor B in the bed friction term is new and should improve accuracy compared with existing models. However, this must be balanced against the increased requirements for topographic data which must be incorporated. This will undoubtedly increase both the computer storage and execution time required.

The assumption of constant eddy viscosity with depth has the advantages of producing effective stress terms which are consistent with the use of unit flow as one of the primary variables and which are simpler than those obtained using more complicated turbulence models. The importance of the velocity distribution factors,  $\alpha$ , in modelling 2-D flow in a river channel and floodplain is unknown and requires clarification.

## 2.5 Derivation of the St Venant equations

In the previous sections of this chapter it has been demonstrated that the 3-D equations of fluid motion can be simplified to give a set of equations which describe the motion of fluids with a free surface. These equations are often referred to as the shallow water equations. In many practical problems even these equations are too complex and further simplifications are necessary to obtain an economical solution. One such case is found when considering flows in open channels. where the width of an open channel is small compared with the length and the lateral discharges across the channel are small (or zero) then it is acceptable to use the 1-D St Venant equations which describe the unsteady motion of fluids in an open channel. The following sections describe the derivation of the St Venant equations from the shallow water equation. The main feature is that the flow is adequately described by sectional average values of the variables, such as discharge.

### 2.5.1 Initial assumptions

In addition to the assumptions underling the Shallow water equations (section 2.3.1) the following two assumptions must also be made.

Consider a channel of arbitrary cross-section, with area  $A$  and width  $B$ . Let the  $x$  axis lie along the centre line of the channel with the  $y$  axis pointing across the channel and the  $z$  axis being vertical. See Figure 2.3 for a definition of the variables.

- 1) There is no lateral flow within the channel.

$$\text{ie. } \left\{ q_y = 0. \quad y: y = 0 \text{ and } y = B \right\} \quad (2.110)$$

- 2) At the lateral edges of the channel the longitudinal flow is zero. This follows from the no slip boundary condition.

$$\text{ie. } \left\{ q_x = 0. \quad y: y = 0, y = B \right\} \quad (2.111)$$

- 3) The water surface is at a ~~uniform~~ elevation at all points across the channel.

This is equivalent to:

$$\frac{\partial h}{\partial y} = 0 \quad (2.112)$$

4) The flow can be described by section averaged discharge and stage.

### 2.5.2 The 1-D continuity equation

Under these assumptions the shallow water continuity equation reduces to:

$$\frac{\partial h}{\partial t} + \frac{\partial q_x}{\partial x} + \frac{\partial q_y}{\partial y} = 0 \quad (2.113)$$

Integrating this equation from  $y = 0$  to  $y = B$  gives:

$$\int_0^B \left( \frac{\partial h}{\partial t} + \frac{\partial q_x}{\partial x} + \frac{\partial q_y}{\partial y} \right) dy = 0 \quad (2.114)$$

Applying Leibnitz law to each term in this equation gives us

$$\frac{\partial}{\partial t} \int_0^B h \, dy + \frac{\partial}{\partial x} \int_0^B q_x \, dy + \left[ q_y - h \frac{\partial y}{\partial t} + q_x \frac{\partial y}{\partial x} \right]_0^B = 0 \quad (2.115)$$

applying the assumptions listed in sections 2.3.1 and 2.5.1 to equation 2.115 this reduces to:

$$B \frac{\partial h}{\partial t} + \frac{\partial Q}{\partial x} + [q_y]_0^B = 0 \quad (2.116)$$

This is usually expressed as:

$$B \frac{\partial h}{\partial t} + \frac{\partial Q}{\partial x} = q_L \quad (2.117)$$

where

$Q$  is the discharge in the cross-section

$q_L$  is the nett lateral inflow per unit length of channel

### 2.5.3 The 1-D dynamic equation

Under these assumptions the  $x$  momentum equation of the shallow water equations reduces to :

$$\frac{\partial q_x}{\partial t} + \frac{\partial \alpha q_x^2}{\partial x} + gD \frac{\partial h}{\partial x} + \frac{Bf}{8D^2} q_x |q_x| - \frac{\partial}{\partial y} [v_t \left[ \frac{\partial q_x}{\partial y} \right]] = 0 \quad (2.118)$$

Integrating this equation across the channel width and applying Leibnitz's law we

obtain:

$$\begin{aligned} & \frac{\partial}{\partial t} \int_0^B q_x dy + \frac{\partial}{\partial x} \int_0^B \alpha q_x^2 dy + g \frac{\partial h}{\partial x} \int_0^B D dy \\ & + \int_0^B \frac{Bf}{8D^2} q_x |q_x| dy \quad (2.119) \\ & + \left[ v_t \left[ \frac{\partial q_x}{\partial y} \right] + q_x \frac{\partial y}{\partial t} + \alpha q_x^2 \frac{\partial y}{\partial t} \right]_0^B = 0 \end{aligned}$$

The boundary terms are zero by the assumptions and boundary conditions applied by the physics of the flow. The internal terms are dealt with as follows.

$$\int_0^B q_x dy = Q \quad (2.120)$$

$$\int_0^B \alpha q_x^2 dy = \iint_A u^2 dA = \beta Q^2 / A \quad (2.121)$$

$\beta$  is the momentum correction factor defined over the whole cross-section. In one dimensional flows the Coriolis factor or energy correction factor ( $\alpha$ ) is also some times referred to and is defined by equation 2.122.

$$\alpha Q^3 / A^2 = \iint u^3 dA \quad (2.122)$$

where

$$\int_0^B D dy = A \quad (2.123)$$

$$\int_0^B (Bf / 8D^2) q_x |q_x| dy = \int_0^B B\tau dy \quad (2.124)$$

This term expresses the effect of the bed friction acting between the channel bed and the flow. As mentioned above, empirical equations are often used to approximate this term. The concept of conveyance is useful in expressing this term. In the case of steady uniform flow it is well known that the channel bed shear stress is related to the square of the discharge:

$$\tau \propto Q^2 = g A S_f \quad (2.125)$$

and

$$Q = K S_f^{1/2} \quad (2.126)$$

so the bed friction integral can be written as:

$$g A S_f \quad (2.127)$$

Equation 2.126 defines the conveyance,  $K$ , of a channel. The hydraulic slope  $S_f$  is equal to the bed slope in uniform flow but in the more normally varies relatively smoothly along a channel. In practice, when solving the St Venant equations  $S_f$  is often taken to be the slope of the water surface profile. The

simple empirical equations which are commonly used to obtain K values are described in Section 2.4.5 and include formulae by Manning, Chezy's and Colebrook White. Further discussion of methods used in calculating K is given in later chapters.

Combining the various approximations to the integral terms we obtain the 1-D dynamic equation 2.128.

$$\frac{\partial Q}{\partial t} + \frac{\partial}{\partial x} \left( \frac{\beta Q}{A} \right)^2 + g A \left( \frac{\partial h}{\partial x} + S_f \right) = 0 \quad (2.128)$$

#### 2.5.4 Summary of the 1-D (St Venant) equations

We have shown that the full equations of 3-D flow can be simplified to give the St Venant equation which describe the gross or overall behaviour of flow in an open channel. The St Venant equations are listed below:

##### Continuity Equation

$$B \frac{\partial h}{\partial t} + \frac{\partial Q}{\partial x} = q_L \quad (2.129)$$

##### Dynamic Equation

$$\frac{\partial Q}{\partial t} + \frac{\partial}{\partial x} \left( \frac{\beta Q}{A} \right)^2 + g A \left( \frac{\partial h}{\partial x} + S_f \right) = 0 \quad (2.130)$$

#### 2.6 Summary and Conclusions

The aims of this chapter were to review the theoretical background to flow in river and flood plain environments. These aims were met by deriving various sets of equations used to model river and flood plain flows. The basic equations of 3-D fluid flow are the Navier-Stokes equations, 2.1 and 2.12. In the case of incompressible turbulent flow the Navier-Stokes equations are converted into the Reynolds' equations, 2.18 and 2.19. The turbulent eddy viscosity concept was introduced in section 2.2.6 and the dynamic Reynolds' equation reduced to equation 2.21.

The so called shallow water equations were derived from the 3-D Reynolds equations, section 2.3. The shallow water equations describe the behaviour of fluid flow with a free surface where the depth of flow is much smaller than the horizontal dimensions of the flow domain. The equations are derived in terms of the unit flows ( $q$ ) rather than the more usual formulation given in the literature in terms of the depth averaged velocity ( $U$ ). A novel approach to the bed friction vector in 2-D flow was followed, sections 2.4.1 to 2.4.3. A factor ( $B$ ) was derived to relate the stresses on a sloping surface to stresses in the horizontal plane. Various empirical approaches to modelling the effects of bed friction were reviewed, section 2.4.5. The shallow water equations are given by 2.107 and 2.108.

In the cases where the flow domain is much larger in the direction of the predominant flow it would be impractical to consider either the 3-D or the 2-D depth integrated behaviour. In these situations (eg. a river or canal) engineers usually consider the flow to be one dimensional. The 1-D equations of flow with a free surface are called the St Venant equations and are derived in section 2.5 and are given by 2.129 and 2.130.

## CHAPTER 3

### FLOW MECHANISMS IN STRAIGHT COMPOUND CHANNELS

#### 3.1 Introduction

The ability to assess or calculate discharge and water levels is one of the foremost needs of the river engineer. It is fundamental to many aspects of river management, from flood forecasting and the design of protection schemes to the licensing of abstractions and the control of water quality. The material covered in this chapter is intended to address the following questions:

- 1) What is a compound channel?
- 2) Are there problems in assessing the conveyance capacity of compound channels?
- 3) What research has been carried out into these problems?
- 4) Is there a clear consensus on which are the important mechanisms and parameters, which control the conveyance capacity of compound channels.

A review of the literature shows that the cases of straight and meandering compound channels are different and most authors consider one or the other of these cases. Consequently this chapter and the following chapter consider the case of straight compound channels. Meandering compound channels are considered in chapters 5 and 6.

#### 3.2 Compound channels and the important mechanisms

##### 3.2.1 Definition of a compound channel

Traditional methods of calculating the discharge or conveyance capacity of channels are based on the assumption that the velocity is uniform within the cross-section. The bed shear stresses are also assumed to be uniform around the wetted perimeter. These assumptions are reasonable in the case of simple channels, Figure 3.1. As mentioned in chapter 2 various empirical formulae are used to relate the discharge,  $Q$ , to the bed roughness. A widely used empirical formulae is Manning's equation:

$$Q = 1/n A R^{2/3} S^{1/2} \quad (3.1)$$

where  $Q$  is the discharge,  $n$  is Manning's roughness coefficient,  $A$  is the channel cross-sectional area,  $R$  is the hydraulic radius defined as  $P/A$ , where  $P$  is the wetted perimeter and  $S$  is the hydraulic slope. Other commonly used empirical formulae are discussed in section 2.4. The assumptions of uniform velocity and discharge within the channel are reasonable for typical simple channels and the straightforward application of the classical techniques gives results of acceptable accuracy.

A compound channel is usually defined as a simple main channel, which carries the normal low flows, with either one or two floodplains or berms at higher elevations on one or both sides of the main channel. The floodplains are usually dry and convey discharge only during flood conditions. Figure 3.2 shows a typical compound channel and defines some physical parameters.

The most obvious aspect of a compound channel is that the flow depths on the floodplain are often significantly smaller than the depths in the main channel, especially during small floods. The bed surface on the floodplains is often much rougher than the bed in the main channel and so the distribution of velocities and bed shear stresses are likely to be non-uniform. Various authors, (eg Myers and Brennan (1990), Knight (1990) and Ackers (1991,1993), have demonstrated that the application of normal simple channel techniques to compound channels is inappropriate.

### **Applying simple channel methods to compound channels**

Knight et al, 1989, analyzed stage discharge data from a river flow gauging site at Montford on the River Severn. Figure 3.3 shows the variation of  $A$ ,  $P$  and  $R$  with stage. Below bankfull all three parameters vary smoothly but at bankfull both the perimeter and hydraulic radius show large discontinuities. Applying normal uniform flow calculations to the stage discharge data results in the Manning's  $n$  and friction factor distributions shown in Figure 3.4. The Manning's  $n$  distribution shows the classic gradual reduction for inbank stages which approaches a constant value at

higher stages. At just overbank stages the discontinuities in P and R affect the back calculated n values and reduce them to about half the bankfull value at low overbank stages. At higher stages the n values increase. The effect on friction factor is to gradually reduce the values until bankfull stage is reached at overbank stages the moody diagram follows a loop, giving a non singular friction factor against Reynolds number distribution. Myers and Brennan (1990) carried out similar calculations for the SERC FCF Phase A data. They found that Manning's n reduced to about 0.01 at bankfull and then reduced sharply to about half this value at just overbank levels, although at larger floodplain depths the value approached the bankfull value. These results are typical of compound channels. These general distributions can be obtained for many examples. The exact geometry of the main channel and floodplains will determine the exact distribution of roughness parameters with stage

These results demonstrate that the simple channel method is not appropriate for computing discharge in compound channels. The variation in roughness values demonstrated above does not reflect a true variation in the bed roughness characteristics as the water level varies. The non-linear interaction of the various geometric parameters in the calculation has produced these spurious results. Engineers recognise that compound channels behave differently to simple channels. The more usual approach followed in many text books is to divide the compound channel into zones. The simple channel equations are then applied to each zone in turn and the total discharge obtained by summing the zonal discharges. This approach is a big improvement over the simple methods. The text book application is usually to divide the floodplain areas from the main channel using vertical division lines at the main channel edges. The division lines are usually not included in the wetted perimeters of the various regions. This approach is usually justified on the grounds that the velocities within each zone are uniform but differ between zones, see Chow (1959), Henderson (1966) or Chadwick and Morfett (1989).

This divided channel approach is based on the assumption that the flows within the individual regions are controlled by bed friction only and that there is no interaction between zones which may affect the discharge capacity of the zones or channel as

a whole. This is obviously a critical assumption which requires further investigation. Classical hydraulics tell us that when co-flowing streams of fluid with markedly different velocities exist then there is usually a turbulent exchange of fluid and momentum between them. This situation is called a shear layer and is a significant mechanism in many flow situations. In the case of compound channels the questions to be answered are as follows:

- 1) Does a shear layer exist between the fast moving main channel flow and the slow moving floodplain flow?
- 2) Is there any other potentially important source of interaction between the flows?
- 3) Do the mechanisms of interaction have significant effects on the discharge capacities of the main channel and floodplain zones?
- 4) What are the parameters which control the strength of the important mechanisms?

Much research has been carried out into these topics in the last thirty years. The following section reviews the important aspects of this research and its conclusions.

### **3.2.2 Research into flows in straight compound channels**

Some of the earliest work in the field was carried out by Sellin (1964). He carried out a laboratory investigation into the overall behaviour of straight compound channels. Stage discharges and longitudinal point velocities were measured in various channel and floodplain geometries. Sellin studied the surface flow patterns using aluminium powder and a moving camera. These photographs revealed the existence of a vortex structure in the region between the main channel and floodplain flows. These vortices were found to have vertical axes and to rotate so that a proportion of the fast moving main channel flow is carried on to the floodplain and vice-versa. Figure 3.4a shows a typical pattern of surface stream lines derived by Sellin from his photographs, The vortices are clear. This exchange of fluid between zones causes a transfer of momentum between the fast and slow moving regions and

represents a significant source of interference. The gross effect is to reduce the velocities in the main channel and increase the velocities in the floodplains

Sellin investigated the importance of this effect by conducting tests with floodplains and main channel separated by impermeable walls. For the geometry investigated the channel with floodplains isolated from the main channel carried discharges between 3% and 4% larger than those in the equivalent compound channel. The channel Sellin used was hydraulically smooth with main channel and floodplains having a Manning's  $n$  of 0.0088. Sellin also carried out some tests with roughened floodplains ( $n$  0.019) and the increase in discharge with separated floodplains was found to be about 9% at just overbank stages and to reduce rapidly for deeper flows. Sellin considered various simple divided channel methods and concluded that applying vertical divisions at the main channel and floodplain boundary modelled the discharge adequately for the conditions investigated. He showed that the relative roughness of the floodplain has a strong effect on the degree of interaction between main channel and floodplain flows. The study covered only a limited range of channel shapes and roughness conditions and so further research was required to confirm these conclusions.

Zhelezneyakov (1965) also used a photographic technique to observe the vertical vortices at main channel and floodplain boundaries. He identified two regions of behaviour: at low overbank stages the main channel velocity decreases and then after a certain depth is reached the main channel velocity increases. He also found that the main channel velocity was reduced more when the floodplain is rougher than the main channel.

The distribution of boundary shear stresses and discharge were studied by Myers and Elsayy (1975). They carried out 10 stage-discharge tests on a laboratory channel about 8.5m long by 0.6m wide. They investigated to boundary shear stress distributions across the wetted perimeter of an asymmetric compound channel, with one floodplain on the right hand side of the main channel. The main channel was 101.6mm deep at bank full and the maximum depth investigated under over bank

conditions was 169mm. They also measured shear stresses for the case where the flow was restricted to the main channel by an impermeable barrier. The results showed that the interaction between main channel and floodplain flows significantly affects the bed shear stress distribution in the main channel. They found that at the lowest overbank depth investigated the mean bed shear stress in the main channel was 22% smaller than the value obtained for the isolated main channel. At higher stages the percentage decrease in mean shear reduced considerably (to about 6% at the deepest stage). In a later study Myers (1978) sought to quantify the mechanism for momentum transfer in compound channels with one floodplain. Myers analyzed his results in terms of a divided channel approach. In each channel element (main channel and floodplain) he identified the following forces: the component of fluid weight acting in the direction of flow and the shear stress acting on the channel bed. In addition to these two forces Myers introduced the concept of apparent shear force, which acts on the interface between the main channel and floodplain. These forces act to retard the main channel flow and enhance the floodplain flow, Figure 3.5. They can be considered to be a convenient method of parameterising the complex interaction produced by the vortices at the main channel edge. For his data set Myers found that the apparent shear force increases to a maximum at relative depths of about 0.3 and then decreases. Apparent shear stress defined as the apparent shear force divided by the area of the vertical division was maximum at the lowest overbank stages and decreased sharply with stage.

Baird and Ervine (1982) also followed the apparent shear stress approach in analyzing results from a physical model study of flow in straight compound channels. In this early paper they considered smooth channels and flood plains. They assumed that the apparent shear stress is related to the velocity gradient at the interface and that this could be expressed in terms of the difference between the mean velocities in the main channel and floodplains. In the case of asymmetric compound channels they found that the apparent shear stress is given by:

$$\tau_a = 50 (\Delta V)^2 \tag{3.2}$$

and for symmetric cases this becomes:

$$\tau_a = 25 (\Delta V)^2 \tag{3.3}$$

In a later paper Baird and Ervine (1984) extended their analysis and suggested that:

$$\tau_a \propto (\Delta V)^{2.2 \sqrt{(B_c/B_f)}} \quad (3.4)$$

where  $B_c$  is the main channel width and  $B_f$  is the floodplain width. They found that  $\tau_a$  varies with non-dimensional depth and produced the following relationship for smooth asymmetric compound channels:

$$\tau_a / (\rho g Y_f S) = (Y_f/Y_c - \beta^*)^{1.5} (B_c/h)^{0.5} (0.5 + 0.3 \ln (B_f/h)) \quad (3.5)$$

Where  $\beta^*$  is the value of relative depth ( $Y_f/Y_c$ ) where the apparent shear stress is zero.  $\beta^*$  is given by the empirical equation:

$$\beta^* = 1.0 + 1.5 (h/B_c)^{1.25} \quad (3.6)$$

$Y_c$  is the flow depth in the main channel,  $Y_f$  is the flow depth on the floodplain and  $h$  is the bankfull depth ( $Y_f = Y_c - h$ ). They also introduced the concept of  $\Phi$  indices to characterise the degree of interaction present.

where:

$$\begin{aligned} V_{mc} &= \Phi_{mc}^{1/2} V'_{mc} \\ V_{fp} &= \Phi_{fp}^{1/2} V'_{fp} \end{aligned} \quad (3.7)$$

and the  $V$  values are the velocities in the regions during interaction and the  $V'$  values are the velocities calculated assuming no interaction occurs. It is possible to show that the  $\Phi$  values for the main channel and floodplain are related to the apparent shear stresses by:

$$\Phi_{mc} = 1 - (\tau_a Y_f / \rho g A_{mc} S) \quad (3.8)$$

and

$$\Phi_f = 1 + (\tau_a Y_f / \rho g A_f S) \quad (3.9)$$

$\Phi_{mc}$  and  $\Phi_f$  are related by the expression

$$A_{mc} (1 - \Phi_{mc}) = A_f (\Phi_f - 1) \quad (3.10)$$

Ervine and Baird proposed that equations 3.5 and 3.6 could be used to evaluate  $\tau_s$  and that equations 3.8 and 3.9 should then be used to calculate the indices for the main channel and floodplain flows. The final discharge in each region is then obtained by applying the indices to the velocities or discharges calculated assuming no interaction (equation 3.7).

Knight, Demetriou and Hamed (1983) also looked at the momentum transfer in terms of apparent shear forces. They derived the equation below for smooth compound channels based on laboratory data.

$$\%ASF = 50 / ((\alpha-1)(\beta+1) - 0.5 [100 - 48(\alpha-0.8)^{0.289} (2\beta)^{1/n} (1+1.02\beta^{0.5} \log_{10}(\gamma))]) \quad (3.11)$$

where

$$n = 0.75e^{0.38\alpha} \quad (3.12)$$

%ASF is the apparent shear force acting on the vertical interface, expressed as a percentage of the mean shear <sup>force</sup> acting over the floodplain segment. The other parameters are based on non-dimensionalized characteristics of the channel:

$$\alpha = (0.5B_c + B_f) / 0.5B_c, \quad \beta = Y_f / Y_c \text{ and}$$

$$\gamma = \text{Manning's } n \text{ for floodplain} / \text{Manning's } n \text{ for main channel.}$$

The experiments were carried out in laboratory channels which were hydraulically smooth, in the main channel at least, so using Manning's  $n$  in the analysis is unsound from a theoretical view point. They concluded that the strength of the apparent shear stress is a function of relative depth, main channel and floodplain geometry and relative roughness of the floodplains. For their data they found that the apparent shear force was approximately 10% of the mean flood plain shear force over a wide range of conditions.

In an investigation into the geometric parameters which affect floodplain flow, James and Brown (1977) carried out a series of experiments in a large scale flume of length 27m and width 1.5m. They investigated the effects of various floodplain widths and roughnesses and present both stage-discharge curves and distributions of depth averaged velocity. Unfortunately they do not supply any calibration data with which to check the basic Manning's n values they quote for the various cases. They analyzed their stage discharge data in terms of the single channel method: ie they applied Manning's equation to the complete compound channel. They used the laboratory data to derive the values of a correction factor ( $\Phi$ ) which can be applied either to the Manning's n value or the hydraulic radius to produce effective values:

$$\Phi = (n_b/n) = (R_{\text{eff}} / R) \quad (3.13)$$

and

$$Q = \Phi^{1/n} A R^{2/3} S^{1/2} \quad (3.14)$$

Where  $n_b$  is the value of Manning's n at bankfull stage. They produced a chart which shows  $\Phi$  to be a function of the channel aspect ratio (Total width of floodplains/ width of main channel) and relative depth. It is rather surprising that  $\Phi$  was not found to be a function of the relative roughness of the floodplains, Figure 3.8. The functions they give are highly unlikely to be at all general, considering the limited range of tests they carried out. This form of analysis is not to be recommended.

Rajaratnam and Ahmadi (1979, 1981) have published the results of a detailed investigation into the distributions of velocity and bed shear stress in straight compound channels. They measured longitudinal velocities and bed shear stresses in a smooth laboratory flume which was about 18m long by 1.22m wide by 0.92m deep. The experiments were carried out with an asymmetric compound channel with only one floodplain. The main channel was 0.711m wide and the bankfull depth was 97.5mm. Longitudinal velocities were measured using a pitot tube, which also doubled as a preston tube during the bed shear stress measurements. The velocity results were presented in two forms:

## Vertical distribution of velocity

In simple channels it is well known that the vertical distribution of point velocity is logarithmic. Rajaratnum and Ahmadi found that the interaction between main channel and floodplain flows disturbs the vertical distribution of velocity. In the main channel close to the floodplain edge the velocities are logarithmic up to a level approximately bankfull. Above this level the velocities are closer to the flow velocities on the flood plain, see figures 3.7 and 3.8. As one moves away from the floodplain boundary the logarithmic profile takes up more of the channel depth and if the channel is wide enough then a central region which is unaffected by the interaction with the main channel exists.

## Distribution of depth averaged velocity and bed shear stress

The measured point velocities and bed shear stresses also show the effect of the interaction between main channel and floodplain. The profiles were non-dimensionalized and empirical equations derived in terms of the free stream values, Figures 3.9, 3.10. The effects of interaction are also obvious on these parameters and Rajaratnum and Ahmadi derived expressions for the widths of the interaction zones in the main channel and floodplains. They found that these shear layer widths are functions of the channel bankfull depths:

$$\begin{aligned}b_{slt} &= 5.97 h \\b_{slm} &= 4.37 h \\b_{slf} &= 1.60 h\end{aligned}\tag{3.15}$$

Where  $b_{slt}$  is the total shear layer width and  $b_{slm}$  and  $b_{slf}$  are the shear layer widths in the main channel and floodplain respectively. The main conclusions drawn from this work are:

- 1) There is a region where the effects of the interaction are felt. The strength of the interaction and the widths of the region are dependent on the channel depths.
- 2) The bed shear stress on the floodplains is increased by the interaction. In the

main channel it is reduced.

- 3) The vertical distributions of velocity showed that the mixing behaviour induced by the interaction is a complex phenomenon and that further research is needed.

Wormleaton <sup>etal</sup> (1985) carried out experimental tests with various floodplain roughnesses. He assessed the apparent shear stresses on the <sup>division plane</sup> and concluded that it is strongly related to the velocity differential between main channel and floodplain flow. He also found that it is a function of the width and depth ratios of the channel.

Prinos and Townsend (1984) present the results of model tests on an asymmetric compound channel. Their flume was 12.2m long by 1.4m wide by 0.4m deep. The symmetric compound channel had a bankfull depth of 102mm. They measured velocities and bed shear stresses and found that the apparent shear stresses are functions of relative depth, width and roughness of main channel and floodplain. They produced an empirical relationship:

$$\tau_a = 0.874 ((Y_c - h)/Y_c)^{-1.129} \alpha^{-0.514} \Delta V^{0.92} \quad (3.16)$$

Where  $\alpha$  is the ratio of half the top width of the whole channel to half the bottom width of the main channel.

Pasche and Rouve (1985) measured the velocity distribution across a compound channel with heavily roughened floodplains. The laboratory experiments were carried out in a flume 25m long by 1m wide by 1m deep. The asymmetric compound channel had a bankfull depth of 124mm with a floodplain of width 500mm. In some tests the floodplain was roughened by placing vertical dowel rods in a regular pattern. The rods were long enough to pierce the free surface. They measured longitudinal velocities with a laser doppler anemometer and drew the following conclusions:

- 1) The momentum exchange between main channel and floodplain must be taken into account.

- 2) In smooth channels the main channel side slope has a significant effect on the strength of the interaction.
- 3) For channels with roughened floodplains the strength of the interaction is not affected by the main channel side slope.

Knight and Lai (1985) investigated the flow structures present in compound channel and duct flow. They conducted experiments with a 17m long flume. They varied floodplain widths and roughnesses. They presented depth averaged velocity profiles and bed shear stresses. The results show that the strength of the interaction mechanisms vary with depth and floodplain roughness.

In a study of the velocity and discharge in compound channels Myers (1987) presents both theoretical considerations and laboratory data collected in a small flume. He concluded that the ratios of velocity and discharge (main channel / floodplain) in smooth compound channels are independent of slope and dependant only on the channel geometry and depth.

Dracos and Hardegger (1987) analyzed laboratory data from James and Brown (1977) and other investigators. They produced a method of estimating the discharge in smooth compound channels. The method is a development of the proposed adjustment to bankfull Manning's  $n$  given by James and Brown. The channel is treated as a single unit and a correction factor ( $\Phi$ ) is calculated. The definition of  $\Phi$  is given by equation 3.9. They found that the correction factor is a function of depth and width ratios:

$$\Phi = 1.65 + 0.976 \alpha^{-0.2854} \ln (R/Y_c) \quad (3.17)$$

where  $\alpha$  is given by:

$$\alpha = (b_{f1} + b_{f2}) / [(1+s_1)^{0.5} (1+s_2)^{0.5} h + b_c] \quad (3.18)$$

where  $b_{f1}$  and  $b_{f2}$  are the widths of the floodplains,  $b_c$  is the bottom width of the main channel,  $s_1$  and  $s_2$  are the slopes of the left and right banks of the main channel. In the case of roughened floodplains Dracos and Hardegger suggest that the correction

factor should be applied to an effective roughness value. They recommend that the weighted average Manning's  $n$  value calculated using the Horton method should be used. The whole theoretical basis of this approach is seriously flawed. It is apparent from the large amount of laboratory work that compound channels do not behave at all like simple channels. Any method based on a single channel approach is very unlikely to have a general range of applicability. The particular method developed by the authors is based on a very small data set which further restricts the utility of their procedure.

Holden and James (1988, 1989) have published the results of a physical model study of compound channel flow. They carried out a series of experiments in a 16m long by 0.92m wide by 0.2m deep flume. The main channel was 545mm wide and they investigated the effect of varying the slope of the main channel. The asymmetric compound channel had a bankfull depth of 106mm and was hydraulically smooth. They measured stage-discharges and bed shear stress distributions. They confirmed that the channel bank slopes have a significant effect on the interaction for smooth compound channels, with the interaction getting stronger as the channel banks become steeper. They used their own and published data to derive modified apparent shear stress methods of calculating flow in compound channels. The main limitation in this work is that they did not consider roughened floodplain cases.

Much of the published research into compound channels up to the late 80's was carried out in relatively small scale facilities, most with hydraulically smooth boundaries. The complex hydraulics observed in these small scale compound channels may not scale up to typical prototype conditions in the field. The only ways to confirm that the laboratory conditions do exist at prototype scales are either to do detailed measurements in the field or to carry out experiments in a very large scale model. The problems involved in collecting a definitive accurate set of field data are such that it would be impractical both because of instrumentation difficulties and due to imperfect knowledge of the various geometric and flow parameters. The Science and Engineering Research Council (SERC) in Britain, along with other government departments and professional bodies identified a strong economic need for improved

methods for estimating discharge in channels with flood plains. Consequently it was decided (see Knight and Sellin, 1987) to fund the construction of a large scale experimental facility which could be used to investigate the behaviour of compound channels. The SERC Flood Channel Facility is situated in HR Wallingford's Laboratory. The flume is 50m long by 10m wide and depths of flow of up to 0.5m can be contained. The instruments available on the facility include a laser doppler anemometer, which allows detailed turbulence measurements to be made, propeller meters to measure longitudinal point velocities and preston tubes to measure bed shear stresses. The maximum discharge available from the four pumps is 1.1 cumecs.

Phase A of the research programme investigated straight compound channels and ran from 1986 to 1989. Phase B, which covered the two years from 1989 to 1990 was designed to study the behaviour of meandering compound channels. A third phase of research into sediment transport in compound channels is due to start in 1993 or 1994.

Four university research teams were involved in Phase A of the FCF work. Each team had particular interests to pursue during the collaborative effort and the following four papers summarize the main findings from the research.

Wormleaton and Merrett (1990) from Queen Mary College, London University were particularly interested in the effects of main channel side slope and scale effects in compound channels. They used the Phase A data to investigate the performance of some simple divided channel methods: with vertical; diagonal and horizontal division lines between main channel and floodplain. They chose the divided channel approach because it is often just as important for the engineer to know the local velocities and discharges in the individual parts of the channel as well as the overall discharge. They applied these methods to 4 out of the 12 data sets collected in Phase A and concluded that these simple methods could be in error by as much as 20% for smooth channels and 60% for roughened floodplain cases. In an attempt to improve the prediction of total and zonal discharges they considered the forces acting on each channel region and concluded that the important forces are: weight of fluid, bed

friction and the apparent shear stress on the interface.

They followed Ervine and Baird (1982, 1984) in proposing the  $\Phi$  index method of accounting for the interaction effects in a discharge calculation. They present an empirical equation for the apparent shear stresses based on four of the data sets collected from the SERC FCF:

$$\tau_a = 3.325 \Delta V^{1.451} (Y_c - h)^{-0.354} b_f^{0.519} \quad (3.19)$$

This expression can then be used to calculate the two  $\Phi$  indices. The main limitation with this expression is that it is based on only a small subset of the available FCF data. The main channel side slope was constant for all four cases at 1:1. Undoubtedly the expression will alter significantly when all the data, for a range of side slopes is considered. The width of floodplain  $b_f$  also appears in this equation in a dimensional form, making the application of this equation to other channels and conditions unfeasible. The authors report improved predictions, compared with the basic divided channel method.

Myers and Brennan (1990) from the University of Ulster concentrated on analyzing the FCF data to investigate flow resistance in compound channels. They show that the smooth trowelled mortar surface of the flume is hydraulically smooth. They treat the channel as a single unit and used the measured stage discharge data to compute the variation of Manning's  $n$  and Darcy friction factor with depth and Reynolds number. The results they present confirm that compound channels should not be treated as a single unit. The resulting variations in the friction parameters, Figure 3.11, are due to the geometry of the channel at over bank stages and not to changes in the bed friction characteristics.

One important aspect of the FCF Phase A work was the study carried out by Knight and Shiono (1990) into the characteristics of turbulence in the shear layer of a compound channel. A two component laser doppler anemometer was used to measure all three components of the primary and fluctuating velocities. Two sets of

readings were required to do this, one to measure longitudinal and transverse components and another to measure longitudinal and vertical components. The turbulent intensities and Reynolds stresses were derived directly from the raw data. Figure 3.12 shows some typical turbulence results for one channel geometry and depth. The channel centre line is at  $y=0$ , with the foot of the channel bank at  $y=0.75\text{m}$  and the channel edge at  $0.9\text{m}$ . The channel bankfull stage is  $0.15\text{m}$ . Figure 3.13 shows the variation in Reynolds stresses which act in the longitudinal direction on the horizontal plane. The longitudinal velocities follow the standard logarithmic profiles in the centre of the main channel and on the floodplain away from the shear layer. In the shear layer the velocity profiles are similar to those observed by Rajaratnam and Ahmadi (1979), the profile follows the logarithmic curve from the bed up to a level where the velocities reduce due to the interaction. The vertical distribution of the shear stresses on the horizontal planes also show that the logarithmic profile holds for regions of the channel out with the shear layer. Where the velocity profile is logarithmic the shear stresses are linear between the bed shear values and the water surface, in the shear layer the shear stresses show a C shaped distribution with depth. The interaction between floodplain and main channel does appear to have a stronger influence on the main channel velocities and stresses than on those in the floodplain. Figure 3.14 shows the lateral and vertical variation of the longitudinal stresses which act on the vertical plane. Out with the shear layers these stresses are zero and the interaction does not affect the flows in either the centre of the main channel or the majority of the floodplains. Knight and Shiono also studied the lateral variation of Darcy friction factors across the channel. The bed shear stress measurements combined with the observed velocities allowed them to calculate the local friction factors based on depth averaged velocities. Figure 3.15 shows that friction factors are constant in the main channel and floodplain zones, where the depths are uniform. The friction factors on the floodplains are consistently larger than those in the main channel and this difference reduces with flow depth. They attempted to evaluate the interaction mechanism by treating it as a viscous shear and deriving values of depth averaged eddy viscosity across the channel according to:

$$\tau_{xy} = \rho \nu_t \partial U / \partial y \quad (3.20)$$

Where  $\tau_{xy}$  is the depth averaged lateral shear stress,  $\rho$  is the density of water,  $v_t$  is the depth average kinematic eddy viscosity and  $U$  is the depth averaged velocity. They also non-dimensionalized the eddy viscosity relative to the bed shear stresses according to:

$$\lambda = v_t / U_* D \quad (3.21)$$

$U_*$  is the local shear velocity defined as:

$$U_* = (\tau_{bx} / \rho)^{1/2} \quad (3.22)$$

The results are shown in Figure 3.16. The values of both eddy viscosity and non-dimensionalized eddy viscosity vary strongly across the shear zone. The values in the main channel are lower than those observed on the floodplain. The computed velocity gradients at the edges of the shear layer approach zero and so small differences in the measured shear stresses result in large errors in the calculated viscosity values. They also show that the plan form vortices observed by Sellin (1964) are present at the floodplain interface. They also plot the distribution of bed shear stress across the channel. They confirmed that the effect of the interaction, secondary currents and lateral shear, induce changes in the bed shear stress distributions. They show that low shear stresses exist in the main channel at the floodplain edge and that high shear stresses exist on the floodplain edge. Figure 3.17 shows typical bed shear stress distributions in compound channels.

The main conclusions that they draw from the data are:

- 1) The primary velocities are logarithmic in the vertical and the corresponding Reynolds stresses are linear in zones out with the shear layer.
- 2) In regions where there is high lateral turbulence imposed on the bed generated turbulence the lateral Reynolds stresses are non linear and include the effects of secondary circulation, both in plan and elevation.

- 3) The lateral variations in the local friction factors show that flows in compound channels may be modelled with constant friction factors in each zone of the flow.
- 4) The interaction between main channel and floodplain flows causes a redistribution of bed shear stresses. The bed stresses are reduced in the main channel shear layer and increased in the floodplain shear layer.

Elliot and Sellin (1990) investigated the discharge capacity of a compound channel which is skewed to the floodplain direction. This case can be regarded as intermediate between straight and meandering channels. They studied the effects of skew angles of  $5^\circ$  and  $9^\circ$ . They found that a channel with a skewed main channel can pass less discharge than an equivalent straight channel. The effect of the skew was larger for the  $9^\circ$  case than for the  $5^\circ$  skew. The capacity of the channel compared to a straight channel is reduced by an amount that varies with depth and is maximum at low overbank stages.

Fukuoka and Fujita (1990) carried out stage discharge measurements in a laboratory channel of width 200mm to 300mm. The main channel widths were between 50mm and 200mm, the bank full depths varied between 30mm and 120mm. The very small size of their laboratory facility means that scale effects must be important and it is unlikely that their results will accurately model prototype channels.

Fukuhara, Fukui and Murota (1990) carried out a set of experiments in a flume 20m long by 0.7m wide by 0.3m deep. The rectangular main channel had widths of 0.2m, 0.3m and 0.4m and bankfull depths of 30mm, 50mm and 70mm. They applied a divided channel method to model the stage discharge relationships. They proposed that adjusted values of hydraulic radius (an effective hydraulic radius) should be used in the calculation. They provided complex functions relating the effective hydraulic radii to the geometric values. They found that these functions varied with channel depth, width and roughness. This form of analysis is unlikely to provide a general model of flow in compound channels.

The behaviour of compound channels during critical flow has been studied by Knight and Yuen (1990). They measured velocity distributions within a laboratory channel under critical flow conditions. They found that local Froude numbers varied across the channel and that supercritical and subcritical flow can exist simultaneously within the same channel. They found that there is a strong tendency for critical flow to first occur on the floodplain at the edge of the main channel, where velocities are high and depths low.

Myers (1990) and Higginson et al (1990) present the results of two model studies of a prototype compound channel. Field measurements of velocity and discharge were also made on the River Main in Northern Ireland. They found that the physical models could accurately reproduce the prototype behaviour (stage-discharges) but that the model floodplains needed to be artificially roughened to achieve this. They found that distorted scale models (larger vertical scale than horizontal scale) do not give accurate predictions of either velocity distributions or total discharge. Further details of the field site and the measurements taken are given by Martin and Myers (1991).

Ackers (1991, 1993) carried out an exhaustive analysis of the data collected on the SERC FCF during Phase A. He developed procedures which allow engineers to use the results from the FCF in designing and analyzing compound channels. This work was carried out at HR Wallingford on behalf of the National River Authority for England and Wales.

The procedures developed by Ackers allow prediction of stage-discharge relationships, division of total discharge into main channel and floodplain components and estimation of boundary shear stresses. The method is based on the divided channel approach (DCM2). A basic discharge is calculated separately for each zone using a conventional resistance equation (such as Manning's) and these are then added together to give the total basic discharge. This is then adjusted to account for the effects of the interactions between the zonal flows. Four regions of flow behaviour were identified, Ackers 1991, within which the variation of the interaction effect with flow depth was different. A different adjustment function is presented for

each region and Figure 3.18 shows the four regions. In region one, where the interaction increases with depth, Ackers (1991) found that the interaction effect was best described by a discharge deficit, DISDEF, which he normalised by the velocity differential and the product of flow depth and main channel depth.

$$Q_{R1} = Q_{\text{basic}} - \text{DISDEF} \quad (3.23)$$

In region 2 the interaction reduces with depth and Ackers developed equations giving the discharge adjustment factor (DISADF). DISADF varies with flow depth, channel geometry and roughness. In region 3 the interaction reduces with stage and again Ackers found that the interaction was best modelled with a discharge adjustment factor.

$$Q_{R2,3,4} = \text{DISADF} Q_{\text{basic}} \quad (3.24)$$

From theoretical considerations Ackers developed the concept of channel coherence (COH). This parameter characterises the behaviour of a compound channel, it is defined as:

$$\text{COH} = \frac{(1+A_*) [(1+A_*) / (1+f_*P_*)]^{0.5}}{1 + A_* (A_* / F_*P_*)^{0.5}} \quad (3.25)$$

Where  $A_*$  is the ratio of total floodplain area to main channel area,  $P_*$  is the ratio of total floodplain wetted perimeter to main channel wetted perimeter and  $f_*$  is the ratio of floodplain friction factor to main channel friction factor.

The available data from the SERC FCF covered only the first three regions. Ackers argued that at higher stages where it is known that the behaviour of compound channels approaches that of simple channels and the value of COH approaches 1 then the basic discharge adjustment factor is given by the value of coherence.

It is not possible to identify the appropriate region and function for a particular water level before hand, but a procedure is given for selecting the correct result from those

obtained using each adjustment function. An additional correction is also given to account for the effect of moderate angles of skewness of the main channel. The total discharge can be divided into main channel and flood plain components using intermediate results from the primary calculations.

The interaction between main channel and flood plain flows also affects the magnitude and distribution of boundary shear stress in a compound section. Ackers (1991) gives procedures for making provisional estimates of the average boundary shear stress in the main channel and the average and local maximum values on the flood plains. Ackers' method for stage-discharge prediction, separation of main channel and flood plain flow and estimation of boundary shear stress has been summarised as a step by step design procedure in Appendix 6.

Most of the work reviewed above has concentrated on the overall behaviour of straight compound channels. The various researchers have limited their laboratory investigations or theoretical modelling efforts to gross features of the flow including: stage-discharges, depth averaged velocity and bed shear stress distributions. In recent years the increasing availability of sophisticated flow measurement techniques based on laser doppler equipment has encouraged researchers to carry out detailed measurements of turbulence in compound channels. The availability of such data has provided the opportunity to develop and test the behaviour of complex numerical turbulence models.

### **3-D turbulence in compound channels**

Krishnappan and Lau (1986) solve the 3-D Reynolds' equations of turbulent flow. They use the  $k$ - $\epsilon$  turbulence model to approximate the turbulent stress terms,  $k$  is the turbulent kinetic energy and  $\epsilon$  is the dissipation rate of turbulent energy. As well as the three momentum equations and the continuity equation two extra equations are introduced which describe the variation of  $k$  and  $\epsilon$  with in the flow. The authors simplified the equations by assuming uniform flow in the longitudinal direction and obtained a set of equations which describe the variation of all three velocity

components with a channel cross-section. They applied the model to some of the laboratory data available from other authors. They showed that the model can give good predictions of total discharge, discharge distribution between main channel and floodplain and boundary shear stress distributions.

Tominaga et al (1989, 1991) carried out detailed turbulence measurements in a laboratory compound channel using a fibre optic laser doppler system. The asymmetric compound channel was hydraulically smooth and was constructed in a flume 12.5m long with a 0.4m by 0.4m cross-section. The rectangular main channel was 0.2m wide and they investigated three bankfull depths of 20mm, 40mm and 60mm (cases S1, S2 and S3 respectively). In all three cases the depth of flow in the main channel was set to approximately 80mm. They found that fairly strong secondary circulation cells exist in both the main channel and floodplain, Figure 3.19. The strength of these cells depends on the relative depth of flow (Floodplain depth/Main channel depth). The maximum secondary velocities within the cross-section were found to be 3.5%, 4% and 2.5% of the maximum longitudinal velocity in cases S-1, S2 and S3. The circulations are such that an upwelling current is developed at the main channel floodplain interface and is inclined into the main channel. The relative strengths of the two counter-rotating circulation cells varies with relative depths. At the highest relative depth (0.75) the main channel cell is very weak but the floodplain cell is strong. In the intermediate case, relative depth 0.5 the two circulation cells are similar in size and strength. In the last case, (relative depth 0.25), the main channel vortex takes up a larger proportion of the main channel width. In all three cases a second counter rotating circulation cell exists in the main channel on the other side of the vortex at the floodplain interface. The strength and size of this vortex also varies with relative depth. They also show some results with a roughened floodplain for a relative depth of 0.5. They show that the general pattern of secondary circulation is the same as in smooth channels but that the strengths of the circulations are reduced, especially in the floodplain region. They also present plots of measured Reynolds stresses in the channel. These distributions are similar to those observed by Knight and Shiono, 1991, They are approximately linear away from the shear zone and increasingly deviate as they approach the main

channel / floodplain edge. The observed bed shear stresses also follow the pattern observed elsewhere, they are low in the main channel at the edge and high on the floodplain side of the boundary. They also present the results of a numerical simulation applied to case S-2 of this data. The assumption of uniform flow in the longitudinal direction was used to simplify the equations and the algebraic stress model due to Launder and Ying (1973) was adopted for its relative simplicity. Their calculations gave good qualitative results in predicting the presence of the various circulation cells but poorly predicted the strengths of the circulations.

Shiono and Knight (1989, 1991) have also measured secondary current distributions in the smooth compound channels constructed in the SERC FCF. The results show the same pattern of secondary currents, namely a strong up welling at the floodplain main channel interface. They observed one circulation cell on the floodplain and two in the main channel. They found that the relative strength and sizes of the two main channel circulations depend on the channel side slopes. Figure 3.20 shows that as the channel sides steepen the upper circulation becomes stronger and covers a larger proportion of the main channel. Figure 3.21 illustrates these different conditions.

Prinos (1991) applies an improved algebraic shear stress model to the data collected by Knight and Demetriou (1983). He shows good agreement between measured and predicted distributions of flow in the main channels and floodplains. His model also predicts the presence of the various secondary circulation cells observed by others.

### **Depth averaged or integrated investigations**

The approaches to modelling compound channel flow followed above are based either on adjusting existing 1-D approaches to account for the effects of interaction on the overall flow or on calculating the complex 3-D behaviour of turbulent flow in compound channel. The first type of approach is more likely to be used by practising engineers due to its relative simplicity. Complex turbulence models are still effectively research tools and it is unlikely that they will ever be an economic option

for the practising engineer involved in the design or analysis of compound channel flows. An intermediate approach between these two types of method has been followed by various authors. This method is based on the depth averaged or depth integrated equations of flow with a free surface, Chapter 2. In the case of steady uniform flow in a straight channel the equations reduce to a single equation which describes the lateral distribution of depth averaged velocity of unit flow across a channel.

Vreugdenhil and Wijnbenga (1982) were amongst the first authors to consider this approach to estimating discharge in compound channels. They solved the simplified depth averaged equation:

$$g D S_{xf} - \frac{gU^2}{C^2 D} + \nu_t \frac{\partial^2 U}{\partial y^2} = 0 \quad (3.26)$$

Where  $g$  is the gravitational acceleration,  $D$  is the local flow depth,  $S_{xf}$  is the longitudinal friction slope,  $U$  is the depth averaged velocity,  $C$  is Chezy's friction number and  $\nu_t$  is the depth averaged lateral turbulent viscosity. They identified the need for a boundary condition at the channel bank and adopted the no-slip condition ( $U=0$ ).

The solution technique was based on finite differences with an iterative procedure to obtain the final solution to the non-linear equation. They identified a problem in determining appropriate values of  $\nu_t$  and proposed a constant value based on an analogy with two dimensional shear layers (Lean and Weare, 1979). This relates  $\nu_t$  to the width,  $\Delta$ , and velocity difference,  $\delta u$ , across the shear layer:

$$\nu_t = 0.01 \Delta \delta u \quad (3.27)$$

They applied this model to field data from the river Maas and reported <sup>that</sup> reasonable agreement can be obtained, provided sufficient information is available for the calibration of both the bed friction term and the viscosity.

Radojkivic and Djordjevic (1985) carried out a set of experiments in a symmetric compound channel. The channel was hydraulically smooth with a rectangular main channel of width 0.152m and bankfull depth 0.076m. Four cases were investigated with total channel width to main channel width ratios of 1, 2, 3 and 4. They solve a different form of the lateral distribution equation:

$$g D S_{xf} - \frac{gn^2U^2}{D^{1/3}} + \frac{\partial}{\partial y} \left[ v_t D \frac{\partial U}{\partial y} \right] = 0 \quad (3.28)$$

The bed shear stresses are evaluated by the Manning's equation and they allow the lateral eddy viscosity and depth to vary across the shear layer. They approximated the lateral eddy viscosity by the depth averaged k-ε model proposed by Keller and Rodi (1985). They reported poor results with this complex turbulence model and ascribed this to the fact that the form of model used is only intended to describe bed generated turbulence and does not adequately describe the effects of secondary currents.

They also used the much simpler empirical relationship relating viscosity to bed shear stresses through a non-dimensional eddy viscosity, λ.

$$v_t = \lambda U_* D \quad (3.29)$$

They found that the appropriate single value of λ varied with the width ratio of the channel. They report good agreement between measured and computed discharges with values of 0.25, 0.45 0.65 for width ratios of 2, 3 and 4 respectively. They concluded that this non-dimensional eddy viscosity could be suitable in practical calculations.

Djordjevic et al (1989) continue this work by drawing an analogy between the lateral diffusion of momentum through the effects of lateral viscosity,  $v_t$ , and the lateral diffusion of dissolved concentrates. They measured both depth averaged velocities and depth averaged concentrations of Rhodamine B dye in an asymmetric compound

channel 34m long by 0.7m wide. They obtained good agreement between measured and computed velocity profiles with a constant  $\lambda$  value of 0.20.

Pashe, Arnold and Rouve (1986) used a laser doppler anemometer to investigate the structure of turbulence in compound channels with vegetatively roughened floodplains. The experiments were carried out in a flume 25m long by 1m wide by 1m deep. The asymmetric compound channel had a width of 0.5m. Vertical dowel rods were used to roughen the floodplain. Velocities and Reynolds stresses were measured directly and confirmed the findings of other investigators described above. The authors carried out depth averaged calculations with a k- $\epsilon$  model and obtained good predictions of both velocity and shear stress distributions. They also carried out calculations with section averaged values of viscosity, derived from the k- $\epsilon$  results and showed that reasonably accurate predictions are possible with very simple turbulence models. However the value of eddy viscosity was found to vary with bed roughness and channel geometry.

Samuels (1988) considered the form of equation:

$$g D S_{xf} - \frac{fU^2}{8} + D \frac{\partial}{\partial y} \left[ \nu_t \frac{\partial U}{\partial y} \right] = 0 \quad (3.30)$$

Where  $f$  is the Darcy friction factor. He derived two analytic solutions for this equation. The first solution is for the velocity distribution in an infinitely wide rectangular channel. He assumed that both  $f$  and  $\nu_t$  are constant across the channel and derived the solution:

$$U = U_0 \left[ 3 \tanh^2 \left\{ (U_0/2\beta)^{1/2} y + 1.1462 \right\} - 2 \right] \quad (3.31)$$

where  $y = 0$  at the channel edge and  $U_0$  is the free stream velocity and  $\beta$  is given by  $(8D\nu_t/f)$ , See Figure 3.22. Assuming the normal definition of the shear layer width, ie the edge of the shear layer is a where  $U = 0.99U_0$ , Samuels derived an expression for the shear layer width:

$$\delta = 5.7 (D / g S_{xf} f)^{0.25} v_t^{0.5} \quad (3.32)$$

He applied this equation with typical values for British rivers and showed that the shear layers can affect the whole width of the main channel. Samuels (1985, 1989) considers some theoretical aspects of depth averaged models. He shows that since the local 3-D velocity vectors ( $u$ ) are continuous across a discontinuity in depth in a channel cross-section then the unit flow vector  $q$  must also be continuous across this step, because of the integral relationship:  $q = \int u \, dz$ . Since  $U = q/D$  then a step discontinuity in depth results in a step discontinuity in depth averaged velocity. It follows that solutions based on the assumption that depth averaged velocity is continuous must be treated with caution where vertical channel banks exist.

Another analytic solution has been derived by Shiono and Knight (1988). They consider the equation:

$$g D S_{xf} - \frac{BfU^2}{8} + \frac{\partial}{\partial y} \left[ v_t D \frac{\partial U}{\partial y} \right] = 0 \quad (3.33)$$

Where the B factor is related to the side slope of the domain by:

$$B = (1 + s_y)^{0.5} \quad (3.34)$$

This is a simplification of the factors derived in section 2.2.4. They use the non-dimensional eddy viscosity given by equation 3.29 to model the lateral shear stresses. They consider the case in which depth varies linearly and assume that  $f$  and  $\lambda$  are constants. They show that when the depth is constant the velocity distribution is given by:

$$U = [ A_1 e^{\gamma y} + A_2 e^{-\gamma y} + 8 g S_{xf} / f ]^{1/2} \quad (3.35)$$

and when the depth varies linearly:

$$U = [ A_3 Y^{\alpha_1} + A_3 Y^{-\alpha_2} + \omega Y ]^{1/2} \quad (3.36)$$

Where

$$\gamma = ( (2/\lambda)^{0.5} (f/8)^{0.25} ) / D$$

$$\alpha_1 = (-0.5 + 0.5 ( 1 + (s_y/\lambda (1+s_y^2)^{0.5}) (8f)^{0.5} )^{0.5}$$

$$\alpha_2 = (0.5 + 0.5 ( 1 + (s_y/\lambda (1+s_y^2)^{0.5}) (8f)^{0.5} )^{0.5}$$

$$\omega = g S_{xf} / ( (1+s_y^2)^{0.5} / (8s_y/f) - \lambda/s_y^2 (f/8)^{0.5} )$$

and Y is the local depth which varies linearly with y.

The solutions are applied to each section of the channel and the boundary conditions allow the constants A to be evaluated in each case. For example in the case of an infinitely wide rectangular channel A1 and A2 become 0 and -U<sub>0</sub> respectively and the solution reduces to:

$$U = U_0 [ 1 - e^{-\gamma y} ]^{1/2} \quad (3.37)$$

Applying the shear layer assumptions it is possible to derive an expression for the width of the shear layer:

$$\delta = 4.658 D f^{0.25} \lambda^{0.5} \quad (3.38)$$

comparing this equation with equation 3.32, derived from Samuels analytic solution :

$$\delta = 5.7 (D / g S_{xf} f)^{0.25} v_t^{0.5} \quad (3.32)$$

We see that the shear layer width in both expressions is related to the square root of the viscosity parameter and  $f^{0.25}$ . The use of the non-dimesionalized viscosity gives a shear layer width which is a linear function of channel depth. Rajaratnum and Ahmadi (1979) also found that the shear layers in a rectangular compound channel are related to channel depth. This tends to confirm that the non-dimensional eddy viscosity approach, which relates viscosity to depth and bed shear stress is a reasonable approximation. Applying equation 3.37 to Rajaratnum and Ahmadi's

geometry and equating the shear layer width to equation 3.15 gives values of  $\lambda$  ranging from 0.13 to 0.17.

In a later paper Shiono and Knight (1991) present further analysis of  $\lambda$  values from the FCF data. They derived values in two ways, firstly they derived values from the measured distributions of bed shear stress and depth averaged velocity and secondly from the measured Reynolds stresses. In both cases they found that the  $\lambda$  values varied strongly across the compound section. Figure 3.23 shows two typical distributions derived by either method. They show that in both cases the  $\lambda$  values are approximately constant in the main channel and on the floodplain. The floodplain values appear to vary with relative depth. Shiono and Knight give an overall value of 0.5 for the main channel and a value of 0.07 derived from the Reynolds stresses. They explain this difference by stating that the overall value includes the effects of secondary flow. They plot distributions of the depth averaged convection terms:  $\rho U V$  and  $\rho U V D$ , Figure 3.23. These distributions were derived from the measured bed shear stress and Reynolds stress distributions and not directly from the measured velocity profiles. Shiono and Knight say this is because they could not orient the LDA probe sufficiently accurately to resolve the  $V$  component. This must call into question the accuracy of their secondary circulation measurements. It is likely that they have measured the position and general direction of the secondary circulation cells but may not have accurate measurements of the strength of the cells. On the basis of these results they conclude that the secondary currents have an important effect on the depth averaged velocity profile. They carried out this analysis only for the cases with a smooth main channel and floodplain and so these conclusions may not be valid for more typical cases with roughened floodplains. They approximate the secondary current convection terms with constant values in the main channel and floodplain regions. The extended equation is:

$$g D S_{xf} - \frac{BfU^2}{8} + \frac{\partial}{\partial y} \left[ v_t D \frac{\partial U}{\partial y} \right] = \Gamma \quad (3.39)$$

where

$$\Gamma = \frac{\partial (\rho U V D)}{\partial y} \quad (3.40)$$

For the SERC FCF Shiono and Knight give values of  $\lambda$  and  $\Gamma$  for four zones: 1) the main channel, 2) the main channel side slope, 3) the floodplain and 4) the floodplain side slope.

zone	$\lambda$	$\Gamma$
1	0.07	0.15
2	0.16	0.00
3	$\lambda_1(2(H-h/H))^4$	-0.25
4	0.16	0.00

Knight, Shiono and Pirt (1989) apply this analytic solution to field data measured on the river Severn at Montford. They split the channel into seven zones, Figure 3.25, and assumed that the secondary current term  $\Gamma$  is small. They calibrated values of  $\lambda$  for each of the seven zones from measured flow profiles:

zone	1	2	3	4	5	6	7
$\lambda$	0.2	3.0	0.2	0.07	0.2	3.0	0.2

They obtained very good correlation between both measured and calculated velocity profiles, Figures 3.26.

Wormleaton (1988) solved equation 3.28 and postulated that the lateral eddy viscosity is given by a sum of bed generated and lateral shear turbulence. He used equation 3.28 with a  $\lambda$  value of 0.16 and assumed that the component of viscosity due to lateral shear is related to the product of a velocity and length scale for the shear layer. He applied this assumption to the SERC FCF data and derived the relationship:

$$v_t = \lambda_s l_s U_s \quad (3.41)$$

He quotes an optimum value of  $\lambda_s$  for the SERC FCF of 0.013. He obtained reasonably good comparisons between computed and measured velocity profiles in one of the SERC FCF geometries.

Keller and Rodi (1989) applied a depth averaged k- $\epsilon$  turbulence model to approximate the lateral shear stresses. They used equation 3.28 with a non-dimensional eddy viscosity of 0.15 to initialise the k- $\epsilon$  model. They applied their model to a selection of small scale laboratory data available in the literature and found that the final solution is sensitive to the  $\lambda$  value used to initialise the model. Figure 3.27 shows some of their results and confirms that reasonable agreement can be obtained.

McKeogh, Kiely and Javan (1990) measured turbulence quantities in a small scale laboratory channel and analyzed this data to provide values of the eddy viscosity. They found that the lateral viscosities vary from main channel to floodplain and with flow depth.

### **3.3 Summary of flow mechanisms in straight compound channels**

There is no doubt that flows in compound channels are affected by complex interactions between main channel and floodplain regions. These interactions reduce the overall discharges and velocities in the main channel and increase them on the floodplain.

The interactions are driven by the velocity differential and non-uniform shear stress distributions which exist across the main channel / floodplain boundary. The most obvious mechanisms are:

- 1) Lateral shear stresses induced by the co-flowing velocity gradients.
- 2) The transfer of mass and momentum between main channel and floodplain is also accomplished by two types of secondary circulation:

a) Vortices which have vertical axes and rotate in plan occur over the main channel floodplain boundary. These vortices move with the general flow and appear intermittent to the stationary observer.

b) Secondary circulation cells which have been observed within the flow cross section. At least three cells exist within each shear layer, two within the main channel and one on the floodplain.

The relative strengths of these circulations, and hence their effect on the overall flow, is known to increase as the main channel side slopes become steeper and be reduced by rough floodplains. The relative strengths of both types of circulation have also been shown to be complex functions of both floodplain and main channel flow depths.

The presence of these secondary circulations affects the distributions of both longitudinal velocity and bed shear stress. In the core regions, away from the bank zone, the vertical distribution of velocity follows the logarithmic profile and the Reynolds stresses are linear. The velocities and bed shear stresses are functions only of local depth and bed roughness and are not affected by the interaction between main channel and floodplain. In the case of relatively narrow main channel or floodplains the interaction or shear zones may cover the whole width of the cross-section.

Within the shear layers the velocity profiles are affected. In the main channel the profile is approximately logarithmic up to some level where the velocities reduce to values roughly equivalent to those on the floodplain. The level at which velocity reduces varies with the position from the channel bank. Close to the bank the level is approximately bankfull and increases as one moves away from the bank. On the floodplain velocities are greater than the logarithmic values through the whole water column.

Bed shear stresses in the main channel shear layer are increased compared to non

compound channel distributions and are distributed differently across the channel bed. On the floodplain the combination of high velocities, low depth and secondary currents induce high bed stresses on the floodplain at the main channel edge. The bed shear stresses rapidly reduce from this peak as one moves away from the channel edge, Figure 3.17.

A theoretical analysis of shear layer widths, based on eddy viscosity concepts, shows that they are proportional to flow depth and fluid viscosity and inversely proportional to bed friction factors. This behaviour has been observed in the laboratory and we can conclude that the eddy viscosity approach is reasonable in modelling the effects of the interaction between main channel and floodplain flows.

It has been demonstrated that the effects of the interaction mechanisms on the gross discharges in the main channel, floodplains and the whole channel are complex functions of:

- 1) channel and floodplain geometry, eg widths, depths, side slopes.
- 2) channel and floodplain bed roughness.
- 3) channel and floodplain depths.
- 4) the velocity difference across the shear layers, this is often related to the difference between the mean velocities in the main channel and floodplain zones.

The strength of the interaction varies strongly with depth. At large floodplain depths, where  $h$  is small compared to the main channel depth of flow. The interaction weakens and the channel begins to behave like a simple channel, ie the coherence of the channel approaches unity.

#### **3.4 Methods for conveyance estimation available in the literature**

In the previous section we have reviewed research work carried out on compound channels. Some of this work has produced specific methods for calculating

discharges in compound channels. It is useful to summarise these methods and to introduce other methods which, though not specifically developed for application to compound channels, are commonly applied in practise.

### **Divided channel methods**

Divided channel methods are often used to calculate discharges in compound channels. The cross-section is divided into main channel and floodplain sections and the classic single channel methods are applied to each section in turn. The simplest division is shown in Figure 3.29, a vertical division line is used to separate main channel and floodplain and this division is not included in any of the wetted perimeters. Various authors have suggested using inclined division lines, Figure 3.29, they argue that a division line should be chosen such that the apparent shear stresses are zero on them. Ramsbottom (1988) investigated the behaviour of various divided channel methods against field data. He found that the best results were obtained using vertical divisions and including the vertical divisions in the wetted perimeter of the main channel but not the floodplains, Figure 3.29.

### **Single channel methods**

Various authors have proposed that the best method of accounting for a variation in velocity and bed roughness across a channel is to derive a weighted mean roughness parameter. Most of these methods are expressed in terms of Manning's  $n$  values. The following methods were identified by HR Wallingford (1988).

*In all the following cases, the channel section is divided into  $N$  parts. The hydraulic radius, wetted perimeter and Manning's roughness coefficient of an arbitrary section  $i$  are  $R_i$ ,  $P_i$  and  $n_i$ , respectively and unsubscripted values apply to the whole section.*

#### **Horton, 1933**

Horton assumed that each part of the cross-section has the same mean velocity, which

at the same time is equal to the mean velocity of the whole section. On the basis of this assumption, the equivalent coefficient of roughness may be obtained by the following equation,

$$n = ( \sum_1^N P_i (n_i^{3/2}) )^{2/3} / P^{2/3} \quad (3.42)$$

The validity of the assumption which allows the derivation of this equation must be questioned. The velocity and thus the mean velocity are functions of roughness and depth, and so the mean velocity of parts with different roughnesses and depths must be different.

### **Lotter, 1933**

By assuming that the total discharge is equal to the sum of the discharges in all the sub-sections, Lotter derived the following equation for the equivalent roughness coefficient,

$$n = P R^{5/3} / \sum_1^N ((P_i R_i^{5/3}) / n_i) \quad (3.43)$$

In deriving this equation it is assumed that the bottom shear stress is constant along the wetted perimeter. It is well known that the shear stress acting on the sloping sides of the channel is less than the shear stress acting on the bed, Chow (1956).

### **Einstein and Banks, 1950**

By assuming that the total force resisting the flow is equal to the sum of the forces resisting the flow developed in the individual areas, a formula for the equivalent roughness coefficient can be derived which is,

$$n = ( \sum_1^N (P_i n_i^2) )^{1/2} / P^{1/2} \quad (3.44)$$

As with the method proposed by Lotter it has been explicitly assumed in deriving this

formula that, in the channel with the constant equivalent roughness coefficient, the bottom shear stress is constant along the wetted perimeter. One more assumption made is that the hydraulic radius of each sub-divided section is equal to the hydraulic radius of the whole section; this need not be the case.

Einstein and Banks tested the above theory by carrying out a series of laboratory experiments. They used a 17ft flume, 12 inches wide and 18 inches deep with sides of painted sheet metal. The bed of the flume comprised concrete blocks into which pegs could be inserted. A series of experiments were carried out with the concrete blocks vertically offset relative to each other and with and without the pegs inserted. By measuring the water surface profile the total resistance was computed. The resistance due to each of the components of the bed was also calculated. It was found that the total resistance exerted by combined types of roughness is equal to the sum of the resistance forces exerted by each type individually.

### **Krishnamurthy and Christensen, 1972**

Krishnamurthy and Christensen derived a method for calculating the equivalent roughness of a composite channel by making the following assumptions:

- (a) the whole cross-section is assumed to be shallow. The section is divided into smaller vertical sub-sections.
- (b) the hydraulic radius,  $R_i$ , of each sub-section can be approximated by the vertical depth,  $d_i$ .
- (c) the vertical velocity distribution in each sub-section follows a logarithmic law.

The formula developed by Krishnamurthy and Christensen is,

$$\ln n = ( \sum_1^N P_i d_i^{3/2} \ln n_i ) / ( \sum_1^N P_i d_i^{3/2} ) \quad (3.45)$$

This formula is not applicable to rectangular channels because it does not take account of side wall effects. However, if the channel is wide and the influence of the side walls is negligible the method of Krishnamurthy and Christensen can be used. Under these conditions the above equation can be modified to give,

$$\ln n = ( \sum_1^N P_i \ln n_i ) / P \quad (3.46)$$

In order to verify their method Krishnamurthy and Christensen used data from the Lower Mississippi river. They showed that for this data their method gave closer agreement with the measured roughness coefficient than the methods of Horton, Lotter or Einstein and Banks.

### **Apparent shear stress methods**

Various authors, eg Baird and Ervine (1982), Knight et al (1983) and Wormleaton and Merrett (1990), have suggested taking account of the interaction mechanisms by including the apparent shear stress on division lines which split the compound channel into main channel and floodplain regions. The division lines are usually taken to be vertical for simplicity's sake. Each of the authors have derived equations which relate apparent shear stress to both geometric and flow variables. The main limitation to these approaches is that these empirical equations are based on limited experiments covering only a small range of conditions. Bearing this in mind the apparent shear stress approaches will not be considered further.

### **Adjustment factor methods**

Various authors have suggested that discharge in compound channels should be calculated using a basic divided channel approach. This basic discharge is then adjusted to take account of the interaction. Baird and Ervine, (1982), Wormleaton and Merrett (1990) and Radojvic (1985) argue that adjustment factors for main channel and floodplain flows are related to the apparent shear stresses and present equations which can be used to calculate adjustment factors from the apparent shear

stresses. These approaches suffer from much the same limitations as the apparent shear stress *methods*.

Ackers (1991, 1993) took a slightly different approach in deriving adjustment factors to a basic discharge calculated assuming no interaction. He used the largest and best data set available (SERC FCF Phase A) to derive the relationships between the adjustment factors and basic geometrical and flow variables.

### **Lateral distribution methods**

Other authors, (eg. Shiono and Knight (1989), Samuels (1985), Wormleaton (1989), Keller and Rodi (1985)) have considered methods based on the shallow water equations. For the case of a straight channel these two dimensional equations reduce to a single one dimensional equation which describes the lateral variation of depth averaged velocity and discharge across a channel. There are three important terms in this equation:

- 1) Bed friction
- 2) Weight of fluid acting in the longitudinal direction and
- 3) Lateral shear stresses.

In addition Shiono and Knight also include a convection term which describes the effect of secondary currents on the distribution of depth averaged velocity. The arguments that the effects of secondary currents should be considered separately from the lateral shear term are not conclusive. Good results have been reported against both laboratory and field data taking account of only bed friction and lateral shear. In these cases the calibrated values of viscosity or non-dimensional viscosity will include the effects of secondary currents. The main problem in applying a lateral distribution method is in choosing an appropriate method of determining the lateral viscosity. Various approaches have been tried or suggested.

### 3.5 A new approach to the lateral distribution equation

The various authors who have considered this approach to conveyance estimation in compound channels have based their calculations on a version of the equation expressed in terms of the depth averaged velocity. The solutions are then produced, either analytically or numerically, assuming that the distribution of depth averaged velocity is continuous. Samuels (1989) has shown that when discontinuities exist in the channel depth, such as at a vertical channel bank, then this assumption is not valid and in fact the depth averaged velocity must also be discontinuous. However the distribution of unit flow must be continuous whatever the shape of the channel bed. A solution based on unit flow rather than depth averaged velocity is a more rational alternative since the assumption that the distribution of  $q$  is smooth and continuous is true in a wider range of circumstances. This is the main reason that the shallow water equations derived in Chapter 2 are expressed in terms of the unit flows rather than depth averaged velocity.

Considering the case of a straight channel with the  $x$ -axis aligned along the channel centreline and that flow is uniform and steady ie  $\partial/\partial x = 0$  and  $\partial/\partial t = 0$  and that the effects of secondary currents can be lumped in to the lateral shear term the  $y$  momentum equation disappears and the  $x$  momentum equation reduces to:

$$g D S_{xf} - \frac{Bfq^2}{8D^2} + \frac{\partial}{\partial y} \left[ v_t \frac{\partial q}{\partial y} \right] = 0 \quad (3.47)$$

where  $q$  is the longitudinal unit flow related to depth averaged velocity by  $q = UD$ . Equation 3.47 is very similar to the form of equation solved by Shiono and Knight :

$$g D S_{xf} - \frac{BfU^2}{8} + \frac{\partial}{\partial y} \left[ v_t D \frac{\partial U}{\partial y} \right] = 0 \quad (3.33)$$

The first two terms are numerically equivalent and any differences between the two solutions must be due to the third (lateral shear term). These two equations have been solved numerically using the same numerical technique described below.

A numerical technique was chosen for two reasons:

- 1) It is easier to apply a numerical solution rather than an analytic solution to a channel with an irregular depth distribution.
- 2) Analytic solutions are available only for particular viscosity models and the use of a numerical model allowed various viscosity models to be evaluated.

For convenience the solution of equation 3.47 is referred to as LDM or LDM1 and solution of equation 3.33 is referred to as LDM2.

Finite differences were chosen as the solution technique along with Newtons' method to linearize the resulting set of nonlinear algebraic equations. The application of finite differences and Newtons method to equations 3.46 and 3.32 is quite straightforward. Any standard text book on numerical methods or numerical analysis provides the details of these techniques, eg Smith (1986) or Conte and De Boor (1981), and the following section only covers the general principles.

In finite differences the flow domain is split into a number of nodes and the various variables are expressed in terms of their values at these nodes. The variables are assumed to vary linearly between nodes. The differential terms:

$\partial F/\partial y$  can then be approximated by:  $\delta F/\delta y$ , where  $\delta F$  is the difference between  $F$  values at near by node points and  $\delta y$  is the grid spacing. Various common methods exist for evaluating the  $\delta f$  terms:

#### **Forward differences**

$$\partial F/\partial y = (F_{i+1} - F_i) / \delta y \quad (3.48)$$

#### **Backward differences**

$$\partial F/\partial y = (F_i - F_{i-1}) / \delta y \quad (3.49)$$

## Central differences

$$\partial F / \partial y = (F_{i+1} - F_{i-1}) / 2\delta y \quad (3.50)$$

Often certain terms in an equation are evaluated at mid-node points and central differences are used to define gradients, such a staggered grid approach was followed when discretizing the lateral shear terms in equation 3.46 and 3.32.

For a domain with N nodes the finite difference technique results in a set of N algebraic equations in terms of the solution vector  $F_i$ . Application of the boundary conditions at nodes  $i=1$  and  $i=N$  results in a set of N-2 equations in N-2 unknowns. The appropriate boundary condition for equation 3.46 and 3.32 is that  $q = U = 0$  at the no-flow boundaries. In matrix notation the resulting set of simultaneous equations are written:

$$[A_{ij}(F_i)] F_j = 0 \quad (3.51)$$

Where the equation is nonlinear the values of the matrix coefficients  $A_{ij}$  depend on the solution vector  $F_j$ . Newton's method is used to linearize these equations as follows, introducing the concept of iteration :

$$F_j^{i+1} = F_j^i + \epsilon_j^i \quad (3.52)$$

Where  $F^i$  is the value of the solution vector at the  $i$ th iteration then the solution is obtained starting from an initial estimate for the solution vector. At each iteration a correction vector ( $\epsilon$ ) is calculated and applied to the existing solution to obtain a new estimate. Newton's method converts equation 3.51 into a set of linear equations for the correction vector by applying a first order expansion in terms of the solution vector. The resulting set of linear equations is :

$$[\partial A_{ij} / \partial F_i] \epsilon_j = -r_j \quad (3.52)$$

Where  $r_j$  is the residual vector.

The solution is progressed from one iteration to the next until the changes in the solution between successive iterations are smaller than some predetermined limit. Various convergence criteria were tried with equations 3.47 and 3.33. The criterion finally adopted was based on the total integrated discharge in the channel, rather than the individual nodal values of  $q$  or  $U$ . Convergence was assumed to have occurred when:

$$\frac{2(Q^i - Q^{i-1})}{(Q^i + Q^{i-1})} \leq 0.1\% \quad (3.54)$$

The following chapter details the work carried out in applying this method to both laboratory and field data.

### 3.6 Conclusions

- 1) A literature search on the behaviour of flows in straight compound channels has been carried out.
- 2) The conveyance capacity of straight compound channels is reduced by complex interactions between the main channel and floodplain flows.
- 3) The main mechanisms which affect the conveyance capacity have been identified as follows:
  - a) The velocity differential between main channel and floodplain flows induces a lateral shear layer between these two regions.
  - b) Secondary circulations, both in plan and within the cross-section, carry fast moving fluid from the main channel to the flood plain and vice-versa. The relative strength of these secondary currents is reduced when the floodplain is rough and when the main channel side slope is slack.

- c) The secondary circulations and lateral shear effects cause the boundary shear stresses to be redistributed around the channel cross-section, with increased values at the edge of the floodplain close to the main channel.
- 4) These mechanisms combine to reduce the discharge in the main channel and increase it on the floodplains.
  - 5) The secondary currents also affect the distribution of longitudinal velocity, particularly in the main channel.
  - 6) The interaction mechanisms are found to affect zones of the main channel and floodplain adjacent to the channel bank. In the case of narrow channels or floodplains these shear layers may extend across the whole channel or floodplain.
  - 7) The width of the shear layers is proportional to the flow depth and turbulent viscosity and is inversely proportional to the bed friction factor.
  - 8) The strength of the interaction is dependent on :  
Main channel / floodplain widths, depths and side slopes  
Main channel / floodplain bed roughness  
The velocity differential across the shear layer
  - 9) Various methods of calculating discharge or conveyance in a straight compound channel have been identified.
  - 10) The lateral distribution method appeared to be the most promising method for application to a wide range of channels and an improved formulation of the LDM equation has been derived.
  - 11) Various models for the lateral eddy viscosity have been identified in the literature.

- 12) The non-dimensional eddy viscosity relates the value of viscosity to bed roughness, flow depth and local flow or velocity. The use of this model can approximate the variation of the interaction effects in a compound channel.
- 13) More work should be carried out to identify appropriate values of viscosity for the evaluation of discharge distributions in compound channels.

## **CHAPTER 4**

### **DISCHARGE ESTIMATION IN STRAIGHT COMPOUND CHANNELS**

#### **4.1 Introduction**

The previous chapter reviewed experimental and theoretical modelling of straight compound channel flows. The important mechanisms, which affect the discharge capacity of compound channels, were distinguished and various procedures which account for these mechanisms were identified. The lateral distribution method (LDM) was found to be very promising and an improved formulation of the equation was derived. The purpose of the material presented in this chapter is to investigate the behaviour of the LDM against the available laboratory and field data from compound channels.

#### **4.2 Summary of data**

Before progressing to an investigation of various aspects of the LDM it is worthwhile to summarize both the laboratory and field data which was available to the author.

##### **4.2.1 Laboratory data**

###### **SERC FCF Phase A**

Data collected during Phase A of the flood channel facility (FCF) test programme was made available to the author by HR Wallingford. This wide range of tests covered a large number of conditions including floodplains of different widths, roughened floodplains and a selection of main channel shapes. The tests were carried out in a large scale flume 50m long by 10m wide by 0.4m deep. Figures 4.1 and 4.2 show the plan lay out of the facility and the compound channel cross-sections constructed.

The full range of tests is detailed in Table 4.1, with the various variables defined in Figure 4.2a. The data available to the author consisted of stage-discharge

measurements for all eleven test series and a small number of velocity profiles for series 2 and 3. The full range of data includes velocity, bed shear stress and turbulence measurements for most of the test conditions.

The experimental program covers relative depths (floodplain depth/bankfull depth) up to 1.0 and relative widths (floodplain widths/main channel width) between 1.0 and 4.6. The main channel cross-sections were trapezoidal with most tests having side slopes of 1.1. Some tests were carried out in rectangular channels, (series 08 and 09) and two with side slopes of 1.2, (10, 11).

### **Bed friction**

Ackers (1991) investigated the behaviour of various relationships used to describe bed friction for the SERC FCF. He concluded that the trowelled mortar surface of the FCF is hydraulically smooth. He derived a modified smooth law from the inbank stage discharge data:

$$f^{1/2} = 2.02 \text{Log}_{10} (\text{Re} f - 1.38)^{1/2} \quad (4.1)$$

This relationship was used to calculate the bed friction term for the smooth tests, where Re is the Reynolds number. Four series of experiments were carried out with roughened floodplains. This roughening was achieved using a regular grid of vertical rods extending through the full water depth. Under these conditions the resistance to flow is composed of the drag of the rods and the bed shear force. Ackers (1991) provided a method of calculating the resulting overall friction factor and this was used to obtain the f value for the roughened floodplains. The method is complex and Appendix 7 provides a summary of its application. The stage-discharge data collected during Phase A of the FCF work are listed in Appendix 3.

### **Myers' laboratory data**

Myers (1990) published details of a combined laboratory and field investigation of

flow in a section of the River Main in Northern Ireland. Both the field and laboratory data was provided to the Author by Dr Myers, whose help is greatly appreciated and gratefully acknowledged. The field data collected on the River Main is considered below and this section is limited to considering only the two sets of laboratory data which Dr Myers provided.

An 800m long reach of the Main was studied in the field. A 1:20 undistorted scale model of the downstream 250m of this reach was constructed and used to investigate the effects of various parameters. The model was set to a longitudinal slope of  $1.906 \times 10^{-3}$ , which matches the observed hydraulic slopes over this part of the reach. The study investigated the effects of roughening the floodplains and removing a floodplain to give an asymmetric cross-section. Only the cases with smooth main channel and floodplain beds, constructed out of perspex, are considered here. Series A is the symmetric channel case and Series F the asymmetric channel case. The inbank stage discharges allowed the quoted Manning's n values to be checked and a value of 0.01 was used for all the work reported here. Figure 4.3 shows the two channel cross-section cases. Stage-discharges and velocity distributions were measured. Details of the experiments and the measured stage-discharges are given in Appendix 4.

### **Kiely's laboratory data**

Kiely (1990) carried out a laboratory investigation into flows in straight and meandering compound channels. His flume was built out of perspex and was 14.4m long by 1.2m wide. The rectangular main channel was 200mm wide by 50mm deep. He presented measured depth averaged velocity profiles at four separate flow depths. The flume was hydraulically smooth and a modified smooth law was used to describe the bed friction terms. As there are only four points on the stage-discharge curve this data has not been used in any of the comparisons with the various discharge estimation methods.

### **Lambert's laboratory data**

Lambert (1992) has carried out a laboratory investigation of flows in straight compound channels. His symmetric compound channels had rectangular main channels, 0.4m wide and were constructed in a flume 1.934m wide. He carried out six experiments with bankfull depths of 0.015m, 0.0827m and 0.0977m and two longitudinal slopes ( $9.4 \times 10^{-4}$  and 0.012). In some tests he roughened the floodplains by gluing gravel to the flume surface, the  $k_s$  value was found to vary with slope and  $k_s$  was taken as 18.43mm and 13.09mm for the mild and steep cases respectively. The smooth cases are modelled with modified smooth laws. The details of the experiments and the measured stage discharges are given in Appendix 4. Figure 4.4 shows the <sup>three</sup> channel cross-sections and six measured stage-discharge curves.

#### 4.2.2 Field data

Gauging data consisting of stage discharge measurements, and in some cases velocity profiles, were available for a number of overbank sites on British rivers. These were identified by Ramsbottom (1989) from a selection of river gauging sites used by the National Rivers Authority for England and Wales (NRA). The best sites were selected from this collection and are used here to evaluate the lateral distribution method. Table 4.2 lists the sites and the types of data available while Tables 4.3 and 4.4 give geometric information. Figures 4.5 to 4.8 show the cross-sections for these sites. The natural channel cross-sections are more variable in shape than the laboratory channels, ranging in total width from less than 30m to over 180m and in depth from about 1m to nearly 6m. The ranges of relative depths and widths are similar to those chosen for the SERC FCF Phase A work. Data from the nine sites listed in Table 4.2 are used here. Stage discharges from seven of the sites were used in evaluating the LDM against other methods. The measurements from the River Penk were omitted from this comparison because there were some doubts about the consistency of these data sets. However the velocity profiles from this site have been used.

The River Main data resulted from an experimental programme carried out on a section of the Main which had been reconstructed to form a compound channel. The

channel was regraded as part of a flood alleviation scheme which was subject to a variety of drainage and environmental constraints. Water levels were measured at sections along the study reach and flow gaugings obtained by propeller meter for inbank and overbank conditions.

At the study reach the main channel was designed to have a width of 12m and depth of 0.9m. The berms are 7.5m wide and slope towards the channel with a lateral gradient of 1 in 25. They are usually covered with heavy weed growth and the channel banks were sown with long grass. Section 14 is situated at a gentle bend in the river which causes a noticeable redistribution of the measured velocities, however the effects are not large and this study provides some of the best field data available for overbank flow in British rivers.

### **Roughness values**

Unlike the experimental data discussed previously, the bed friction values for the river sites are not known accurately and must be estimated on the basis of either published guidelines or measurements. In general the floodplains of a compound channel are significantly rougher than the main channel and separate roughness values must be used. The roughness is characterised by Mannings 'n' here since this is most familiar to river engineers.

The assessment of Mannings 'n' is difficult and subjective. Its value was calculated for several inbank stages using values of stage and discharge from the rating curve. It was therefore possible to observe the variation of 'n' with stage. Generally 'n' decreases with stage and this was evident for four of the seven sites. 'n' remained approximately constant for one site and rose with stage for the Blackwater at Ower and Tees at Low Moor. The station at Ower is a crump weir site and Low Moor is just upstream of a low flow weir. Plots of the variation of 'n' with stage are shown in Figures 4.9 and 4.10

It was decided to use the bankfull value of Mannings 'n' ( $n_b$ ) as the roughness

parameter for the main channel when assessing overbank flow, as it is relatively easy to obtain and represents a fixed point on 'n' against stage curve. Values of  $n_b$  are shown in Table 4.5 for the nine sites. The slope is the average longitudinal bed slope evaluated from ordnance survey maps of the sites. In the case of the River Main, in Northern Ireland, the slope quoted is the average water surface slope observed over a wide range of conditions, Myers (1990) and Higginson et al (1990).

The estimation of floodplain roughness ( $n_f$ ) is difficult because of the mixture of roughness components which may occur. These include walls, fences, hedges, tracks, trees, bushes, other vegetation, buildings etc. Floodplains may also change in section and character in the direction of flow. The values used in this study are listed in Table 5. Where ~~ver~~ possible these values are based on velocity gauging data which allowed the proportion of flow on the floodplain to be estimated. In the other cases the guidelines given in Chow (1956) and by Sellin (1991) were followed.

Chow gives typical 'n' values for grassed channels of between 0.03 and 0.05 where the grass is short, rising to 0.04 to 0.10 as the growth gets longer or denser. Sellin et al (1990) investigated the effects of various vegetation management techniques on the discharge capacity of a man made compound channel. He recommends 'n' values of between 0.04 to 0.06 for grassed floodplains which are cut annually and higher values of 0.06-0.08 if the maintenance is less regular, or the flow occurs in the summer season before the annual cut. Following these guidelines, values of 0.04 or 0.06 were assigned to the sites where it was impossible to estimate the values from the available flow data. In general, for the sites used, the predicted discharges are much more sensitive to the main channel roughness since the floodplains carry a comparatively small portion of the total discharge.

### 4.3 Comparison between analytic and numerical solutions for the LDM

The Lateral distribution method (LDM) developed in chapter 3 is based on the equation:

$$g D S_{xf} - \frac{Bfq^2}{8D^2} + \frac{\partial}{\partial y} \left[ v_t \frac{\partial q}{\partial y} \right] = 0 \quad (4.2)$$

Other authors, eg. Shiono and Knight (1988) and Samuels (1988) have solved equation 4.3.

$$g D S_{xf} - \frac{BfU^2}{8} + \frac{\partial}{\partial y} \left[ v_t D \frac{\partial U}{\partial y} \right] = 0 \quad (4.3)$$

These equations and the differences between them are discussed in Section 3.5. Both equations have been solved using the same finite difference scheme with Newton's method to linearize the resulting algebraic equations, . The solutions to 4.2 and 4.3 are referred to as the LDM and LDM2 respectively.

Some preliminary work with these equations showed that the non-dimensional form of the eddy viscosity (4.4), which was used by Shiono and Knight (1988) was the most promising and it was decided that this relationship for the lateral eddy viscosity would be used in all further work.

$$v_t = \lambda U_* D \quad (4.4)$$

As a check on the accuracy of the numerical solutions to 4.2 and 4.3 two test cases were considered and compared with the analytic solutions provided by Shiono and Knight (1988).

The first case was a rectangular channel, depth 2m with the bed roughness calculated using the rough turbulent law with a  $k_s$  value of 0.1m. Solutions for a range of  $\lambda$  or (NEV) values were considered. Figure 4.11 shows a typical set of results for an NEV value of 0.75. The top figure compares the analytic solution to equation 4.3 and the numerical solution to 4.2 and shows that the two solutions are identical. This

Where the gradient of  $v \ll \frac{\partial D}{\partial y}$  is zero then the two equations give identical results. Where  $v \ll \frac{\partial D}{\partial y}$  is positive then the LDM will give larger values of velocity, and where  $v \ll \frac{\partial D}{\partial y}$  is negative then the LDM model gives smaller values of velocity than the LDM2 model. This can be seen in Figure 4.12.

is not surprising since in the case of constant depth it is possible to show that 4.3 and 4.2 are logically equivalent. The lower figure shows the comparison between the numerical and analytic solutions to equation 4.3, again these solutions are identical and this confirms that the numerical scheme used to obtain the solution is accurate.

The second case was similar to the first except that the flow depth in the channel varied linearly between 2m at the left hand side to 1m at the right hand side. Figure 4.12 shows that the numerical and analytic solutions to equation 4.3 are identical. However there are slight differences between the solution to 4.2 and 4.3. The LDM gives larger velocities on the deeper side of the channel and smaller velocities on the shallow side of the channel. The reason for this difference is related to the lateral shear terms in 4.2 and 4.3. This is demonstrated by replacing  $q$  with  $UD$  in 4.2 and expanding the differential to obtain:

$$\frac{\partial}{\partial y} \left[ v_t \frac{\partial q}{\partial y} \right] = \frac{\partial}{\partial y} \left[ v_t D \frac{\partial U}{\partial y} + v_t U \frac{\partial D}{\partial y} \right] \quad (4.5)$$

It is apparent that in the case of uniform depth ( $\partial D/\partial y = 0$ ) and the two equations (4.2 and 4.3) are identical. |



#### 4.4 Application of LDM to SERC FCF Phase A data

As mentioned above Ackers (1991) used the large amount of calibration data collected on the FCF to derive definitive relationships for this flume. Hence the bed friction terms for the FCF Phase A data were not subject to calibration and this data set provided the opportunity to investigate the effect of variations in NEV on the flows predicted using the LDM.

The analysis fell into three main parts

- a) The calculation of optimum NEV values for each observation and averaging

these values for each test series

- b) Discharge estimation using fixed values of NEV
- c) Comparison of LDM with other methods of discharge estimation

#### 4.4.1 Investigation of NEV values

A preliminary application of the LDM to the SERC FCF data was to calculate stage - discharges for a range of fixed  $\lambda$  or NEV values. The results are shown in Figures 4.13 to 4.15. These results are encouraging in that the general trend of the stage-discharge curves are predicted well. For an individual case it is apparent that the optimum value of NEV varies with stage. Comparing results from one series to another it is also likely that channel conditions such as aspect ratio and relative roughness will affect the optimum values of NEV. Thus in general it is likely that the optimum NEV values for any channel will vary both with cross-section shape and stage. This provided the motivation for the work described below.

In order to obtain optimum values of NEV for each observed stage-discharge, the LDM was applied iteratively giving an updated estimate of NEV at each iteration. The optimum value, NEVC, was judged to have been found when the observed and predicted flows differed by less than 0.1%.

NEVC was found to vary strongly with both channel shape and stage. Table 4.6 gives the mean values and standard deviations for NEVC, averaged over each series. The differences in the means from series to series show the effect of shape and roughness condition. The large values of the standard deviations is not due to random scatter but systematic variation of NEVC with stage. Figure 4.16 shows the change in NEVC with stage for the smooth tests. The distributions are roughly 's' shaped: at low stages the values of NEVC tend to increase; at intermediate stages they reduce and at higher stages they tend to become constant or start to increase slowly. The curves are systematically displaced to the <sup>top</sup> as the floodplains become wider. The roughened test results are shown on Figure 4.17 and display the same general trends as the smooth results. The variation with stage is not so

pronounced as in the smooth case, although the three zones of rising and falling trends are still present.

There is quite a wide variation in the averaged optimum values of NEV, ranging from 0.03 for series 7 to 0.43 for series 10. In general NEVC reduces with falling relative widths and rougher floodplains. The values of NEVC for inbank flows also show variation both with stage and channel shape, the mean values are listed in Table 4.7.

Table 4.8 gives values of NEVC averaged over the whole data set. The smooth floodplain tests gave an average value of 0.27 or 0.29 if series 4 data was omitted. Series 4 was not strictly speaking a compound channel but extends the inbank results to higher stages. The rough tests gave the lower value of 0.22 and the inbank value was found to be 0.12. It is interesting that the inbank value falls within the range  $0.16 \pm 0.08$  quoted in the literature, (eg Okoye, 1970 and Lean and Weare 1979), while the overbank results are considerably larger. This is undoubtedly due to the more complex turbulent flow structure generated by the interaction between the main channel and floodplain flows.

The above procedure is not the only one which can be followed when investigating variations of NEV. Shiono and Knight (1989, 1990) used the measured velocity profiles from the SERC FCF to produce optimized values for main channel, side slope and floodplain areas, see section 3.2.2. These values are based on the analytic solution to equation 4.3 rather than the version used by the author (4.2).

Having seen that the optimum NEV value is a function of geometry, stage and relative roughness it was not clear whether it is necessary to include the variation in NEV in order to obtain useful predictions of discharge. This point is considered in the following section.

#### **4.4.2 Discharge estimation with fixed NEV values**

The objects of the work described in this section are:

- a) To estimate the sensitivity of discharge estimates produced by LDM to changes in NEV
- b) To assess whether it is necessary to include variable NEV in order to obtain accurate predictions of discharge and velocity.

The procedure adopted was to apply the LDM with various fixed values of NEV and to compare the resulting mean errors and standard deviations in the computed discharges. Tables 4.9, 4.10 and 4.11 list the mean errors for smooth, rough and inbank tests respectively and Tables 4.12 and 4.13 give the results averaged over the whole data set.

The values of NEV chosen were the optimum values found previously: 0.27, 0.29 for the smooth tests; 0.22 for the rough tests and 0.12 for the inbank results. In addition the mean value quoted in the literature, 0.16, was also used, as was the intermediate value 0.24.

The effect of increasing NEV is to reduce the predicted discharge. The mean errors show a systematic reduction as NEV increases both for individual test series and the whole data set. The standard deviations do not show any consistent variation with NEV for the individual tests and are roughly constant for the whole set. For a given series the value of NEV closest to the optimum value for that series gave the best accuracy. For series 5 a value of 0.24 gave a mean error -0.1% which rose to -1.0% and -1.6% with NEV's of 0.27 and 0.29. Averaging over all the data produced similar results: a value of 0.24 gave the smallest mean error for the smooth data; 0.22 minimised the error in the roughened case and inbank the error was smallest with NEV of 0.12.

As can be seen from Figures 4.18 and 4.19 the variation, of the errors in the calculated discharges, around the means shows some systematic trends, similar to those found for back calculated NEVC. The plots are roughly 's' shaped with the

results for wider floodplains displaced to the right. Results are shown only for one value of NEV, (0.16), but increasing NEV tends to move the 's' curves to the left.

The overall error appears to be relatively insensitive to the NEV value used. For the smooth case increasing NEV by 70% from 0.16 to 0.27 changed the mean error in the predicted flows from 3.4% to -0.5%, a reduction of about 4% and the standard deviations were similar at 3.5% and 4.1% respectively. The standard value of 0.16 gave very good predictions with a mean error of 3.4% and a variance of 3.5%, hence two thirds of the predictions lie in the range -0.1% to 7% similarly for the rough case the standard value gave mean error and variance of 3.7% and 5.5%. With NEV of 0.24 the mean error for the smooth tests dropped to 0.5% and for the rough case the value 0.22 reduced the mean error to -0.7%.

The optimum value of NEV for the SERC FCF is about 0.24 to 0.27 for the smooth floodplain cases and 0.22 for roughened floodplains. The inbank value of 0.12 is similar to the typical value of 0.16. The overall error in discharge estimation using a fixed value of 0.16 was between 3% and 4% with a standard deviation of about 4% and 6% for the smooth and rough tests respectively. These errors can be reduced by using the optimum values of NEV although the variances remain approximately constant. In view of the relative insensitivity of the method to changes in NEV it is recommended that the standard value of 0.16 be used.

#### **4.4.3 Calculated distributions of velocity and discharge**

The LDM is based on computing the distribution of flow across the channel. It is implicit that in order to produce accurate estimates of total discharge the method should accurately predict the lateral flow distributions. Figures 4.20 and 4.21 show measured and predicted depth average velocity profiles for series 2 and 3 respectively. Predicted velocities are plotted for NEV values of 0.0 and 0.24, series 2, or 0.16, series 3. These values were the optimum NEV's found for these series. Overall the predicted velocities are good, especially in the centre main channel or on the floodplain away from the channel boundary. The predictions are not so good at

the channel/floodplain interface. Large peaks in the velocities are produced at the high floodplain depths but get smaller and narrower as the depth reduces. The peaks result from dividing the smoothly varying unit flow profile by the depths which change suddenly at the channel boundary. Depth averaged velocity is not a true physical parameter, it is obtained by dividing the discharge per unit width by the local depth.

Figures 4.22 and 4.23 show the velocity profiles computed by both the LDM and the LDM2. The LDM2 profiles do not show the peaks at the floodplain edges which are such an obvious feature of the LDM solutions. However both equations give the same velocities on the floodplain where there are no lateral gradients and the effects of interaction are small. The solution in the main channel given by the LDM2 is consistently too high and this is probably because equation 4.3 under predicts the lateral shear stresses in the shear layer between floodplain and main channel. This would explain why Shiono and Knight (1991) found that they required large values of NEV within the shear layer in order to predict the measured velocity profiles.

The peaks in the velocity profiles produced by the LDM are of minor importance. The calculations are all carried out in terms of  $q$ , the unit flow. Figures 4.24 and 4.25 show comparisons between the measured and calculated unit flow distributions for series 2 and series 3. The agreement between calculations and measurements are very close for the lowest stages and get slightly worse as the depths get larger. In general the computed distributions are too smooth. The distributions calculated using the sum of segments method (SSGM), which is equivalent to neglecting the lateral shear terms ( $v_t = 0$ ) in equation 4.2, are very close to the measured unit flows on the floodplains and show the same sharp change in values at the edge of the main channel. The values predicted are generally too high in the rest of the main channel. The distributions calculated with non zero NEV values tend to over predict unit flows in the shear layer on the floodplain and under predict in the shear layer in the main channel. These deficiencies obviously need further work to improve the choice of NEV values but the method can give useful results even with such a crude approximation for the viscosity.

#### **4.4.4 Conclusions**

- 1) The LDM has been applied to the best data set available to determine typical values of  $\lambda$  or NEV.
- 2) NEV was found to vary with channel geometry, roughness and depth.
- 3) For the purposes of stage discharge-estimation a single value of NEV was found to be sufficient, although the optimum value varied from geometry to geometry.
- 4) The errors introduced by using the standard value of NEV = 0.16 quoted in the literature were found to be small and it is recommended that this value should be used.
- 5) The LDM can accurately predict both stage-discharge distributions and the lateral distributions of flow in a compound channel.

#### **4.5 Application of LDM to Laboratory and field data**

Previously the LDM has been applied to discharge and velocity data available from the SERC FCF. Optimum values of the NEV were identified and comparisons made with the other form of the LDM. This section describes the application of the LDM to other laboratory and river data and covers three main topics.

- a) Calculation of stage-discharge curves
- b) Evaluation of the computed velocity and unit flow profiles
- c) Evaluation of the sensitivity of the LDM to changes in bed roughness and NEV values.

##### **4.5.1 Laboratory data**

###### **Myers' Data**

Myers provided stage discharges and measured velocity profiles for two smooth boundary compound channels. Figure 4.3 shows the two cross-section geometries and Figure 4.26 shows the stage-discharge curves calculated with a range of NEV

values. The inbank stage-discharge curves are almost identical for the NEV values between 0.0 and 0.5. In both geometries they start to spread out at overbank stages. It appears that the optimum value increases and then decreases at higher stages. The calculated velocity profiles are shown in Figures 4.27 and 4.28 for series A and F respectively. The profiles calculated with  $NEV = 0$  predict velocities which are too large in the main channel but the results obtained with  $NEV = 0.16$  are much better. The predicted velocities on the floodplain are generally good for the lowest overbank depths but are poor for the cases with larger depths. This effect may be exaggerated compared to the SERC FCF by the relatively narrow floodplains in Myers' laboratory channels.

### **Lambert's data**

Figure 4.4 shows the cross-section geometries which Lambert used. Figure 4.29 show calculated stage-discharge curves for all six geometries. Curves are shown for NEV values of 0.08, 0.16 and 0.24. For the tests with small bankfull levels there is very little difference between the results for the three values. It is apparent that the optimum value of NEV varies from geometry to geometry and with stage. However over all this data the standard value of 0.16 gives reasonable results.

### **Kiely's data**

Kiely (1990) presented four sets of velocity profiles measured in laboratory channel. Figure 4.30 shows the channel cross-section and the measured and calculated stage-discharge results. The kinks in the plotted stage-discharges are due to the plotting program and not the results. The velocity profiles are shown in Figure 4.31. In order to obtain this degree of agreement between the measurements and the calculations it was necessary to vary the floodplain Manning's  $n$  values with stage and to set  $NEV = 0$  over the floodplain regions.

## **4.5.2 Field data**

Figures 4.32 and 4.33 show measured and computed stage discharges for the eight gauging sites. The NEV was varied between 0.0 and 0.5, increasing NEV gives lower discharges and the curves show this by shifting to the left. Most of the sites are relatively insensitive to NEV and the various curves fall in a tight band around the observations. It is difficult to explain the wide variation seen in the other cases but channel shape and roughness both appear to have an effect. It has been suggested, Knight et al (1989), that it is necessary to use different values of NEV across the channel in order to obtain acceptable predictions. They showed that for the Severn at Montford NEV values of 0.2, 3.0 and 0.07 were appropriate for intermediate side slopes, the floodplains and the main channel respectively.

Figure 4.34 shows the stage discharges predicted with both single and multiple values of NEV for the Severn at Montford. The stage-discharge curves shown in the top plot give very similar results at inbank levels but these spread out at just overbank and converge again at higher stages. A typical NEV value in the range 0.16 to 0.24 appears to be appropriate. From the bottom plot it is clear that the fixed value of about 0.16 gives very similar discharges as using the variable NEV values suggested by Knight et al (1989). A much bigger difference is obvious between the results from the LDM, based on equation 4.2 and the LDM2, based on equation 4.3. The range of curves predicted by the LDM2 is displaced to the right and are much closer together. In order to make these curves match the data Knight et al found that it was necessary to use unusually high values of NEV on the flood plains.

The predicted velocity profiles for the LDM with a constant and variable NEV values are shown in Figure 4.36 for three stages. The use of different NEV values across the channel appears to accentuate the 'peaks' at the channel floodplain boundaries, making them both narrower and larger. Overall little practical difference is evident in the distributions: they are very similar in the main channel and over most of the wide floodplain. The predicted discharges for these three velocity profiles are listed below.

NEV	LDM		
Stage	0.16	Varies	Difference
mAOD	m <sup>3</sup> /s	m <sup>3</sup> /s	%
6.087	346.0	344.3	0.5
5.20	235.2	235.2	0.0
4.73	197.3	197.3	0.0

Again there is no practical difference and the extra work required to identify the NEV values appropriate for each part of the channel does not result in improved prediction for either the velocity profile or the total discharge.

Figure 4.37 shows the velocity profiles obtained with the LDM2 and the LDM methods. In the case of a constant NEV value the LDM2 method give similar profiles on the floodplain but the main differences occur in the main channel predictions. The LDM2 predictions have too broad a distribution of high velocities in the main channel, the LDM predictions give a much narrower peak which matches the data better. The three lower plots show the same pattern with the LDM2 method consistently over predicting velocities in the main channel.

Velocity profiles for the River Main are shown in Figure 4.38. Section 14 lies on a slight bend and the measured velocity profiles are mildly skewed and increase from left to right. Velocities on the right hand floodplain, which lies on the outside of the bend, are consistently higher than those on the left floodplain. The predicted velocity profiles are good for the wide range of stages, both inbank and out of bank. In general the distribution in the main channel is close to the measurements which explains the excellent discharge results. It would have been possible to improve the agreement on the floodplains by adjusting the roughness values. This has not been done since the skewed velocities are the result of bend induced secondary currents and not differential bed roughness.

Similar results for the Ouse at Skelton are shown on Figure 4.39. In this case both the discharge and velocity results are poor. The velocities are consistently high over

the left channel edge and low in the centre. Some attempts were made to improve the agreement by varying the roughnesses across the main channel but these were only partially successful. The channel at Skelton is relatively deep and narrow and the flow within the main channel may be quite strongly three dimensional. The LDM is based on the assumption that the flow can be adequately described with a 2-D depth integrated approach, which is not appropriate when strong secondary currents are present. Alternatively the poor agreement may be due to inaccurate or inconsistent data.

The four velocity profiles for the River Penk, Figure 4.40, show good agreement with the observations. The main channel velocities are under predicted slightly, although this is only significant at the highest stage. The corresponding discharges are given below and it is clear that the LDM gave excellent results in this case.

Stage	Qobs	Qcalc	Error
mAOD	m <sup>3</sup> /s	m <sup>3</sup> /s	%
1.94	32.8	29.4	-10.4
1.90	28.2	28.2	0.0
1.84	26.5	26.6	0.4
1.66	21.8	22.3	2.3

The results at 1.94m was obviously out of step with the other results and when the original current metering data, provided by the NRA, was checked it turned out that this one set of data was unreliable. This highlights the problems in collecting accurate and consistent discharge data for real rivers.

The River Trent at North Muskham has a relatively deep main channel and again the LDM did not give particularly good predictions when the bankfull Mannings 'n' value of 0.033 was used, Figure 4.41. By adjusting the roughness values improved agreement was obtained, Figure 4.42.

Current metering was carried out over the main channel and on the berm up to the

flood bank. At stages higher than 8.5mAOD the flood bank becomes inundated and water spreads out over the whole floodplain which is approximately 300m wide. This by-pass flow is not gauged and the total discharge is unknown although the slope of the measured discharge curve changes noticeably above the flood bank level.

### **Calculated unit flow profiles**

The computed depth averaged velocity profiles discussed above all show peaks at the main channel - floodplain interfaces. These peaks get taller as the main channel is roughened and wider if the NEV value is increased. In some cases the peaks are quite large and raise doubts about the accuracy of the results. In general these doubts are misplaced, the effect of the peaks on the total discharge and overall flow distribution is small. Figures 4.43 and 4.44 show the unit flow distributions from which the velocity profiles shown in Figures 4.36 and 4.37 were derived.

The large discontinuities in the velocity profiles are not visible in the unit flow profiles, which vary smoothly across the channel. The agreement between the computed and measured unit flows is excellent, except at the edges of the floodplain where the calculated profile overpredicts slightly. An attempt was made to improve the agreement between the calculated and observed velocities by varying the roughness values on the main channel banks with the constant value of NEV, 0.16. The resulting velocity and unit flow profiles are shown in Figures 4.45 and 4.46. The peaks in the velocity profiles have been reduced and the predicted unit flow profile over the channel banks is closer to the observed distribution, although the prediction is worse in the centre of the main channel. These plots were obtained by varying the roughness values in up to five zones over the channel banks and were arrived at by trial and error.

The computed discharges using a constant nb and a variable nb were 351 cumecs and 363 cumecs. Hence there is little doubt that calibration of the roughness values in order to match measured velocity profiles more closely will result in better discharge estimates. However the amount of work required to do this may be out of proportion

to the benefit in improved accuracy. In this example a single value of roughness in the main channel gave an error in estimated discharge of 6%. Considering that the errors in the measured discharge are probably of this order then this estimate is quite accurate enough for most practical purposes

#### **4.6 Comparison of different methods of calculating discharge**

The previous sections of this chapter have evaluated the lateral distribution method against both laboratory and field data. The LDM is now compared with various other methods in terms of :

- 1) Errors in discharge estimation
- 2) Errors in depth estimation
- 3) Errors in predicting the distribution of discharge between main channel and floodplains.

##### **4.6.1 The methods**

The methods detailed below were identified as appropriate for application to measured stage discharges in straight compound channels.

LDM	Lateral Distribution Method with $NEV = 0.16$
DCM	Divided Channel Method, using vertical division lines which are included in the wetted perimeter of the main channel but omitted from the wetted perimeter of the flood plains
SCM	Single Channel Method, applying the bankfull main channel Manning's n value to the whole compound channels
SCM2	Horton's Composite Roughness Method
SCM3	Lotter's Composite Roughness Method
SCM4	Einstein and Banks Composite Roughness Method
SCM5	Krishnamurthy and Christensen Composite Roughness Method
SSGM	Sum of Segments Method

DCM2	Divided Channel Method, using vertical division lines which are not included in the wetted perimeter of either the main channel or the flood plains
ACKM	Ackers' Method, based on Flood Channel Facility Phase A data. Main channel slope used for main channel flow.

These methods for calculating discharge in straight compound channels fall into four broad categories: divided channel methods; method of segments; composite roughness methods and more complex physically based methods. These methods have been applied to the various data sets available.

#### 4.6.2 SERC FCF Phase A

##### Total Discharge

The various composite roughness methods are not applicable to the SERC FCF, since the bed roughness terms are not approximated with Manning's equation and the comparison was carried out with the single channel and divided channel methods only. Each method was applied to individual discharge observations and the error in predicted discharge calculated. The standard NEV value, 0.16, was used with the LDM.

Table 4.14 gives the mean errors and variances for each test series. All three methods are sensitive to channel geometry and give smaller errors as the floodplain widths are reduced. Both the LDM and the two divided channel methods tend to over predict flows while the SCM under predicts, as expected Ackers' method performs the best overall on this data set. Figures 4.47 and 4.48 show the variation of error in the calculated flows with depth for the various methods.

At low floodplain depths the DCM gives approximately zero error which rises to between 10% and 15% at relative depths of about 0.15 as the depth increases further the error drops back towards zero. The other divided channel method (DCM2) gives a very similar distribution of errors but displaced upwards by about 5%. The SCM

gives much larger errors at low relative depths than either the DCM or DCM2. Maximum errors of between -50% and -30% were found, with the wider floodplain cases giving the larger errors. As the depth increases the errors reduce, tending towards zero at relative depths of about 0.75. The hydraulic behaviour of compound channels at low floodplain depths is quite different from compact channels but at large depths the main channel becomes a minor local area of increased depth. The lateral velocity gradients, which generate considerable turbulence and flow resistance at low depths, are reduced and the flow starts to approach the compact channel state. Ackers' method was developed using this data and, not surprisingly, it gives the most consistently accurate results.

Overall the LDM performs slightly better than the DCM and significantly better than the SCM. Table 4.15 shows the mean errors and variances taken over the whole data set. On average the LDM gave errors of about 3.4% compared to the DCM with 5.0%, the DCM2 at 7.7%, the SCM at -13.7% and Ackers' method at 0.3%. In terms of standard deviation the LDM and the two divided channel methods are similar with values close to 4.0%, the SCM is much worse at 14.0% and Ackers' method had a standard deviation of 1.7%. For the rough floodplain case the LDM gave mean error and standard deviation of 3.7% and 5.5% respectively; the DCM 24.7% and 14.0%; DCM2 12.1 and 11.8 and Ackers' method was best at -2.0% and 3.8%.

It was also possible to calculate the errors in predicted depth using these data. The measured discharge values were used to interpolate between the discharges calculated at the measured stages to obtain the predicted depths for a given discharge. In general these results show similar distributions to the discharge results. Where a method over-predicts discharge then it under-predicts depth. The mean errors in calculated depth for each series are shown in Table 4.16 and Figures <sup>4.49 and 4.50.</sup> The mean errors over the whole data set in Table 4.17. In general the errors in depth are considerably smaller than the equivalent errors in discharge, for example the LDM gives a mean error in discharge of 4.7% with a SD of 5.9% for series 1. The equivalent mean error and SD in terms of predicted depth are -1.3% and 1.1%. Thus the calculation of discharge in compound channels is far more sensitive to the method used than the

calculation of stage or depth. This is probably due to the general shape of compound channel rating curves, which often have relatively mild slopes. It also explains why it has been possible to use and calibrate 1-D river models with a sufficient degree of accuracy even when a relatively crude method is used to calculate the conveyance of compound channels. These models are generally calibrated against water levels and the calculated water levels are relatively insensitive to the method used to compute the conveyances.

Figure 4.51 shows the mean errors and standard deviations in both the calculated discharges and depths for the SERC FCF Phase A data sets. Figure 4.52 shows a comparison between the measured and calculated distribution of flow between the main channel and floodplains for this data set. All the methods tend to over predict the proportion of flow in the main channel at low overbank depths but improve as depths become greater, except for Ackers' method which gives good results at all levels. This is clearer in Figure 4.53 where the difference between calculated and measured ( $Q_{mc}/Q_{tot}$ ) is plotted for the various methods. It is obvious that Ackers' method predicts the main channel flow to within 1% consistently while the LDM gives it to about 2% and the two divided channel methods give good predictions at low overbank stages but get worse as the flow gets deeper.

It is not surprising that Ackers' method and the LDM give good results when applied to this data set. Both of these methods have been developed based on (ACKM), or modified after application to (LDM), this data set. A far better test of these methods is to apply them to data sets not used in their derivation or development.

### 4.6.3 Myers' data

Because Myers (1991) provided a bed friction calibration in terms of Manning's  $n$  it was possible to apply all the composite roughness methods. The results in terms of the errors in the computed discharges and depths are shown in Tables 4.18 and 4.19 and Figure 4.54. The LDM, DCM, DCM2, SCM3 and ACKM gave the best results with mean errors in discharge over both sets of data of 0.2%, -1.0%, 1.7%,

5.7% and -5.2% respectively. The standard deviations for all the methods were similar at about 6%-7%. The results for the calculated depths are similar with these five methods giving the best overall results.

Myers (1991) also provided velocity profiles which have been integrated to provide the proportion of the total flow in the main channel. Figure 4.55 shows the measured and calculated proportion of flow in the main channel and the differences between the calculated and measured  $Q_{mc}/Q_{tot}$  values. For both series A and F all the methods tend to under predict the proportion of flow in the main channel at low overbank stages and to over predict at high stages. The LDM method gives consistently better results than the other methods.

#### **4.6.4 Lambert's data**

Because the bed friction terms are evaluated with either a modified smooth law or the rough turbulent colebrook-white equation the various composite roughness methods have not been applied to this data set. The errors in the calculated discharges are shown in Figure 4.56 for the LDM, DCM, SCM, SSGM, DCM2 and ACKM. All of the methods tend to over predict discharge at low stages but show similar linear reductions in the over prediction as the depth increases. The SCM is the exception to this, giving an increase in the error in predicted discharge as depth increases. The errors in predicted depth shown in Figure 4.57 show the opposite trend as expected. The errors in predicted depth reduce as the depth increases and are of an order of magnitude smaller than the equivalent errors in discharge.

None of the methods is particularly accurate for this data set, with some giving errors for discharge and depth in excess of 150% and -30% respectively. The two best methods are the lateral distribution method and Ackers' method. At the higher stages Ackers method does seem to be more consistent than any of the other methods. The mean errors in discharge and depth, averaged over all six series of Lambert's data, are shown in Figure 4.58 and Tables 4.20 and 4.21. The lateral distribution method and Ackers' method perform significantly better than the other methods with mean

errors in discharge of -0.5% and 9.4% and SD values of 16.2% and 14.9%, compared with values between 30% and 55% with SD values of about 25% for the other methods. As with the other data sets the errors in the calculated depths are much smaller and show less sensitivity to method.

#### **4.6.5 Field data**

River gauging data at sites with compound channels was supplied to HR by various NRA regions as part of a study into methods of improving flood discharge assessment (Ramsbottom 1989). In total eight sets of field gauging data were obtained. As is to be expected with data collected under field conditions none of the information is perfect and all of the sites show some deviation from the ideal cases studied in the laboratory. In particular not all the cases are truly straight prismatic channels with uniform flow. The various sites and the data collected from them are described in detail by Ramsbottom (1989) and Ackers (1991). As can be seen from Figures 4.5 and 4.6 it is difficult to define the bankfull level exactly for some of these sites. In these cases each engineer must apply his own judgement. When applying the ACKM procedures it may be difficult to define the geometric parameters used to idealise the main channel.

#### **Bed roughness values**

The various methods were applied to the data using two basic estimates of the main channel and flood plain roughness values. The authors' estimates of main channel roughness values vary from about 0.025 to 0.046 and the flood plain roughnesses from 0.025 to about 0.100. The main channel roughness values were obtained by back calculation using the inbank measured flows. The bankfull value was used at all higher stages. The flood plain roughness for the Blackwater, Main, Severn and the Tees were estimated by comparing measured and calculated distributions of depth averaged velocity profiles across the flood plains. The LDM method with a NEV value of 0.16 was used to simulate the measured flood plain velocities and the values of Manning's  $n$  which gave the best fit between the calculated and measured velocity

profiles was adopted. In the case of the Torridge an estimated value of 0.06 was assumed. In general the values adopted are similar to those obtained by Ramsbottom (1989) on the basis of the divided channel method (DCM).

Ackers (1991) applied his method to some of the sites listed in Table 4.2, Main sections 6 and 14, Severn, Torridge and the Trent. Table 5.3 of Ackers (1991) reports the mean discrepancies, defined as :  $(1.0 - Q_{meas}/Q_{calc})$  obtained for each site with a range of roughness values for both main channel and floodplain. The second set of roughness values listed in Table 4.5 are the values which Ackers found to give the minimum mean discrepancy for each site, in effect optimum values of flood plain Manning n for Ackers' method. In a corrigenda to his report Ackers makes the following observations:

*The actual geometry of the river Main cross section 14 differs from that based on published information available (December 1991). The reach is now known to be of irregular gradient, with non-uniform flow, so the hydraulic gradients used in the analysis are not valid. The information on the River Main should be disregarded as unsuitable for this type of analysis.*

The application reported in this section was carried out using the corrected cross-section and the average hydraulic slope reported by Myers et al (1990). Hence the back calculated main channel Manning's n value for section 14 is now 0.0278 rather than 0.0248. Flow in the study reach on the River Main is known to be non-uniform, the hydraulic slope varies along the reach. The reach also includes several bends, the bends are not particularly tight and straight channel techniques are regularly applied by engineers to rivers with this type of plan form. There has been some debate as to whether these differences from laboratory data should preclude the River Main data from any further analysis. The stage discharge data from the two River Main sections is included in the analysis described here since the Author felt that in practice engineers regularly deal with channels of this type. The roughness values derived using this average hydraulic slope are not valid for other hydraulic slopes. The other sites used are gauging stations operated by the NRA and water surface

slopes are not regularly measured when gauging flows at these sites. The implicit assumption is made that the gauging sites are situated where steady, uniform and normal flow conditions operate. No information exists to confirm or refute this assumption but it should be noted that natural flows are rarely steady, uniform or normal. Indeed a close inspection of the rating sheets from some of these sites shows that during the two or three hours required to measure the discharge by the point velocity method the water level could rise or fall by significant amounts. Other causes of uncertainty also exist for some of these sites and the various authors noted above have discounted some of these sites as unsuitable. For example, the River Blackwater section has flood banks at the main channel edges which may affect the degree of interaction. The River Ouse section has very small floodplains and may act more like a simple channel. Both the Rivers Tees and Torridge sections have irregular floodplains with flood banks. The analysis reported here has been carried out using all eight sites and only the Severn, Torridge and Trent sites.

In an earlier version of this work, Wark et al (1991), the discharge observations used were derived from rating curves developed at each of the gauging sites, which were developed by Ramsbottom (1989) and Myers, rather than the individual observations. This procedure was said to average out measurement errors and seasonal changes in vegetation and cross-section. Between 5 and 12 points were selected on each stage-discharge curve. This procedure has been criticised and in the work reported here the actual observed pairs of stage and discharge were used. In the cases of the Severn and the Tees these data points were smoothed using running averages over three consecutive data points. Between five and thirty six data points were obtained for each site. All of the discharge estimation methods were applied with identical conditions, such as the cross-section geometry and roughness values.

The idealised cross-sections shown in Figures 4.5 and 4.6 are approximate and are included only as illustration. They are based on the estimated main channel side slopes. The main channel side slopes and corresponding idealised depth were estimated following the procedure described in section 6.4 of the summary to Ackers (1991). These two parameters were only used in the ACKM method and appear in

the calculations for the correction factors. The basic flows were calculated with the actual channel and flood plain cross-sections as recommended by Ackers (1991). Ackers also recommends that the factor  $Q_{2,c}$  should have a lower limit of 0.5 and this limit was used in this work.

The mean errors averaged over each river site are shown in Table 4.22 and the mean percentage errors for the various methods, averaged over various subsets of the data, are shown in Table 4.23. These averages and standard deviations were obtained from the individual results and not by averaging the mean values for each site. As mentioned there was some debate over the usefulness of some of this data and the following discussion is limited to the three sets of data collected from the Severn, Torridge and Trent. The variation of errors in calculated discharge with depth for each of the methods are shown in Figures 4.60 to 4.65. It is interesting to note that the variation of errors with stage for natural channel data do not show the systematic variations present in the laboratory channel data. This is probably partly due to the greater errors in the measured values and partly due to the more irregular and rougher channel cross-sections.

### **Results with Author's $n$ values**

The roughness values used for the flood plains in this work were derived, in the main, by adjusting them to give good agreement between the measured depth averaged velocity profiles and the velocity distribution predicted by the LDM. In general these values agreed reasonably closely with those obtained by Ramsbottom (1989), who integrated the velocity profiles to obtain the actual flood plain discharge and then estimated the flood plain roughness using a divided channel method

The two divided channel methods perform well over all the natural (Severn, Torridge and Trent) data with mean errors in the range -0.3% to 0.3%. The LDM gave the next best accuracy with a mean error of 0.1%. The ACKM method follows in fourth place with a mean error of -2.2%. The single channel methods all show much greater mean errors and standard deviations than the four best methods and will not be

considered further. The mean errors over each individual river site in Table 4.22 tend to confirm these conclusions, although the ranking of the various methods varies from site to site. These differences are probably due, in part at least, to the wide range of channel cross section type, scale and shape. It is worth noting that the standard deviations reported are partly due to random errors in the measured data and partly due to systematic differences between the predictions and the measurements.

### **Results with Ackers' n values**

Ackers (1991) reports broadly similar results with the authors n values for his method. However he also reported results obtained with roughness values optimised to reduce these errors for his method. The main limitation of Ackers application is that he didnot to compare his method with existing techniques. The analysis reported above has been repeated using Ackers Manning n values. The mean errors for the LDM and the two divided channel methods have increased from between -1% and +1% to between 2% and 5%. The mean error for the ACKM method is actually slightly worse at -3.1%. Figure 4.59 shows these errors and standard deviations. The errors reported by Ackers for his method with these data sets are slightly better and this is probably due, in part, to different approaches in applying the method to non-symmetric natural channels. The author has treated each flood plain separately in order to calculate velocities and basic discharges. This has the advantage of allowing different roughness values to be assigned to the two flood plains. Ackers, 1991, takes averaged floodplain widths and elevations to define an average floodplain geometry, which combined with an average floodplain roughness value is used to derive average floodplain velocity and basic discharge.

### **Discussion**

The above results show that of the methods investigated four are worthy of further consideration, namely: The LDM, DCM, DCM2 and the ACKM method. It is difficult to make definitive statements as to which is best on the basis of these results from natural rivers. The lack of independent calibration data means that the bed

friction calibrations have been based on the obtained results. It has been shown that the bed roughness values for natural rivers and flood plains are not well defined, the choice of value is often influenced by the method used to compute the channel conveyance. Therefore these results are inconclusive and do not confirm (in the strict scientific definition) that any of the four methods gives more accurate results than the others. It has been demonstrated that all four methods can be calibrated to match field data.

#### **4.6.6 Comparison with backwater calculations.**

The LDM has also been used to calculate the conveyance tables used by 1-D river models which solve the St Venant equations. Results are available from three independent studies:

##### **River Thames at Wallingford 1**

The back water program CHANNEL, developed by Dr G Pender of the Department of Civil Engineering, The University of Glasgow was used in a study into the effects of developing the floodplain of the river Thames at Wallingford. A proposed golf course on a site to the north of Wallingford involved the construction of raised tees and greens on the existing floodplain. The consultant Travers Morgan retained the University of Glasgow to carry out a before and after study of the effects of these alterations to the floodplain on water levels at the site. Travers Morgan gave their permission for the use of this material in this thesis and this is gratefully acknowledged.

Figure 4.66 shows the backwater profiles for the before case. The ONDA results came from a much larger unsteady computational model constructed by the NRA. The ONDA program uses a divided channel approach (DCM2) to calculate conveyances. As can be seen from Figure 4.66 there are no practical differences between the profile computed on the basis of the DCM2 approach and the LDM. However the velocity profiles available from the LDM, Figure 4.67, provide an

indication of where high velocity and bed shear stress are to be expected and so aid the design of bed protection measures.

### **River Thames at Wallingford 2 and the River Tees at Low Moor**

A version of the river model LORIS, which was developed by HR Wallingford, was altered to use the LDM to compute the conveyance tables. The standard version of LORIS uses the Sum of Segments Method (SSGM) to calculate conveyances. Two existing steady state LORIS studies were identified and the results obtained with the two versions compared.

Figure 4.68 shows various backwater profiles for the River Thames at Wallingford. This model covers the reach of the river which passes through the town of Wallingford. There is a medieval arched bridge over the Thames at Wallingford and the large steps in the backwater profiles at chainage 1500 are caused by the severe head losses through this constriction. Again the differences in the computed water levels are small and well within the calibration accuracy of this type of model. The backwater results from the River Tees at Low Moor are similar with very little difference between the two versions, although the LDM version gives slightly higher water levels along the whole reach.

#### **4.7 Summary and Conclusions**

- 1) The numerical solution technique used to solve the lateral distribution equations (4.2) and (4.3) has been verified by comparison with analytic solutions (section 4.3).
- 2) The SERC FCF data set has been used to evaluate values of the Non dimensional Eddy Viscosity parameter (NEV). The optimum NEV values for the SERC FCF Phase A data set were found to depend on the relative depth, width and roughness condition of the channel (4.4.1).

- 3) The average values of NEV for the FCF Phase A channels were found to be 0.29, 0.22 and 0.12 for smooth floodplains, roughened floodplains and inbank flows respectively.
- 4) The LDM was applied to the FCF data with several fixed values of NEV. The errors in calculated discharge were found to vary with relative depth, width and roughness (4.4.2). The mean errors in calculated discharge were minimised when the optimum values of NEV for each series, identified in Section 4.41, were used.
- 5) The predicted discharges were found to be relatively insensitive to NEV value and it is recommended that the value 0.16 should be used in practice (4.4.4).
- 6) When bed roughness values are well known the LDM can produce adequate predictions of the lateral distribution of flow, or velocity, across the channel (4.4.3)
- 7) The LDM has been applied to other laboratory data and field data. Good agreement between measured unit flows, velocities, stage discharges and the proportion of total flow in the main channel were obtained with NEV values close to 0.16 (4.5.1).
- 8) Predicted unit flow and velocity profiles for the laboratory and natural channels have been produced. In general these are better for wider, shallower main channels than for narrow, deep channels (4.4.4 and 4.5.1).
- 9) The LDM method gives good results with a single value of NEV. It is not necessary to use variable values of NEV across the channel to achieve good agreement with measurements (4.4.3 and 4.5.2)
- 10) The two versions of the LDM (equations 4.2 and 4.3) have been compared and the author's version, based on equation 4.2, was found to give superior

predictions of velocity and discharge (4.5.2).

- 11) The LDM has been compared with other methods applied to the FCF data. On average the LDM and Ackers' methods gave better predictions of discharge and depth than the other methods (4.6.2).
- 12) The LDM has been compared with other methods of calculating the conveyance capacity of compound channels. These comparisons have been carried out over the various sets of laboratory data. Two methods, LDM and Ackers' method, gave much better predictions of both discharge and depth in the laboratory channels than the other methods considered (4.6.3, 4.6.4)
- 15) The LDM has been compared with other methods of estimating discharge in natural river channels. The results were inconclusive with the best four methods (LDM, DCM, DCM2 and ACKM) giving mean errors which are within the measurement errors of the data (4.6.5).
- 16) The main problem in applying any method of calculating discharge is in estimating appropriate values of bed roughness. When the roughness values are known the LDM is expected to give acceptable predictions of both velocity distribution and total discharge. More work should be directed towards improving the accuracy of methods of estimating bed roughness values (4.6.5).

## CHAPTER 5

### FLOW MECHANISMS IN MEANDERING CHANNELS

#### 5.1 Introduction

The opening four chapters of this thesis concentrated on the flow behaviour and modelling of straight compound channels. These have been investigated in some detail over the last three decades but are less important in practical terms, compared with sinuous and meandering compound channel flows. The remainder of this thesis considers the topic of flow in meandering compound channels.

Any study of flows in meandering compound channels is handicapped by the relative sparseness of the available laboratory and field data. The main purpose of this chapter is to review the data available and summarise the main conclusions and findings from these studies. A secondary purpose is to review the effect of channel meanders on the inbank conveyance capacity of a channel, this is a logical precursor to the more complex situation of overbank flow in meandering compound channels.

#### 5.2 Laboratory investigations into meandering flow

At least eight laboratory studies into aspects of flow in meandering compound channels <sup>have been carried out</sup> These studies include: SERC FCF Phase B (1989 - 1990); Willetts et al (1991); US Army Vicksburg (1956); Kiely (1989); Toebes and Sooky (1967); James and Brown (1977); Smith (1977) and Stein and Rouve (1989). In addition Rajaratnam and Ahmadi (1981) published some details of laboratory tests and Dr Shiono of the University of Bradford is currently carrying out laboratory experiments with a meandering compound channel, although these are as yet unpublished. A large scale model of meandering compound channels is known to exist in Bucharest, although very little has been published in english language journals. A combination of field and laboratory work has been carried out by Sellin et al (1990) in to the behaviour of a man made meandering compound channel on the River Roding. Lorena (1992) has carried out experiments with a single meander bend constructed in a laboratory flume, however details of this work are yet to be published.

The main characteristics and findings of each of the laboratory investigations identified in the literature are detailed below.

### 5.2.1 Phase B SERC FCF

Phase B of the SERC FCF programme ran from 1989 to 1990 and dealt with flows in meandering compound channels. Phase B followed on directly from Phase A, which investigated straight compound channel flows. The FCF at HR Wallingford provided the primary set of data used in this work and is a high quality and consistent laboratory data set. The details of the experiments and the data collected were made available to the author by the various university researchers involved in the experiments. Recently Sellin et al (1993) and Greenhill and Sellin (1993) have published details of the test programme, the results and some analysis.

The Phase B geometries were constructed with a smooth mortar finish. The basic surface roughness size was identical within the main channel and on the flood plains. In general the full flood plain width of 10m was used although tests with a reduced flood plain width were also undertaken. Two basic meander geometries with different sinuosities were constructed for the Phase B experiments. The first geometry had a sinuosity of 1.37 (60° meander) and included four complete meanders. The second geometry had a sinuosity of 2.04 (110° meander) and included four and a half meander wavelengths, as shown Figures 5.1, 5.2, 5.3 and 5.4.

The design longitudinal slope of the flood plain was  $1.0 \times 10^{-3}$ . The actual longitudinal slope of the flood plain surface for the first channel geometry was  $0.996 \times 10^{-3}$  and  $1.021 \times 10^{-3}$  for the second. Two main channel cross-section geometries were used with the 60° meander geometry. The first was a simple trapezium with a base width of 0.90m, side slopes of 45° and a depth of 0.15m. The second was an approximation to a typical natural geometry, reproducing the relatively deep pools which form on the outsides of the bends and the symmetric geometry at the cross-over sections. Only the natural main channel cross-sectional geometry was used with the 110° meander geometry. Figures 5.2 and 5.4 show details of the plan and cross-

section geometries. The natural cross-sections were derived from a parametric analysis of cross-sections obtained from seventeen natural channel bends. The procedure is described by Lorena (1992). Due to scale considerations the cross-sections adopted in the FCF work have a vertical distortion of approximately 2:1, compared to the natural channels analyzed.

The full flood plain width of 10.0m was used for most experiments, but stage-discharges were measured with the flood plain edges tangential to the meander bends. This was carried out for both the meander geometries with natural main channel cross sections. The flood plain sides were sloped at 45° (1:1) in these cases.

In general the experiments included no artificial roughening of the flood plains or main channel, the surfaces being left as trowelled mortar. However, a few experiments did include artificial roughening on the flood plains by utilising vertical dowel rods placed in differing geometric patterns. The rod roughened tests had the rods placed over the whole flood plain, while the partially roughened tests had only the inner flood plain or meander belt covered with rods.

Additional tests were also carried out by introducing a blockage to the flood plain flow. Concrete blocks aligned in the flow direction were used to approximate the behaviour of bridge piers on the flood plain. In the case of the 110° geometry these blocks were also used to construct walls across the full widths of the flood plains to the inner bend apices. This simulated the effect of complete development on the flood plain, which would restrict the flow to the main channel. This data has not been used since no reliable method of calculating the flow resistance of the blocks or walls exists. The smooth and rod roughened cases correspond to calibration tests carried out during Phase A of the FCF work into straight compound channels and Ackers (1991) provides accurate bed friction calibrations for these two conditions.

The test programme included investigation of in-bank and out of bank flows. Measurements of stage, velocity (magnitude and direction), boundary shear stress, turbulence and dispersion were all included in the programme. Separate

measurements of angles and velocities were made in the main channel and flood plain areas. For the main channel measurements were taken on eleven cross sections along a quarter of a wave length of the 60° channel and on fourteen cross sections over half a wave length of the 110° channel. These main channel sections were taken perpendicular to the main channel centre line and extended 300mm on to the flood plains on either sides. Measurements were made on a grid with horizontal spacings of 150mm or 50mm and vertical spacing of 15mm. On the flood plain measurements were made at 13 (60°) or 11 (110°) traverses covering half a wave length. Readings were taken at spacings of 0.5m laterally and 10mm vertically. Only the main channel velocity data were used in this project. There was insufficient time available to allow the flood plain velocities to be collated and analyzed.

Boundary shear stresses were measured in both geometries using a Preston tube on the smooth surfaces, Knight et al (1992) . The shear stress measurements were made at the same sections in the main channel and on the flood plain as the point velocity data. A two component Laser Doppler Anemometer was used to measure turbulence data across the flood plain and main channel at one bend apex. Detailed water surface levels were measured using a Churchill probe both in the main channel and across the flood plain over one meander wave length. Dye dispersion tests were carried out at inbank flow conditions. These experiments involved injecting dye at various points across the channel and monitoring the concentrations at selected positions downstream. Flow visualisation experiments involved photographing the movements of either injected dye or floating bodies. The visualisation experiments provide qualitative indications of the complexity of the flow structures present. Because this project put a high priority on the estimation of both the total discharge and the distribution of discharge none of the turbulence, water surface level, dispersion of flow visualisation information was not used in this project.

A full listing of the experiments undertaken in the Phase B tests is given in Table 5.1 and Table 5.2 lists the stage-discharge experiments carried out. The test numbering system followed was devised by researchers from the University of Bristol. Tests one to nineteen were carried out during phase A of the FCF work into compound

channels. To ease data handling the stage-discharge data available from other sources were also assigned serial numbers. The Aberdeen stage-discharge data were assigned numbers between 100 and 199. The Vicksburg data were assigned numbers between 200 and 299. Kiely's one set of stage-discharge data was given the test number 301 and Sooky's data were assigned numbers 400 to 499.

Sellin et al (1993) present stage-discharge data collected during the experiments. They only list 8 sets of stage-discharge data out of the 12 sets that were collected. They attempt to demonstrate the effect of a meandering channel on overbank flow by calculating the distributions with depth of two bed friction parameters, Manning's  $n$  and Darcy friction factor. The cases with smooth floodplains give similar  $n$  distributions as straight compound channels, the values increase sharply at just overbank levels and drop gradually towards the inbank values as the flow depths increase. The roughened floodplain tests do not display this gradual return to a limiting value but increase with depth. This is mainly due to the inappropriate use of Manning's equation in these cases. The flow resistance due to the rod roughening is caused by: the constricted flow area between the rods; drag on the rods and wave effects as the rods pierce the water surface. The use of a single channel form of analysis for straight compound channels has been shown to be deficient many times in the literature and it is not surprising that the more complex case of overbank flow in meandering channels should also require a more careful and reasoned approach.

In a discussion of the detailed velocity and flow visualisation measurements Sellin et al (1993) highlight important aspects of flow in meandering compound channels in the cases with smooth floodplains.

- 1) The primary velocities in the main channel and flood plain are aligned in different directions. In the main channel below bank full the velocities are generally follow the direction of the sinuous channel banks. On the flood plain, away from the main channel the primary velocities are in the direction of the valley walls or centre line. The direction of velocities above bankfull levels over the main channel is often between these two conditions. In the

straight channel crossover reaches between bends the velocities are skewed across the main channel and dye dispersion tests show that a significant proportion of the flow enters from the upstream floodplain travels across the channel in a skewed path to leave the channel just before the next bend.

- 2) There is a vigorous interaction between flows on the floodplain and in the main channel. Flows from the floodplain enter the main channel in a region up stream of a meander bend. Some of <sup>the</sup> fluid from the floodplain plunges down into the main channel and becomes entrained in the general main channel flow. In addition significant volumes of fluid from low down in the main channel are displaced out on to the floodplain.
- 3) The effects of this cross-over of flow from the flood plain on one side of the main channel to the other is to induce shear stresses acting on the horizontal plane. These shear stresses interact with the plunging flows to induce secondary currents in the channel bends which rotate in the opposite sense to those observed during inbank flow.
- 4) The strength of the interaction is affected by the cross-sectional shape of the main channel. The strength of the secondary currents and the plunging flow were smaller in the cases where the main channel cross-section approximated a natural river channel and was varied through each meander. The case with a trapezoidal main channel showed stronger secondary currents and interaction compared to the natural channel cases.
- 5) The strength of the interaction is affected by the sinuosity of the main channel and the over bank flow depth. The more sinuous channel actually 'turned back' so that over part of the meander the main channel velocities are in the upstream direction for the whole flow and the interaction was stronger than for the less sinuous channel. The variation of the interactions with depth are not clear from this analysis but these will probably vary with depth.

Figure 5.10 summarizes these mechanisms.

## 5.2.2 Aberdeen

The Aberdeen flume, Willetts et al (1991) and Willetts and Hardwick (1993) was constructed as a scale model of the SERC FCF. Although due to space limitations a larger vertical scale was used leading to the model having distorted channel cross-sections when compared to the equivalent geometry on the SERC FCF. The meandering channels were formed in expanded polystyrene and painted. In all cases the flood plain width was 1.20 m and the flood plain and main channel roughnesses were identical. Experiments were conducted with four different channel sinuosities, viz. 1.00, 1.21, 1.40 and 2.04. An identical trapezoidal cross-section for the main channel was used for all sinuosities with a base width of 0.139m, a depth of 0.050m and side slopes of 70.7° (0.35:1).

Two additional experiments were conducted with 'natural' main channel cross sections. These were created by infilling the trapezoidal channels to a depth of 20 mm with bakelite powder. This moveable bed was subjected to bankfull flow until a stable bed topography had evolved, which was then fixed and painted. The water temperature was  $14^{\circ}\text{C} \pm 1^{\circ}\text{C}$  in all experiments.

The experimental conditions are summarized in Table 5.3. Stage-discharge measurements were taken for all conditions except for inbank flows in the 2.04 sinuosity channel with the natural cross-section. Figures 5.5 and 5.6 show the various plan and cross section geometries.

Willetts et al (1991) and Willetts and Hardwick (1993) report the main observations and conclusions. The study included measurement of stage-discharge relationships, point velocities within the main channel and water surface levels over a wavelength of the meander pattern. The objects of the investigation were:

- 1) To identify the flow structures associated with channel-flood plain interaction.

- 2) To explore the dependency of these structures on channel cross section shape.
- 3) To determine whether main channel sinuosity and cross-section shape have significant influence on stage-discharge relationships.

The stage-discharge measurements show that the discharge capacity of the floodway reduces as the sinuosity of the main channel increases. For a given sinuosity the main channel cross section has a strong effect on the capacity. The 'natural' cases had larger total discharges than the equivalent trapezoidal channels at high stages, even though the trapezoidal channels had larger cross sectional areas. An explanation of this unexpected phenomenon was indicated by dye dispersion tests. The trapezoidal channels exhibited far stronger secondary currents and more interaction between main channel and flood plain flows than the natural cases. Thus channel cross section shape has a strong effect on the conveyance capacity of a flood way.

A complete set of stage-discharge data was supplied to the author by Willetts (1991) and this assistance is gratefully acknowledged. Only the data collected in the trapezoidal main channel and meandering cases have been used here. The inbank stage-discharges collected in the straight channel were used to calibrate a modified smooth friction law.

### **5.2.3 US Army Vicksburg**

A series of stage-discharge experiments were conducted on compound meandering channels by the United States Army Corps of Engineers (1956) at the Waterways Experiment Station in Vicksburg, Mississippi, USA. The main purpose of these experiments was to determine the effects on floodway capacity of: radius of curvature of bends; sinuosity of main channel; depth of overbank flow; ratio of overbank area to main channel area and flood plain roughness. Two basic sizes of main channel cross section were constructed. The smaller channel was constructed with a trapezoidal cross section of base width one foot (0.305m) and was 0.5 feet (0.152m) deep. Stage-discharge relationships were measured for ten basic conditions. The results obtained with the one foot wide channel were inconclusive and a further

set of tests were carried out with a larger main channel (two feet wide).

The main channel cross-section was trapezoidal in all cases, with side slopes of 63.4°. The bottom width was two feet (0.610m). The tests were conducted in a flume 30.5 m long and 9.2 m wide. Main channels with three planform geometries were moulded in sand and stabilized with a concrete veneer. The flood plain width was varied by installing temporary brick walls. The basic flood plain roughness was plain brushed concrete. Two additional roughnesses were obtained by covering the surface with expanded metal grating, laid with the openings oriented parallel and normal to the flow direction.

The three different meander planforms were constructed with this 2 ft wide channel, all with arcs of circles connected tangentially, with no straight reaches between them. The meander wave length was held constant at twenty four feet (7.315m). Three and a half full wave lengths were constructed for the three sinuosities. The valley slope was  $1.0 \times 10^{-3}$  in all cases. For each condition the discharge was measured at bankfull and three overbank stages. The main conclusions of the study were :

- 1) Where the main channel is narrow (and small) compared to the flood plain, the effect of channel sinuosity on the total discharge capacity is small.
- 2) The effect of increasing main channel sinuosity is to reduce the total discharge capacity of the channel.
- 3) When the flood plain is more than three times the width of the meander belt the effect of channel sinuosity on the total discharge capacity is small.
- 4) The effect of increased flood plain roughness is to reduce the total discharge capacity.

Stage-discharge relationships were measured for eleven separate conditions with the 2 ft wide main channel but it was found that the roughened flood plain cases could not be used since the quoted Manning's n values of 0.025 and 0.035 could not be verified. The smooth surface of the Vicksburg flume was similar to the SERC FCF and both facilities were constructed at similar scales. The Vicksburg flume had a

quoted Manning's  $n$  of 0.012 but this could not be verified and it was decided to model bed friction using the modified smooth turbulent law developed for the SERC FCF. Thus only three of the measured stage-discharge curves could be used. The experimental conditions for the 2ft wide channel are listed in Table 5.4 and Figure 5.7.

#### 5.2.4 Toebes and Sooky

Toebes and Sooky (1967) and Sooky (1964) carried out a laboratory study of overbank flow with a meandering channel of low sinuosity, 1.090. They varied only the main channel depth and recorded stage-discharges as well as data on water surface and velocity variations across the channel and flood plains. The modelled geometry covered 5.5 meander wave lengths. The sinuous main channel was constructed with a sinusoidal plan form and a rectangular cross section in a flume 7.3m long and 1.18m wide, Figure 5.8. Two separate channel depths and seven longitudinal slopes were tested to give eleven individual stage-discharge cases. Calibration tests were also carried out in straight rectangular channels and this provided the necessary information to calibrate a modified smooth law for Sooky's flume.

Sooky analyzed these stage-discharge relationships based on division of the cross section in to two zones by a horizontal line at bankfull. He assumed that flows in both regions are controlled by the longitudinal valley slope. Applying basic frictional losses and calculating the discharges in these two regions separately over-predicted discharge and so did not account for all energy losses. In order to account for these extra energy losses Sooky introduced an extra length of wetted perimeter ( $T$ ) to both the main channel and flood plain calculations. He used his laboratory data to back-calculate the values of  $T$  required to give zero error in the predicted discharges.  $T$  was found to be a complicated function of:

- 1) overbank flow depth
- 2) mean velocities in the two zones

### 3) longitudinal slope

On the basis of this analysis it was concluded that the additional energy losses (other than bed friction) introduced in overbank flow in meandering channels will depend on these parameters. In addition the following conclusions were also drawn:

- 1) The additional losses increase (from zero) with over bank stage up to some maximum. As depth increases beyond this point the extra losses then reduce.
- 2) The deeper and narrower the main channel then the smaller are the extra energy losses.
- 3) For the purposes of calculating discharge in meandering compound channels, cross sections are best divided by a horizontal division at bankfull.

The measured velocities also provided useful information on the flow structure within the channel. It is well known that flow around channel bends induces spiral currents and super elevation. Inbank secondary currents are known to rotate with the surface currents directed to wards the outside of the bend. During overbank flow Sooky observed that the secondary currents rotate in the opposite sense, ie the surface currents are directed towards the inside of the bend. This observation has been confirmed by other researchers (SERC FCF, Stein et al, 1989). In addition, the velocities were integrated to provide discharge values in the various regions of the channel.

#### 5.2.5 Smith

Smith (1978) has published details of a laboratory investigation into overbank meandering flow. He carried out stage-discharge experiments for three cases including a straight compound channel, a meandering compound channel and for the flood plain alone. The flume was set at a longitudinal slope of  $1 \times 10^{-3}$  and in both cases the main channel was trapezoidal with a top width of 0.27m and bankfull depth 0.076m. The model channel had 7 meander wave lengths and all three cases were constructed of trowelled mortar in a flume 24m long by 1.2m wide. The meandering

planform was constructed with a sinuosity of 1.172 and filled the full width of the flume. Smith carried out some analysis of the meandering case using the straight channel divided channel method (DCM2). He concluded that straight channel methods are inappropriate for calculating the discharge in meandering compound channels. He carried out some dye injection tests to investigate flow patterns and found that the flow in the main channel varied along the wave length, spilling out of the channel onto the flood plain and back. The flow in the channel was observed to be lowest at the cross-over reach, half way between meander bends. At deep overbank stages the valley flow was observed to pass over the main channel. A separation zone occurred and a spiral eddy in the main channel was induced.

The main conclusions of Smith's work were:

- 1) Straight channel methods are inappropriate for calculating discharge in meandering compound channels.
- 2) For meandering overbank discharges the main channel and flood plain flows interact. This interaction has a strong effect on the discharge capacity and varies strongly with stage.
- 3) The flow in the main channel varies along a meander wavelength and is minimum at some point between bends.

Smith provided a bed friction calibration for Manning's  $n$  of about 0.01, although this did appear to vary for the various cases. During later work on verifying the authors method this data set was found to behave differently from the other data available. This was attributed to the poor bed friction calibration and it was decided that Smith's bed friction calibration is unreliable and so this data set should not be used in any numerical work.

### **5.2.6 James and Brown**

James and Brown (1977) carried out measurements to determine the geometric parameters which influence flood plain flow in a tilting flume 26.8m long by 1.5m

wide. Out of fourteen tests they conducted nine with straight channels, three with single skewed crossovers, one with two cross-overs and one with three cross-overs. Only the last case even approaches a meandering geometry but is rather unrealistic when compared to typical natural planforms. The bend radius was too small and the length of straight cross-over too large. The straight and meandering channel stage-discharge data was analyzed in terms of Manning's  $n$  values. On the basis of this they concluded that 'The resistance factor increased as the crossover or meander length decreased'. This is equivalent to saying that the conveyance capacity was reduced as the sinuosity increased.

This data set was not used in any comparisons because of the relatively poor meandering geometry and the lack of adequate bed friction calibration data.

### 5.2.7 Kiely

Kiely et al (1989<sup>1,2,3</sup> and 1990) carried out experimental work into flows in straight and meandering compound channels. Discharges, point velocities and turbulence measurements were made in a 14.4m long by 1.2 m wide flume. A straight, single meander wave length and multiple meander (4.5 wave lengths and sinuosity 1.224) cases were investigated, see Figure 5.9. The flume was hydraulically smooth with a test section constructed of glass and perspex for use with a single component Laser Doppler system. The main channel was rectangular in all three cases and the flume was set at a valley slope of  $1.0 \times 10^{-3}$ . McKeogh and Kiely (1989) provide a modified smooth law which gives the bed friction in this flume. The laser system was used to investigate detailed flow structures in both the main channel and the flood plain. Kiely identified the following mechanisms in overbank meandering flow.

- 1) Secondary currents in the main channel during overbank flow were observed to rotate in the opposite direction to those seen during inbank flow. A detailed examination of the secondary current patterns suggests that the mechanisms producing these different patterns are both present during over bank flow but that the curvature induced currents are less intense and become

nullified. The energy losses due to secondary currents during overbank flow are greater than the losses during inbank flow.

- 2) Velocities within the main channel were generally observed to follow the direction of the main channel side walls. The direction of velocities at points over the main channel and above bankfull level were observed to vary with level. Above bank level the direction of flow changes from being parallel to the main channel at bankfull to being almost parallel to the flood plain, close to the water level. This change in the direction of local velocity through the water column indicates the presence of a horizontal shear layer between the main channel and flood plain flows.
- 3) At the crossover reaches the water on the flood plain is observed to pass into and across the main channel. Thus fluid from the left hand flood plain crosses the main channel and ends up on the right hand flood plain. As the flow crosses into the channel the depth increases and as it passes out onto the flood plain the depth decreases. This expansion and contraction of the flow area is known to induce energy losses in analogous situations.
- 4) Velocities were seen to vary strongly across the flood plain. Outwith the meander zone the velocities were approximately uniform. Within the meander zone an area of reduced velocity was observed. It was felt that this was caused by the interaction of the main channel and flood plain flows, with relatively low velocity fluid leaving the channel at the cross over reaches and passing down the flood plain.

The multiple meander data has been used by the author to test and verify various methods of calculating the conveyance capacity of meandering compound channels.

### **5.2.8 Stein and Rouve**

Stein and Rouve (1988, 1989) have investigated the detailed flow structures present

over one meander wave length for overbank flow conditions. Sophisticated laser doppler anemometry was used to measure all three point velocity components within the flow for one water level and discharge. The meandering channel was constructed in a flume 15.0m long by 3.0m wide. The main channel was rectangular with a width of 0.4m and a bankfull depth of 0.1m. The preliminary results presented allowed the following conclusions to be drawn.

- 1) Secondary currents in the main channel rotate in the opposite direction to those for inbank flow.
- 2) Fluid 'welling out of' the main channel slows the discharge on the flood plain.
- 3) A horizontal shear layer exists between the lower and upper parts of the main channel.

### 5.3 General Comments

Experimental work on flows in meandering channels during over bank conditions has been identified from the literature. The investigators and the main characteristics of their experiments are summarized below.

SERC FCF Phase B Multiple meander, two sinuosities, two cross sections, two flood plain roughnesses, stage-discharges, velocity, water surface and bed shear stresses.

Willettts et al Multiple meander, three sinuosities, two cross sections, stage-discharges, water surface levels and velocities.

US Army Vicksburg Multiple meander, three sinuosities, three flood plain roughnesses, stage-discharges.

Kiely Single and multiple meander, one sinuosity, stage-discharges, velocity, water surface and turbulence measurements.

Toebe and Sooky	Multiple meander, one sinuosity, two cross sections, seven slopes, stage-discharges, water surface levels and velocities.
James and Brown	Multiple meander, stage-discharges and velocities.
Smith	Multiple meander, stage-discharges.
Stein and Rouve	Single meander, water surface levels, velocities and turbulence measurements.

The key physical dimensions of the test channels are given in Table 5.5. Table 5.6 shows the relationships between the key geometric parameters for the laboratory flume tests. Various authors have published details of empirical equations derived by regression analyses carried out on natural meander patterns. The exact equations vary from author to author but in general it is possible to say that in natural, fully developed, meander bends: the wave length is approximately ten times the channel width; the channel width is approximately ten times the channel bankfull depth and the radius of curvature of the bends is between two to three times the channel width.

A study of Table 5.6 shows that most laboratory studies have been carried out with main channel width to depth ratio's ( $B/h$ ) which lie between 3.5 and 5.0. Only the SERC FCF geometries have channel cross sections which approximate to natural cross sections with an aspect ratio of 8.0. Toebe and Sooky (1967) and the work carried out at Vicksburg (1956) demonstrated that main channel cross section shape can have a strong effect on the discharge capacity of meandering channels during overbank flow. These observations have been confirmed by Willetts et al (1991). Most of the investigations have used meanders with wavelength to channel width ratios which are close to the natural ratio of 10. Only the meander investigated by James and Brown (1977) with a ratio of about 33 is unrealistic in terms of this ratio. The final geometric ratio between the bend radius and channel width generally falls within the natural range of 2 to 3. Sooky, James and Brown and Smith all constructed channels with low sinuosity and this produced  $r_c/B$  ratios of about 4.0.

However this is not a serious deviation since the relationships for natural channels were derived for fairly sinuous channels.

It has been demonstrated that all three of these geometric ratios effect the stage-discharge capacity during overbank flow. Since only the large scale experiments carried out in the SERC FCF satisfied all three relationships it is likely that the flow patterns and stage-discharge relationships for the FCF will be closer to those observed in nature than for the other experimental data collected in small scale models. Most investigators identified well defined structures within the flow including: secondary currents within the main channel and bulk exchanges of flow between main channel and flood plain. One major limitation is that all of the above laboratory work was carried out on models with horizontal floodplain topography. Natural floodplains usually slope inwards to the main channel banks and this side slope may significantly affect the behaviour of a meandering compound channel. Figure 5.10 shows the flow processes taking place during over bank flow in meandering channels.

#### **5.4 Bed friction**

In later chapters stage-discharge data, from these laboratory studies, is used to develop and verify methods of estimating discharge in meandering channels. In order to carry out this work it is necessary to calculate energy losses due to bed friction. All of the laboratory models were constructed with hydraulically smooth surfaces. One of the conclusions arising from the earlier work by Ackers (1991) is that the bed friction in hydraulically smooth conditions should be obtained from a smooth turbulent expression. This expression correctly predicts the effect of viscosity on friction factor. In any given case it may be appropriate to derive a modified version of the smooth turbulent law which fits the data better than the general version quoted in the literature. This approach to determining bed friction has been followed and for each of the various data sets a modified smooth law has been obtained.

The original references either gave the appropriate modified smooth law or stage-discharge measurements in straight simple channels which could be used to calibrate

the constant values in the smooth law. The general form of the modified smooth law is :

$$1/f^{1/2} = A \log (\text{Re } f^{1/2}) + B \tag{5.1}$$

Where Re is the Reynolds number of the flow defined by:  $\text{Re} = 4RV/\nu$ , V is the flow velocity, R is the hydraulic radius, and  $\nu$  is the kinematic viscosity of the water. The kinematic viscosity can be calculated from recorded temperatures by the equation

$$\nu = ( 1.741 - 0.0499 T + 0.00066 T^2 ) \times 10^{-6} \tag{5.2}$$

in which T is the temperature in °C and the values of the constants A and B derived for each of the data sources are listed below.

Data source	A	B	Comments
Vicksburg	2.02	-1.38	The SERC FCF smooth law was used
Toebees and Sooky	0.68	2.42	Values calibrated to given stage-discharges
Kiely	2.10	-1.56	Values provided by Kiely
Serc FCF	2.02	-1.38	Values provided by Ackers
Aberdeen	2.48	-2.91	Values calibrated to given stage-discharges

Some of the experiments carried out on the SERC FCF involved roughening the flood plains with vertical rods extending through the full depth of water. The pattern of rods consisted of a triangular distribution of angle 60°. This was designed to have a density of 12 rods per square metre. Under these conditions the resistance to flow is made up of drag of the rods and the shear force at the channel boundaries. Ackers (1991) has analyzed some calibration tests carried out during phase A of the SERC FCF work and developed a method of obtaining the total friction factor due to rod roughness.

He assumed that the rod drag and bed friction can be treated separately, accounting for the blockage effect of the rods on the mean velocity. The drag of the rods is related to the square of the mean flow velocity past the rods. Ackers calibrated an

expression for the drag coefficient which depends on the ratio of rod diameter to flow depth. The expression is quite complex and in order to obtain friction factor values for a specific depth iteration is required. The equations and data for the method are given in Appendix 7.

## 5.5 Summary

The sections above present the results of a literature search in to overbank flow in meandering compound channels. The main purposes of this review were:

- a) To identify laboratory data to use in developing and verifying a new procedure for discharge estimation in overbank flow in meandering channels.
- b) To summarize the current state of knowledge on the detailed flow structures present during overbank meandering flow and to gauge the effect these might have on the discharge capacity of the channel.

Eight laboratory investigations were identified, including the SERC FCF. The two most modern and extensive data sets (SERC FCF and Aberdeen) were considered to represent the best quality data available and it was decided to use these two sets in developing a new procedure. Three other investigations (Vicksburg, Kiely and Sooky) were deemed appropriate to use in verification of the new procedure.

The internal structure of currents during overbank flows has been found to be highly complex. The most important observations are:

- 1) The longitudinal velocities below bankfull tend to follow the main channel side walls while the floodplain velocities are generally in the valley direction. Thus the floodplain flows pass over the main channel and induce a horizontal shear layer.
- 2) The energy loss due to secondary currents in the main channel is greater than for an equivalent simple channel and the currents rotate in the opposite sense

compared to inbank flows.

- 3) Fluid passes from the main channel onto the flood plain and back into the main channel in the following meander bend. Hence the proportion of discharge passed by the main channel and flood plain varies along a meander wavelength. These bulk exchanges of fluid between slow and fast moving regions of flow introduce extra flow resistance.
- 4) Flows on the flood plain outwith the meander belt are usually faster than those within the meander belt. It would appear that the extra flow resistance induced by the meandering main channel has a relatively small effect on the outer flood plain.

The following sections examine the topic of energy losses during inbank flow in channel bends and meanders. Although the main thrust of the work was to deal with overbank flow it is important to examine the inbank case as well. The transition from inbank to overbank flow is often the critical aspect of practical problems and it would be impossible to study it properly with out some knowledge of the characteristics of inbank flow.

## **5.6 Inbank meandering flow**

### **5.6.1 Background**

It has been recognised for many years that meandering can increase the effective resistance of channels significantly for inbank flows. Laboratory and theoretical investigations into the characteristics of flow in channel bends have shown that complicated flow structures form and that these can have a large effect on the discharge capacity of the channel.

Secondary or spiral currents are induced by differences in centripetal accelerations acting on a vertical column. The longitudinal velocities are greater for particles close to the water surface. This implies that the lateral forces on the water column are not in equilibrium and so lateral movements of particles are induced. The currents move towards the outside of the bend at the water surface and towards the inside at the

channel bed. These secondary currents also affect the water surface profile across the channel. In straight channels the water surface is uniform but in bends the surface is displaced and slopes down from the outside to the inside of the bend to balance the non-uniform lateral pressure distribution introduced by the secondary currents. These secondary currents affect the distribution of longitudinal flow within the channel cross section by advecting the faster moving fluid towards the outer bank. The flow distribution and associated longitudinal bed shear stresses becomes non-uniform across the channel. The secondary currents also induce a lateral component of bed shear stress which obviously increases the total shear stress acting on the bed.

The strength of such secondary currents is known to vary along a bend. In the case where a single bend has straight reaches both up and down-stream then it has been observed that there are no secondary currents at the inlet to the bend. The strength of the currents increases along the bend until they become fully developed and are then uniform until the bend exit is reached. The secondary currents persist in the straight reach down stream, becoming less and less intense with distance from the bend exit. Where the straight reaches between bends are not long enough to fully dissipate the secondary currents then the residual currents at the bend entrance can have a strong effect on the flow in the bend. The growth and decay of secondary currents has a strong influence on the flow distribution within a channel bend.

It is known that the bend tightness (radius of curvature/width) has a strong influence on the secondary currents described above. The tighter the bend then the more pronounced the secondary currents. Tight bends also induce zones of flow separation particularly against the inner bank. The effect of this is to introduce a 'dead zone' close to the inner bank in which there is no significant longitudinal flow. A shear layer is induced and large horizontal vortices are induced within the zone. The effective width of the bend is reduced and the effect of secondary currents in displacing the longitudinal flow outwards is enhanced.

The topography of a natural channel is formed by the typical discharges and sediments it passes. The size and shape of the channel varies both with discharge

and plan geometry. It is generally accepted that the important channel forming discharge for natural channels is close to the bankfull capacity of the channel. In straight channels the flow induces sediment movement which deepens and widens the channel until some equilibrium state is reached. The processes which induce the formation of river meanders are not well understood but it is likely that they are related to efficiency of the resulting geometry in terms of both discharge and sediment transport. That is to say the resulting geometry is the most efficient shape for passing the bankfull discharge and sediment load, Chang (1988).

Given that a meander has developed, then the secondary currents will develop up to some maximum strength and then decay away. These currents strongly affect the local bed shear stresses and form a channel cross section that varies strongly along the bend. At the entrance to the bend where the flow distribution and bed shear stresses are approximately uniform across the channel, the cross section is approximately rectangular or trapezoidal. The secondary currents tend to deepen the channel on the outside and transport the material towards the inside of the bend where the lower velocities allow it to settle out. Thus many natural bends exhibit deep pools at the outside banks with shallow regions along the inner banks. The pools are deepest and the shallow area widest at about, or just beyond, the apex of the bends. Although the shape of a channel varies along a meander it has been observed that the cross sectional area remains approximately constant throughout the bend.

### **5.6.2 Energy loss in channel bends**

It is apparent that the presence of bends in a channel will affect the discharge capacity of the channel. In straight channels the only significant loss mechanism is bed friction but in curved channels other loss mechanisms may also be important. It was decided to investigate the relative effect of bends on stage-discharge relationships. The inbank stage-discharge data from phase B of the FCF work was available and was used in the following work.

### 5.6.3 Methods of evaluating non-friction losses

The available data was collected for uniform flow conditions. The rate or gradient of energy dissipation along the channels was constant and can be assumed to be represented by the bed slope ( $S_o$ ). The total energy loss is composed of friction loss, bend losses and all other losses. The rate of energy dissipation induced by these various mechanisms are all assumed to be constant and the total energy gradient is the sum of the individual gradients. The friction gradient ( $S_f$ ) can be calculated from the Darcy equation,

$$S_f = f V^2 / (8 g R) \quad (5.3)$$

Subtracting the friction loss from the total loss gives the sum of all other losses. This can be represented by the difference between the total energy and friction gradients,  $S_o - S_f$ , or as a bend loss coefficient  $K_L$ , where

$$K_L = h_L / (V^2/2g) \quad (5.4)$$

in which  $h_L$  is the head loss through the bend. This can be evaluated as

$$h_L = (S_o - S_f) l \quad (5.5)$$

in which  $l$  is the length of the channel through the bend. The losses associated with bends can also be accounted for in terms of a resistance coefficient, most commonly Manning's  $n$ . The ratio of the value including bend losses ( $n'$ ) to the basic value ( $n$ ) can be expressed in terms of the energy gradients through Manning's equation, i.e.

$$(n'/n) = (S_o/S_f)^{1/2} \quad (5.6)$$

### 5.6.4 Data sets

The effect of meandering on flow resistance can be inferred from the stage-discharge

data obtained from the inbank Phase B experiments in the SERC Flood Channel Facility. Three sets of data are available, one for each of the geometries tested, i.e.

- the 60° meander geometry with trapezoidal cross-section,
- the 60° meander geometry with the natural cross-section, and
- the 110° meander geometry with the natural cross-section.

The measurements were all taken under uniform flow conditions (for the natural geometries the bed undulates considerably and uniformity is assumed to imply identical flow conditions at the same positions on successive bends).

### 5.6.5 Results and conclusions

For the 60° meander geometry with the trapezoidal cross-section the difference between total energy loss and friction loss can be wholly ascribed to effects associated with the meander planform. This loss has been calculated for each measured stage-discharge pair and expressed in each of the forms outlined above, Table 5.7. The bed slope of the channel is given by

$$S_o = S_{of} / s \tag{5.7}$$

in which  $S_{of}$  is the slope of the flume, and  $s$  is the channel sinuosity.

For the 60° meander geometry the slope of the flume was  $0.996 \times 10^{-3}$  and the sinuosity was 1.374, giving a channel slope of  $0.7248 \times 10^{-3}$ . The length of the channel through the bend,  $L$ , was assumed to be measured through half a meander wavelength, i.e. 8.245 m. This distance includes the straight section of channel at the cross-over.

Estimation of bend losses for the 60° meander geometry with the natural cross-section is complicated by the variation of the cross-section shape along the channel. The flow distortions associated with this variation can be expected to cause additional

energy losses, and so the difference between the average bed gradient and the friction gradient cannot be attributed to the effects of the meander planform alone. No experiments were performed with a straight channel with this natural geometry and the natural cross-section was about half the area of the trapezoidal one, so the losses associated with the meander planform and the cross-section variation cannot easily be separated.

Because the hydraulic radius varies along the channel the friction gradient, as calculated using equations 5.1 and 5.3, will also vary. A value of  $S_f$  at each of the defined cross-sections was therefore computed and an average obtained, weighted by the relative distances represented by each cross-section. For the 60° meander geometry the weighted average is given by

$$S_{fv} = ( 1.25 S_{f5} + 0.5745 ( S_{f4} + S_{f3} + S_{f2} + S_{f1} + S_{f0} ) ) / 4.1225 \quad (5.8)$$

in which  $S_{f5}$  is the value calculated for the cross-section at the cross-over and  $S_{f0}$  to  $S_{f4}$  are the values calculated at the cross-sections defined at equal displacements through the bend.

The water level was measured at the cross-over section only. When calculating flow areas and wetted perimeters at the other sections it was assumed that the water surface was linear, with a slope equal to the average channel slope of  $0.7248 \times 10^{-3}$ . This assumption is reasonable because the cross-sections were designed with a constant cross-sectional area. An energy balance between the crossover and apex sections for one discharge confirmed that the change in water level associated with the cross-section variation was negligible.

Each natural cross-section was compound, with a deep section and a horizontal berm. It was assumed for these calculations that the discharge in the channel was the sum of the discharges in the deep and berm sections, with any interaction between the two regions unaccounted for. The friction gradient is then given by

$$S_f = [ Q / ( A_d (8 g R_d / f_d)^{1/2} + A_b (8 g R_b / f_b)^{1/2} ) ]^2 \quad (5.9)$$

in which Q is the total discharge, A is the flow area, and the subscripts d and b refer to the deep and berm sections respectively.

The friction factors were calculated using the appropriate modified smooth law, see section 5.4. Equation 5.1 was modified slightly by expressing the velocity in the Reynolds number in terms of the friction gradient through equation 5.3, i.e.

$$1 / f^{1/2} = 2.02 \log ( ( 4 (8 g)^{1/2} / v ) R^{3/2} S_f^{1/2} ) - 1.38 \quad (5.10)$$

Equations 5.9 and 5.10 were solved iteratively to obtain the necessary values of  $S_f$  for each section and the average value then calculated by equation 5.8.

The non-friction losses for the 60° meander geometry with the natural cross-section are presented in Table 5.8. The losses represent the sum of those associated with curvature and the varying cross-section.

The losses for the 110° meander geometry with the natural cross-section were evaluated in the same way as for the 60° meander geometry with the natural cross-section. In this case the slope of the flume was  $1.021 \times 10^{-3}$  and the channel sinuosity was 2.043, and hence the bed slope was  $0.49972 \times 10^{-3}$ , by equation 5.7. The length of the channel through each bend, L, was 10.532 m. For this geometry there was no straight cross-over reach and the cross-sections were defined at equal displacements through the bend. The average friction slope was therefore calculated directly, without weighting.

The non-friction losses for the 110° meander geometry with the natural cross-section, which again include losses associated with channel curvature and varying cross-section, are presented in Table 5.9.

The mean values of  $S_o - S_f$ , K and  $n/n$  for the three cases are listed below. The

standard deviations are in brackets.

Channel	$S_o - S_f$ ( $\times 10^{-3}$ )	K	$n'/n$ ( $= (f'/f)^{1/2}$ )
60° trapezoidal	0.107 (0.032)	0.081 (0.026)	1.078 (0.029)
60° natural	0.236 (0.012)	0.415 (0.113)	1.217 (0.013)
110° natural	0.186 (0.005)	0.594 (0.108)	1.262 (0.010)

It is interesting to note that the standard deviations on the energy gradients are much less in the case of the natural cross-sections. This implies that the rate of energy dissipation due to bend effects is more uniform with stage for natural channels than for trapezoidal channels. These sections were designed to mimic typical natural rivers and so in real channels the bend losses may not vary as strongly with depth as in the case of trapezoidal or rectangular channels. By comparing the results for the two 60° geometries we can see that channel cross-section shape strongly affects the non-friction losses and that these are approximately twice as large for the natural channel as for the trapezoidal channel. The differences between the results for the 60° and 110° are less conclusive but the non-friction losses appear to vary with channel sinuosity.

In order to assess the significance of these extra losses the mean gradients above have been normalised by the total energy gradients and are quoted below. These results show that non-friction losses can be very significant. In the cases examined the non-friction losses formed between 15% to 40% of the total energy losses. It is impossible to draw general conclusions from these data but they do indicate that further investigation of non-friction losses in channel bends is required.

Channel	$(S_o - S_f) / S_o$
60° trapezoidal	0.15
60° natural	0.32
110° natural	0.37

### 5.6.6 Energy loss mechanisms in channel bends

The results presented above confirm that the presence of bends in open channel flows affect the energy loss compared to straight channels. The question which still remains to be answered is: How significant are these non-friction energy losses and what are the important parameters which affect them? The following authors have tried to identify and quantify the mechanisms which induce this extra flow resistance.

Shukry (1950) carried out a set of experiments in rectangular channel bends. He constructed single bends which turned through angles ( $\theta$ ) of  $90^\circ$ ,  $135^\circ$  and  $180^\circ$ . The experiments were conducted for depth to width ratios ( $y/B$ ) of 0.6, 0.8, 1.0 and 1.2 and also for bend radius to width ratios ( $r_f/B$ ) of 0.5, 1.0, 2.0 and 3.0. Shukry analyzed the extra energy loss induced by the presence of the bend using a bend loss coefficient ( $K_L$ ), defined as:

$$h_L = K_L (V^2/2g) \quad (5.11)$$

in which  $h_L$  is the head loss due to bends only, and  $V$  is the overall mean velocity. He showed that the bend loss coefficient is a function of:

- 1) The Reynolds number
- 2) Depth ratio ( $y/B$ )
- 3) Radius of curvature ( $r_f/b$ )
- 4) The angle subtended by the bend ( $\theta/180$ )

In addition he found that the proportion of these extra energy losses induced during development of the secondary currents were approximately constant at 40%.

Rozovskii (1957) published the seminal analytical work on flows in channel bends. He examines the theory of many of the mechanisms described above and compares predictions with both field and laboratory measurements. He identified the following sources of energy loss:

- 1) The redistribution of longitudinal flow across the channel
- 2) Energy lost in initiating secondary currents
- 3) Increased bed friction due to the secondary currents
- 4) Increased internal energy dissipation due to internal friction caused by the secondary currents
- 5) The redistribution of longitudinal flow in the vertical
- 6) Separation and the formation of eddy zones in sharp bends.

Rozovskii analyzed the energy dissipated by each of these mechanisms in a wide rectangular channel and concluded that the important mechanisms which significantly increase energy dissipation in bends are the increased bed and internal friction due to the secondary currents.

He provided the following expression for the extra energy losses:

$$h_L = (24 g^{1/2}/C + 60 g/C^2) (y/r_c)^2 (l/y) (V^2/2g) \quad (5.12)$$

where  $h_L$  is the total extra energy loss in a bend of length  $l$  and radius  $r_c$ .  $y$  is the flow depth,  $g$  the acceleration due to gravity,  $V$  is the average flow velocity and  $C$  is the Chezy bed friction parameter. This equation was derived assuming a logarithmic distribution of the longitudinal velocities in the vertical and that the secondary currents are fully developed. In general this analysis shows that the energy losses due to a bend increase with channel roughness and the squares of flow velocity and depth to radius ratio. Hence the tighter a bend, the larger the energy dissipated.

Much of Rozovskii's analysis was approximate: he was forced to make many assumptions and he concluded that further experimental and theoretical work is required.

Leopold et al (1960) explained the resistance behaviour of meandering channels by identifying three major types of resistance.

- 1) Skin resistance is associated with the surface roughness of the channel and varies with the square of the flow velocity.
- 2) Internal distortion resistance results from energy dissipation by eddies, secondary circulation and increased shear rate, wherever any boundary feature deflects part or all of the flow from its former direction. It will also vary with the square of the flow velocity.
- 3) Spill resistance is associated with local accelerations followed by sudden expansions in the flow and can be related to Froude number.

Leopold et al conducted experiments with inbank flows and moderately sinuous channels. They found that channel curvature could, by internal distortion, induce energy loss of the same order as that due to skin friction, and double that amount in tight curves. This type of loss could be related to radius of curvature of the bends and the ratio of channel width to radius.

Energy loss associated with spill resistance appears to be just as significant but only comes into effect at a critical value of Froude number (which is substantially less than 1.0). It appears that the Froude number at bankfull depth is generally less than this critical value in natural channels. This mechanism may be responsible for determining channel width by inducing bank erosion at its onset. It is unlikely to be a major loss mechanism for inbank flows in natural rivers and will be neglected.

Form resistance associated with flow around small-scale alluvial bed forms can be considered together with skin resistance by estimating a combined resistance coefficient. As noted by Onishi et al (1976), skin resistance is not independent of internal distortion and may be enhanced by the non-uniformity induced by secondary currents.

Internal distortion resistance results from energy dissipation by eddies, secondary circulation and increased shear rate wherever any boundary feature deflects part or all of the flow from its former direction. The secondary circulation induced by meandering is a major contributor to this type of resistance.

Onishi et al (1976) investigated inbank flows in meandering, alluvial channels. They attributed head loss to the following four categories of flow resistance.

- 1) Surface resistance or boundary stress, which may be enhanced by the nonuniform distribution induced by secondary currents.
- 2) Form drag, resulting from the unsymmetrical distribution of normal pressure around curves and deformations on the boundary. These losses are due primarily to separation but are also influenced by secondary currents. They depend on the Froude number, channel width, and the stream-wise and transverse non-uniformity of the channel geometry.
- 3) Superelevation, which causes additional asymmetry of the normal pressure distribution on walls and large scale bed forms, resulting in 'wave resistance'. These losses depend on the channel geometry and the Froude number.
- 4) Bed forms, in alluvial channels.

Onishi et al (1976) described the total loss due to bends using a bend loss coefficient, defined as:

$$h_L = K_L (V^2/2g) \quad (5.13)$$

in which  $h_L$  is the head loss due to bends only, and  $V$  is the overall mean velocity. They showed that this could be expressed as:

$$K_L = L / 4R_b (f_{bc} - f_{bs}) \quad (5.14)$$

in which  $L$  is the length of the bend,  $R_b$  is the bed hydraulic radius,  $f_{bc}$  is the bed friction factor for the meandering channel and  $f_{bs}$  is the bed friction factor for a similar but straight channel. The bed loss coefficient could be related to channel and flow characteristics by:

$$K_L = f ( V / (g R_b)^{0.5} , R_b/D_{50} , B/r_c ) \quad (5.15)$$

in which  $D_{50}$  is the median size of the bed material,  $B$  is the channel width and  $r_c$  is the centre-line radius of curvature.

The results obtained by Onishi et al showed  $K_L$  to be strongly dependent on the Froude number. In some cases  $K_L$  was negative, implying an energy gradient less than for corresponding straight channels. This was attributed to a relative decrease in bedform drag and possible decreases in wave resistance and boundary shear.

Hayat (1965) obtained value of  $K_L$  (as defined above) for meandering channels with rectangular cross-sections and rigid beds. In contrast to the alluvial channel results of Onishi et al (1976),  $K_L$  was found to be approximately constant with Froude number.

The variation of cross-sectional geometry along a channel has also been identified as a source of energy loss (e.g. Chow, 1959). Kazemipour and Apelt (1979, 1983), however, have shown that such irregularity contributes no additional energy loss provided that no flow separation or broken surges occur.

From the above it is apparent that the main sources of energy loss in channel bends are:

- 1) Bed friction
- 2) Increased bed friction due to secondary currents
- 3) Internal energy dissipation due to increased turbulence induced by secondary currents.

The energy loss in a bend has been found to depend on the following parameters

Bed roughness ( $f$ ,  $C$ ,  $n$  etc)

Flow depth ( $y$ )

Bend radius ( $r_c$ )

Length of bend ( $l$ ) or Angle of bend ( $\theta$ ,  $l = r_c \theta$ )

The cross-sectional shape of the channel.

Any general method for predicting flows in bends should account for these three processes and be formulated in terms of the five parameters above. Many methods have been identified in the literature. The majority of them have been derived empirically from laboratory data and may not include all of the important parameters. The following section describes methods which have been identified in the literature and in addition two methods have been modified to improve the predictions. The more promising of these methods are then applied to the available laboratory data.

### 5.6.7 Stage-discharge prediction methods

Although there is now better understanding of the mechanisms of energy loss, most hydraulics text books still recommend accounting for their effects together by a simple adjustment to the value of Manning's  $n$  for a similar but straight channel. Such adjustments have been proposed by Cowan (1956) and the Soil Conservation Service (1963). These methods are very similar and only the latest one is covered below.

#### The Soil Conservation Service (SCS) (1963) Method

The Soil Conservation Service (1963) proposed accounting for meander losses by adjusting the basic value of Manning's  $n$  on the basis of sinuosity ( $s$ ), as follows.

$$\begin{aligned} n'/n &= 1.0 && \text{for } s < 1.2 \\ n'/n &= 1.15 && \text{for } 1.2 \geq s < 1.5 \\ n'/n &= 1.30 && \text{for } s \geq 1.5 \end{aligned} \tag{5.16}$$

in which  $n'$  is the adjusted value and  $n$  is the basic value. Because  $n$  is proportional to  $f^{1/2}$ , the adjustment should be squared when using the Darcy-Weisbach equation.

#### The Linearized SCS (LSCS) Method

The step nature of the SCS recommendation introduces discontinuities at the limits of the defined sinuosity ranges, with consequent ambiguity and uncertainty. To overcome this problem the relationship has been linearized and is expressed as

$$\begin{aligned} n'/n &= (f'/f)^{1/2} = 0.43 s + 0.57 && \text{for } s < 1.7 \\ n'/n &= (f'/f)^{1/2} = 1.30 && \text{for } s \geq 1.7 \end{aligned} \quad (5.17)$$

in which  $f'$  is the adjusted Darcy-Weisbach friction factor.

### **The Method of Scobey (1933)**

On the basis of flume tests Scobey suggested that the value of Manning's  $n$  should be increased by 0.001 for each 20 degrees of curvature in 100 ft of channel. These recommendations are not expressed in terms of dimensionless channel characteristics and are unlikely to have consistent accuracy at different scales.

### **The Method of Mockmore (1944)**

Mockmore (1944) analyzed data from artificial channels and rivers for bend angles between 90° and 180° and proposed the relationship

$$h_L = (2 b/r_c) V^2 / 2g \quad (5.18)$$

in which  $h_L$  is the energy lost through a bend, in excess of the friction loss. The friction loss is obtained from normal hydraulic calculations, eg the Darcy-Weisbach equation, i.e.

$$V = (8 g R S_f / f)^{1/2} \quad (5.19)$$

in which  $g$  is gravitational acceleration,  $R$  is the hydraulic radius of the cross-section,  $S_f$  is the energy gradient, and  $f$  is the friction factor. For uniform flow  $S_f$  can be

equated to  $S_o$ , the bed gradient. The energy loss due to friction along a length of channel  $l$  is given by:

$$h_f = (f l / 4 R) V^2 / 2g \quad (5.20)$$

Combining these gives the total head loss:

$$h_L + h_f = ((f l / 4 R) + 2B / r_c) V^2 / 2g \quad (5.21)$$

on re-arranging this becomes :

$$h_L + h_f = (f + 8 R B / l r_c) (l / 4 R) V^2 / 2g \quad (5.22)$$

by comparing with equation 5.19 it is apparent that the extra bend head losses can be considered as an adjustment to the straight channel friction factor with

$$f' = f + 8 R B / l r_c \quad (5.23)$$

This form of the method is easier to apply to stage-discharge data from meandering channels where a bed friction calibration for an equivalent straight channel is available.

### **The Method of Leopold et al (1960)**

From a set of laboratory experiments carried out on meandering channels formed in sand Leopold et al (1960) presented a graphical relationship between the ratio of the additional boundary shear induced by channel curvature ( $\tau_i$ ) to the boundary shear associated with friction ( $\tau_s$ ) and the ratio of flow width ( $B$ ) to mean radius of curvature ( $r_c$ ). This can be expressed as

$$\tau_i / \tau_s = 2.632 (B/r_c) - 0.526 \quad (5.24)$$

and applies below a critical value of Froude number (approximately 0.5). At higher Froude numbers the additional shear was a function of Froude number. By relating boundary shear stresses to velocity, equation 5.24 can be interpreted as an adjustment to the friction factor as follows. The basic Darcy equation relates shear stress to the square of velocity with the coefficient  $f$ :

$$\tau = \rho f V^2 / 2g \quad (5.25)$$

Assuming that the total shear stress is composed of the two components defined and that each component has a corresponding friction factor then equation 5.24 becomes

$$f_i/f = 2.632 (B/r_c) - 0.526 \quad (5.26)$$

the total friction factor is given by

$$f' = f + f_i \quad (5.27)$$

rearranging and dividing by  $f$  gives

$$f_i / f = f' / f - 1 \quad (5.28)$$

substituting in equation 5.26 gives

$$f' / f = 2.632 (B / r_c) + 0.474 \quad (5.29)$$

### **The Toebes and Sooky (1967) Method**

From experimental results in a small laboratory channel with a sinuosity of 1.09, Toebes and Sooky (1967) proposed an adjustment to  $f$ . Below a critical value of the Froude number the adjustment depends solely on the hydraulic radius (in metres) according to

$$f' / f = 1.0 + 6.89 R \quad (5.30)$$

They confirmed the conclusions of Leopold et al that above the critical Froude number the increase in losses due to channel curvature is a function of Froude number. The critical value of the Froude number was found to depend on hydraulic radius but was not exceeded in any of the applications reported here.

#### **The Method of Agarwal et al (1984)**

Agarwal et al (1984) performed a regression analysis on previously published data from alluvial channels to define a correction for bend losses. The actual flow velocity is determined by dividing the velocity calculated according to Ranga Raju's (1970) resistance law by  $\xi$  where:

$$\xi = 2.16 f_{*R}^{-0.042} \quad (5.31)$$

with

$$f_{*R} = \text{Re} (\theta / 180^\circ)^{-4.65} (b / y)^{1.11} (r_m / b)^{1.38} \text{Fr}^{9.29} \quad (5.32)$$

in which  $\theta$  is the bend angle,  $y$  is the flow depth,  $\text{Fr}$  is the Froude number, in terms of the hydraulic radius, i.e.  $V / (gR)^{1/2}$ , and  $\text{Re}$  is the Reynolds number,  $(4RV / \nu)$ , where  $\nu$  is the kinematic viscosity.

Ranga Raju's (1970) resistance law is intended for use in alluvial channels. The adjustment for bend losses is independent of the friction loss computation and it is assumed that it applies to rigid boundary channels as well, with any appropriate resistance law. It is unclear whether  $\text{Re}$  and  $\text{Fr}$  in equation 5.32 are in terms of the actual velocity or that calculated from friction losses only, and the latter has been assumed.

#### **The Method of Pacheco-Ceballos (1983)**

Pacheco-Ceballos (1983) re-analyzed the results collected by Shukry (1950). He

related the head loss due to the bend to the velocity at the bend entrance. Other authors express head loss in terms of the average velocity through the bend. By assuming that the lateral distribution of velocity within the bend follows the free vortex profile he produced the following equation for  $K_L$ :

$$K_L = ( y_1 - y_m + V_1^2 / 2g - ( N y^2 V^2 / y_m^2 2g ) ) 2g / V^2 \quad (5.33)$$

Where  $y_1$  and  $V_1$  are the flow depth and velocity in an equivalent straight channel;  $y$  and  $V$  are the flow depth and velocity at the bend entrance and  $y_m$  is the average depth at the position along the bend where the secondary flow becomes fully developed.  $N$  is a parameter related to free vortex flow:

$$N = [ ( \ln r_o / r_i )^2 r_o r_i / B^2 ]^{-1} \quad (5.34)$$

where  $r_o$  and  $r_i$  are the radii of the outer and inner channel banks. The term  $y_1 - y_m$  in equation 5.33 is approximated by :

$$\log (y_1 - y_m) = 2.11 V - ( \phi + 0.7 r_c / B - 0.06(r_c / B)^2 + y ) \quad (5.35)$$

$\phi$  is a parameter which varies with the bend angle ( $\theta$ ). For Shukry's bends of 45°, 90° and 180° it has values 2.98, 2.70 and 2.64 respectively. Intermediate values can be obtained by interpolation.

### **The Method of Chang (1983)**

Chang (1983) derived a general analytical model for the rate of energy expenditure per unit channel length associated with transverse flow. This model is based on the conceptual model developed by Rozovskii (1957) and assumes that the extra energy loss is due to increased bed friction and internal turbulence related to the secondary currents. Chang (1983) assumed a power law for the vertical distribution of longitudinal velocity. This gave a different expression for the secondary current compared to Rozovskii's.

For the case of a wide rectangular channel where super elevation and the lateral variation of secondary currents are small, Chang approximated the secondary currents with a linear distribution and produced a simplified expression for the energy loss in a bend where the secondary currents are fully developed.

$$S'' = \left( \frac{2.86 f^{1/2} + 2.07 f}{0.565 + f^{1/2}} \right) \left( \frac{y}{r_c} \right)^2 Fr^2 \quad (5.36)$$

in which  $S''$  is the energy gradient associated with transverse flow ( $h_t/l$ ), for uniform flow.

$$S_o - S_f = S''$$

or

$$1 - S_f / S_o = S'' / S_o \quad (5.37)$$

since the rates of energy loss are linearly dependent on the friction factors

$$1 - S_f / S_o = 1 - f / f' \quad (5.38)$$

Rearranging and substituting it is possible to see that Chang's (1983) method can be interpreted as an adjustment to the basic straight channel friction factor.

$$f'/f = 1 / (1 - S'' / S_o) \quad (5.39)$$

Chang (1988) reports a slightly different form of equation 5.36

$$S'' = \left( \frac{2.07 f + 4.68 f^{1/2} - 1.83 f^{3/2}}{0.565 + f^{1/2}} \right) \left( \frac{y}{r_c} \right)^2 Fr^2 \quad (5.40)$$

However both forms were found to give very similar results in preliminary calculations and the simpler equation 5.36 has been used throughout.

## The Modified Chang Method

Chang's (1983) method was developed for wide, rectangular channels. Because most rivers and flood channels have large width to depth ratios this was not considered a major limitation, but the effect of shape warrants investigation at a later stage to confirm the method's validity.

Chang's (1983) method also assumes that secondary circulation is fully developed. In fact, the circulation takes considerable distance to develop through a bend and begins to decay once the channel straightens out. For meanders, the circulation must reverse between successive bends and the associated energy gradient must drop to zero at two points over each wavelength. The average energy gradient associated with secondary circulation along the channel must therefore be substantially less than predicted assuming full development. Rozovskii (1957) studied this growth and decay of secondary currents analytically. He assumed that the distribution of the circulations remains constant during the process of decay. He showed that the angle of bend required for the secondary currents to become fully developed is:

$$\theta = 2.3 C y / (g^{1/2} r_c) \quad (5.41)$$

where  $C$  is the Chezy coefficient. This can be written in terms of Darcy  $f$ :

$$\theta = 6.5 y / (f^{1/2} r_c) \quad (5.42)$$

The corresponding length of channel required for fully developed secondary currents is

$$l_c = 6.5 y / f^{1/2} \quad (5.43)$$

Applying this criterion to the SERC channel geometry showed that under some flow conditions the circulation would never develop fully. Significantly, the degree of development varied greatly with stage in the same channel. For example, for the 60°

trapezoidal channel, secondary circulation would be fully developed only after  $152^\circ$  of curvature at bankfull and after  $54^\circ$  for a flow depth of 0.06 m, which is approximately the lowest depth tested. The curvature of each bend in this geometry is  $120^\circ$ , so secondary circulation would probably be fully developed over a considerable proportion of the channel length at low stages, but not at all at relatively high stages.

Chang (1984) accounted for the effects of growth and decay of secondary circulation by applying his full secondary circulation loss model together with nonuniform flow calculations to predict the distribution of losses and boundary shear stresses, as well as water levels through bends. This requires integration of stream-wise and transverse velocities at each computational section and would be impractical to use. As an alternative, his approach was simplified to apply to uniform flow through a sequence of identically repeated meanders. Because the energy gradient varies with the growth and decay of secondary circulation, flow can not actually be uniform. Also the bed slope is unlikely to be constant; it will vary over a meander wavelength even for idealized laboratory meanders. The assumption of uniformity is therefore a simplification, but the primary velocity and flow depth will not vary greatly. For determining the effective resistance in meandering channels average conditions are sufficient and minor departures from uniformity are unlikely to influence the conclusions. This approach enables a correction factor to be computed which can be applied to the energy gradient predicted by his wide-rectangular equation (5.44), to account for growth and decay of circulation.

Chang (1983) presented an Equation for the energy gradient associated with fully developed transverse circulation,  $S''_{fd}$ .

$$S'' = \left( \frac{2.86 f^{1/2} + 2.07 f}{0.565 + f^{1/2}} \right) \left( \frac{y}{r_c} \right)^2 Fr^2 \quad (5.44)$$

It is assumed, as by Chang (1984), that the pattern of secondary circulation remains constant during growth and decay. The strength of the circulation, and its variation, can then be represented by the transverse velocity at one position on the profile, and particularly at the water surface at the centre of the channel. If it is further assumed that the local value of energy gradient associated with secondary circulation,  $S''$ , is proportional to transverse velocity (longitudinal velocity is constant by the uniformity assumption), then  $S''$  can be related to the fully developed value by

$$S'' = S''_{fd} (v_{rc} / v_{rc\ fd}) \quad (5.45)$$

in which  $v_{rc}$  is the transverse velocity at the water surface in the centre of the channel, and the subscript fd denotes the fully developed value. Similarly, the average value of  $S''$  through a meander wavelength is given by

$$S''_{ave} = S''_{fd} (v_{rc\ ave} / v_{rc\ fd}) \quad (5.46)$$

In equation 5.46  $v_{rc\ ave}$  is the average of absolute values because the sense of  $v_{rc}$  reverses between successive bends.

The total gradient of energy losses is the sum of friction gradient ( $S_f$ ) and the secondary circulation loss gradient (it is assumed here that there are no other sources of energy loss, or that these are accounted for in the basic friction factor). Under uniform flow conditions the total gradient of losses is equal to the bed gradient  $S_o$ , and  $S''$  can be represented by  $S''_{ave}$ . Therefore

$$S_f + S''_{ave} = S_o \quad (5.47)$$

$S_f$  can be estimated using the Darcy-Weisbach Equation, i.e.

$$S_f = (f V^2)/(8 g R) \quad (5.48)$$

in which  $V$  is the mean flow velocity and  $R$  is the hydraulic radius.

Substituting equation 5.48 for  $S_f$  and equation 5.46 for  $S''_{ave}$  in equation 5.47 and rearranging gives

$$V = ( (g S_o) / ( (f/(8R) ) + K ) )^{1/2} \quad (5.49)$$

with

$$K = ( (2.86 f^{1/2} + 2.07 f) / (0.565 + f^{1/2}) ) (y/r_c)^2 (B/A) (v_{rc\ ave}/v_{rc\ fd})$$

in which  $A$  is the cross-sectional area and  $B$  is the surface width of the flow.

Equation 5.49 can also be expressed as:

$$V = ((8 g R S_o)/f')^{1/2}$$

with

$$f' = f / (1 - S''_{ave}/S_o) \quad (5.50)$$

For evaluation of equation 5.49 or 5.50,  $v_{rc\ fd}$  can be calculated from the equation for the distribution of transverse velocity ( $v_r$ ) under fully developed conditions given by Kikkewa et al (1976), i.e.

$$v_r/V = F^2 (y/r) (1/\kappa) ( F_1(z/y) - (1/\kappa) (V_* / V) F_2(z/y) ) \quad (5.51)$$

with

$$F = ((y/y_c)(r/r))^{1/2}$$

$$F_1(z/y) = - 15( (z/y)^2 \ln(z/y) - 1/2 (z/y)^2 + 15/24 )$$

$$F_2(z/y) = 15/2 ( (z/y)^2 \ln(z/y) - (z/y)^2 \ln(z/y) + 1/2 (z/y)^2 - 19/54 )$$

in which  $\kappa$  is the von Karman constant,  $V_*$  is the shear velocity,  $y_c$  is the flow depth at the channel centre,  $z$  is the vertical direction, and  $r$  is the radial direction.

At the channel centre  $y = y_c$  and at the water surface  $z = y$ , and so  $F = 1$ ,  $F_1 = 10/3$ ,

and  $F_2 = 10/9$ . Substituting these values in equation 5.51 gives the fully developed transverse velocity at the water surface at the channel centre,

$$v_{rc\ fd}/V = (y/r_c)(1/\kappa)(10/3 - (1/\kappa)(V_* / V)(10/9)) \quad (5.52)$$

The von Karman constant has a value of 0.4 and the shear velocity can be determined by:

$$V_* = (g R S_f)^{1/2} \quad (5.53)$$

with  $S_f = S_o$  for uniform flow.

The average surface transverse velocity,  $v_{rc\ ave}$  is also required for evaluating equations 5.49 and 5.50. Chang (1984) presented an equation for computing the transverse velocity at the water surface along the centre line through a bend. The velocity is computed at discrete cross sections along the channel, and the value at any section is related to that at the preceding section by

$$(v_{rc})_{j+1} = (v_{rc})_j + (f/2)^{1/2} (10/3 - (1/\kappa)(5/9)(f/2)^{1/2}) (V/r) \exp(-(\kappa/y)(f/2)^{1/2} \Delta s) \Delta s \quad (5.54)$$

in which the subscript  $j$  is the cross section index, and  $\Delta s$  is the distance between sections  $j$  and  $j + 1$ .

Equation 5.54 includes two terms, one describing the growth and the other the decay of secondary circulation. The full equation applies to flow through a bend but along a straight reach after a bend only the decay term applies and

$$(v_{rc})_{j+1} = (v_{rc})_j \exp(-(\kappa/y)(f/2)^{1/2} \Delta s) \quad (5.55)$$

Calculation of  $v_{rc\ ave}$  requires solution of equations 5.54 and 5.55, with  $V$  given by equation 5.49 or 5.50 and  $v_{rc\ fd}$  is obtained from equation 5.52. Because of the implicit nature of this set of equations the solution is iterative and is obtained as follows.

- 1) A first estimate of the mean velocity is calculated neglecting losses associated with secondary circulation, using the Darcy-Weisbach equation and an appropriate formula for the friction factor.
- 2) This velocity and  $(v_{rc})_1 = 0$  are used in equations 5.54 and 5.55 to compute an initial distribution of  $v_{rc}$  through one complete meander wavelength.
- 3) The value of  $v_{rc}$  at the last section is substituted for  $(v_{rc})_1$  and the distribution is recomputed iteratively until the value of  $v_{rc}$  at the first and last sections are identical, within a specified tolerance. This corresponds to uniform conditions through a series of identical meanders.
- 4) The average value of absolute  $v_{rc}$  through the wavelength is calculated as

$$(v_{rc})_{ave} = (\sum v_{rc} \Delta s) / (\sum \Delta s) \quad (5.56)$$

- 5) The mean flow velocity is recalculated, accounting for losses associated with secondary circulation, using equation 5.49 or 5.50.
- 6) The recalculated mean velocity is then used in equations 5.54 and 5.55 to compute a new distribution of  $v_{rc}$  through the wavelength.
- 7) This procedure is repeated until the recalculated mean velocity is the same as the previous one, within a specified tolerance.

This method is obviously not suitable for direct application in practice, but could be applied to different hypothetical situations to develop relationships between  $S''_{ave}$  and geometric and hydraulic parameters. This would provide a method for estimating head losses without the limitations of the LSCS method.

## 5.7 Application of prediction methods

### 5.7.1 The Methods

Various methods have been identified for accounting for the additional resistance to flow induced by channel curvature. These are as proposed by :

Scobey (1933)

Cowan (1956)  
Soil Conservation Service (SCS) (1963)  
Toebe and Sooky (1967)  
Leopold et al (1960)  
Shukry (1950)  
Mockmore (1944)  
Onishi et al (1976)  
Agarwal et al (1984)  
Rozovskii (1957)  
Chang (1983)  
Chang (1988)  
Pacheco-Ceballos (1983)

Some of these were not considered further for various reasons. Scobey's method gave unrealistic predictions for the data sets used, probably because it is not expressed in terms of dimensionless variables and suffers from scale effects. Cowan's approach is similar to the SCS method, which allows better quantitative description of channel characteristics. Shukry's method could not be applied to the data sets available because his curves for some parameters did not extend to these conditions. The method proposed by Onishi et al was intended for mobile bed channels and requires specification of sediment size; it is therefore not appropriate for the conditions under which the available data sets were obtained. Rozovskii's Equation is very similar to Chang's and it was not thought worthwhile to consider both. Chang's equation produced better results in preliminary applications and is also extended in subsequent publications; it was therefore selected in preference to Rozovskii's. Chang's 1983 and 1988 equations are virtually identical and the 1988 version was rejected as it performed slightly worse in the preliminary applications. The method of Pacheco-Ceballos is difficult to apply and has not been considered at this stage. Thus the following methods have been considered:

Soil Conservation Service (SCS) (1967)  
Toebe and Sooky (1967)

Leopold et al (1960)  
Mockmore (1944)  
Agarwal et al (1984)  
Chang (1983)  
Modified Chang (1984)  
Linearized Soil Conservation Service (LSCS)

To demonstrate the effect of meandering on channel conveyance and to provide a basis for comparison of the other methods, stage-discharge relationships were calculated ignoring non-friction losses.

### Friction loss only

For a given stage the discharge is given by

$$Q = A V \quad (5.57)$$

in which  $A$  is the cross-sectional area and  $V$  is the flow velocity, given by the Darcy-Weisbach equation, i.e.

$$V = (8 g R S_f / f)^{1/2} \quad (5.58)$$

in which  $g$  is gravitational acceleration,  $R$  is the hydraulic radius of the cross-section,  $S_f$  is the energy gradient, and  $f$  is the friction factor. For uniform flow  $S_f$  can be equated to  $S_o$ , the bed gradient.

### 5.7.2 Data set

The selected prediction methods were applied to the following three sets of data, none of which were used in the development of any of the methods.

- 1) A full inbank stage-discharge relationship for a trapezoidal channel

constructed in the SERC Flood Facility at HR Wallingford, UK. This channel had a base width of 0.90 m, side slopes of 45°, a depth of 150 mm and a bed gradient of 0.00073. The sinuosity was 1.374 and four complete meanders were installed.

- 2) Full stage-discharge relationships for trapezoidal channels at the University of Aberdeen (Willetts, personal communication). These channels all had base widths of 139 mm, side slopes of 71°, and depths of 50 mm. Sinuosities were 1.21, 1.41 and 2.043 with bed slopes of 0.00083, 0.00071, and 0.00030 respectively.
- 3) Bankfull discharges for trapezoidal channels measured by the US Army Corps of Engineers at the Waterways Experiment Station, Vicksburg. The channels had side slopes of 63°, depths of 0.152 m and base widths of either 0.305 m or 0.610 m. For the wide channel sinuosities of 1.20, 1.40 and 1.57 were tested. For the narrow channel the sinuosities tested were 1.17, 1.22, 1.33, 1.49, 1.50, 1.75 and 2.54. In all cases the valley slope was 0.001. Full details of the channels and experiments are reported by the US Army Corps of Engineers (1956).

### 5.7.3 Results and conclusions

Each of the methods described above was applied to predict the discharge for every flow condition in these data sets. The friction factor for the SERC and Aberdeen channels varied with Reynolds number and were calculated by the appropriate modified smooth law, see section 5.4. This required that the equations representing the different methods be solved iteratively. There were no data to establish variations of friction factor for the Vicksburg channels, and a constant value for each channel type was calculated from the bankfull flows in the corresponding straight channel.

The percentatge error in each prediction was calculated as:

$$\%Error = 100 (Q_p - Q_m) / Q_m$$

where  $Q_p$  is the predicted discharge and  $Q_m$  is the measured discharge. The average error and standard deviation of errors for each data set and for all the data together, are listed for each method in Table 5.10. Two values were computed for some of the Vicksburg data with the SCS Method. This was because the sinuosities fell on the thresholds of the correction factor defined by equation 5.16. Values on either side of the thresholds were used and averages including both results presented. The first column gives the error obtained by ignoring bend losses and therefore gives an indication of the effect of meandering on resistance.

In terms of average error and the standard deviation of errors, the Modified Chang and SCS Methods appear to perform best with mean errors within the range -5% to +5% and standard deviations of less than 10%. Ignoring the energy loss induced by meandering gives unacceptably high errors in the prediction of discharge for inbank flows. Of the methods considered, those of Agarwal et al (1984), Mockmore (1944) and Chang (1983) appear to be unsatisfactory. The Chang methods are the only methods with a sound theoretical base, but the Modified Chang Method is not easy to apply in its present form. All the other methods are empirical and based largely on laboratory data; their generality is therefore not assured.

The overall performance of the SCS method is surprisingly good, and suggests that adjusting Manning's  $n$  by a factor related simply to sinuosity is reasonable. The relationship between the adjustment factor and sinuosity as recommended by SCS and as derived from the data used here is shown in Figure 5.11. (The values derived from the data are approximate. They were calculated from the discharges as measured and as calculated assuming friction loss only. The variation of friction coefficient with Reynolds number as bend losses are introduced are therefore not accounted for.)

One undesirable feature of the SCS recommendation is that it is a step function. The consequences of this are apparent in the prediction of the Vicksburg channel discharges. For the wide channel with a sinuosity of 1.2 the error is 30.71% or 13.66%, depending on which side of the step the sinuosity is assumed to lie.

Similarly, for the narrow channel with sinuosity of 1.50 the error could be -8.10% or -18.71%. It would obviously be advisable to replace the SCS step function with a smooth curve. It is difficult to know where this curve should lie because the data are fairly spread out. One reason for the data spread is that bend losses are not caused by sinuosity per se, but rather by the degree of curvature. This is well demonstrated by the Vicksburg narrow channel data for sinuosities of 1.49 and 1.50. Although the sinuosities are almost identical, the bends in the 1.49 sinuosity channel are tighter, with longer straight reaches between bends. The tighter bends cause greater energy loss and the adjustment factor is 1.23, compared with 1.06 for the other, more gently curving channel. This effect is accounted for by the Modified Chang Method, as shown in Figure 5.12 where it was used to compute the adjustment factor for each data point. The spread of the predicted values is still considerable, confirming that it is associated with factors not accounted for by sinuosity alone, rather than experimental scatter. The range bars for the SERC and Aberdeen data points in Figures 5.11 and 5.12 show that the adjustment factor also varies considerably with stage, and that this is reproduced by the Modified Chang Method. It is therefore not entirely satisfactory to account for bend losses in meandering channels in terms of sinuosity alone. A more reliable adjustment function in terms of radius of curvature and bend angle could be determined using the Modified Chang Method in hypothetical applications.

Using the SCS method as it stands would not lead to major errors, however. To make it more satisfactory, the steps in the relationship could be eliminated by using the curve shown in Figure 5.12, although the inherent limitations remain. This has been done and the resulting method is referred to as the Linearized Soil Conservation Service method (LSCS). Prediction errors using this linearization are listed in Table 5.10 in the column headed LSCS Method, These reduced errors show that the linearized version is superior.

The following limitations remain with a relationship between an adjustment to Manning's  $n$  and sinuosity.

- 1) It cannot account for the variation of the adjustment with stage and radius of curvature.
- 2) It cannot account for the effects of cross-sectional shape. This can be significant, as shown by the SERC results : the ratio of total to friction losses in terms of Manning's  $n$  for the 1.37 sinuosity channel was 1.078 with a trapezoidal section and 1.22 with a pseudo-natural section.
- 3) An adjusted  $n$  value is useful for rivers and other channels with fairly uniform planforms which can be characterised by sinuosity. In many cases the planform is irregular and it would be preferable to account for losses in individual bends separately in non-uniform profile computations.

The relationship between bend radius and sinuosity is probably not highly variable in natural rivers, however, and this may not be cause for concern. The same comment applies to artificial channels designed in accordance with regime relationships.

Chang's theory could be applied to address these issues directly. The form used in this study already accounts for stage and bend radius effects. The complete form (Chang, 1984) would account for cross-sectional shape effects (but probably not for variations of cross-section along a reach). It would not be necessary to simulate the flow through each bend using the full theory. Rather, the theory could be used to generate general corrections to  $n$ , or preferably to the Darcy-Weisbach  $f$ , to account for these effects. It could also be used to develop a general relationship for the loss coefficient for single bends.

## **5.8 Conclusions**

- 1) A literature review of overbank flow in meandering compound channels has been carried out (5.2). The main purposes of this review were:
  - a) To identify laboratory data to use in developing and verifying a new procedure for discharge estimation in overbank flow in meandering

channels.

- b) To summarize the current state of knowledge on the detailed flow structures present during overbank meandering flow and to gauge the effect these might have on the discharge capacity of the channel.
- 2) Eight laboratory investigations were identified, including the SERC FCF (Section 5.2). The two most recent and extensive data sets (SERC FCF and Aberdeen) were considered to represent the best quality data available and it was decided to use these two sets in developing a new procedure for estimating the conveyance of meandering compound channels. Three other investigations (Vicksburg, Kiely and Sooky) were deemed appropriate to use in verification of the new procedure.
- 3) The internal structure of currents during overbank flows has been found to be highly complex. The most important observations are:
- a) The longitudinal velocities below bankfull tend to follow the main channel side walls while the floodplain velocities are generally in the valley direction. Thus the floodplain flows pass over the main channel and induce a horizontal shear layer.
  - b) The energy loss due to secondary currents in the main channel is greater than for an equivalent simple channel and the currents rotate in the opposite sense compared to inbank flows.
  - c) Fluid passes from the main channel onto the flood plain and back into the main channel in the following meander bend. Hence the proportion of discharge passed by the main channel and flood plain varies along a meander wavelength. These bulk exchanges of fluid between slow and fast moving regions of flow introduce extra flow resistance.

- d) Flows on the flood plain outwith the meander belt are usually faster than those within the meander belt. It would appear that the extra flow resistance induced by the meandering main channel has a relatively small effect on the outer flood plain.
- 4) The behaviour of flow in meandering channels during inbank flow has been investigated using the SERC FCF Phase B data (5.6.3 and 5.6.4). The relative strengths of the bed friction and non-friction energy loss mechanisms were calculated for the three sets of inbank stage-discharges.
- 5) The non-friction losses were found to vary both with channel sinuosity and cross-sectional geometry (5.6.5). The 'natural' channel cross-sections induce approximately twice as much non-friction loss as the equivalent trapezoidal channel.
- 6) A literature search was carried out to identify the important processes which induce this extra flow resistance to flows in channel bends (5.6.7). The main sources of flow resistance in a channel bend are:
- a) bed friction;
  - b) increased bed friction due to secondary currents
  - c) internal energy dissipation due to increased turbulence induced by secondary currents.
- 7) The flow resistance in a bend depends on:
- a) bed roughness ( $f$ ,  $C_n$  etc);
  - b) flow depth ( $y$ );
  - c) bend radius ( $r_c$ );
  - d) length of bend ( $l$ ) or angle of bend ( $\theta$ ,  $l = r_c \theta$ );
  - e) The cross-sectional shape of the channel and its variation along the length of the channel.

- 8) Flow resistance in a set of meander bends is likely to differ from the resistance induced by a single bend in an otherwise straight channel, due to the interaction (growth and decay) between the secondary currents induced in the individual bends.
- 9) Various methods which account for the extra flow resistance were identified in the literature and a selection of methods were applied to the available laboratory data (5.7.2).
- 10) The methods were evaluated by comparing the mean errors in predicted discharge. The SCS method was found to give acceptable results for most practical purposes even though it does not account for the important mechanisms explicitly (5.7.3).
- 11) An improved version of the SCS method was formulated to remove the undesirable step function (LSCS) and this linearized version gave better predictions. Although these methods, which adjust Manning's  $n$  based on the channel sinuosity, gave acceptable results they are empirical and their generality is not assured (5.7.2 and 5.7.3).
- 12) Chang's approach, in explicitly modelling the resistances due to secondary currents combined with backwater calculations along the channel, is based on sound theoretical considerations. This approach is applicable to both single bends and series of meanders and further work should be carried out to prove it against more general cases (5.7.3).

## CHAPTER 6

### DISCHARGE ESTIMATION IN MEANDERING COMPOUND CHANNELS

#### 6.1 Introduction

The purpose of this Chapter is to devise a new and robust method for discharge estimation in meandering compound channels. The previous chapter reviewed the previous laboratory work which has been carried out into meandering compound channels, and identified some important mechanisms which affect the discharge capacity of these channels. Earlier chapters reviewed similar work for straight compound channels and some of these methods for calculating discharge in straight compound channels were applied to a selection of the meandering channel data collected during Phase B of the SERC FCF work. The purpose of this was to confirm that straight channel methods are inappropriate for use when analyzing meandering channels with overbank flow.

A further literature review is presented covering proposed methods of calculating discharges in meandering compound channels. A promising method is then developed on the basis of the SERC FCF Phase B data and data from the University of Aberdeen. These methods are then tested and verified against a range of other laboratory and field data.

#### 6.2 Application of straight channel methods to meandering data.

##### 6.2.1 The methods

The methods used in this work are listed below. These are simple methods which are practical to apply by hand. The Lateral Distribution Method which was found to give good results for straight channels has not been included in this assessment since it is a computational model and the research programme put a high priority on hand calculation methods. The various composite roughness methods have not been included here since their performance against straight channel data was poor.

DCM            Divided Channel Method, using vertical division lines which are

included in the wetted perimeter of the main channel but omitted from the wetted perimeter of the floodplains. Main channel slope used for main channel flow.

- SCM Single Channel Method, using main channel slope.
- SSGM Sum of Segments Method. Main channel slope used for main channel segments.
- DCM2 Divided Channel Method, using vertical division lines which are not included in the wetted perimeter of either the main channel or the floodplains.  
Main channel slope used for main channel flow.
- FCFAM Method developed by Ackers, based on Flood Channel Facility Phase A data. Main channel slope used for main channel flow.
- HOR1 Divided Channel Method, using a horizontal division line at bankfull stage. Division line is included in floodplain wetted perimeter but not in main channel wetted perimeter. Floodplain slope used for main channel and floodplain flows.
- HOR2 Divided Channel Method, using a horizontal division line at bankfull stage. Division line is included in floodplain and main channel wetted perimeters.  
Floodplain slope used for main channel and floodplain flows.
- HOR3 Divided Channel Method, using a horizontal division line at bankfull stage. Division line is included in floodplain wetted perimeter but not in main channel wetted perimeter. Main channel slope used for main channel flow.
- HOR4 Divided Channel Method, using a horizontal division line at bankfull stage. Division line is included in floodplain and main channel wetted perimeters. Main channel slope used for main channel flow.

The two divided channel methods (DCM and DCM2); the single channel method (SCM); the sum of segments method (SSGM) and the FCFAM method (ACKM) were all applied as described above. These are the standard simple methods which could be used to calculate flows in compound channels. The various horizontal

division line methods (HOR1, HOR2, HOR3, HOR4) are simplifications of the methods proposed by Toebees and Sooky (1967) and Smith (1977). The main channel and floodplains are considered to be split by a horizontal line at bankfull level. The region above the dividing line is included in the floodplain area when calculating the floodplain flow. The sinuosity of a meandering channel is the ratio of the curvilinear distance along the channel to the straight distance between the two points.

### **6.2.2 The data set**

The SERC FCF Phase B stage-discharge test programme is summarized in Table 5.1 and the results of stage and discharge are presented in detail in Appendix 5. Of this data series numbers B32, B33, B46 and B48 have been excluded from this analysis for the following reasons.

- B32, B46 Floodplain roughened with rows of isolated breeze blocks, special methods must be used to account for the head losses due to these blocks.
- B33 Floodplain only partially roughened. The roughness zones were limited to the 'meander belt', creating two distinct roughness regions on the floodplains. The methods described above are suitable for floodplains which are homogeneously roughened.
- B48 Floodplains are totally blocked by breeze block walls which run from the inner bend apices to the outer edge of the floodplain. This simulates the case were development has occurred over the whole floodplain. Again the simple methods used here are not suitable for this geometry.

The series B21, B26, B31, B34, B39, B43 and B47 from Phase B of the FCF were all analyzed using the methods described above. In total 107 data points were used in this analysis. The full details of the experiments are given in Section 5.2. The bed friction terms for the various tests were calculated using a modified smooth law for the smooth cases and the Ackers rod roughness method for the roughened cases.

### 6.2.3 Results

The mean errors and standard deviations in the mean errors for the various methods are listed in Table 6.1. The results differed considerably depending whether the floodplains were roughened or not and so mean errors are given over the smooth data, the roughened data and over all the smooth and rough data. Table 6.1 shows that for the whole data set the mean errors for the various methods vary from 7.3% to 70.1%. All the methods over-predict discharge by significant amounts. The corresponding standard deviations vary between 16.8% and 56.7% showing that the errors vary by very large margins about the mean values.

It is worth looking more closely at the results averaged over the smooth and rough data sets. The mean error for the fourth horizontal division line method (HOR4) taken over all the data is 7.3% and so this method would appear to give the best results. However when the mean error is calculated over the smooth and rough data sets the mean errors are 19.5% and -19.8% respectively. Thus the relatively low mean error achieved by considering the whole data set is actually the result of large positive errors for the smooth cases and large negative errors for the rough cases. This wide band of errors is highlighted by the large values of the standard deviations.

The results discussed above show that the simple methods developed for straight compound channels are likely to give rise to large errors in estimated discharges if applied to meandering compound channels. The range of errors to be expected will vary with the following parameters:

- 1 sinuosity
- 2 floodplain width / main channel width
- 3 floodplain roughness / main channel roughness
- 4 floodplain depth / main channel depth

For cases similar to the Phase B geometries considered, the errors in calculated discharges may be as large as 100%. Hence a different method is required to

calculate the discharge in meandering compound channels.

The four methods based on a simple two way division with a horizontal line at bankfull stage appear to perform slightly better overall than the other methods. This suggests that horizontal divisions are most appropriate for meandering channels. In straight compound channels the best divisions are based on vertical divisions at the edges of the main channel.

Of the methods applied to the meandering laboratory data the horizontal division methods gave marginally more accurate predictions. In general straight channel methods are not appropriate for the analysis of meandering compound channels. This confirmed that the development of a new procedure for discharge estimation in meandering compound channels is worthwhile.

### **6.3 Procedures for discharge estimation in meandering compound channels**

The main objectives of this chapter are to develop and verify a procedure for calculating the conveyance of a meandering channel during overbank flow. The mechanisms which affect the conveyance capacity of meandering channels were identified in Chapter 5 and are summarized below. A further literature search was carried out to identify the means by which other authors have accounted for these mechanisms. Armed with this knowledge of physical processes and modelling techniques it was then possible to decide on an appropriate approach to be followed in developing a new procedure.

#### **6.3.1 Important mechanisms**

The internal structure of currents during overbank flows has been found to be highly complex. The available laboratory data has been reviewed in chapter 5 and the most important observations are:

- 1) The longitudinal velocities below bankfull tend to follow the main channel

side walls while the floodplain velocities are generally in the valley direction. Thus the floodplain flows pass over the main channel and induce a horizontal shear layer.

- 2) The energy loss due to secondary currents in the main channel is greater than for an equivalent simple channel and the currents rotate in the opposite sense compared to inbank flows.
- 3) Fluid passes from the main channel onto the floodplain and back into the main channel in the following meander bend. Hence the proportion of discharge passed by the main channel and floodplain varies along a meander wavelength. These bulk exchanges of fluid between slow and fast moving regions of flow introduce extra flow resistance.
- 4) Flows on the floodplain outwith the meander belt are usually faster than those within the meander belt. It would appear that the extra flow resistance induced by the meandering main channel has a relatively small effect on the outer floodplain.

### 6.3.2 Methods available in the literature

**Toebe and Sooky (1967)** account for the interaction losses by separating the main channel and floodplain flows by a horizontal plane at bankfull level. The apparent shear on this plane is accounted for by adding a solid boundary equivalent to the wetted perimeters of both flow regions. The discharges in the two regions are then calculated separately and added. Experimental data were obtained from small-scale rectangular channels and these were used to evaluate the solid boundary addition. The addition was found to vary in a rather complex way with overbank flow depth, main channel depth, and channel gradient, but no general, practically usable relationship was proposed.

**James and Brown (1977)** proposed accounting for the interaction losses in straight and meandering compound channels by adjusting the value of Manning's  $n$ . From laboratory test results they developed an adjustment to the bankfull  $n$  value, dependent on relative flow depth and the ratio of floodplain width to main channel

width. The adjusted  $n$  value is then applied to the cross-section considered as a single channel. Their experiments were conducted mainly with straight channels, however, and the data for meandering channels are very limited.

**Yen and Yen (1983)** also considered the compound section as a unit and treated the main channel as a resistance element. They proposed a Darcy-Weisbach type resistance coefficient which accounts for expansion and contraction losses induced by the main channel. This model does not account for flow in the main channel, and depends on empirical information obtained for closed conduits which is unverified for channels.

**Ervine and Ellis (1987)** also proposed division of the cross-section into three zones, viz. the main channel below bankfull level, the floodplain within the meander width, and the floodplain beyond the meander belt. They identified the main sources of energy losses in each of these zones. In the main channel these are :

- 1) friction on the wetted perimeter,
- 2) boundary resistance due to transverse shear and internal friction associated with secondary currents induced by the meander bends,
- 3) the turbulent shear stress generated by the velocity difference between the main channel and the co-linear component of the floodplain flow at the horizontal interface at bankfull level, and
- 4) form resistance associated with the undulating riffle-pool sequence.

Over the floodplain within the meander belt the main sources of energy loss are :

- 1) friction on the wetted perimeter,
- 2) expansion of the flow as it enters the main channel, and
- 3) contraction of the flow as it re-enters the floodplain.

The only loss over the floodplain beyond the meander belt is due to friction on the wetted perimeter.

Ervine and Ellis proposed a model for predicting stage-discharge relationships by quantifying the more important of these loss mechanisms. Friction losses are estimated using the Darcy-Weisbach equation with the friction factor given by the Colebrook-White equation. Losses associated with secondary currents in the main channel are estimated using the method proposed by Chang (1983) for fully developed circulation in wide, rectangular channels. Subsequent experimental observations have shown the secondary circulation to be generally opposite in sense for overbank flows compared with inbank flows. This is because it is driven by the horizontal shear at the bankfull level, rather than by centripetal acceleration. Chang's method was derived for the inbank mechanism, and is therefore inappropriate for overbank cases. Ervine and Ellis account for the growth and decay of secondary currents by applying only half of the head loss predicted by Chang's 1983 model.

Expansion losses for the floodplain flow are determined by application of the force-momentum principle, and contraction losses by using loss coefficient values presented by Rouse (1950) and used by Yen and Yen (1983). The losses in the main channel associated with the shear across the horizontal interface and with pool-riffle undulation were considered minor and not accounted for. They applied the model to the experimental conditions of the US Army Corps of Engineers, Waterways Experiment Station (1956) and Toebes and Sooky (1967) and produced fairly accurate predictions. The method is summarized below and the zonal definitions are shown in Figure 6.1.

#### Total discharge

$$Q_T = Q_1 + Q_2 + Q_3 + Q_4 \quad (6.1)$$

#### Main channel

$$Q_1 = A_1 V_1 \quad (6.2)$$

$$V_1 = \left( \frac{2 g (S_o / s) R_1}{(f_1 / 4) + ((2.86 f_1^{1/2} + 2.07 f_1) / (5.565 + f_1^{1/2})) (R_1 / r_c)^2} \right)^{1/2}$$

Where  $A_1$  is the area of the main channel  $V_1$  is the mean velocity in the main channel,  $r_c$  is the bend radius of curvature,  $S_o$  is the valley slope and  $s$  is the sinuosity.

### Inner floodplain

$$Q_2 = A_2 V_2 \quad (6.3)$$

$$V_2 = \left( \frac{2 g S_o W_2}{(f_2 / 4) (W_2 - B s) / y_2 + s \sin^2(\theta_m) ( (1 - y_2 / (y_2 + h))^2 + K_c )} \right)^{1/2} \quad (6.4)$$

Where  $W_2$  is the width of the inner floodplain,  $B$  is the width of the main channel,  $y_2$  is the depth of flow on the floodplain,  $h$  is the bankfull depth,  $\theta_m$  is the mean angle between the main channel and the valley centre lines and  $K_c$  is the contraction coefficient. The values of contraction coefficient given by Rouse are listed in Table 6.2.

### Outer floodplain

The flows ( $Q_3$  and  $Q_4$ ) are calculated assuming only bed friction with the division lines omitted from the definition of the wetted perimeters and the floodplain slope  $S_o$  is used in the calculation.

**Greenhill (1992)** has tried various different methods of calculating discharges for a selection of the SERC FCF data (Tests 26, 31 and 39). No attempt was made to identify or model individual loss mechanisms and the methods are based on dividing the channel into the four zones and calculating the discharge in each zone assuming only bed friction. The two 'best' methods: Greenhill4 and Greenhill5) have been considered here.

The main channel discharge is calculated assuming that the horizontal division is

included in the wetted perimeter of the main channel and the inner floodplain zone. Greenhill's method 4 applies vertical divisions at the meander belt edges and method 5 is based on division lines inclined outward at 45°. These division lines are included in the wetted perimeter of the inner floodplain zone but not the outer zones. The main channel hydraulic slope ( $S_o/s$ ) is used when calculating the main channel and meander belt discharges while the floodplain gradient ( $S_o$ ) is used in calculating the outer floodplain flows.

These approaches were derived by empirical trial and error based on one set of stage discharge data collected on the FCF during Phase B (60° smooth trapezoidal). Greenhill used Manning's equation, with a value of 0.01, although the surface is hydraulically smooth and a modified smooth law has been developed for this laboratory facility, Ackers 1991. The best of the methods were then applied to two other sets of Phase B data with smooth floodplains (60° narrow floodplain and 110°); one set from James and Brown (1977); three sets from the Vicksburg investigation (1956) and Smith's data (1978).

Errors in discharge estimation of between 16% for the FCF 110° geometry at low stages and -10% were reported. The variation in these errors with depth are shown to vary radically from data set to data set. In order to obtain accurate results with Smith's data, Greenhill was forced to adjust the given  $n$  value from 0.01 to 0.015. These methods were only applied to three out of the 9 usable stage discharge data sets collected on the FCF and have not been verified against data with roughened floodplains.

## **6.4 Approach to conveyance estimation**

### **6.4.1 Introduction**

The methods identified above are all based on relatively simple conceptual models based on traditional engineering concepts for flows in straight channels. Flow in compound meandering channels is very complex and the development of methods to analyze it accurately will probably follow directions that are highly computational.

The development of suitable 3-D models including sophisticated turbulence models is the ultimate goal of much research and the SERC FCF Phase B data is an important data set to use in the validation of such models. A slightly simpler approach would be to develop a 2-D depth integrated model with turbulence terms. This approach has proved to be useful in the case of straight compound channels. However 2-D modelling may not be suitable for the more complex 3-D nature of flows in meandering channels.

The work involved in developing complex numerical models was prohibitive and it was felt that it would be useful to develop a simple hand calculation technique which would provide the engineer with a method of obtaining a first estimate of the discharge capacity of meandering compound channels.

It was felt that the methods should be developed to be design oriented and expressed in terms of physical parameters which are meaningful in a design context. For example, the dependence of channel capacity on design variables, such as cross-section shape and size, should be fairly explicit.

The SERC Phase B tests were limited to just two different planform geometries, with sinuosities of 1.37 and 2.04. The Phase A tests, carried out in straight channels, represent the limiting case of sinuosity 1.0. This wide range of sinuosities is such that it would be unreasonable to expect to be able to interpolate flow characteristics between them. This makes a purely empirical, descriptive approach unrealistic, as it could be applied only to new situations which are very similar to the experimental ones.

To ensure a degree of generality in the design methods, it was decided to base them on conceptual models of the physical processes involved in dissipating energy and determining flow structure. The SERC data will be used to quantify these processes, in terms of geometric and fluid state parameters. This will involve theoretical and empirical formulations. The relative importance of the individual processes is expected to vary with the scale of the physical system, and possibly also with the

flow condition. Separation and individual treatment of the processes should account for the effects of these variations on the required predictions (of stage-discharge relationships, for example) better than if these were made in terms of the geometries and fluid state parameters directly. The approach will also have the advantage of being able to include data from different sources and obtained under different conditions, and will allow the methods to be easily modified as new results and analyses become available.

The division of the channel in to four zones as proposed by Ervine and Ellis (1987) was adopted as the most flexible approach. The stage-discharge relationship for a compound meandering channel will be predicted by dividing the cross-section into zones and calculating the zonal discharges separately. The division will be by a horizontal line at bankfull level and a vertical line on either side of the meander belt. This approach also recognises the limited scope of the present investigation and allows improved models to be substituted for the various zonal calculations in the future, which would be difficult in a method based on a lumped calculation of total discharge.

#### **6.4.2 Formulation zone 1**

The flow mechanisms in this zone are complex, as shown by Willetts (1992) and Sellin et al (1993), for example. The major mechanisms responsible for energy dissipation are :

- 1) friction,
- 2) secondary circulation driven by the shear imposed by the floodplain flow,
- 3) the apparent shear stress on the horizontal interface associated with the gradient of colinear velocity components across it,
- 4) the bulk exchange of water between the main channel and the floodplain.

Losses associated with variations in cross-section geometry and flow separation have been shown to be insignificant for the conditions likely to occur (Kazemipour and

Apelt, 1979, 1982 and 1983).

It was originally intended to develop physically-based deterministic models to account for the effects of the various loss mechanisms on stage-discharge relationships. This has proved not to be possible, at least for the main channel zone, owing to the current lack of understanding of the mechanisms and their effects. An empirical approach has therefore been resorted to, based on the Phase B data and a rational selection of dimensionless variables. The procedure is to calculate the bankfull discharge ( $Q_{br}$ ) using an appropriate method for inbank flows, and then to adjust this to account for the effects of overbank flow. The bankfull discharge includes allowance for the effects of bend losses. This was used rather than an equivalent straight channel value to separate the inbank bend losses from the ultimate adjustment factor. This will allow future developments in inbank flow assessment to be incorporated. Also, it is likely that in some design applications inbank stage-discharge measurements will be available for the specific site, and these can then be used to evaluate  $Q_{br}$  directly.

Discharges in this zone have been obtained by integration of the velocity magnitude and direction measurements taken in some of the Phase B experiments. The relevant experiments and integrated discharge values are listed in Table 6.3. The discharges were found to vary along the channel below bank-full in a way consistent with the descriptive observations reported by Willets (1992), Figure 6.2.

A study of Figure 6.2 shows that for both the 60° and 110° geometries the discharges vary along a meander, being maximum at the bend apices ( $2X/L = 0.0, 1.0$ ) and minimum at some point in between. Figure 6.2A shows that cross-section shape does not affect the distribution strongly, with the trapezoidal and natural cases giving similar variations of discharge. Figures 6.2B and 6.2C show that while the roughness of the floodplain may affect the magnitudes of the main channel discharges it does not have a significant effect on the flow distribution. The effect of channel sinuosity is apparent from Figures 6.2B and 6.2C. The more sinuous channel was found to have a much wider variation in main channel discharge at similar depths compared to the less sinuous channel. For example at a flow depth of 200mm, the 110° main

channel discharge varied between about 0.4 and 1.3 of the mean while for the 60° main channel the variation is between 0.8 and 1.2 of the mean. The effect of depth is more pronounced for the more sinuous channel. The 60° main channel discharges vary between about 0.8 and 1.2 of the mean for all three depths while for the 110° main channel the variation was between 0.9 and 1.1 at low depth (165 mm) and 0.3 and 1.3 at high depth (200 mm).

These variations are ignored in this analysis as neither they, nor their effects will be explicitly accounted for in the stage-discharge predictions. The values listed in Table 6.3 are averages of the integrations at all the measurement sections, weighted by the channel lengths represented by the sections.

The main channel bankfull discharges were not measured during the experiments, and have been determined indirectly. For the trapezoidal channel, the modified version of Chang's (1984) method for accounting for bend losses has previously been found to predict the stage-discharge relationship very accurately (-1.76% average error over all measured values). It was therefore used to predict the bankfull discharge. The stage-discharge relationship is shown in Figure 6.3. No method has yet been found which predicts the stage-discharge relationships sufficiently accurately for the pseudo-natural channels. The bankfull discharges were therefore determined for these cases by graphically extending the measured stage-discharge relationships, as shown in Figures 6.4 and 6.5. The bankfull discharges for each channel type are also listed in Table 6.3.

The ratios of main channel discharge to bankfull discharge ( $Q/Q_{br} = Q_1'$ ) are plotted against floodplain flow depth ( $y_2$ ) on Figure 6.6. This shows that as the water level rises above the floodplain, the discharge initially decreases below the bankfull value and then gradually rises and may exceed the bankfull value at high stages. The relationship between main channel discharge and overbank flow depth is clearly affected by the channel cross-section geometry, the channel sinuosity ( $s$ ) and the floodplain roughness. It is obviously desirable to express these characteristics in non-dimensional terms and appropriate measures have been selected. The flow depth is

normalized by the hydraulic depth of the main channel at bankfull, i.e.  $A/B$ , where  $A$  is the cross-sectional area and  $B$  is the surface width. This has been chosen rather than a flow depth or hydraulic radius because it probably varies least along natural channels and will require the least field survey information. The data have been replotted in Figure 6.7 in terms of the dimensionless flow depth,  $y_2/(A/B)$  ( $= y'$ ). The cross-section geometry is characterized by the ratio of surface width to hydraulic depth. This is a physically meaningful parameter because it represents the ratio of the area on which the apparent shear stress on the horizontal interface is applied to a measure of the volume affected. Expressed as  $B^2/A$  it is also a shape factor, describing the deviation of the channel cross-section from square. The floodplain roughness is expressed as the ratio of floodplain and main channel Darcy-Weisbach friction factors,  $f_2/f_1$  ( $= f'$ ). For the main channel, both the basic straight channel value and the effective value accounting for bend resistance were considered, and the final results found to be indistinguishable. The basic value will be more meaningful to most engineers and has therefore been used.

Quantitative interpretation of the relationships between the channel discharge and the various physical characteristics is severely constrained by the amount of data available. In most cases effects are presented by only two data points. The exclusive use of linear functions to describe the relationships in this analysis is a consequence of the lack of data; it is unlikely that the processes are actually linear.

Figure 6.7 suggests that for any particular channel the relationship between  $Q_1'$  and  $y'$  can be represented by two straight lines. At low overbank stages the slope of the line is negative and not appreciably affected by channel geometry, sinuosity or floodplain roughness. At higher stages the slope is positive and both the slope and position of the line are affected by these characteristics.

The straight line describing the variation of  $Q_1'$  with  $y'$  at low overbank stages must obviously pass through the point (1.0, 0.0), which defines the constant in the relationship. The slope is defined by the four points at  $y'$  approximately equal to 0.2. These points are very close together although they represent widely different

conditions, suggesting that the variation is not appreciably affected by these conditions. The effect of sinuosity appears to be similar to that for higher values of  $y'$ , but there are insufficient data to distinguish the effect reliably and a common slope has been assumed. This was calculated as the average of the slopes for all four data points. The variation for low stages is then defined by

$$Q_1' = 1.0 - 1.69 y' \quad (6.5)$$

For overbank stages higher than  $y'$  equal to approximately 0.2, the relationship between  $Q_1'$  and  $y'$  is more complex and is clearly affected by channel geometry, sinuosity and floodplain roughness. These characteristics had to be quantified for all data points. Both channel geometry (as represented by the ratio  $B^2/A$ ) and sinuosity were constant in all experiments for each channel type, but the floodplain friction factor varied with flow depth for both smooth and rod-roughened experiments. As described before, floodplain roughness was accounted for in terms of the ratio ( $f'$ ) of the Darcy-Weisbach friction factor for the floodplain ( $f_2$ ) and the equivalent straight channel value for the main channel at bankfull stage ( $f_c$ ). The main channel and smooth floodplain values were calculated using the relationship for smooth channels derived by Ackers (1991) from straight channel data, equation 5.1. For the rod-roughened floodplain, values were obtained from the procedure developed by Ackers (1991) and summarized in Appendix 7. The variable values are listed in Table 6.4.

The relationship between  $Q_1'$ ,  $y'$ ,  $B^2/A$ ,  $s$  and  $f'$  for values of  $y'$  greater than about 0.2 was determined in seven different ways. These are discussed in the following paragraphs.

### Method 1

As there are no more than two data points on the curve for each channel type on Figure 6.7, it is assumed that all relationships are linear. The basic relationship is

$$Q_1' = m y' + c \quad (6.6)$$

in which  $m$  is the slope of the line and  $c$  defines its position. Both  $m$  and  $c$  may be functions of  $B^2/A$ ,  $s$  and  $f'$ . It is impossible to determine the effect of sinuosity on  $m$  because only two sinuosities were used (1.37 and 2.04), and only one floodplain flow depth was used for the 2.04 sinuosity channel in this range of  $y'$ . The accelerating effect of the apparent shear stress on the horizontal interface must decrease with sinuosity and the rate of increase of  $Q_1'$  with  $y'$  will be less, implying a smaller value of  $m$ . However, assigning a value of  $m$  to a sinuosity of 2.04 would be totally speculative without additional data, and it was assumed that it would be the same as for a sinuosity of 1.37. It was assumed, therefore, that  $m$  depends on  $B^2/A$  and  $f'$  only, i.e.

$$m = m ( B^2/A, f' ) \quad (6.7)$$

Because no experiments were performed with the trapezoidal channel with rod-roughened floodplains, there is no evidence that the effects of  $B^2/A$  and  $f'$  on  $m$  are not independent, and they are assumed to be so.

The positions of the lines (and hence the values of  $c$ ) are clearly dependent on  $B^2/A$ ,  $s$  and  $f'$ . The dependence on  $B^2/A$  can be seen by comparing the points for the 60° trapezoidal and pseudo-natural channels with smooth floodplains. The dependence on sinuosity can be seen by comparing the points for the 60° and 110° pseudo-natural channels with smooth floodplains. The dependence on  $f'$  can be seen by comparing the points for the 60° pseudo-natural channels with smooth and rod-roughened floodplains. It was assumed, therefore, that

$$c = c ( B^2/A, s, f' ) \quad (6.8)$$

As for  $m$ , there is no evidence that the effects of  $B^2/A$  and  $f'$  are not independent. No experiments were done with the trapezoidal channel with different sinuosities, so there is also no evidence that the effects of  $B^2/A$  and  $s$  are not independent. However, the effects of  $s$  and  $f'$  are clearly not independent, as can be seen by comparing the points for the smooth and rod-roughened floodplains for the 60° and

110° pseudo-natural channels : the effect of roughening the floodplain is much less if the sinuosity is greater. To account for this dependence,  $f'$  was initially omitted from the expression for  $c$ , i.e. it was assumed that

$$c = c ( B^2/A, s ) \quad (6.9)$$

The combined effect of  $s$  and  $f'$  was accounted for by a subsequent adjustment to  $Q_1'$ .

It can be seen in Table 6.4 that  $f'$  is substantially different at different flow depths, even when the floodplains are not roughened and the physical surface roughness are identical. For example, for the 60° pseudo-natural channel with smooth floodplains,  $f'$  varies by a factor of two over the range of  $y'$  tested. If the dependence on  $f'$  is being sought, it is therefore not correct to connect the points for each channel geometry, as done in Figure 6.6, because they have different  $f'$  values. This difficulty was addressed by adjusting the positions of the points so that points with identical  $f'$  values could be connected to define the relationships. Points with the same  $y'$ ,  $s$  and  $B^2/A$  were used to define the gradient of  $Q_1'$  with  $f'$  for that channel and  $y'$ . Assuming this gradient to be constant with  $Q_1'$ , the position of a point could be adjusted to represent the same  $f'$  as another point with the same  $s$  and  $B^2/A$  but different  $y'$ . The line through these points would then represent the relationship between  $Q_1'$  and  $y'$  for a given channel with constant  $f'$ . As no data were obtained for the trapezoidal channel with roughened floodplains, the points for the trapezoidal channel were adjusted using the gradient of  $Q_1'$  with  $f'$  as calculated for the 60° pseudo-natural channel. The adjusted points and resulting linear relationships are shown in Figure 6.7 and Table 6.5. This diagram forms the basis of the discharge relationship for  $y'$  greater than about 0.2.

It was assumed that equation 6.7 has the form

$$m = a_1 B^2/A + a_2 f' + a_3 \quad (6.10)$$

One point and the line through it were selected to represent equation 6.10 for each

of the 60° trapezoidal, 60° pseudo-natural with smooth floodplain, and 60° pseudo-natural with roughened floodplain channels. The average value of  $f'$  for each channel was used. Three equations for  $m$  were therefore set up and these were solved simultaneously to determine values for  $a_1$ ,  $a_2$  and  $a_3$ . The resulting equation for  $m$  is

$$m = 0.0147 B^2/A + 0.0320 f' + 0.169 \quad (6.11)$$

The same approach was followed to evaluate  $c$ , with equation 6.9 assumed to have the form

$$c = b_1 B^2/A + b_2 s + b_3 \quad (6.12)$$

The same points and lines as used to define  $m$  were again used to set up three equations for  $c$ , which were solved simultaneously to determine values for  $b_1$ ,  $b_2$ , and  $b_3$ . The resulting equation for  $c$  is

$$c = 0.0132 B^2/A - 0.302 s + 0.851 \quad (6.13)$$

The initial adjustment to bankfull discharge is therefore given by

$$Q_1' = ( 0.0147 B^2/A + 0.0320 f' + 0.169 ) y' + 0.0132 B^2/A - 0.302 s + 0.851 \quad (6.14)$$

Equation 6.14 does not account for the joint effect of  $s$  and  $f'$  on  $c$ . A further adjustment was derived by calculating the ratios of measured  $Q_1'$  to the values calculated by equation 6.14, and relating them to  $s$  and  $f'$ . The predicted ( $Q_{1p}'$ ) and measured ( $Q_1'$ ) values for those experiments in the appropriate range of  $y'$  are listed in Table 6.6.

The adjustment required to the discharge ratio predicted by equation 6.14 is plotted in Figure 6.9. The data for high values of  $f'$  are too sparse to infer a variation with

s. It was assumed that the adjustment varies linearly with  $f'$  and linear regression was used to obtain the relationship

$$Q_1'/Q_{1p}' = K = 1.07 - 0.0698 f' \quad (6.15)$$

The adjustment factor for  $y'$  greater than about 0.2 is then given by

$$Q_1' = (m y' + c) K$$

with

$$m = 0.0147 B^2/A + 0.032 f' + 0.169$$

$$c = 0.0132 B^2/A - 0.302 s + 0.851$$

$$K = 1.07 - 0.0698 f' \quad (6.16)$$

## Method 2

The second adjustment in Method 1, represented by  $K$ , was intended to account for the interdependence of the effects of  $s$  and  $f'$  on  $Q_1'$ . As it turned out to be a function of  $f'$  only, which is accounted for in  $m$ , it need really only be applied to  $c$ . The adjustment to  $c$  (as predicted by equation 6.13) was derived by calculating the ratios of the required values to these predicted values, and relating them to  $s$  and  $f'$ . The values of  $c$  required were calculated using equation 6.6 with  $m$  given by equation 6.11. The predicted ( $c_p$ ) and required ( $c$ ) values for those experiments in the appropriate range of  $y'$  are listed in Table 6.7.

The adjustment required to  $c$  as predicted by equation 6.13 is plotted against  $f'$  in Figure 6.10. Again, the data are too sparse to infer a variation with  $s$ , and the following linear relationship with  $f'$  was obtained and is assumed to apply for all sinuosities.

$$c/c_p = 1.14 - 0.136 f' \quad (6.17)$$

The adjustment factor for  $y'$  greater than about 0.2 is then given by

$$Q_1' = m y' + K c$$

with

$$m = 0.0147 B^2/A + 0.032 f' + 0.169$$

$$c = 0.0132 B^2/A - 0.302 s + 0.851$$

$$K = 1.14 - 0.136 f' \quad (6.18)$$

### Method 3

Methods 1 and 2 were derived by simultaneous solution of one equation for each of the channel types. Some of the data were therefore not used, and a more accurate formulation might be obtained from a regression analysis on all the data. In Method 3 a straight forward multiple linear regression analysis was performed, giving the following relationship.

$$Q_1' = 0.469 y' + 0.0392 B^2/A - 0.0645 f' - 0.195 s + 0.382 \quad (6.19)$$

### Method 4

Figure 6.8 presents a set of straight lines for  $y'$  greater than about 0.2, the slopes and positions of which appear to depend on  $B^2/A$ ,  $f'$  and  $s$ . In this method multiple linear regression analyses were performed separately on the slopes and intercepts of the lines.

Because there is only one data point for the 110° crossover angle channel for each roughness condition, no slope could be determined. Slopes were therefore known for only one sinuosity and consequently no variation with sinuosity could be considered. It was therefore assumed that the slopes of the lines depend only on  $B^2/A$  and  $f'$ . Using the data for the channels with a 60° crossover angle, the following relationship for slope was found.

$$m = 0.0183 B^2/A + 0.0128 f' + 0.159 \quad (6.20)$$

The intercepts ( $c$ ) of the lines were assumed to depend on  $B^2/A$ ,  $f'$  and  $s$ . Values of  $c$  for each line were calculated using equation 6.6, with  $Q_1'$  as given in Table 6.4 and  $m$  measured on Figure 6.8. For the  $110^\circ$  crossover angle channels  $m$  was calculated using equation 6.20. The resulting relationship for  $c$  is

$$c = 0.00768 B^2/A - 0.0708 f' + 0.0672 s + 0.435 \quad (6.21)$$

The adjustment factor for  $y'$  greater than about 0.2 is then given by

$$Q_1' = m y' + c$$

with (6.22)

$$m = 0.0183 B^2/A + 0.0128 f' + 0.159$$

$$c = 0.00768 B^2/A - 0.0708 f' - 0.0672 s + 0.435$$

### Method 5

The slopes of the lines for  $y'$  greater than about 0.2 on Figure 6.8 do not vary greatly, and a simpler equation for  $Q_1'$  would result if the slope were assumed constant. It was assumed that the average slope ( $m = 0.433$ ) applies to all lines and values of  $c$  were calculated using equation 6.6 and this value. The relationship between  $c$  and the channel variables was reanalysed and the relationship for  $Q_1'$  is then given by

$$Q_1' = 0.433 y' + 0.00715 B^2/A - 0.0532 f' + 0.0246 s + 0.459 \quad (6.23)$$

### Method 6

There are only two data points for the  $110^\circ$  crossover channel for  $y'$  greater than 0.2. The point for the experiment with roughened floodplains suggests that sinuosity has no effect on  $Q_1'$ , while the point for the experiment with smooth floodplains suggests a significant effect. Methods 1 to 5 attempted to reconcile this information.

In Method 6 it was assumed that  $Q_1'$  is independent of sinuosity, as suggested by the

experiments with roughened floodplains. Although intuitively unappealing, there is some justification for this assumption. Sinuosity is accounted for in the estimate of  $Q_{br}$ , and the implication is that the magnitude of main channel energy loss associated with meandering is similar for inbank and overbank flows, although it is recognised that the mechanisms are radically different. The validity of this assumption needs to be investigated using a data set with a wider range of sinuosities.

This method is therefore similar to Method 4, but the regression analysis for  $c$  excluded the data for the 110° crossover channel, resulting in a different formulation. The adjustment factor is given by

$$Q_1' = m y' + c$$

with

$$m = 0.0183 B^2/A + 0.0128 f' + 0.159$$

$$c = 0.00888 B^2/A - 0.0729 f' + 0.402 \quad (6.24)$$

### Method 7

In this method it was assumed (as for Method 5) that  $m$  is constant, and that (as for Method 6)  $c$  is independent of sinuosity. Values of  $c$  were determined as in Method 5 and the regression analysis revised. The adjustment factor is then given by

$$Q_1' = 0.433 y' + 0.0182 B^2/A - 0.0614 f' + 0.402 \quad (6.25)$$

### Evaluation of the methods

The errors in reproducing the data by each of the methods are listed in Table 6.8. The selection of the most appropriate method or methods was based on the magnitude, nature and distribution of errors, with some consideration of simplicity. Errors are most acceptable at high values of  $y'$  because the main channel contribution to total discharge becomes relatively less significant as stage increases. Errors are considered more acceptable at high sinuosities than at moderate sinuosities, as the

latter are more common in design applications. Negative errors are preferable to positive errors because they would introduce conservative underestimation of main channel conveyance in design applications.

On the basis of the above criteria, Method 2 was selected, its worst performance is for high  $y'$  and high sinuosity with rough floodplains and the error for the latter condition is negative. It should be noted that the experimental floodplain roughness was extreme, and the error decreases for smoother floodplains.

## Summary

The procedure is to calculate the bankfull discharge ( $Q_{bf}$ ), and then to adjust this to account for the effects of overbank flow. The bankfull discharge can be estimated using inbank flow methods or obtained by measurement, if possible. The hydraulic slope which controls the flow in the main channel zone ( $S$ ) is related to the floodplain or valley hydraulic slope by the channel sinuosity, (ie  $S = S_o / s$ ). It should be noted that  $S_o$  can either be a ground slope if uniform flow is assumed or a water surface slope.

The adjustment factor was determined from the SERC FCF Phase B data. Actual discharges in this zone were obtained by integrating the velocity magnitude and direction measurements taken in some of the experiments. The ratio of actual to bankfull discharge defines the adjustment factor,  $Q_1'$ .

$Q_1'$  was found to depend on:

- 1) the floodplain flow depth at the edge of the main channel ( $y_2$ );
- 2) the channel sinuosity ( $s$ );
- 3) the cross-section geometry and
- 4) floodplain roughness.

These characteristics are represented by dimensionless parameters which were chosen

as being both meaningful and easy to measure. The flow depth is normalized by the hydraulic depth of the main channel at bankfull, equation 6.26, where A is the cross-sectional area and B the surface width of the main channel at bankfull.

$$y' = y_2 / (A/B) \quad (6.26)$$

The cross-section geometry is characterized by  $B^2/A$ . The floodplain roughness is expressed as the ratio of floodplain and main channel Darcy-Weisbach friction factors, i.e.

$$f' = f_2 / f_1 \quad (6.27)$$

The Darcy-Weisbach friction factor can be calculated using the Colebrook-White equation. If Manning's n is used then f is related to n by

$$f = \frac{8 g n^2}{R^{1/3}} \quad (6.28)$$

The ratio  $f'$  can therefore also be expressed in terms of Manning's n

$$f' = (n_2/n_1)^2 (R_1/R_2)^{1/3} \quad (6.29)$$

The relationship between the adjustment factor and these variables is shown schematically in Figure 6.8. This shows that the main channel discharge is initially reduced as stage rises above bankfull, and that this reduction is independent of channel characteristics. At higher stages the discharge increases with stage at a rate which depends strongly on  $B^2/A$ , s and  $f'$ . Various expressions for the relationship at high stages were derived by different methods. The relationship derived by method 2 above was chosen as the best.

Thus the variation in main channel discharge with overbank stage can be accounted for by choosing the adjustment factor to be the greater of :

$$Q_1' = 1.0 - 1.69 y' \quad (6.30)$$

or

$$Q_1' = m y' + K c$$

with

$$m = 0.0147 B^2/A + 0.032 f' + 0.169$$

$$c = 0.0132 B^2/A - 0.302 s + 0.851$$

$$K = 1.14 - 0.136 f' \quad (6.31)$$

and the correct flow in zone 1 is given by

$$Q_1 = Q_{br} Q_1' \quad (6.32)$$

### 6.4.3 Formulation zone 2

This section describes two alternative methods for predicting the discharge in the inner floodplain zone. The first method attempts to account for the principal loss mechanisms using physically-based deterministic formulations. The formulations are based on a very simple conceptual model of the loss mechanisms and require empirical adjustment to account for the additional complexities involved.

The second method is purely empirical and follows an approach similar to that used for the main channel zone. A basic discharge is calculated assuming friction losses only, and this is then adjusted to account for the effects of flow interaction with the main channel. The adjustment is based on data obtained from the SERC Phase B experiments and data provided by Professor B B Willetts (personal communication) obtained from experiments conducted under his supervision at the University of Aberdeen.

#### Expansion contraction model

The major energy loss mechanisms in the inner floodplain zone have been identified previously by other researchers (for example, Ervine and Ellis 1987, McKeogh and

Kiely 1989) as

- 1) friction on the wetted perimeter,
- 2) expansion of the flow as it enters the main channel, and
- 3) contraction of the flow as it re-enters the floodplain.

The energy loss due to friction ( $h_f$ ) over one meander wavelength ( $L$ ) can be estimated using the Darcy-Weisbach equation,

$$h_f = \frac{f_2 L V_2^2}{8 g R_2} \quad (6.33)$$

in which

$f_2$  is the Darcy-Weisbach friction factor for the inner floodplain,

$g$  is the acceleration due to gravity,

$V_2$  is the flow velocity, and

$R_2$  is the hydraulic radius.

The hydraulic radius is defined as the ratio of the cross-sectional area to the wetted perimeter. The inner floodplain zone is rectangular and so the cross-sectional area is the product of the inner floodplain width ( $W_2$ ) and the flow depth on the floodplain ( $y_2$ ). The wetted perimeter includes the floodplain surface only, and not the horizontal plane dividing the inner floodplain and main channel zones. By considering the areas of the floodplain and division plane over a wavelength, it can be shown that the effective wetted perimeter is the width less the product of the sinuosity ( $s$ ) and the main channel top width ( $B$ ). The hydraulic radius for friction loss calculations is therefore given by

$$R_2 = \frac{W_2 y_2}{W_2 - B s} \quad (6.34)$$

Expansion and contraction losses depend on the pattern of flow across the main

channel, which is complex. The flow expansion is accompanied by deviation of the primary flow direction and entrainment of some of the floodplain flow into the main channel along the cross-over reach (Jasem, 1990). There are also bulk exchanges of water between the main channel and floodplain associated with the bend apex regions (Willettts, 1992). The model developed here assumes straight flow across a slot in which there is no transverse flow, and is therefore a very simplified representation of the real situation. A complete, quantitative description of the interactions between floodplain and channel flows would require detailed computational modelling. Appropriate models do not exist at present, nor do the understanding and quantitative information necessary for their development in the short term. For present purposes, however, only the energy loss associated with the floodplain - main channel interaction is to be predicted and the model does not need to be complete and accurate in all respects. It is assumed, therefore, that the magnitude of energy loss and its dependence on the main flow and geometric properties is similar for the simplified and real situations. In fact, insufficient information is available at present even to provide a good, general description of energy loss for the simple case and some broad assumptions are necessary.

The expansion loss over a simple downward step (as shown in Figure 6.11) can be estimated by application of energy and momentum equations between sections 1 and 2. This gives

$$h_e = \left( \frac{4 y_2 (y_2/y_1 - 1)}{y_2 + h + y_1} + (1 - (y_2/y_1)^2) \right) \frac{V_2^2}{2g} \quad (6.35)$$

in which

- $h_e$  is the energy lost in expansion of the flow,
- $y_1$  is the flow depth in the main channel,
- $h$  is the step height,

If it is assumed that the water surface is flat and unaffected by the step, then  $y_1 = y_2 + h$  and equation 6.35 reduces to

$$h_c = (1 - y_2/y_1)^2 \frac{V_2^2}{2g} \quad (6.36)$$

Equations 6.35 and 6.36 have both been applied to some data obtained by Jasem (1990) and the differences in their predictions found to be negligible. Equation 6.36 is therefore accepted as an adequate description. Note that this result is independent of  $\theta$ , the inclination of the downward step to the direction of flow.

The flow pattern for contraction over an upward step is shown in Figure 6.12. The step induces a vena contracta a short distance downstream of the step, beyond which the flow expands to the normal flow conditions. The loss of energy associated with this pattern is concentrated in the expansion region, i.e. between sections 3 and 4. The contraction loss ( $h_c$ ) could therefore be described by an expansion loss equation similar to equation 6.36, i.e.

$$h_c = (1 - y_3/y_2)^2 \frac{V_3^2}{2g} \quad (6.37)$$

Equation 6.37 cannot be used, however, without knowledge of the contraction coefficient necessary to define the flow conditions at section 3. This cannot be determined analytically and has not been investigated experimentally. Yen and Yen (1983) recommended accounting for the contraction loss between a meandering channel and its floodplain with the relationship

$$h_c = K_c \frac{V_2^2}{2g} \quad (6.38)$$

in which  $K_c$  is a contraction loss coefficient which varies with the ratio of floodplain to main channel flow depths, as given in Table 6.2. These values for  $K_c$  were given by Streeter in Rouse (1950) and are apparently based on data obtained from experiments in pipes conducted by Weisbach in 1855. Jasem's (1990) results for

wide rectangular slots agree well with these values and they can therefore be accepted as reasonably accurate for free surface flows as well.

Both expansion and contraction losses can be expected to depend on the width of the main channel (B). The expansion develops over some distance from the downward step. If this development is incomplete before the upward step is encountered, then clearly the associated expansion loss will be proportionately reduced. Incomplete development will also mean that the flow contraction does not begin from the bed of the main channel, but some distance above it, and the associated loss will be less. Flow patterns for wide and narrow channels are illustrated in Figure 6.13.

Jasem (1990) measured expansion and contraction losses over slots with width to depth ratios ranging from 2 to 20. His results have been used to derive corrections to the expansion and contraction loss coefficients to account for width to depth ratio. The ratios of measured expansion loss coefficient to  $(1 - y_2/y_1)^2$  are plotted against width to depth ratio (B/h) in Figure 6.14. The ratios of measured contraction loss coefficient to interpolated values from Table 6.2 are plotted against B/h in Figure 6.15. As the loss coefficients are additive a correction could be applied to both together, and the ratios of the sums of the measured values to the sums of  $(1 - y_2/y_1)^2$  and values from Table 6.2 are plotted against B/h in Figure 6.16. In each case linear regression was used to obtain a relationship between the correction factor and width to depth ratio. These relationships are given on the figures. They are remarkably similar, and it would therefore be most practical to apply a single correction to the two coefficients together, i.e.

$$\text{Width to Depth Ratio Correction} = 0.02 (B / h) + 0.69 \quad (6.39)$$

For a channel angled across the floodplain the width presented to the flow would be greater than B and would vary with the angle. Attempts to refine equation 6.39 to account for this are not worth while at the current state of knowledge of the processes.

Both expansion and contraction losses can also be expected to vary with the side slopes of the main channel. The effect on the contraction loss should be particularly significant because of the influence the bank slope must have on the contraction coefficient. These effects cannot be described analytically and no directly applicable experimental results can be found. Chow (1959), however, has presented results obtained by Formica (1955) for energy losses in lateral expansions and contractions in channels. These have been used to obtain first estimates of the effects of the transition geometries.

Formica measured energy losses across an abrupt contraction in width and a contraction with a straight taper of 30°. The energy loss varied considerably with discharge but on average the loss with the tapered contraction was about 0.3 times that with the abrupt contraction. If the contraction loss is assumed to decrease linearly with the cotangent of the side slope, a correction function can be written as

$$\text{Contraction Side Slope Correction} = 1 - (S_s / 2.5) \quad (6.40)$$

in which  $S_s$  is the cotangent of the side slope. It would be realistic to set a minimum value above zero, say 0.1, to this correction.

Formica also conducted experiments with an abrupt expansion in width and expansions with straight tapers of 1:1, 1:2, 1:3 and 1:4. For the 1:4 taper the energy loss was about 0.3 times that for the abrupt expansion, and decreased quite uniformly over this range. Assuming a linear decrease of the expansion loss coefficient with side slope, the correction would be

$$\text{Expansion Side Slope Correction} = 1 - (S_s / 5.7) \quad (6.41)$$

Again, it would be advisable to set a lower limit of, say, 0.1 to this correction.

Both downward and upward steps between the main channel and floodplain extend over a width of  $(W - B)$  over the inner floodplain between consecutive bend apices.

Over a meander wavelength there will be two downward and two upward steps. If the losses are assumed proportional to the width over which expansion and contraction take place, then the losses should be further corrected by

$$\text{Step Length Correction} = 2 (W_2 - B) / W_2 \quad (6.42)$$

The head loss over one wavelength associated with expansion and contraction,  $h_L$ , is therefore estimated as

$$h_L = h_e + h_c \quad (6.43)$$

i.e.

$$h_L = C_{sl} C_{wd} (C_{sse} (1 - y_2/y_1)^2 + C_{ssc} K_c) V_2^2 / 2g \quad (6.44)$$

in which

$C_{sl}$  is the step length correction  
 $= 2 (W_2 - B) / W_2$ ,

$C_{wd}$  is the width to depth ratio correction  
 $= 0.02 B / h + 0.69$ ,

$C_{sse}$  is the expansion side slope correction  
 $= 1 - s / 5.7$ ,

$C_{ssc}$  is the contraction side slope correction  
 $= 1 - s / 2.5$ ,

$K_c$  is the basic contraction coefficient, as given in Table 6.2.

The total energy loss over one meander wavelength is the sum of the friction and expansion and contraction losses, i.e.  $h_f + h_L$ . Each of these major loss components can be expressed as a multiple of the velocity head, so that

$$h_f + h_L = (f_2 L / 4 R_2 + K_e) V_2^2 / 2g \quad (6.45)$$

in which  $K_e$  is the total expansion-contraction loss coefficient, as defined by equation 6.44. Under uniform flow conditions the total energy gradient is equal to the floodplain bed gradient,  $S_o$ , so that

$$h_f + h_L = S_o L \quad (6.46)$$

Equations 6.45 and 6.46 can be combined to give

$$V_2 = \left( \frac{2 g S_o L}{(f_2 L)/(4 R_2) + K_e} \right)^{1/2} \quad (6.47)$$

Considering the complexities of the flow mechanisms equation 6.47 could not be expected to account for all the energy losses under all conditions. A comparison of the SERC Phase B and Aberdeen data showed the non-friction losses to be strongly influenced by the cross-sectional geometry of the main channel. The basic model, equation 6.47, was found to predict stage-discharges reasonably well for the SERC 60° channels but to underpredict discharge quite badly (errors ~20%) for the Aberdeen channel with a similar sinuosity.

Apart from the scale the only significant difference between the two channels is the cross sectional shape. This has been described in the zone 1 model by the factor ( $B^2 / A$ ) and was assumed to be an appropriate measure here as well.

It was assumed that the friction part of the model is adequate and that the non-friction term should be adjusted. Also it was assumed that the error in total discharge would most likely arise in the zone 2 model because its contribution is most significant at higher stages.

The correction is based on the SERC 60° trapezoidal channel ( $B^2 / A = 9.14$ ) and the Aberdeen 1.4 sinuosity channel ( $B^2 / A = 3.84$ ). It was found by trial that the shape effect observed in these two channels could be accounted for by multiplying the non-friction term in equation 6.47 ( $K_e$ ) by a factor defined by:

by a factor,  $F1$  where  $F1$  took the values 0.984 for the Aberdeen 1.4 sinuosity and 0.914 for the SERC 60° case

Equation 6.48 has been removed.

in which  $A$  is the cross-sectional area of the main channel below bankfull.

The SERC Phase B results suggest a further effect associated with main channel sinuosity ( $s$ ). Application of the basic model (equation 6.47) to this data showed that, for smooth floodplains, the predictions were reasonable for both the 60° trapezoidal and natural channels. The errors in calculated discharge over the whole range of stages are shown in Figure 6.17.

The cause of the high positive errors at low relative depth ( $y'$ ) is not known. They are not consistent, being clearly present for the 60° trapezoidal and 110° natural channels, but not for the 60° natural channel.

A correction for sinuosity was made based on the difference in errors for the different sinuosities at higher values of  $y'$ . The prediction for sinuosity 2.04 needs to be reduced by about 10%, while for sinuosity 1.37 no adjustment is required.

As for the shape correction factor it was assumed that the non-friction term should be adjusted and that the non-friction component of the zone 2 model. It was found by trial that this can be accounted for by multiplying  $K_e$  by another factor, defined by

$$F_2 = s / 1.4 \quad (6.49)$$

The discharge in the inner floodplain zone is therefore given by

$$Q_2 = W y_2 V_2 \quad (6.50)$$

with  $V_2$  given by

$$V_2 = \left( \frac{2 g S_o L}{(f_2 L)/(4 R_2) + F_1 F_2 K_e} \right)^{1/2} \quad (6.51)$$

Preliminary applications of this model showed it to be quite insensitive to estimation of the step height,  $h$ . It is recommended that this be approximated by the hydraulic depth ( $= A/B$ ).

### **Empirical Model**

The physically-based model described above is unable to account adequately for the energy losses in the inner floodplain without empirical adjustment based on the SERC Phase B and Aberdeen data. Even then, the errors in predicting discharge over a range of overbank stages are inconsistent for some geometries and there is a case for considering further empirical adjustment. Because of the significant empirical content that would be required anyway, it would be practically expedient to apply empirical corrections to a basic discharge calculated in a simpler way than as required by the previous method.

The simplest empirical approach might be to disregard the horizontal division between the main channel and inner floodplain zones and consider the two together. This would be physically realistic considering the significant interaction and exchange of flows observed between the zones (e.g. Willetts, 1992); the separation of the zones is acknowledged to be rather artificial. However, knowledge of the zonal distribution of the discharge, albeit longitudinally averaged, would be most useful in design applications. The analysis for the main channel zone exposed significant variations of conveyance with stage which, although based on limited data, are significant. This information would be lost in a method which did not separate the zones. Subdivision of the cross-section into the previously defined zones has therefore been retained.

Empirical analysis of the inner floodplain zonal discharge is compromised by the lack of directly measured discharges. Velocity measurements were taken over the floodplains for only five conditions in the SERC Phase B experiments : at two flow depths for each of the 60° trapezoidal and pseudo-natural channels, and at one flow depth for the 110° pseudo-natural channel. There were no measurements for the rod-roughened floodplains. Where velocities were measured, they could not easily be

used to compute discharges over the defined zone. This was because the measuring sections above the plain surfaces and above the main channel did not fit together to provide single, continuous sections across the whole zone. There were therefore no practically usable velocity measurements for this zone. Inner floodplain discharges were estimated by subtracting calculated discharges for the main channel and outer floodplain zones from the total measured discharge. The main channel discharges were calculated using the method developed earlier. The outer floodplain discharges were calculated assuming friction losses only, using the Darcy-Weisbach equation. The friction factors were estimated using the appropriate modified smooth law for the particular experiments, see section 5.4.

The use of calculated, rather than measured, discharges for analyzing the inner floodplain flows has obvious disadvantages. The method for calculating main channel discharges is based on very limited data from the SERC Phase B experiments only. As discussed in the section on the main channel analysis, only a limited range of stages and channel characteristics were included. There is, as yet, no evidence to confirm that the main channel model applies to the Aberdeen channels, as has been assumed in this analysis. On the other hand, obtaining discharges by calculation enables all the stage-discharge data to be incorporated in the analysis, rather than just the few conditions for which velocities were measured. This makes trends very much easier to detect and provides additional information for interpretation.

The Aberdeen data were included in this analysis because they represent some conditions (an extra sinuosity and different main channel geometry) which were not covered by the SERC Phase B experiments, and which were shown in the development of the physically-based model to be significant.

The basic discharge for the inner floodplain zone was calculated assuming friction to be the only loss mechanism. It was further assumed that the plane separating this zone from the main channel would offer the same resistance as the floodplain surface. An analysis was also done with the separating plane subtracted from the wetted perimeter. This did not reduce the final adjustment required and the simpler

calculation was therefore adopted.

The flow in the inner floodplain zone can be expected to be affected by much the same characteristics as that in the main channel. This is supported by inspection of the variables appearing in the physically-based model. The same dimensionless parameters were therefore used. The flow depth was made nondimensional ( $y'$ ) by dividing by the hydraulic depth of the main channel at bankfull, and the cross-sectional shape of the main channel was accounted for by the value of  $B^2/A$ .

The data used in the analysis were the overbank stage discharge measurements for the SERC Phase B standard geometries with smooth and rod-roughened floodplains, and the overbank stage-discharge measurements for the Aberdeen trapezoidal channels. The geometric conditions for these sets are listed in Table 6.9.

For each measured stage the actual and basic inner floodplain discharges were calculated as described above. The ratio of these values ( $Q_2'$ ) defines the adjustment to be applied to the basic discharge.  $Q_2'$  is plotted against  $y'$  for the SERC Phase B data in Figure 6.19 and for the Aberdeen data in Figure 6.20. The numbered points on Figure 6.19 are calculated directly from the integrated main channel discharges used for deriving the prediction model; the numbers indicate the relevant experiments. These points provide checks on the accuracy of the main channel model for some conditions.

Both Figures 6.19 and 6.20 show a clear pattern. For small values of  $y'$  there is a rapid increase of  $Q_2'$  with  $y'$ , in which no distinct variation with channel characteristics can be discerned. For larger values of  $y'$ ,  $Q_2'$  decreases with  $y'$  nonlinearly and at a rate dependent on  $B^2/A$ ,  $s$  and roughness. The ranges of  $y'$  less than and greater than 0.2 were treated separately. It would have been difficult to establish relationships between the variables for the SERC data alone because only two sinuosities are represented and the two values of  $B^2/A$  are not greatly different. The inclusion of the Aberdeen data contributed considerable supplementary information.

The relationship between  $Q_2'$  and  $y'$  for  $y'$  less than about 0.2 is difficult to quantify because of the limited amount of data and their considerable scatter. Much of the scatter can be ascribed to the procedure used to determine the zonal discharge. At low overbank stages the inner floodplain contribution to total discharge is very small. As it was calculated as a small difference between relatively large quantities, errors can be expected to be significant. For the SERC Phase B data, shown on Figure 6.19, it is only for the 60° trapezoidal channel that there are sufficient values to define a trend. Data for the other channels suggest a decrease in  $Q_2'$  for low values of  $y'$  but there are insufficient points to establish the effects of the channel characteristics on the trend. The data for the Aberdeen experiments, shown on Figure 6.20, also show a distinct and similar trend, but again this is not sufficiently well-defined to quantify the effects of channel characteristics. The data for the 1.215 sinuosity channel are particularly widely scattered and some  $Q_2'$  values for very low  $y'$  are too high to appear on the graph. As it was not possible to establish multiple correlations, a single straight line was drawn through all the data, passing through the origin to ensure positive adjustment in all cases. This gave the relationship

$$Q_2' = 6.0 y' \quad (6.52)$$

For values of  $y'$  greater than about 0.2 the relationship between  $Q_2'$  and  $y'$  is nonlinear and clearly dependent on  $B^2/A$  and  $s$ . The dependence on  $f'$  ( $= f_2/f_1$ ) is questionable. The curves for the 60° crossover angle channels with smooth and rod-roughened floodplains coincide fairly closely, although the measured points suggest that roughness has some influence which is opposite at relatively low and high values of  $y'$ . The value of  $f'$  varies over the range of  $y'$  being considered from about 1.8 to 0.78 for the smooth floodplain cases, and from about 3.1 to 11.9 for the rod-roughened floodplain cases. Considering these variations and the close coincidence of the curves, it would appear that floodplain roughness has negligible effect. However, the curves for the 110° crossover angle channels with smooth and rod-roughened floodplains suggest that roughness has a very considerable effect. It would be extremely difficult to quantify this effect because no two points have the same value of  $f'$  and, if roughness is significant, each point actually lies on a different

curve. A comparison of the SERC and Aberdeen data suggested that the curve for the rod-roughened case is consistent and that the curve for the smooth case is out of character.

The curves in Figures 6.19 and 6.20 can best be represented by an equation with the form

$$Q_2' = a y'^b \quad (6.53)$$

Values of  $a$  and  $b$  were determined for each case by plotting the data on logarithmic paper and fitting straight lines through them, as shown in Figures 6.21 and 6.22. The resulting values are listed in Table 6.10.

Visual assessment of Figures 6.21 and 6.22 suggests that  $a$  depends strongly on  $s$ , only slightly and not consistently on  $B^2/A$ , and on  $f'$  for high sinuosities. As discussed above, the dependence on  $f'$  is very difficult to establish. The parameter  $b$  depends strongly on  $B^2/A$ . The combined dependence of  $b$  on  $s$  and  $f'$  suggested by the data for the  $110^\circ$  channel with smooth floodplains is again problematic and cannot be accounted for without further information. The slope of the line representing this condition was assumed to be inconsistent and disregarded. It could then be assumed that  $a$  depends only on  $s$ , and  $b$  depends only on  $B^2/A$ .

The dependence of  $a$  on  $s$  was determined by calculating the average of the values of  $a$  in Table 6.10 for each sinuosity represented. These are plotted in Figure 6.23 and the relationship can be described by

$$a = 1.02 s^{-0.915} \quad (6.54)$$

The dependence of  $b$  on  $B^2/A$  was determined in the same way, ignoring the value for Run B39. The average values of  $b$  are plotted against  $B^2/A$  in Figure 6.24. The relationship for  $b$  is given by

$$b = -0.81 (B^2/A)^{-0.477} \quad (6.55)$$

The adjustment factor, as predicted by equations (6.52) to (6.55), is plotted together with the SERC data in Figure 6.25 and with the Aberdeen data in Figure 6.26.

The discharge for the inner floodplain zone should therefore be obtained by first calculating a basic discharge using an appropriate resistance equation (e.g. Darcy-Weisbach, Chezy or Manning). For this calculation the wetted perimeter should be equal to the width of the meander belt and the friction factor should be appropriate for the inner floodplain surface. The basic discharge should then be adjusted by multiplying by the lesser of

$$Q_2' = 6.0 y' \quad (6.56)$$

and

$$Q_2' = a y'^b \quad (6.57)$$

with

$$a = 1.02 s^{-0.915} \quad (6.58)$$

$$b = -0.81 (B^2/A)^{-0.477} \quad (6.59)$$

#### 6.4.4 Formulation zones 3 and 4

The important mechanisms which affect discharge in the outer zones are

- 1) Friction
- 2) Shear on the interfaces with zone 2

Unfortunately there was not enough data to evaluate the relative importance of each of these mechanisms. However other authors work tends to indicate that shear on the division lines will be relatively unimportant. Hence flow in the outer floodplain zones is assumed to be solely controlled by friction. The zonal discharges are calculated using an appropriate friction equation with the division lines separating

these zones from Zone 2 excluded from the wetted perimeter.

$$\begin{aligned} Q_3 &= A_3 V_3 \\ Q_4 &= A_4 V_4 \end{aligned} \tag{6.60}$$

where

$$\begin{aligned} V_3 &= \left( \frac{8 g R_3 S_o^{1/2}}{f_3} \right) \\ V_4 &= \left( \frac{8 g R_4 S_o^{1/2}}{f_4} \right) \end{aligned} \tag{6.61}$$

#### 6.4.5 Boundary shear stresses

Boundary shear stresses were also measured for some conditions during Phase B of the SERC FCF work. These data have been analyzed by Knight et al (1992) and Lorena (personal communication) and form the basis of the provisional recommendations presented here.

There is no simple, general method for predicting boundary shear for inbank flows in meandering channels, but several simulation models have been developed which can be used for this purpose (for example, by Bridge, 1992, and Nelson and Smith, 1989).

For overbank flows, Knight et al have shown that the sectional average boundary shear stress in the main channel is less than would occur at bankfull stage at all cross-sections through a meander wavelength. Sectional average values are insufficient for designing scour protection, however, because the distributions of boundary shear across the sections are not uniform and vary with flow condition.

The measured distributions suggest that during overbank flows the shear stress on the main channel banks may be higher than for inbank flows at some locations through the meander. The shear stress on the bed, however, is less than for inbank flows. Design shear stresses for scour protection should therefore be based on inbank flows for the bed and on overbank flows for the banks.

Under overbank flow conditions the bank shear stress on the upstream bank does not exceed  $1.6 \gamma y_2 S_o$  in any of the measured distributions, where  $\gamma$  is the unit weight of water defined by  $\rho g$  ( $9.81 \times 10^3 \text{ N/m}^3$ ). On the downstream bank a high, localised stress concentration was observed downstream of each bend apex, associated with the expulsion of water from the main channel to the floodplain (see Figure 5.10). This concentration is shown in Figure 6.27, which presents Lorena's plot of contours of shear stress for the 2.04 sinuosity channel with a flow depth on the floodplain of 50 mm. The concentrations were centred at points between  $60^\circ$  and  $70^\circ$  downstream of the apex section for all the experimental conditions. The maximum observed shear stresses in the concentrations approached  $5 \gamma y_2 S_o$ . The stress concentrations are very localised and decrease rapidly with distance but, because of the limited experimental conditions and consequent uncertainty regarding locations, they should be assumed to be more extensive when designing scour protection. The enhanced shear stresses also extend for some distance over the floodplain on the downstream side of the channel.

For the design of scour protection, it is recommended that boundary shear stresses be determined for the main channel bed and banks for the full range of inbank stages, using currently available methods. In addition, the banks should be able to resist stresses of

$$\tau = 1.6 \gamma y_2 S_o \quad (6.62)$$

on the upstream side, and

$$\tau = 5 \gamma y_2 S_o \quad (6.63)$$

on the downstream side.

The observed shear stress distributions suggest that the sediment transport capacity in the main channel will be lower for overbank flows than for inbank flows. Net deposition of sediment may therefore occur in the main channel during prolonged flood events. The shear concentrations on the downstream banks during overbank flows suggest enhancement of meander migration in the valley direction during prolonged flood flows, and also corroborate the mechanism of meander cutoff by opening chutes across point bars.

#### 6.4.6 Summary

Experimental data from Phase B of the SERC FCF has been analyzed to produce a methods for the estimation of discharges in compound channels. The best approach was found to be based on dividing the cross-section into zones and calculating the discharge in each zone independently. The four zones chosen are:

- 1) The main channel below bankfull level.
- 2) The floodplain within the meander belt.
- 3) The floodplain beyond the meander belt on the left bank.
- 4) The floodplain beyond the meander belt on the right bank.

The zones are illustrated in Figure 6.28

For a given stage the total discharge will be calculated as the sum of the component discharges, i.e.

$$Q = Q_1 + Q_2 + Q_3 + Q_4 \quad (6.64)$$

The zonal discharges will be calculated independently, accounting for the appropriate energy loss mechanisms in each.

## **Zones 3 and 4**

The discharges in zones 3 and 4 are assumed to be controlled by bed friction only and are given by equations 6.60 and 6.61.

## **Zone 1**

The loss mechanisms which affect the main channel discharge are complex. It was not possible to develop a physically based description of these mechanisms and an empirical procedure was developed. A correction factor is applied to the bankfull discharge to obtain the variation in the main channel discharge with over bank stage. The form of the correction factor is given by equations 6.30, 6.31 and 6.32.

## **Zone 2**

Two alternative methods for predicting the discharge in the inner floodplain zone were developed. The first method attempts to account for the principal loss mechanisms using physically-based deterministic formulations. The formulations are based on a very simple conceptual model of the loss mechanisms and required empirical adjustment to account for the additional complexities involved. The model explicitly accounts for bed friction and expansion / contraction over the main channel and is described by equations 6.51, 6.50, 6.49, 6.48, 6.41, 6.40 and 6.34.

The second method is purely empirical and follows an approach similar to that used for the main channel zone. A basic discharge is calculated assuming friction losses only, and this is then adjusted to account for the effects of flow interaction with the main channel. The form of the correction factor is given by equations 6.56, 6.57, 6.58 and 6.59.

These two approaches to computing the inner floodplain discharges give two separate methods of calculating discharges in meandering compound channels. For convenience the model incorporating the expansion contraction losses will be referred

to as the James and Wark method while the empirical procedure for zone 2 will be referred to as the James and Wark 2nd method.

## **Bed shear stresses**

Bed shear stress data was measured under overbank conditions during Phase B of the FCF work. The analysis carried out by the investigators is summarised above. The main channel bed shear stresses are reduced during overbank flow compared to bank full conditions. The shear stresses on the floodplains adjacent to the main channel show peak values which are associated with the exchange of flow between the main channel and the floodplain. Equations 6.62 and 6.63 give a rough estimate of the likely peak bed shear stresses.

## **6.5 Verification of the procedure**

### **6.5.1 Background**

The previous chapter details the development of two new procedures for estimating the conveyance of meandering compound channels. One procedure (James and Wark) includes a semi-empirical model of the inner floodplain flows, while the other is based on a purely empirical approach to the inner floodplain discharge. Other methods were also identified in the literature. The work reported in this chapter was carried out to compare the new and existing methods. A selection of the laboratory data available from various sources described in chapter 5 was obtained and the methods were applied to predict the stage discharge values. In some cases zonal discharges were also measured and these provide a check on the predicted distribution of flows in addition to total discharges.

### **6.5.2 Methods**

Of the methods listed in chapter 5 the following have been used in this verification:

Bed friction only (BFO)                  James and Wark (JW)

James and Wark 2	(JW2)	Ervine and Ellis	(EE)
Greenhill 4	(GH4)	Greenhill 5	(GH5)

The James and Wark; Ervine and Ellis and the Greenhill methods are described in detail in section 6.3.2. The bed friction only method is based on the James and Wark channel subdivision. The discharges are calculated assuming only bed friction is acting and the areas, wetted perimeters and hydraulic slopes for each zone are as defined for the James and Wark method.

### 6.5.3 Application to laboratory data

#### Data

The available laboratory data is reviewed in Chapter 5. Five of the eight available data sets are considered to be of good enough quality for use in the development and verification processes. Two of these sets were used to develop the new procedures (SERC and Aberdeen). The data sets which have been used in this verification work are listed in Table 6.11 and 6.12. These are stage discharge data collected under overbank flow conditions. The test numbers have been assigned for ease of data handling. Tables 6.11 and 6.12 also list the values of parameters required for the various calculations, such as the width of zones 2 and the whole floodplain; the side slopes of the floodplain edges and radius of curvature of the channel centerline. These are shown on Figure 6.1. Table 6.13 lists the values of parameters required when calculating the main channel discharges.  $\theta_m$  is the mean angle between the channel centerline and the floodplain centreline, averaged over a wave length. This mean angle is required for the Ervine and Ellis calculations. Because most of the geometries were constructed using a combination of straight reaches and circular arcs these parameters were easily calculated. In the case of Sooky's sinusoidal geometry a numerical integration was carried out to determine  $\theta_m$ .

#### Total discharge and stage

Each of the above methods were applied to the available data as follows.

- 1) The predicted discharges were calculated for the measured stages. This allowed the error in the predicted discharges to be calculated according to:

$$\% \text{Error in predicted flow} = 100 (Q_{\text{calc}} - Q_{\text{meas}}) / Q_{\text{meas}}$$

- 2) The calculated stage discharge curves were then used to obtain calculated stage values by linear interpolation using the measured discharges. The error in the predicted stage was calculated in terms of the depth of flow in the main channel (H) according to:

$$\% \text{Error in predicted depth} = 100 (H_{\text{calc}} - H_{\text{meas}}) / H_{\text{meas}}$$

The mean values of these errors were calculated for each condition. In addition means were calculated over combinations of the data as follows:

- 1) All SERC data
- 2) Smooth floodplain SERC data
- 3) Rod roughened SERC data
- 4) Vicksburg data
- 5) Kiely data
- 6) Sooky data
- 7) All data
- 8) All data not used in the development of the methods.

### Errors in discharges

The mean errors in the predicted discharges for the SERC FCF data are shown in Table 6.14. The BFO method over predicts by considerable margins with mean errors of 44.8%, 12.3% and 32.5% for the smooth, rough and all the data. The JW method gives errors of less than 5% for all three subsets (-3.3%, -5.3% and -4.0%) although it is tending to under predict. JW2 gave good results for the smooth data, -5.2%, but gave poor results for the rod roughened data, -22.8%, which shows up in a larger error of -11.8% over all of the data. EE also gave reasonable results over both the smooth and rough data with errors of 4.9%, 8.2% and 6.1% respectively. GH4 tends to over predict for the smooth data and under predict for the rough data

with errors of -22.5%, -0.2% and 13.9% over all the FCF data. GH5 does reduce these errors slightly to 12.7%, -7.5% and 5.1% overall.

Four of these methods (JW, JW2, GH4 and GH5) were developed based on the SERC FCF Phase B data. It is not surprising that these four methods give good accuracy when applied to this data set. The main conclusion is that the JW method is more accurate than the JW2 method for cases with roughened floodplains. None of the other data was collected with roughened floodplains and so it has been impossible to verify this conclusion against independent information. Future experimental work into conveyance of meandering overbank flow should cover conditions with rough floodplains.

Table 6.15 gives the mean errors for the various methods over the Aberdeen, Vicksburg and Kiely data sets. It is clear from the Aberdeen and Vicksburg results that the BFO method becomes less accurate for more sinuous channels. In general typical errors of about 30% to 40% were obtained with these data. Both the JW and JW2 methods give very similar results for the Aberdeen data with average errors of 0.6% and 0.8% respectively. This is not surprising since this data was used to develop both of the models for the inner floodplain flows. Again the EE method gave reasonable predictions with a mean error of -2.3%. GH4 and GH5 over predicted discharge by 16.9% and 12.7% respectively. There are too few data for each individual condition of the Vicksburg and Kiely data sets to make any detailed conclusions but it is possible to say that the JW, JW2 and the EE methods gave similar overall predictions.

The application to Sooky's data is summarized in Table 6.16. Again there are too few data for each individual condition to make any meaningful conclusions but over all 63 data points the BFO method gave a mean error in discharge of 20.8%. The JW and JW2 methods gave errors of -1.9% and 1.2% and the EE method an error of 14.6%. The GH4 and GH5 performed well on this data set with mean errors of -1.4% and 5.2% respectively.

Table 6.17 summarises the mean errors over the various sub sets and all the data. The BFO method over predicted discharge by 34.1% on average over all the laboratory data available. The JW and JW2 methods generally gave similar results for the smooth data and this is reflected in the mean errors of -2.1% and -4.3% respectively. The EE method gave a mean error of 5.3% and GH4 and GH5 gave mean errors of 11.5% and 8.0% respectively. Given these results Table 6.18 shows the six methods ranked in order of accuracy of predicted discharge for the various sub sets of the data. It is obvious that the bed friction only method is the worst of all six methods followed by Greenhill's methods 4 and 5 respectively. It is more difficult to distinguish between the best three methods.

The above discussion has concentrated on the mean errors and has ignored the standard deviations (SD) in these means. In general the JW and JW2 methods have SD's of between 5% and 10% for the various sub sets of the data. The Ervine and Ellis method although giving roughly equivalent mean errors shows SD's between 15% and 20%. These quite large standard deviations are not caused by random scatter about the means but are due to systematic trends in the errors with depth, this is discussed in detail below but it is possible to say that the JW and JW2 methods gave slightly more accurate predictions. Over all the data the JW method performed better with a mean error and standard deviation of -2.1% and 9.7% compared to -4.3% and 13.2% for the JW2 method. In addition it has been shown to be more accurate for the data with roughened floodplains, mean error and SD -4.0% and 8.4% compared to -11.8% and 14.4% for the JW2 method.

### **Errors in stage**

The results shown in Tables 6.19 to 6.22 are the mean % errors in calculated depth for the various data sets. In general these results follow the discussion of the errors in discharges with two important exceptions.

- 1) Where a method over predicts discharge then it under predicts water level.
- 2) The values of errors in calculated stage are much less than the corresponding

errors in discharge.

This can be demonstrated by comparing the values in Tables 6.17 and 6.22. The Bed Friction Only method over predicted discharge by 34.1% on average but under predicted the channel depth by 4.7%. Similar comparisons can be made for the other methods.

The variation of errors in predicted discharge and stage for the six methods with relative depth are shown in Figures 6.29 to 6.35. Ignoring all losses except bed friction gave errors in the predicted discharges which fall mainly in the range 10% to 50%, with corresponding errors in depth between -10% and -2%. It is apparent from Figure 6.29 that the errors depend on the geometry of the channel with the various cases displaying different distributions of errors with the depth of over bank flow. In general the errors show strong trends with stage. The JW method gives a much smaller range of errors, Figure 6.30. Most of the data falls in the range -10% to 0% for discharge and -2% to 3% for the water depth. At low over bank stages ( $H-h/H < 0.15$ ) the method tends to over predict discharges with the errors reducing at higher stages.

Figure 6.31 shows the error distributions for the JW2 method. The majority of the errors in predicted discharge fall in the range -20% to 10% with the corresponding errors in depth lying between 2% and 15%. There are more noticeable trends in the errors for this method compared to the JW method. The rod roughened data (33, 34 and 43) show a strong increase in the under prediction of discharge with depth.

The Ervine and Ellis method gave errors in predicted discharge in the range -30% to 50% with the corresponding errors in water depth lying in the range -8% to 10%, Figure 6.32. This method tends to over predict discharge (and under predict water level) at low relative depths and under predict discharge at high depths with an approximately linear graduation between. This agrees with the limited number of results quoted by Ervine and Ellis (1987). It is interesting to note from Table 6.15 that for the data collected from the Vicksburg flume the Ervine and Ellis method is

the most accurate of all the methods. Ervine and Ellis only applied their method to the Vicksburg data and reported good agreement.

Figures 6.33 and 6.34 show the variation of errors for Greenhill's methods 4 and 5 respectively. Both these methods give variations of error for the various cases which are similar to those obtained with the bed friction only method but shifted towards the zero error line. Greenhill's method 4 shows errors in discharge which are shifted by approximately 20% - 22% while method 5 gives errors in discharge shifted by about 25 - 27%. Both of these methods display quite wide ranges of errors.

The results above show that the semi-empirical expansion contraction model developed by the authors (JW) is more accurate than the other methods with a mean error that is well within experimental tolerances. The tendency of the method to under predict discharges is a conservative fault. In a design situation a channel is usually sized to have a required discharge capacity at a given water level. The authors method gives a slightly larger channel size than actually required hence water levels will be slightly lower than predicted. The Ervine and Ellis method, which is based on a similar conceptual model, gives a mean error which is probably acceptable in practice but the larger standard deviation indicates a wider and more systematic spread of errors about the mean. The alternative empirical model developed by the authors (JW2) was found to be less accurate when the floodplains are rougher than the main channel and is not recommended. By ignoring the effects of loss mechanisms other than bed friction the above results indicate that errors in total discharges in the order of 35% may be expected. The empirical attempts by Greenhill to reduce these errors do succeed to a limited extent but do not significantly reduce the spread of the errors. The James and Wark method has the additional advantage over the others that it is based on measured velocities and discharges for zone 1, and should give more reliable predictions of the zonal distribution of conveyance. There is limited independent information available on zonal distributions of flow and this is considered below.

### **Sensitivity analysis**

The James and Wark method requires values of geometric parameters which are well defined in laboratory channels but usually poorly defined in natural channels. The values of meander wavelength and main channel side slopes (required for the zone 2 model) in particular are difficult to define exactly for natural channels. The following sensitivity analysis was carried out to determine the degree of precision required when estimating these parameters in practice.

The values of the wave length ( $L$ ) and side slopes ( $S_s$ ) for the available laboratory data are known exactly. Errors in the predicted discharges are not due to uncertainties in  $L$  or  $S_s$  but to other causes. The effects of uncertainties in  $L$  and  $S_s$  were investigated as follows.

The known values of  $L$  and  $S_s$  for all of the available data were factored up or down by fixed amounts. The JW method was applied using these factored values of  $L$  or  $S_s$  in the calculation. The mean errors in predicted discharge were calculated over all 279 data points. Thus the variation in errors could be related to the known errors in  $L$  or  $S_s$ .

The effect of uncertainties in wave length are summarized in Table 6.23. The mean error in the predicted discharges is reduced from -2.1% to -10.3% by the 50% reduction in wave length and increases to 2.3% for a 50% increase in wave length. Thus an error in wave length of  $\pm 50\%$  results in a  $\pm 10\%$  change in the mean error in predicted discharge. Similar results are shown in Table 6.24 for changes in side slope. The mean error is reduced from -2.1% to -5.3% by a 100% reduction in side slope and increases to 2.4% for a 100% increase in side slope. Thus changes of  $\pm 100\%$  in side slope values results in a  $\pm 5\%$  change in the mean error. These results, although not conclusive, indicate that predicted discharges are relatively insensitive to errors in wave length and main channel side slope and great accuracy in their estimation is not necessary. However similar sensitivity test should be carried out in any practical application to confirm these findings.

### **Discharge distributions**

The results above demonstrate the overall accuracy of the various methods. The methods are based on similar channel subdivisions. The discharges in the various parts or zones of the channel are calculated separately and summed together to obtain the total discharge. Hence the methods give the distribution of flow between the zones in addition to the total discharge.

There is very little independent information available on the distribution of discharge in meandering overbank flow. Sooky (1966) carried out detailed velocity measurements in shallow (403, depth 0.0613 m) and deep (409, depth 0.080 m) meandering channels which were otherwise identical. These experiments were carried out in a channel which was built at a scale approximately 8-9 times smaller than the SERC FCF Phase B geometries. Sooky integrated these velocity measurements to obtain the proportion of the total discharge within each zone. Kiely (1989) gives similar information for two depths (Test 301, 0.060m and 0.080m). The measured discharges in all four zones for these four cases are given in Table 6.25. Table 6.26 gives the errors in the predicted discharges for these four cases. The BFO method over predicts by up to 50% while the JW method gave results accurate to within  $\pm 10\%$ , the JW2 was accurate to  $\pm 17\%$ , EE 30% and Greenhill's two methods to 30%. The JW method gave very good overall accuracy for Kiely's data while none of the methods were particularly accurate for Sooky's two conditions. The main reason was probably a poor definition of bed friction for Sooky's data.

Table 6.27 shows the measured and calculated distribution of flows between the various zones as percentages of the total discharge. The results obtained for Sooky's data show little difference between the various methods, they all give similar distribution of flows. This may be a function of the very low sinuosity of Sooky's channel. Kiely's results show more differences between the methods. The JW method gives excellent predictions of total discharge (within 4% and 1%). At the lower depth the JW method gives the distribution of flows almost exactly but under predicts the zone 1 discharge for the higher depth, this is coupled with a general over prediction for the other zones. The JW2 method gave similar results to the JW method for the flow distributions. It gave excellent results for the smaller depth case

and under predicted the main channel discharge for the deeper case. In fact all the methods under predict the zone 1 discharges for the deeper case and this would indicate that the bed friction law is a better fit to the data at low stages. The EE and the two GH methods over predicted the zone 1 discharge and under predicted the zone 2 discharges.

These measured distributions of flow were derived from integrating point velocity measurements and the derived zonal flows are probably accurate to about 5%. The comparisons show that in general both the JW and JW2 methods give flow distributions which agree with the measured distributions. On the basis of this very limited data it can be concluded that the author's method (JW) gives superior predictions of both the total and zonal flows in meandering compound channels. It is hoped that future experimental work will concentrate on the collection of data giving the zonal distribution of discharges to confirm these conclusions.

#### **6.5.4 Application to straight laboratory data**

The SERC FCF work has been carried out in two phases. Phase A dealt with straight compound channels and Phase B dealt with meandering compound channels. The Phase A data has already been used to develop a method of calculating conveyance in straight compound channels, Ackers (1991). The work reported in section 6.2 demonstrates that these straight channel methods cannot be used to predict discharges in meandering compound channels.

The James and Wark method was developed based on the Phase B data. The independent data available for verification included : the Vicksburg data with sinuosities of 1.57, 1.40 an 1.2; Kiely's data with sinuosity 1.22 and Sooky's data with sinuosity of 1.09. The author's method gave reasonable predictions for all of these data. Since the straight channel methods are known to give inaccurate predictions for meandering channels it is to be expected that the meandering channel methods will give poor predictions of discharge in straight compound channels.

The performance of the James and Wark method applied to data from straight compound channels has been investigated. The Phase A data set was available and was used in this evaluation along with the straight channel data available from the Aberdeen flume (100) and Kiely's results (300). The details of the various tests and results from Phase A are reported in full by Ackers (1991). Of the Phase A data tests 1,2,3,5,7,8,9,10 were used in this evaluation, a total of 198 data points were available. The appropriate modified smooth law or Ackers' rod roughness method were used to obtain the bed friction factors.

When applying the meandering channel methods to straight channel data the inner floodplain zone disappears. Zone 2 has the same width as the main channel and it was assumed that the zones 1 and 2 could be considered as a single unit. The channel division therefore has reduced to the straight channel division method (DCM2).

The James and Wark method gave an average error in predicted discharge of -27.3% with a standard deviation of 17.0%. This general under prediction of discharges by up to 50% demonstrates that although the method can accurately predict discharges in channels with sinuosities as low as 1.09 it cannot be applied to straight compound channels. Obviously further work is required to investigate the conveyance of compound channels with sinuosity between 1.0 and 1.09.

### **6.5.5 Application to field data**

The procedure presented above was developed and verified using laboratory model data. There is very little field information available regarding the performance of full scale meandering channels with floodplains. The only detailed field investigation known at present was carried out on the River Roding in Essex, see Sellin and Giles (1989) or Sellin et al (1990). One other site is also currently being investigated by Sellin. A physical model of a 250m long section of the River Blackwater in Hampshire has been constructed in the SERC FCF at a scale of 1:5. Field measurements are scheduled to commence in early 1993 and are to run for three

years. The results of this study were not available at the time of writing but should provide improved validation data.

### **The Roding study**

The Roding is a relatively small river with a channel width and depth of about 7m and 1.5m respectively. Full details of the field and laboratory measurements carried out on this site are available in Sellin and Giles (1988) and Sellin et al (1990). The study reach lies downstream of Abridge and as part of a flood alleviation scheme a two stage channel was formed by excavating approximately 30m wide berms on either side of the main channel, Figures 6.34 and 6.35. The original channel was untouched and remained in the natural state with a bankfull capacity of approximately 3 cumecs. The resulting flood channel has a low flow channel which meanders within the berm limits with a sinuosity of 1.38 and a wave length of approximately 96m. Hence the channel does not possess outer floodplain zones. The berms were formed at a level below the surrounding floodplain and were intended to provide extra flood discharge capacity and so relieve flooding on the existing floodplain for flows with a return period of up to thirty years. Shortly after completion of the scheme it became clear that the actual capacity of the channel was less than the design value. This was partly assigned to the difference between the assumed berm vegetation (short grass) and the actual vegetation which was extremely dense. The design case assumed that the berm would be grazed by farm animals but in fact this did not happen and the National Rivers Authority (NRA) were forced to cut the growth mechanically at considerable cost.

The field and laboratory projects investigated the effects of different maintenance policies on the channel capacity. Most of the conditions investigated were with the flood berms covered, totally or partially, with extremely dense vegetation and verification of calibrated bed roughness values was not possible. The roughness values varied strongly both with stage and during the growing season. The data recorded after a full cut on the berm showed much less variation in berm roughness values and so were felt to provide the best information for validation of the author's

procedure. The method was applied to the stage-discharge data from the following two cases.

- P2 The berm growth was cut immediately after the summer growing season and so the berms were covered in short grass.
- M2 The laboratory model data corresponding to the smooth berm case (P2 on the prototype).

In order to apply the procedure to these measurements the seven available surveyed sections were used to provide reach averaged areas, widths etc for both flow zones at stages up to 1.0m above the berm level and these are given in Table 6.28. The information provided by Sellin and Giles (1988) and Sellin et al (1990) combined with widely accepted guidelines, Chow (1959) and Henderson (1966) allowed the berm Manning's  $n$  values for the two cases, P2 and M2 to be estimated as 0.050 and the main channel Manning's  $n$  was estimated as 0.044. The longitudinal slope of the berm was  $1.405 \times 10^{-3}$ .

The mean errors in the predicted discharges given by the BFO, JW and JW2 methods are shown in Table 6.29. It is apparent that the recommended method (JW) improves the overall accuracy of the predicted discharges to about -2% and that by ignoring the non-friction head losses discharge will be over-predicted by about 10% on average. The empirical JW2 method gave very poor predictions resulting in a mean error of approximately -30%. These results are confirmed by Figure 6.36, the JW and BFO methods give stage discharge curves which follow the general trend of the data. The JW method tends to under predict discharge at low floodplain depths and over predict at high floodplain depth, while the BFO method over predicts for all stages.

Some sensitivity tests were carried out to investigate the effect of berm roughness on the total channel capacity. Table 6.30 shows the variation of mean errors in predicted discharges, for the BFO and JW methods, with berm roughness for case P2. Both methods over-predict discharges with low berm roughness and under-predict with

high berm roughness. The author's method always gives smaller discharges because the non-friction energy losses in the two zones are explicitly accounted for. The difference between the mean errors for the two methods reduces from >100% at very low roughness to about 10% at the calibrated roughness. At higher roughnesses the difference between the two methods remains approximately constant at about 10%.

These results show that as the floodplain becomes smoother the two methods diverge more. Thus the effect of increased floodplain roughness is to make the non-friction head losses less important. Bed friction is likely to be the most important single source of energy loss in natural rivers and remains a potential source of significant error in conveyance predictions. The estimation of bed friction factors is largely subjective even given the comprehensive guidelines presented in standard texts such as Chow (1959) and Henderson (1966). Thus it is not possible to give general guidelines on the choice of bed friction value as site specific aspects are likely to govern the relative importance of the various loss mechanisms. Tests should be carried out for each application to gauge the sensitivity of the solution to variations in roughness values.

## **6.6 Summary and conclusions**

- 1) Various methods suitable for the determination of flow in straight compound channels have been applied to a selection of stage-discharge data collected in meandering compound channels. The poor predictions obtained confirm that straight channel techniques are not suitable for meandering channels (section 6.2).
- 2) A literature search was carried out to identify methods proposed by previous authors (6.3.2).
- 3) On the basis of a knowledge of the important mechanisms which affect the discharge capacities of meandering compound channels and an appreciation of modelling techniques a strategy was devised for developing an improved

method of discharge estimation (6.4.1).

4) Experimental data from Phase B of the SERC FCF has been analyzed to produce methods for the estimation of discharges in compound channels. The best approach was found to be based on dividing the cross-section into zones and calculating the discharge in each zone independently. The four zones chosen are:

- 1) The main channel below bankfull level.
- 2) The floodplain within the meander belt.
- 3) The floodplain beyond the meander belt on the left bank.
- 4) The floodplain beyond the meander belt on the right bank.

The zones are illustrated in Figure 6.28 and for a given stage the total discharge will be calculated as the sum of the component discharges. These will be calculated independently, accounting for the appropriate energy loss mechanisms in each (6.4.1).

5) The loss mechanisms which affect the main channel (zone 1) discharge are complex and an empirical procedure has been developed to account for these mechanisms (6.4.2). A correction factor is applied to the bankfull discharge to obtain the variation in the main channel discharge with over bank stage. The form of the correction factor ( $Q_1'$ ) is given by equations 6.30, 6.31 and 6.32.

6)  $Q_1'$  was found to depend on:

- 1) the floodplain flow depth at the edge of the main channel ( $y_2$ );
- 2) the channel sinuosity ( $s$ );
- 3) the cross-section geometry and
- 4) floodplain roughness.

7) Two alternative methods for predicting the discharge in the inner floodplain (zone 2) were developed (6.4.3). The first method attempts to account for the principal loss mechanisms using physically-based deterministic formulations. The formulations are based on a very simple conceptual model of the loss mechanisms and required empirical adjustment to account for the additional complexities involved. The model explicitly accounts for bed friction and expansion / contraction over the main channel and is described by equations 6.51, 6.50, 6.49, 6.48, 6.41, 6.40 and 6.34.

The second method is purely empirical and follows an approach similar to that used for the main channel zone. A basic discharge is calculated assuming friction losses only, and this is then adjusted to account for the effects of flow interaction with the main channel. The form of the correction factor is given by equations 6.56, 6.57, 6.58 and 6.59.

8) The discharges in zones 3 and 4 are assumed to be controlled by bed friction only and are given by equations 6.60 and 6.61 (6.4.4).

9) Bed shear stress data was measured under overbank conditions during Phase B of the FCF work (6.4.5). The analysis carried out by the investigators is summarised above. The main channel bed shear stresses are reduced during overbank flow compared to bank full conditions. The shear stresses on the floodplains adjacent to the main channel show peak values which are associated with the exchange of flow between the main channel and the floodplain. Equations 6.62 and 6.63 give a rough estimate of the likely peak bed shear stresses.

10) The two methods developed by the authors and four other methods have been used to predict discharges and stages for the available laboratory data. The author's semi-empirical method (JW) was found to give the most accurate predictions of total discharge and acceptable predictions of the distribution of discharges (6.5.3).

- 11) The available data used in this verification covered a limited range of conditions. Further experimental work is required to look at both total discharges and the distribution of discharges for :
  - a) Meandering channels with low sinuosities ( $<1.09$ ).
  - b) Meandering compound channels with rough floodplains.
  - c) Low over bank depths ( $y' < 0.2$ )
  
- 12) The sensitivity of the James and Wark method to variations in the values of both meander wave length and main channel side slope has been investigated. The results indicate that in great precision in estimating these values is not required (6.5.3).
  
- 13) The procedure has been applied to the best field data available and has been shown to give improved predictions compared to current practice. The sensitivity of the results to variations in bed roughness value has been investigated. The non-friction energy losses are shown to be less important as the floodplain is roughened. Bed friction remains the most significant source of energy loss in rivers with overbank flow (6.5.5).
  
- 14) The JW method has been applied to stage-discharge data from straight laboratory channels and gave very poor predictions of discharge. The JW method gave adequate predictions for Sooky's data which had sinuosity of 1.09. Further research is required to provide discharge estimation methods for meandering compound channels of low sinuosities (6.5.4).

## **CHAPTER 7**

### **RECOMMENDATIONS FOR FUTURE RESEARCH**

#### **7.1 Introduction**

The present investigation into flows in compound channels has concentrated on developing improved methods for stage discharge estimation in both straight and meandering channels. In general the available laboratory and field information was used to develop conceptual models of the important processes. Suitable methods of approximating these processes were identified and developed. The research which still remains to be carried out falls into two main categories:

- 1) The collection of independent information to use in verifying the available laboratory and field data for a wider range of conditions.
- 2) The development of two and three dimensional numerical models and their application to the available data and the improvement of existing simplified one dimensional techniques.

#### **7.2 Straight compound channels**

##### **7.2.1 Background**

The problem of flow in straight compound channels has been extensively studied. The vast majority of laboratory data sets have been collected in small scale compound channels with hydraulically smooth boundaries. Ackers (1991) reviewed a wide selection of the data available in the literature. He concluded that much of it is not suitable for use in validating methods of calculating conveyances in prototype compound channels for the following reasons:

- 1) The measurements were carried out in small scale flumes and at smaller depths may have been prone to laminar flow.
- 2) Typically channel cross-section geometries are distorted, width/depth ratios

are typically too low compared to natural channels. This stems from practical difficulties in taking measurements in shallow depths.

- 3) In short flumes it is often difficult to ensure completely uniform flow and this makes it difficult to accurately calibrate the bed friction values. In addition many investigators do not publish sufficient calibration data to use in checking the calibrated roughness values. The use of rough turbulent roughness indicators such as Manning's  $n$  or  $k_s$  with hydraulically smooth facilities is to be discouraged. A single value is unlikely to be accurate at all depths or slopes.

### **7.2.2 Laboratory studies**

Given that much of the existing laboratory data is not of sufficient quality to use in confirming the new methods of discharge estimation it is still worth while to carry out accurate measurements in laboratory compound channels.

This work should concentrate on providing detailed information for the validation of the simpler 1-D methods (eg. Ackers' method and the LDM) and complex 3-D turbulence models. There is a particular need to undertake experiments to measure stage-discharge, velocity (both longitudinal and secondary currents) and bed shear stresses for compound channels under the following conditions.

- 1) In compound channels with floodplains roughened to various degrees. The method of using vertical dowel rods produces extreme floodplain roughness compared with the main channel and also may distort the internal turbulent structure of the flow since most of the 'extra' resistance is caused by the constriction of the flow area and the wave effects from the free surface. Lambert's approach in roughening the floodplain with various sizes of gravel has been tried at HR Wallingford and does provide a relatively simple way of obtaining an intermediate roughness condition.

- 2) In compound channels with a non-hydraulically smooth bed. All of the laboratory data available was collected in flumes with a hydraulically smooth main channel, even data sets with roughened floodplains. The strength of the various interaction mechanisms may be reduced in the case of rougher main channels and further data is required.
- 3) In compound channels with floodplains which slope transversely away from the main channel. The majority of the experimental data available was collected in channels with horizontal floodplain surfaces. Only Myers' has studied laboratory channels with sloping floodplains and further work under a wider range of conditions is required.

### **7.2.3 Further development of discharge estimation techniques**

Chapter 4 shows that two methods of discharge estimation in straight compound channels were superior than the others when applied to the available laboratory data. These two methods are considered below and strategies to further improve them are identified.

Ackers' method is purely empirical but is based on a very detailed analysis of the best laboratory data available. In order to improve this method in the light of new information it would be necessary to repeat much of the empirical analysis including new data sets. Should sufficient data of a suitable quality become available this would be worthwhile.

The lateral distribution method is based on a depth averaged description of the flow distribution across a channel. Of the two forms of the equation (one in terms of depth averaged velocity and one in terms of unit flow) the unit flow form appears to perform better in a wider range of conditions.

The main source of uncertainty in the method arises in the choice of lateral eddy viscosity model. The use of the non-dimensional viscosity model which relates

lateral viscosity to local bed shear stress conditions is attractive and has been found to give reasonable results by various authors. There is no doubt that the form of equation strongly influences the required values of non-dimensional eddy viscosity. Other authors who use the depth averaged velocity form have found it necessary to use several values across a compound cross-section in order to obtain reasonable predictions of flow distribution, while it is shown in chapter 4 that a single value of NEV with the unit flow form of the equation can give adequate results.

The unit flow form of the method has only been applied to six velocity profiles from two cases of the SERC FCF Phase A data. It would be useful to repeat the work of Shiono and Knight (1989, 1990 and 1991); and carry out a detailed comparison of measured and predicted depth averaged velocity, unit flow and bed shear stress distributions; using the unit flow version of the method applied to all of the available velocity and bed shear stress data.

### **7.3 Meandering compound channels**

There has been much less work carried out for flow in meandering compound channels compared with straight compound channels. Consequently there are far more opportunities for further work. In general these opportunities cover both the physical and theoretical modelling of flow in meandering compound channels.

#### **7.3.1 Stage-discharge prediction for inbank flows**

It is clear from Chapter 5 that the effect of meandering on inbank channel conveyance is considerable, and the importance of main channel capacity in a two-stage channel design or analysis is obvious. The SCS and LSCS methods of adjusting the friction factor to account for meander effects has been shown to be reasonable. They have no theoretical basis, however, and suffer from the main limitation of relating bend energy losses to only one parameter. In order to circumvent these limitations it is recommended that Chang's (1984) approach be further developed to provide simple guidelines for estimating losses that account for

a wide range of all the relevant parameters. The guidelines should allow losses to be evaluated for individual bends as well as for a meander train. The effect of variation of cross-section along the channel should also be investigated, but this would require a more complete description of flow in bends.

### **7.3.2 Laboratory studies**

#### **Extension of existing data sets**

Existing laboratory studies cover a relatively narrow range of conditions in meandering compound channels. Further laboratory work is required either to verify or extend the present method (James and Wark) for conditions other than those covered by the existing data. In particular the following list of experiments would fill gaps in the available laboratory data. This list is not in any particular order or importance.

- 1) Undertake experiments to measure stage-discharge, velocity and bed shear stresses for meandering channels with sinuosities between 1.0 and 1.09. This is important because there is a need to establish at what sinuosity a compound channel analysis treatment should switch from straight to meandering.
- 2) Undertake experiments to measure stage-discharge, velocity and bed shear stresses for low overbank stages, ie ( $y_2/h$ ) values between 0.0 and 0.1. There are few data points in this region and it is probably the most common range of overbank flow conditions which occur in nature.
- 3) Undertake experiments to measure stage-discharge, velocity and bed shear stresses for floodplains with transverse slope away from the main channel. There are few laboratory data for this condition and natural floodplains tend to slope laterally in this manner. There is some conjecture that it may be more realistic to analyze overbank flow in these geometries using straight channel techniques, as the flow will be constrained parallel to the main channel.

- 4) Undertake experiments to measure stage-discharge, velocity and bed shear stresses for sinuosities between 1.09 and 1.20; 1.20 and 1.40; 1.40 and 2.01 and for sinuosities greater than 2.01. All known laboratory experiments have been carried out at or very close to sinuosities of 1.09, 1.20, 1.40 and 2.01 and this is obviously leaves gaps in the available information.
- 5) Undertake experiments to measure stage-discharge, velocity and bed shear stresses in meandering channels for a range of channel to floodplain widths and for cases with asymmetric floodplains on either side of the main channel. All existing data have been collected for a limited range of channel to floodplain width ratios and with symmetric floodplains.
- 6) In order to confirm the SERC Phase B data it would be useful to conduct experiments in small scale flumes with geometries which are exact scale models of the phase B tests. If such experiments were carried out and proved to be positive then the gaps in the Phase B results could be filled using data collected in much smaller laboratory facilities.
- 7) Undertake experiments to measure stage-discharge, velocity and bed shear stresses in meandering channels with roughened floodplains. The only information currently available was obtained from the SERC FCF for only two channel sinuosities. The method of using vertical dowel rods to roughen the floodplain also produced extreme floodplain roughnesses. Independent information is required to confirm the SERC FCF data.
- 8) Undertake experiments to measure stage-discharge, velocity and bed shear stresses in meandering channels with different cross-sections. The SERC FCF phase B investigation covered trapezoidal and pseudo natural cross-sections. Other studies have been conducted either with rectangular or trapezoidal main channel cross-sections. Further information on the effects of varying channel side slopes in trapezoidal channels and the effects of changes in cross-section shape along a meander would be useful.

Laboratory work intended to extend existing information should be carried out in channels with idealized geometries similar to those from which the existing laboratory data were obtained. For example the floodplains should be uniform in width along the length of the channel and the meandering main channel plan geometry should be a simple repeating geometric shape.

### **Laboratory studies of loss mechanisms**

The formulation of models of loss mechanisms has exposed some surprising gaps in experimental results. Some useful information could be obtained from relatively simple and inexpensive laboratory studies. The following studies would contribute to the descriptions of losses in the identified flow zones :

- 1) A quantification of contraction loss over an upward step.
- 2) A study of the effect of slot alignment on expansion and contraction losses.

### **7.4 Field data collection**

The lack of adequate and reliable field data has been a major constraint in the verification of analysis methods for both straight and meandering compound channels. The methods presented above are based on results from laboratory experiments. While this is appropriate because of the high degree of control of the relevant variables, the correspondence between laboratory and field conditions is not firmly established. The relative importance of different energy loss mechanisms may change with scale. Some information was available both for straight and meandering channels. These field data for straight channels proved to be inconclusive but provided good initial verification of the meandering channel method developed in Chapter 6. However further field data should be sought to fully verify methods of estimating conveyance in straight and meandering compound channels.

#### **7.4.1 Strategy for field data collection**

It is apparent that the analysis methods for both straight and meandering channels have not yet been fully verified against field data because very few relevant field measurements have been made. Given that it is desirable to collect more field data it is important that the correct types of information are obtained in order to make the most efficient use of resources.

In general there are two levels of validation possible and these differ in the amount of hydraulic information to be measured at each site.

- 1) Collect only stage-discharge information at each site.
- 2) Collect stage-discharges, point velocities, and water levels both along and across the study reach.

Obviously it will be possible to carry out measurements at a larger number of sites if only total discharges are to be measured. This would provide a wide range of data for the validation of the overall method but would not provide information to validate the calculated flow distributions. If the more detailed validation is required then it is likely that fewer sites would be considered due to the increased costs.

It will either be possible to partially validate the overall methods on a relatively large number of sites, or carry out more detailed validation on a limited number of sites. The detailed validation would require that at least three or four projects be set up and the costs of running these projects over three or four years are likely to be considerable.

Partial validation of the method using stage-discharge data from a wider set of sites would probably be sufficient in the short term combined with the long term aim of collecting sufficient information to carry out full validation over a number of sites.

## 7.4.2 Suitable sites

Much of what follows is equally relevant to straight or meandering sites, only the first two recommendations are specific to meandering channels. The type of reach to be considered for field data collection should conform to the following guidelines.

- 1) Sites should have significant meanders or bends. The meander zone should form a significant part of the floodplain and the meanders should be distinct and well developed.
- 2) Sites should preferably have a fairly regular meander pattern. The meander wave length and amplitude should not vary significantly within each site.
- 3) Land usage, (vegetation etc) on each floodplain should be reasonably uniform.
- 4) The presence of buildings or other obstructions on the floodplain should not disqualify a site provided that the obstruction has a minor effect of the flow pattern through the site.

In order to carry out any hydraulic calculations relating to a chosen site certain information is required detailing both the plan and cross section geometries.

- 5) Enough survey data should be available from maps and channel cross sections to estimate both the main channel and floodplain longitudinal slopes. Where the local bed slopes at the site differ from the overall reach slopes both should be given.

### 7.4.3 Hydraulic data

In order to provide enough validation data for either a partial or a full validation then the following hydraulic data should be measured.

- 1) Water surface slopes. The important hydraulic slope which controls flow in open channels is the water surface slope. In uniform flow this slope will be equal to the valley or floodplain slope. Water surface slopes should be measured over the reaches of interest. It may be possible to do this relatively easily and cheaply using maximum water level recorders set at intervals along the reach.
- 2) Pairs of measured stage and corresponding discharge. These should be provided at both inbank and out of bank stages. It may be possible to identify suitable sites which are close to existing inbank gauging stations. Maximum water level recorders would provide stage values with discharges being obtained from the nearby gauging sites. This would probably be the most efficient method of collecting stage discharge data in meandering overbank reaches. In suitable reaches not close to existing gauging stations special arrangements would be required to measure discharge.
- 3) Velocity profiles. These may be either just in the main channel regions or across the whole channel and floodplain. This would require a cableway to be set up at selected sites in the reach.

To provide information for a partial validation items 1 and 2 above should be measured at as many sites as possible. If a more complete validation is required then item 3 above should also be measured at each site. In the immediate future it is recommended that suitable sites should be identified and, if possible, a partial validation carried out. In the longer term detailed measurements should be sought to add to the data set provided by the Blackwater project.

## **7.5 Computational modelling**

### **7.5.1 Turbulence modelling**

Three dimensional turbulence modelling is the most promising approach for developing methods to describe the complex mechanics of flow in both straight and meandering compound channels. It is not envisaged that turbulence models will be used directly for routine design applications, but rather that they could be used in parametric studies to generate general results for incorporation in standard design methods. By following such an approach the results of experimental work (such as the SERC FCF Phase A and B studies) and field studies could be extended and generalized. The procedure would be to calibrate the model on the existing laboratory data and then to use the computational model rather than the laboratory to generate information about a wider range of conditions. Turbulence modelling should be used to complement laboratory studies rather than replace them.

In design applications use of a 3-D flow and turbulence model is unlikely to be practical for the foreseeable future. However useful information may be obtained from a two dimensional, depth integrated model. This type of approach has proved to be useful in the simpler straight channel case, for example the lateral distribution method (LDM). Development of suitable 2-D models should be encouraged.

### **7.5.2 One dimensional modelling**

Many one dimensional models of river flows exist which are based on the St Venant equations of 1-D flow. They generally use the computational technique of finite differences to solve the St Venant equations and so provide the variation of water level and discharge along a reach of channel. Typically these models are based on the use of pre-computed tables of conveyance which are accessed during the calculations.

## Existing methods used to calculate conveyance

One dimensional models require channel cross-sections to be supplied at locations along the river. These cross-sections and other data describing the bed roughness of the channel are then used to calculate the conveyance of each cross-section within the model. Conveyance is a convenient measure of a rivers' capacity to pass discharge. Typically the methods used to compute conveyance are based on variants of the divided channel or sum of segment methods. These methods are appropriate for straight compound channels but have been found to give poor results when applied to meandering compound channels.

Some work is presented above on the effects of replacing the existing conveyance calculation with the LDM further work should be carried out to extend this by including Ackers' method and the James and Wark method for conveyance calculations in a steady state backwater program. The effects of the various methods should be evaluated against each other by application to a wide range of idealized and natural river reaches.

## CHAPTER 8

### SUMMARY AND CONCLUSIONS

#### Chapter 2

- 1) The aims of this chapter were to review the theoretical background to flow in river and flood plain environments. These aims were met by deriving various sets of equations used to model river and flood plain flows.
- 2) The basic equations of 3-D fluid flow are the Navier-Stokes equations, 2.1 and 2.12. In the case of incompressible turbulent flow the Navier-Stokes equations are converted into the Reynold's equations, 2.18 and 2.19. The turbulent eddy viscosity concept was introduced in section 2.2.6 and the dynamic Reynold's equation reduced to equation 2.21.
- 3) The so called shallow water equations were derived from the 3-D Reynolds equations, section 2.3. The shallow water equations describe the behaviour of fluid flow with a free surface where the depth of flow is much smaller than the horizontal dimensions of the flow domain.
- 4) The shallow water equations are derived in terms of the unit flows ( $q$ ) rather than the more usual formulation given in the literature in terms of the depth averaged velocity ( $U$ ).
- 5) A novel approach to the bed friction vector in 2-D flow was followed, sections 2.4.1 to 2.4.3. A factor ( $B$ ) was derived to relate the stresses on a sloping surface to stresses in the horizontal plane. Various empirical approaches to modelling the effects of bed friction were reviewed, section 2.4.5. The shallow water equations are given by 2.107 and 2.108.
- 6) In the cases where the flow domain is much larger in the direction of the predominant flow it would be impractical to consider either the 3-D or the 2-D depth integrated behaviour. In these situations (eg. a river or canal) engineers usually consider the flow to be one dimensional.

- 7) The 1-D equations of flow with a free surface are called the St Venant equations and are derived in section 2.5 and are given by 2.129 and 2.130.

## **STRAIGHT COMPOUND CHANNELS**

### **Chapter 3**

- 8) A literature search on the behaviour of flows in straight compound channels has been carried out.
- 9) The conveyance capacity of straight compound channels is reduced by complex interactions between the main channel and floodplain flows.
- 10) The main mechanisms which affect the conveyance capacity have been identified as:
  - a) The velocity differential between main channel and floodplain flows. This induces a lateral shear layer between these two regions.
  - b) Secondary circulations, both in plan and within the cross-section carry fast moving fluid from the main channel to the flood plain and vice-versa. The relative strength of these secondary currents is reduced when the floodplain is rough and when the main channel side slope is slack.
  - c) The secondary circulations and lateral shear effects cause the boundary shear stresses to be redistributed around the channel cross-section, with increased values at the edge of the floodplain close to the main channel.
- 11) These mechanisms combine to reduce the discharge in the main channel and increase it on the floodplains.
- 12) The secondary currents also affect the distribution of longitudinal velocity, particularly in the main channel.
- 13) The interaction mechanisms are found to affect zones of the main channel and

floodplain adjacent to the channel bank. In the case of narrow channels or floodplains these shear layers may extend across the whole channel or floodplain.

- 14) The width of the shear layers is proportional to the flow depth and turbulent viscosity and is inversely proportional to the bed friction factor.
- 15) The strength of the interaction is dependent on :
  - a) Main channel / floodplain widths, depths and side slopes
  - b) Main channel / floodplain bed roughness
  - c) The velocity differential across the shear layer
- 16) Various methods of calculating discharge or conveyance in a straight compound channel have been identified.
- 17) The lateral distribution method appeared to be the most promising method for application to a wide range of channels and an improved formulation of the LDM equation has been derived.
- 18) Various models for the lateral eddy viscosity have been identified in the literature.
- 19) The non-dimensional eddy viscosity relates the value of viscosity to bed roughness, flow depth and local flow or velocity. The use of this model can approximate the variation of the interaction effects in a compound channel.
- 20) More work should be carried out to identify appropriate values of viscosity for the evaluation of discharge distributions in compound channels

#### **Chapter 4**

- 21) The numerical solution technique used to solve the lateral distribution

equations (4.2) and (4.3) has been verified by comparison with analytic solutions (section 4.3).

- 22) The SERC FCF data set has been used to evaluate values of the Non Dimensional Eddy Viscosity parameter. The optimum NEV values for the SERC FCF Phase A data set were found to depend on the relative depth, width and roughness condition of the channel (4.4.1).
- 23) The average values of NEV for the FCF Phase A channels were found to be 0.29, 0.22 and 0.12 for smooth floodplains, roughened floodplains and inbank flows respectively.
- 24) The LDM was applied to the FCF data with several fixed values of NEV. The errors in calculated discharge were found to vary with relative depth, width and roughness (4.4.2). The mean errors in calculated discharge were minimised when the optimum values of NEV for each series, identified in Section 4.4.1, were used.
- 25) The predicted discharges were found to be relatively insensitive to NEV value and it is recommended that the value 0.16 should be used in practice (4.4.4).
- 26) When bed roughness values are well known the LDM can produce adequate predictions of the lateral distribution of flow, or velocity, across the channel (4.4.3)
- 27) The LDM has been applied to other laboratory data and field data. Good agreement between measured unit flows, velocities, stage discharges and the proportion of total flow in the main channel were obtained with NEV values close to 0.16 (4.5.1).
- 28) Predicted unit flow and velocity profiles for the laboratory and natural channels have been produced. In general these are better for wider, shallower

main channels than for narrow, deep channels (4.4.4 and 4.5.1).

- 29) The LDM method gives good results with a single value of NEV. It is not necessary to use variable values of NEV across the channel to achieve good agreement with measurements (4.4.3 and 4.5.2)
- 30) The two versions of the LDM (equations 4.2 and 4.3) have been compared and the author's version, based on equation 4.2, was found to give superior predictions of velocity and discharge (4.5.2).
- 31) The LDM has been compared with other methods applied to the FCF data. On average the LDM and Ackers' methods gave better predictions of discharge and depth than the other methods (4.6.2).
- 32) The LDM has been compared with other methods of calculating the conveyance capacity of compound channels. These comparisons have been carried out over the various sets of laboratory data. Two methods, LDM and Ackers' method, gave much better predictions of both discharge and depth in the laboratory channels than the other methods considered (4.6.3, 4.6.4)
- 33) The LDM has been compared with other methods of estimating discharge in natural river channels. The results were inconclusive with the best four methods (LDM, DCM, DCM2 and ACKM) giving mean errors which are within the measurement errors of the data (4.6.5).
- 34) The main problem in applying any method of calculating discharge is in estimating appropriate values of bed roughness. When the roughness values are known the LDM is expected to give acceptable predictions of both velocity distribution and total discharge. More work should be directed towards improving the accuracy of methods of estimating bed roughness values (4.6.5).

## MEANDERING CHANNELS

### Chapter 5

- 35) A literature search in to overbank flow in meandering compound channels has been carried out (5.2). The main purposes of this review were:
- a) To identify laboratory data to use in developing and verifying a new procedure for discharge estimation in overbank flow in meandering channels.
  - b) To summarize the current state of knowledge on the detailed flow structures present during overbank meandering flow and to gauge the effect these might have on the discharge capacity of the channel.
- 36) Eight laboratory investigations were identified, including the SERC FCF (5.2). The two most modern and extensive data sets (SERC FCF and Aberdeen) were considered to represent the best quality data available and it was decided to use these two sets in developing a new procedure for estimating the conveyance of meandering compound channels. Three other investigations (Vicksburg, Kiely and Sooky) were deemed appropriate to use in verification of the new procedure. The key physical dimensions of the test channels are given in Table 5.5. Table 5.6 shows the relationships between the key geometric parameters for the laboratory flume tests.
- 37) Natural, fully developed, meander bends have geometric ratios: the wave length is approximately ten times the channel width; the channel width is approximately ten times the channel bankfull depth and the radius of curvature of the bends is between two to three times the channel width.
- 38) Most laboratory studies have been carried out with main channel aspect ratio's ( $B/h$ ) which lie between 3.5 and 5.0. Only the SERC FCF geometries have channel cross sections which approximate to natural cross sections with an aspect ratio of 8.0.

- 39) It has been demonstrated that all three of these geometric ratios effect the stage discharge capacity during overbank flow. Since only the large scale experiments carried out in the SERC FCF satisfied all three relationships it is likely that the flow patterns and stage discharge relationships for the FCF will be closer to those observed in nature than for the other experimental data collected in small scale models.
- 40) Most investigators identified well defined and complex structures within the flow including: secondary currents within the main channel and bulk exchanges of flow between main channel and flood plain. Figure 10 shows the flow processes taking place during over bank flow in meandering channels. The most important observations are:
- a) The longitudinal velocities below bankfull tend to follow the main channel side walls while the floodplain velocities are generally in the valley direction. Thus the floodplain flows pass over the main channel and induce a horizontal shear layer.
  - b) The energy loss due to secondary currents in the main channel is greater than for an equivalent simple channel and the currents rotate in the opposite sense compared to inbank flows.
  - c) Fluid passes from the main channel onto the flood plain and back into the main channel in the following meander bend. Hence the proportion of discharge passed by the main channel and flood plain varies along a meander wavelength. These bulk exchanges of fluid between slow and fast moving regions of flow introduce extra flow resistance.
  - d) Flows on the flood plain outwith the meander belt are usually faster than those within the meander belt. It would appear that the extra flow resistance induced by the meandering main channel has a relatively small effect on the outer flood plain.
- 41) The behaviour of flow in meandering channels during inbank flow has been investigated using the SERC FCF Phase B data (5.6.3 and 5.6.4). The relative

strengths of the bed friction and non-friction energy loss mechanisms were calculated for the three sets of inbank stage discharges.

- 42) The non-friction losses were found to vary both with channel sinuosity and cross-sectional geometry (5.6.5). The 'natural' channel cross-sections induce approximately twice as much non-friction loss as the equivalent trapezoidal channel.
- 43) A literature search was carried out to identify the important processes which induce this extra flow resistance to flows in channel bends (5.6.7). The main sources of flow resistance in a channel bend are:
- a) bed friction;
  - b) increased bed friction due to secondary currents
  - c) internal energy dissipation due to increased turbulence induced by secondary currents.
- 44) The flow resistance in a bend depends on:
- a) bed roughness ( $f$ ,  $C_n$  etc);
  - b) flow depth ( $y$ );
  - c) bend radius ( $r_c$ )
  - d) length of bend ( $l$ ) or angle of bend ( $\theta$ ,  $l = r_c \theta$ )
  - e) The cross-sectional shape of the channel and its variation along the length of the channel.
- 45) Flow resistance in a set of meander bends is likely to differ from the resistance induced by a single bend in an otherwise straight channel, due to the interaction (growth and decay) between the secondary currents induced in the individual bends.
- 46) Various methods which account for the extra flow resistance were identified

in the literature and a selection of methods were applied to the available laboratory data (5.7.2).

- 47) The methods were evaluated by comparing the mean errors in predicted discharge. The SCS method was found to give acceptable results for most practical purposes even though it does not account for the important mechanisms explicitly (5.7.3).
- 48) An improved version of the SCS method was formulated to remove the undesirable step function (LSCS) and this linearized version gave better predictions. Although these methods, which adjust Manning's  $n$  based on the channel sinuosity, gave acceptable results they are empirical and their generality is not assured (5.7.2 and 5.7.3).
- 49) Chang's approach, in explicitly modelling the resistances due to secondary currents combined with backwater calculations along the channel, is based on sound theoretical considerations. This approach is applicable to both single bends and series of meanders and further work should be carried out to prove it against more general cases (5.7.3).

## Chapter 6

- 50) Various methods suitable for the determination of flow in straight compound channels have been applied to a selection of stage-discharge data collected in meandering compound channels. The poor predictions obtained confirm that straight channel techniques are not suitable for meandering channels (section 6.2).
- 51) A literature search was carried out to identify methods proposed by previous authors (6.3.2).
- 52) On the basis of a knowledge of the important mechanisms which affect the

discharge capacities of meandering compound channels and an appreciation of modelling techniques a strategy was devised for developing an improved method of discharge estimation (6.4.1).

53) Experimental data from Phase B of the SERC FCF has been analyzed to produce methods for the estimation of discharges in compound channels. The best approach was found to be based on dividing the cross-section into zones and calculating the discharge in each zone independently. The four zones chosen are:

- a) The main channel below bankfull level.
- b) The floodplain within the meander belt.
- c) The floodplain beyond the meander belt on the left bank.
- d) The floodplain beyond the meander belt on the right bank.

54) The loss mechanisms which affect the main channel (zone 1) discharge are complex and an empirical procedure has been developed to account for these mechanisms (6.4.2). A correction factor is applied to the bankfull discharge to obtain the variation in the main channel discharge with over bank stage. The form of the correction factor ( $Q_1'$ ) is given by equations 6.30, 6.31 and 6.32.

55)  $Q_1'$  was found to depend on:

- a) the floodplain flow depth at the edge of the main channel ( $y_2$ );
- b) the channel sinuosity ( $s$ );
- c) the cross-section geometry and
- d) floodplain roughness.

56) Two alternative methods for predicting the discharge in the inner floodplain (zone 2) were developed (6.4.3). The first method attempts to account for the principal loss mechanisms using physically-based deterministic formulations.

The formulations are based on a very simple conceptual model of the loss mechanisms and required empirical adjustment to account for the additional complexities involved. The model explicitly accounts for bed friction and expansion / contraction over the main channel and is described by equations 6.51, 6.50, 6.49, 6.48, 6.41, 6.40 and 6.34.

The second method is purely empirical and follows an approach similar to that used for the main channel zone. A basic discharge is calculated assuming friction losses only, and this is then adjusted to account for the effects of flow interaction with the main channel. The form of the correction factor is given by equations 6.56, 6.57, 6.58 and 6.59.

- 57) The discharges in zones 3 and 4 are assumed to be controlled by bed friction only and are given by equations 6.60 and 6.61 (6.4.4).
- 58) Bed shear stress data was measured under overbank conditions during Phase B of the FCF work (6.4.5). The analysis carried out by the investigators is summarised above. The main channel bed shear stresses are reduced during overbank flow compared to bank full conditions. The shear stresses on the floodplains adjacent to the main channel show peak values which are associated with the exchange of flow between the main channel and the floodplain. Equations 6.62 and 6.63 give a rough estimate of the likely peak bed shear stresses.
- 59) The two methods developed by the authors and four other methods have been used to predict discharges and stages for the available laboratory data. The author's semi-empirical method (JW) was found to give the most accurate predictions of total discharge and acceptable predictions of the distribution of discharges (6.5.3).
- 60) The available data used in this verification covered a limited range of conditions. Further experimental work is required to look at both total

discharges and the distribution of discharges for :

- a) Meandering channels with low sinuosities ( $<1.09$ ).
- b) Meandering compound channels with rough floodplains.
- c) Low over bank depths ( $y' < 0.2$ )

- 61) The sensitivity of the James and Wark method to variations in the values of both meander wave length and main channel side slope has been investigated. The results indicate that great precision in estimating these values is not required (6.5.3).
- 62) The procedure has been applied to the best field data available and has been shown to give improved predictions compared to current practice. The sensitivity of the results to variations in bed roughness value has been investigated. The non-friction energy losses are shown to be less important as the floodplain is roughened. Bed friction remains the most significant source of energy loss in rivers with overbank flow (6.5.5).
- 63) The JW method has been applied to stage-discharge data from straight laboratory channels and gave very poor predictions of discharge. The JW method gave adequate predictions for Sooky's data which had sinuosity of 1.09. Further research is required to provide discharge estimation methods for meandering compound channels of low sinuosities (6.5.4).

## Chapter 7

- 64) The present investigation into flows in compound channels has concentrated on developing improved methods for stage discharge estimation in both straight and meandering channels. In general the available laboratory and field information was used to develop conceptual models of the important processes. Suitable methods of approximating these processes were identified and developed. The research which still remains to be carried out falls into two main categories:
- a) The collection of independent information to use in verifying the available laboratory and field data for a wider range of conditions.
  - b) The development of two and three dimensional numerical models and their application to the available data and the improvement of existing simplified one dimensional techniques.
- 65) Chapter 7 gives a detailed list of future research and lays out possible strategies for the collection of field data.

## REFERENCES

ACKERS P (1991) The Hydraulic Design of Straight Compound Channels, Report SR 281, HR Wallingford, October.

ACKERS P (1993) Hydraulic Design of Two-Stage Channels, Proc. Instn. Civ. Engrs., Wat. Marit. & Energy, 1992, 96, Dec, 247-257.

AGARWAL V C, GARDE R J and RANGA RAJU K G (1984) Resistance to flow and sediment transport in curved alluvial channels, Fourth Congress, Asian and Pacific Division, IAHR, Thailand, 11-13 September, pp 207-218.

AHMADI R (1979) An Experimental Study of Interaction Between Main Channel and Flood Plain Flows, Ph D Thesis, Dept Civil Engineering, The Univ of Alberta, Canada.

ARNOLD U, PASCHE E, and ROUVE G (1985) Mixing in Rivers with Compound Cross-Section, 21st IAHR Congress, Melbourne, Australia, pp 168,172.

ARNOLD U, HOTTAGES J and ROUVE G (1988) Combined Digital Image and Finite Element Analysis of Mixing in Compound Open Channel Flow, Proc 3rd Intl Symp Refined Flow Modelling and Turb Measurements, Tokyo.

ARNOLD U, STEIN J and ROUVE G (1989) Sophisticated Measurement Techniques for Experimental Investigation of Compound Channel Flow, Hydro Comp 89, Dubrovnik, Yugoslavia, 13-16th June 89, pp 11,21.

ARNOLD U, ROUVE G and STEIN J (1989) A Review of Investigations on Compound Open Channel Flow, Hydro Comp 89, Dubrovnik, Yugoslavia 13-16th June 89, Supplements pp 19,40.

BAIRD J I and ERVINE D A (1982) Rating Curves for Rivers with Overbank Flow, Proc. Instn. Civ. Engrs., Part 2, 1982, 73, June, pp 465-472.

BAIRD J I and ERVINE D A (1984) - Resistance to Flow in Channels With Overbank Flood-Plain Flow, Proc, 1st Int Conf Channels and Channel Control Struct, Computational Mechanics Centre, Southampton, England, and Springer Verlag, Heidelberg, Germany, pp 4 137,4 150.

BATCHELOR G K (1967) - Introduction to Fluid Dynamics, Cambridge Univ Press.

CARLING P A (1992) Personal communication.

CHADWICK A and MORFETT J (1986) - Hydraulics in Civil Engineering, Allen and Unwin, London, ISBN 0-04-627004-3.

CHANG H H (1983) - Energy Expenditure in Curved Open Channels, Jml Hydr Engineering, Vol 109, No 7, July.

CHANG H H (1984) Variation of Flow Resistance Through Curved Channels, Journal of Hydraulic Engineering, Vol 110, No 12, pp 1772-1782.

CHANG H H (1984) - Analysis of River Meanders, Jnl Hydr Eng, Vol 110, No 1.

CHANG H H (1984) - Regular Meander Path Model, Jnl Hydr Eng, Vol 110, No 10, Oct.

CHANG H H (1988) - Fluvial Processes in River Engineering, John Wiley and Sons Inc ISBN 0-471-63139-6.

CHOW V T (1956) - Open Channel Hydraulics, McGraw-Hill, London, International Student Edition, ISBN 0-07-Y85906-X.

CONTE S D and de BOOR L - Elementary Numerical Analysis, McGraw-Hill Inc, Singapore ISBN 0-07-012447-7.

CORPS of ENGINEERS U S ARMY, Waterways Experiment Station, Vicksburg, Mississippi, (1956) - Hydraulic Capacity of Meandering Channels in Straight Floodways, CWL ITEM 807.

COWAN W L (1956) Estimating Hydraulic Roughness, Agricultural Engineering, Vol 37, No 7, pp 474-475.

DJORDJEVIC J, PETROVICI J, MAKSIMOVIC C and RADOJKOVIC M - (1989) Experimental Tracer Investigations in a Compound Laboratory Channel, HydroComp 89, Dubrovnik, Yugoslavia, 13-16th June pp 269-278.

DRACOS T , HARDEGGER P (1987) Steady Uniform flow in Prismatic Channels with Flood Plains, Jnl Hydr Resch, Vol 25, No 2.

DROLET J and GRAY W G (1989) On the Well Posedness of Some Wave Formulations of the Shallow Water Equations, Adv Water Resources, Vol 11, June.

EINSTEIN H A and BANKS R B, (1950). Fluid resistance of composite roughness, Transactions, American Geophysical Union, Vol 31, No 4, pp 606-610.

ELLIOTT S C A and SELLIN R H J (1990) SERC Flood Channel Facility : Skewed Flow Experiments, Jnl Hydr Resch, Vol 28, No 2, pp 197,214.

ERVINE D A and BAIRD J I (1982) Rating Curves for Rivers with Overbank Flow, Proc Instn Civ Engrs, Part 2, 73, June, pp 465,472.

ERVINE D A and ELLIS J (1987) Experimental and Computational Aspects of Overbank Flood Plain Flow, Transactions of the Royal Society of Edinburgh : Earth Sciences, 78, pp 315,325.

ERVINE D A AND JASEM H K (1991) Personal communication

FALCONER R A (1977) Mathematical Modelling of Jet-Forced Circulation in Reservoirs and Harbours, Ph D Thesis, Dept Civil Engineering, Imperial College, London.

FUKUHARA T and MUROTA A (1990) Discharge Assessment in Compound Channel with Floodplain Roughness, Paper E2, Proc Intl Confr on River Flood Hydraulics, Wallingford, England, 17,20th Sept.

FUKUOKA S and FUJITA K (1990) Prediction Method of Flow Resistance in Rivers with Compound Channels and Application to River Course Design, Paper D2, Proc Intl Confr on River Flood Hydraulics, Wallingford, England, 17,20th Sept, pp 113,122.

GREENHILL R K (1992) An Investigation into Compound Meandering Channel Flow, PhD thesis, Department of Civil Engineering, University of Bristol.

GREENHILL R K and SELLIN R H J (1993) Development of a Simple Method to Predict Discharges in Compound Meandering Channels, Proc. Instn. Civ. Engrs., Wat., Marit & Energy, 101, pp 37-44, Paper 10012.

HAYAT S (1965) The Variation of Loss Coefficient with Froude Number in an Open Channel Bend. Thesis presented to the University of Iowa in partial fulfilment of the requirements for the degree of Master of Science.

HEAPS N S (1969) A Two-dimensional Numerical Sea Model, Phil Trans Roy Soc Vol 265, pp 93,137.

HENDERSON F M (1966) Open Channel Flow, Macmillan, New York.

HIGGINSON N N J, JOHNSTON H T and MYERS W R C (1990) The Effect of Scale Distortion in a Compound River Channel Model Study, Paper L2, Proc Intl Confr on River Flood Hydraulics, Wallingford, England, 17,20th Sept.

HOLDEN A P and JAMES C S (1989) Boundary Shear Distribution on Flood Plains, Jml of Hydr Res, Vol 27, No 1.

HOLDEN A P and JAMES C S (1988) Discharge Computation for Compound Channels, The Civil Engineer in South Africa, Vol 30, No 8, pp 371-376.

HORTON R E (1933) Separate Roughness Coefficients for Channel Bottom and Sides, Engineering News-Record, Vol 111, No 22, pp 652-653.

HR WALLINGFORD (1988) Assessing the Hydraulic Performance of Environmentally Acceptable Channels, Report EX 1799, HR Wallingford, September.

HR Wallingford (1991) Phase A & B Flood Channel Facility Manual, Inception Report, HR Wallingford, Report EX 2485 (November)

- HR Wallingford (1992) Phase A & B Flood Channel Facility Manual, Interim Report, HR Wallingford, Report EX 2548 (March)
- HR Wallingford (1992) Phase A & B Flood Channel Facility Manual, Final Report, HR Wallingford, Report EX 2606 (July)
- HUNTER S C (1983) Mechanics of Continuous Media, 2nd Edition Ellis Horwood Ltd, Chichester, Sussex ISBN 0-470-27384-4.
- JAMES and BROWN (1977) Geometric Parameters that Influence Floodplain Flow, Hydraulics Laboratory, U S Army Engineer Waterways Experiment Station, Vicksburg, Miss.
- KAZEMIPOUR A K and APELT C J (1979) Shape Effects on Resistance to Uniform Flow in Open Channels, Journal of Hydraulic Research, Vol 17, No 2, pp 129-148.
- KAZEMIPOUR A K and APELT C J (1983) Energy Losses in Irregular Channels, Journal of Hydraulic Engineering, Vol 109, No 10, pp 1374-1379.
- KAY D C (1988) Tensor Calculus, McGraw-Hill Inc, ISBN-0-07-033484-6.
- KELLER R J and RODI W (1988) Prediction of Flow Characteristics in Main Channel/Flood Plain Flows, Jnl of Hydr Resch, Vol 26, No 4.
- KIELY G K (1989) An Experimental study of Overbank Flow in Straight and Meandering Compound Channels, Ph D Thesis, Dept of Civ Eng, Univ College, Cork.
- KIELY G, JAVAN M and McKEOGH E J (1989) A Comparison of Turbulence Measurements in Straight, Single Meander and Multiple Meander Channels, Int'l. Confr. on Channel Flow and Catchment Runoff, Centennial of Manning's and Kuichlings Rational Formula, University of Virginia, May.
- KIELY G (1989) Experimental Study of the Mechanisms of Flood Flow in Meandering Channels, Proc. of the 23rd IAHR Congress, Ottawa, Canada, August.
- KIELY G (1990) Overbank Flow in Meandering Channels the Important Mechanisms, Proc of Intl Conf on River Flood Hydraulics, Wallingford, 17-20 September.
- KIKKEWA H, IKEDA S and KITAGAWA A (1976) Flow and Bed Topography in Curved Open Channels, Journal of the Hydraulics Division, ASCE, Vol 102, No HY9, pp 1327-1342.
- KNIGHT D W, DEMETRIOU J D and HAMED M E (1983) Hydraulic Analysis of Channels with Flood Plains, Int'l Congress Hydr Aspects of Floods and Flood Control, September 13-15.

KNIGHT D W and LAI C J (1985) Turbulent Flow in Compound Channels and Ducts, Int'l Symp on 'Refined Flow Modelling and Turbulence Measurements', Iowa, U S A, Sept.

KNIGHT D W AND SELLIN R H J (1987) The Serc Flood Channel Facility, Journal of the Institution of Water and Environmental Management, Vol 1, No 2, pp 198-204.

KNIGHT D W, SHIONO K and PIRT J (1989) Prediction of Depth Mean Velocity and Discharge in Natural Rivers with Overbank Flow, Int'l Conf of Coastal, Estuarine and River Waters, Bradford, England, 19-21 Sept .

KNIGHT D W and SAMUELS P G (1989) River Flow Simulation: Research and Developments, Paper 18, IWEM Annual Conference.

KNIGHT D W and SHIONO, K (1990) Turbulence Measurements in a Shear Layer Region of a Compound Channel, Jnl Hydr Resch, Vol 28, No 2, pp 175,196.

KNIGHT D W, YUAN Y M and FARES Y R (1992) Boundary Shear in Meandering Channels, Proc. Int. Symp. on Hydraulic Research in Nature and Laboratory, Wuhan, China, November, 1992.

KRISNAMURTHY M and CHRISTENSEN B A (1972) Equivalent Roughness for Shallow Channels, Journal of Hydraulics Div, ASCE, Vol 98, HY12, pp 2257-2262.

KRISHNAPPAN B G and LAU Y L (1986) Turbulence Modelling of Flood PlainFlows, Jnl Hyd Eng, Vol 112, No 4.

KUIPERS and VREUGDENHIL C B (1973) Calculation of 2-Dimensional Horizontal Flow, Delft Hydraulics Laboratory, Report S163 part 1.

LAMBERT M (1992) Personal Communication

LEAN G H and WEARE J T (1979) Modelling Two Dimensional Circulating Flow, Jnl Hydr Div, Proc ASCE, Vol 105, No HV1.

LEENDERTSE J J (1967) Aspects of a Computational Model for Long Period Water Wave Propagation, Memorandum RM-5294-PR, Rand Corporation, Santa Monica, California.

LEOPOLD L B, BAGNOLD R A, WOLMAN M G and BRUSH L M (1960) Flow Resistance in Sinuous or Irregular Channels, Geological Survey Professional Paper 282-D, U S Gov Printing Office, Washington.

LORENA M L (1991) Personal Communication

LOTTER G K (1933) Considerations on Hydraulic Design of Channels with Different Roughness of Walls, Transactions, All-Union Scientific Research Institute, Leningrad, Vol 9, pp 238-241.

McKEOGH E J and KIELY G (1989) A Comparison of Velocity Measurements in Straight, Single meander and Multiple Meander Channels, Int'l. Confr. on Channel Flow and Catchment Runoff, Centennial of Manning's and Kuichlings Rational Formula, University of Virginia, May.

McKEOGH E J, KIELY G K and JAVAN M (1989) Velocity and Turbulence Measurements in a Straight Channel with Interacting Floodplains using Laser Doppler Anemometry, Hydr & Environ Modelling of Coastal Estuarine and River Waters, Proc Int'l Conf, Bradford, 19-21 Sept, pp 429,440.

MILES G V and WEARE T J (1973) On the Representation of Friction in Two-Dimensional Numerical Models, Numerical Methods in Fluid Dynamics, Proc Int'l Conf Univ of Southampton, England, 26-28 Sept.

MOCKMORE C A (1944) Flow Around Bends in Stable Channels, Transactions, ASCE, Vol 109, pp 593-618.

MYERS W R C and ELSAWY E M (1975) Boundary Shear in Channel with Flood Plain, Jnl Hydr Div, Proc, ASCE, Vol 101, No HY7.

MYERS W R C (1978) Momentum Transfer in a Compound Channel, Jnl Hydr Resch, 16, No2.

MYERS W R C (1987) Velocity and Discharge in Compound Channels, Jnl Hydr Eng, Vol 113, No 6, pp 753,766.

MYERS W R C and BRENNAN E K (1990) Flow Resistance in Compound Channels, Jnl Hydr Resch, Vol 28, No 2, pp 141,156 .

MYERS W R C (1990) Physical Modelling of a Compound River Channel, Paper L1, Proc Intl Confr on River Flood Hydraulics, Wallingford, England, 17,20th Sept.

MYERS W R C (1990) Personal communication

NATIONAL RIVERS AUTHORITY (1991) Design Method for Straight Compound Channels, R&D Note 44, NRA.

ODGAARD J A (1984) Flow and Bed Topography in Alluvial Channel Bend, Jnl Hydr Engr, Vol 110, No 4, April.

ODGAARD J A (1986) Meander Flow Model 1: Development, Jnl Hydr Eng, Vol 112, No 12, Dec.

OGINK H J M (1985) The Effective Viscosity Coefficient in 2-D Depth Averaged Flow Models, 21st IAHR Congress, Melbourne, Australia.

OKOYE J K (1970) Characteristics of Transverse Mixing in Open Channel Flows, California Institute of Technology, Pasadena, California, Report No KH-R-23, Nov.

- ONISHI Y, JAIN S C and KENNEDY J F (1976) Effects of Meandering in Alluvial Streams, Journal of the Hydraulics Division, ASCE, Vol 102, No HY7.
- PASCHE E and ROUVE G (1985) Overbank Flow with Vegetatively Roughened Flood Plains, Jnl Hydr Eng, Vol 111, No 9.
- PASCHE E, ARNOLD A and ROUVE G (1986) Review of Overbank Flow Models, Advancements in Aerodynamics, Fluid Mechanics and Hydraulics, ASCE, June 3-6, Minneapolis, Minnesota.
- PRINOS P and TOWNSEND R D (1983) Estimating Discharge in Compound Open Channels, in Proceedings of the 6th Canadian Hydrotechnical Conference, Ottawa, Canada. R D Townsend (Ed), vol 1, pp129-146.
- PRINOS P and TOWNSEND R D (1984) Comparison of Methods for Predicting Discharge in Compound Channels, Proc. of the 1st Int Conf on Channels and Channel Control Structures, Southampton.
- PRINOS P, TOWNSEND R and TAVOULARIS S (1985) Structure of Turbulence in Compound Channel Flows, Jnl Hydr Eng, Vol 111, No 9.
- PRINOS P (1989) Experiments and Numerical Modelling in Compound Open Channel and Duct Flows, Hydro Comp 89, Dubrovnik, Yugoslavia, 13-16th June, pp 255,269.
- PRINOS P (1990) Turbulence Modelling of Main Channel - Floodplain Flows with an algebraic stress Model, Proc. of Intl. Conf. on River Flood Hydraulics, Wallingford, pp 164- 172.
- RADOJKOVIC B E and DJORDJEVIC B E (1985) Computation of Discharge Distribution in Compound Channels, 21st IAHR Cong, Melbourne, Australia, 19,23rd Aug.
- RAJARATNAM N and AHMADI R M (1979) Interaction between Main Channel and Floodplain Flows, Jnl Hydr Div Proc ASCE, Vol 105, No HY5.
- RAJARATNAM N and AHMADI R M (1981) Hydraulics of Channels with Flood Plains, Jnl Hydr Resch, Vol 19, No 1.
- RAMSBOTTOM D M (1989) Flood Discharge Assessment, Interim Report, Hydraulics Research Ltd, Report SR 195, March.
- RANGA RAJU, K G (1970) Resistance relations for alluvial streams, La Houille Blanche, No 1.
- ROUSE H (Ed) (1950) Engineering Hydraulics, John Wiley and Sons, New York.
- ROZOVSKII I L (1957) Flow of Water in Bends of Open Channels, The National Science Foundation Washington D C, The Israel Program for scientific translations

(1961).

SAMUELS P.G (1985) Modelling of River and Flood Plain Flow using the Finite Element Method, Ph D Thesis, Department of Mathematics, Univ of Reading, Hydraulics Research Report No SR61, Nov

SAMUELS P G (1988) Lateral Shear Layers in Compound Channels, Int's Congr on Fluvial Hydraulics, Budapest

SAMUELS P G (1989) Some Analytical Aspects of Depth Averaged Flow Models, Intl Conf Hydraulic and Environmental Modelling of Coastal, Estuarine and River Waters, Bradford, England, 19-21, Sept.

SCOBEY F C (1983) The Flow of Water in Flumes. US Department of Agriculture, Tech Bull No 393.

SELLIN R H J (1964) A Laboratory Investigation into the Interaction Between the Flow in the Channel of a River and that over its Flood Plain, La Houille Blanche/No 7.

SELLIN R H J, GILES A and VAN BEESTEN D P (1990) - A Post Implementation Appraisal of a Two Stage Channel in the River Roding, Essex, Report submitted to The Thames Division NRA.

SELLIN R H J, GILES A and BEESTEN D P (1990) Post-Implementation Appraisal of a Two Stage Channel in the River Roding, Essex, Jrnl IWEM, 1990, 4, April.

SELLIN R H J, ERVINE D A, WILLETTS B B (1993) Behaviour of Meandering Two-stage Channels, Proc. Instn. Civ. Engrs., Wat., Marit & Energy, 101, pp 99-111, Paper 10106.

SHIONO K and KNIGHT D W (1988) Two Dimensional Analytical Solution for a Compound Channel, Third Int'l Symp Refined Flow Modelling and Turbulence Measurements Tokyo, Japan, July.

SHIONO K and KNIGHT D W (1989) Transverse and Vertical Reynolds Stress Measurements in a Shear Layer Region of a Compound Channel, Seventh Symposium on Turbulent Shear Flows, August 21-23, Stanford.

SHIONO K and KNIGHT D W (1990) Mathematical Models of Flow in Two or Multi Stage Straight Channels, Paper G1, Proc Intl Confr on River Flood Hydraulics, Wallingford, England, 17,20th Sept.

SHUKRY A (1950) Flow around Bends in an Open Flume, Trans ASCE, Vol 115, pp 751,788.

SMITH C D (1978) Effects of Channel Meanders on Flood Stage in Valley, Jrnl Hydr Div, Proc ASCE, Vol 104, No HY1.

SMITH G D (1986) Numerical Solution of Partial Differential Equations - Finite Difference Methods, Third Edition Clarendon Press, Oxford.

SOIL CONSERVATION SERVICE (1963) Guide for Selecting Roughness Coefficient 'n' Values for Channels, US Department of Agriculture, Soil Conservation Services, Washington.

SOOKY A A (1964) The Flow Through a Meander Flood Plain Geometry, Ph D Thesis, Purdue Univ, 65-2647, Univ Microfilms Inc, Ann Arbor, Michigan.

STEIN C J and ROUVE G (1988) 2D-LVU-Technique for Measuring Flow in a Meandering Channel with Wetted Flood Plains - A New Application and First Results, Proc Int'l Conf on Fluvial Hydr Budapest, June, pp 5,10.

STEIN C J and ROUVE (1989) 2D Depth-Averaged Numerical Predictions of the Flow in a Meandering Channel with Compound Cross Section, Hydrosoft, Vol 2, No 1, pp 2,7.

TOEBES G H and SOOKY A A (1967) Hydraulics of Meandering Rivers with Flood Plains, Jnl of Waterways and Harbours Div, Proc ASCE, Vol 93, No WW2, pp 213,237.

TOMINAGA A, NEZU I and KOBATAKE (1989) Experimental and Numerical Investigations on Turbulent Structure in Compound Open-Channel Flow, Hydrocomp 89, Dubrovnik, Yugoslavia, 13-16th June, pp 244,254.

TONG G D (1982) Computation of Turbulent Recirculating Flow, Ph D Thesis, Dept Civil Eng, Univ College of Swansea, Univ of Wales C/Ph/63/82.

VREUGDENHIL C B, WIJBENGA J H A (1982) Computation of Flow Patterns in Rivers, Jnl Hydr Div, ASCE, Vol 108, No HY11, Nov.

WARK J B (1988) - The Equations of River and Floodplain Flow, A Technical Report submitted to the Dept of Civil Engineering, The Univ of Glasgow, Dec.

WARK J B, SAMUELS P G and ERVINE D A (1990) A Practical Method of Estimating Velocity and Discharge in Compound Channels, Intl Confr on River Flood Hydraulics, Wallingford, Oxfordshire, Sept.

WARK J B, RAMSBOTTOM D M and SLADE J E (1991) Flood Discharge Assessment by the Lateral Distribution Method, Report SR 277.

WEBBER N B (1971) Fluid Mechanics for Civil Engineers, Chapman and Hall, London ISBN 0-412-10600-0.

WILLETTS B B, HARDWICK R I and MACLEAN A G (1990) Model Studies of Overbank Flow from a Meandering Channel, Proc of Intl Conf on River Flood Hydraulics, Wallingford, 17-20 September.

WILLETTS B B and HARDWICK R I (1991) Personal Communication

WILLETTS B B (1992) The Hydraulics of Overbank Flow in Meandering Rivers, Seminar on Multiple Stage Channels, HR Wallingford Ltd., Wallingford, UK.

WILLETTS B B and HARDWICK R I (1993) Stage Dependency for Overbank Flow in Meandering Channels, Proc. Instn. Civ. Engrs., Wat., Marit & Energy, 101, pp 45-54, Paper 10049.

WORMLEATON P R, ALLEN J and HADJIPANOS P (1982) Discharge Assessment in Compound Channel Flow, Journal of the Hydraulics Division, ASCE, Vol 108, No HY9, pp975-994.

WORMLEATON P R, and HADJIPANOS P (1985) Flow Distribution in Compound Channels, Jnl., Hydr. Eng, ASCE, 111(2), pp357-361.

WORMLEATON P R (1988) Determination of Discharge in Compound Channels using the Dynamic Equation for Lateral Velocity Distribution, Intl Conf on Fluvial Hydraulics, Budapest.

WORMLEATON P R and MERRIT D J (1990) An Improved Calculation for Steady Uniform Flow in Prismatic Main Channel Flood Plain Sections, Jnl Hydr Resch, Vol 28, No 2, pp 157,174.

YEN B C and WENZEL H G (1970) Dynamic Equations for Steady Spatially Varied Flow, Jnl Hydr Div, ASCE, Vol 96, No HY3 YEN B C (1971) - Spatially Varied Open Channel Flow Equations, Department of the Interior, Washington, D C.

YEN B C and YEN C L (1983) Flood Flow over Meandering Channels, Proceedings, Rivers '83, River Meandering, ASCE, pp 554-561.

YUEN K W H and KNIGHT D W (1990) Critical Flow in a Two Stage Channel, Paper G4, Proc Intl Confr on River Flood Hydraulics, Wallingford, England, 17,20th Sept.



**UNIVERSITY OF GLASGOW**  
**DEPARTMENT OF CIVIL ENGINEERING**

**DISCHARGE ASSESSMENT IN STRAIGHT AND  
MEANDERING COMPOUND CHANNELS**

**JAMES BINNING WARK B. Eng**

**July 1993**

**Volume 2**

**A thesis submitted in fulfilment of the regulations governing the award of the  
degree of Doctor of Philosophy**

**© James B. Wark 1993**

---

Thesis  
9616  
copy 1  
vol 2

## CONTENTS VOLUME 2

### Chapter 1

#### Figures

- 1.1 Simple channel
- 1.2 Compound channel

### Chapter 2

#### Figures

- 2.1 Rotation about y axis
- 2.2 Rotation about  $\bar{x}$  axis
- 2.3 Definitions for a river channel

### Chapter 3

#### Figures

- 3.1 Simple channel
- 3.2 Compound channel
- 3.3 Variation of A, P and R for the River Severn at Montford, after Knight et al (1989)
- 3.4 Variation of Manning's n and friction factor with stage
- 3.4a Surface streamlines for a straight compound channel, after Sellin (1964)
- 3.5 Definition of apparent shear forces for compound channels
- 3.6 James and Brown's correction factor for straight compound channels, after James and Brown (1977)
- 3.7 Definition sketch for Rajaratnum and Ahmadi's channel, after Rajaratnum and Ahmadi (1981)
- 3.8 The vertical distribution of velocity in compound channels, after Rajaratnum and Ahmadi (1981)
- 3.9 Depth averaged velocity in the main channel, after Rajaratnum and Ahmadi (1981)
- 3.10 Depth averaged velocity and bed shear stress on the floodplain, after Rajaratnum and Ahmadi (1981)
- 3.11 Variations in friction parameters for the SERC FCF Phase A data, after Myers and Brennan (1990)
- 3.12 Turbulence data from the SERC FCF, after Knight and Shiono (1990)
- 3.13 Distribution of Reynolds stresses in the horizontal plane, after Knight and Shiono (1990)
- 3.15 Lateral variation of local friction factor for the SERC FCF, after Knight and Shiono (1990)
- 3.16 Lateral variation of depth averaged lateral eddy viscosity, after Knight

- and Shiono (1990)
- 3.17 Bed shear stress distributions for SERC FCF, after Knight and Shiono (1990)
  - 3.18 Example distribution of discharge adjustment factors for SERC FCF, after Ackers 1991.
  - 3.19 Secondary current distributions, after Tominaga et al (1989, 1991)
  - 3.20 Secondary current distributions, after Shiono and Knight (1989, 1991)
  - 3.21 Illustration of secondary currents, after Shiono and Knight (1989)
  - 3.22 Shear layer width in a rectangular channel, after Samuels (1988)
  - 3.23  $\lambda$  values for FCF derived by Shiono and Knight (1991)
  - 3.24 Lateral distribution of convection terms in FCF, after Shiono and Knight (1991)
  - 3.25 Cross-section for the River Severn at Montford, after Knight et al (1991)
  - 3.26 Calculated lateral distributions of velocity for the Severn at Montford, after Knight et al (1991)
  - 3.27 Calculated lateral distributions of velocity and shear stress after Keller and Rodi (1988)
  - 3.28 Summary of mechanisms in a straight compound channel, after Knight et al (1983)
  - 3.29 Divided channel methods

## Chapter 4

### Tables

- 4.1 Summary of Phase A experiments on SERC FCF
- 4.2 Overbank gauging sites
- 4.3 Overbank gauging sites, channel and floodplain widths
- 4.4 Overbank gauging sites, channel and floodplain depths
- 4.5 Overbank gauging sites, Manning's n values
- 4.6 Mean values of back calculated NEV SERC FCF
- 4.7 Mean values of back calculated NEV inbank SERC FCF
- 4.8 Mean values of back calculated NEV all data SERC FCF
- 4.9 Mean errors with NEV fixed smooth floodplains SERC FCF
- 4.10 Mean errors with NEV fixed rough floodplains SERC FCF
- 4.11 Mean errors NEV fixed inbank SERC FCF
- 4.12 Mean errors NEV fixed all data SERC FCF
- 4.13 Mean errors NEV fixed all inbank data SERC FCF
- 4.14 Mean errors in discharge for various methods SERC FCF
- 4.15 Mean errors in discharge for various methods SERC FCF all data
- 4.16 Mean errors in depth for various methods SERC FCF
- 4.17 Mean errors in depth for various methods SERC FCF all data
- 4.18 Mean errors in discharge Myers lab data
- 4.19 Mean errors in depth Myers lab data
- 4.20 Mean errors in discharge Lambert lab data
- 4.21 Mean errors in depth Lambert lab data
- 4.22 Mean errors in discharge for each overbank gauging site
- 4.23 Mean errors in discharge overbank gauging sites



## Figures

- 4.1 Layout of the SERC FCF during Phase A, after Knight and Sellin (1989)
- 4.2 Channel cross-sections, SERC FCF Phase A
- 4.2a Compound channel definitions
- 4.3 Myers' laboratory cross-sections
- 4.4 Lambert's laboratory cross-sections
- 4.5 Natural channels cross-sections
- 4.6 Natural channels cross-sections
- 4.7 Cross-sections for the River Penk
- 4.8 Cross-sections for the River Trent
- 4.9 Main channel Manning's n values natural channels
- 4.10 Main channel Manning's n values natural channels
- 4.11 Analytic and numerical solutions (LDM, LDM2) rectangular channel
- 4.12 Analytic and numerical solutions (LDM, LDM2) quadrilateral channel
- 4.13 Computed stage-discharges (LDM) for SERC FCF Phase A smooth data
- 4.14 Computed stage-discharges (LDM) for SERC FCF Phase A smooth data
- 4.15 Computed stage-discharges (LDM) for SERC FCF Phase A rough data
- 4.16 Computed distributions of NEVC for SERC FCF Phase A smooth data
- 4.17 Computed distributions of NEVC for SERC FCF Phase A rough data
- 4.18 Distributions of %error in Qcalc with NEV = 0.16 for SERC FCF Phase A smooth data
- 4.19 Distributions of %error in Qcalc with NEV = 0.16 for SERC FCF Phase A rough data
- 4.20 Calculated depth averaged velocity profiles LDM Series 2 SERC FCF Phase A data
- 4.21 Calculated depth averaged velocity profiles LDM Series 3 SERC FCF Phase A data
- 4.22 Calculated depth average velocity profiles LDM and LDM2 Series 2 SERC FCF Phase A data
- 4.23 Calculated depth average velocity profiles LDM and LDM2 Series 3 SERC FCF Phase A data
- 4.24 Calculated unit flow profiles LDM Series 2 SERC FCF Phase A data
- 4.25 Calculated unit flow profiles LDM Series 3 SERC FCF Phase A data
- 4.26 Stage discharge curves for Myers' lab data LDM
- 4.27 Calculated depth averaged velocity profiles LDM Myers' Series A
- 4.28 Calculated depth averaged velocity profiles LDM Myers' Series F
- 4.29 Stage discharge curves for Lambert's lab data LDM
- 4.30 Cross-section and stage discharge curve for Kiely's lab data LDM
- 4.31 Calculated depth averaged velocity profiles LDM Kiely
- 4.32 Stage-discharge curves for field data LDM
- 4.33 Stage-discharge curves for field data LDM
- 4.34 Stage-discharge curves with fixed and variable NEV values LDM, Severn at Montford

4.35	Stage-discharge curves LDM and LDM2, Severn at Montford
4.36	Velocity profiles fixed and variable NEV, Severn at Montford
4.37	Velocity profiles fixed and variable NEV LDM2, Severn at Montford
4.38	Velocity profiles River Main section 14
4.39	Velocity profiles River Ouse at Skelton
4.40	Velocity profiles River Penk at Penkridge
4.41	Velocity profiles River Trent at North Muskham, bankfull n values
4.42	Velocity profiles River Trent at North Muskham, calibrated n values
4.43	Unit flow profiles, fixed NEV, Severn at Montford
4.44	Unit flow profiles, variable NEV, Severn at Montford
4.45	Unit flow profiles, n constant and variable, Severn at Montford
4.46	Depth averaged velocities, n constant and variable, Severn at Montford
4.47	Errors in calculated discharges SERC FCF Phase A, Smooth data
4.48	Errors in calculated discharges SERC FCF Phase A, Rough data
4.49	Errors in calculated depths SERC FCF Phase A, Smooth data
4.50	Errors in calculated depths SERC FCF Phase A, Rough data
4.51	Mean errors in discharge and depth SERC FCF Phase A
4.52	Proportion of flow in main channel, SERC FCF Phase A
4.53	Differences in calculated and measured proportions of flow in main channel, SERC FCF Phase A
4.54	Mean errors in discharge and depth Myers' lab data
4.55	Differences in calculated and measured proportions of flow in main channel, Myers' lab data
4.56	Errors in calculated discharges Lambert's lab data
4.57	Errors in calculated depths Lambert's lab data
4.58	Mean errors in discharge and depth Lambert's lab data
4.59	Mean errors in discharge river gauging data
4.60	Variation of errors in discharge with stage river gauging data, LDM
4.61	Variation of errors in discharge with stage river gauging data, DCM
4.62	Variation of errors in discharge with stage river gauging data, SCM
4.63	Variation of errors in discharge with stage river gauging data, SCM3, SSGM
4.64	Variation of errors in discharge with stage river gauging data, DCM2
4.65	Variation of errors in discharge with stage river gauging data, ACKM
4.66	Backwater profiles for the River Thames at Wallingford reach 1
4.67	Example velocity profiles River Thames at Wallingford
4.68	Backwater profiles for the River Thames at Wallingford reach 2
4.69	Backwater profiles for the River Tees at Low Moor

## Chapter 5

### Tables

5.1	Summary of SERC Phase B tests
5.1	(cont) Summary of SERC Phase B tests
5.2	Summary of SERC Phase B stage discharge tests
5.3	Summary of Aberdeen experiments
5.4	Summary of Vicksburg experiments 2ft wide channel

- 5.5 Geometric parameters lab studies meandering channels
- 5.6 Non-dimensional geometric parameters meandering channels
- 5.7 Bend losses for 60° meander geometry, trapezoidal cross-section
- 5.8 Non-friction losses for 60° meander geometry, natural cross-section
- 5.11 Non-friction losses for 110° meander geometry, natural cross-section
- 5.12 Summary of mean errors in bend loss predictions

## Figures

- 5.1 Detailed plan geometry of FCF 60° meander
- 5.2 Plan of flume and natural cross-section geometry for 60° meander
- 5.3 Detailed plan geometry for FCF 110° meander
- 5.4 Plan of flume and natural cross-section geometry for 110° meander
- 5.5 Plan geometries of the Aberdeen flume with channel sinuosities of 1.40 and 2.04 (after Willetts 1992)
- 5.6 Plan geometry of the Aberdeen flume with channel sinuosity of 1.21 (after Willetts 1992)
- 5.7 Plan and cross-sections for Vicksburg flume (after US Army 1956)
- 5.8 Plan and cross-sections for Sooky's flume (after Sooky 1964)
- 5.9 Plan and cross-sections for Kiely's flume (after Kiely 1990)
- 5.10 Flow processes in a meandering compound channel (after Ervine and Jasem)
- 5.11 Adjustment to Manning's n for bend losses: measured and predicted
- 5.12 Predicted adjustments to n for bend losses: modified Chang method

## Chapter 6

### Tables

- 6.1 Mean errors straight methods meandering data
- 6.2 Contraction loss coefficients (Rouse, 1950)
- 6.3 Main channel integrated discharges
- 6.4 Variables for defining main channel flow
- 6.5 Adjusted variables for defining main channel flow
- 6.6 Roughness and sinuosity adjustment to  $Q1'$
- 6.7 Roughness and sinuosity adjustment to c
- 6.8 Errors (%) in reproducing  $Q1'$  for high values of  $y'$
- 6.9 Data sets for inner flood plain analysis
- 6.10 Equation parameters for  $y'$  greater than 0.2
- 6.11 Geometric data overbank laboratory studies
- 6.12 Geometric data Sooky's laboratory study
- 6.13 Main channel geometric data
- 6.14 Mean % errors in discharge FCF data
- 6.15 Mean % errors in discharge Aberdeen, Vicksburg and Kiely data
- 6.16 Mean % errors in discharge Sooky data
- 6.17 Mean % errors in discharge all data
- 6.18 Ranking of methods
- 6.19 Mean % errors in stage FCF data
- 6.20 Mean % errors in stage Aberdeen, Vicksburg and kiely data

- 6.21 Mean % errors in stage Sooky data
- 6.22 Mean % errors in stage all data
- 6.23 Sensitivity tests : effect of errors in wave length
- 6.24 Sensitivity tests : effect of errors in channel side slope
- 6.25 Measured zonal discharges, Sooky and Kiely data
- 6.26 Errors (%) in calculated total flows, Sooky and Kiely data
- 6.27 Measured and calculated flow distributions
- 6.28 Reach averaged geometric parameters Roding study
- 6.29 Errors in predicting overbank discharges
- 6.30 Sensitivity tests on the effect of floodplain roughness

## Figures

- 6.1 Cross-section subdivision for overbank flows Ervine and Ellis method
- 6.2 Variation of main channel discharge along a meander during overbank flow (FCF Phase B)
- 6.3 Inbank stage-discharge relationship for 60° trapezoidal channel
- 6.4 Inbank stage-discharge relationship for 60° natural channel
- 6.5 Inbank stage-discharge relationship for 110° natural channel
- 6.6 Variation of dimensionless main channel discharge with flow depth
- 6.7 Variation of dimensionless main channel discharge with dimensionless flow depth
- 6.8 Variation of dimensionless main channel discharge with dimensionless flow depth with points adjusted for friction factor ratio
- 6.9 Additional adjustment to discharge for relative roughness
- 6.10 Adjustment to  $c$  for relative roughness
- 6.11 Flow expansion over a downward step
- 6.12 Flow contraction over an upward step
- 6.13 Expansion and contraction flow patterns
- 6.14 Width to depth ratio correction for expansion losses
- 6.15 Width to depth ratio correction for contraction losses
- 6.16 Width to depth ratio correction for combined expansion and contraction losses
- 6.17 Errors for SERC predictions before sinuosity predictions
- 6.18 Errors for Aberdeen predictions before sinuosity predictions
- 6.19 Adjustment factor for inner flood plain discharges for SERC Phase B experiments
- 6.20 Adjustment factor for inner flood plain discharges for Aberdeen experiments
- 6.21 Adjustment factor for inner flood plain discharges for  $y' > 0.2$ , SERC Phase B data
- 6.22 Adjustment factor for inner flood plain discharges for  $y' > 0.2$ , Aberdeen data
- 6.23 Variation of  $a$  with  $s$
- 6.24 Variation of  $b$  with  $B^2/A$
- 6.25 Comparison of predicted zone 2 adjustment factor with SERC data
- 6.26 Comparison of predicted zone 2 adjustment factor with Aberdeen data
- 6.27 Example of boundary shear stress distribution in a meandering compound channel (after Lorena)
- 6.28 Cross-section subdivision for overbank flows, James and Wark

- 6.29 Errors in predicted discharge and depth BFO
- 6.30 Errors in predicted discharge and depth JW
- 6.31 Errors in predicted discharge and depth JW2
- 6.32 Errors in predicted discharge and depth EE
- 6.33 Errors in predicted discharge and depth GH4
- 6.34 Errors in predicted discharge and depth GH5
- 6.35 Location plan of study area on River Roding at Abridge (after Sellin et al 1990)
- 6.36 Roding at Abridge sample cross-section
- 6.37 Roding at Abridge measured and calculated stage-discharges

## **APPENDICES**

- 1 SUMMARY OF TENSOR MATHEMATICS
- 2 THE STRESS VECTOR ON AN ARBITRARY SURFACE
- 3 SERC PHASE A DATA
- 4 RIVER GAUGING SITES AND LABORATORY DATA
- 5 MEANDERING LABORATORY DATA
- 6 SUMMARY OF THE ACKERS METHOD
- 7 SUMMARY OF THE ACKERS ROD ROUGHNESS METHOD
- 8 PUBLISHED PAPERS

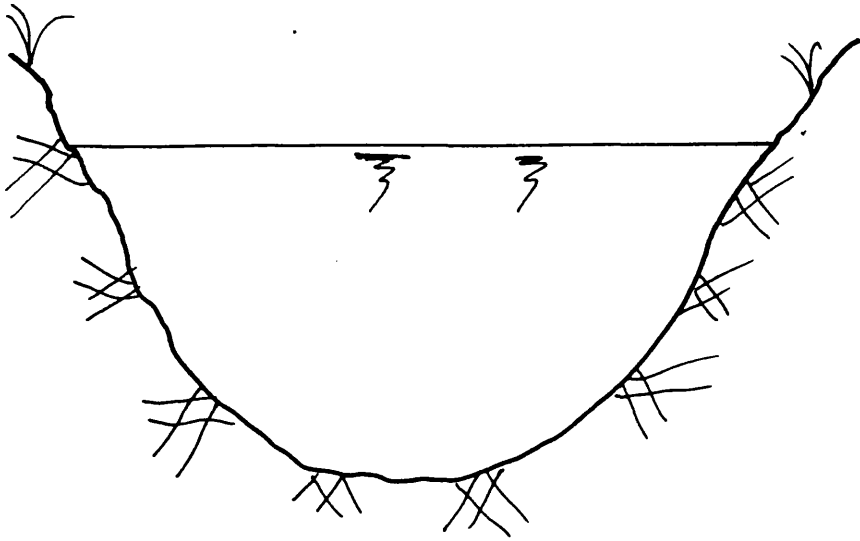


**Figure 1.1** Simple channel

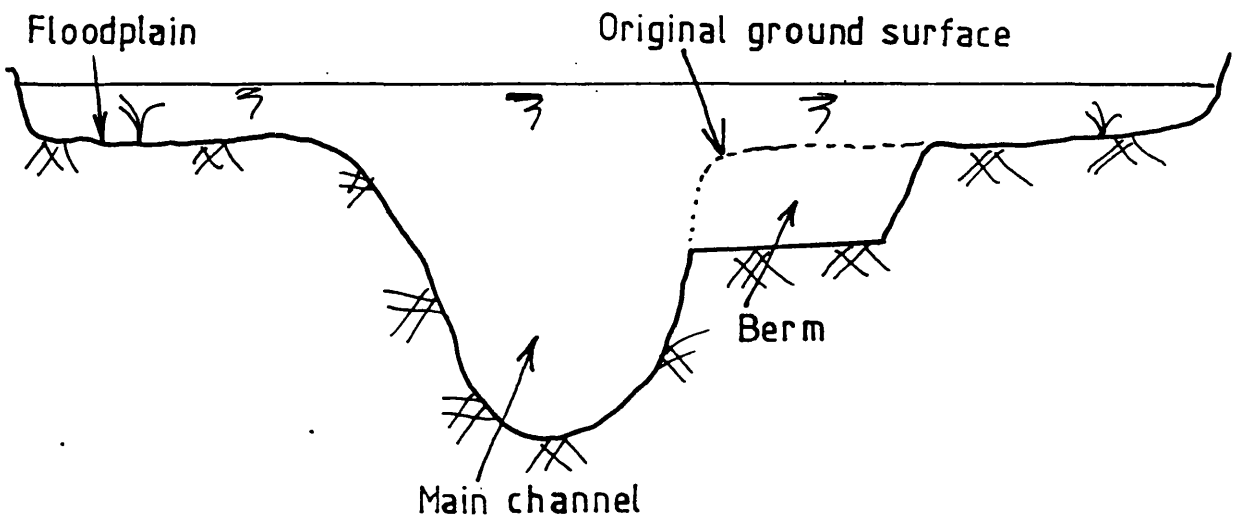


**Figure 1.2** Compound channel

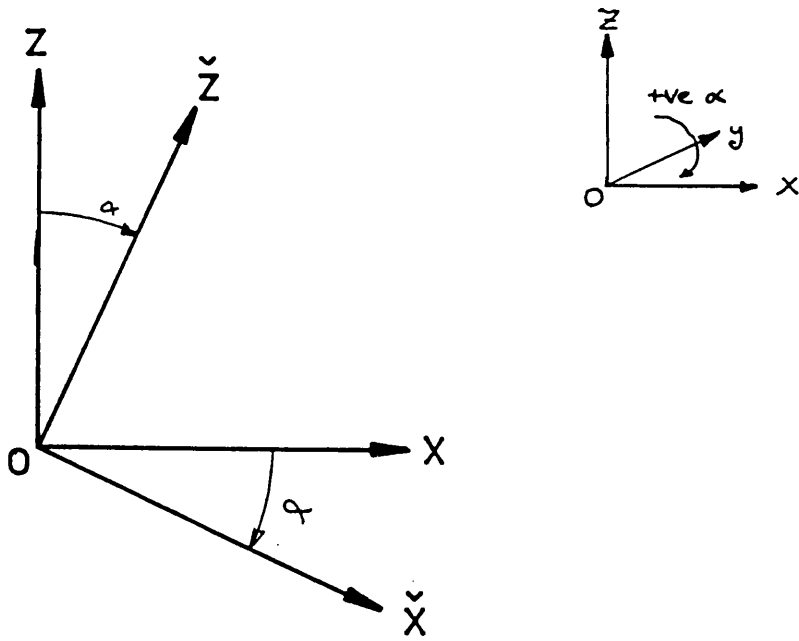


Figure 2.1 Rotation about y axis

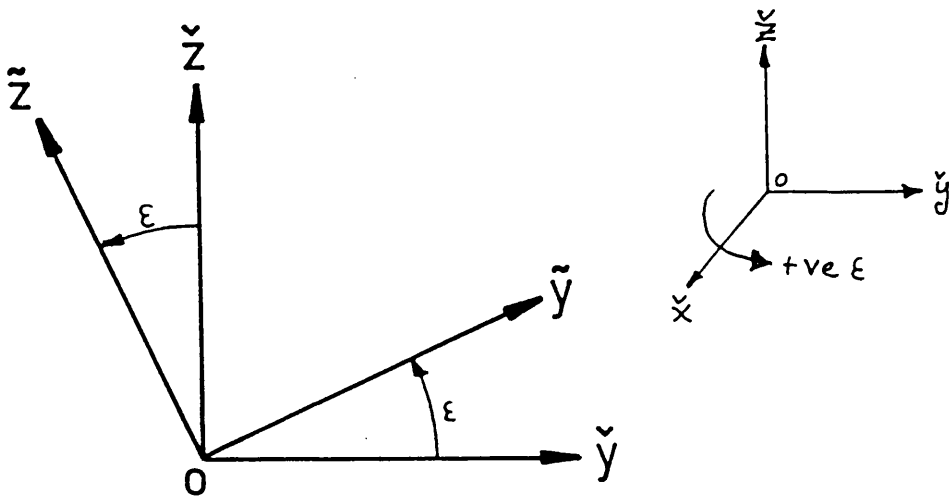


Figure 2.2 Rotation about x axis

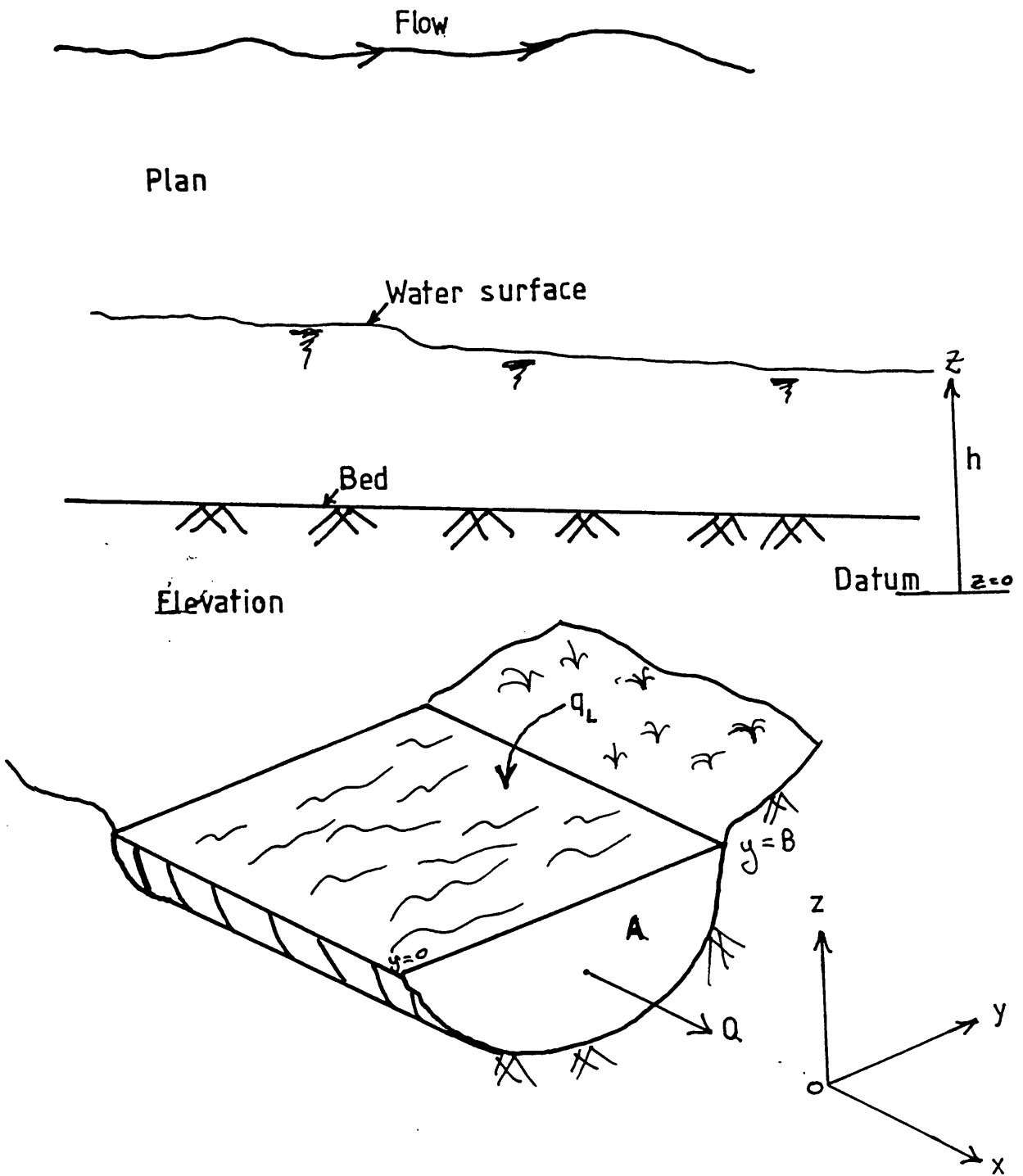
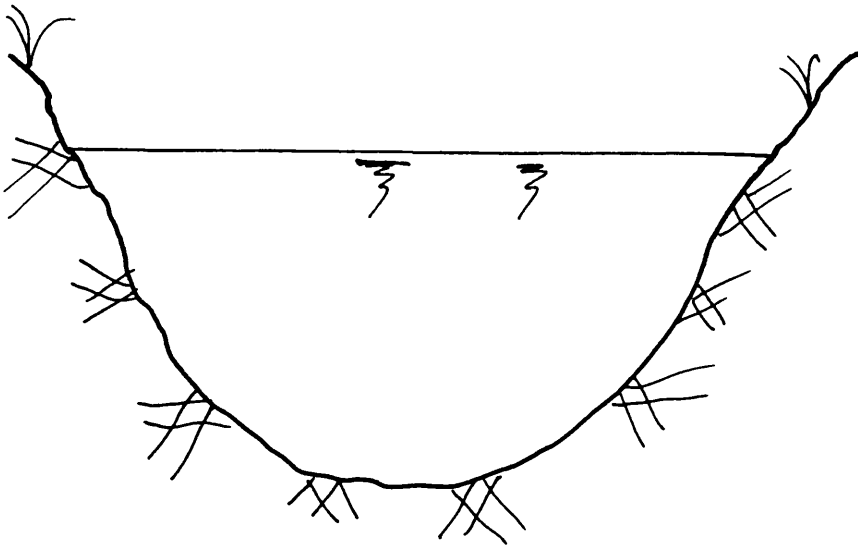
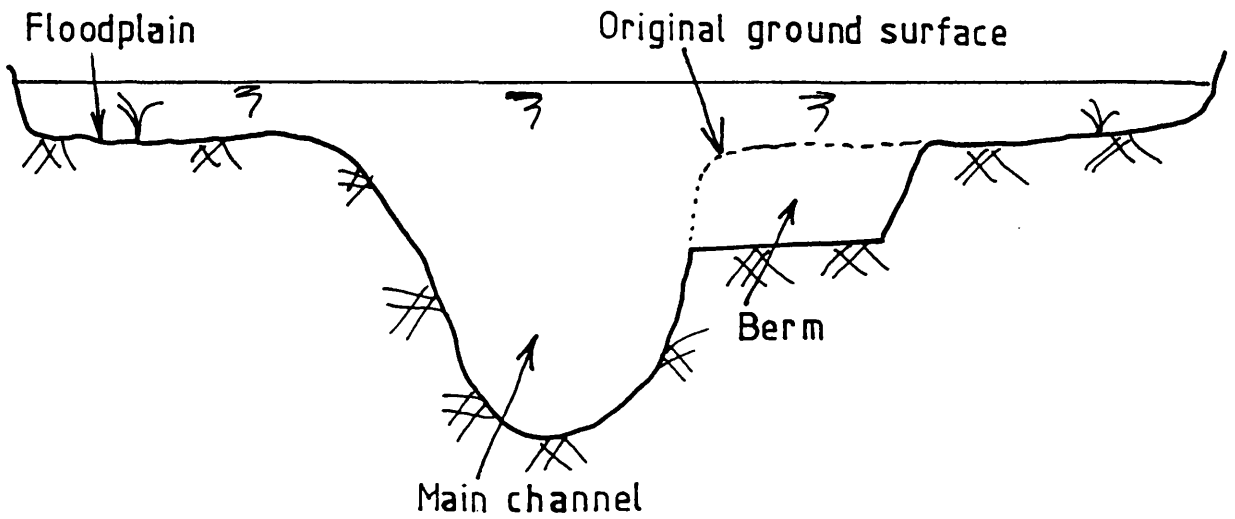


Figure 2.3 Definitions for a river channel



**Figure 3.1 Simple channel**



**Figure 3.2 Compound channel**

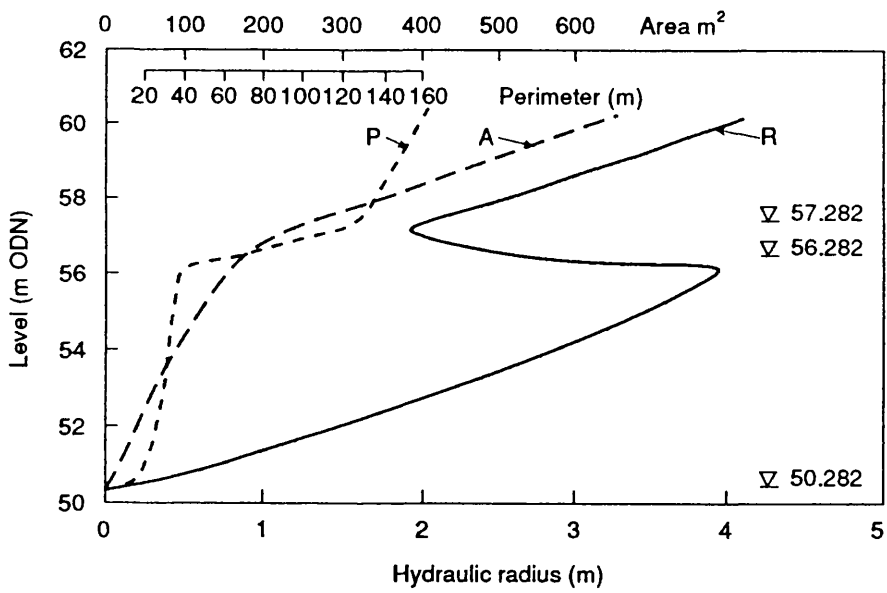
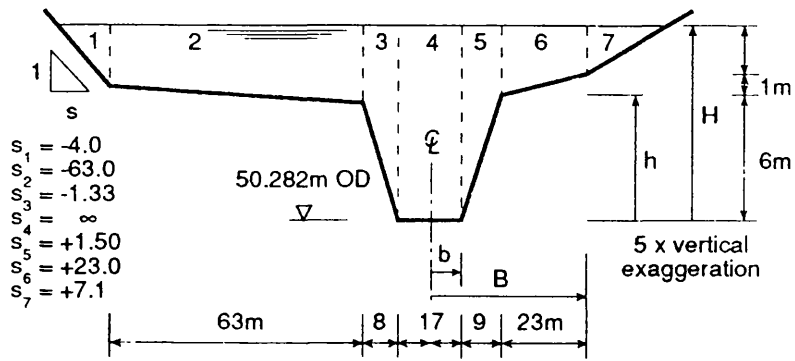


**Figure 3.3** Variation of A, P and R for the River Sever at Montford (after Knight et al, 1989)

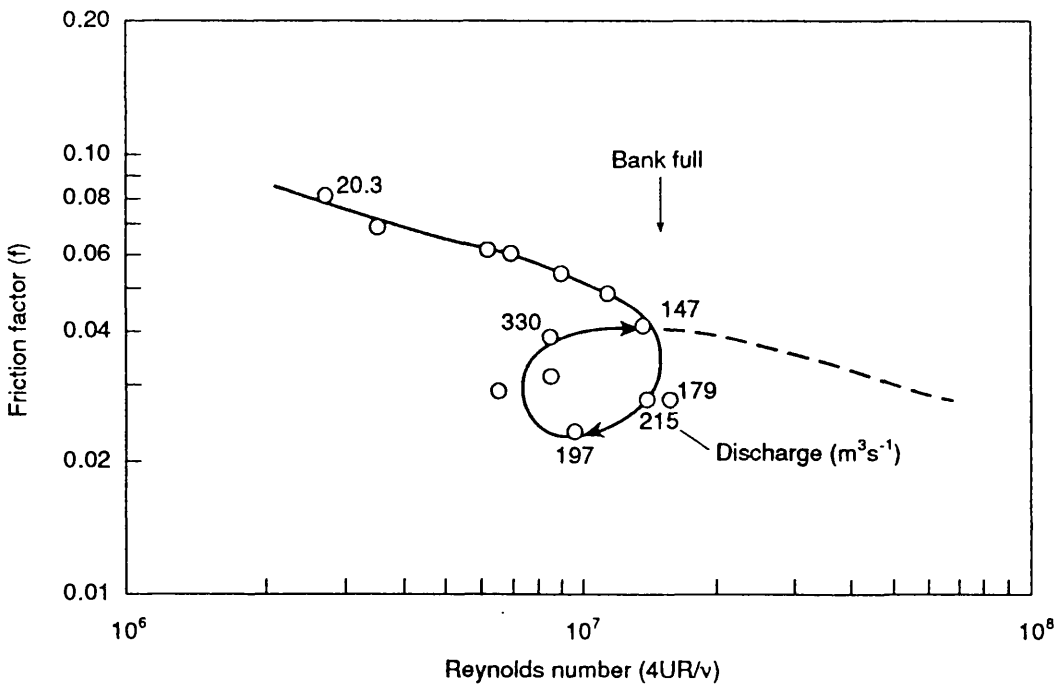
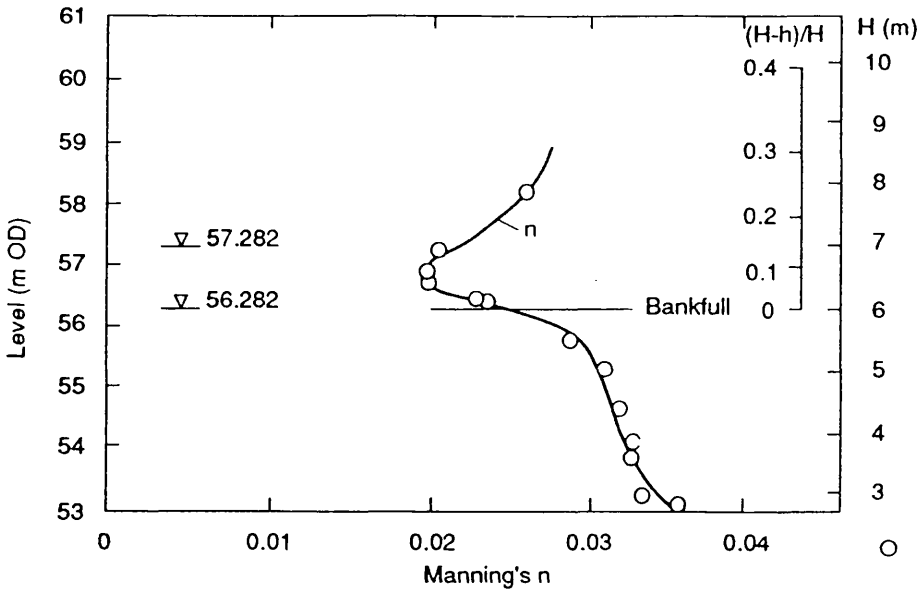
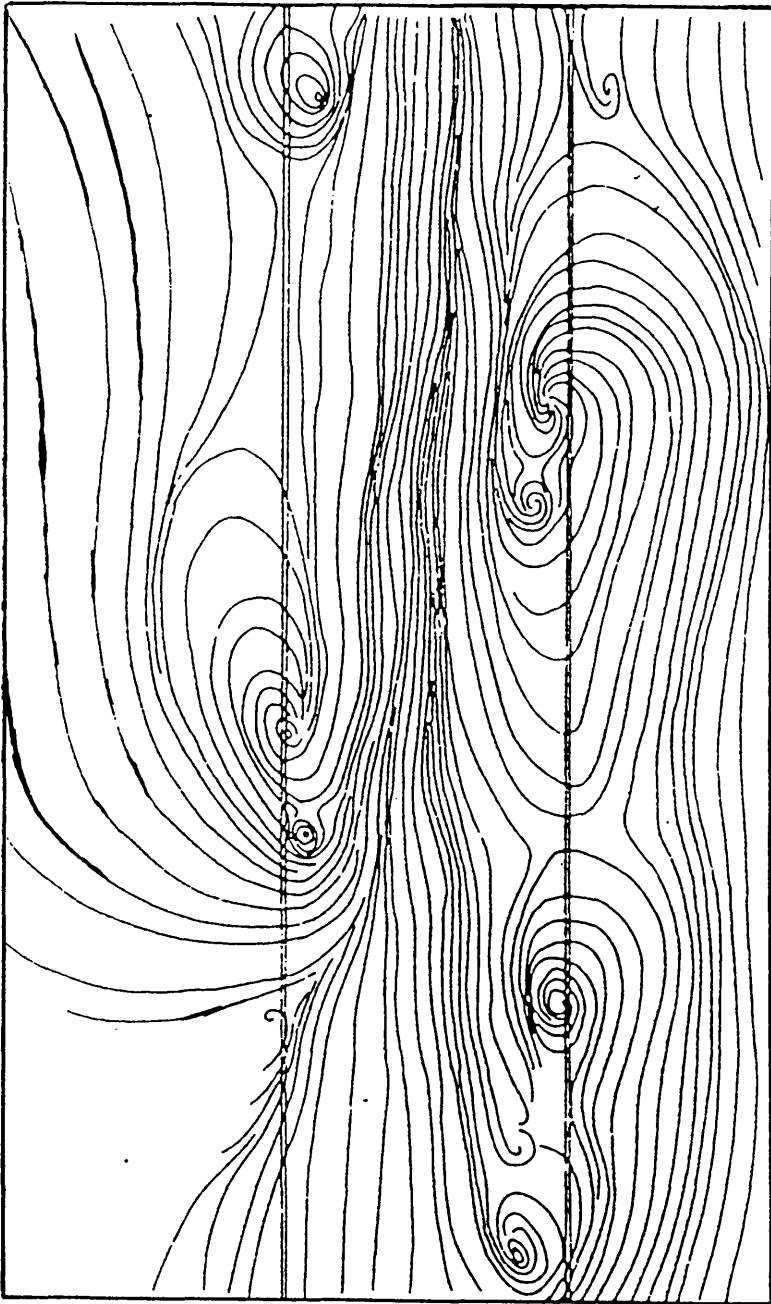


Figure 3.4 Variation of Manning's  $n$  and friction factor with stage



Surface streamlines relative to moving camera

Figure 3.4a Surface stream lines for a straight compound channel, after Sellin (1964)

$F_{bf}$  Bed shear force on floodplain  
 $F_{bc}$  Bed shear force on main channel  
 $F_1$  Apparent shear force

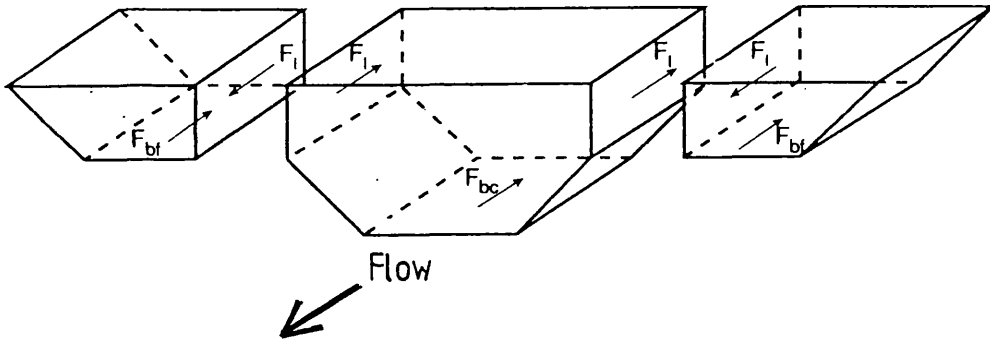


Figure 3.5 Definition of apparant shear forces for compound channels

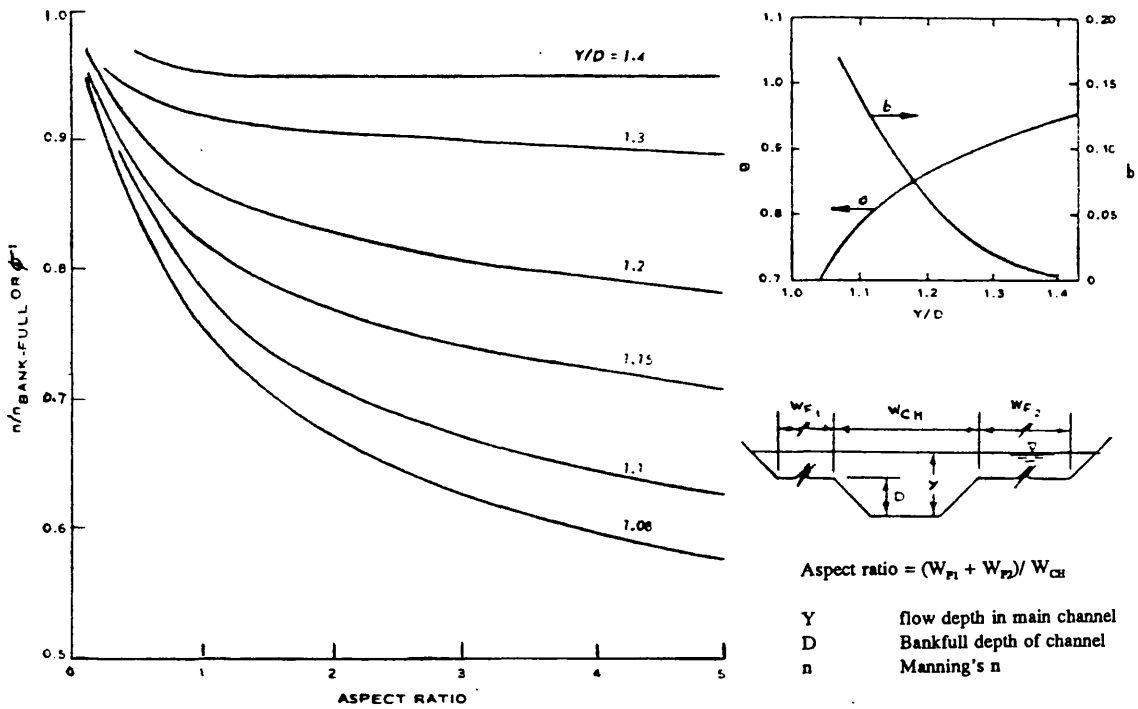


Figure 3.6 James and Brown's correction factor for straight compound channels, after James and Brown (1977)

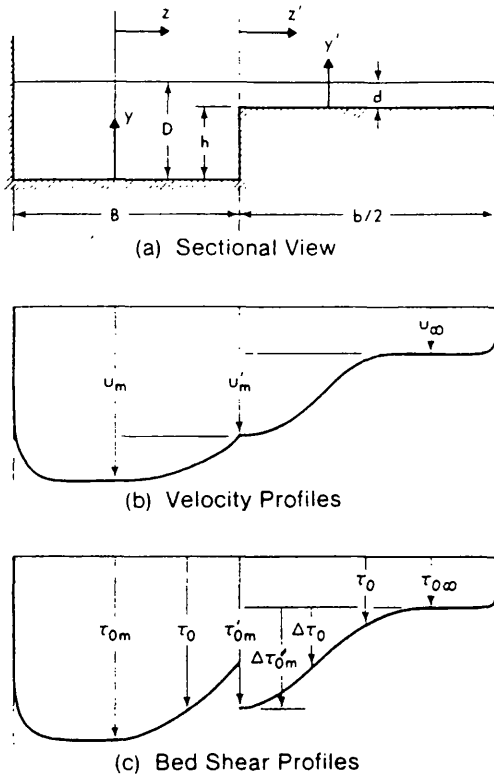


Figure 3.7 Definition sketch for Rajaratnum and Ahmadi's channel, after Rajaratnum and Ahmadi (1981)

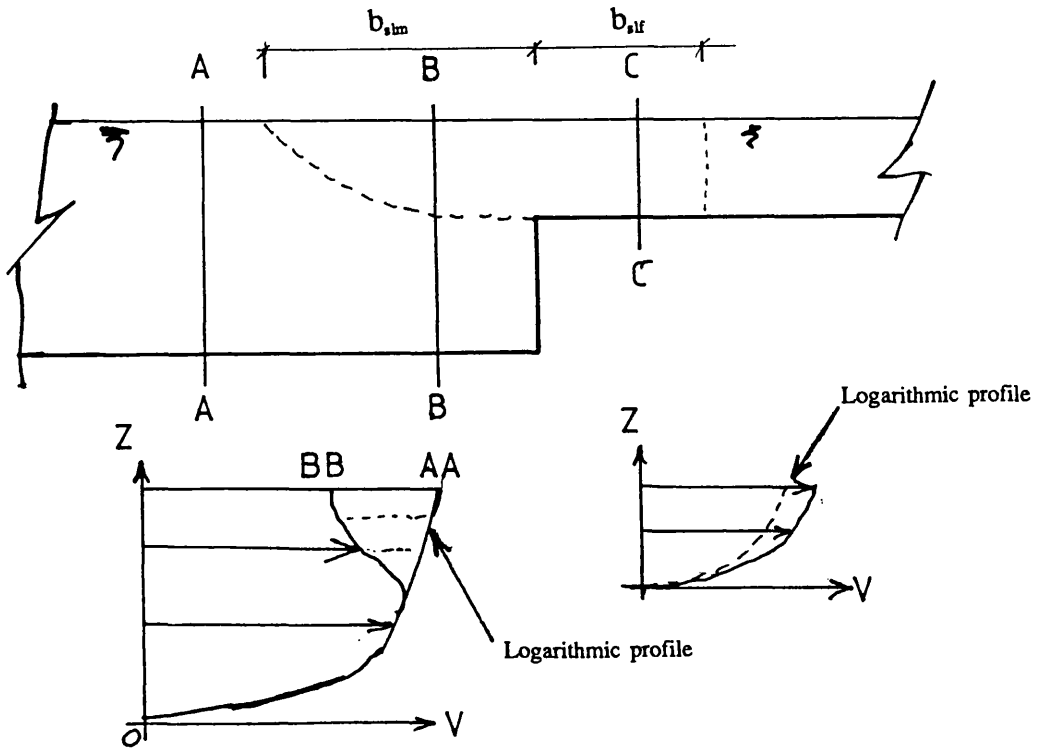
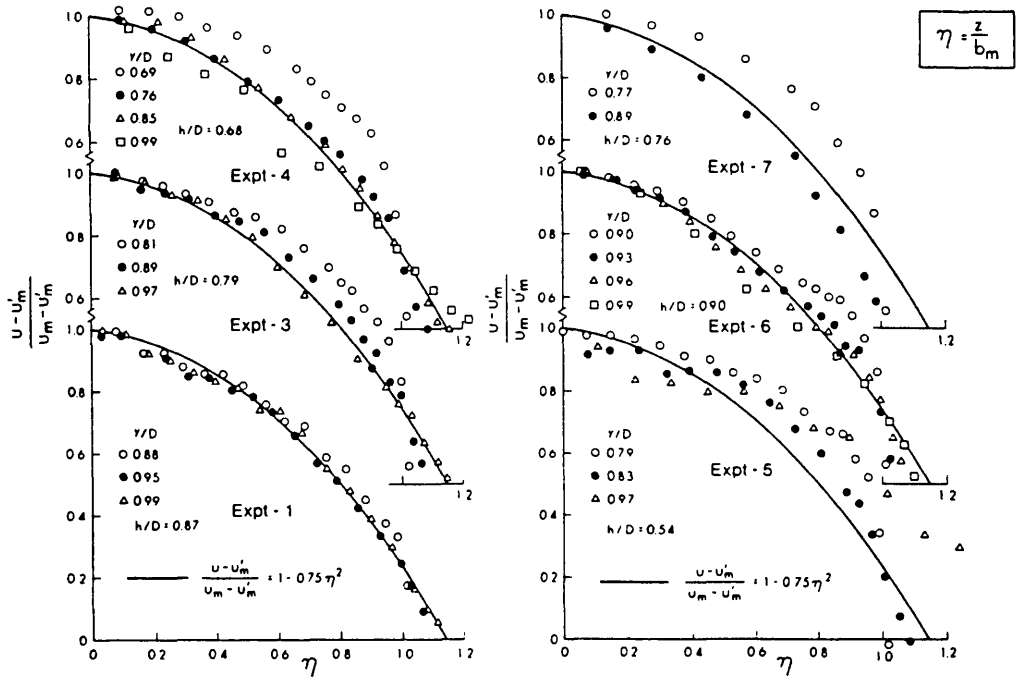


Figure 3.8 The vertical distribution of velocity in compound channels, after Rajaratnum and Ahmadi (1981)



$$\frac{u_m - u_\infty}{u_\infty} = \frac{\sqrt{\frac{D}{d} \frac{C_{*m}}{C_{*f}} \log\left\{C_{*m} \left(\frac{y'D}{d'd} - 1\right) \frac{d\sqrt{gd}S_o}{v} \sqrt{\frac{D}{d}}\right\}} - \log\left\{C\sqrt{C_{*f}} \frac{y'}{d} \frac{d\sqrt{gd}S_o}{v}\right\}}{\log\left\{C\sqrt{C_{*f}} \frac{y'}{d} \frac{d\sqrt{gd}S_o}{v}\right\}}$$

Figure 3.9 Depth averaged velocity in the main channel, after Rajaratnum and Ahmadi (1981)

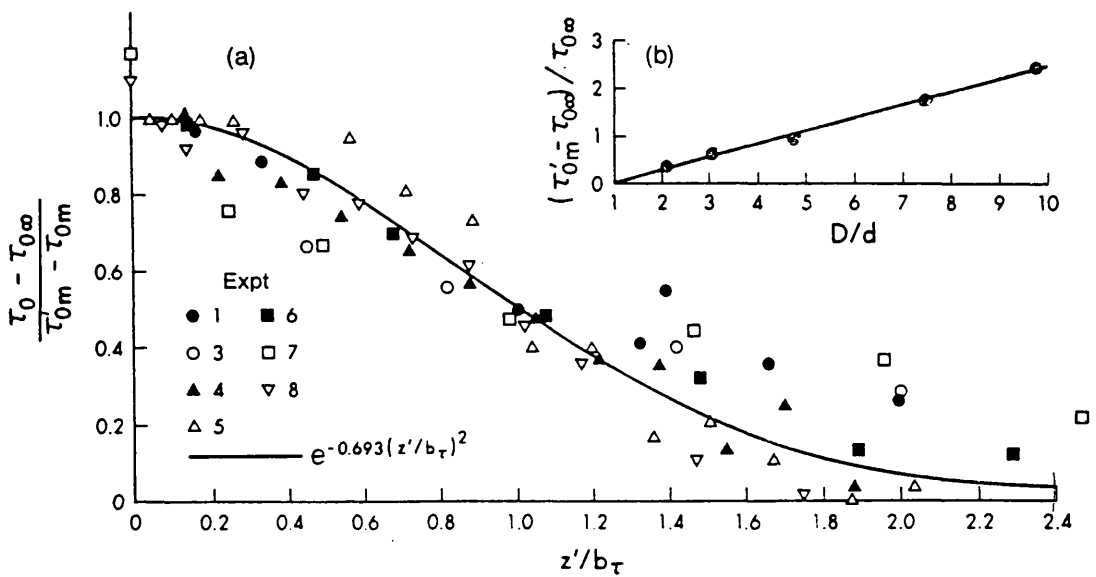
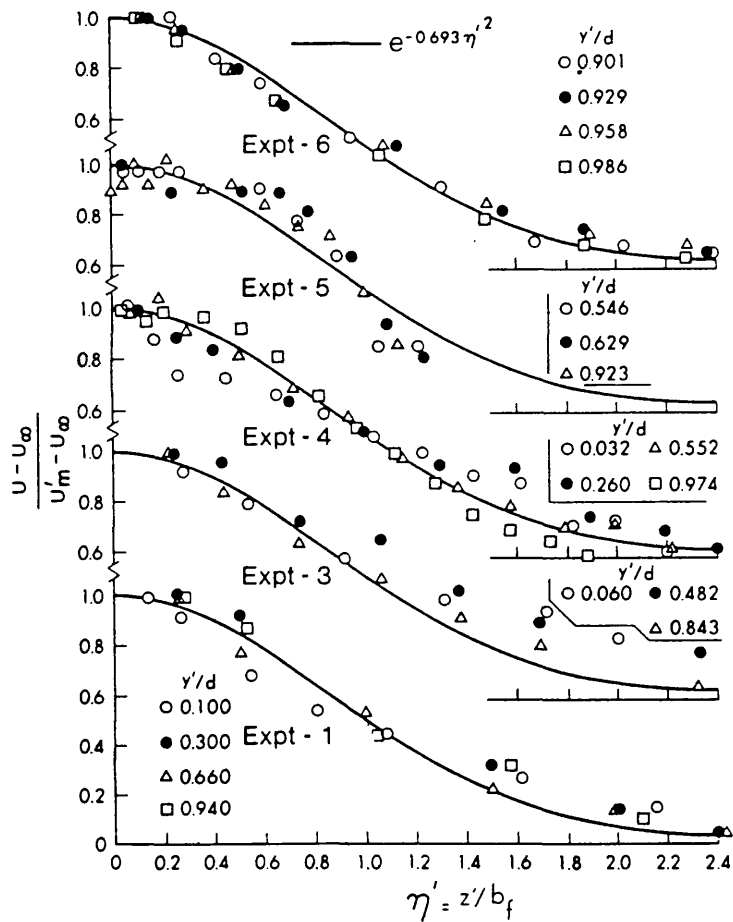


Figure 3.10 Depth averaged velocity and bed shear stress on the floodplain, after Rajaratnum and Ahmadi (1981)

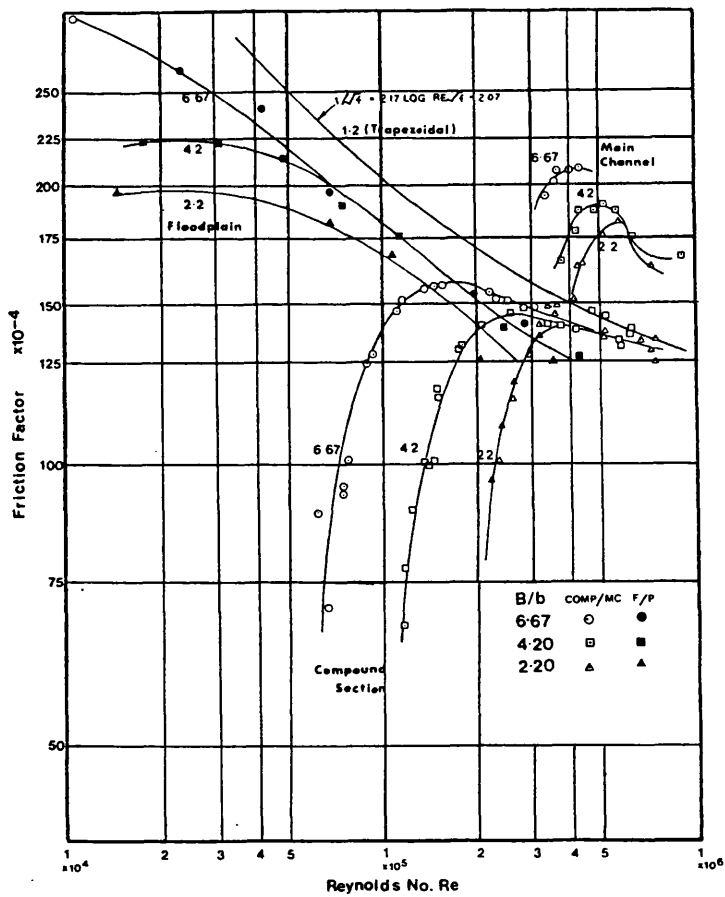
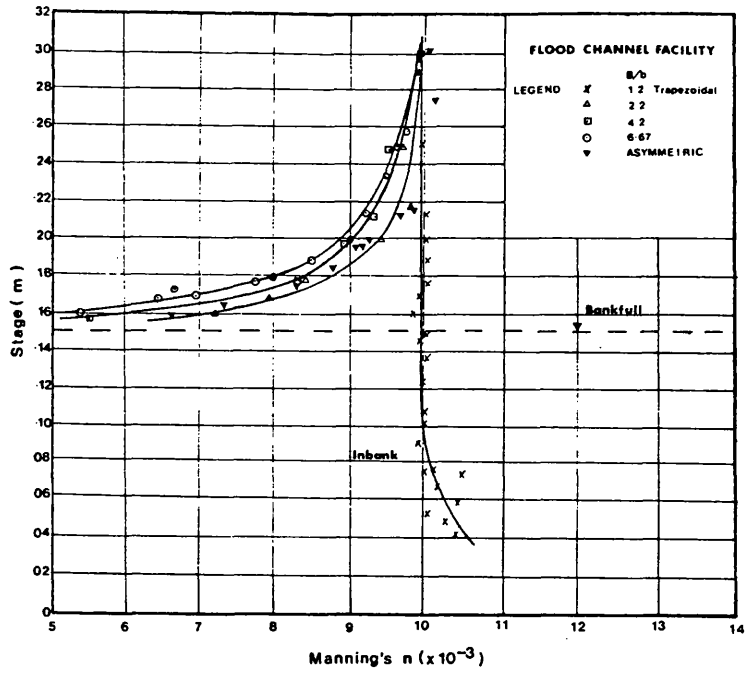
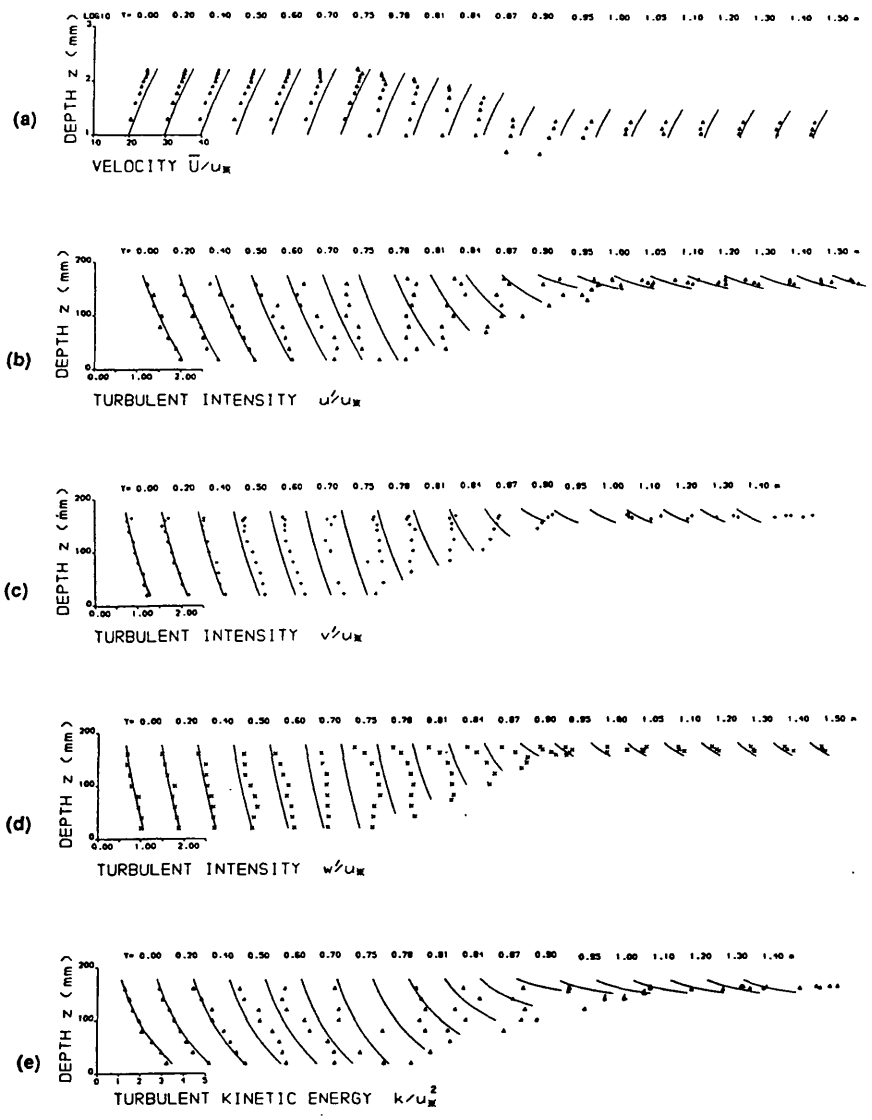
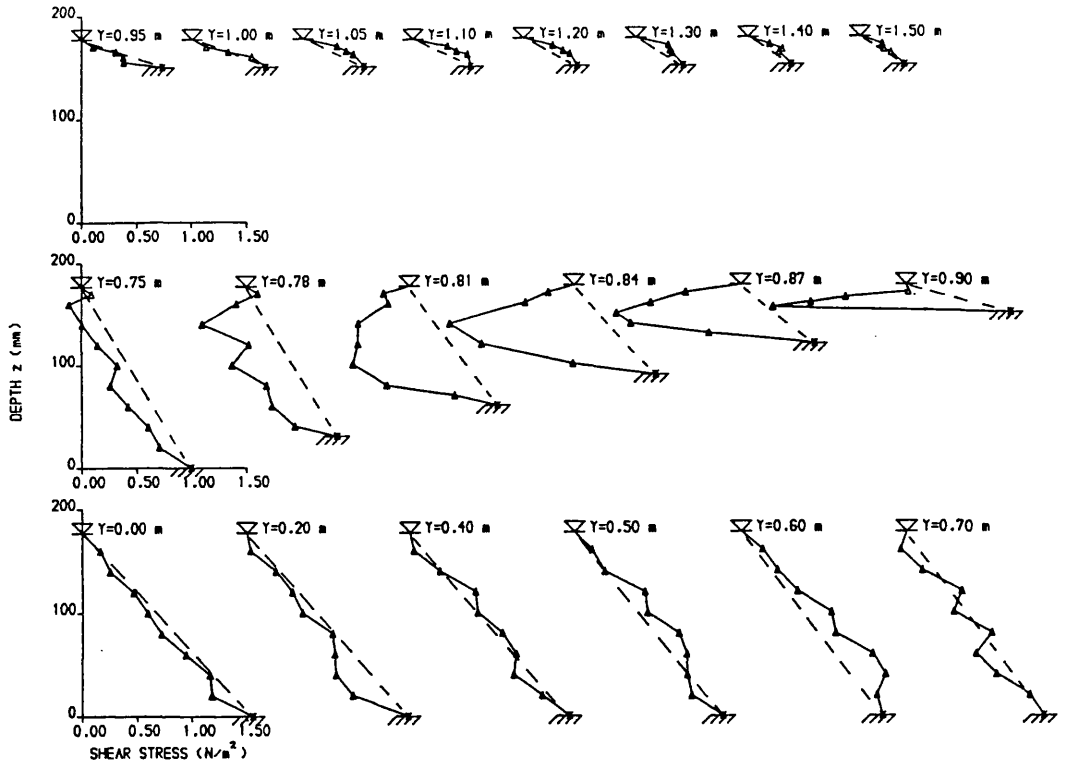


Figure 3.11 Variations in friction parameters for the SERC FCF Phase A data, after Myers and Brennan 1990.



**Figure 3.12 Turbulence data from the SERC FCF , after Knight and Shiono (1990)**



**Figure 3.13** Distribution of Reynolds stresses in the horizontal plane, after Knight and Shiono (1990)

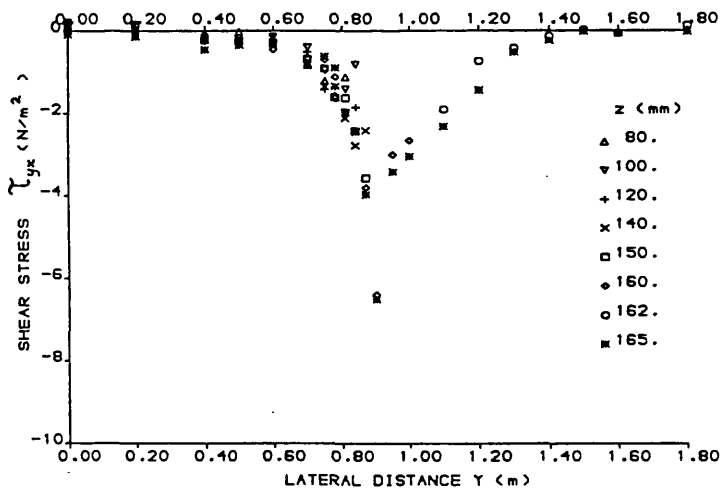


**Figure 3.14** Distribution of Reynolds stresses in the vertical plane, after Knight and Shiono (1990)

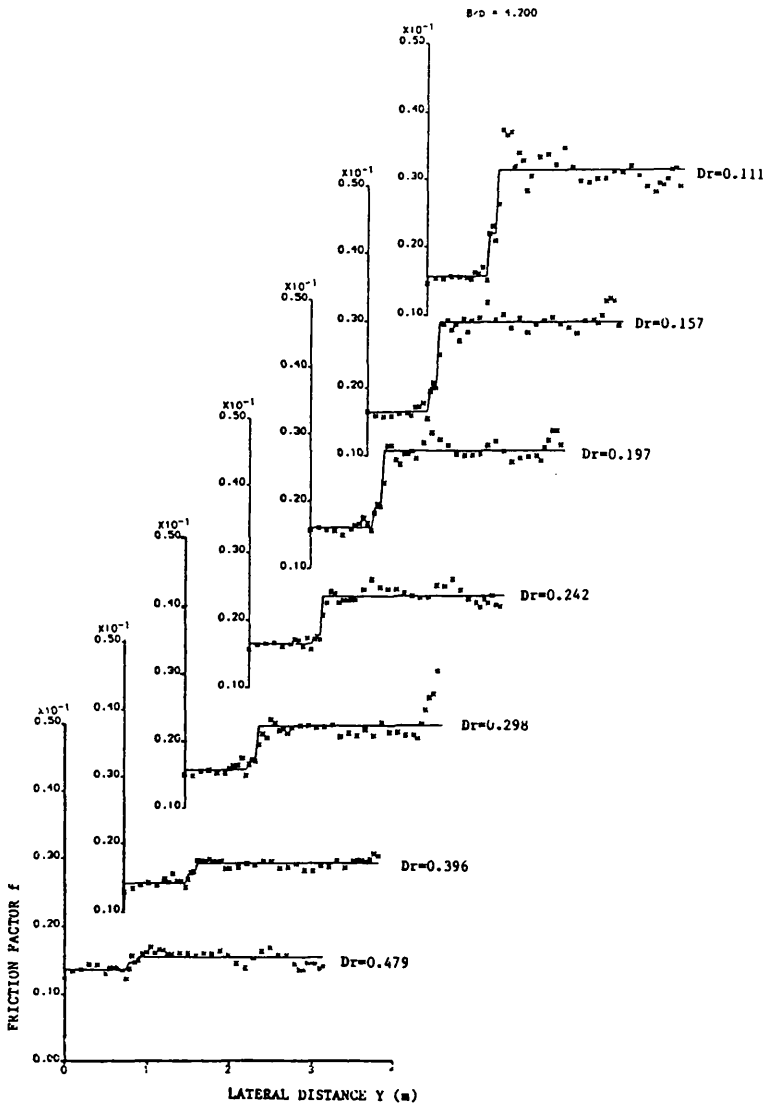
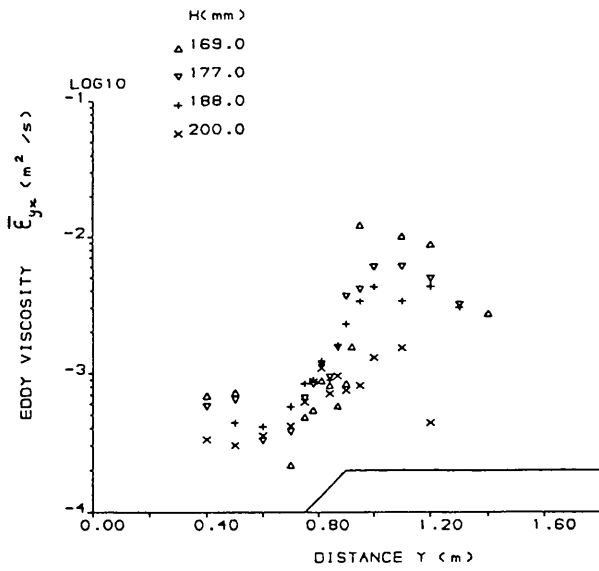
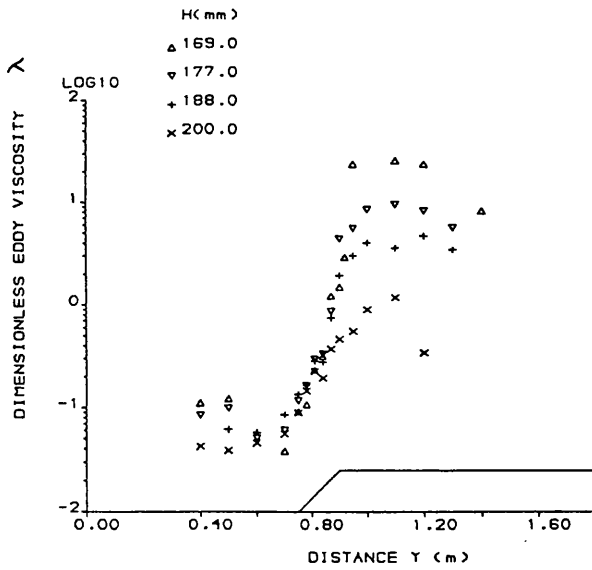


**Figure 3.15 Lateral variation of local friction factor for the SERC FCF, after Knight and Shiono (1990)**



a) Eddy viscosity



b) Non-dimensionalized eddy viscosity

Figure 3.16 Lateral variation of depth averaged lateral eddy viscosity, after Knight and Shiono (1990)

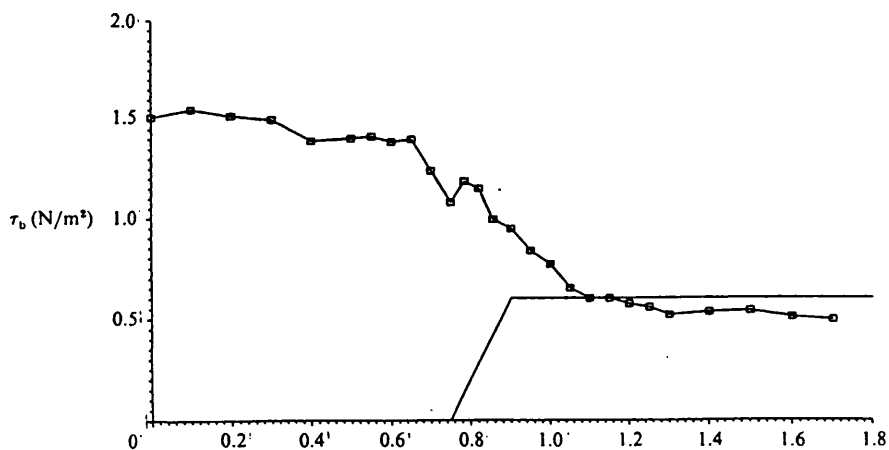
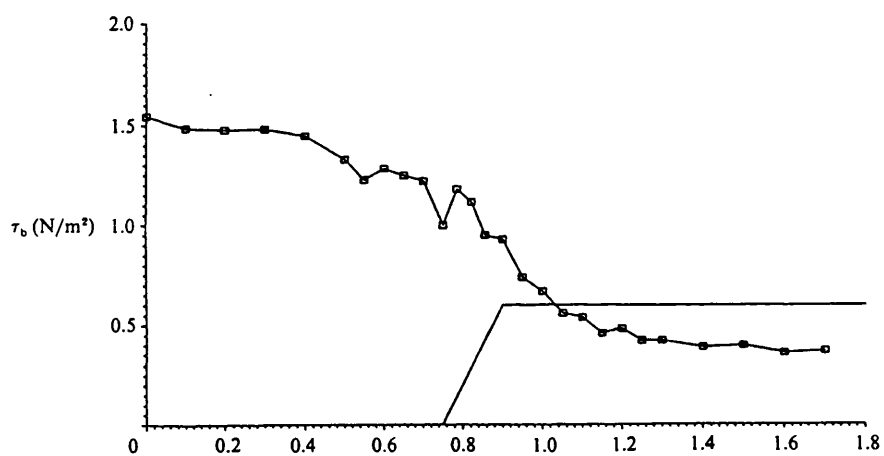
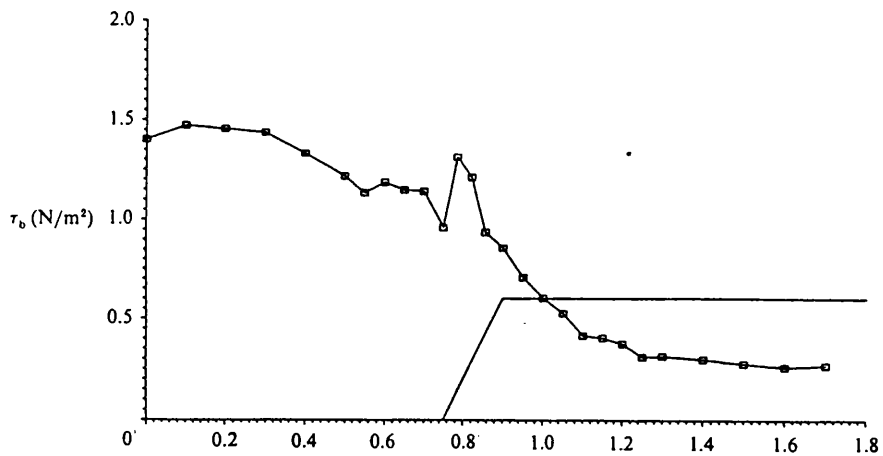


**Figure 3.17 Bed shear stress distributions for SERC FCF, after Knight and Shiono (1990)**

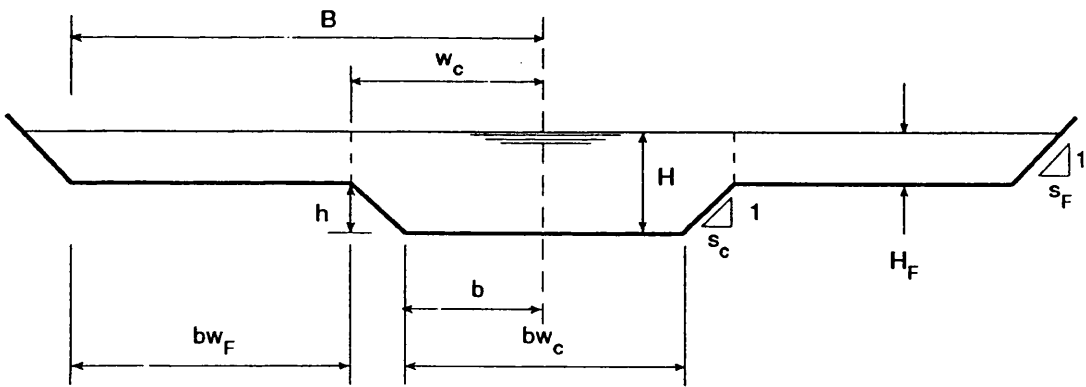
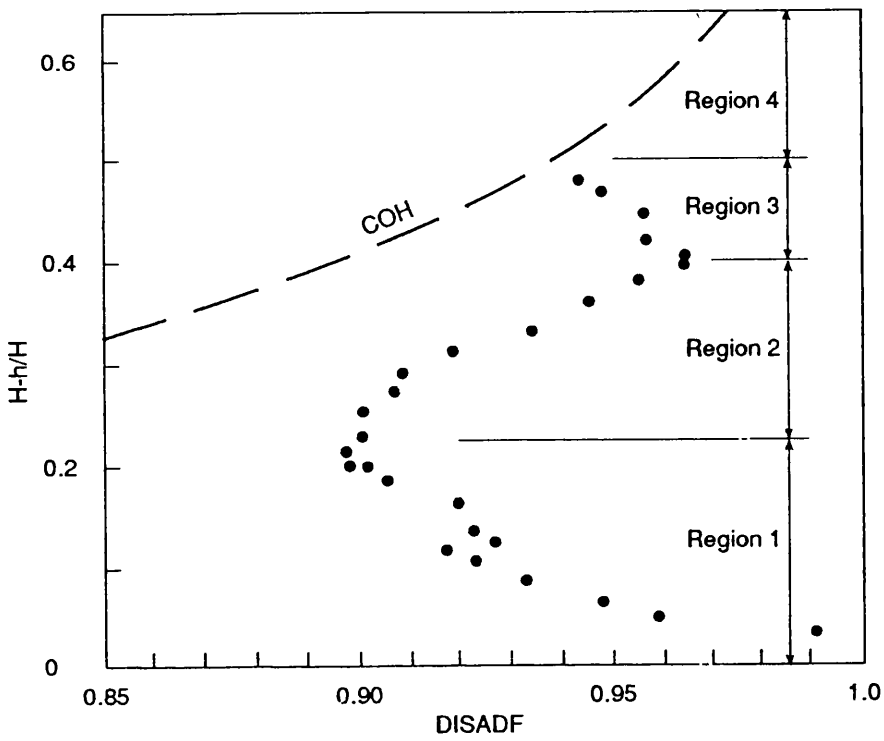
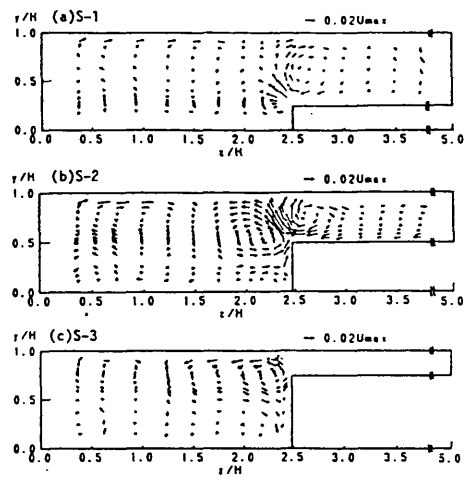


**Figure 3.18 Example distribution of discharge adjustment factors for SERC FCF, after Ackers 1991.**



$$1 - \frac{h}{H} = 0.75$$

$$= 0.6$$

$$= 0.25$$

Figure 3.19 Secondary current distributions, after Tominaga et al (1989, 1991)

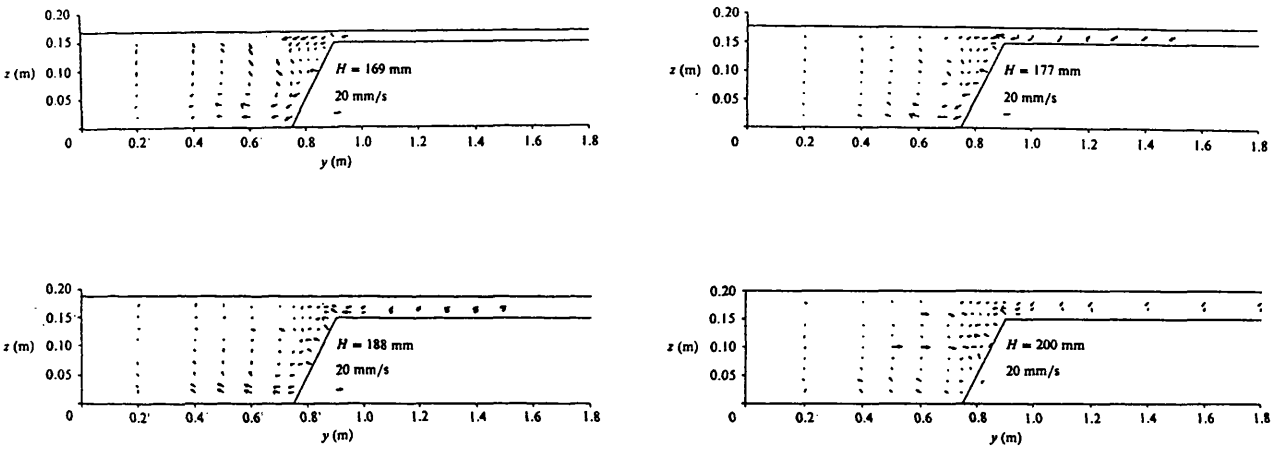


Figure 3.20 Secondary current distributions, after Shiono and Knight (1989, 1991)

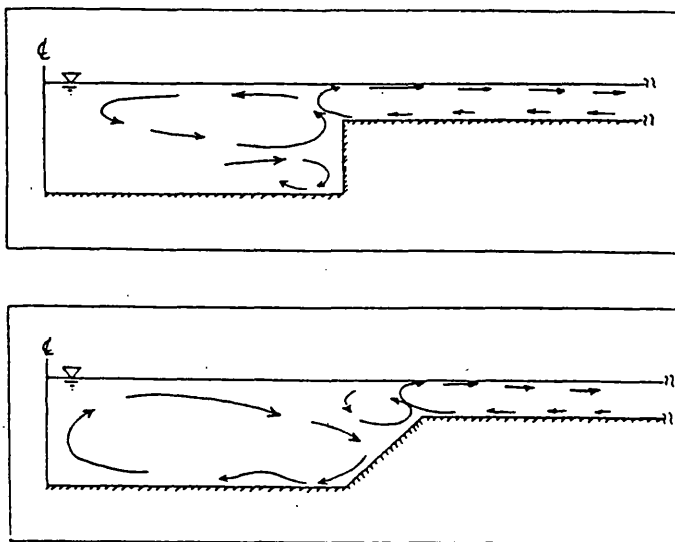


Figure 3.21 Illustration of secondary currents, after Shiono and Knight (1989)

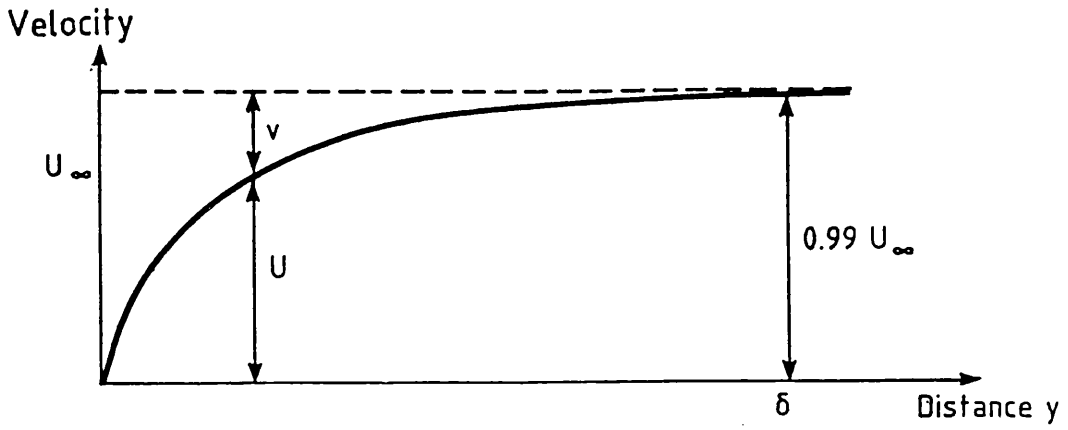
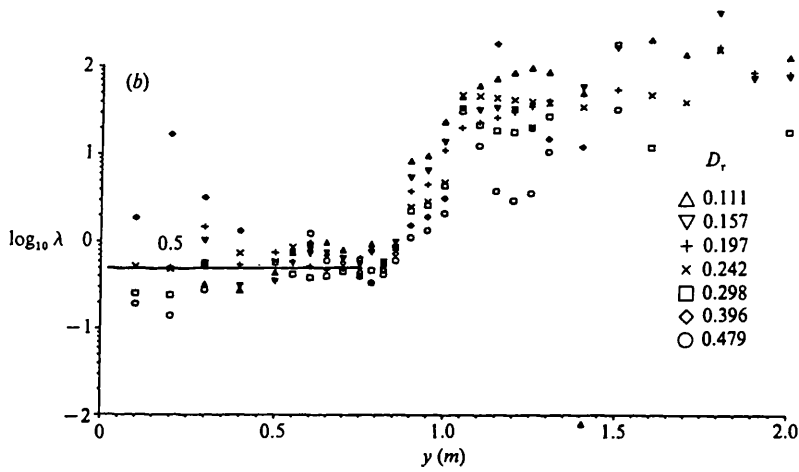
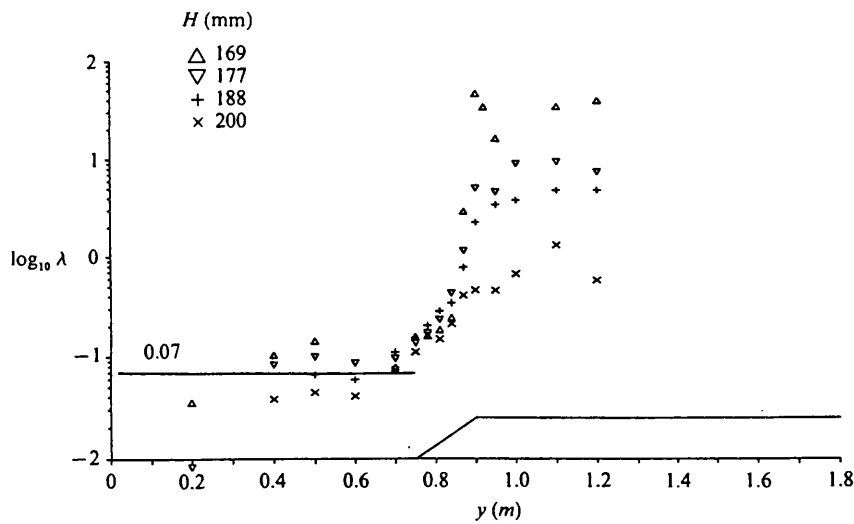


Figure 3.22 Shear layer width in a rectangular channel, after Samuels (1988)



a) based on measured bed shear and depth averaged velocities



b) based on measured Reynolds stresses

Figure 3.23  $\lambda$  values derived by Shiono and Knight (1991)



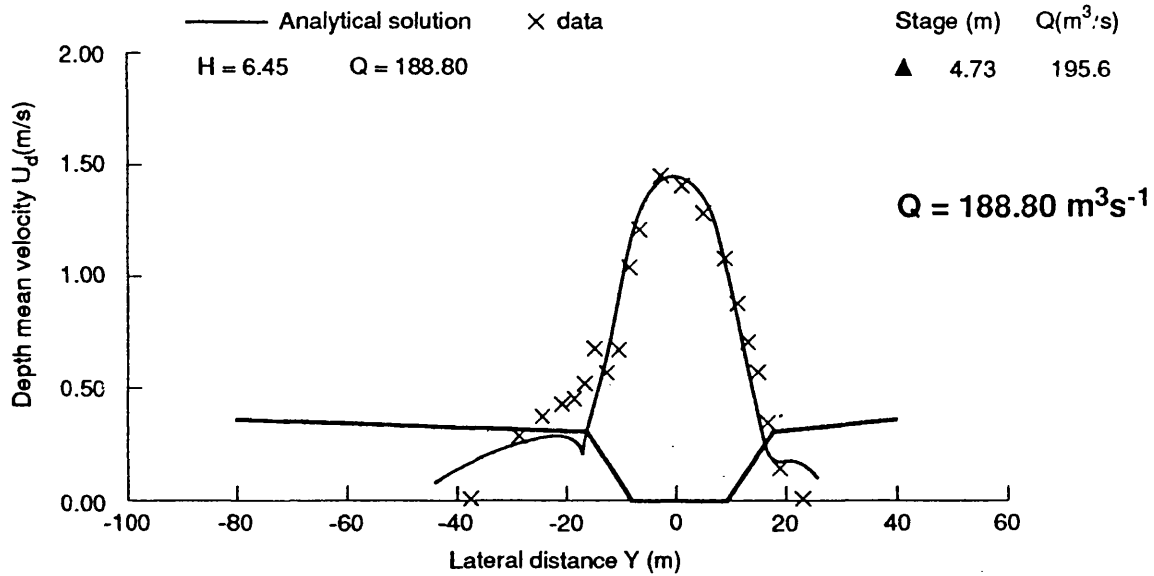
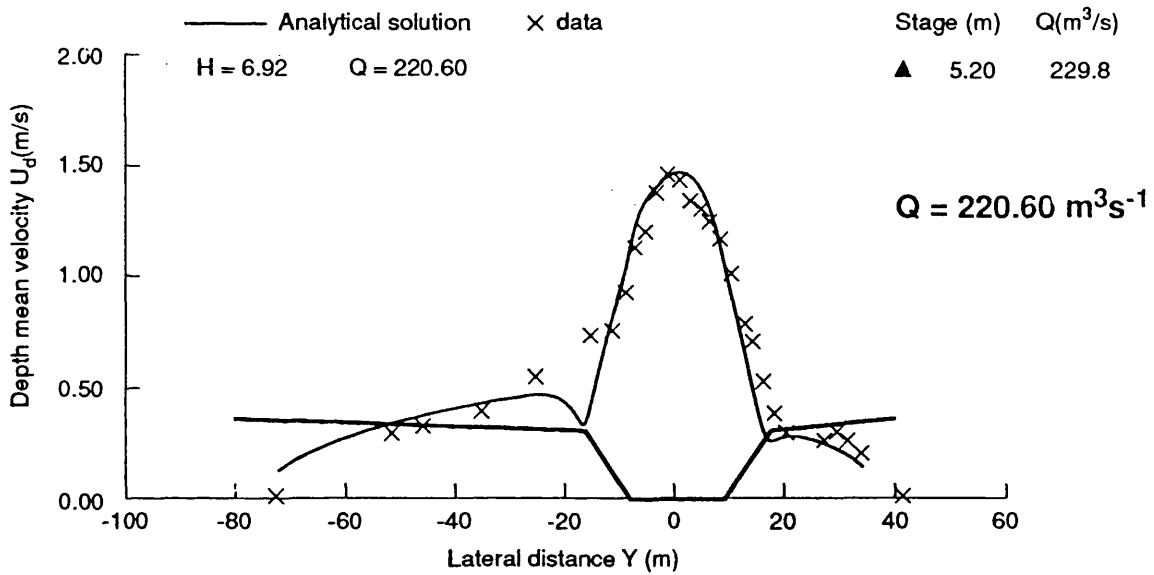
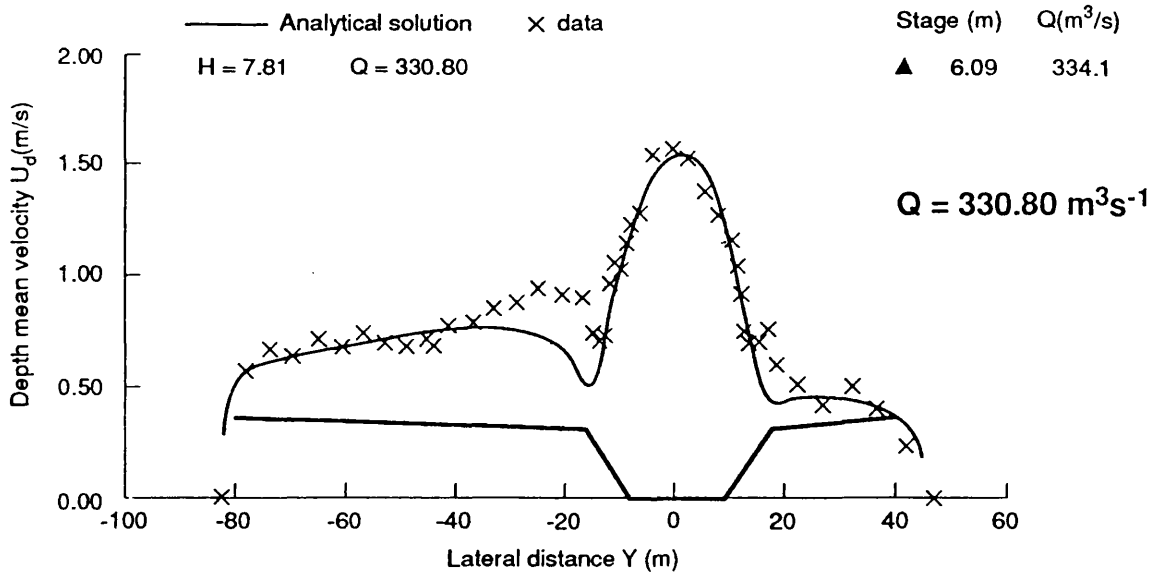


Figure 3.26 Calculated lateral distributions of velocity for the Severn at Montford, after Knight et al (1991)

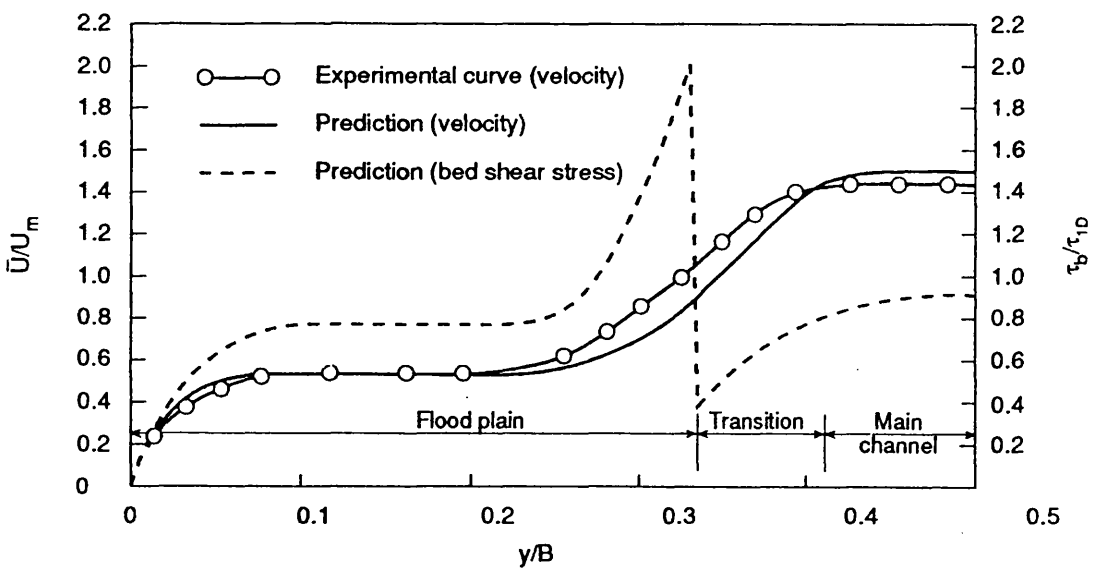
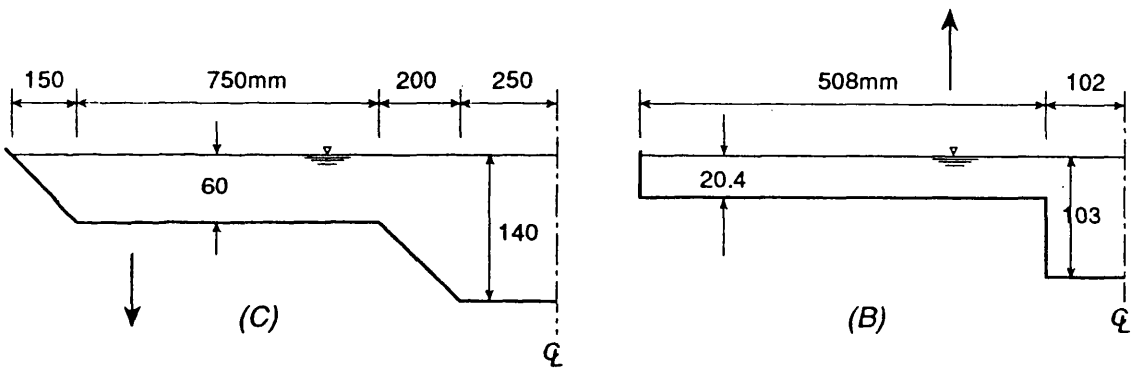
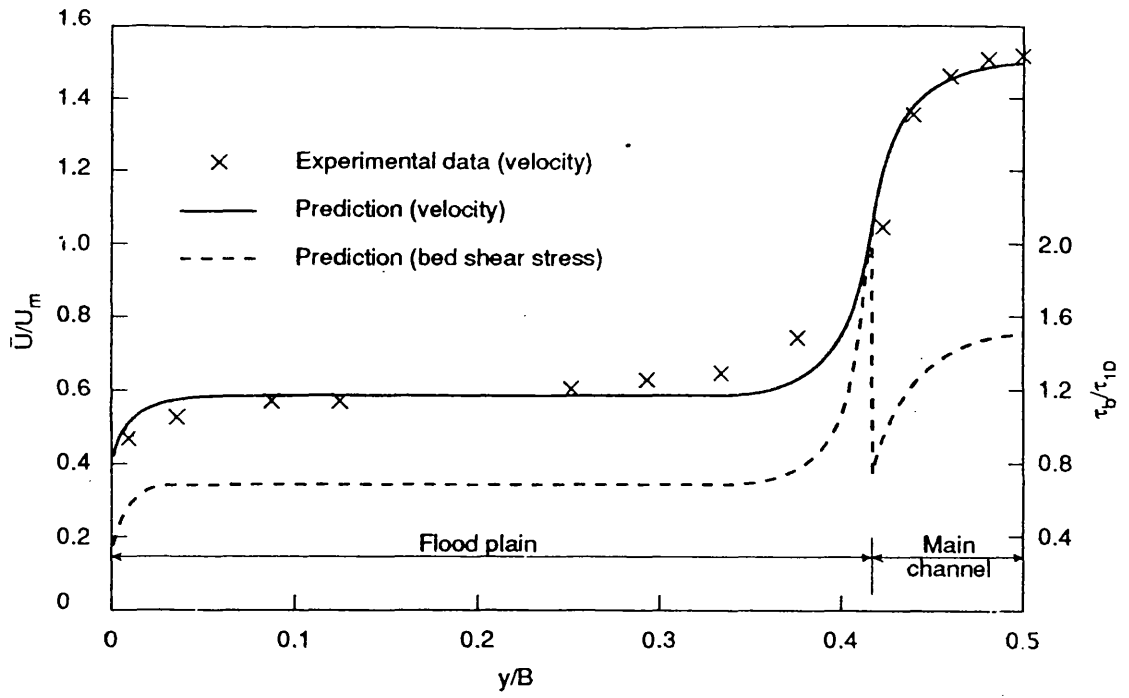
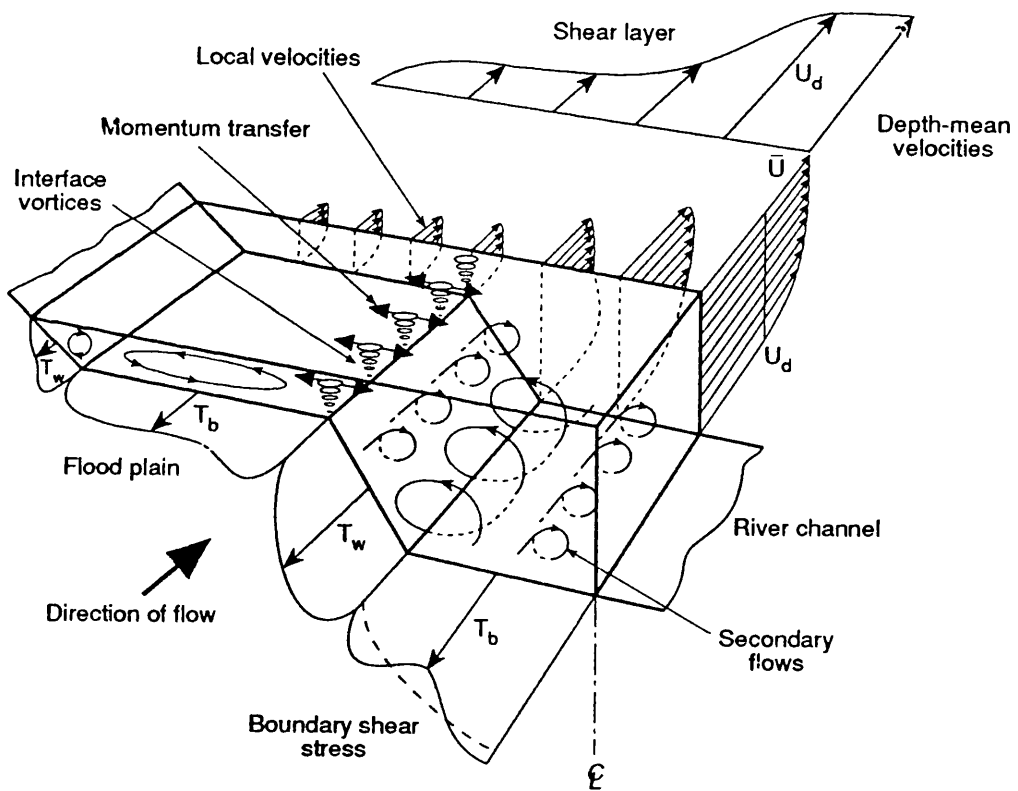
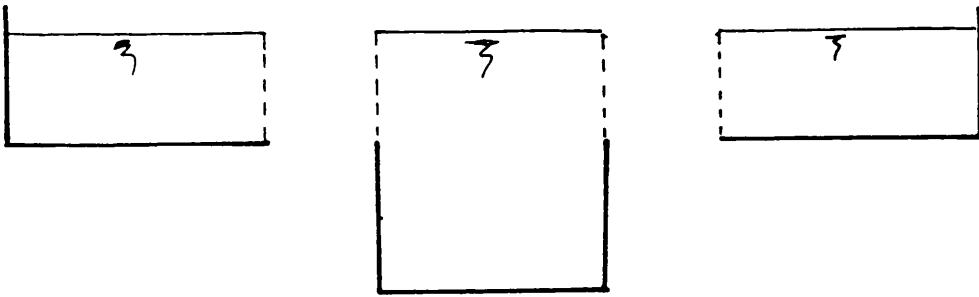


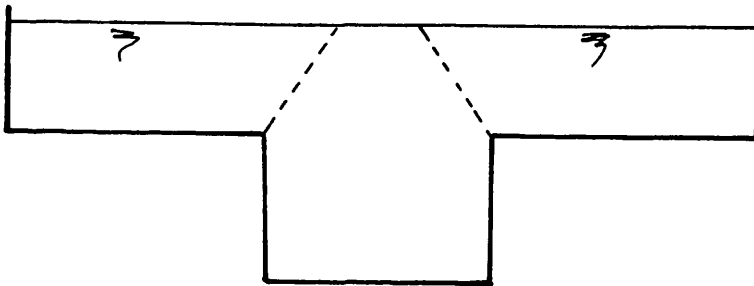
Figure 3.27 Calculated lateral distributions of velocity and shear stress, after Keller and Rodi (1988)



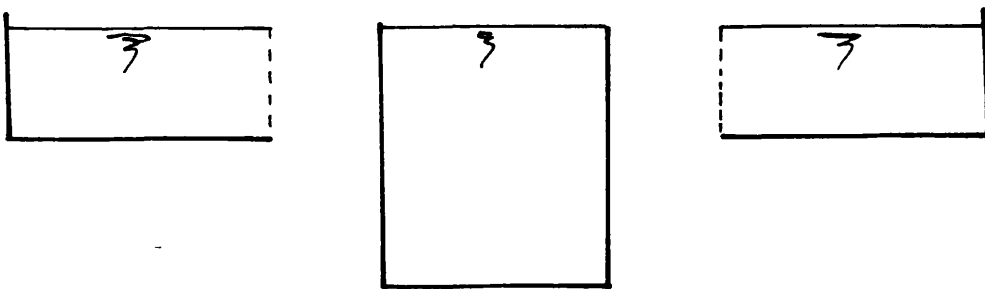
**Figure 3.28 Summary of mechanisms in a straight compound channel, after Knight et al (1983)**



a) Divided channel method (DCM2)



b) Inclined surface divided channel methods



c) Divided channel method (DCM)

Figure 3.29 Divided channel methods

**Table 4.1 Summary of Phase A experiments on SERC FCF**

Series	BT	Bmc m	Bfp m	BT/Bmc m	Bfp/Bmc	Qbankfull m <sup>3</sup> /s
01	10.00	1.80	8.20	5.55	4.56	0.20
02	6.60	1.80	4.80	3.67	2.67	0.20
03	3.60	1.80	1.80	2.00	1.00	0.20
04	2.10	2.10	0.00	1.00	0.00	0.20
05	4.05	1.80	2.25	2.25	1.25	0.20
06	4.35	1.95	2.40	2.23	1.23	0.20
07, 071	6.60	1.80	4.80	3.67	2.67	0.20
08, 09	6.30	1.50	4.80	4.20	3.20	0.18
10, 11	6.90	2.10	4.80	3.29	2.29	0.22

**Notes**

- 1 Definitions are given in Figure 4.2a
- 2 Bankfull depth h = 0.15m
- 3 Bed slope =  $1.029 \times 10^{-3}$
- 4 Maximum depth Hmax = 0.30m
- 5  $(H_{max} - h)/h = 1.0$
- 6 07, 071, 09 and 11 had roughened floodplains

**Table 4.2 Overbank gauging sites**

River	Site	Stage discharge	Velocity
Blackwater	Blackwater	Y	N/A
Main	Section 6	Y	N/A
Main	Section 14	Y	Y
Ouse	Skelton	Y	Y
Penk	Penkridge	N	Y
Severn	Montford	Y	Y
Tees	Low Moor	Y	N/A
Torrige	Torrington	Y	N/A
Trent	N. Muskham	N	Y

**Notes**

- 1 Y - Data used
- 2 N - Data not used
- 3 N/A - Data not available

**Table 4.3 Overbank gauging sites, channel and floodplain widths**

Rivers	Bankfull Stage m AOD	BT m	Bmc m	Bfp m	BT/Bmc	Bfp/Bmc
Blackwater	1.70	72.0	6.0	66.0	12.00	11.00
Main 6	0.90	27.5	13.7	13.8	2.01	1.01
Main 14	0.92	26.3	12.8	13.5	2.05	1.05
Ouse	4.30	68.5	41.8	26.7	1.64	0.64
Penk	1.58	40.0	18.3	21.7	2.19	1.19
Severn	4.17	125.0	35.0	90.0	3.57	2.57
Tees	8.50	186.0	56.0	130.0	3.32	2.32
Torridge	17.20	120.0	30.0	90.0	4.00	3.00
Trent	7.60	180.0	72.0	36.0	2.50	0.50

**Table 4.4 Overbank gauging sites, channel and floodplain depths**

River	h m	Hmax m	(Hmax-h)/h
Blackwater	1.70	3.58	1.10
Main 6	0.90	2.20	1.45
Main 14	0.92	2.00	1.10
Ouse	9.36	13.45	0.12
Penk	1.94	2.31	0.19
Severn	5.75	7.75	0.35
Tees	4.36	6.67	0.55
Torridge	2.78	5.29	0.90
Trent	5.70	8.21	0.44

**Table 4.5 Overbank gauging sites, Manning's n values**

River	Slope	m <sup>3</sup> /s Qb	Authors Estimate			Ackers Estimate		
			nb	nfl	nfr	nb	nfl	nf
Blackwater	1.60x10 <sup>-3</sup>	8.50	0.046	0.094	0.099	-	-	-
Main 6	1.906x10 <sup>-3</sup>	12.75	0.032	0.040	0.040	0.030	0.050	0.050
Main 14	1.906x10 <sup>-3</sup>	16.06	0.0278	0.040	0.040	-	0.02	0.020
Ouse	1.46x10 <sup>-4</sup>	250.20	0.0448	-	0.060	-	-	-
Penk	1.50x10 <sup>-3</sup>	17.00	0.046	0.060	0.060	-	-	-
Severn	1.95x10 <sup>-4</sup>	183.30	0.031	0.025	0.045	0.0307	0.0338	0.0338
Tees	8.00x10 <sup>-4</sup>	266.20	0.056	0.100	0.100	-	-	-
Torridge	1.45x10 <sup>-3</sup>	190.00	0.027	0.060	-	0.024	0.026	0.026
Trent	3.20x10 <sup>-4</sup>	389.60	0.032	-	0.032	0.032	-	0.032

Notes: h - Bankfull depth  
 See Figure 2 for definitions  
 nb - Main channel bankfull Manning's n  
 nfl, nfr - Left and right floodplain Manning's n  
 Hmax - Maximum depth  
 Qb - Bankfull discharge

**Table 4.6 Mean values of back calculated NEV SERC FCF**

Series	Type	NOP	NEVC	SD
01	Smooth	26	0.31	0.11
02	Smooth	29	0.25	0.08
03	Smooth	22	0.20	0.04
04	Smooth	14	0.09	0.01
05	Smooth	08	0.23	0.04
06	Smooth	20	0.21	0.07
08	Smooth	25	0.36	0.14
10	Smooth	19	0.43	0.09
07	Rough	18	0.03	0.23
071	Rough	04	0.15	0.01
09	Rough	10	0.14	0.02
11	Rough	16	0.30	0.06

**Notes**

- 1 Smooth refers to smooth floodplains
- 2 Rough refers to roughened floodplains
- 3 NOP - Number of data points
- 4 SD - Standard deviation in mean value

**Table 4.7 Mean values of back calculated NEV inbank SERC FCF**

Series	NOP	NEVC	SD
04	09	0.18	0.11
08	11	0.10	0.10
10	08	0.09	0.05

**Table 4.8 Mean values of back calculated NEV all data SERC FCF**

Data set	NOP	NEVC	SD
All smooth	163	0.27	0.14
Series 4 omitted	149	0.29	0.13
All rough	48	0.22	0.08
Inbank smooth	28	0.12	0.10

**Table 4.9 Mean errors with NEV fixed smooth floodplains SERC FCF**

NEV SERIES	NOP	0.16		0.24		0.27		0.29	
		ACC	SD	ACC	SD	ACC	SD	ACC	SD
01	26	4.7	5.9	2.2	3.7	1.4	3.1	0.9	2.7
02	29	2.8	4.4	-0.1	3.5	-1.7	3.8	-1.7	4.1
03	22	1.1	2.5	-2.1	3.3	-3.1	4.1	-3.7	4.7
04	14	-6.1	0.1	-11.3	12.0	-13.0	13.7	-14.1	14.8
05	08	2.8	3.5	-0.1	1.6	-1.0	1.9	-1.6	2.3
06	20	2.1	4.3	-1.7	4.1	-3.2	4.9	-4.0	5.5
08	25	4.2	5.7	1.0	5.2	0.0	5.5	-0.7	5.8
10	19	5.8	6.3	3.8	4.5	-3.0	3.8	2.6	3.5

## Notes

1. ACC is the mean percentage accuracy ie the mean of :  $100*(QCALC-QMEAS)/QMEAS$
2. Series 4 was a simple channel without floodplains.

**Table 4.10 Mean errors with NEV fixed rough floodplains SERC FCF**

NEV SERIES	NOP	0.16		0.22		0.24	
		ACC	SD	ACC	SD	ACC	SD
07	18	3.9	5.6	-0.7	3.1	-2.1	3.3
071	04	-0.9	3.2	-6.6	8.2	-8.8	10.2
09	10	-2.1	3.2	-7.8	8.1	-9.2	9.6
11	16	8.2	9.6	5.1	6.8	3.8	5.5

**Table 4.11 Mean errors NEV fixed inbank SERC FCF**

NEV SERIES	NOP	0.16		0.12	
		ACC	SD	ACC	SD
04	09	-0.7	2.9	0.5	2.4
08	11	-4.7	1.0	-3.0	5.5
10	13	-2.7	3.4	-1.9	2.9

**Table 4.12 Mean errors NEV fixed all data SERC FCF**

DATA SET	NOP	NEV	ACC	SD
All smooth	163	0.16	2.6	4.4
All smooth	163	0.24	-0.5	5.1
All smooth	163	0.27	-1.6	5.4
Series 4 omitted	149	0.16	3.4	3.5
Series 4 omitted	149	0.24	0.5	3.9
Series 4 omitted	149	0.27	-0.5	4.1
Series 4 omitted	149	0.29	-1.1	4.2
All rough	48	0.16	3.7	5.5
All rough	48	0.22	-0.7	6.0
All rough	48	0.24	-2.2	5.9

**Table 4.13 Mean errors NEV fixed all inbank data SERC FCF**

DATA SET	NOP	NEV	ACC	SD
All inbank smooth	33	0.16	-2.8	3.7
All inbank smooth	33	0.12	-1.6	3.3

**Table 4.14 Mean errors in discharge for various methods SERC FCF**

SERIES	TYPE	NOP	LDM		DCM		SCM		DCM2		ACKM	
			ACC	SD	ACC	SD	ACC	SD	ACC	SD	ACC	SD
01	Smooth	26	4.7	5.9	6.4	4.9	-15.0	12.8	8.7	4.2	-0.7	1.1
02	Smooth	29	2.8	4.4	4.7	3.8	-17.4	15.9	7.3	3.7	-0.7	2.1
03	Smooth	22	1.1	2.5	2.3	2.8	-7.6	8.0	6.5	2.4	-0.7	1.5
04	Smooth	14	-6.1	0.1	0.2	1.2	0.2	1.2	0.2	1.2	0.2	1.2
05	Smooth	08	2.8	3.5	4.2	3.2	-7.6	7.6	8.1	2.0	0.3	2.4
06	Smooth	20	2.1	4.3	5.6	3.9	-11.9	12.3	7.1	4.1	0.4	2.3
08	Smooth	25	4.2	5.7	5.4	4.0	-10.5	14.9	8.6	3.2	-0.2	1.1
10	Smooth	19	5.8	6.3	5.0	2.8	-14.1	14.7	7.6	3.0	-0.1	1.7
07	Rough	18	3.9	5.6	20.2	14.3			24.6	17.8	-7.5	2.7
071	Rough	04	-0.9	3.2	28.7	9.2			37.5	11.4	-17.7	2.8
09	Rough	10	-2.1	3.2	22.6	14.5			27.9	18.5	-5.3	1.6
11	Rough	16	8.2	9.6	19.1	13.3			23.2	16.0	-5.6	1.1

## Notes

1. NEV = 0.16 LDM

**Table 4.15 Mean errors in discharge for various methods SERC FCF all data**

SERIES	NOP	LDM		DCM		SCM		DCM2		ACKM	
		ACC	SD	ACC	SD	ACC	SD	ACC	SD	ACC	SD
All smooth	163	2.6	4.4	4.5	4.0	-11.6	13.4	7.1	3.9	-0.3	1.7
Series 4 omitted	149	3.4	3.5	4.9	3.9	-12.7	13.4	7.7	3.5	-0.3	1.7
All rough	48	3.7	5.5	21.0	13.5			25.9	16.9	-7.3	3.9
All data (not 4)	197	3.5	4.1	8.8	10.2			12.1	11.8	-2.0	3.8

## Notes

1. NEV = 0.16 LDM

**Table 4.16 Mean errors in depth for various methods SERC FCF**

SERIES	TYPE	NOP	LDM		DCM		SCM		DCM2		ACKM	
			ACC	SD	ACC	SD	ACC	SD	ACC	SD	ACC	SD
01	Smooth	26	-1.3	1.1	-1.9	1.4	3.4	2.4	-2.5	1.1	0.3	0.5
02	Smooth	29	-0.9	1.4	-1.6	1.5	4.9	4.4	-2.5	1.3	0.4	1.0
03	Smooth	22	-0.6	1.1	-1.1	1.6	3.2	3.2	-3.0	1.1	0.4	0.8
04	Smooth	14	4.6	2.9	0.0	1.0	0.0	1.0	0.0	1.0	0.0	1.0
05	Smooth	08	0.4	5.0	-0.3	5.6	4.3	4.5	-3.4	0.7	1.4	4.6
06	Smooth	20	-0.8	1.7	-2.3	1.6	4.3	4.4	-2.9	1.6	0.0	1.1
08	Smooth	25	-1.4	1.3	-2.0	1.4	2.8	4.0	-3.0	0.9	0.1	0.5
10	Smooth	19	-2.2	0.8	-1.8	1.0	4.1	4.2	-2.7	1.0	0.1	0.7
07	Rough	18	-2.3	2.4	-8.6	5.6			-9.5	6.2	6.9	3.2
071	Rough	04	0.5	2.3	-12.4	3.5			-14.5	3.9	18.8	3.4
09	Rough	10	1.4	1.7	-9.8	5.7			-11.0	6.5	4.9	2.2
11	Rough	16	-4.5	2.7	-7.9	5.2			-8.9	5.7	5.0	3.2

Notes

1. NEV = 0.16 LDM

**Table 4.17 Mean errors in depth for various methods SERC FCF all data**

SERIES	NOP	LDM		DCM		SCM		DCM2		ACKM	
		ACC	SD	ACC	SD	ACC	SD	ACC	SD	ACC	SD
All smooth	163	-0.6	2.4	-1.5	1.9	3.5	3.8	-2.5	1.4	0.3	1.3
Series 4 omitted	149	-1.1	1.7	-1.7	1.9	3.8	3.9	-2.8	1.2	0.3	1.3
All rough	48	-2.1	3.2	-8.9	5.3			-10.0	6.0	6.8	4.8
All data (not 4)	197	-1.3	2.2	-3.5	4.4			-4.5	4.4	1.9	3.8

Notes

1. NEV = 0.16 LDM

**Table 4.18 Mean errors in discharge Myers lab data**

NOP METHOD	Series A + F 20		Series A 12		Series F 8	
	ACC	SD	ACC	SD	ACC	SD
LDM	0.2	7.2	3.4	7.0	-4.3	4.3
DCM	-1.0	6.8	1.8	6.9	-5.2	4.4
SCM	-13.2	6.3	-12.3	7.4	-14.6	4.3
SCM2	-13.2	6.3	-12.3	7.4	-14.6	4.3
SCM3	5.7	7.2	8.6	7.4	1.4	4.4
SCM4	-13.2	6.3	-12.3	7.4	-14.6	4.3
SCM5	-13.2	6.3	-12.3	7.4	-14.6	4.3
SSGM	5.7	7.2	8.6	7.4	1.4	4.4
DCM2	1.7	7.7	5.2	7.6	-3.4	4.2
ACKM	-5.2	5.2	-3.3	5.0	-8.8	3.7

## Notes

- 1 NEV = 0.16 in LDM
- 2 nb = 0.01 nf = 0.01 slope =  $1.906 \times 10^{-03}$
- 3 Cross sections are shown on figure

**Table 4.19 Mean errors in depth Myers lab data**

NOP METHOD	Series A + F 20		Series A 12		Series F 8	
	ACC	SD	ACC	SD	ACC	SD
LDM	1.0	4.8	-0.8	4.4	3.6	4.3
DCM	-1.6	5.0	-0.1	4.8	4.0	4.6
SCM	8.4	5.3	8.2	6.4	8.8	3.4
SCM2	8.4	5.3	8.2	6.4	8.8	3.4
SCM3	-2.1	4.8	-3.1	4.3	-0.7	2.2
SCM4	8.4	5.3	8.2	6.4	8.8	3.4
SCM5	8.4	5.3	8.2	6.4	8.8	3.4
SSGM	-2.1	4.8	-3.1	4.3	-0.7	2.2
DCM2	0.3	3.7	-1.5	4.5	3.0	4.2
ACKM	4.2	4.3	2.7	3.8	6.4	4.4

## Notes

- 1 NEV = 0.16 in LDM
- 2 nb = 0.01 nf = 0.01 slope =  $1.906 \times 10^{-03}$
- 3 Cross sections are shown on figure

**Table 4.20 Mean errors in discharge Lambert lab data**

SERIES	ALL		1		2		3		4		5		6	
	85		14		11		21		7		22		10	
METH	M	SD	M	SD	M	SD	M	SD	M	SD	M	SD	M	SD
LDM	-0.5	16.2	7.1	4.3	22.3	4.9	-15.9	10.4	3.5	7.0	-11.2	6.4	17.1	11.4
DCM	23.5	13.1	2.9	4.8	21.6	5.4	8.2	11.0	36.2	9.3	25.2	8.1	73.8	16.6
SCM	55.0	45.8	81.1	6.2	116.7	4.5	-2.2	12.1	6.7	12.3	64.3	29.9	84.1	26.8
SSGM	55.0	34.6	21.7	5.2	35.1	3.6	34.2	15.2	68.7	13.5	68.0	9.4	129.0	21.1
DCM2	31.8	22.8	13.4	4.2	29.4	4.3	13.8	9.5	40.6	7.8	35.9	6.2	82.7	13.9
ACKM	9.4	14.9	-5.7	2.9	3.6	2.2	5.8	4.7	25.8	5.9	6.2	3.0	40.1	16.4

Notes

1 NEV = 0.16 in LDM

**Table 4.21 Mean errors in depth Lambert lab data**

SERIES	ALL		1		2		3		4		5		6	
	85		14		11		21		7		22		10	
METH	M	SD	M	SD	M	SD	M	SD	M	SD	M	SD	M	SD
LDM	1.3	8.8	-3.6	1.9	-9.5	1.4	9.0	8.0	-0.5	3.3	6.6	5.7	-6.8	4.6
DCM	-7.4	6.6	-1.0	3.2	-9.3	1.6	-2.2	3.6	-9.4	1.9	-9.0	2.3	-20.8	3.1
SCM	-13.0	11.7	-26.4	3.1	-28.9	3.2	0.3	2.7	1.6	2.5	-13.4	7.0	-12.2	4.7
SSGM	-15.3	6.5	-9.8	2.3	-13.5	0.9	-9.4	3.0	-15.5	1.7	-19.2	1.8	-28.3	1.6
DCM2	-9.8	5.4	-6.5	1.8	-11.8	1.1	-4.0	2.4	-9.8	1.4	-11.5	1.3	-20.9	2.0
ACKM	-3.1	6.1	3.8	2.9	-1.7	1.0	-1.7	1.8	-6.9	2.1	-2.5	1.3	-16.0	7.0

Notes

1 NEV = 0.16 in LDM

**Table 4.22 Mean errors in discharge for each overbank gauging site**

SITE METHOD	Blackwater		Main 6		Main 14		Ouse		Severn		Tees		Torrige		Torrige <sup>3</sup>		Trent	
	ACC	SD	ACC	SD	ACC	SD	ACC	SD	ACC	SD	ACC	SD	ACC	SD	ACC	SD	ACC	SD
<b>Authors n values</b>																		
LDM	2.1	6.0	5.0	11.0	3.0	4.7	-3.5	7.9	4.5	3.1	4.9	6.7	-2.2	6.9	-7.1	5.9	5.6	8.4
DCM	3.6	6.1	1.0	9.5	0.6	4.9	-10.9	7.4	2.0	3.0	-0.8	6.3	-4.3	6.7	-8.7	5.7	3.0	8.2
SCM	-29.7	5.3	-8.5	14.8	-9.6	8.5	-12.5	7.5	-26.0	5.8	-14.2	11.4	-10.8	13.1	-24.2	8.2	-16.4	7.0
SCM2	-61.9	3.0	-15.7	12.4	-20.9	12.5	-18.0	7.8	-25.8	5.2	-27.6	18.4	-21.1	24.2	-48.2	10.6	-16.4	7.0
SCM3	39.3	8.5	7.4	12.0	6.8	4.8	5.0	8.4	14.4	3.4	7.0	6.8	-5.9	6.9	6.4	11.3	8.8	
SCM4	-62.6	2.9	-15.9	12.4	-21.4	12.6	-18.2	7.6	-26.6	5.2	-28.6	18.6	-22.0	25.0	-50.0	10.3	-16.4	7.0
SCM5	-39.6	4.9	-10.3	12.3	-11.7	9.7	-13.4	7.6	-25.4	5.8	-15.4	12.8	-12.1	14.7	-27.4	8.7	-16.4	7.0
SSGM	39.3	8.5	7.4	12.0	6.8	4.8	5.0	8.4	14.4	3.4	7.0	6.9	5.9	6.9	1.6	6.3	11.3	8.8
DCM2	3.6	6.1	4.1	12.1	3.2	4.6	-0.2	7.8	5.5	4.1	0.4	6.4	-3.9	6.5	-7.9	5.7	3.4	8.2
ACKM	-11.4	10.3	-6.9	9.9	-11.0	10.8	-0.4	7.8	-3.1	3.0	-8.9	8.0	-9.3	10.6	-14.1	5.6	-2.2	8.4
<b>Ackers n values</b>																		
LDM	2.1	6.0	10.0	9.6	7.5	6.7	-3.5	7.9	3.8	2.7	4.9	6.7	9.5	7.4	4.5	6.6	5.6	8.4
DCM	3.6	6.1	6.4	8.6	4.0	5.6	-10.9	7.4	1.8	2.7	-0.8	6.3	8.0	7.3	3.5	6.4	3.0	8.2
SCM	-29.7	5.3	-2.4	15.7	-9.6	8.5	-12.5	7.5	-25.4	5.8	-14.2	11.4	0.4	14.7	-14.7	9.2	-16.4	7.0
SCM2	-61.9	3.0	-20.8	11.7	-1.0	8.0	-18.0	7.8	-29.5	6.5	-27.6	18.4	-0.6	15.8	-17.1	9.5	-16.4	7.0
SCM3	39.3	8.5	13.1	10.9	10.2	6.5	5.0	8.4	14.3	3.1	7.0	6.8	19.5	7.5	15.1	7.2	11.3	8.8
SCM4	-62.6	2.9	-21.9	11.6	-1.5	8.0	-18.2	7.6	-29.5	6.5	-28.6	18.6	-0.7	15.8	-17.1	9.5	-16.4	7.0
SCM5	-39.6	4.9	-6.7	10.7	-7.6	8.6	-13.4	7.6	-26.4	6.0	-15.4	12.8	0.2	14.9	-15.1	9.2	-16.4	7.0
SSGM	39.3	8.5	13.1	10.9	10.2	6.5	5.0	8.4	14.3	3.1	7.0	6.9	19.5	7.5	15.1	7.2	11.3	8.8
DCM2	3.6	6.1	9.7	11.1	6.5	6.7	-0.2	7.8	5.4	3.5	0.4	6.4	8.4	7.1	4.4	6.5	3.4	8.2
ACKM	-11.4	10.3	-5.6	8.1	1.1	7.6	-0.4	7.8	-4.1	3.3	-8.9	8.0	3.2	10.0	-1.1	6.0	-2.2	8.4
NOP	.7		14.		11.		13.		36.		5.		15.		6.		28.	

**Notes**

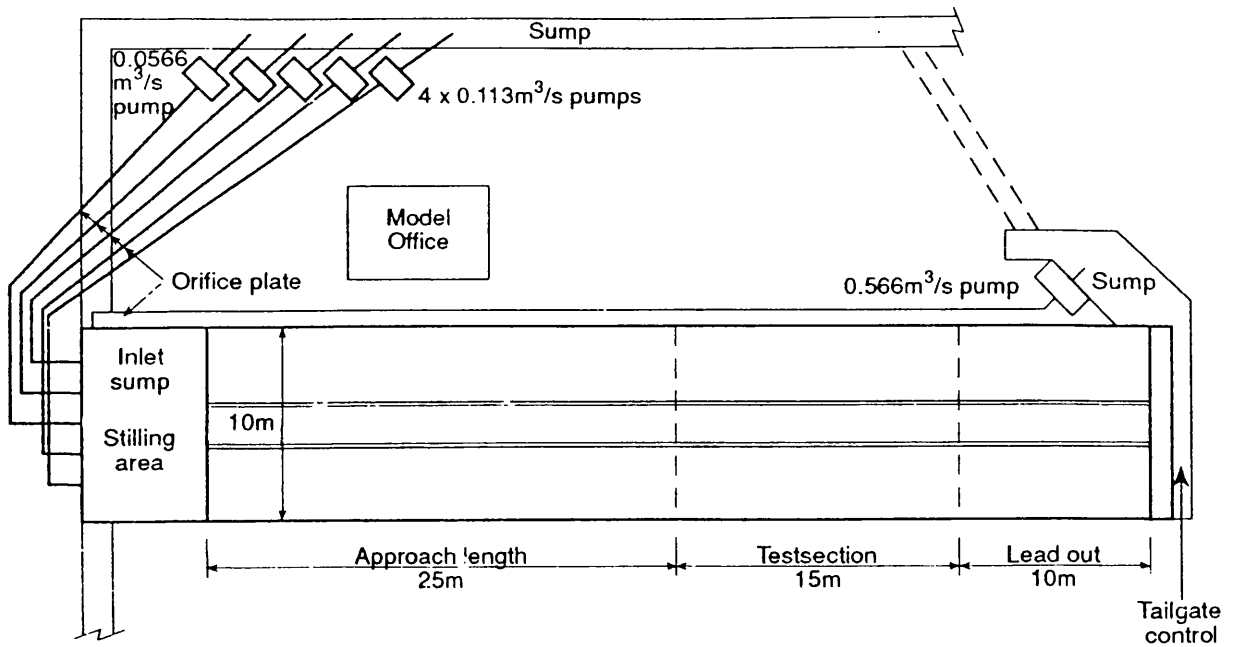
- 1 NOP Number of data points at each site
- 2 ACC = 100\*(Qcalc-Qmeas)/Qmeas, SD = Standard Deviation
- 3 Results using Ackers estimate of bankfull stage

**Table 4.23 Mean errors in discharge overbank gauging sites**

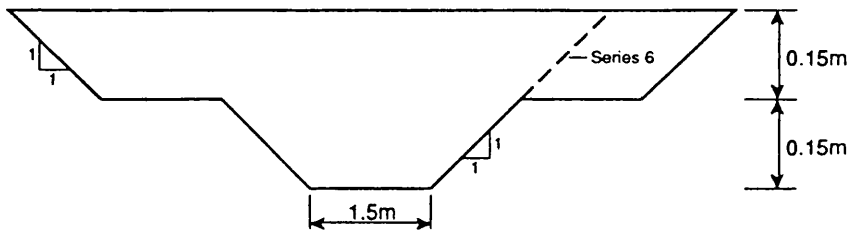
Data Set	A		B		C		D	
NOP	127		118		77		68	
METHODM	SD	M	SD	M	SD	M	SD	
Authors n values								
LDM	1.2	6.7	1.2	6.8	0.7	5.2	0.7	5.2
DCM	-1.0	6.6	-1.0	6.7	-0.4	4.5	-0.3	4.4
SCM	-11.9	15.6	-12.6	15.9	-10.9	17.5	-12.1	18.2
SCM2	-17.6	20.3	-18.7	20.6	-12.8	19.8	-14.1	20.6
SCM3	8.1	11.9	8.0	12.2	6.1	9.6	5.8	9.9
SCM4	-18.2	20.6	-19.3	20.9	-13.3	20.4	-14.7	21.2
SCM5	-12.9	16.2	-13.8	16.5	-10.8	17.5	-12.0	18.2
SSGM	8.1	11.9	8.0	12.2	6.1	9.6	5.8	9.9
DCM2	1.0	7.4	1.1	7.5	0.1	6.6	0.3	6.7
ACKM	-4.4	8.4	-4.2	8.0	-2.8	6.8	-2.2	5.5
Ackers n values								
LDM	5.0	6.9	4.5	6.6	5.5	4.9	4.6	3.9
DCM	2.2	7.4	1.5	7.0	3.5	5.0	2.5	3.8
SCM	-15.0	13.1	-16.9	11.4	-17.2	12.5	-20.9	7.4
SCM2	-20.5	16.9	-22.8	15.0	-19.4	13.9	-23.3	8.9
SCM3	14.0	9.6	13.4	9.5	14.4	5.4	13.3	4.3
SCM4	-20.7	17.0	-23.1	15.0	-19.4	13.9	-23.3	9.0
SCM5	-16.3	13.4	-18.4	11.4	-17.8	12.8	-21.5	7.8
SSGM	14.0	9.6	13.4	9.5	14.4	5.4	13.3	4.3
DCM2	5.0	6.8	4.6	6.6	5.3	4.9	4.6	4.1
ACKM	-2.8	7.6	-3.4	6.8	-2.0	6.3	-3.1	4.5

**Notes:**

- 1 M - mean SD - Standard deviation in mean
- 2  $\text{Error} = 100 \cdot (Q_{\text{Calc}} - Q_{\text{meas}}) / Q_{\text{meas}}$
- 3 The data for the Severn and Trent has been smoothed using running averages of three consecutive data points
- 4 Means taken over following subsets of available stage discharge data:
  - A Blackwater, Main 6, Main 14, Ouse, Severn, Tees, Torridge, Trent
  - B As A with Ackers estimate of Bankfull Stage for Torridge
  - C Severn, Torridge and Trent only
  - D As C with Ackers estimate of Bankfull Stage for Torridge

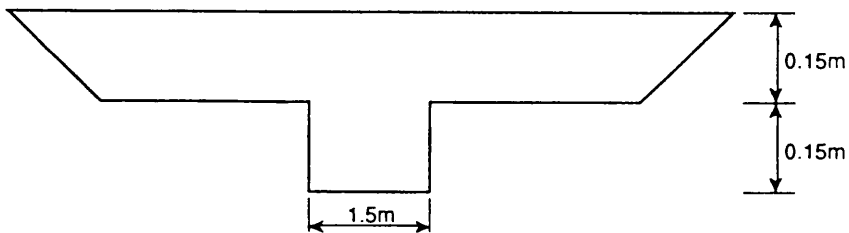


**4.1 Layout of the SERC FCF during Phase A, after Knight and Sellin (1989)**

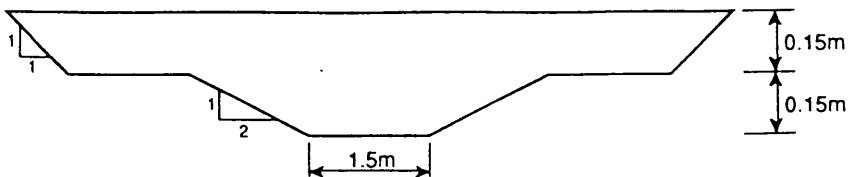


**a) Series 01, 02, 03, 04, 05, 06**

*Note: Series 06 Asymmetric Flood Plain*

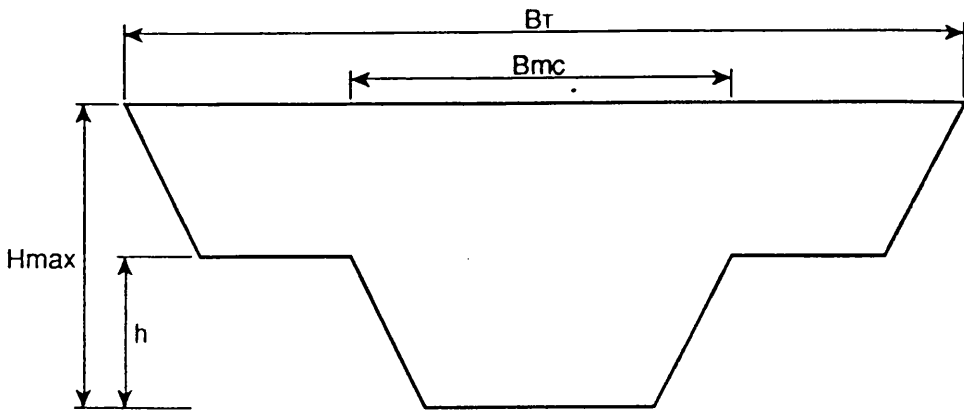


**b) Series 08, 09**

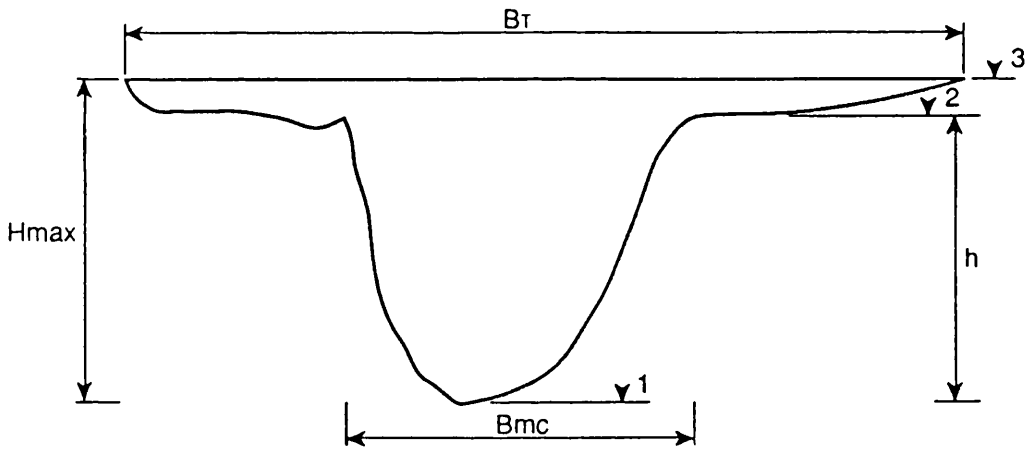


**c) Series 10, 11**

**4.2 Channel cross-sections, SERC FCF Phase A**



a) SERC FCF

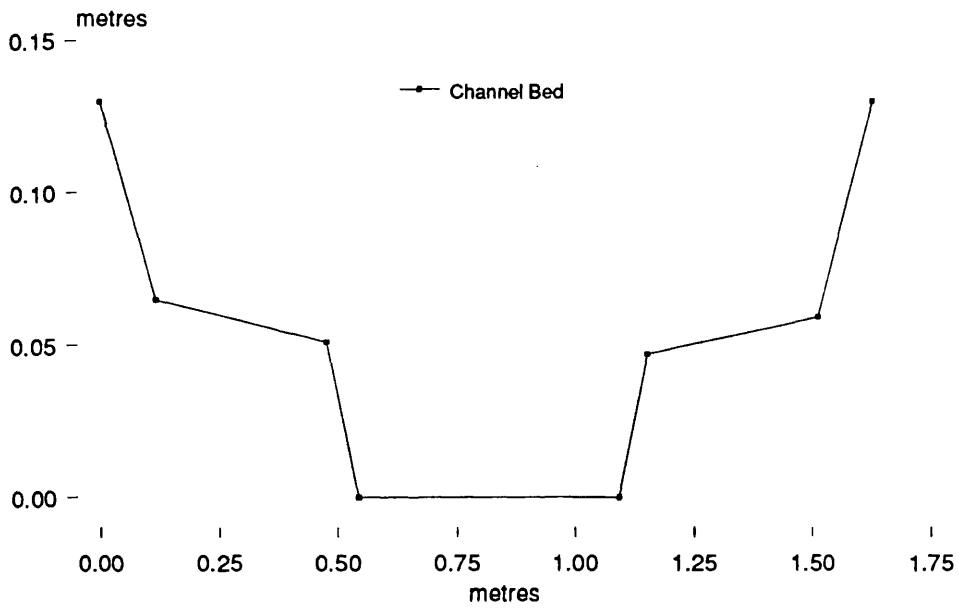


- ▼ 1 Lowest Point in Section
- 2 Bankfull Stage
- 3 Maximum Stage
- $B_t$  Total Width
- $B_{mc}$  Banktop Width Main Channel
- $h$  Bankfull Depth
- $H_{max}$  Maximum Depth

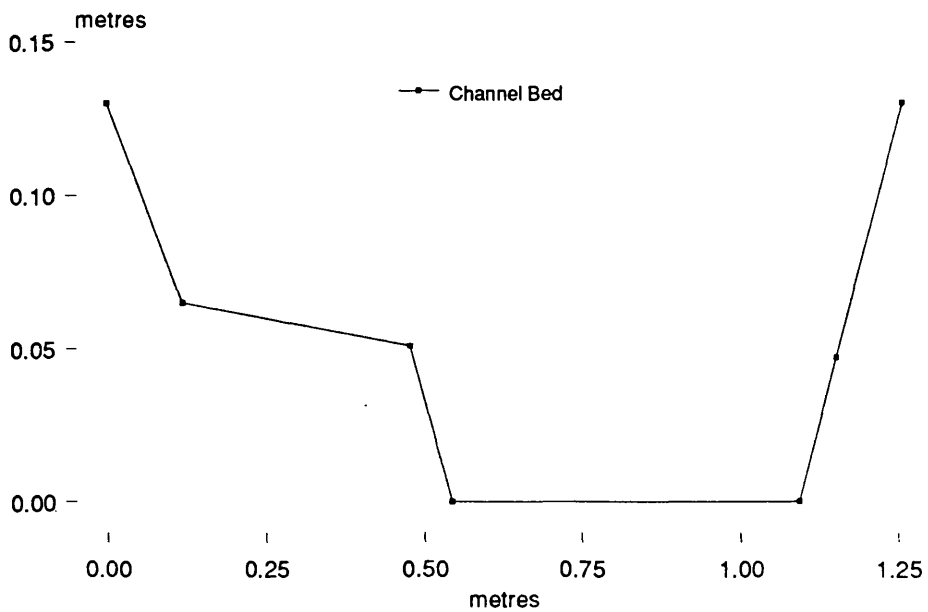
b) Natural Channel

Figure 4.2a Compound channel definitions

## Myers Laboratory Flume Series A Cross Section Geometry

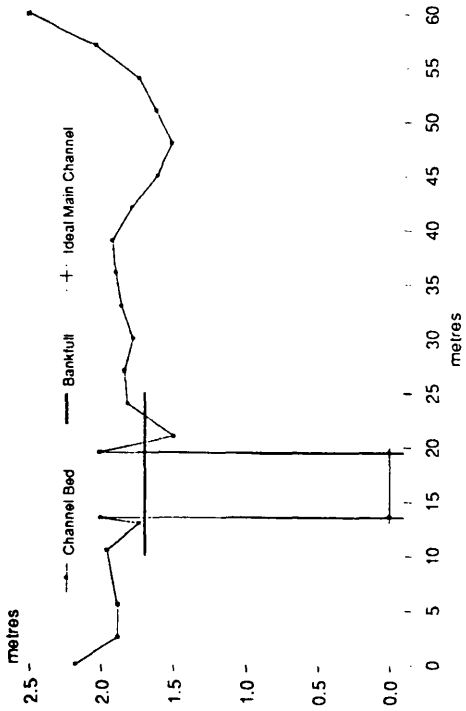


## Myers Laboratory Flume Series F Cross Section Geometry

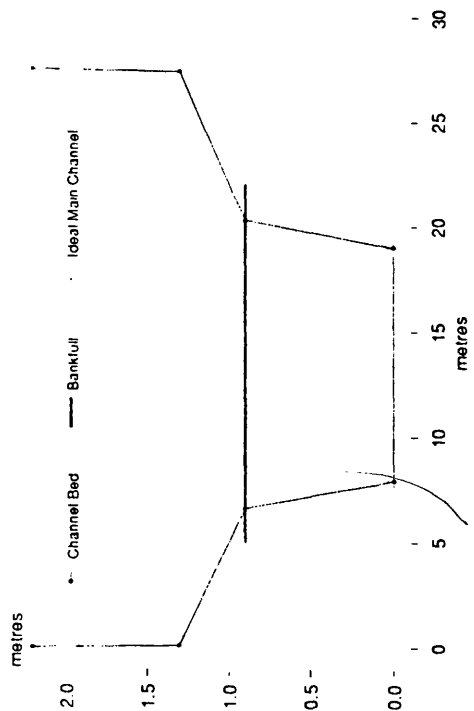


**Figure 4.3** Myers' laboratory cross-sections

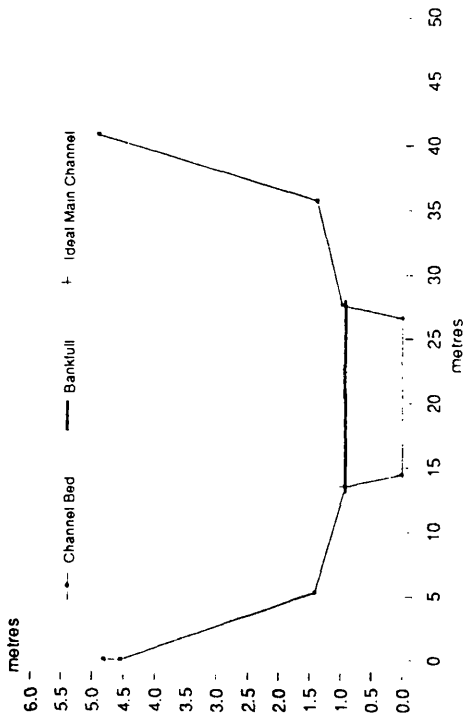
### Cross Section Geometry



### River Main Section 6 Cross Section Geometry



### Cross Section Geometry



### River Ouse at Skelton Cross Section Geometry

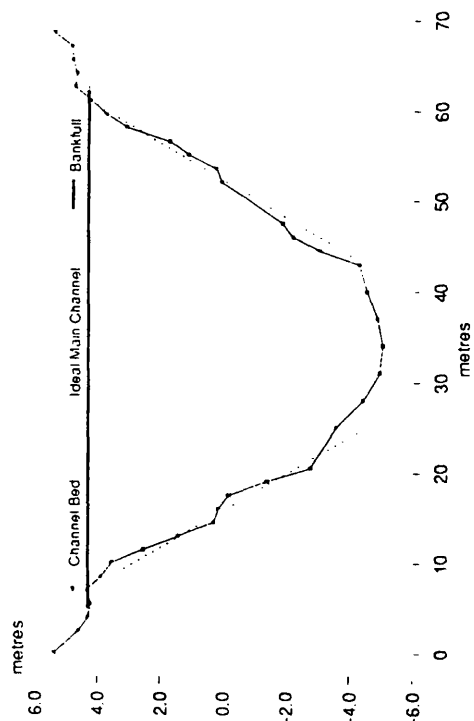
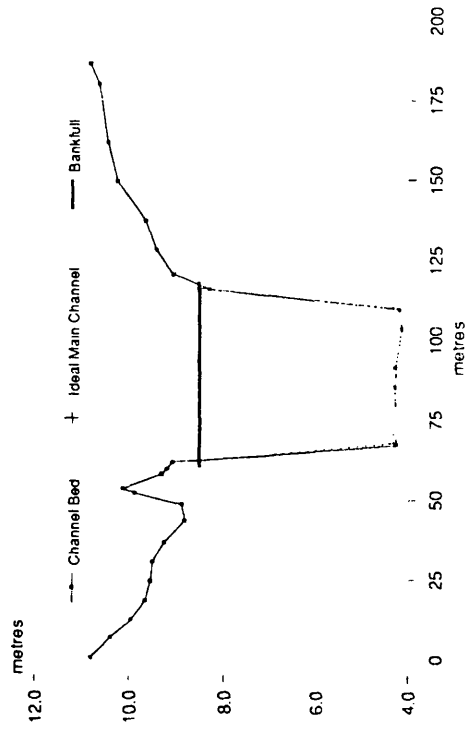
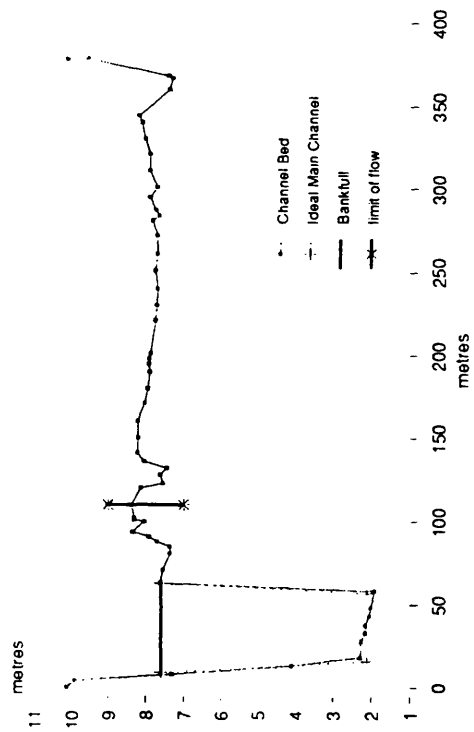


Figure 4.5 Natural channels cross-sections

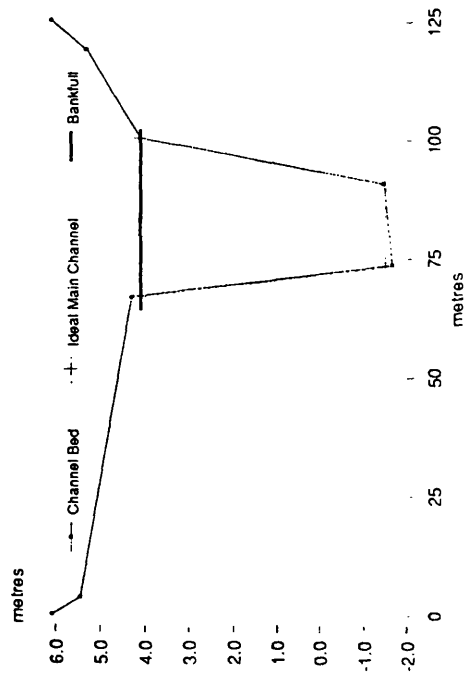
**RIVER TEES AT LOW MOOR  
Cross Section Geometry**



**River Trent at North Muskham  
Cross Section Geometry**



**RIVER TORRIDGE AT TORRINGTON  
Cross Section Geometry**



**River Torridge at Torrington  
Cross Section Geometry**

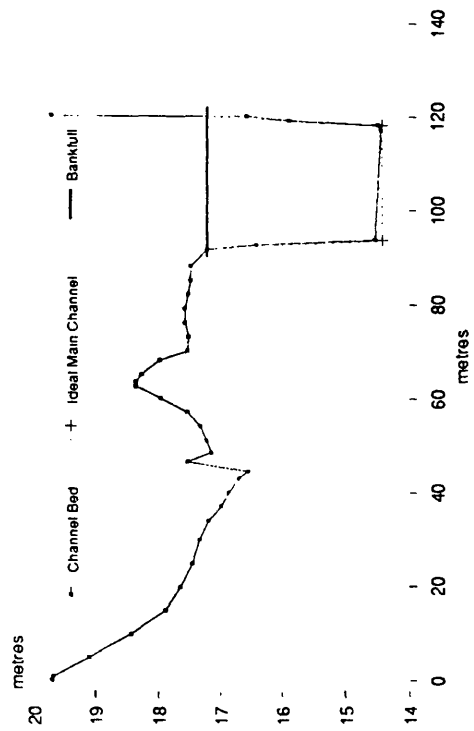
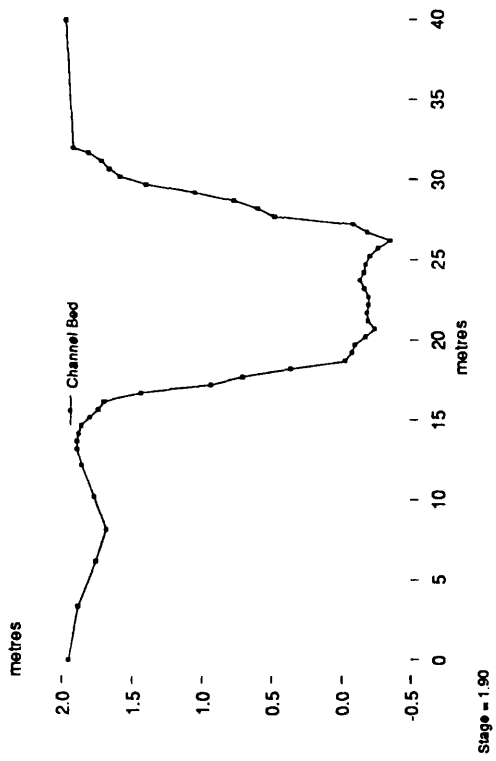
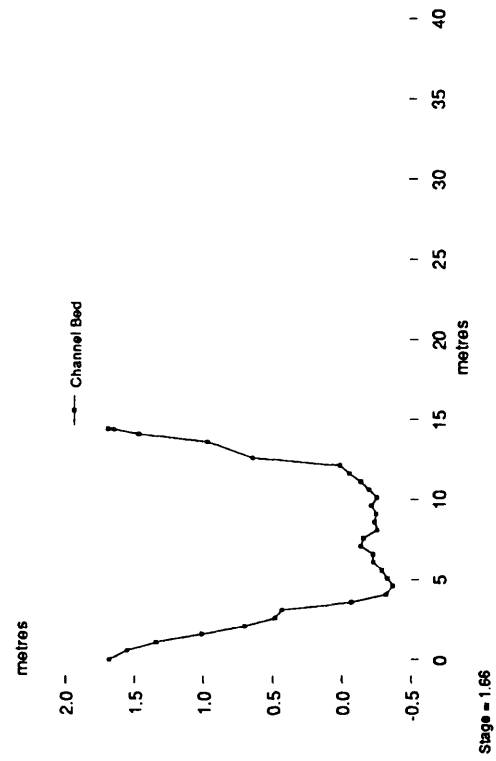


**Figure 4.6 Natural channels cross-sections**

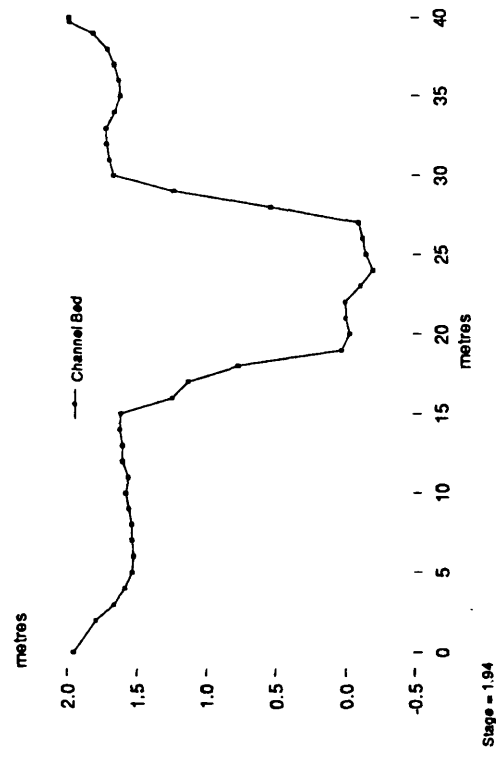
River Penk at Penkridge  
Cross Section Geometry



River Penk at Penkridge  
Cross Section Geometry



River Penk at Penkridge  
Cross Section Geometry



River Penk at Penkridge  
Cross Section Geometry

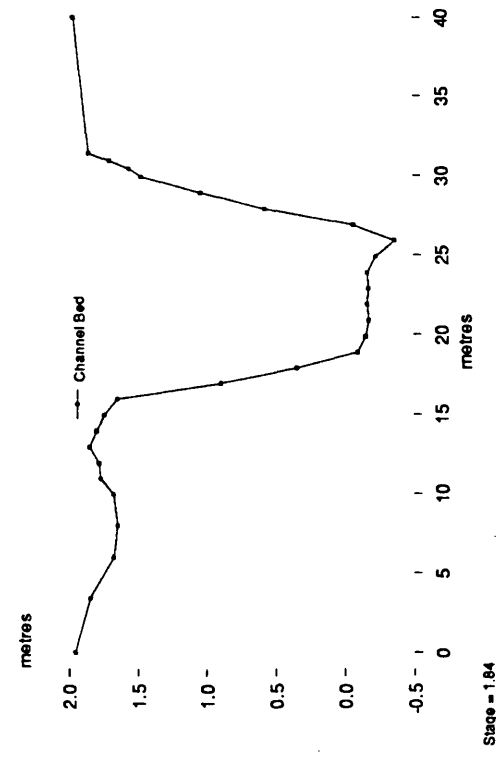
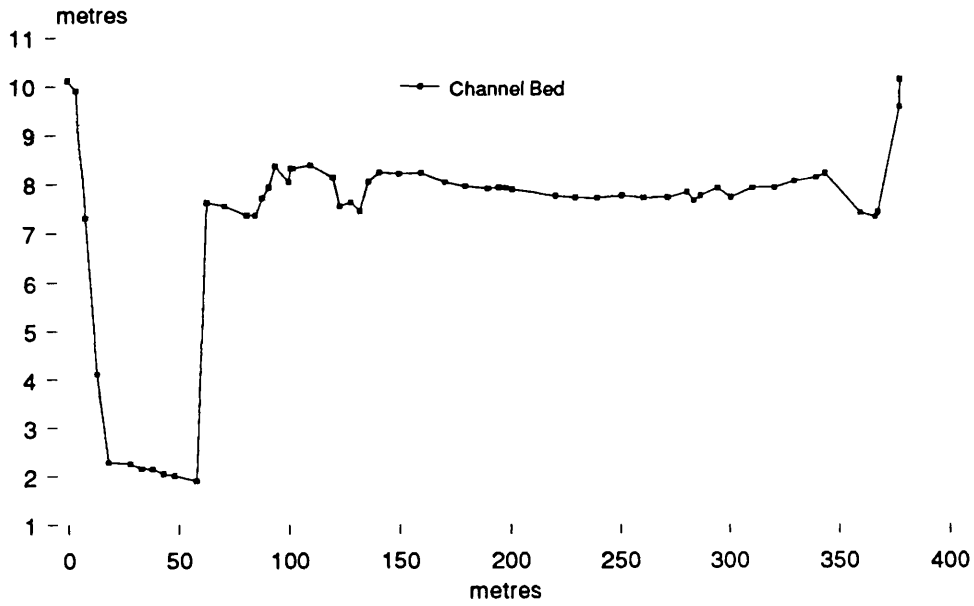
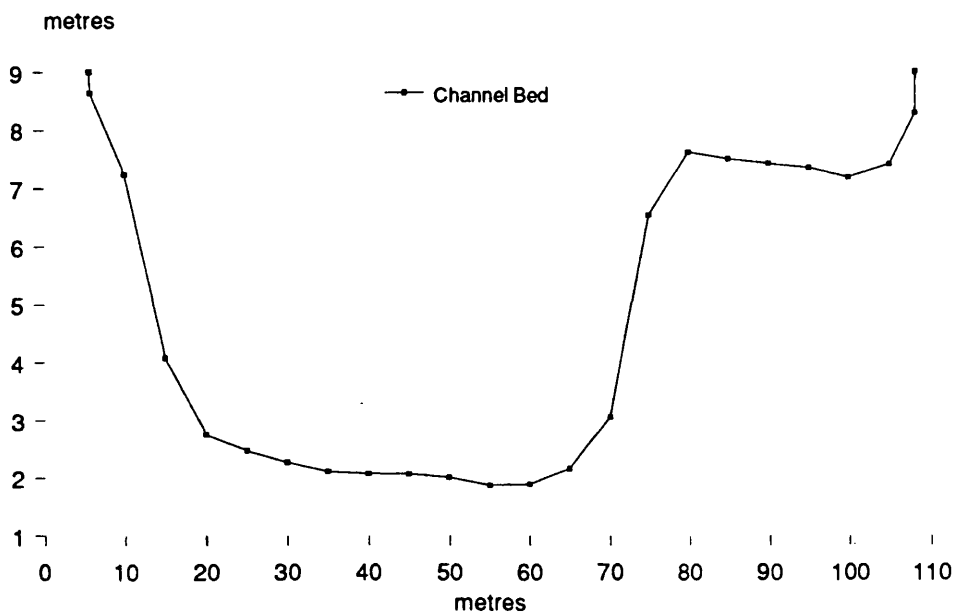


Figure 4.7 Cross-sections for the River Penk

## River Trent at North Muskham Cross Section Geometry

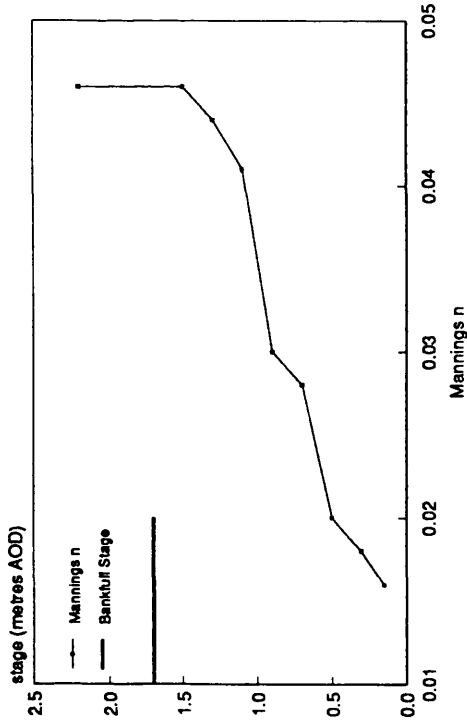


## River Trent at North Muskham Cross Section Geometry

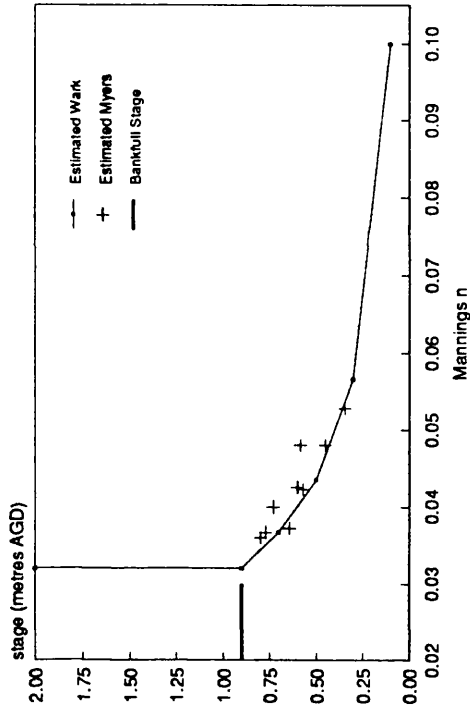


**Figure 4.8** Cross-sections for the River Trent

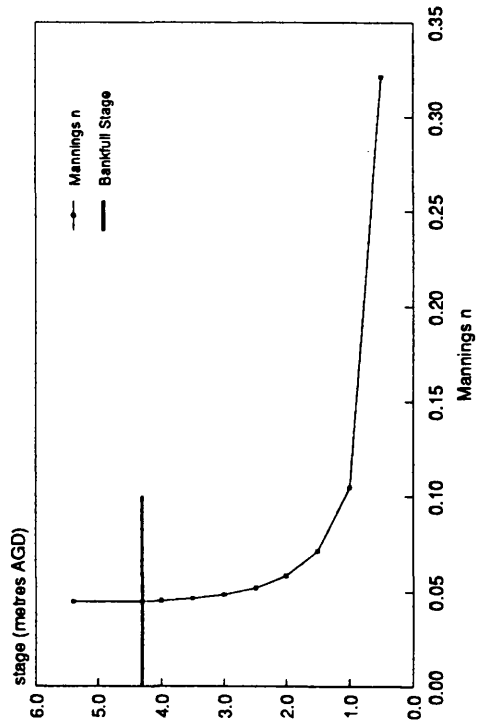
River Blackwater at Ower  
Main Channel Mannings n



River Main Section 6  
Main Channel Mannings n



River Ouse at Skelton  
Main Channel Mannings n



River Severn at Montford  
Main Channel Mannings n

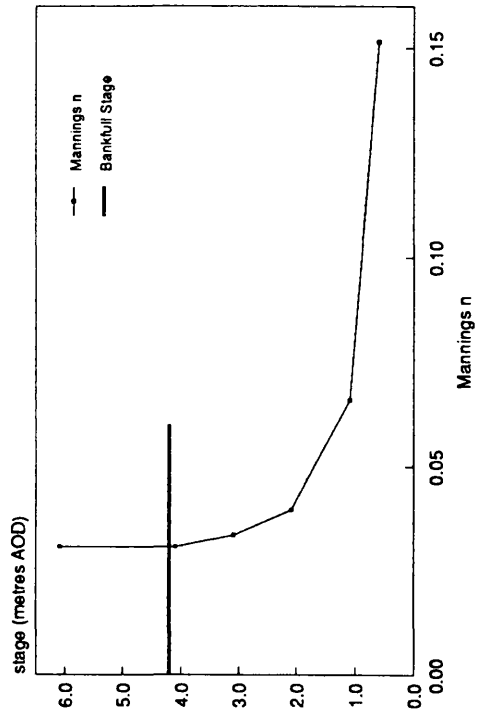
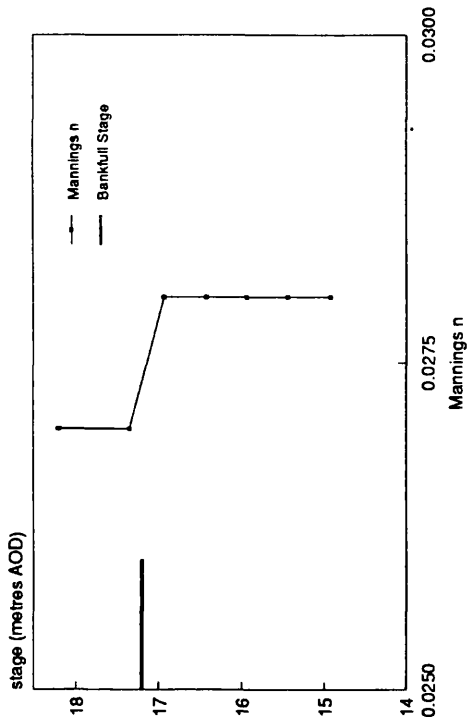
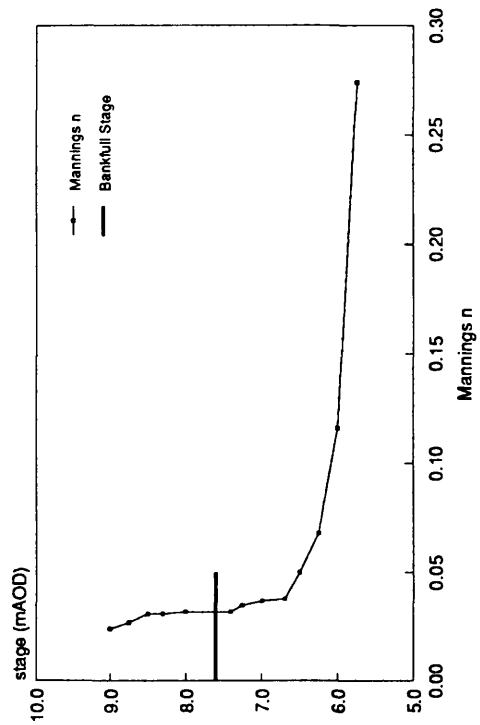


Figure 4.9 Main channel Manning's n values natural channels

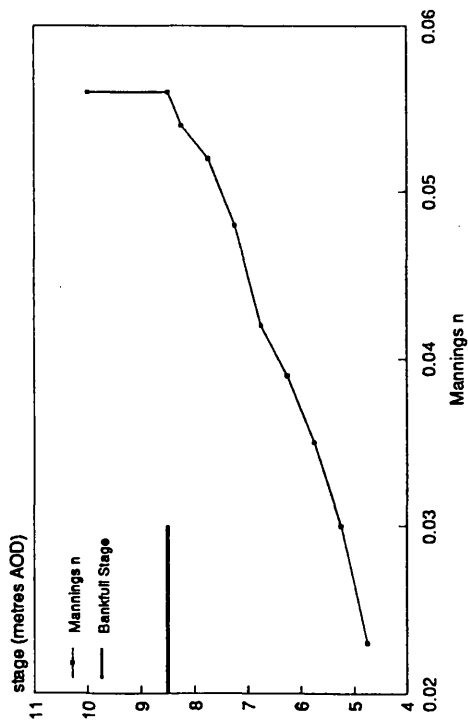
River Torridge at Iorrington  
Main Channel Mannings n



River Trent at North Muskham  
Main Channel Mannings n



River Tees at Low Moor  
Main Channel Mannings n



River Ouse at Skelton  
Main Channel Mannings n

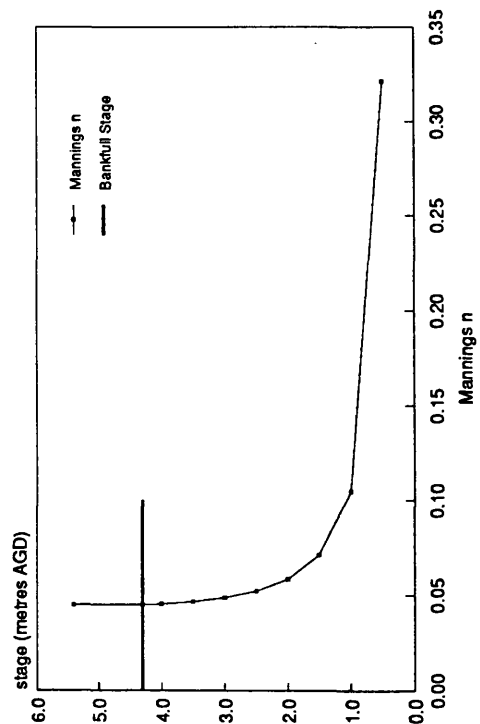
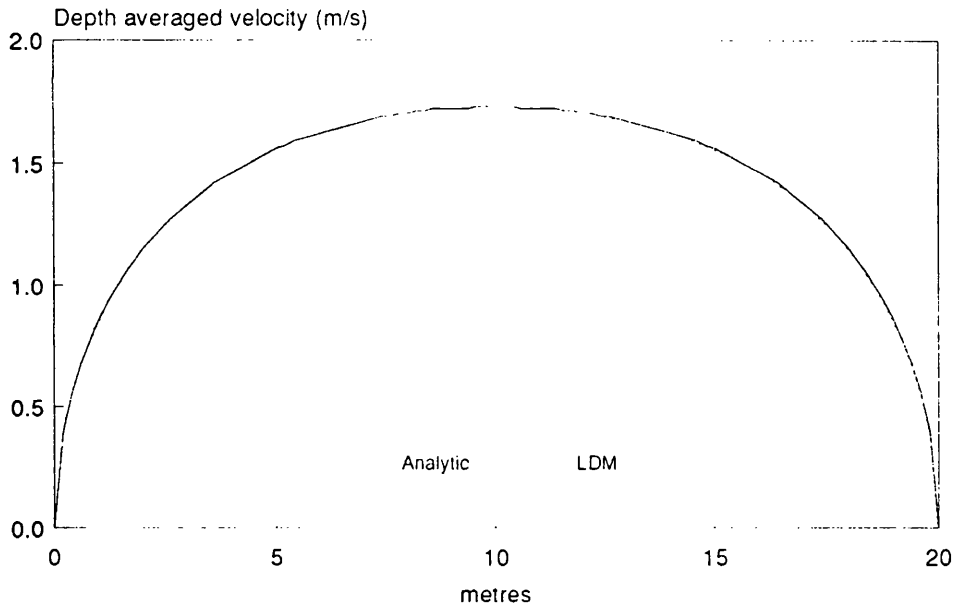
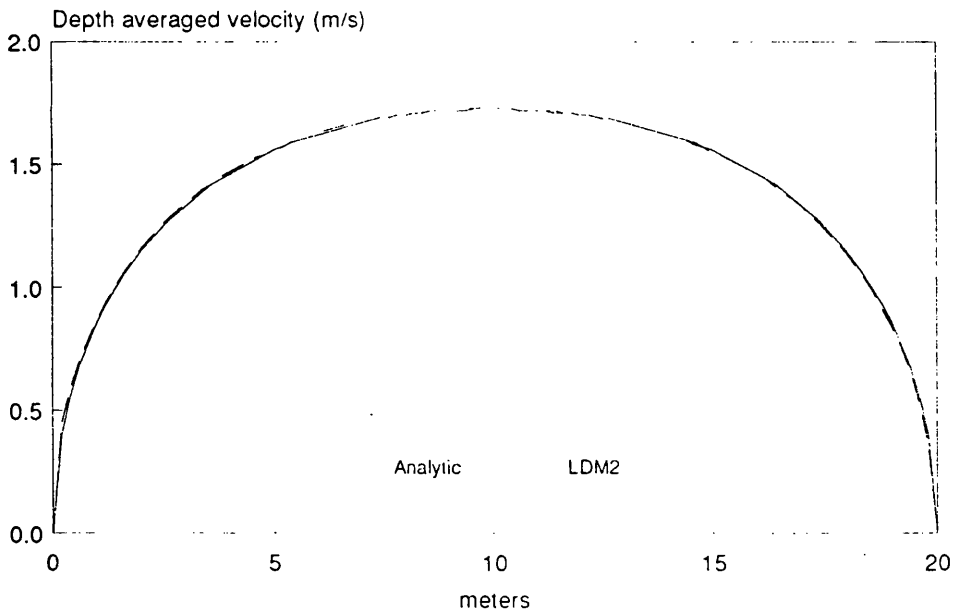


Figure 4.10 Main channel Manning's n values natural channels

### Rectangular Channel Depth 2m ks 0.1m NEV 0.75

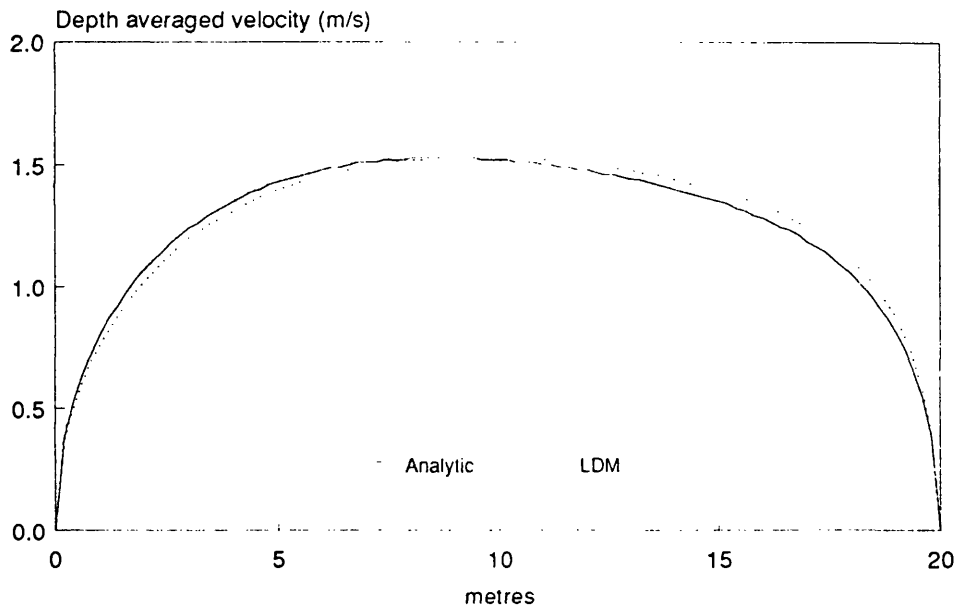


### Rectangular Channel Depth 2m ks 0.1m NEV 0.75



**Figure 4.11. Analytic and numerical solutions (LDM, LDM2) rectangular channel**

Quadrilateral Channel  
Depth 2m 1m ks 0.1m NEV 0.75



Quadrilateral Channel  
Depth 2m 1m ks 0.1m NEV 0.75

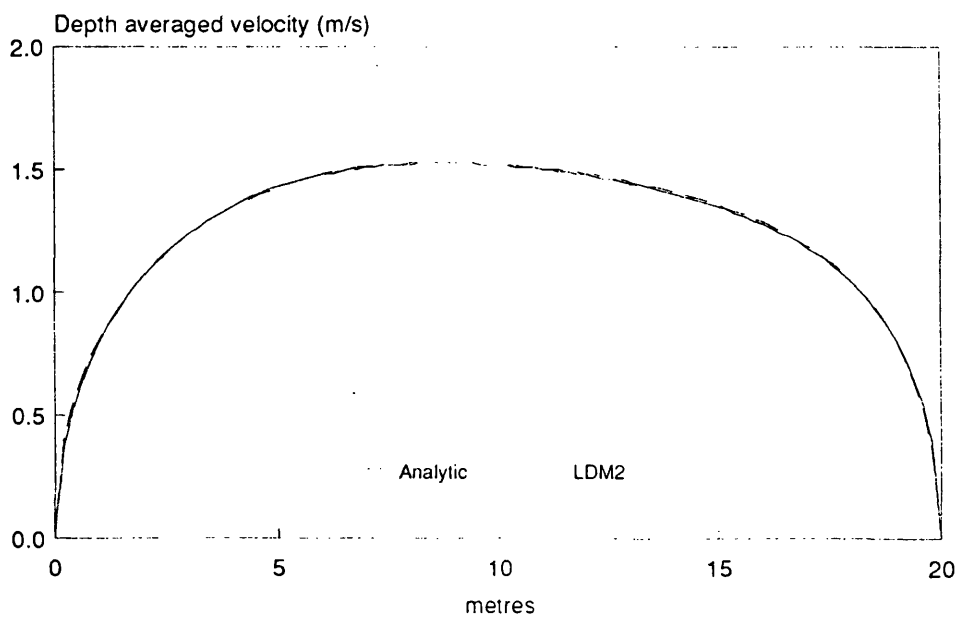
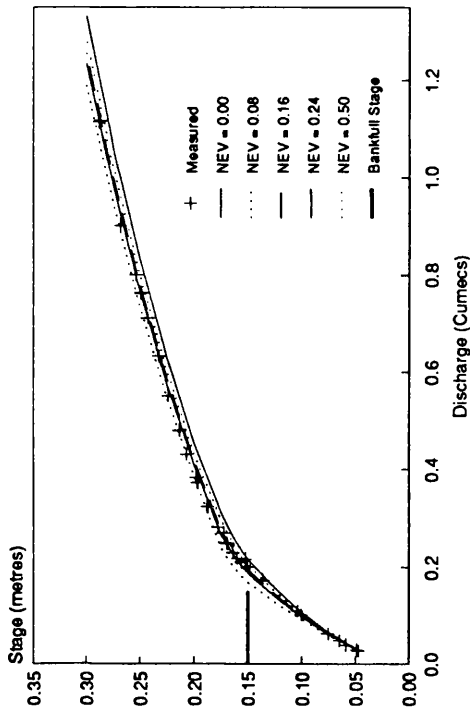
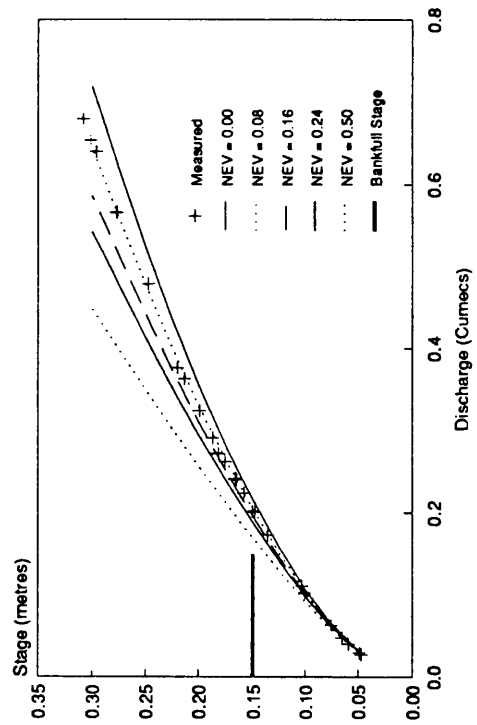


Figure 4.12 Analytic and numerical solutions (LDM, LDM2) quadrilateral channel

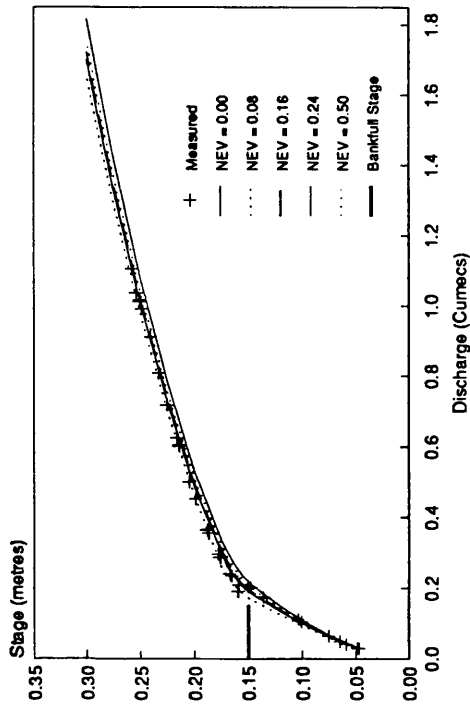
SERC Flume Series U2  
Stage Discharge



SERC Flume Series O4  
Stage Discharge



SERC Flume Series U1  
Stage Discharge



SERC Flume Series O3  
Stage Discharge

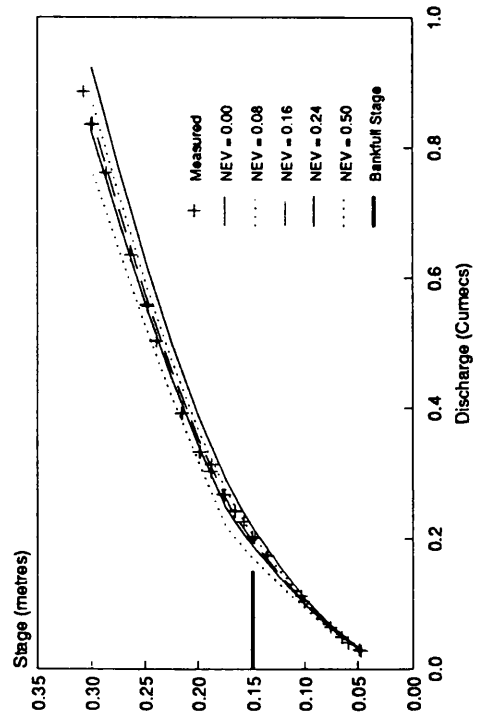
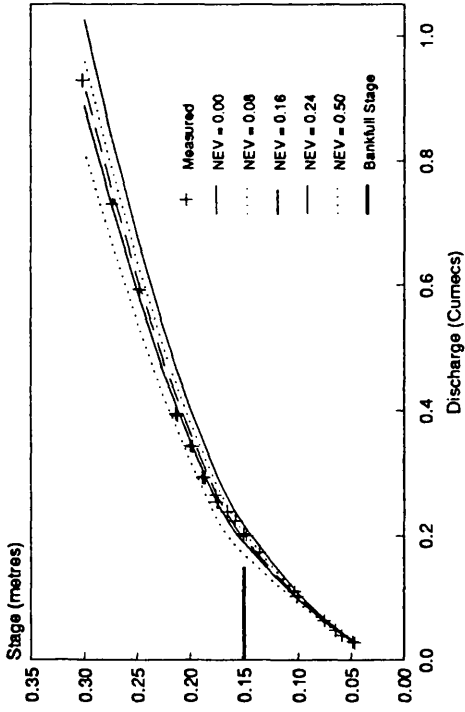
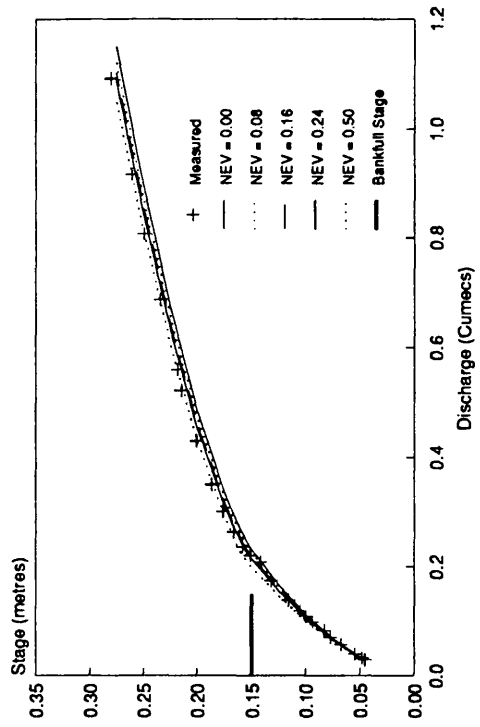


Figure 4.13 Computed stage-discharges (LDM) for SERC FCF Phase A smooth data

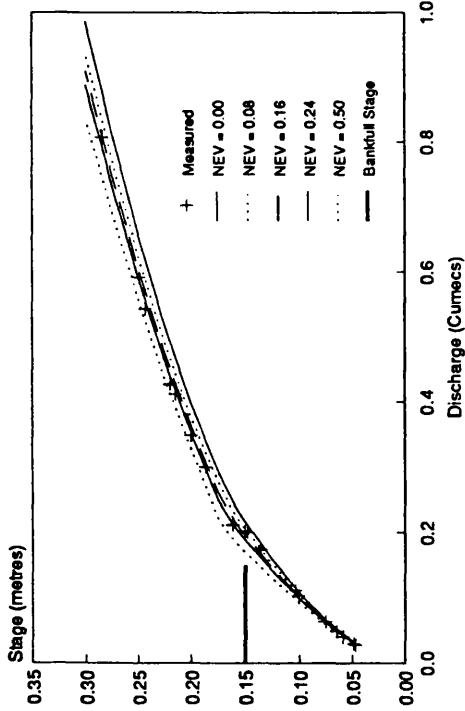
SERC Flume Series 06  
Stage Discharge



SERC Flume Series 10  
Stage Discharge



SERC Flume Series 05  
Stage Discharge



SERC Flume Series 08  
Stage Discharge

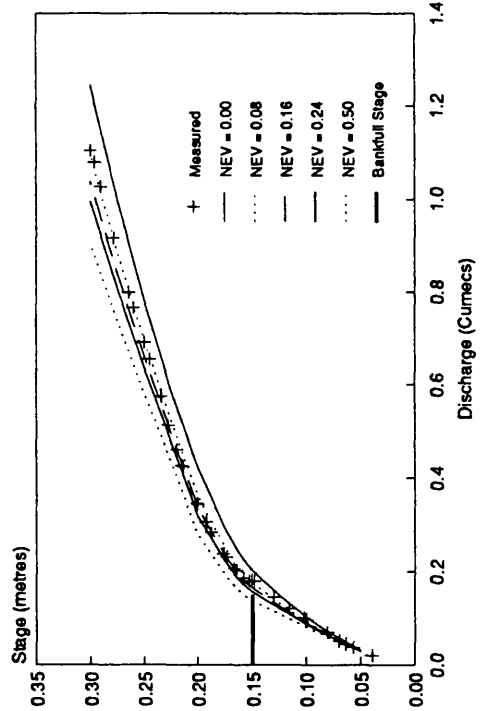
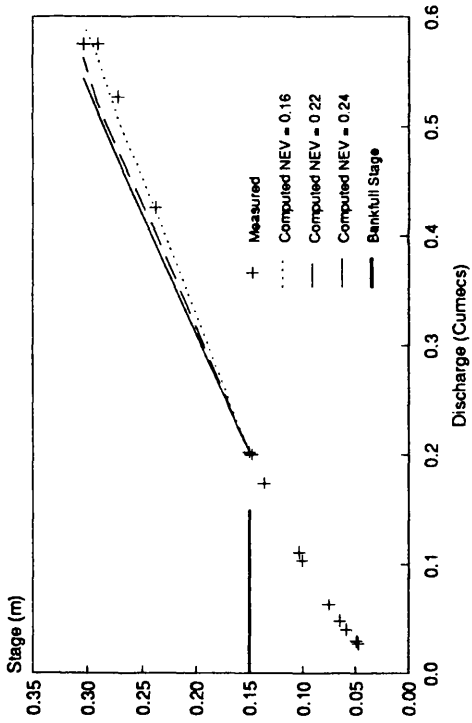
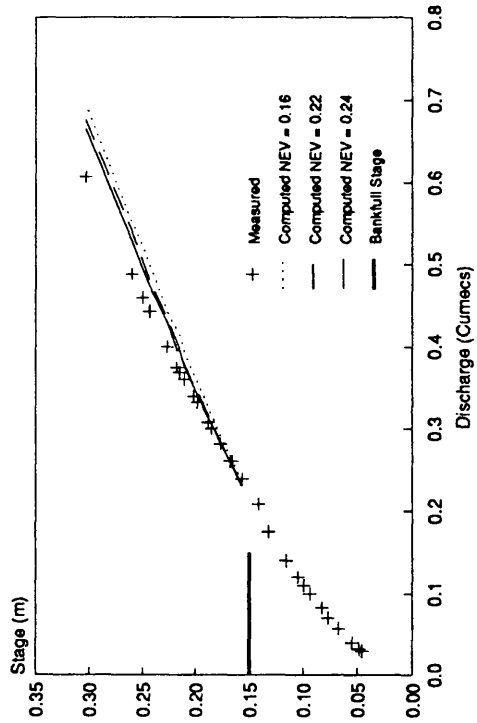


Figure 4.14 Computed stage-discharges (LDM) for SERC FCF Phase A smooth data

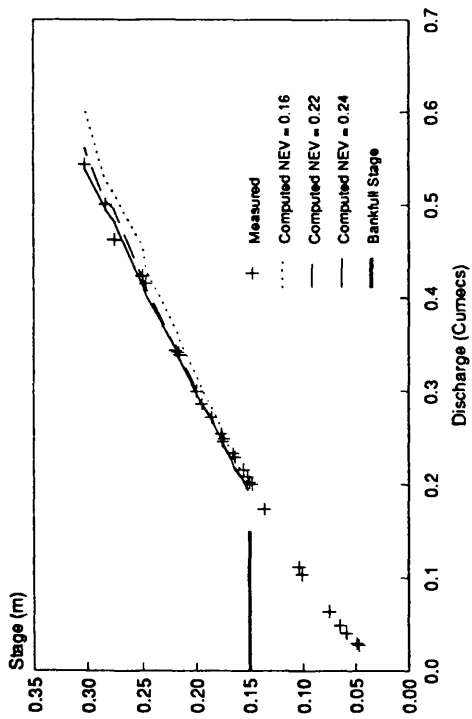
SERC Flume Series U/a  
Stage Discharge



SERC Flume Series 11  
Stage Discharge



SERC Flume Series 07  
Stage Discharge



SERC Flume Series 09  
Stage Discharge

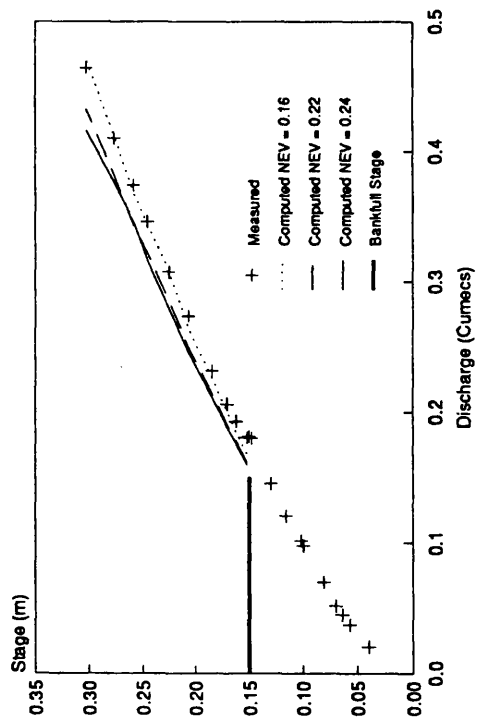
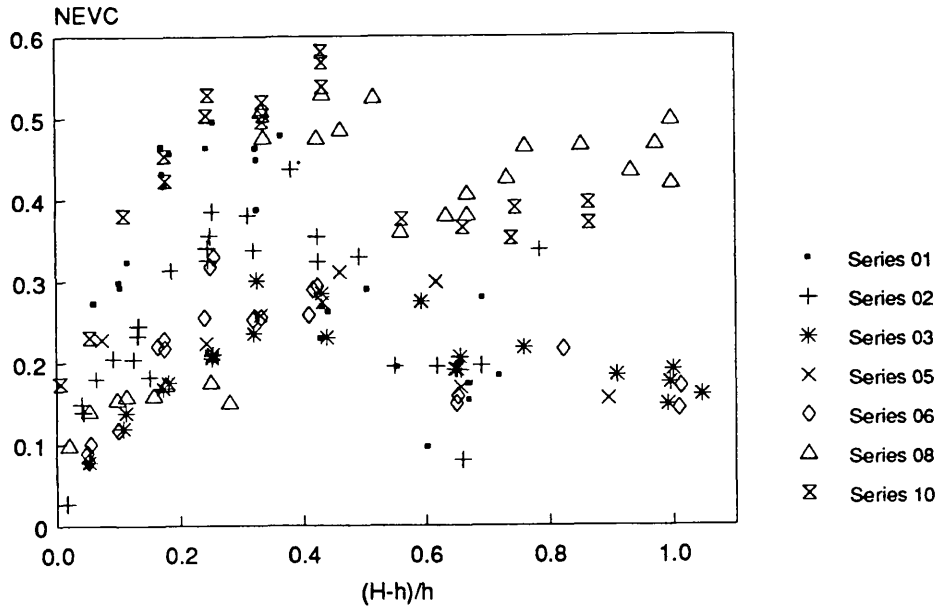


Figure 4.15 Computed stage-discharges (LDM) for SERC FCF Phase A rough data

## Back Calculated NEV Values SERC Flume Smooth Case



**Figure 4.16** Computed distributions of NEVC for SERC FCF Phase A smooth data

## Back Calculated NEV Values SERC Flume Rough Case

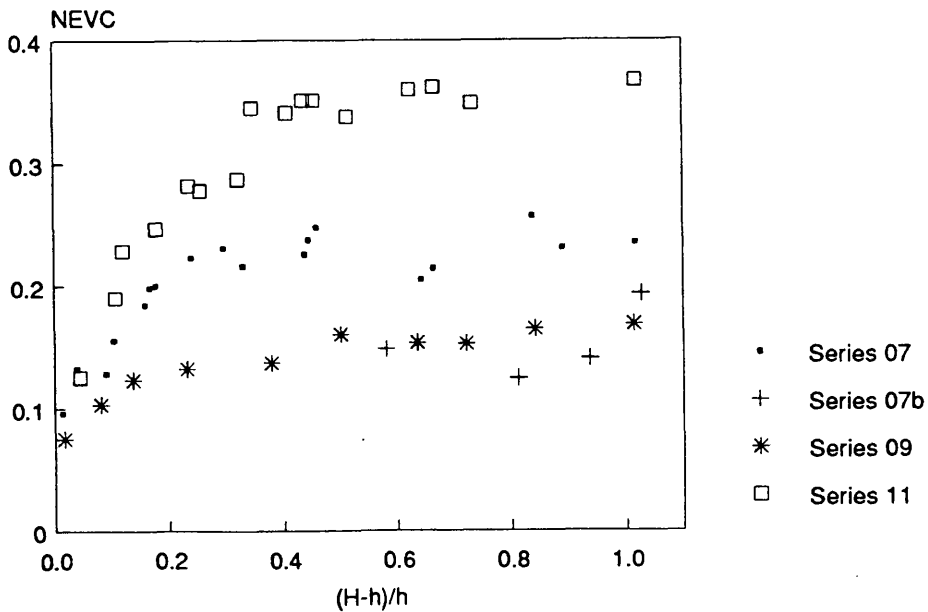


**Figure 4.17** Computed distributions of NEVC for SERC FCF Phase A rough data

## Lateral Distribution Method SERC Flume Smooth Case

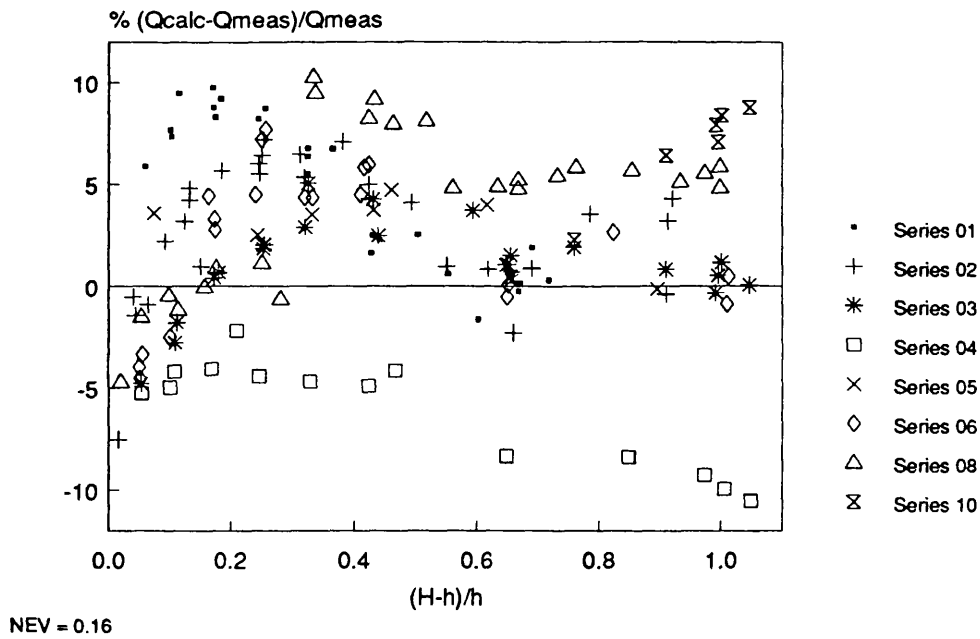


**Figure 4.18** Distributions of %error in  $Q_{calc}$  with NEV = 0.16 for SERC FCF Phase A smooth data

## Lateral Distribution Method SERC Flume Rough Case

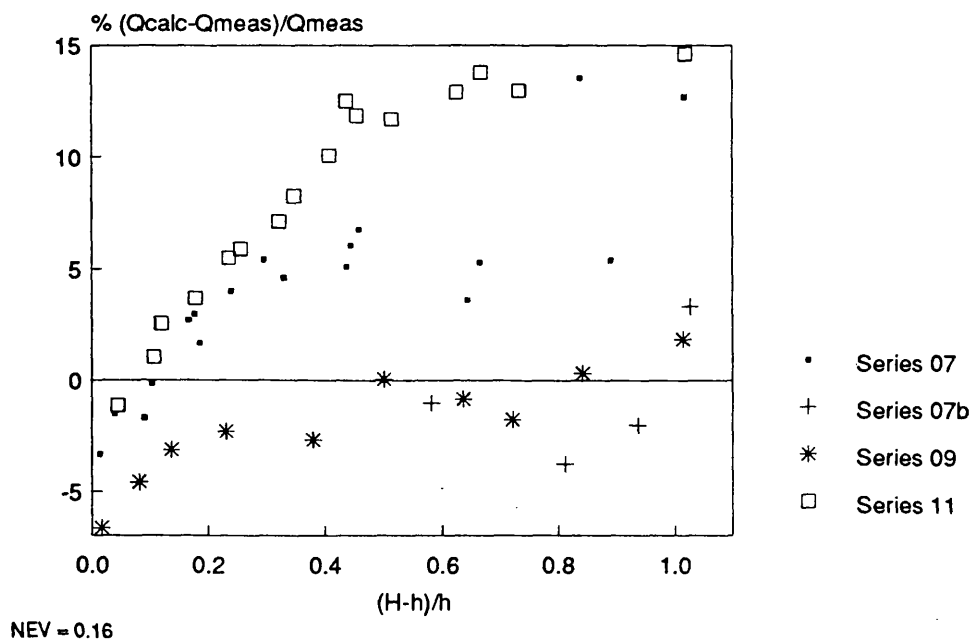
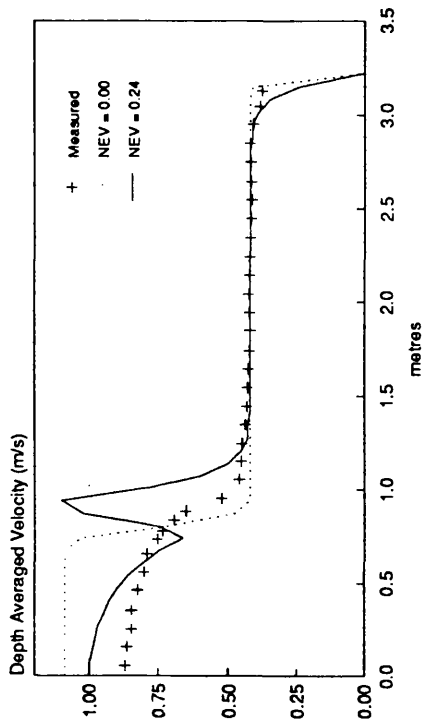


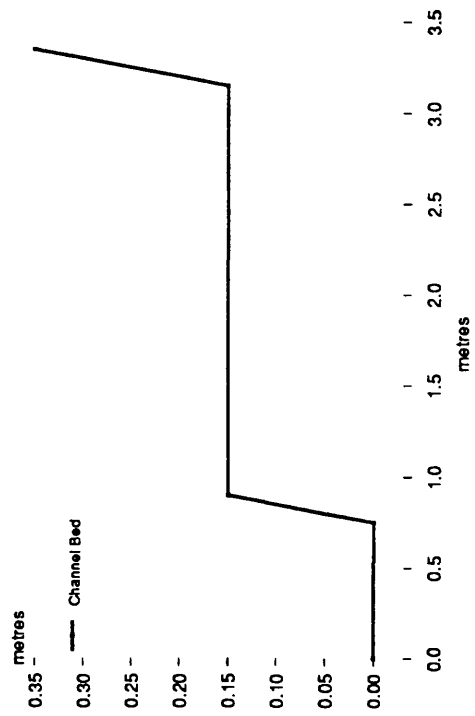
**Figure 4.19** Distributions of %error in  $Q_{calc}$  with NEV = 0.16 for SERC FCF Phase A rough data

SERC Flume Series 02

Velocity Distribution  
Stage = 0.198m

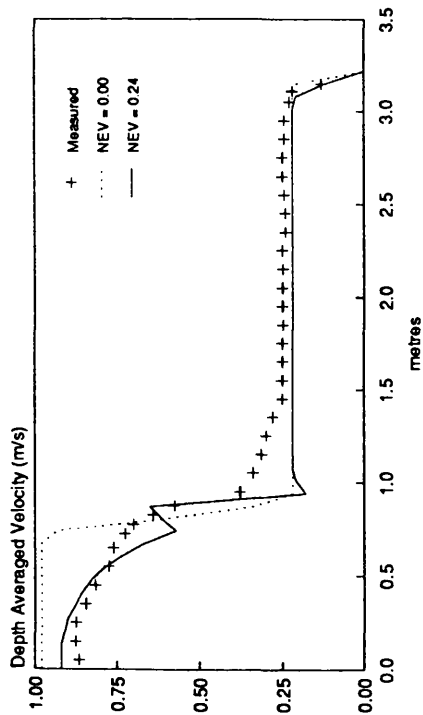


SERC Flume Series 02  
Cross Section Geometry



SERC Flume Series 02

Velocity Distribution  
Stage = 0.169m



SERC Flume Series 02  
Velocity Distribution  
Stage = 0.288m

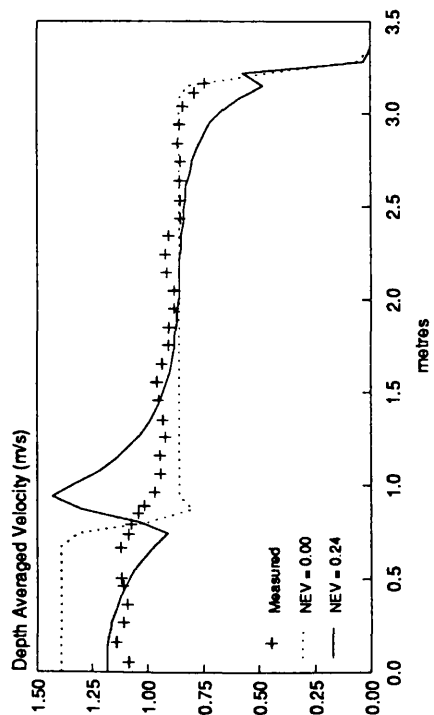
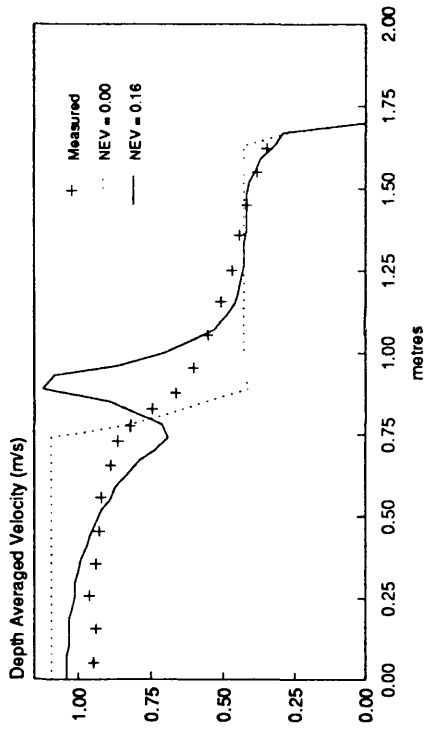
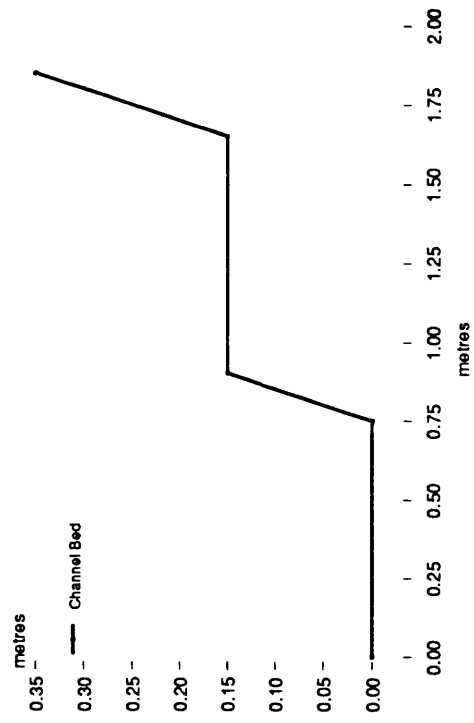


Figure 4.20 Calculated depth averaged velocity profiles LDM Series 2 SERC FCF Phase A data

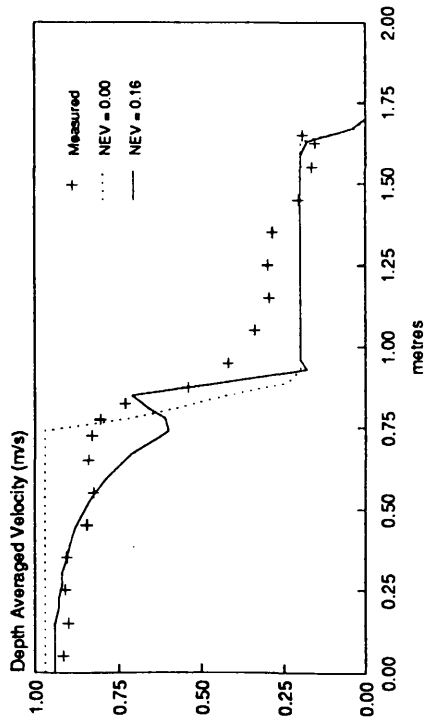
Velocity Distribution  
Stage = 0.199m



SERC Flume Series 03  
Cross Section Geometry



Velocity Distribution  
Stage = 0.167m



SERC Flume Series 03  
Velocity Distribution  
Stage = 0.300m

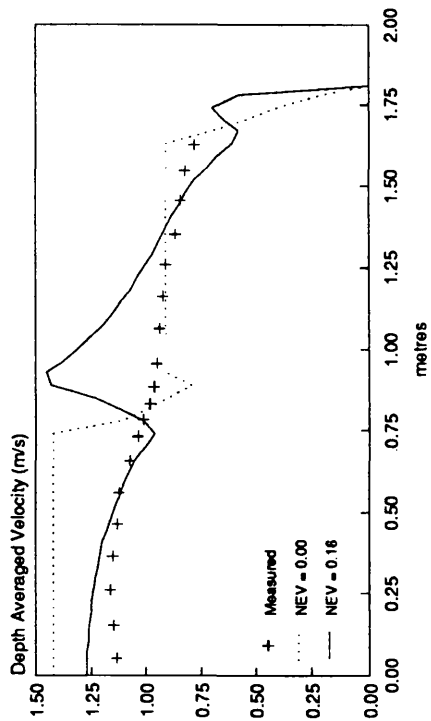
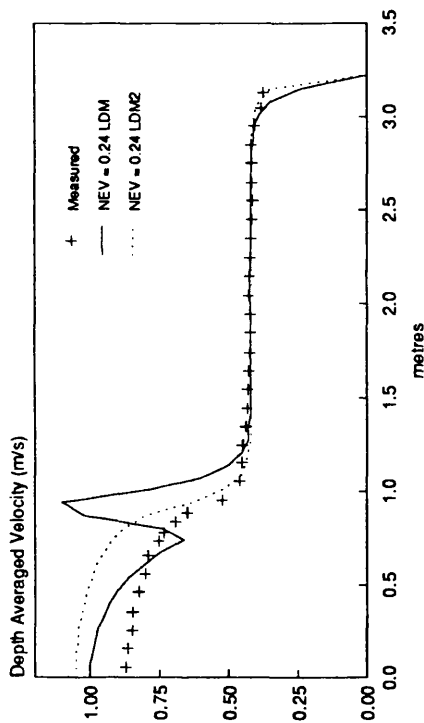
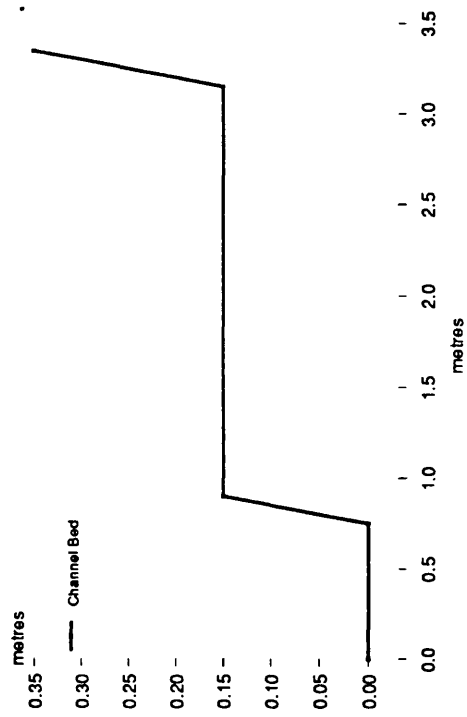


Figure 4.21 Calculated depth averaged velocity profiles LDM Series 3 SERC FCF Phase A data

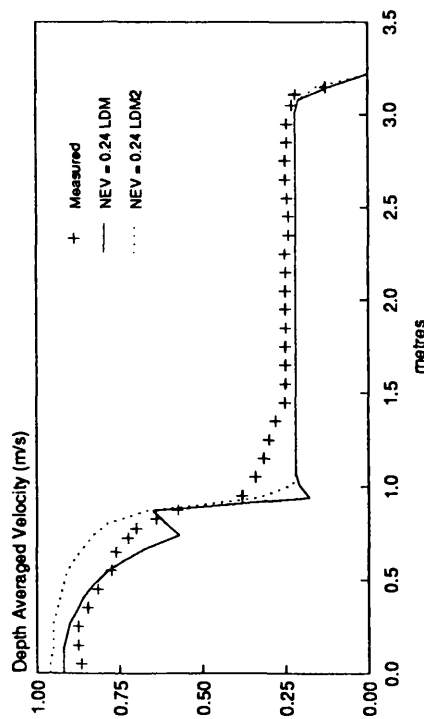
Velocity Distribution  
Stage = 0.198m



SERC Flume Series O2  
Cross Section Geometry



Velocity Distribution  
Stage = 0.169m



SERC Flume Series O2  
Velocity Distribution  
Stage = 0.288m

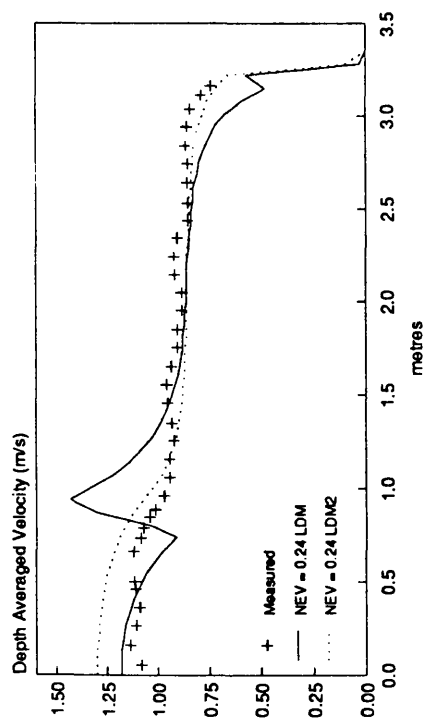
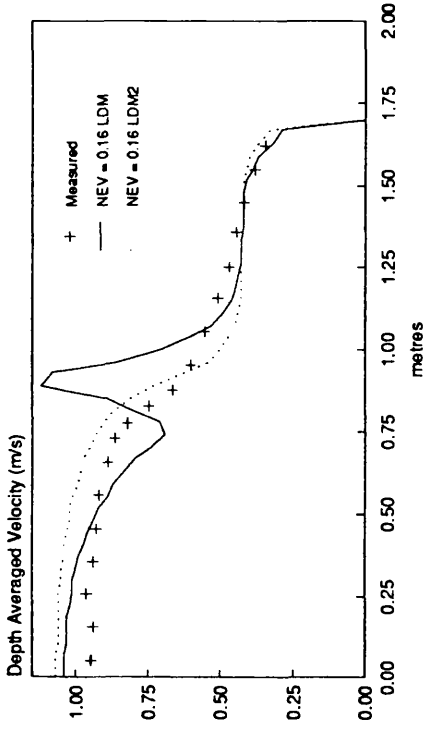


Figure 4.22 Calculated depth average velocity profiles LDM and LDM2 Series 2 SERC FCF Phase A data

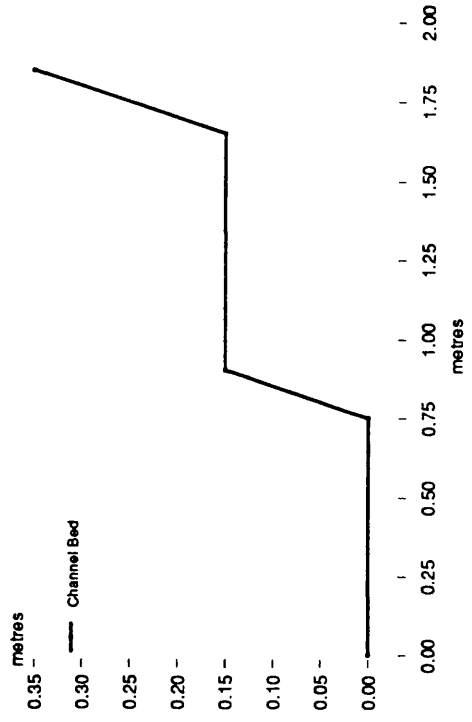
SERC Flume Series 03

Velocity Distribution

Stage = 0.199m



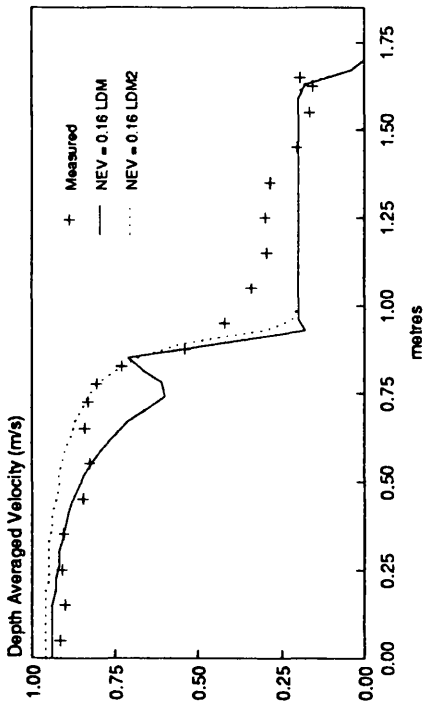
SERC Flume Series 03  
Cross Section Geometry



SERC Flume Series 03

Velocity Distribution

Stage = 0.167m



SERC Flume Series 03  
Velocity Distribution

Stage = 0.300m

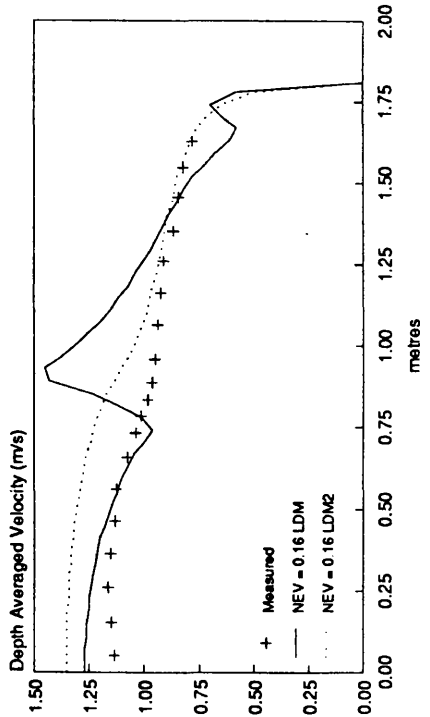
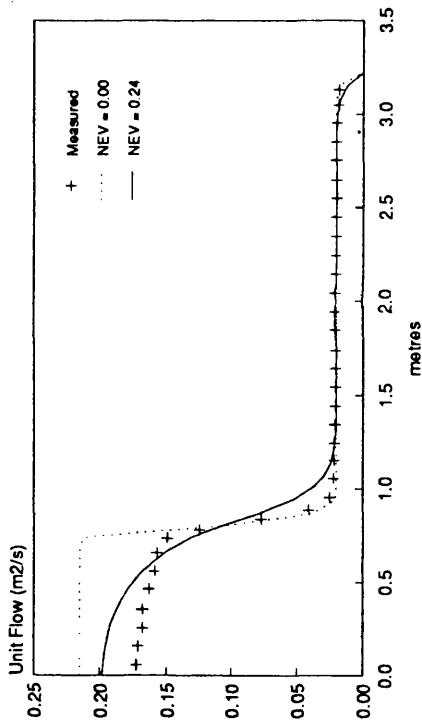
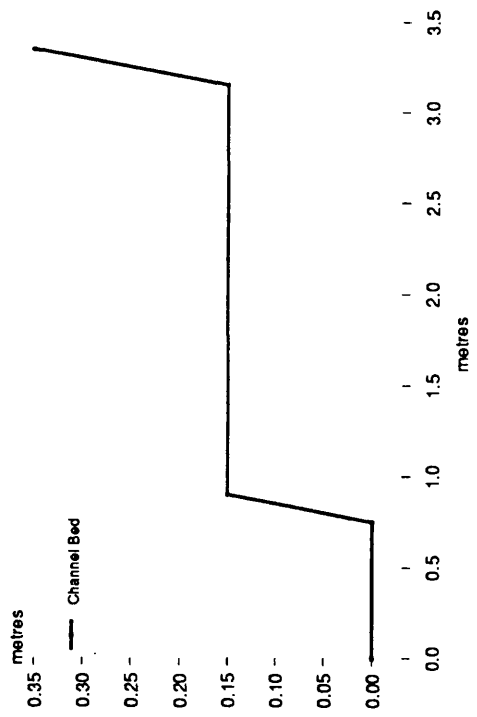


Figure 4.23 Calculated depth average velocity profiles LDM and LDM2 Series 3 SERC FCF Phase A data

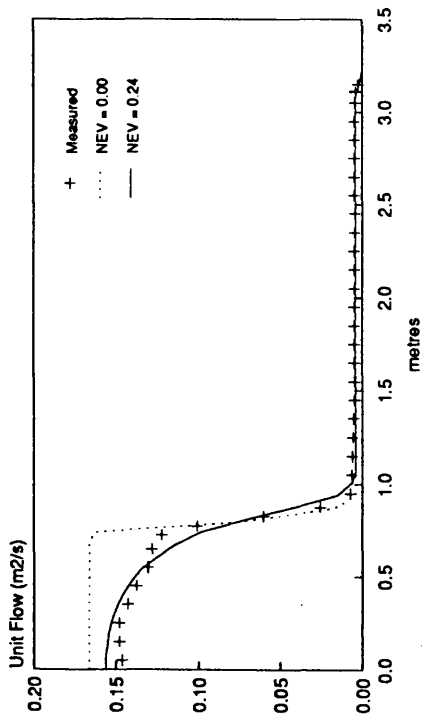
SERC Flume Series 02  
Unit Flow Distribution  
Stage = 0.198m



SERC Flume Series 02  
Cross Section Geometry



SERC Flume Series 02  
Unit Flow Distribution  
Stage = 0.169m



SERC Flume Series 02  
Unit Flow Distribution  
Stage = 0.288m

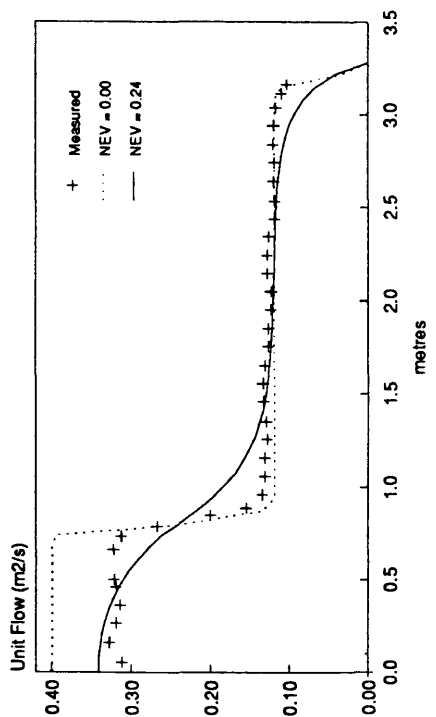
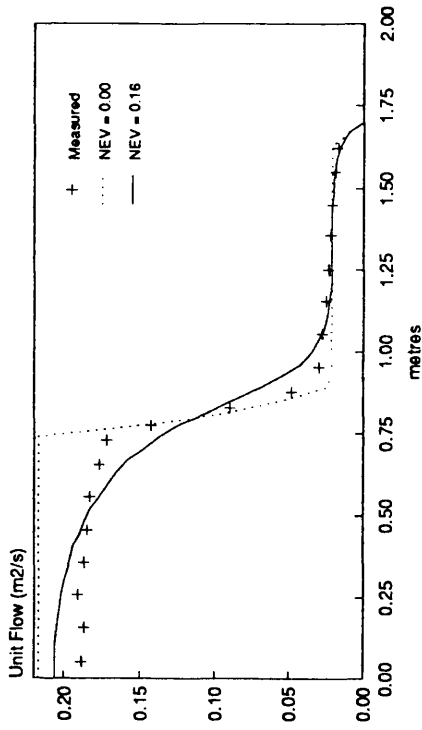
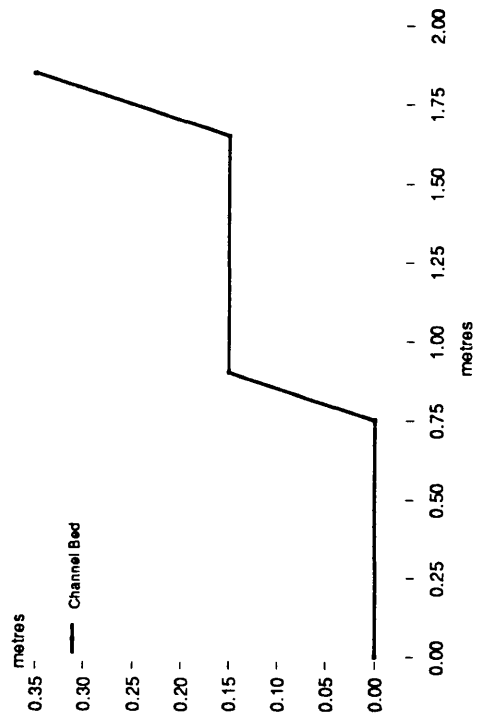


Figure 4.24 Calculated unit flow profiles LDM Series 2 SERC FCF Phase A data

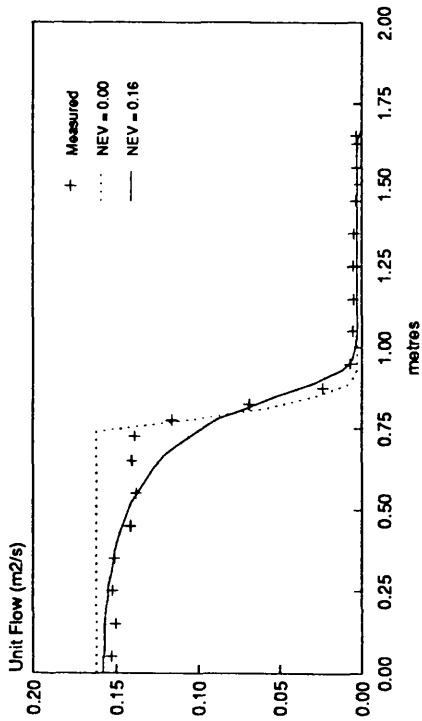
**SERC Flume Series 03**  
**Unit Flow Distribution**  
**Stage = 0.199m**



**SERC Flume Series 03**  
**Cross Section Geometry**



**SERC Flume Series 03**  
**Unit Flow Distribution**  
**Stage = 0.167m**



**SERC Flume Series 03**  
**Unit Flow Distribution**  
**Stage = 0.300m**

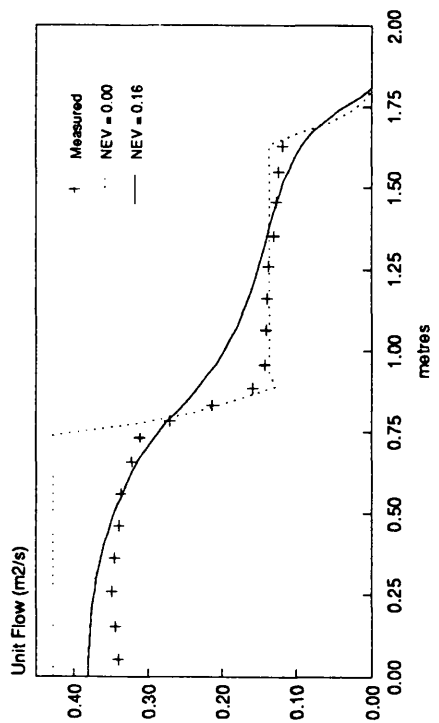
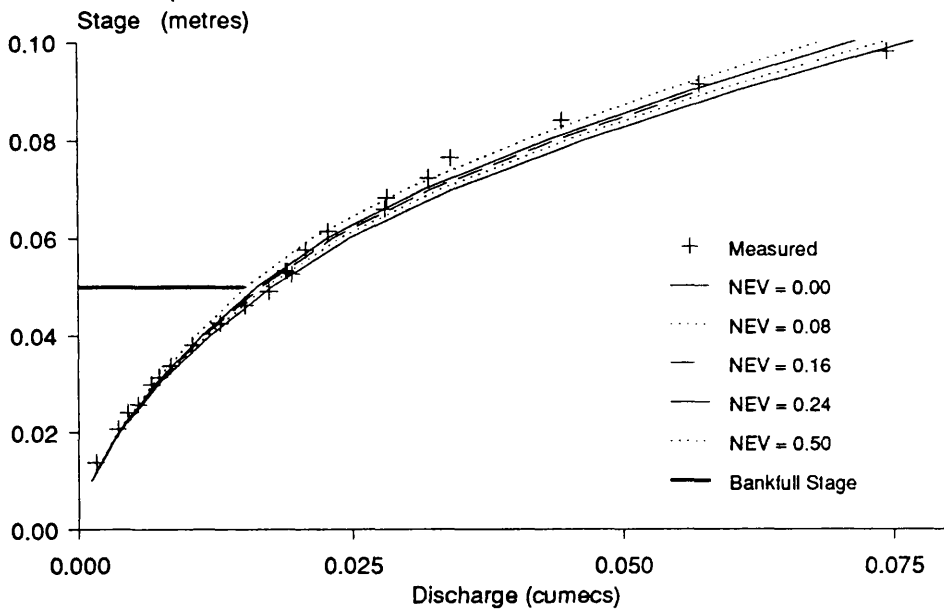


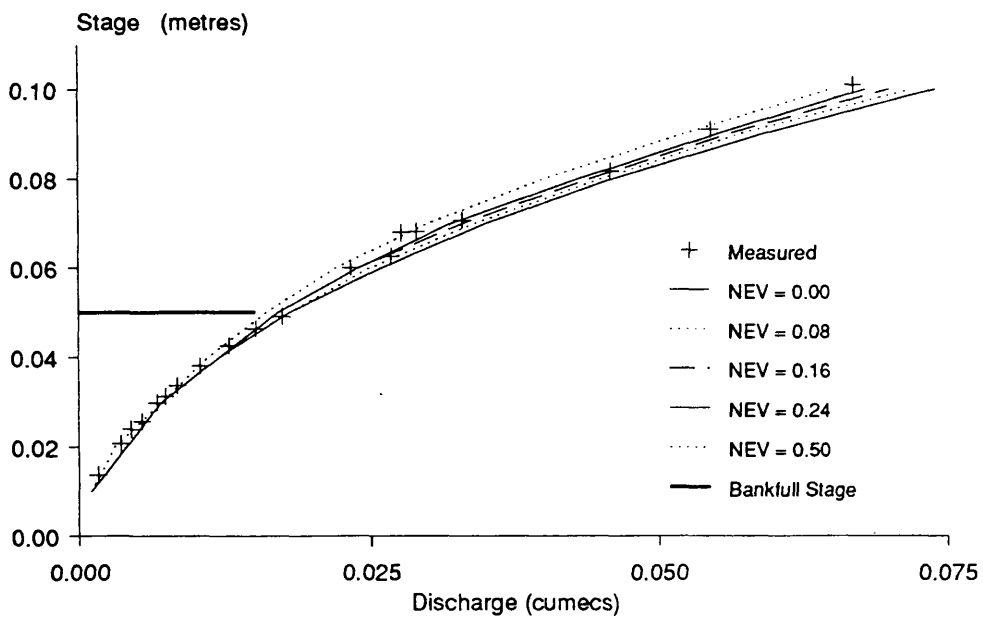
**Figure 4.25** Calculated unit flow profiles LDM Series 3 SERC FCF Phase A data

## Myers Laboratory Flume Stage Discharge Series A



nb = 0.010 nf = 0.010

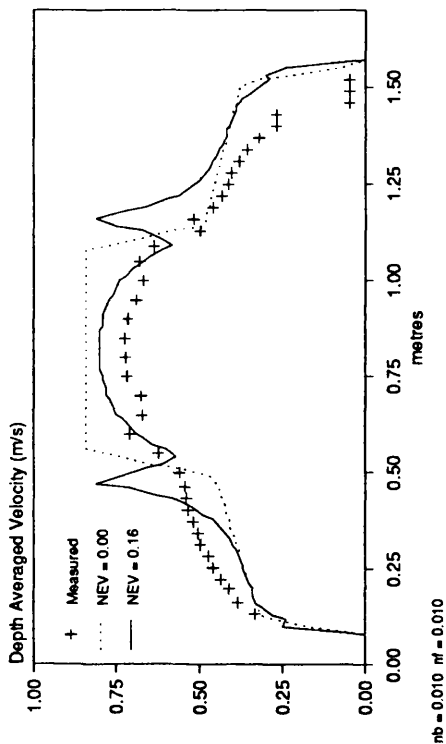
## Myers Laboratory Flume Stage Discharge Series F



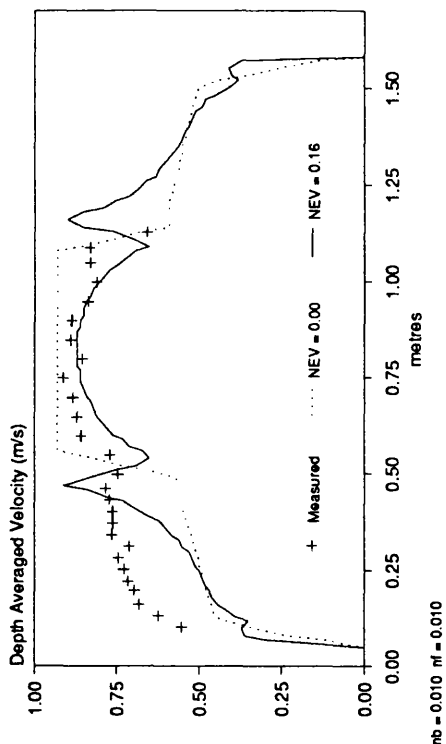
nb = 0.008 nf = 0.008

**Figure 4.26 Stage discharge curves for Myers' lab data LDM**

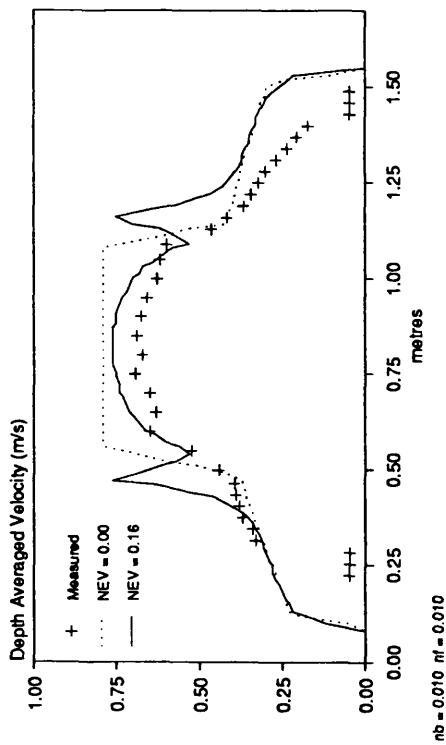
Velocity Distribution  
Stage = 0.08395 m



Myers Laboratory Flume Series A  
Velocity Distribution  
Stage = 0.09793 m



Velocity Distribution  
Stage = 0.07641 m



Myers Laboratory Flume Series A  
Velocity Distribution  
Stage = 0.09131 m

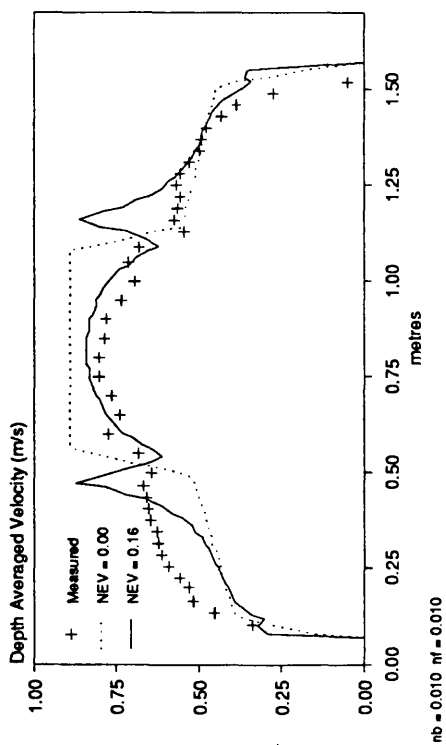
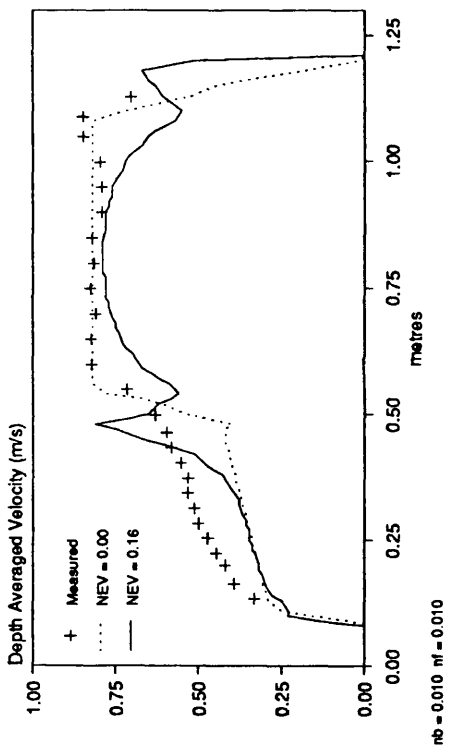
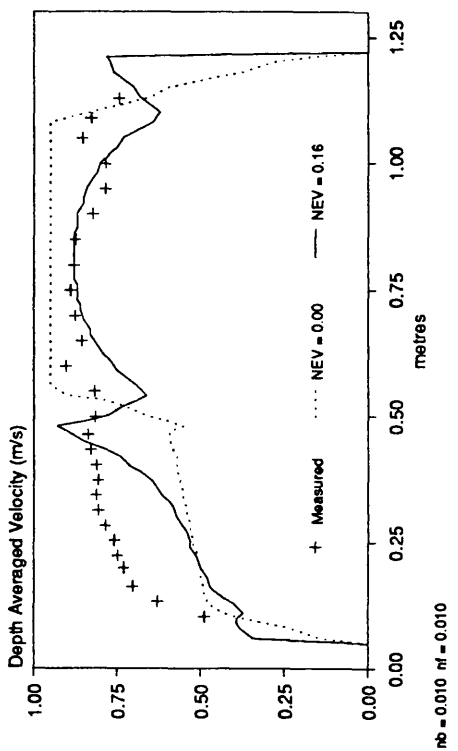


Figure 4.27 Calculated depth averaged velocity profiles LDM Myers' Series A

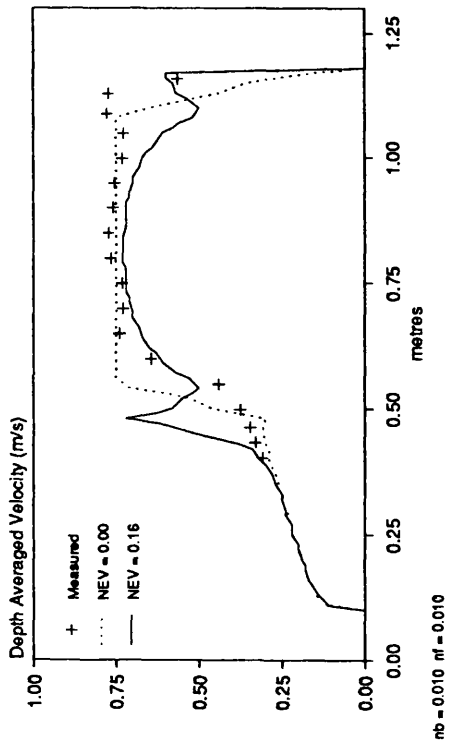
Velocity Distribution  
Stage = 0.08177 m



Myers Laboratory Flume Series F  
Velocity Distribution  
Stage = 0.1010 m



Velocity Distribution  
Stage = 0.07074 m



Myers Laboratory Flume Series F  
Velocity Distribution  
Stage = 0.09115 m

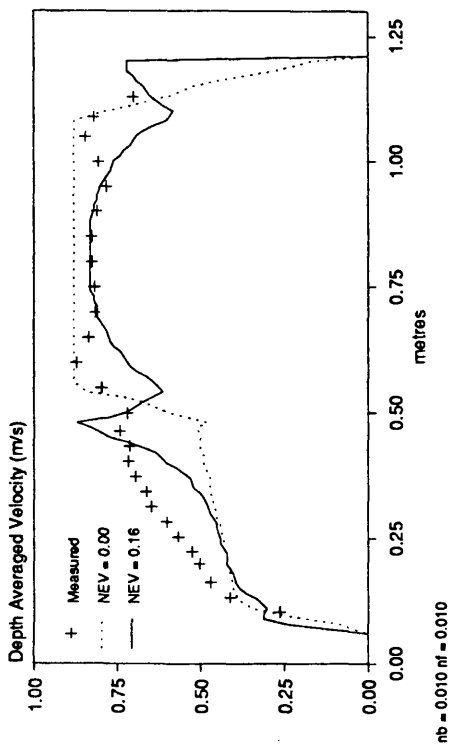


Figure 4.28 Calculated depth averaged velocity profiles LDM Myers' Series F

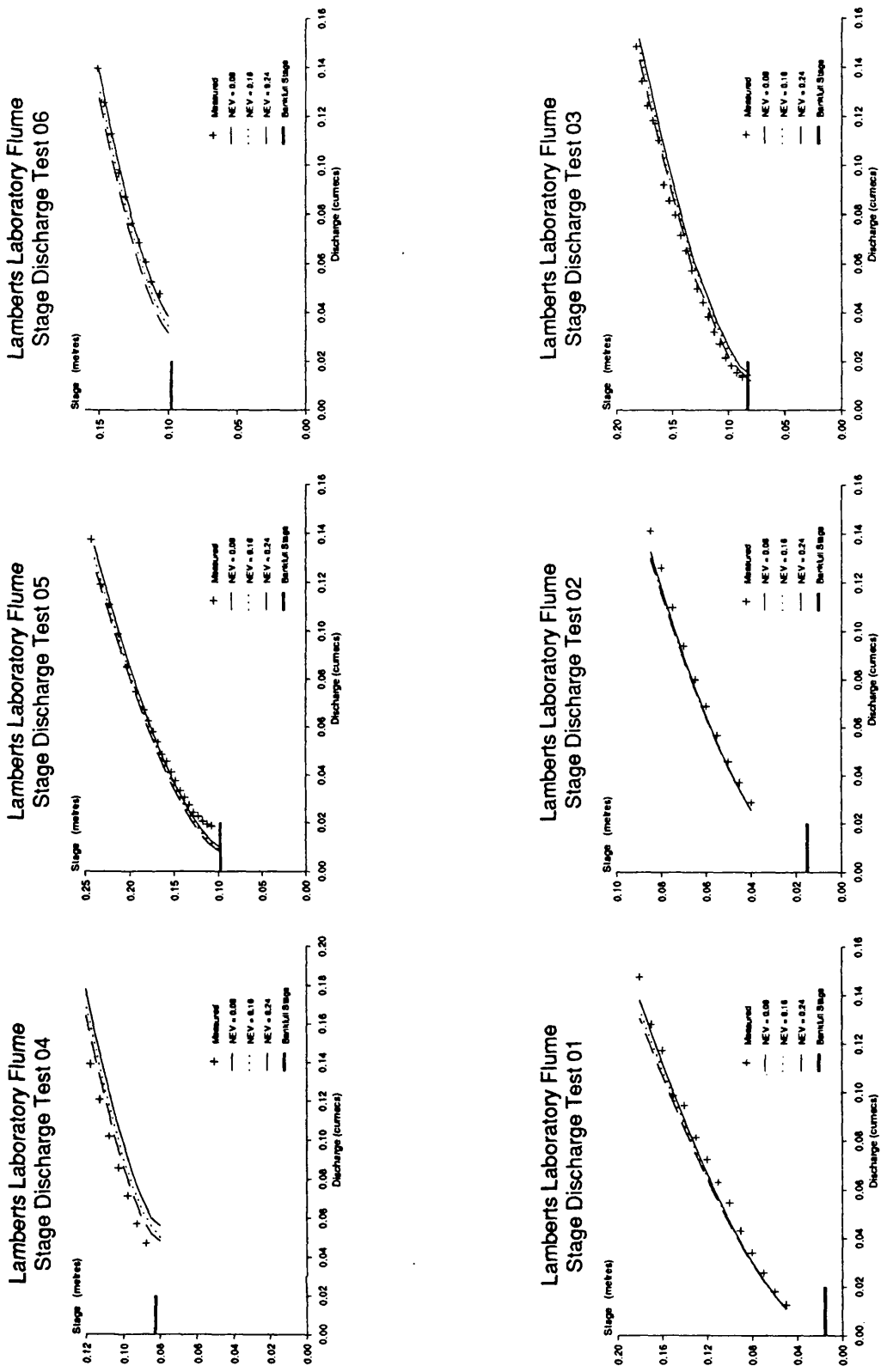
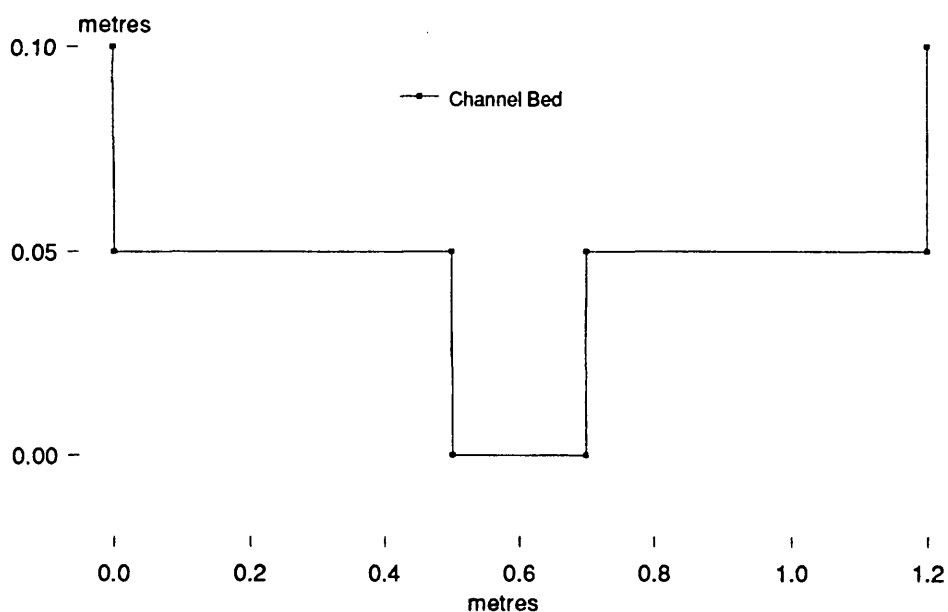
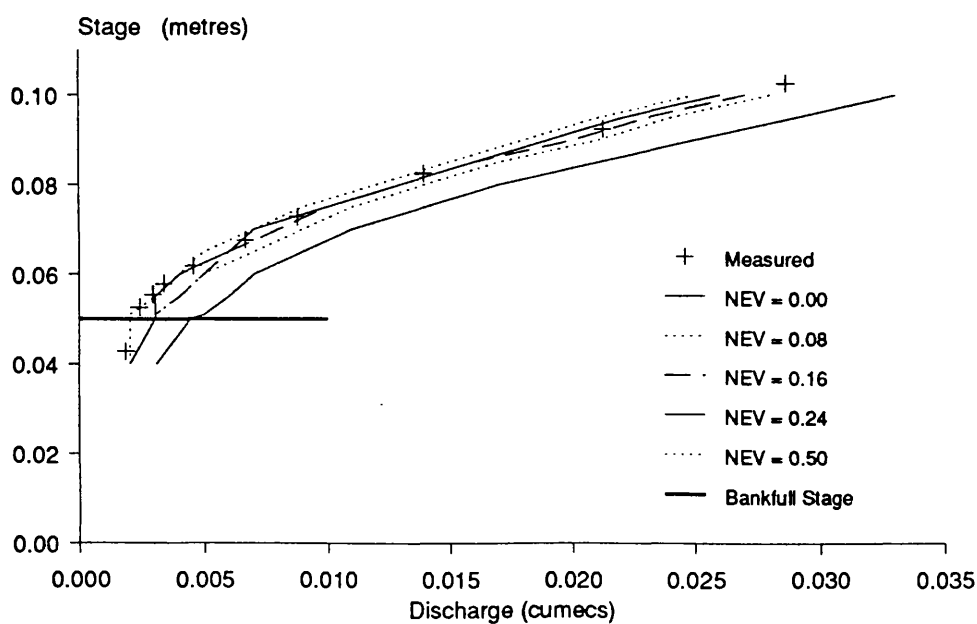


Figure 4.29 Stage discharge curves for Lambert's lab data LDM

## Kiely Laboratory Flume Cross Section Geometry



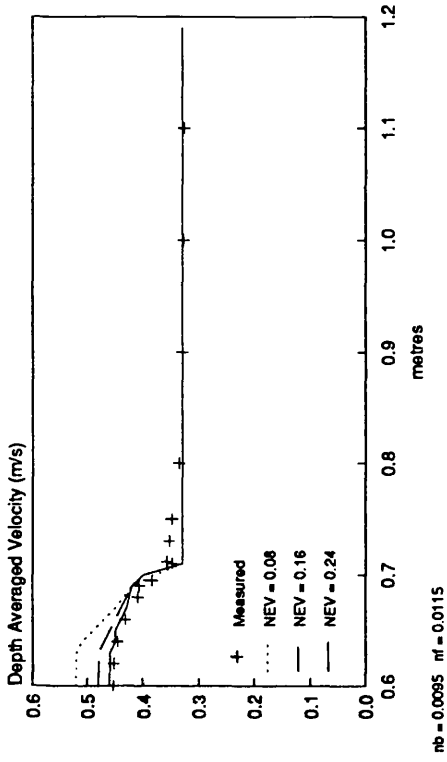
## Kiely Laboratory Flume Stage Discharge



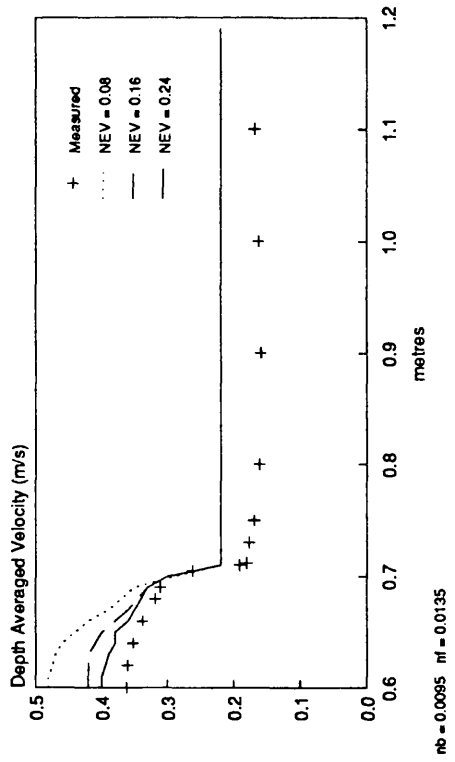
nb = 0.0095 nf = 0.014 - 0.012

**Figure 4.30** Cross-section and stage discharge curve for Kiely's lab data LDM

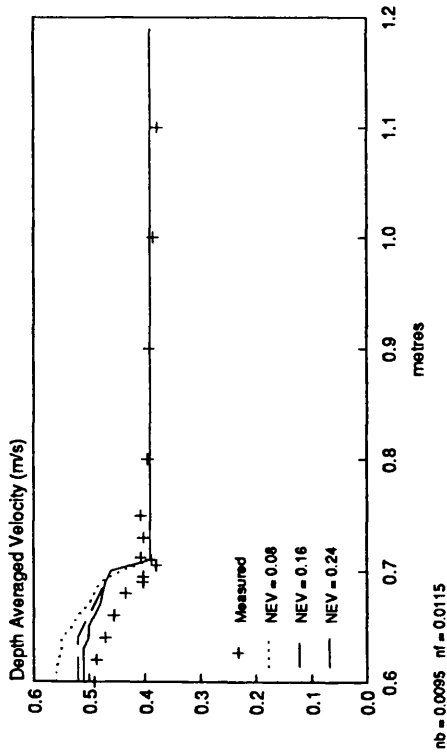
### Velocity Distribution Stage = 0.0918 m



### Kiely Laboratory Flume Velocity Distribution Stage = 0.0697 m



### Velocity Distribution Stage = 0.1029 m



### Kiely Laboratory Flume Velocity Distribution Stage = 0.0806 m

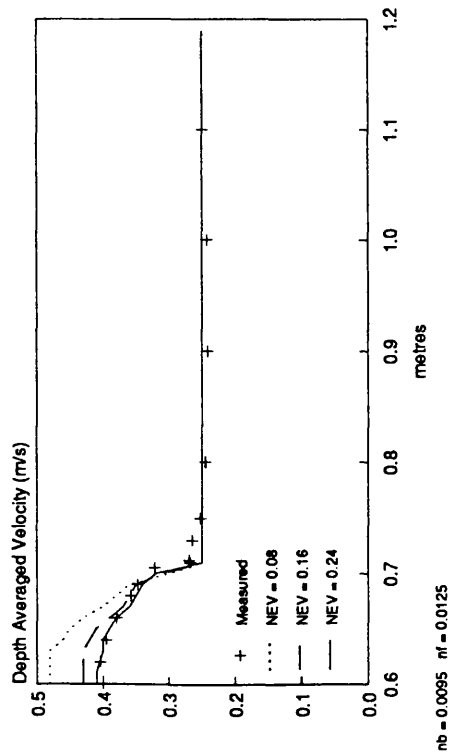
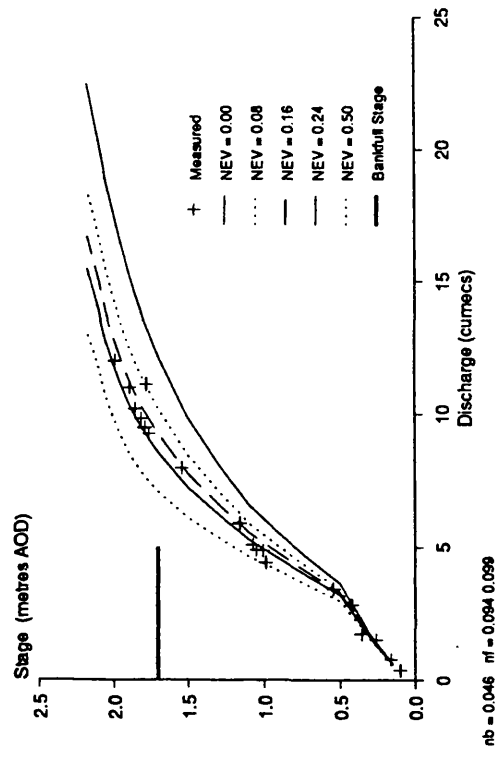
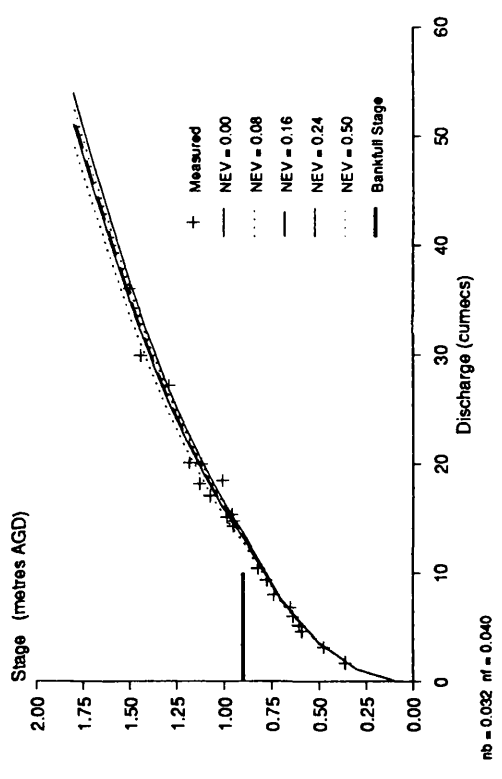


Figure 4.31 Calculated depth averaged velocity profiles LDM Kiely

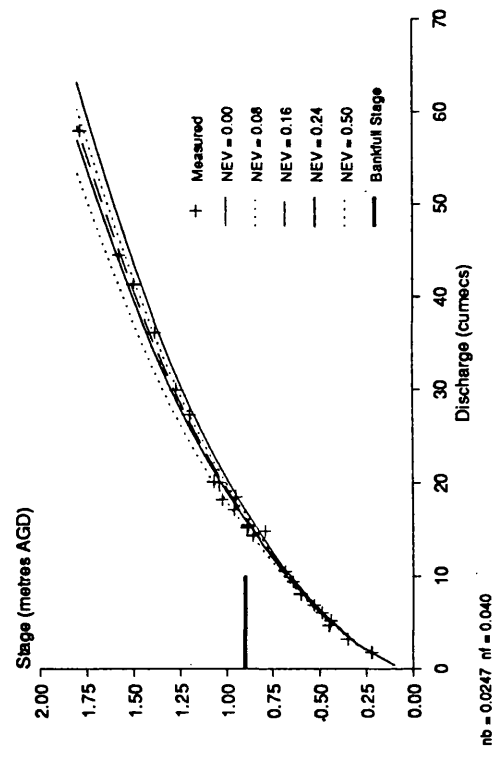
### River Blackwater at Ower Stage Discharge



### River Main Section 6 Stage Discharge



### River Main Section 14 Stage Discharge



### River Ouse at Skelton Stage Discharge

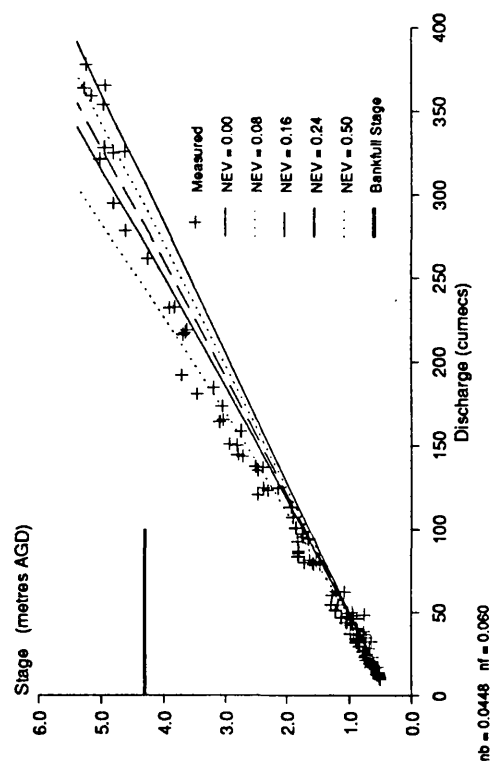
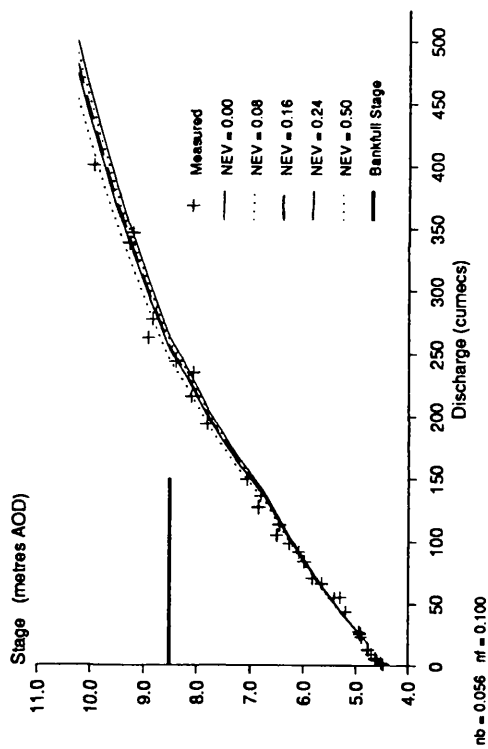
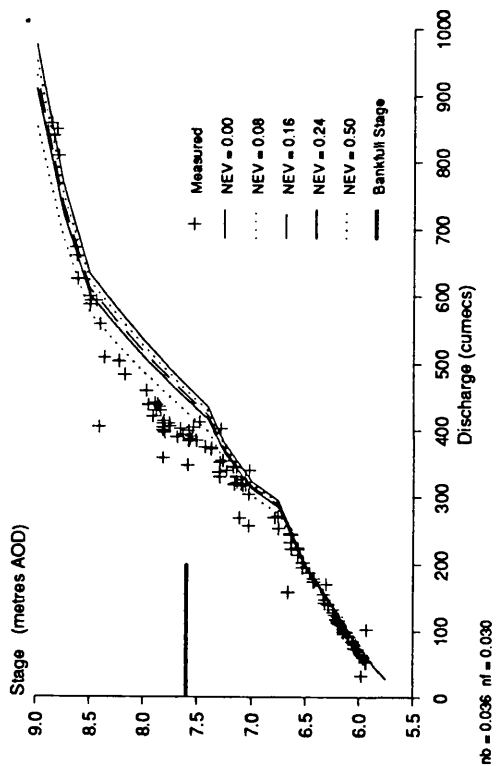


Figure 4.32 Stage-discharge curves for field data LDM

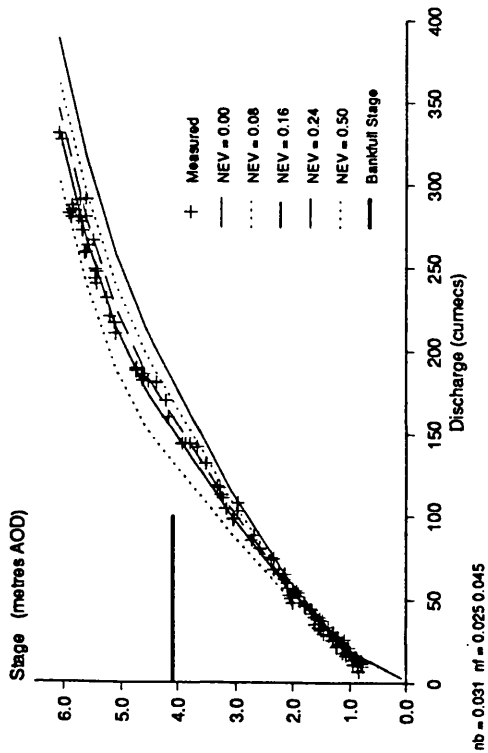
### River Tees at Low Moor



### River Trent at North Muskham



### River Severn at Montford



### River Torridge at Torrington

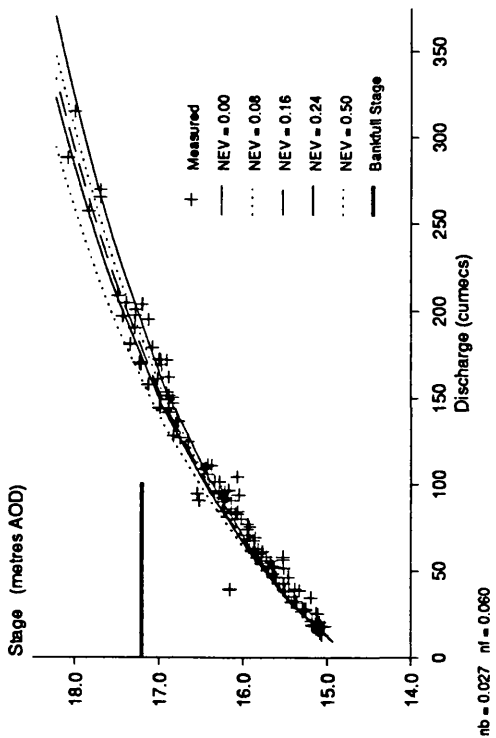
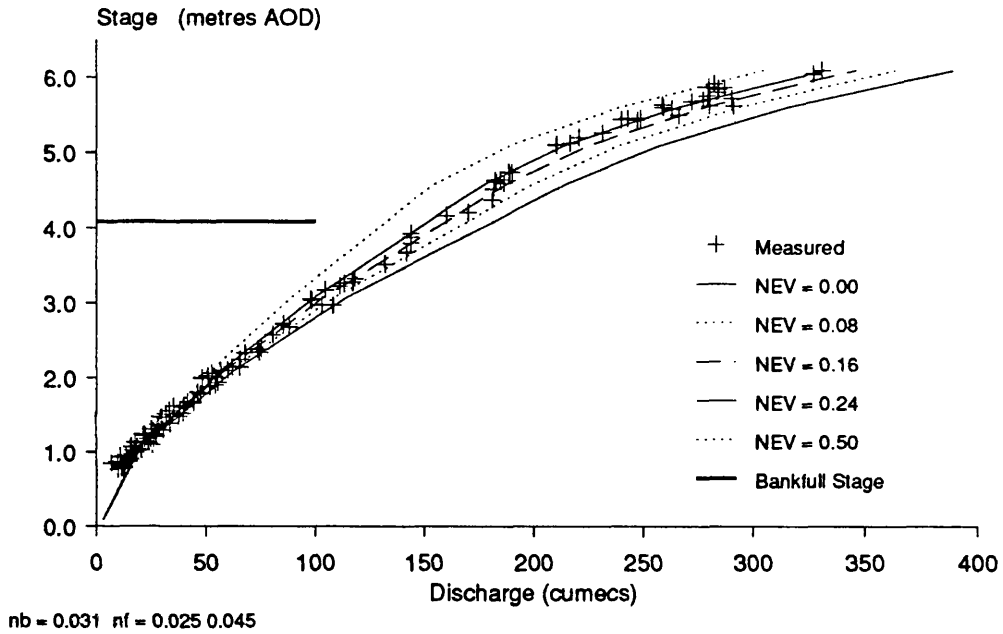
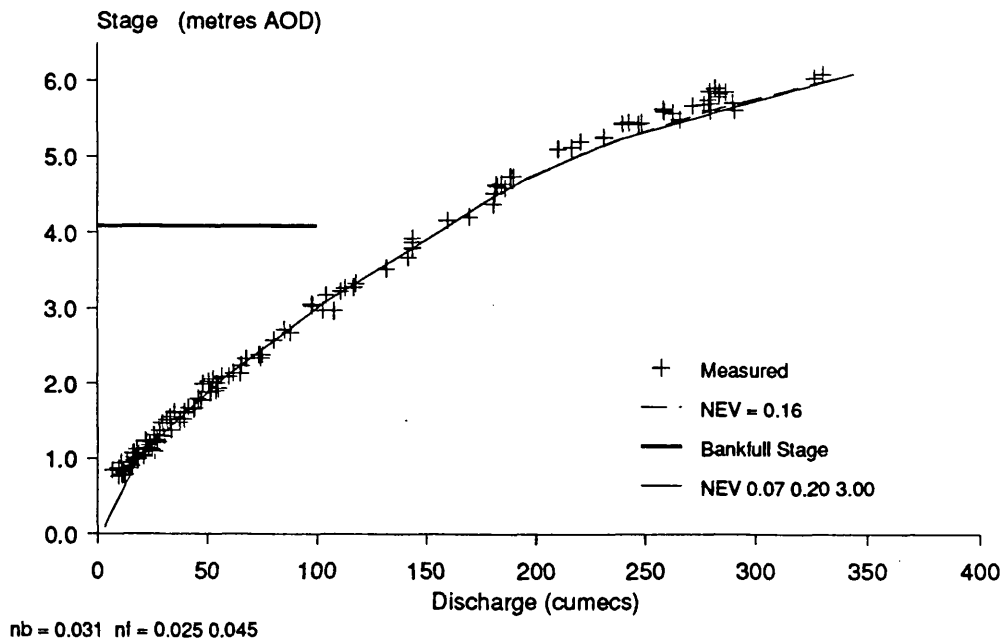


Figure 4.33 Stage-discharge curves for field data LDM

## River Severn at Montford Stage Discharge

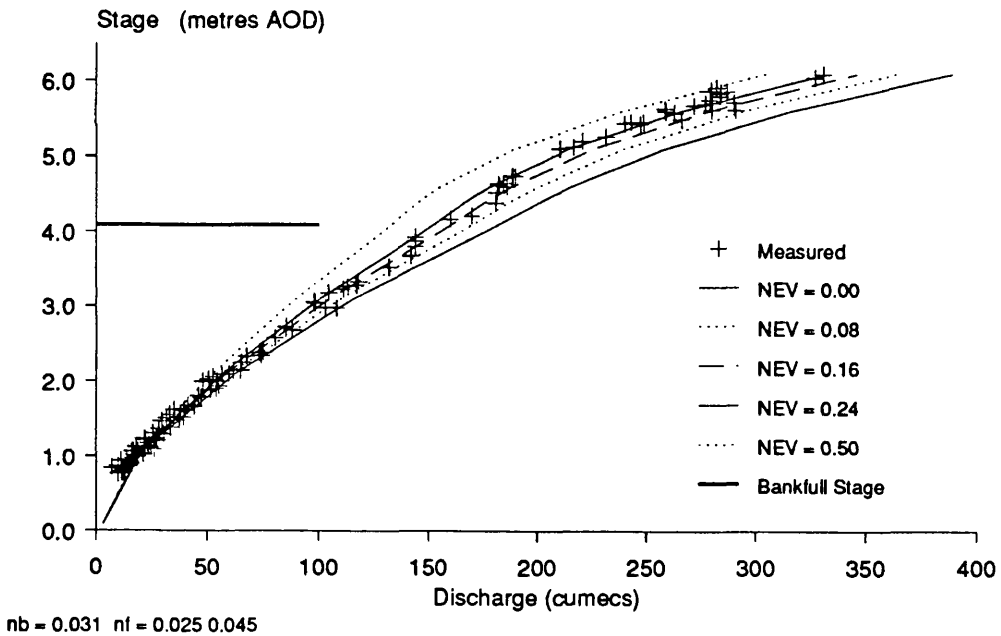


## River Severn at Montford Stage Discharge



**Figure 4.34 Stage-discharge curves with fixed and variable NEV values LDM, Severn at Montford**

## River Severn at Montford Stage Discharge



## River Severn at Montford Stage Discharge LDM2

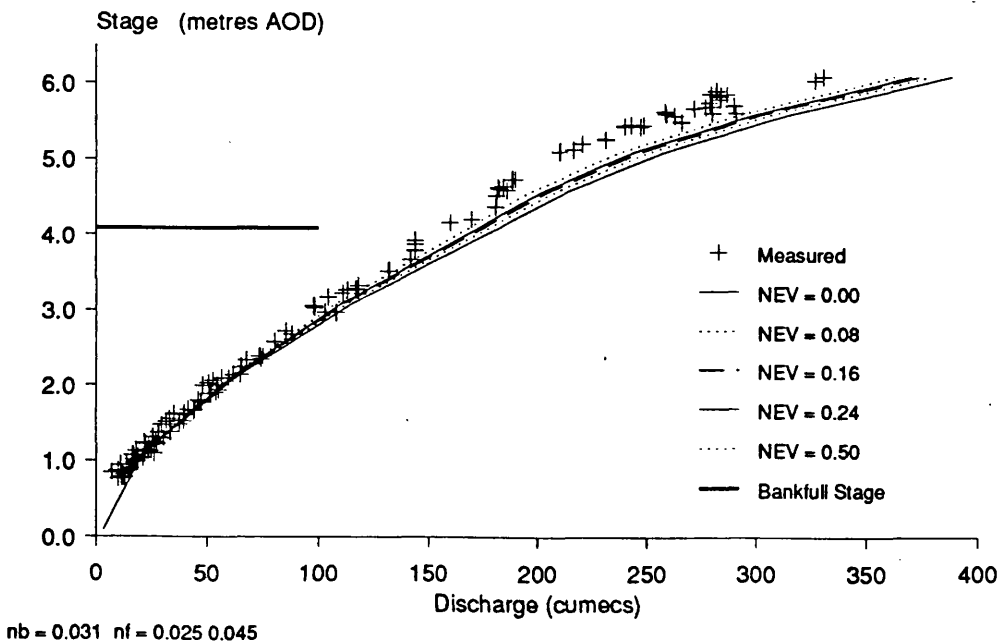
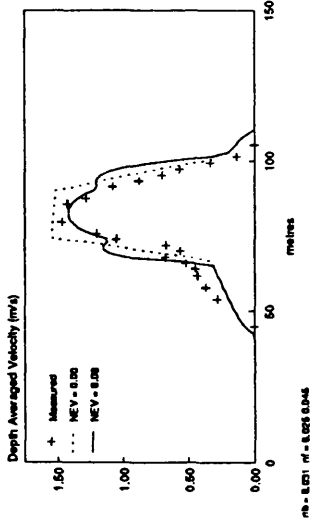
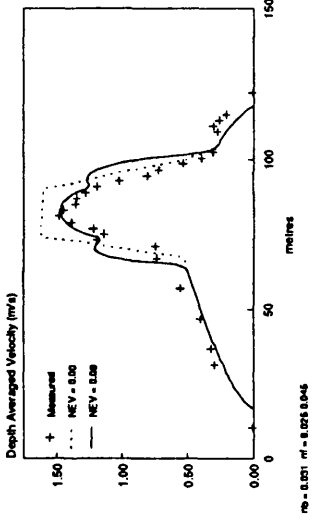


**Figure 4.35 Stage-discharge curves LDM and LDM2, Severn at Montford**

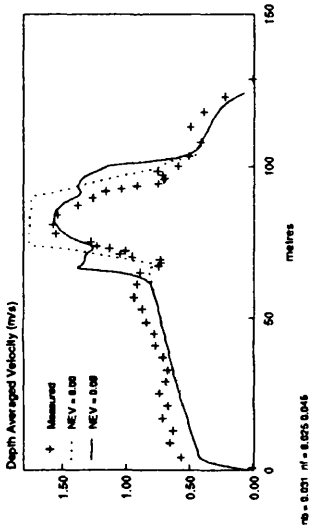
River Severn at Montford  
Velocity Distribution  
Stage = 4.73 m AOD



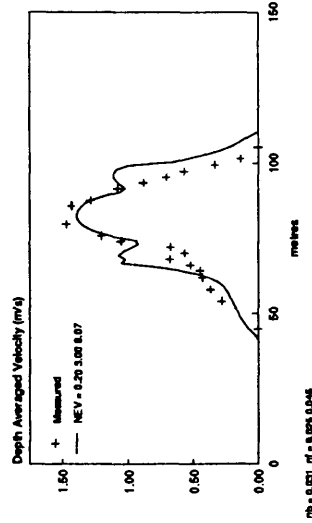
River Severn at Montford  
Velocity Distribution  
Stage = 5.20 m AOD



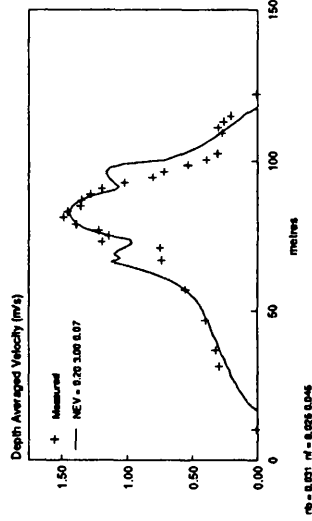
River Severn at Montford  
Velocity Distribution  
Stage = 6.087 m AOD



River Severn at Montford  
Velocity Distribution  
Stage = 4.73 m AOD



River Severn at Montford  
Velocity Distribution  
Stage = 5.20 m AOD



River Severn at Montford  
Velocity Distribution  
Stage = 6.087 m AOD

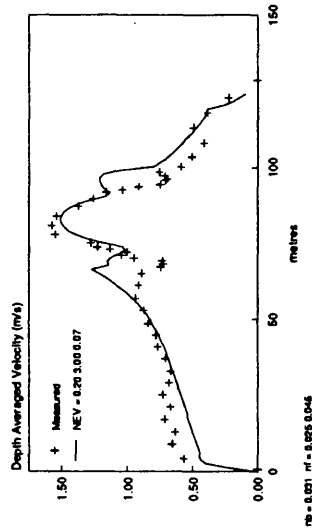
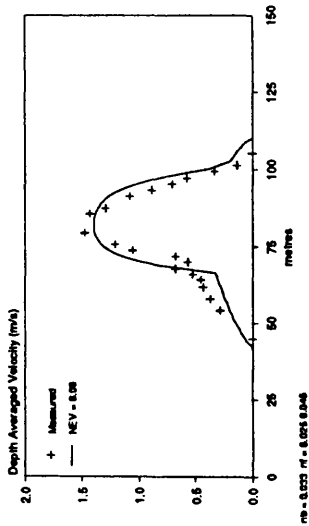
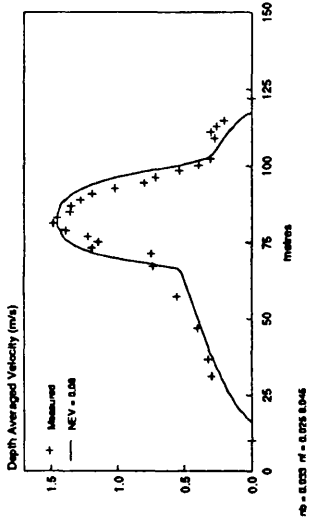


Figure 4.36 Velocity profiles fixed and variable NEV, Severn at Montford

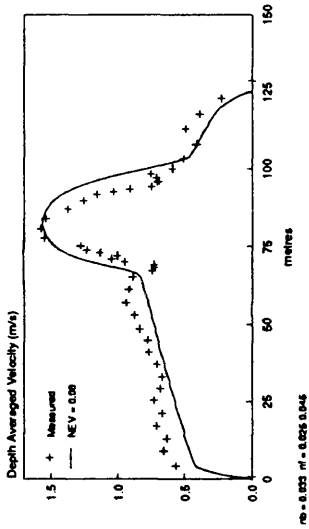
River Severn at Montford  
Velocity Distribution LDM2  
Stage = 4.73 m AOD



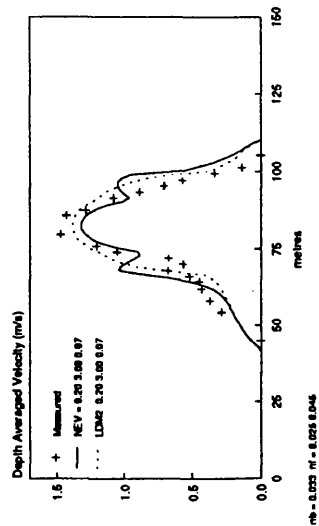
River Severn at Montford  
Velocity Distribution LDM2  
Stage = 5.20 m AOD



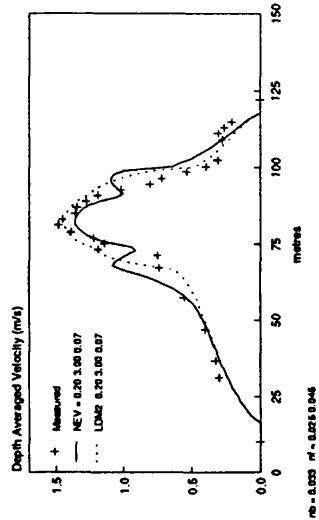
River Severn at Montford  
Velocity Distribution  
Stage = 6.087 m AOD



River Severn at Montford  
Velocity Distribution  
Stage = 4.73 m AOD



River Severn at Montford  
Velocity Distribution  
Stage = 5.20 m AOD



River Severn at Montford  
Velocity Distribution  
Stage = 6.087 m AOD

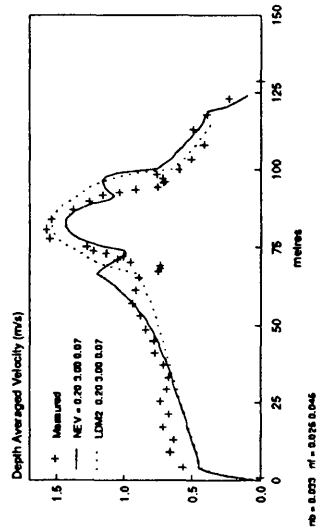
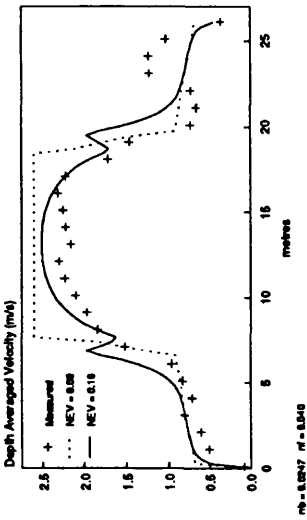
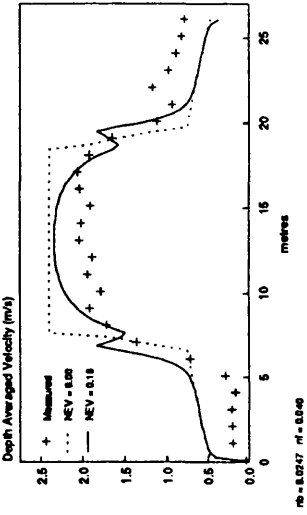


Figure 4.37 Velocity profiles fixed and variable NEV LDM2, Severn at Montford

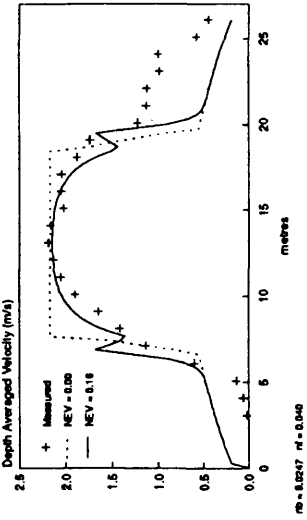
River Main Section 14  
Velocity Distribution  
Stage = 1.785m AGD



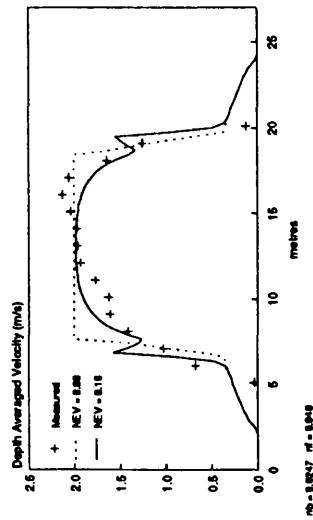
River Main Section 14  
Velocity Distribution  
Stage = 1.580m AGD



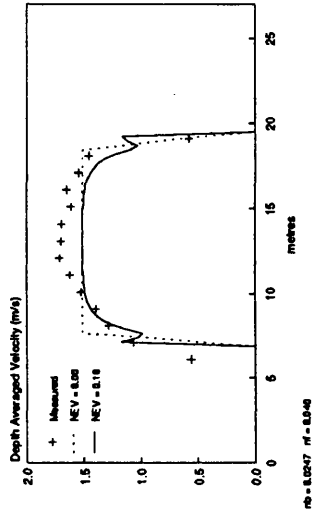
River Main Section 14  
Velocity Distribution  
Stage = 1.365m AGD



River Main Section 14  
Velocity Distribution  
Stage = 1.200m AGD



River Main Section 14  
Velocity Distribution  
Stage = 0.790m AGD



River Main Section 14  
Velocity Distribution  
Stage = 0.490m AGD

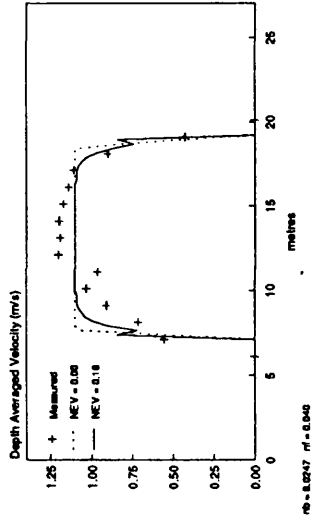
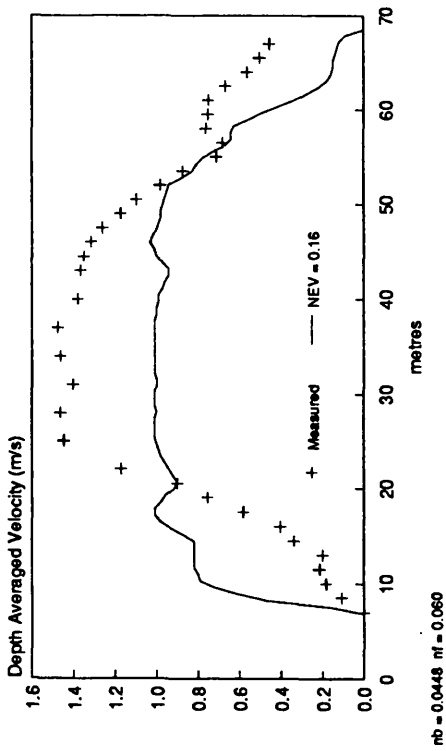
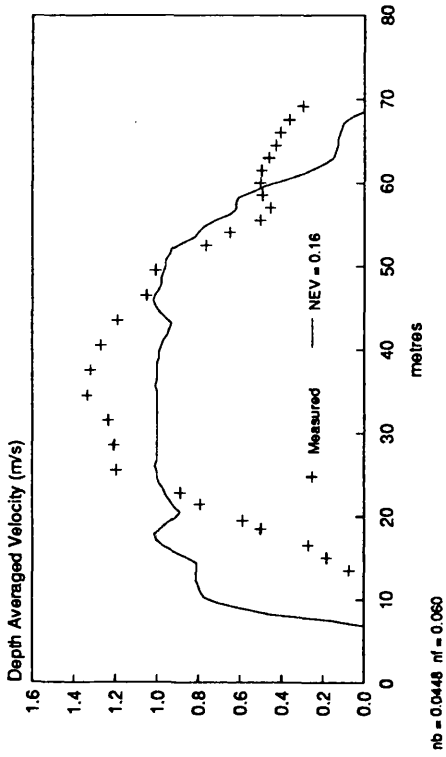


Figure 4.38 Velocity profiles River Main section 14

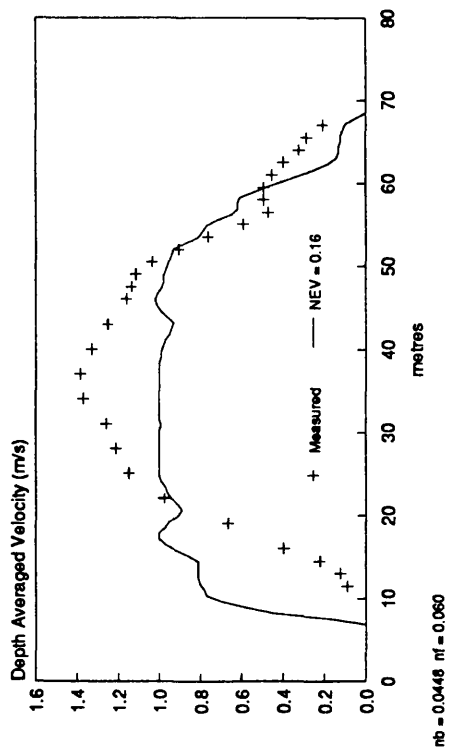
River Ouse at Skelton  
 Depth Averaged Velocity  
 Stage = 5.391m AGD



River Ouse at Skelton  
 Depth Averaged Velocity  
 Stage = 5.269m AGD



River Ouse at Skelton  
 Depth Averaged Velocity  
 Stage = 5.241m AGD



River Ouse at Skelton  
 Depth Averaged Velocity  
 Stage = 4.806m AGD

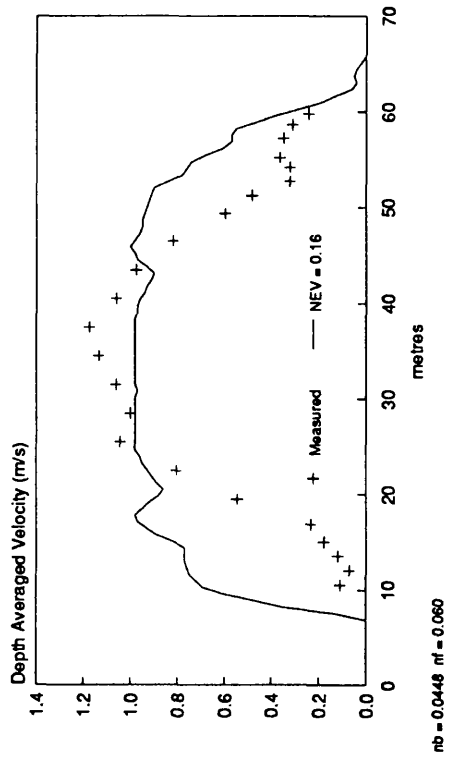
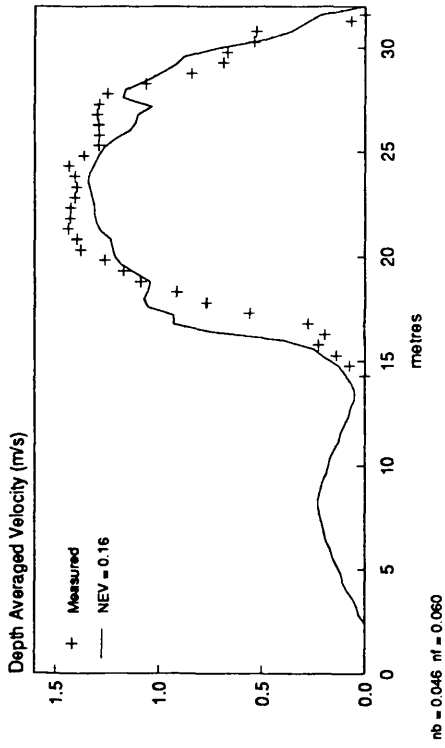


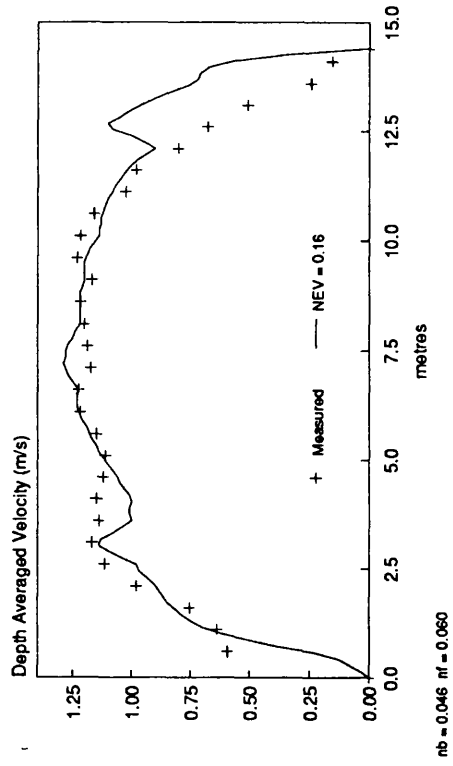
Figure 4.39 Velocity profiles River Ouse at skelton

RIVER PENK AT PENKRIDGE

Velocity Distribution  
Stage = 1.90m AGD

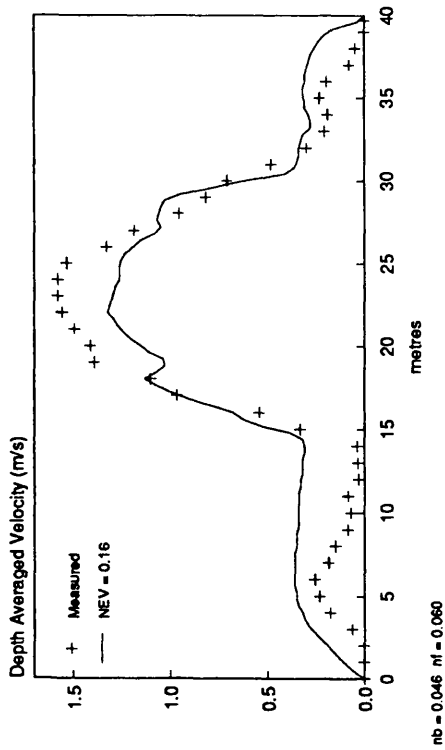


River Penk At Penkrige  
Velocity Distribution  
Stage = 1.66m AGD



RIVER PENK AT PENKRIDGE

Velocity Distribution  
Stage = 1.94m AGD



River Penk At Penkrige  
Velocity Distribution  
Stage = 1.84m AGD

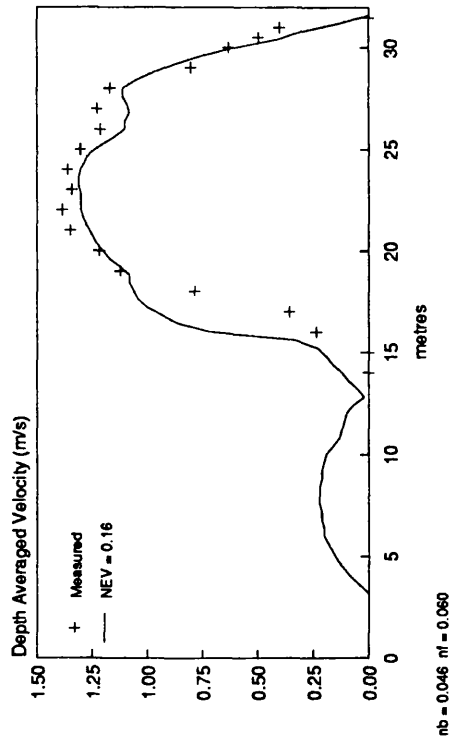


Figure 4.40 Velocity profiles River Penk at Penkridge

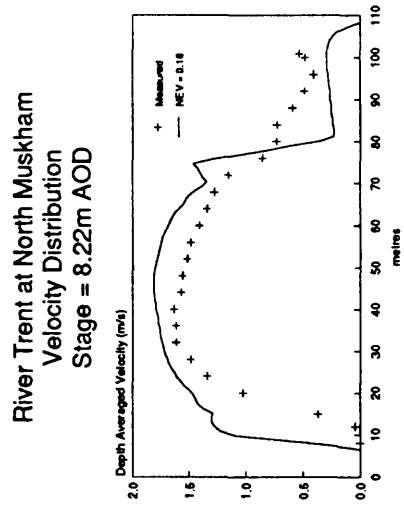
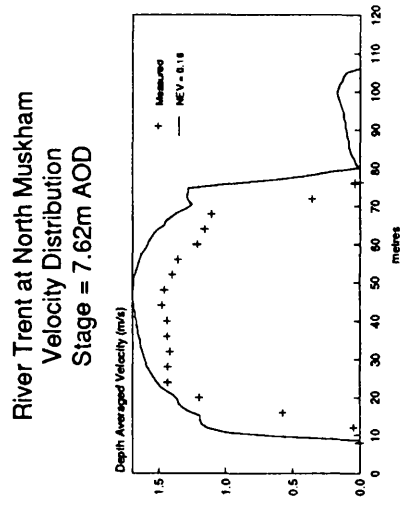
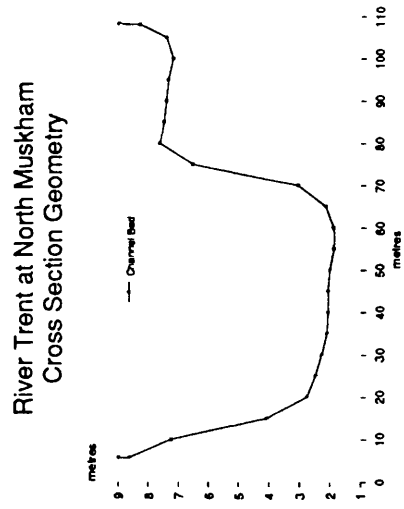
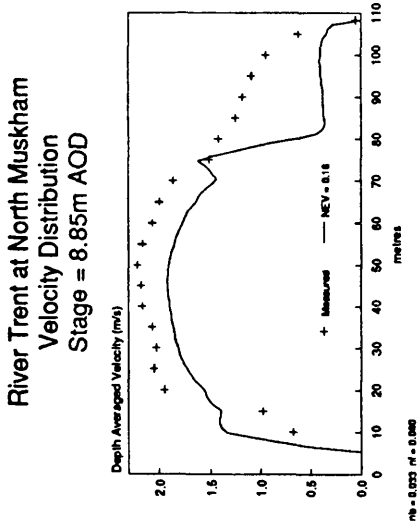
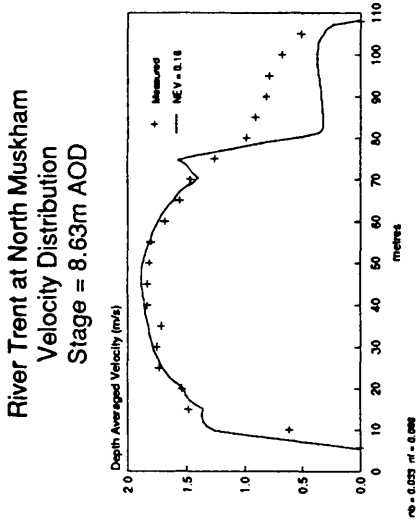
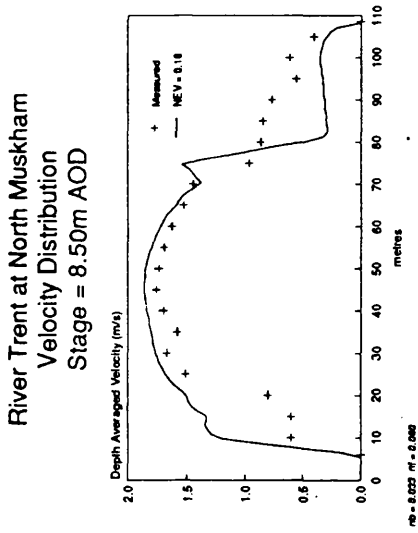


Figure 4.41 Velocity profiles River Trent at North Muskham, bankfull n values

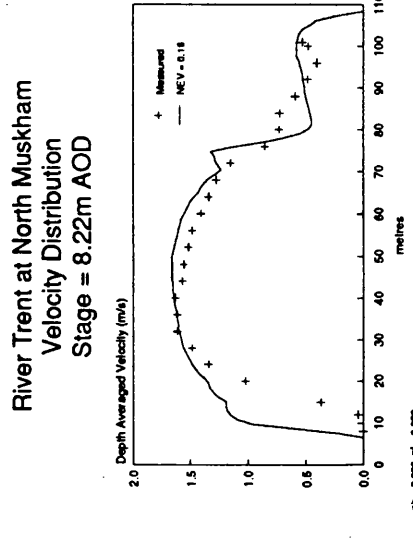
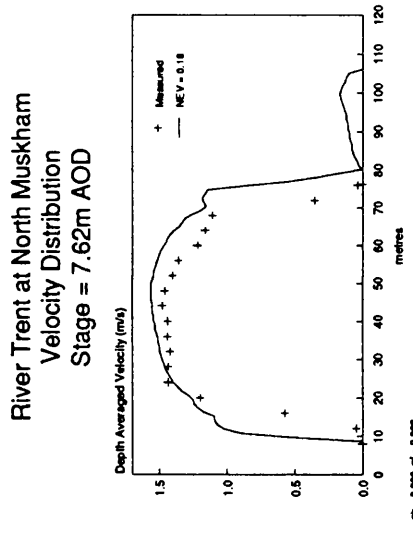
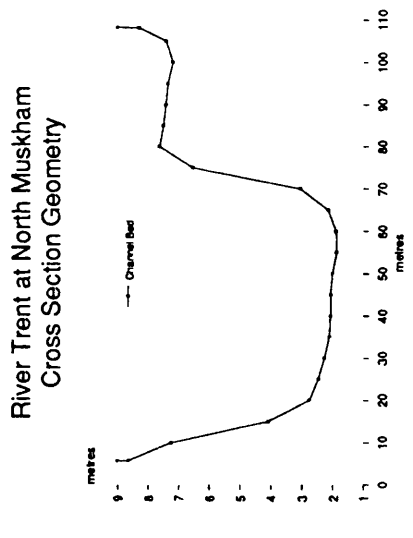
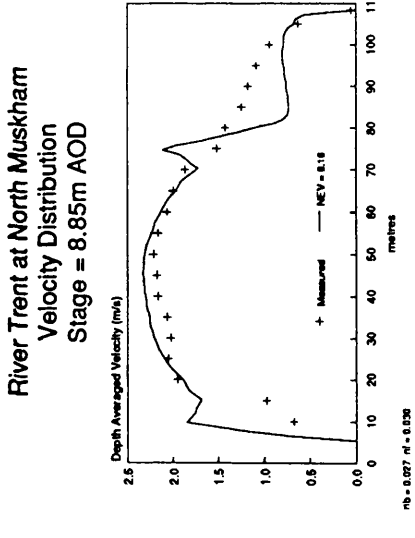
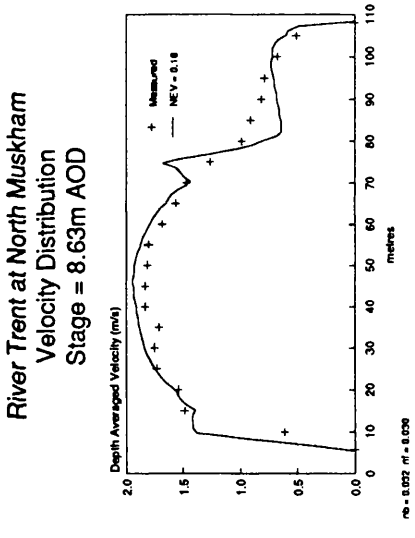
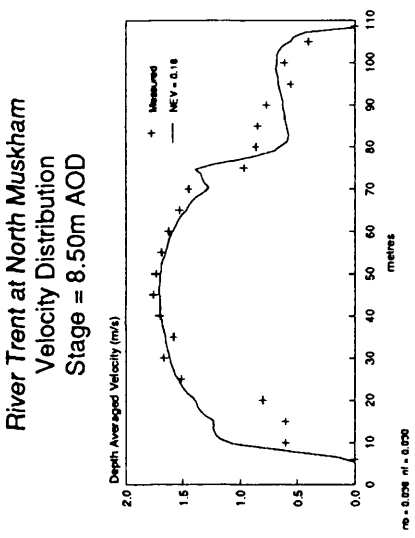
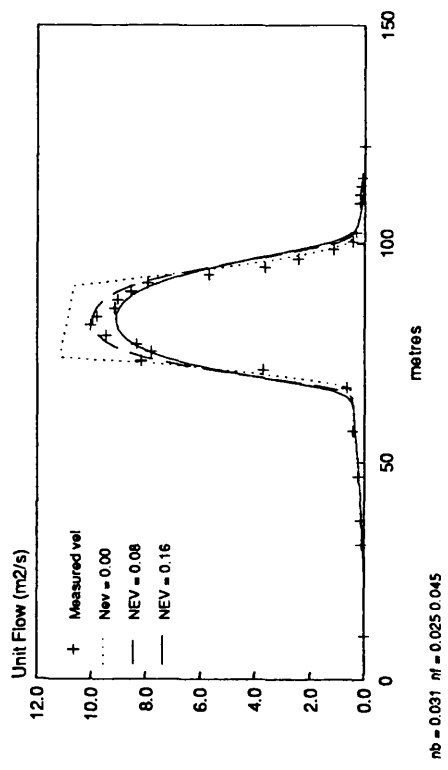
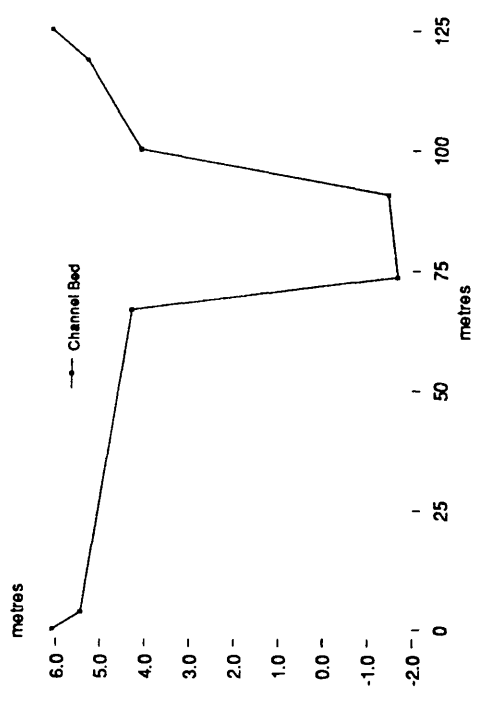


Figure 4.42 Velocity profiles River Trent at North Muskham, calibrated n values

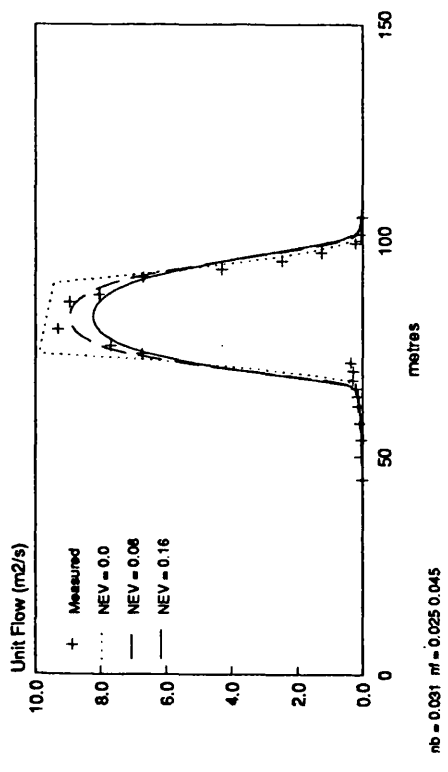
River Severn at Montford  
Unit Flow Distribution  
Stage = 5.20 m AOD



River Severn at Montford  
Cross Section Geometry



River Severn at Montford  
Unit Flow Distribution  
Stage = 4.73 m AOD



River Severn at Montford  
Unit Flow Distribution  
Stage = 6.087 m AOD

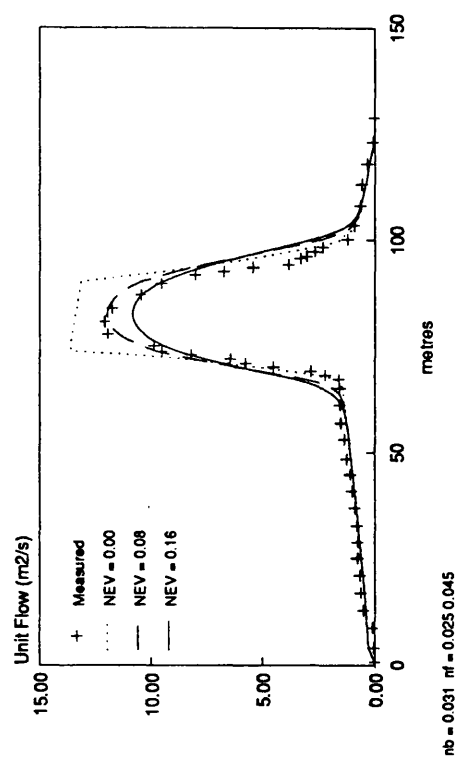
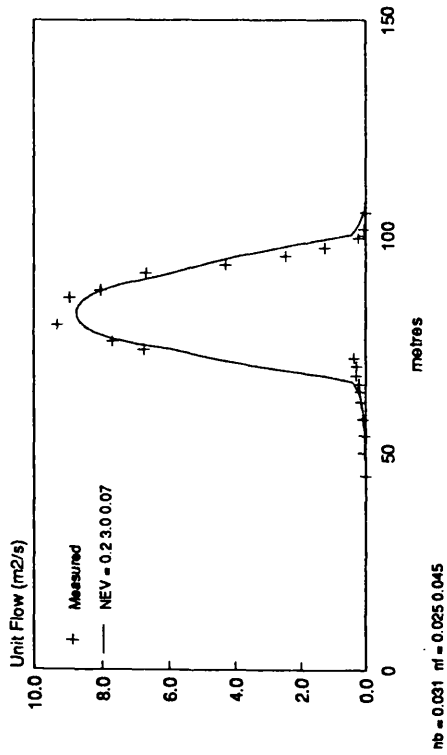
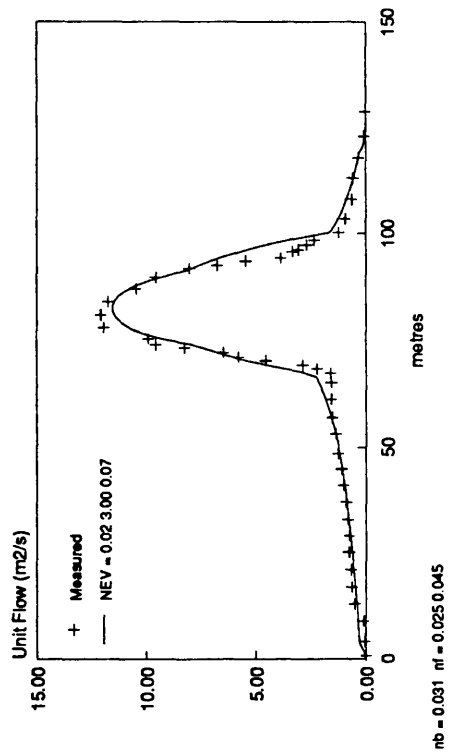


Figure 4.43 Unit flow profiles, fixed NEV, Severn at Montford

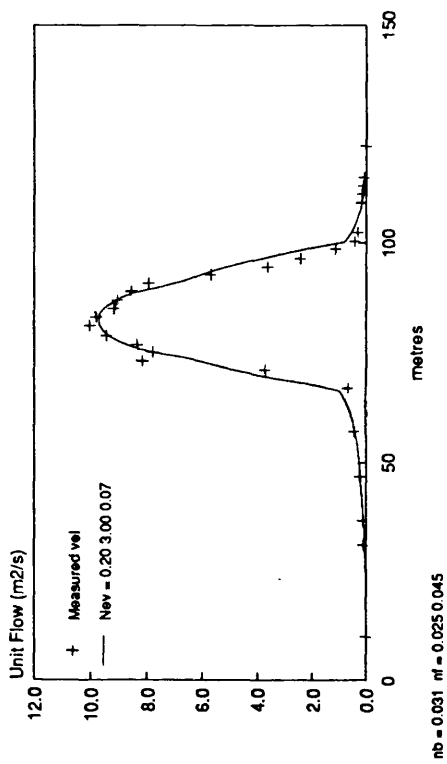
**River Severn at Montford  
Unit Flow Distribution  
Stage = 4.73 m AOD**



**River Severn at Montford  
Unit Flow Distribution  
Stage = 6.087 m AOD**



**River Severn at Montford  
Unit Flow Distribution  
Stage = 5.20 m AOD**



**River Severn at Montford  
Cross Section Geometry**

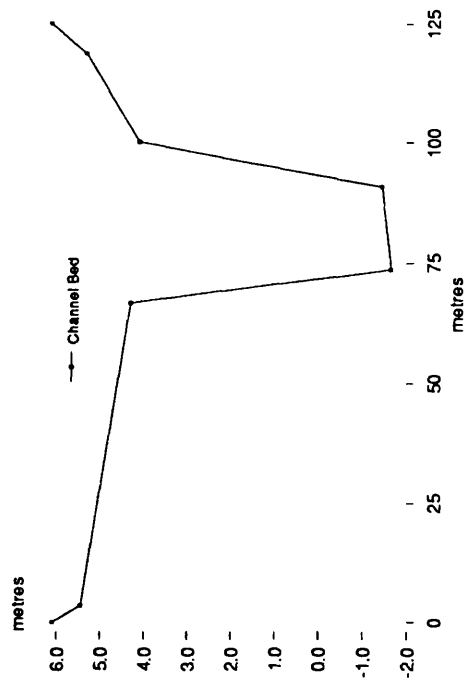
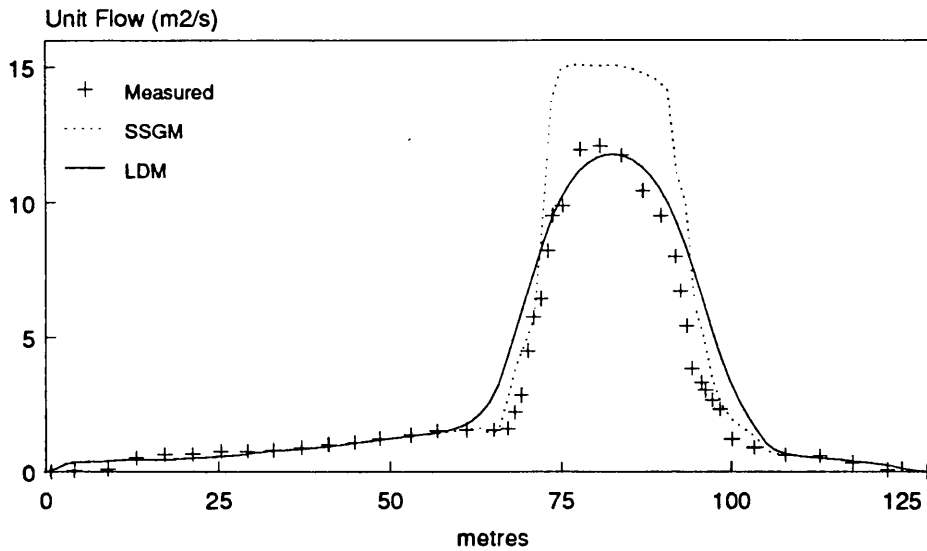


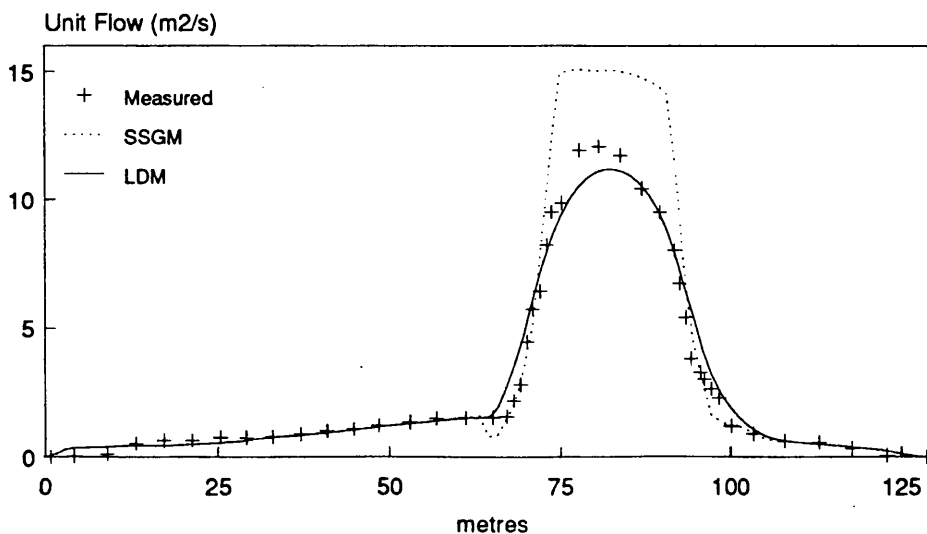
**Figure 4.44 Unit flow profiles, variable NEV, Severn at Montford**

## River Severn at Montford Unit Flow Distribution Stage = 6.087 m AOD



nb = 0.028 nf = 0.023 0.040

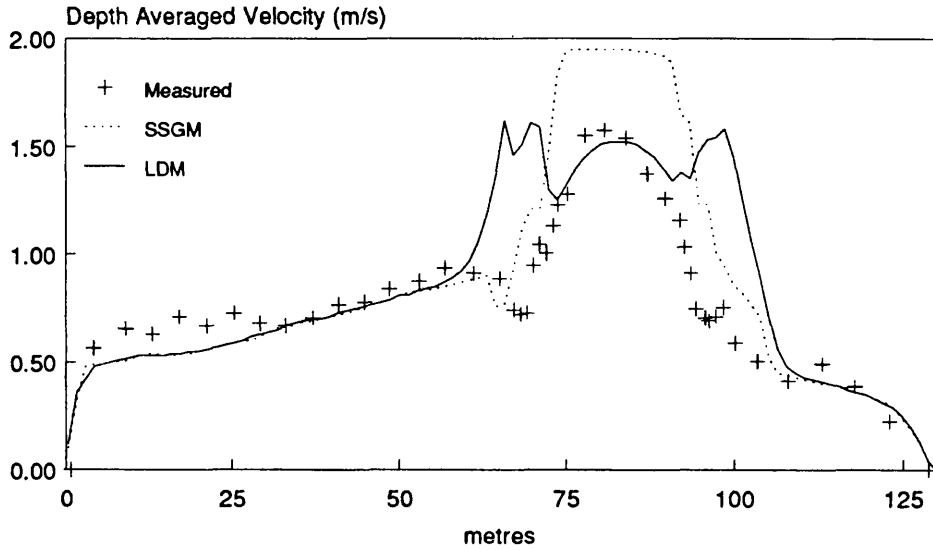
## River Severn at Montford Unit Flow Distribution Stage = 6.087 m AOD



nb = 0.028 nf = 0.023 0.040  
n varied on channel banks

**Figure 4.45 Unit flow profiles, n constant and variable, Severn at Montford**

## River Severn at Montford Velocity Distribution Stage = 6.087 m AOD



## River Severn at Montford Velocity Distribution Stage = 6.087 m AOD

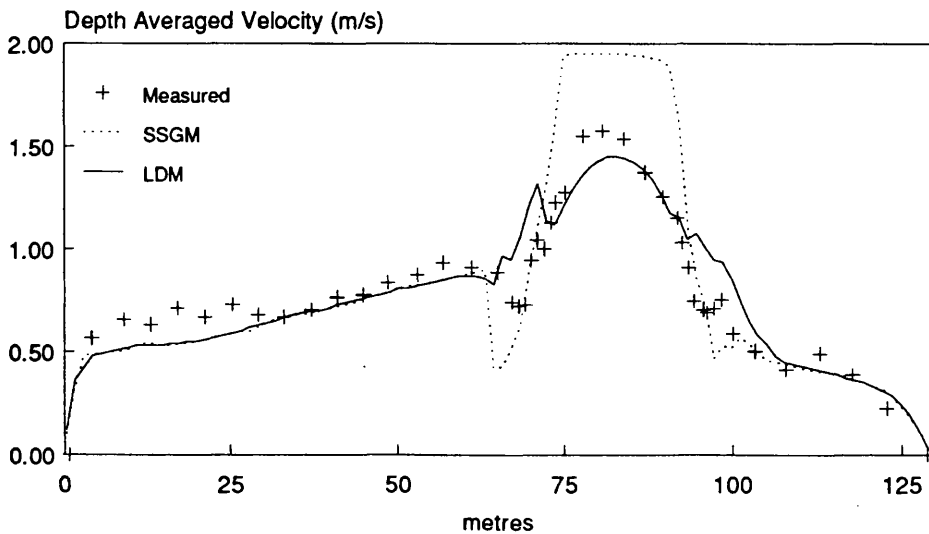
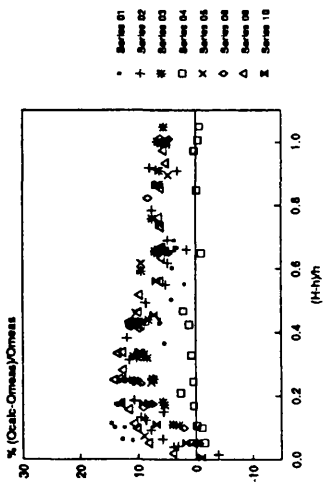
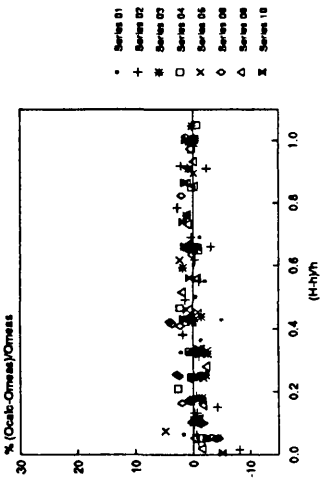


**Figure 4.46** Depth averaged velocities, n constant and variable, Severn at Montford

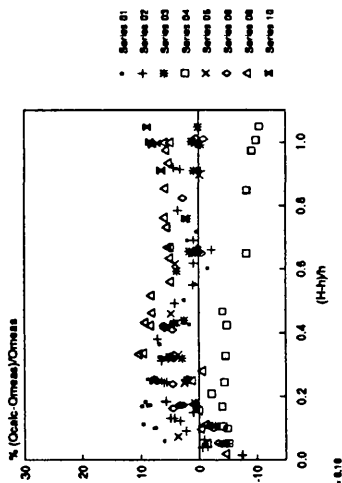
Divided Channel Method2  
SERC Flume Smooth Case



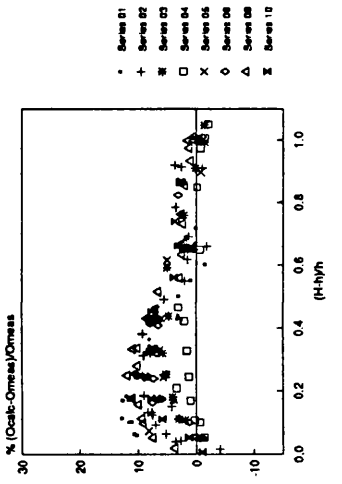
Ackers Method  
SERC Flume Smooth Case



Lateral Distribution Method  
SERC Flume Smooth Case



Divided Channel Method  
SERC Flume Smooth Case



Single Channel Method  
SERC Flume Smooth Case

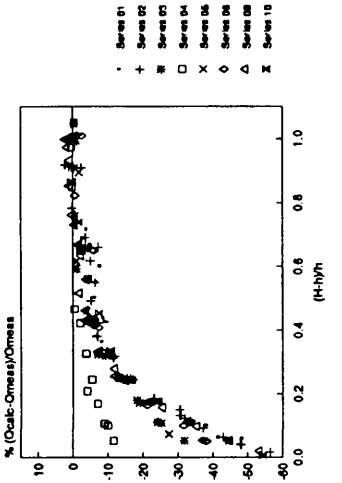
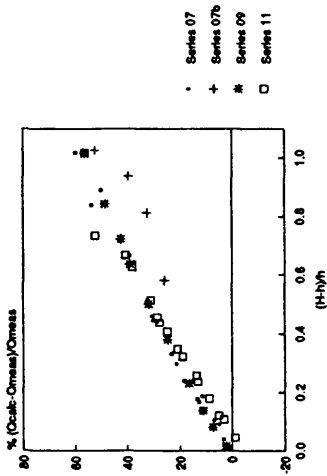
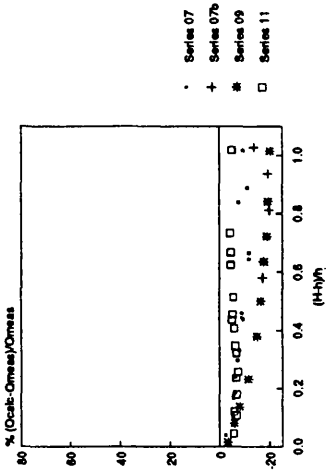


Figure 4.47 Errors in calculated discharges SERC FCF Phase A, Smooth data

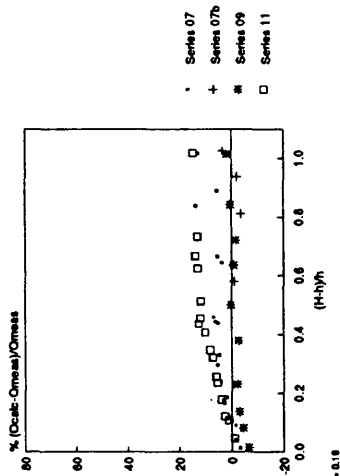
Divided Channel Method2  
SERC Flume Rough Case



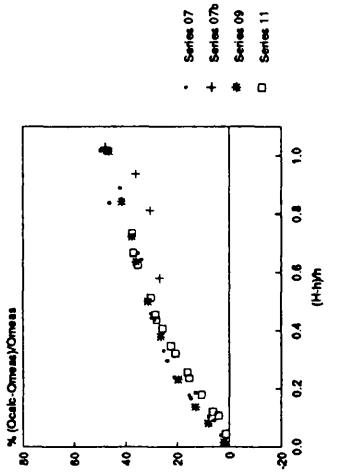
Ackers Method  
SERC Flume Rough Case



Lateral Distribution Method  
SERC Flume Rough Case



Divided Channel Method  
SERC Flume Rough Case



Single Channel Method  
SERC Flume Rough Case

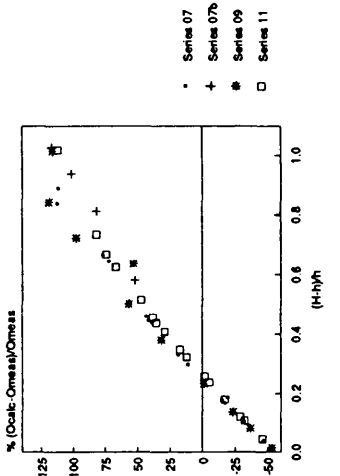
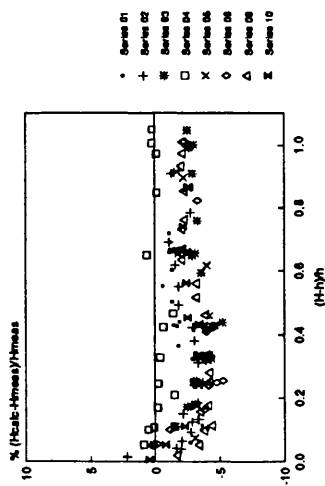
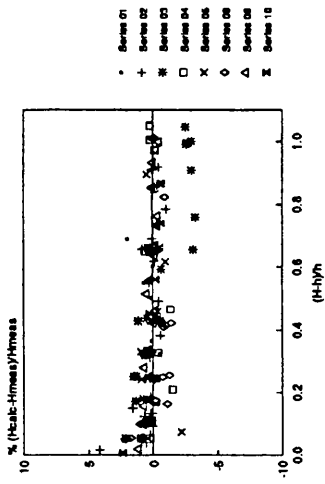


Figure 4.48 Errors in calculated discharges SERC FCF Phase A, Rough data

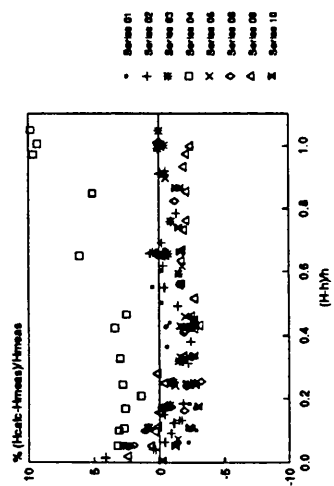
Divided Channel Method2  
SERC Flume Smooth Case



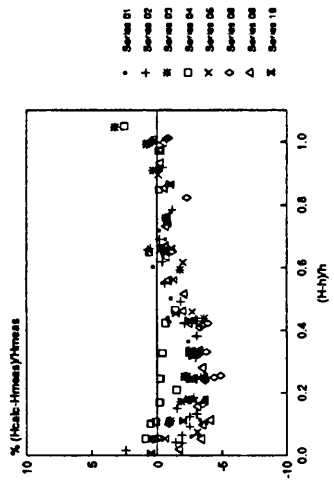
Ackers Method  
SERC Flume Smooth Case



Lateral Distribution Method  
SERC Flume Smooth Case



Divided Channel Method  
SERC Flume Smooth Case



Single Channel Method  
SERC Flume Smooth Case

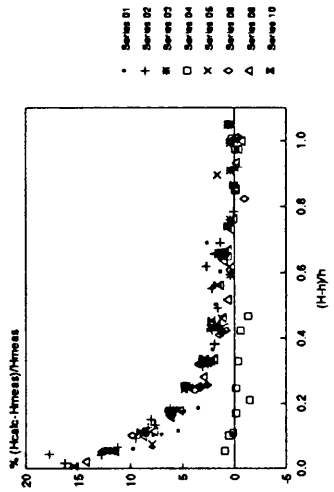
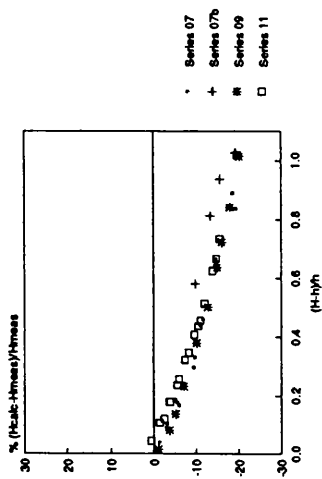


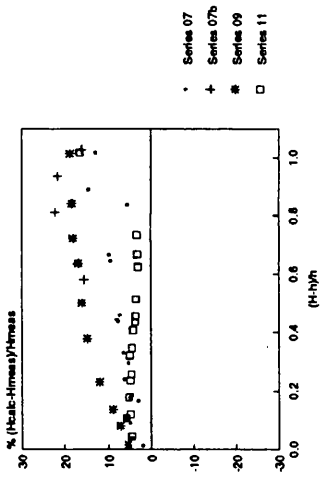
Figure 4.49 Errors in calculated depths SERC FCF Phase A, Smooth data

NEV-0118

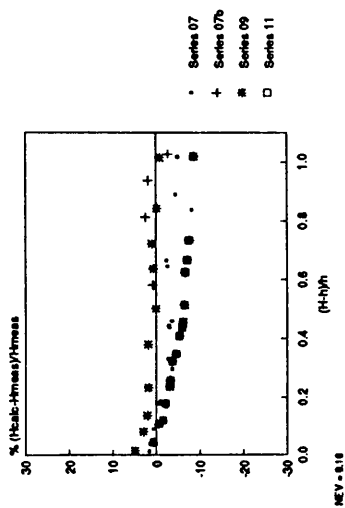
Divided Channel Method2  
SERC Flume Rough Case



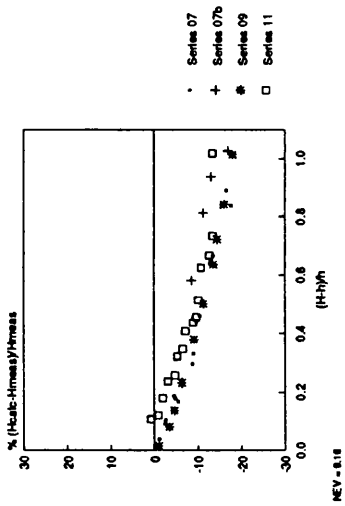
Ackers Method  
SERC Flume Rough Case



Lateral Distribution Method  
SERC Flume Rough Case



Divided Channel Method  
SERC Flume Rough Case



Single Channel Method  
SERC Flume Rough Case

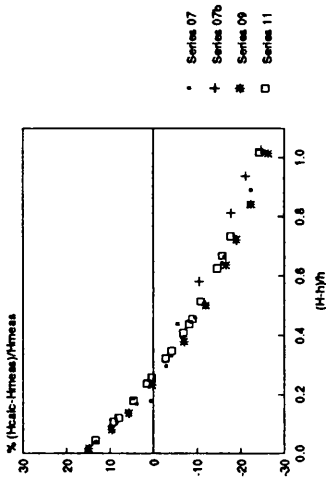
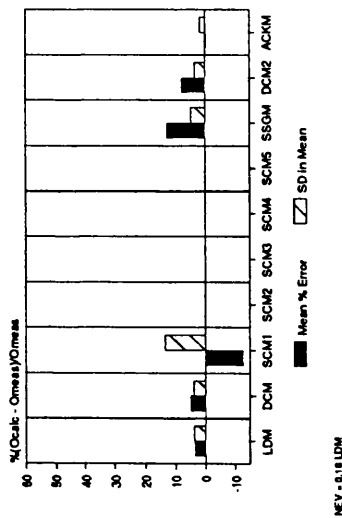
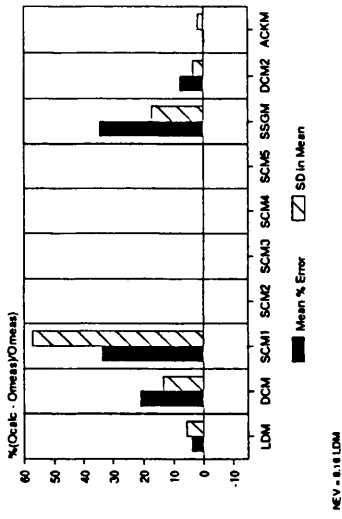


Figure 4.50 Errors in calculated depths SERC FCF Phase A, Rough data

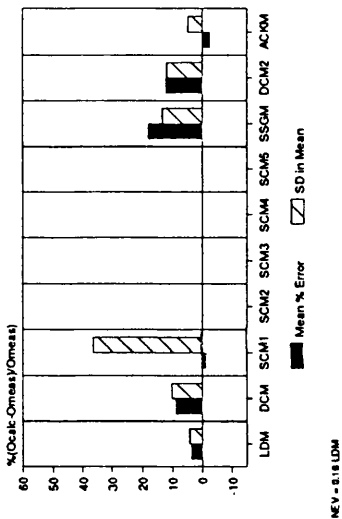
Mean % Errors in Calculated Flows  
SERC Flume Smooth Case (149)



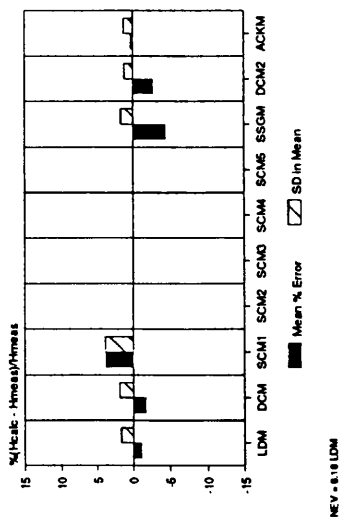
Mean % Errors in Calculated Flows  
SERC Flume Rough Case (48)



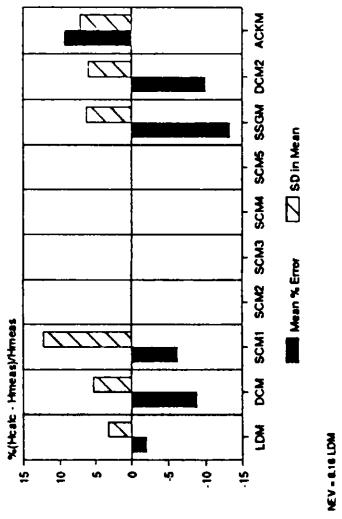
Mean % Errors in Calculated Flows  
SERC Flume Smooth and Rough (197)



Mean % Errors in Calculated Depth  
SERC Flume Smooth Case (149)



Mean % Errors in Calculated Depths  
SERC Flume Rough Case (48)



Mean % Errors in Calculated Depth  
SERC Flume Smooth and Rough (197)

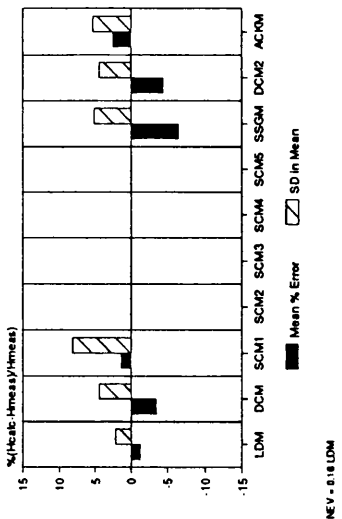
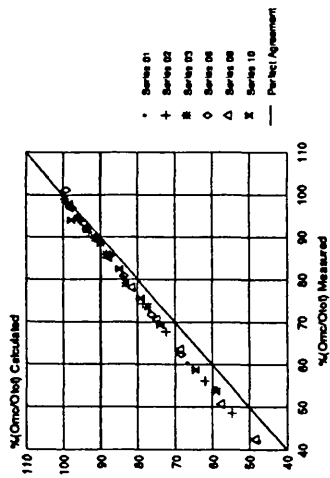
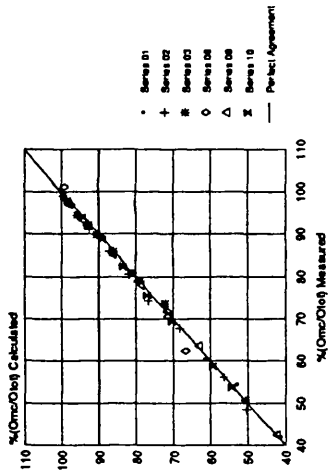


Figure 4.51 Mean errors in discharge and depth SERC FCF Phase A

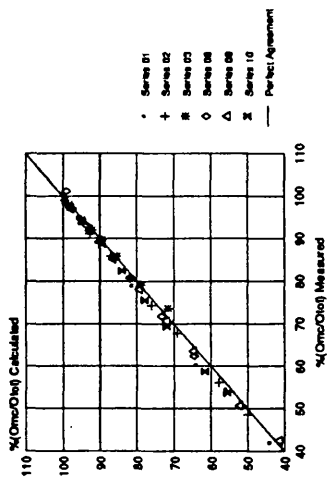
Divided Channel Method 2  
SERC Flume Smooth Case



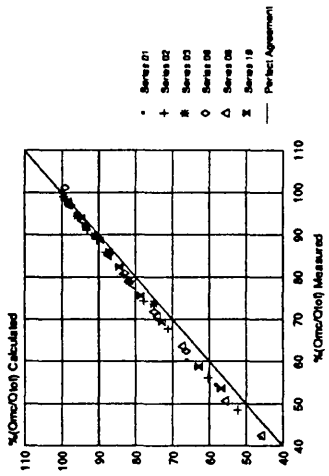
Ackers Method  
SERC Flume Smooth Case



Lateral Distribution Method NEV = 0.16  
SERC Flume Smooth Case



Divided Channel Method  
SERC Flume Smooth Case



Sum of Segments Method  
SERC Flume Smooth Case

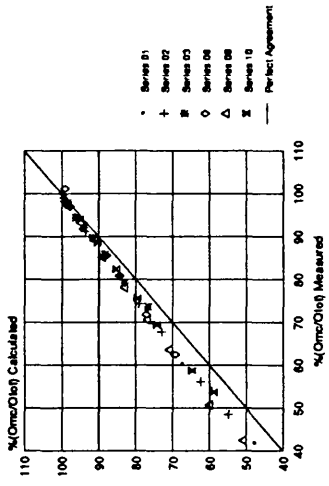
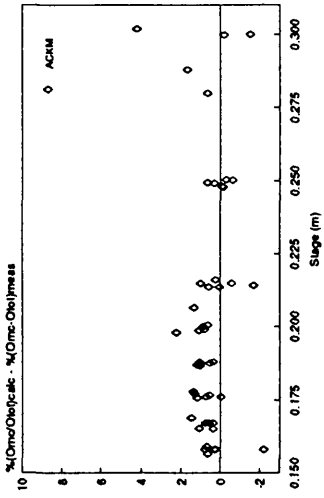
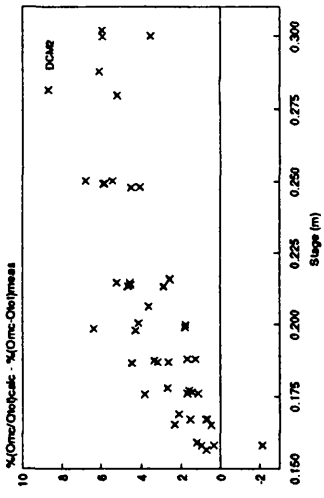


Figure 4.52 Proportion of flow in main channel, SERC FCF Phase A

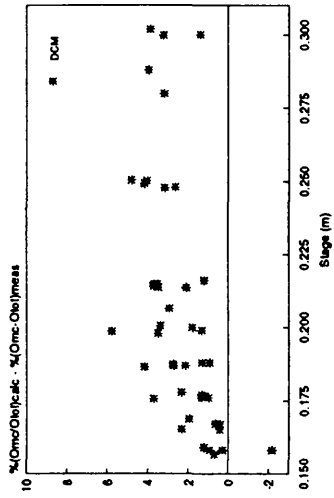
Differences in Qmc Calc and Meas  
SERC Flume Smooth Case ACKM



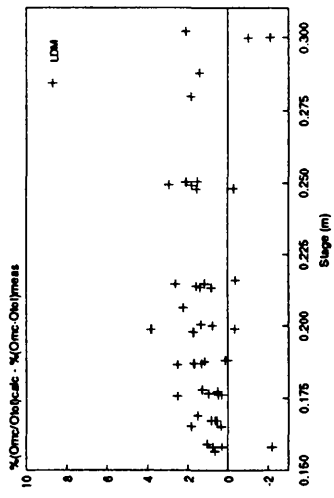
Differences in Qmc Calc and Meas  
SERC Flume Smooth Case DCM2



Differences in Qmc Calc and Meas  
SERC Flume Smooth Case DCM



Differences in Qmc Calc and Meas  
SERC Flume Smooth Case LDM



Differences in Qmc Calc and Meas  
SERC Flume Smooth Case

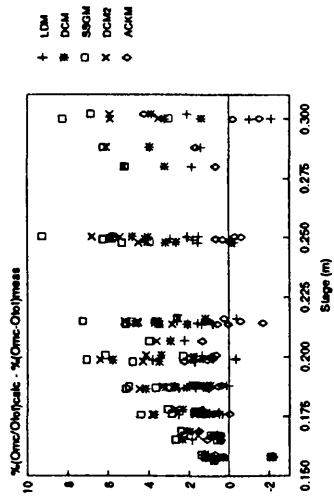
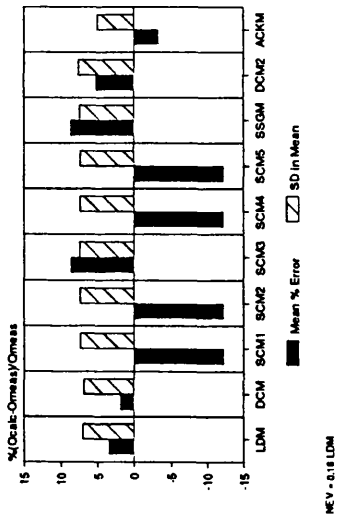
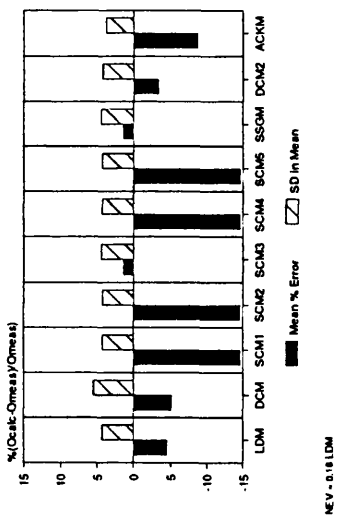


Figure 4.53 Differences in calculated and measured proportions of flow in main channel, SERC FCF Phase A

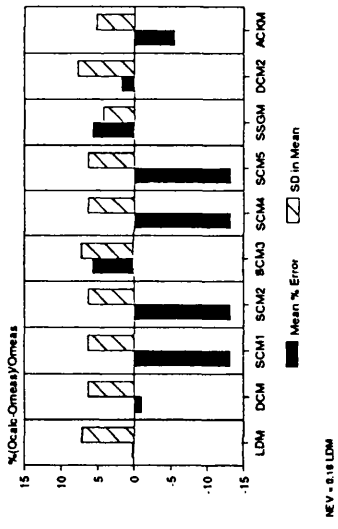
Mean % Errors in Calculated Flows  
Myers Laboratory Flume Series A



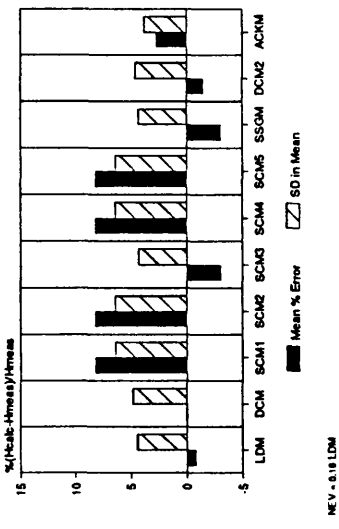
Mean % Errors in Calculated Flows  
Myers Laboratory Flume Series F



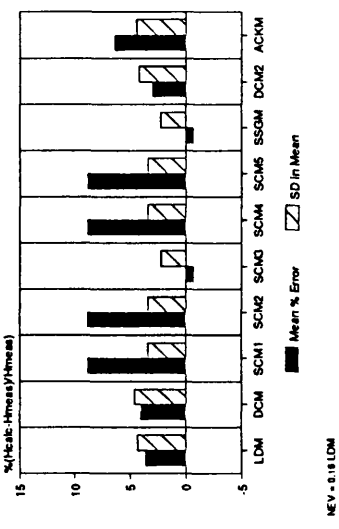
Mean % Errors in Calculated Flows  
Myers Laboratory Flume Series A and F



Mean % Errors in Calculated Depth  
Myers Laboratory Flume Series A



Mean % Errors in Calculated Depth  
Myers Laboratory Flume Series F



Mean % Errors in Calculated Depth  
Myers Laboratory Flume Series A and F

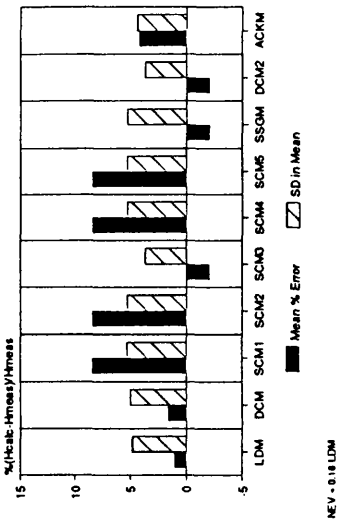
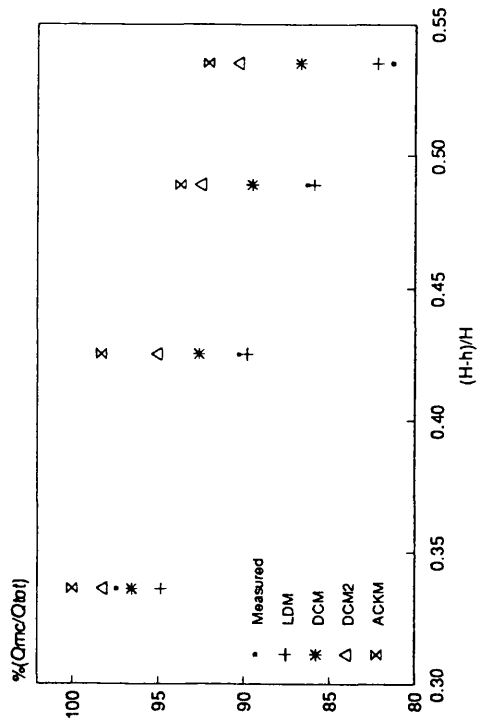
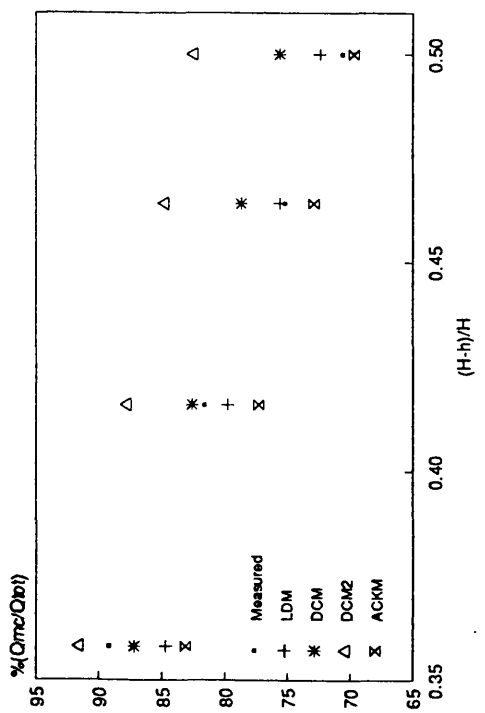
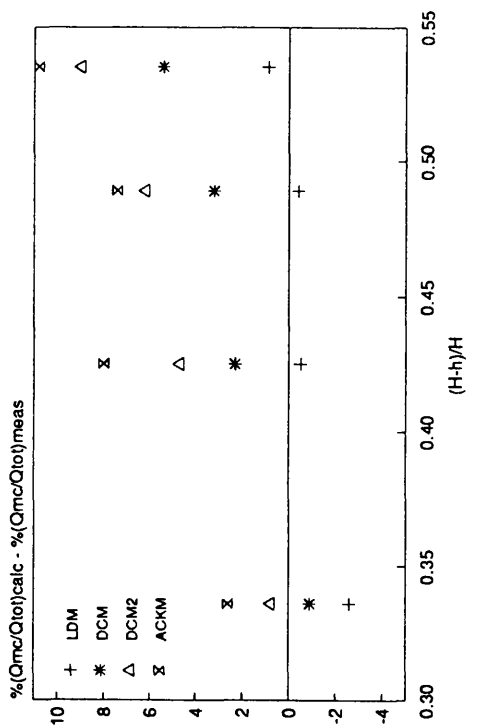


Figure 4.54 Mean errors in discharge and depth Myers' lab data



Differences in Qmc Calc and Meas  
Myers Laboratory Flume Series F



Differences in Qmc Calc and Meas  
Myers Laboratory Flume Series A

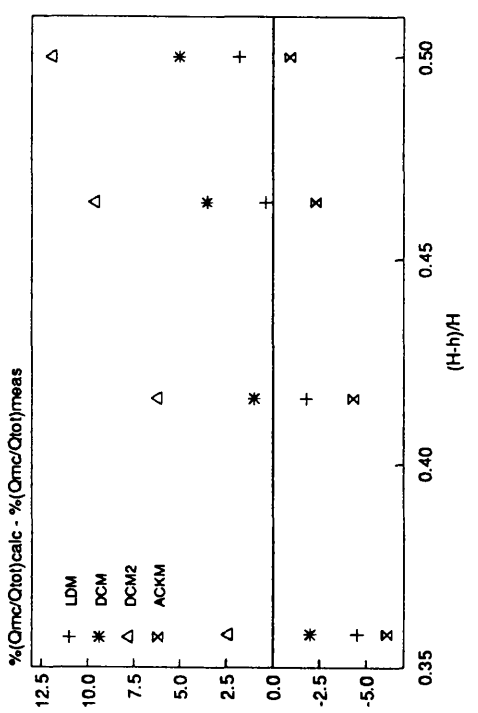


Figure 4.55 Differences in calculated and measured proportions of flow in main channel, Myers' lab data

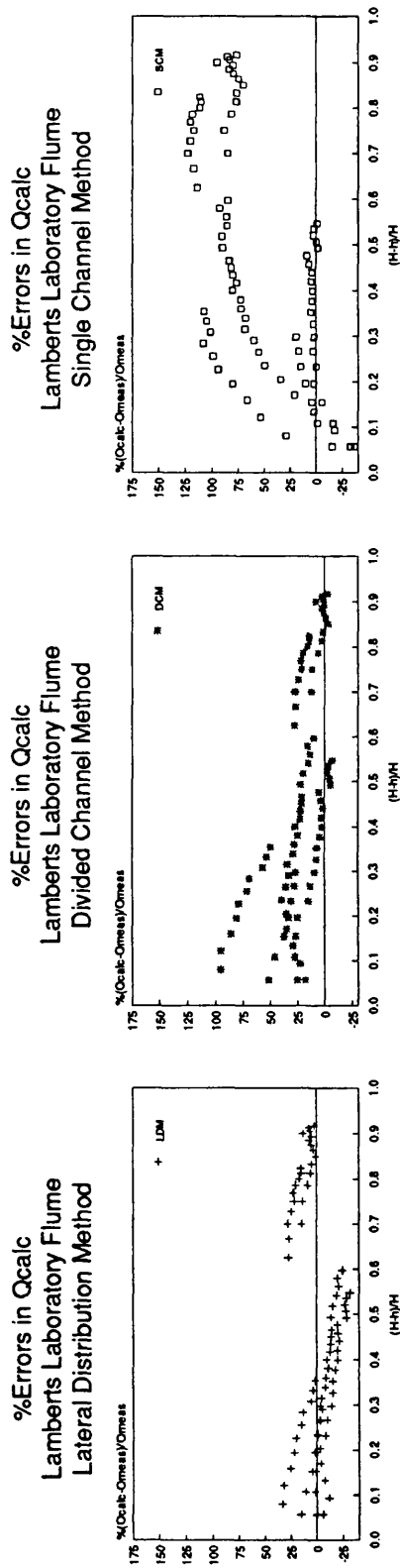
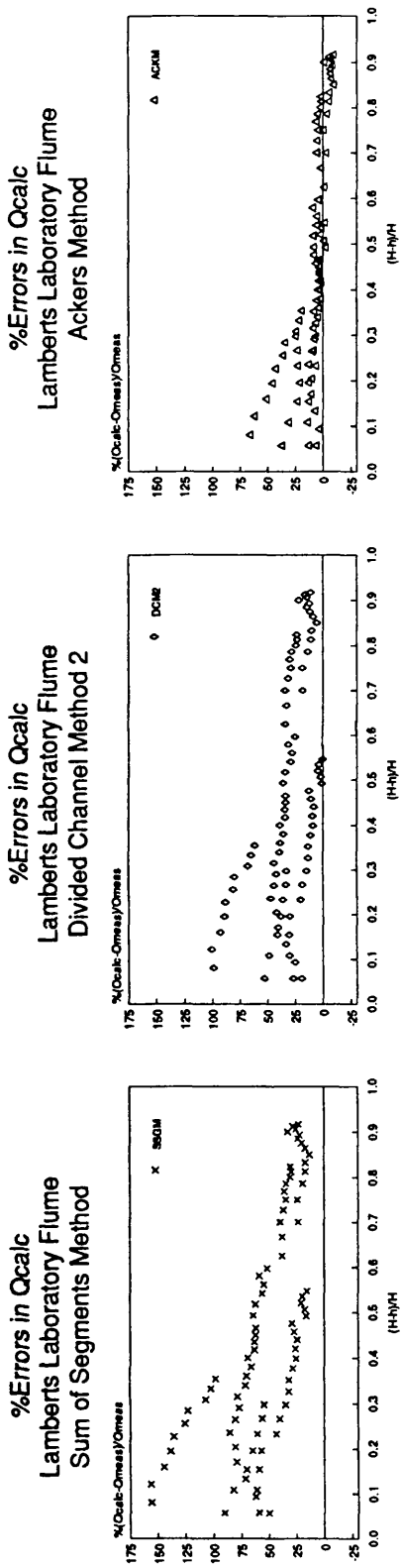
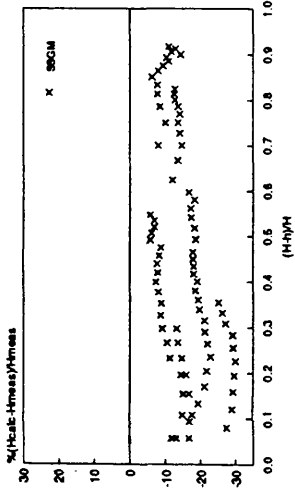
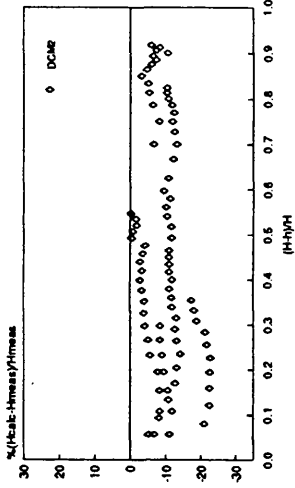


Figure 4.56 Errors in calculated discharges Lambert's lab data

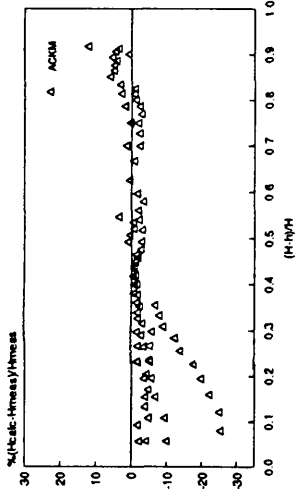
**%Errors in Hcalc  
Lamberts Laboratory Flume  
Sum of Segments Method**



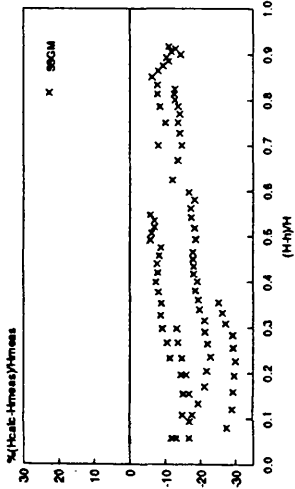
**%Errors in Hcalc  
Lamberts Laboratory Flume  
Divided Channel Method 2**



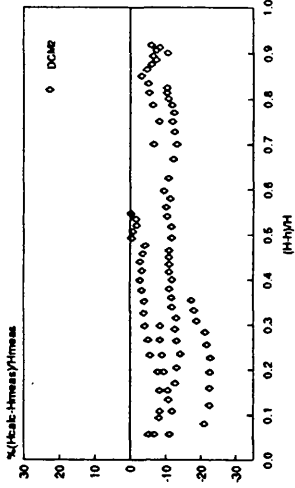
**%Errors in Hcalc  
Lamberts Laboratory Flume  
Ackers Method**



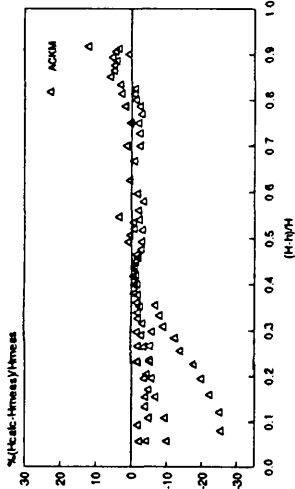
**%Errors in Hcalc  
Lamberts Laboratory Flume  
Lateral Distribution Method**



**%Errors in Hcalc  
Lamberts Laboratory Flume  
Single Channel Method**



**%Errors in Hcalc  
Lamberts Laboratory Flume  
DCM**



**%Errors in Hcalc  
Lamberts Laboratory Flume  
LDM**

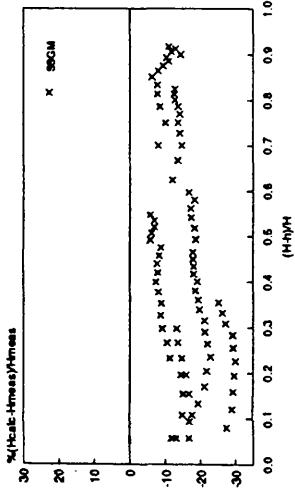
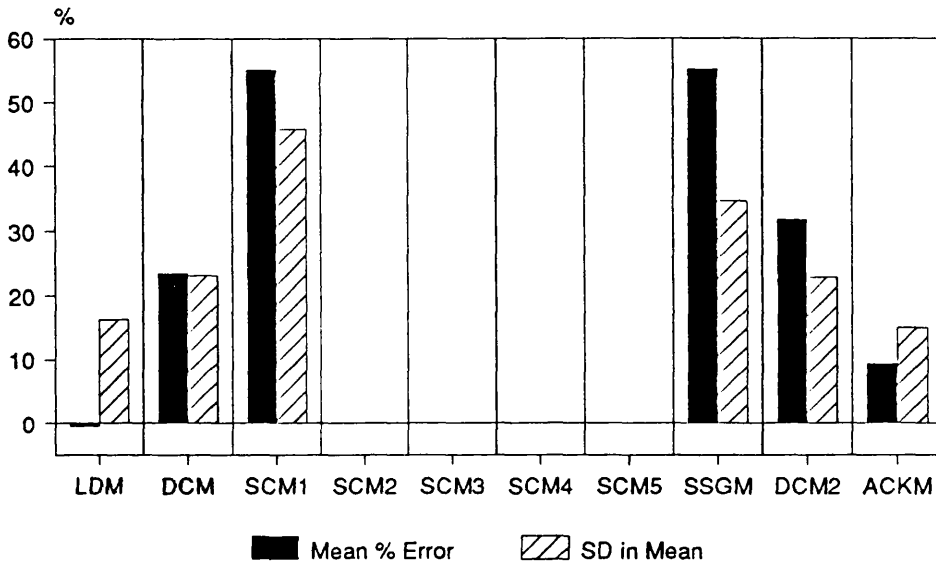


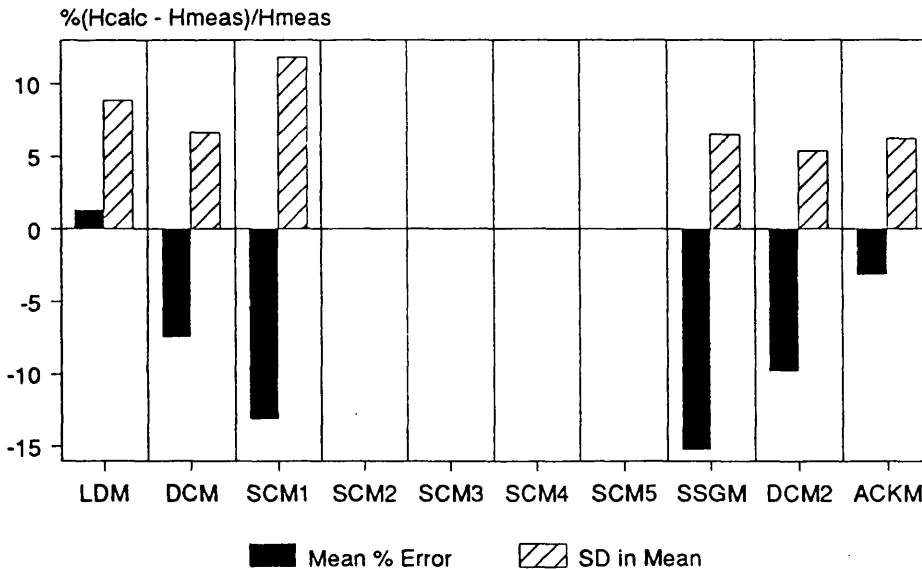
**Figure 4.57 Errors in calculated depths Lambert's lab data**

## Mean % Errors in Calculated Flows Lamberts Laboratory Flume All Data (85)



NEV = 0.16 LDM

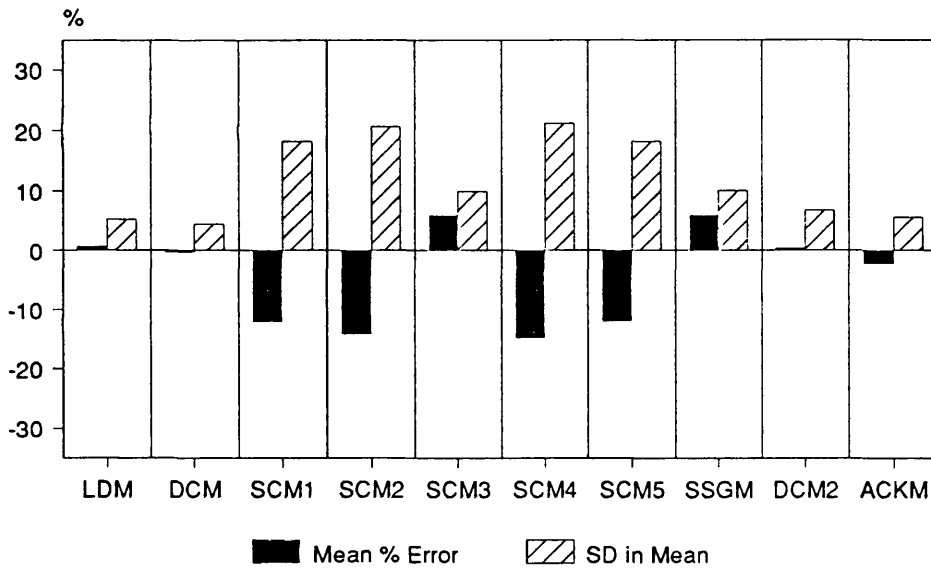
## Mean % Errors in Calculated Depth Lamberts Laboratory Flume All Data (85)



NEV = 0.16 LDM

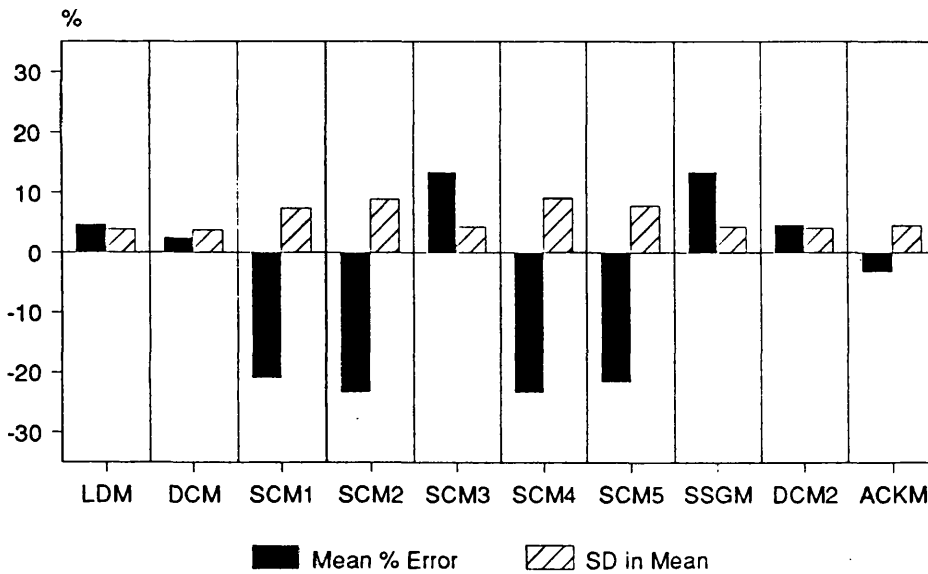
**Figure 4.58 Mean errors in discharge and depth Lambert's lab data**

## Mean % Errors in Calculated Flows River Data Authors n Values



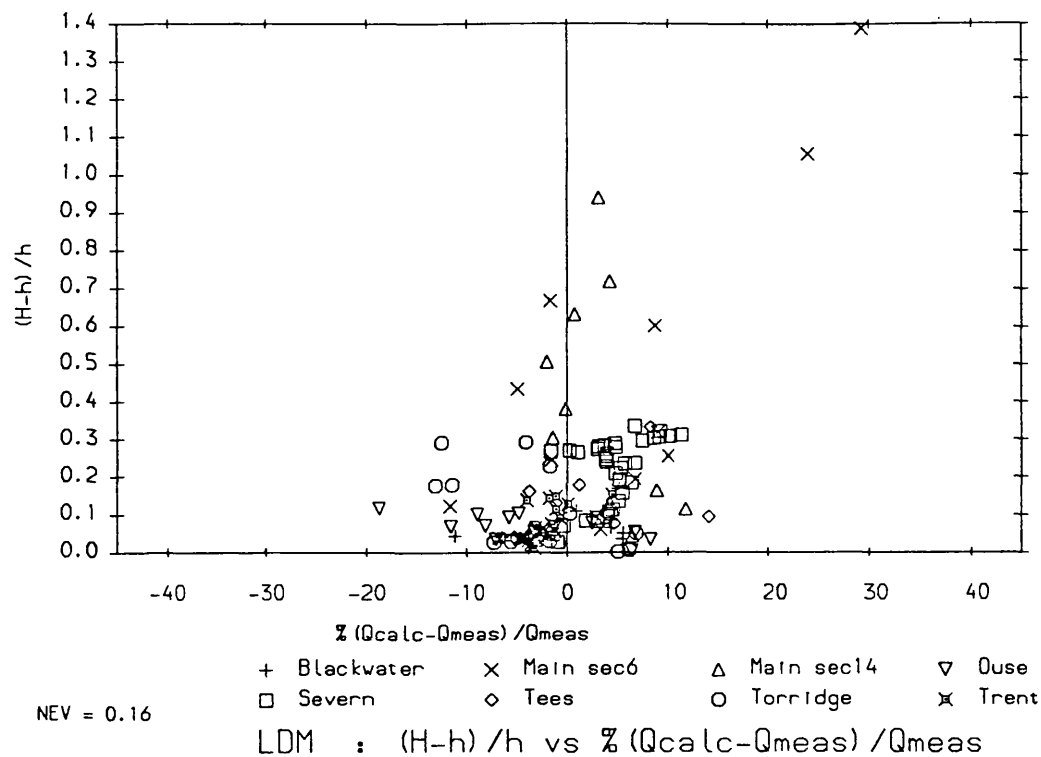
NEV = 0.16 LDM

## Mean % Errors in Calculated Flows River Data Ackers n Values

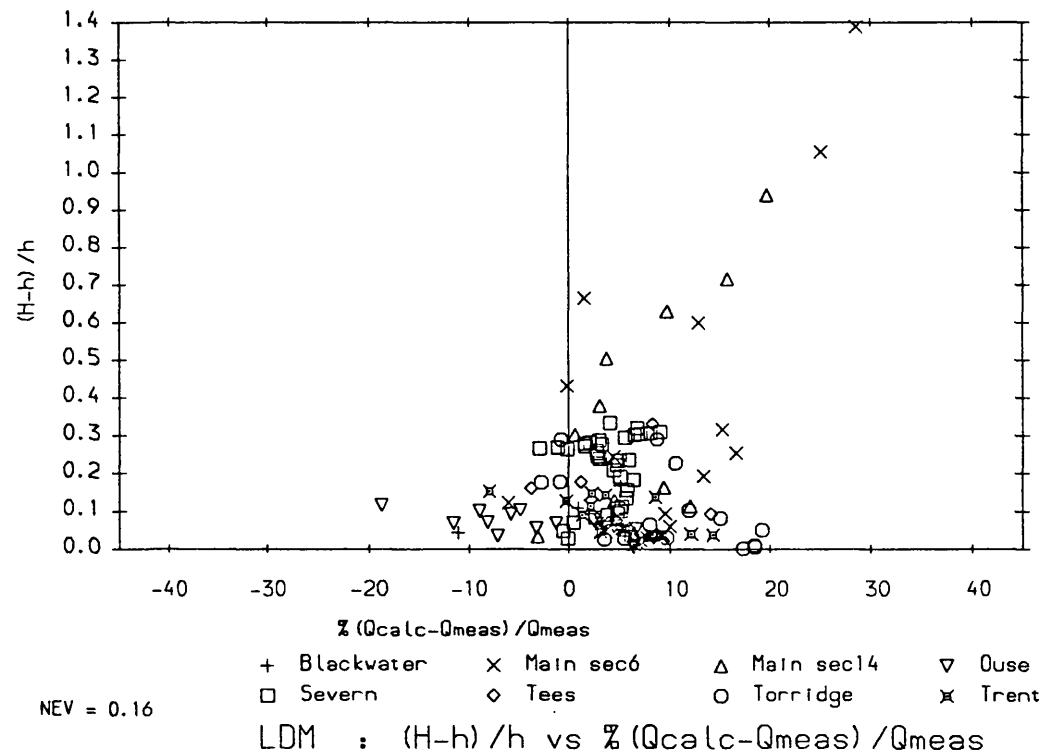


NEV = 0.16 LDM

**Figure 4.59 Mean errors in discharge river gauging data**

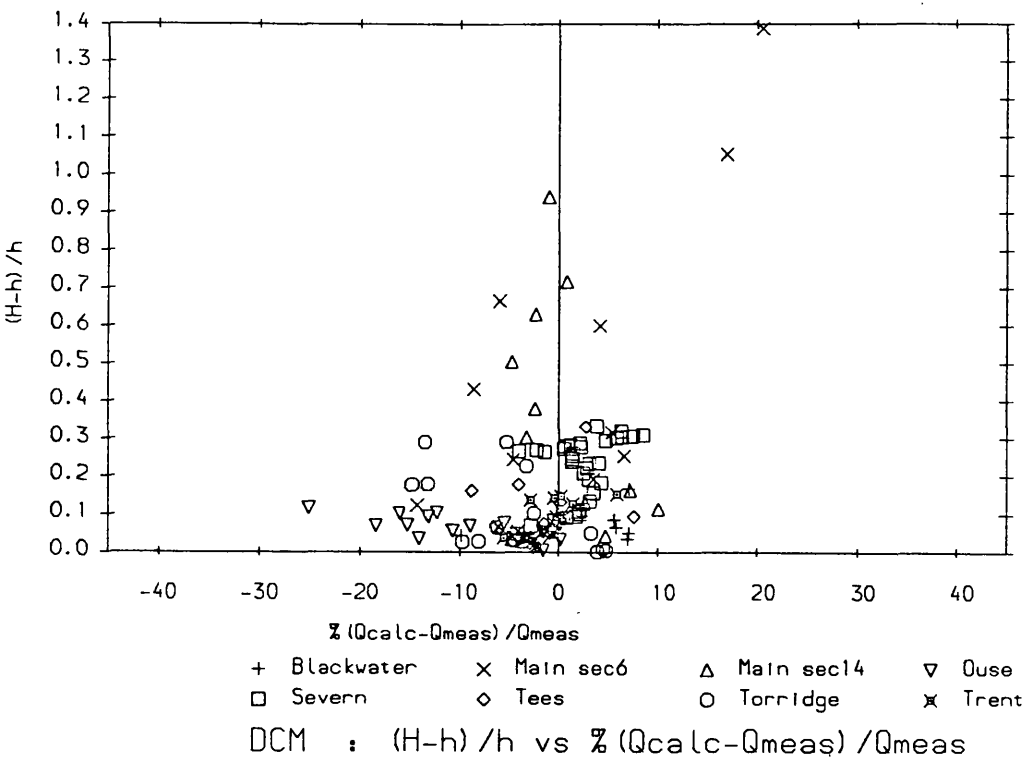


**a) Author's Manning's n values**

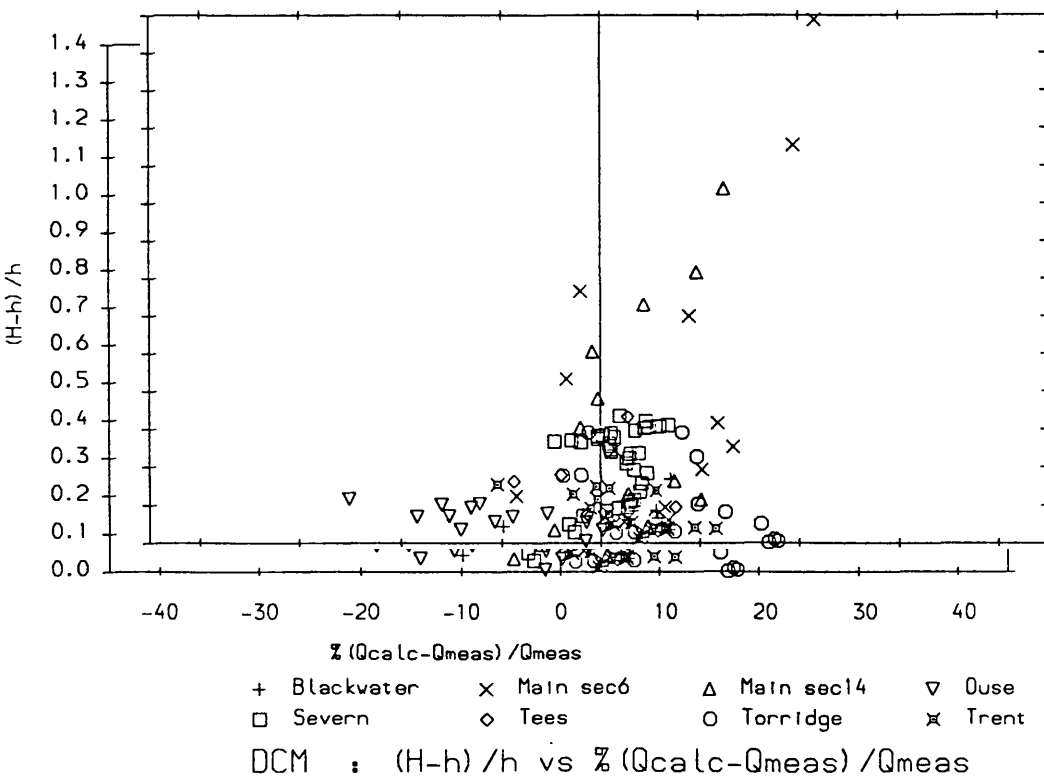


**b) Ackers' Manning's n values**

**Figure 4.60 Variation of errors in discharge with stage river gauging data, LDM**

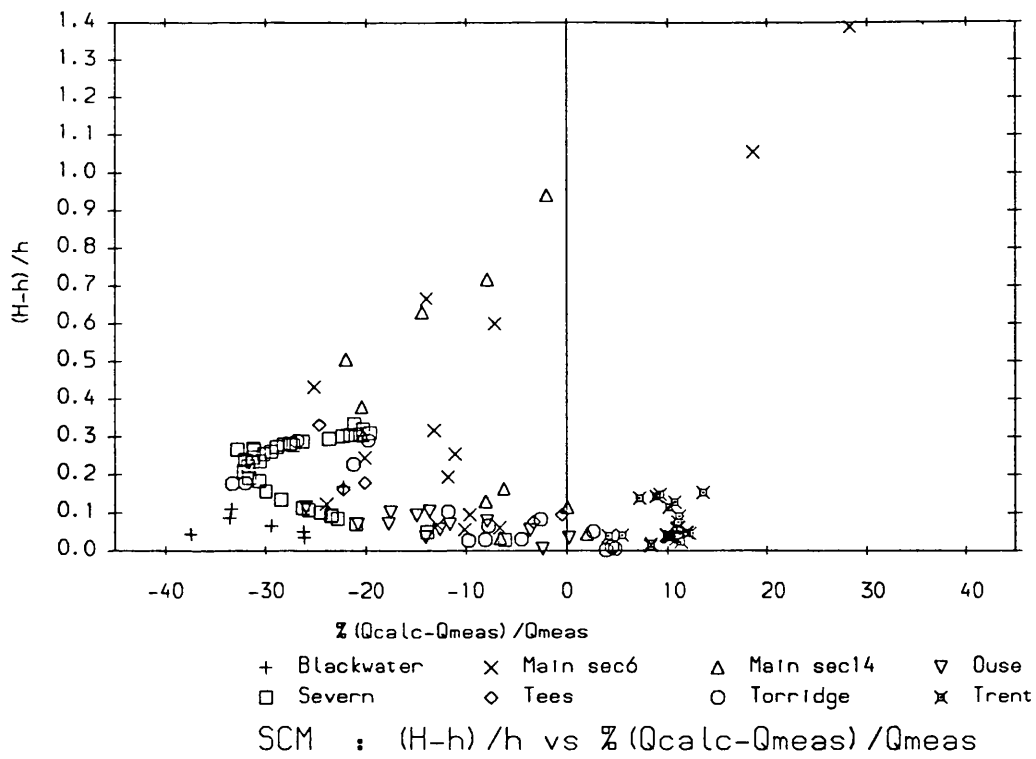


a) Author's Manning's n values

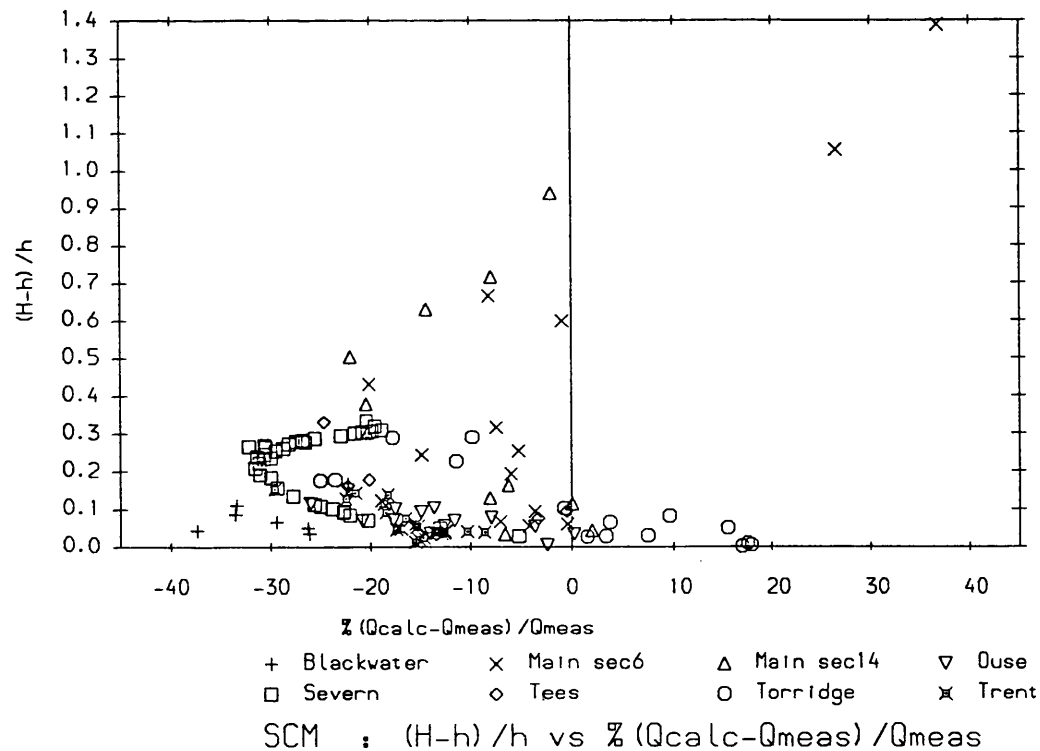


b) Ackers' Manning's n values

Figure 4.61 Variation of errors in discharge with stage river gauging data, DCM

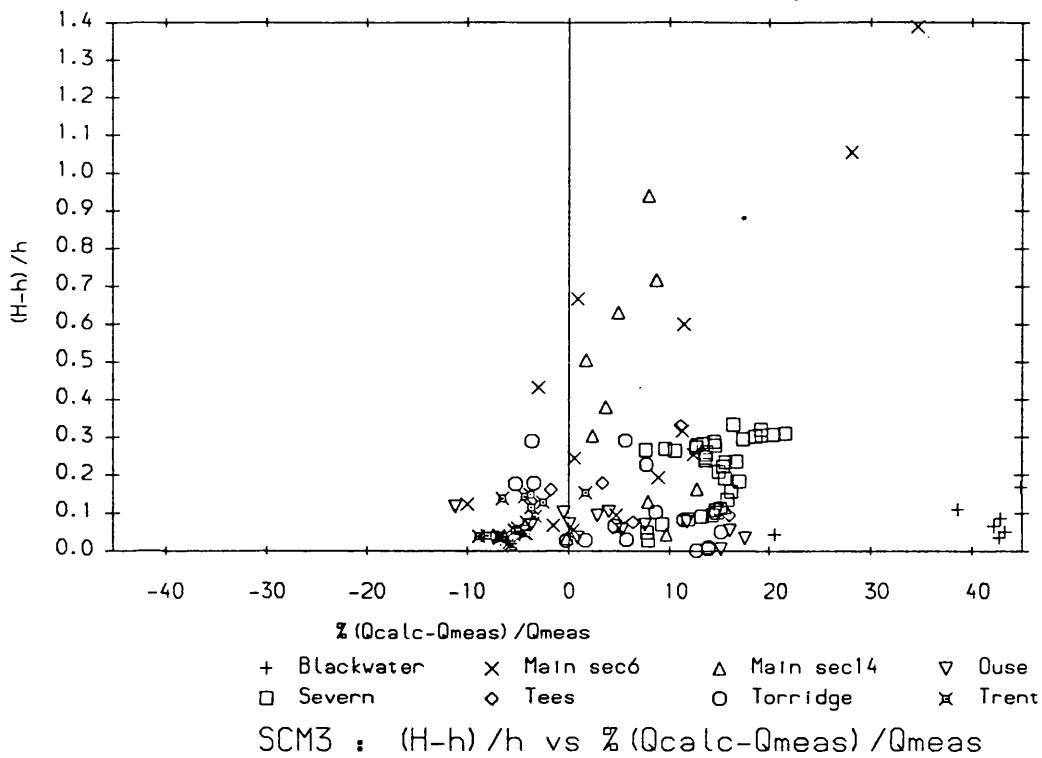


a) Author's Manning's n values

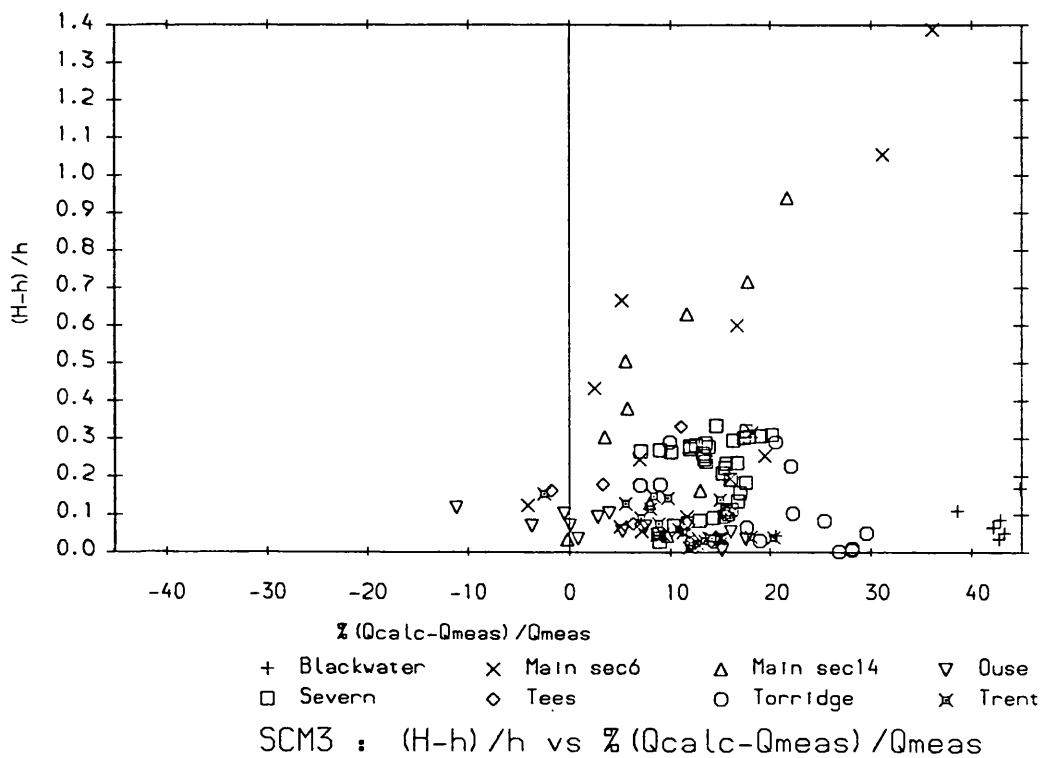


b) Ackers' Manning's n values

Figure 4.62 Variation of errors in discharge with stage river gauging data, SCM

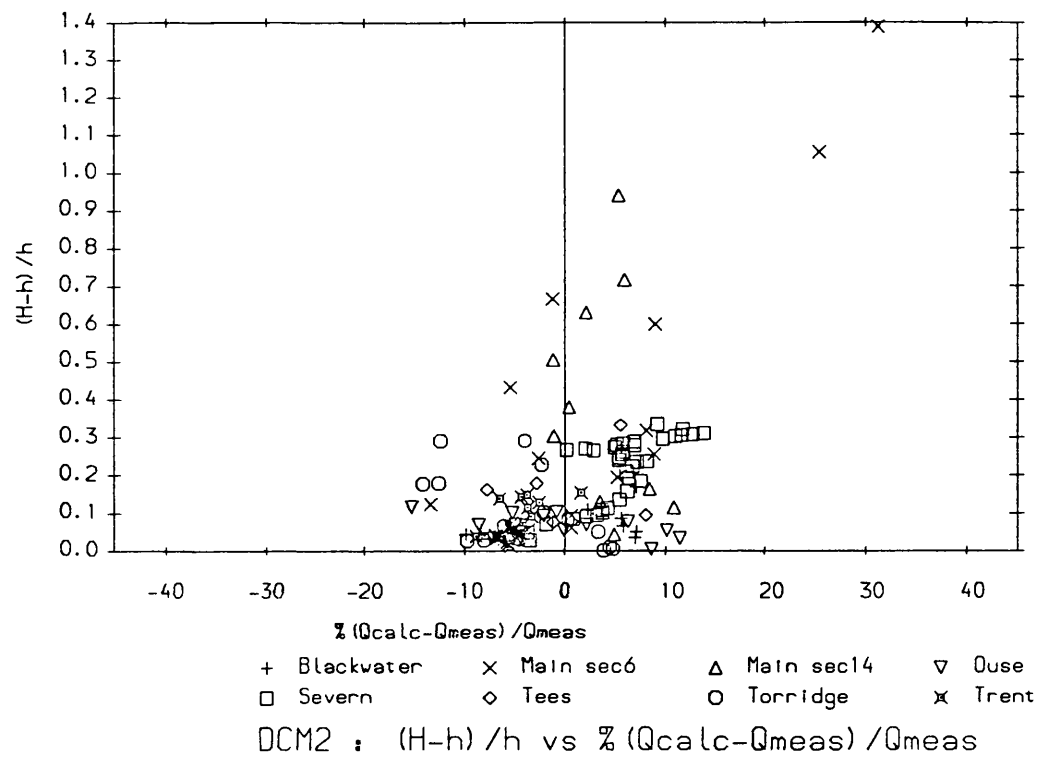


a) Author's Manning's n values

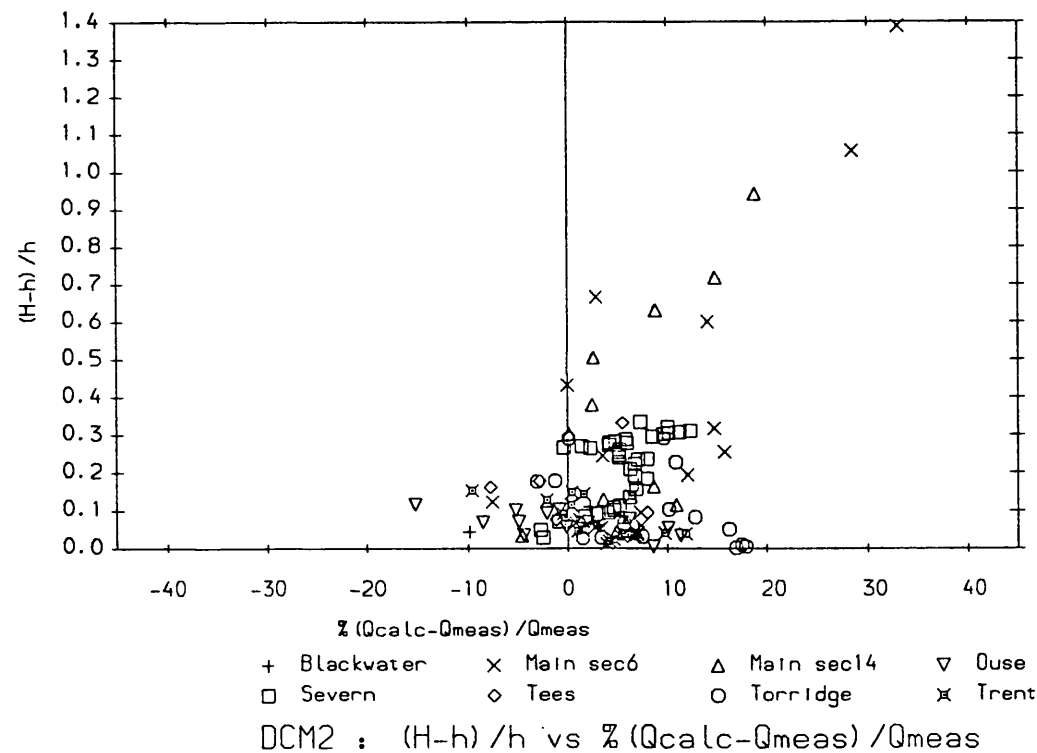


b) Ackers' Manning's n values

Figure 4.63 Variation of errors in discharge with stage river gauging data, SCM3, SSGM

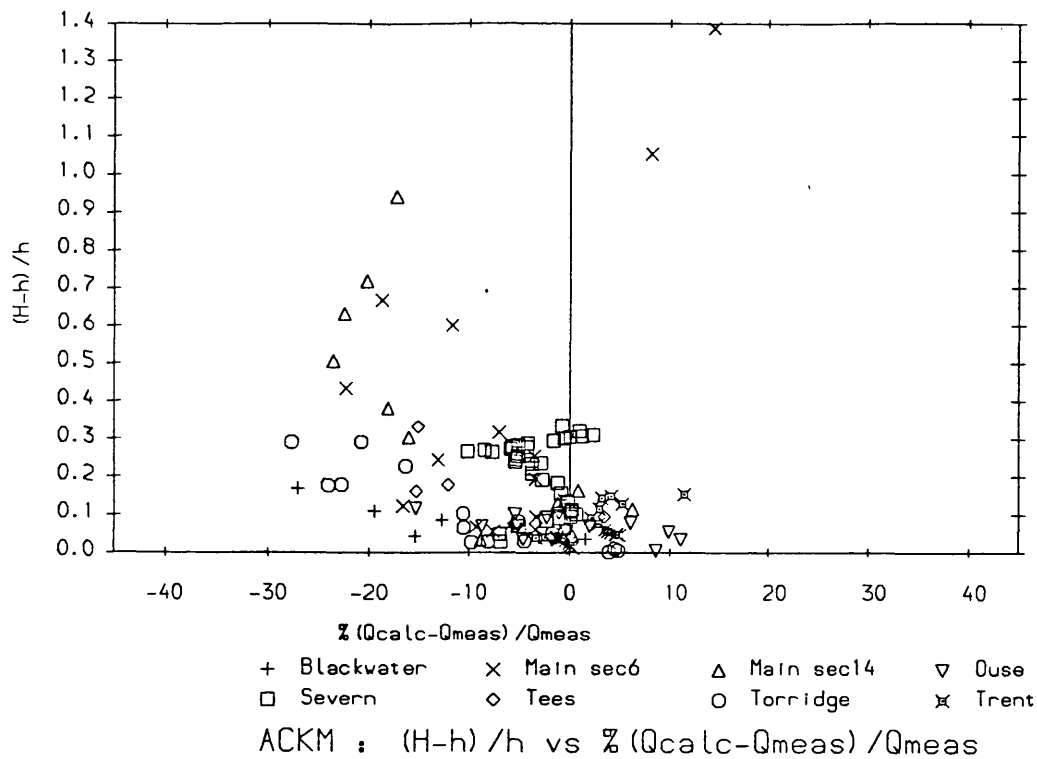


**a) Author's Manning's n values**

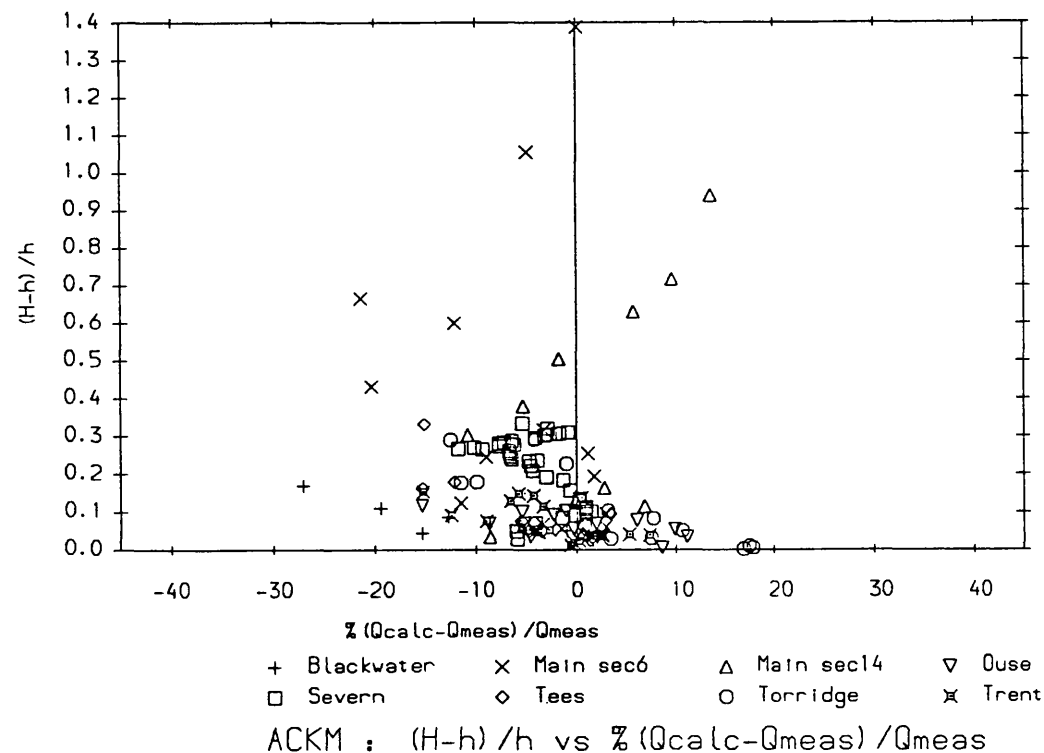


**b) Ackers' Manning's n values**

**Figure 4.64 Variation of errors in discharge with stage river gauging data, DCM2**



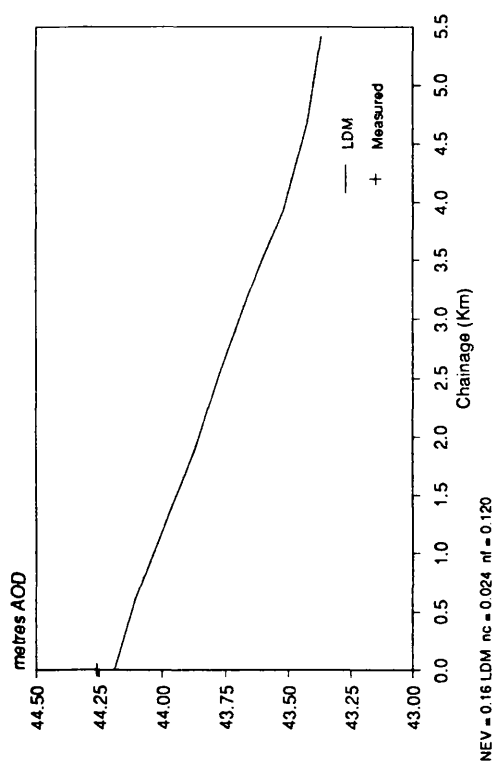
**a) Author's Manning's n values**



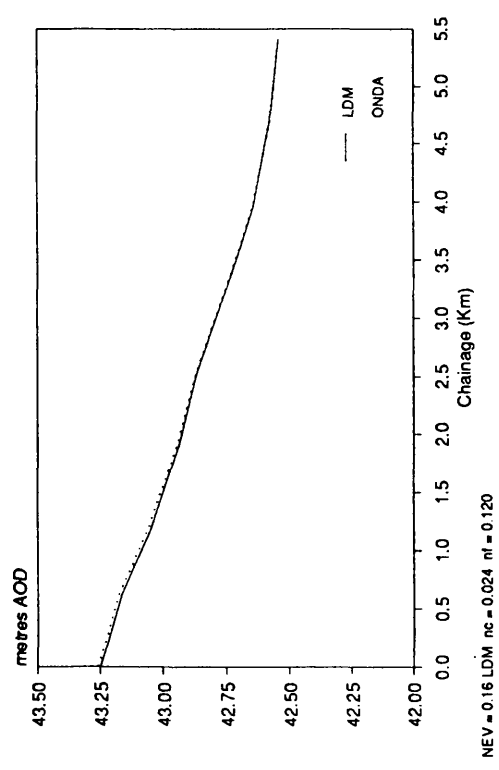
**b) Ackers' Manning's n values**

**Figure 4.65 Variation of errors in discharge with stage river gauging data, ACKM**

### Backwater Profile 190 cumecs



### Backwater Profile 120 cumecs



### River Thames at Wallingford Backwater Profile 190 cumecs

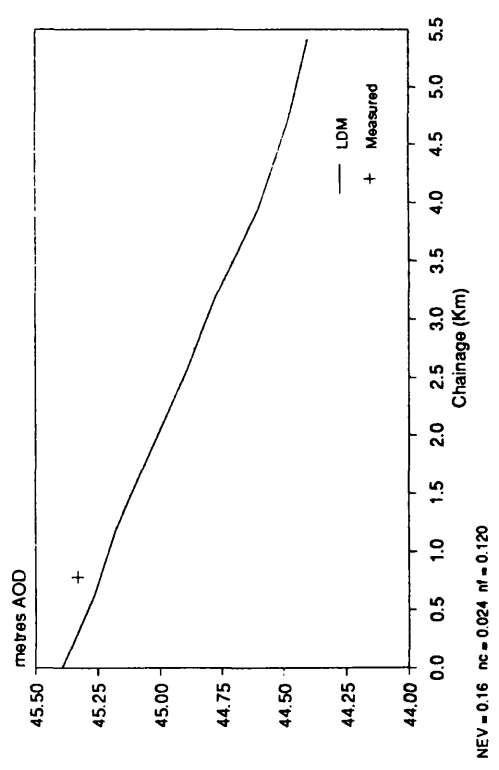
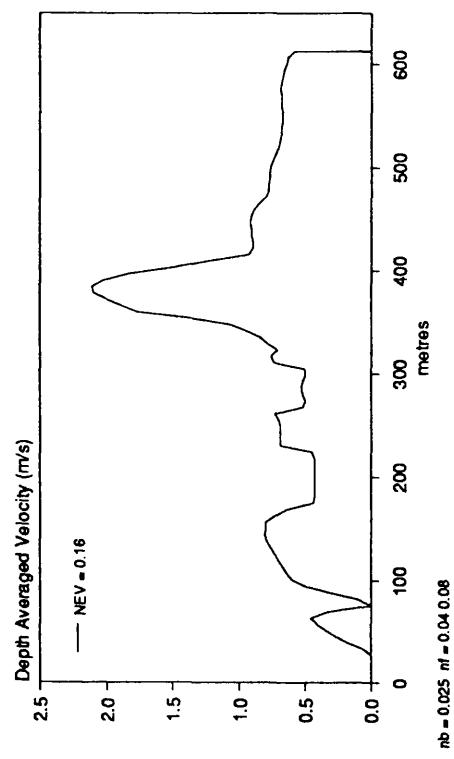
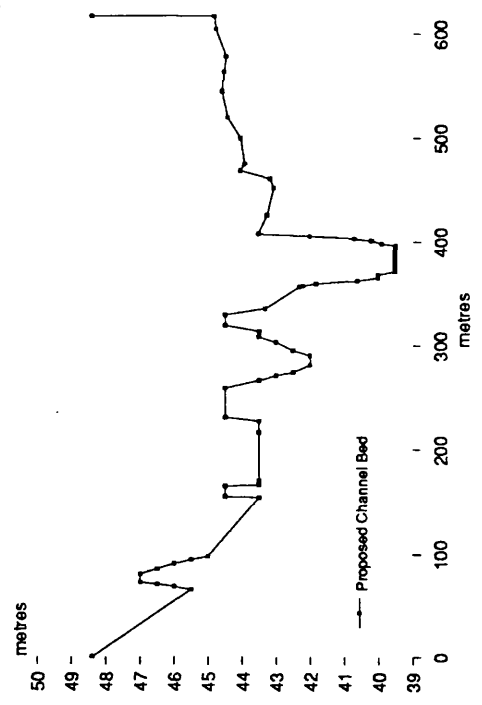


Figure 4.66 Backwater profiles for the River Thames at Wallingford reach 1

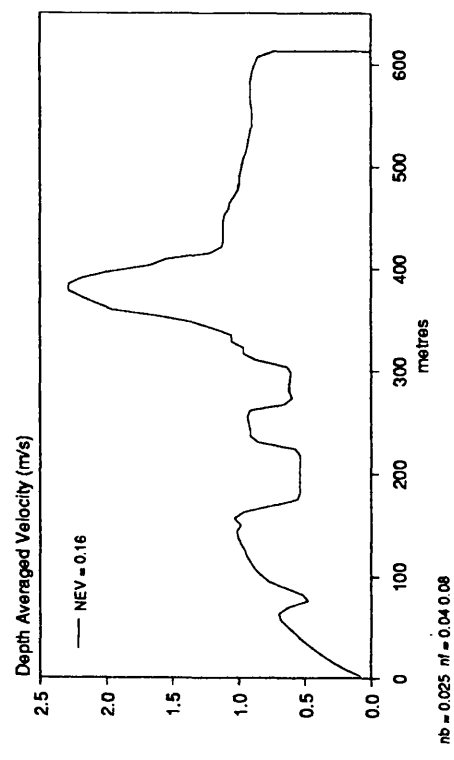
River Thames at Wallingford  
 Velocity Distribution  
 Section C Stage = 47.0 m AOD



River Thames at Wallingford  
 Section C : Proposed Geometry



River Thames at Wallingford  
 Velocity Distribution  
 Section C Stage = 48.4 m AOD



River Thames at Wallingford  
 Velocity Distribution  
 Section C Stage = 44.5 m AOD

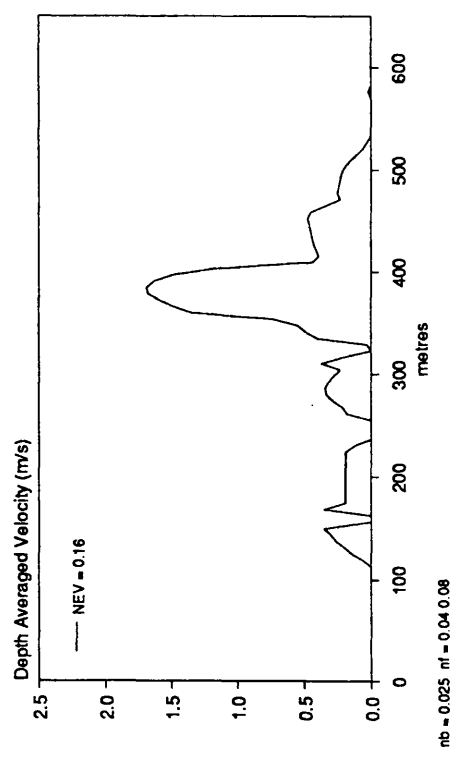
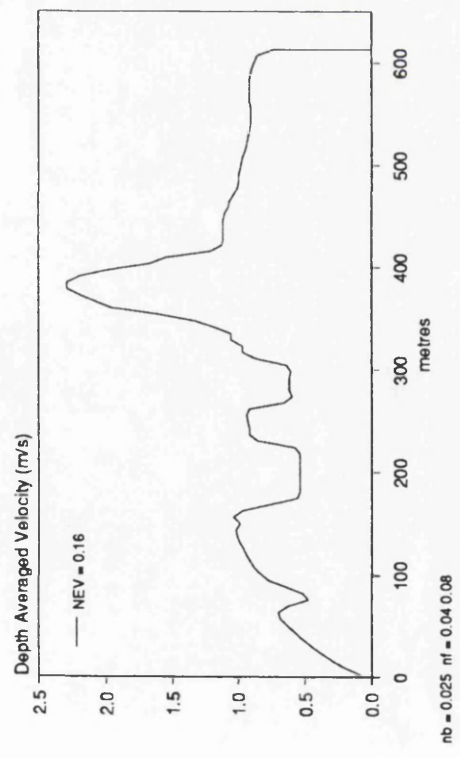
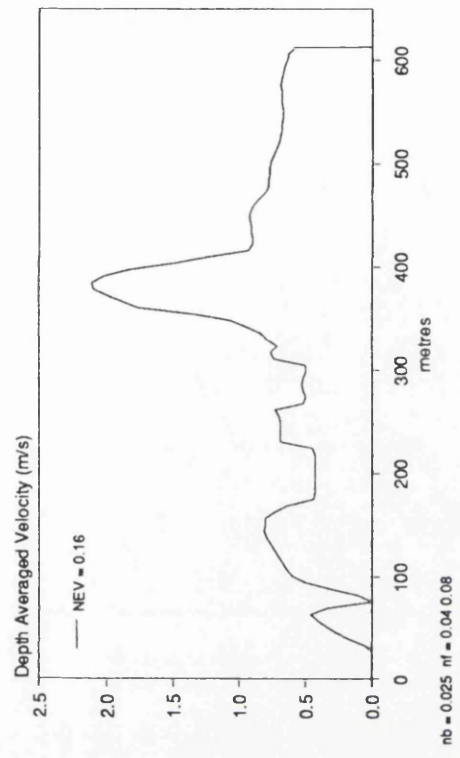


Figure 4.67 Example velocity profiles River Thames at Wallingford

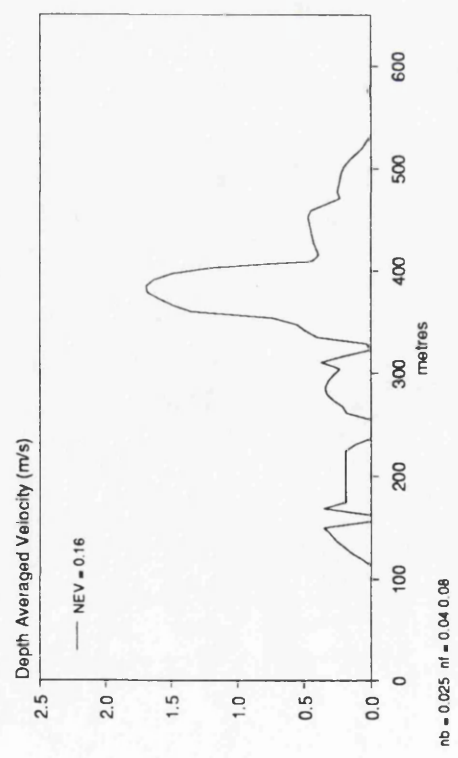
Velocity Distribution  
Section C Stage = 48.4 m AOD



Velocity Distribution  
Section C Stage = 47.0 m AOD



River Thames at Wallingford  
Velocity Distribution  
Section C Stage = 44.5 m AOD



River Thames at Wallingford  
Section C : Proposed Geometry

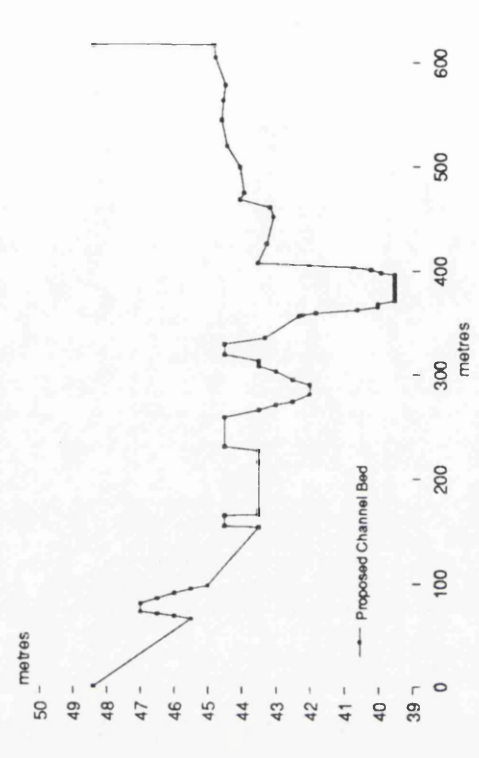
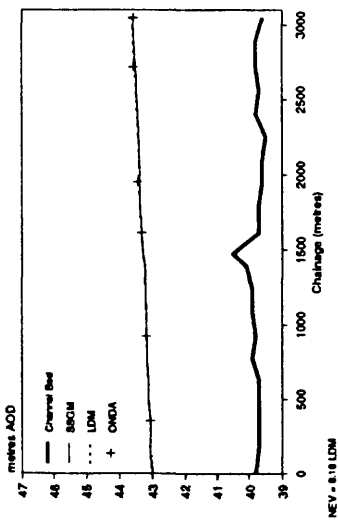
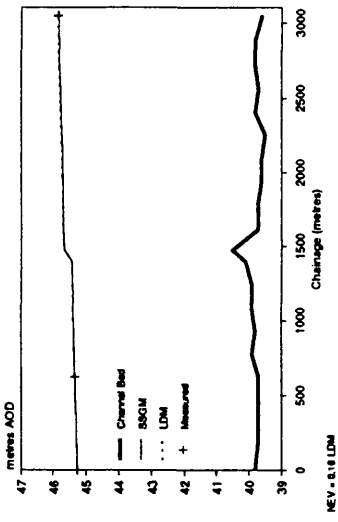


Figure 4.67 Example velocity profiles River Thames at Wallingford

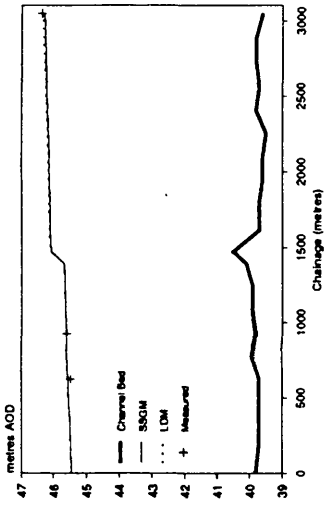
River Thames at Wallingford  
Backwater Profiles 120 cumecs



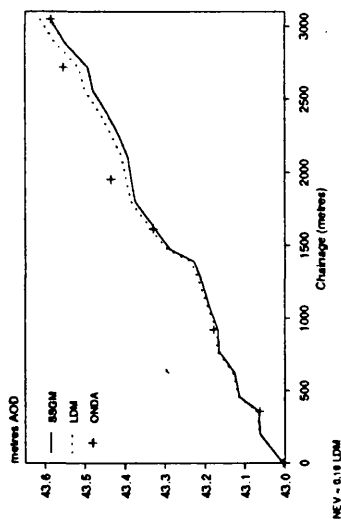
River Thames at Wallingford  
Backwater Profiles 374 cumecs



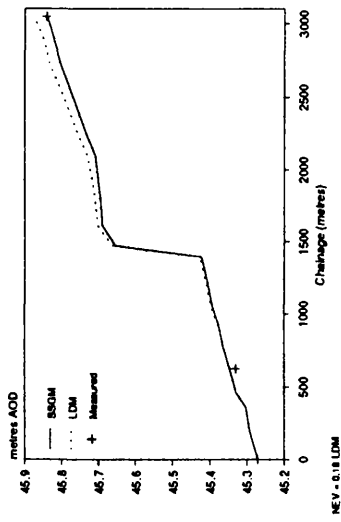
River Thames at Wallingford  
Backwater Profiles 500 cumecs



River Thames at Wallingford  
Backwater Profiles 120 cumecs



River Thames at Wallingford  
Backwater Profiles 374 cumecs



River Thames at Wallingford  
Backwater Profiles 500 cumecs

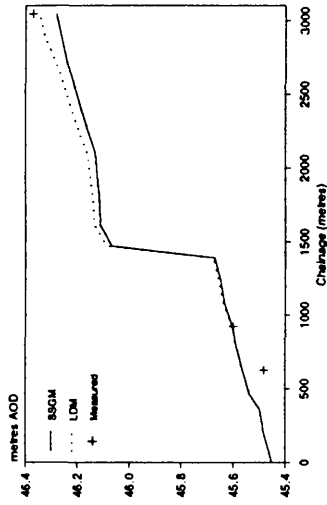
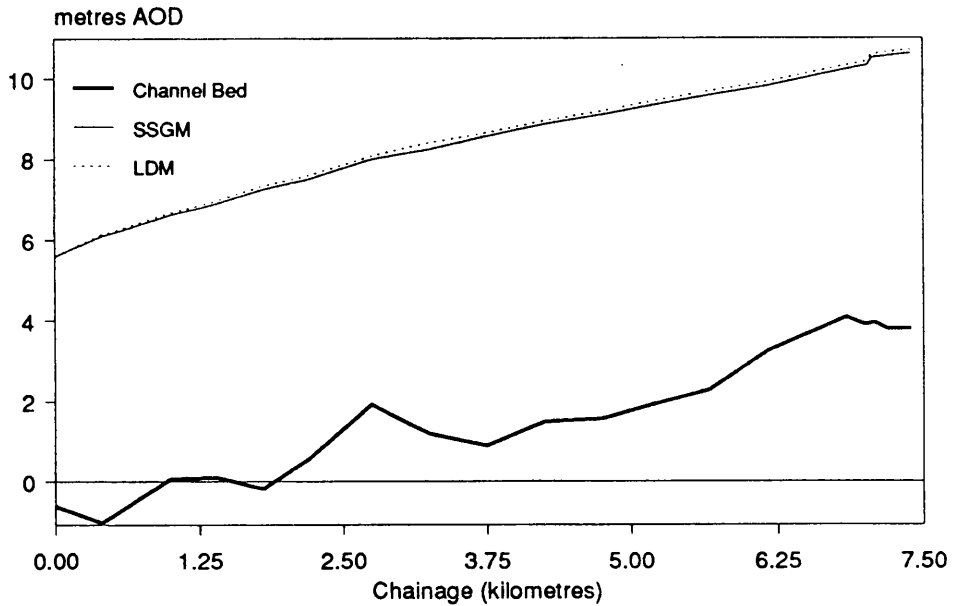


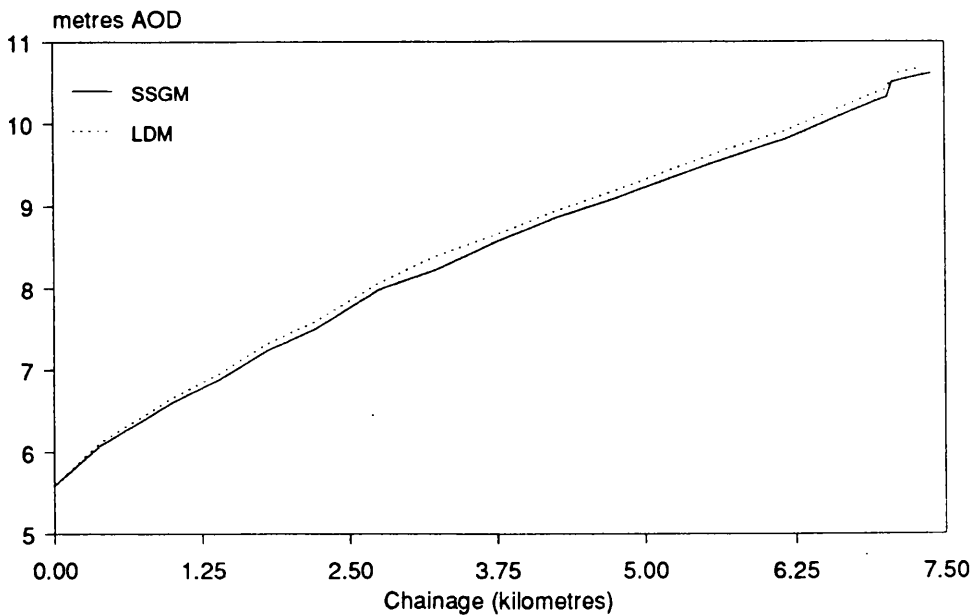
Figure 4.68 Backwater profiles for the River Thames at Wallingford reach 2

## River Tees at Low Moor Backwater Profiles 450 cumecs



NEV = 0.16 LDM

## River Tees at Low Moor Backwater Profiles 450 cumecs



NEV = 0.16 LDM

**Figure 4.69** Backwater profiles for the River Tees at Low Moor

**Table 5.1 Summary of SERC Phase B tests**

Run No	Angle	Flow	X-Sn	FP Type	FP Config	S/D	U $\theta$ Chan	U $\theta$ FP	Lev	BS	Turb	Vis	Disp
B20	60	Inbank	T	S	N/A	*							*
B21	60	Overbank	T	S	St	*							
B22	60	D=100mm	T	S	St	N/A	*	N/A	*	*	*		
B23	60	D=200mm	T	S	St	N/A	*	*	*	*	*	*	*
B24	60	D=250mm	T	S	St	N/A	*	*	*	*	*	*	*
B25	60	Inbank	N	S	St	*							*
B26	60	Overbank	N	S	St	*							
B27	60	D=140mm	N	S	St	N/A	*	N/A	*	*	*		
B28	60	D=165mm	N	S	St	N/A	*	N/A	*	*	*	*	*
B29	60	D=200mm	N	S	St	N/A	*	*	*	*	*	*	*
B30	60	D=250mm	N	S	St	N/A	*	*	*	*	*	*	*
B31	60	Overbank	N	S	Na	*							
B32	60	Overbank	N	R-BB	St	*							
B33	60	Overbank	N	R-PD	St	*							
B34	60	Overbank	N	R-D	St	*							
B35	60	D=165mm	N	R-D	St	N/A	*	N/A	*	*	*		
B36	60	D=200mm	N	R-D	St	N/A	*	*	*	*	*		
B37	60	D=250mm	N	R-D	St	N/A	*	*	*	*	*		

**Notes**

- 1 S/D = Stage-discharge data
- 2 U $\theta$  = Magnitudes and directions of velocities over test sections
- 3 Lev = Water surface levels
- 4 BS = Boundary shear stress
- 5 Turb = Turbulence data
- 6 Vis = Flow visualization tests
- 7 Disp = Dispersion tests
- 8 T = Trapezoidal
- 9 N = Natural
- 10 S = Smooth
- 11 R-D = Roughened dowel rods
- 12 R-PD = Partially roughened dowel rods
- 13 R-BB = Roughened with breeze blocks
- 14 St = Standard
- 15 Na = Narrow
- 16 W = Walled
- 17 N/A = Not Applicable
- 18 In = In main channel only

**Table 5.1 (cont) Summary of SERC Phase B tests**

Run No	Angle	Flow	X-Sn	FP Type	FP Config	S/D	U $\theta$ Chan	U $\theta$ FP	Lev	BS	Turb	Vis	Disp
B38	110	Inbank	N	S	N/A	*							*
B39	110	Overbank	N	S	St	*							
B40	110	D=140mm	N	S	St	N/A	*	N/A	*	*	*	*	
B41	110	D=165mm	N	S	St	N/A	*	N/A	*	*	*	*	
B42	110	D=200mm	N	S	St	N/A	*	*	*	*	*	*	
B43	110	Overbank	N	R-D	St	*							
B44	110	D=165mm	N	R-D	St	N/A	*		In				
B45	110	D=200mm	N	R-D	St	N/A	*		In				
B46	110	Overbank	N	R-BB	St	*							
B47	110	Overbank	N	S	Na	*							
B48	110	Overbank	N	S	W	*							

**Notes**

- 1 S/D = Stage-discharge data
  - 2 U $\theta$  = Magnitudes and directions of velocities over test sections
  - 3 Lev = Water surface levels
  - 4 BS = Boundary shear stress
  - 5 Turb = Turbulence data
  - 6 Vis = Flow visualization tests
  - 7 Disp = Dispersion tests
  - 8 T = Trapezoidal
  - 9 N = Natural
  - 10 S = Smooth
  - 11 R-D = Roughened dowel rods
  - 12 R-PD = Partially roughened dowel rods
- 13 R-BB = Roughened with breezeblocks
- 14 St = Standard
- 15 Na = Narrow
- 16 W = Walled
- 17 N/A = Not Applicable
- 18 In = In main channel only

**Table 5.2 Summary of SERC Phase B stage discharge tests**

Run No	Angle	Flow Type	X-Sn	FP	FP Config	No of Data Points
B20	60	Inbank	T	S	N/A	17
B21	60	Overbank	T	S	St	16
B25	60	Inbank	N	S	St	10
B26	60	Overbank	N	S	St	16
B31	60	Overbank	N	S	Na	14
B32	60	Overbank	N	R-BB	St	13
B33	60	Overbank	N	R-PD	St	12
B34	60	Overbank	N	R-D	St	18
B38	110	Inbank	N	S	N/A	11
B39	110	Overbank	N	S	St	14
B43	110	Overbank	N	R-D	St	15
B46	110	Overbank	N	R-BB	St	14
B47	110	Overbank	N	S	Na	14
B48	110	Overbank	N	S	W	8

**Notes**

1	T = Trapezoidal	6	R-BB = Roughened with breeze blocks
2	N = Natural	7	St = Standard
3	S = Smooth	8	Na = Narrow
4	R-D = Roughened dowel rods	9	W = Walled
5	R-PD = Partially roughened dowel rods	10	N/A = Not Applicable

**Table 5.3 Summary of Aberdeen experiments**

Sinuosity	Cross-section	Valley Slope	Test no
1.00	Trapezoidal	0.00100	AB100
1.00	Trapezoidal	0.00071	AB100A
1.21	Trapezoidal	0.00100	AB101
1.40	Trapezoidal	0.00100	AB102
1.40	Natural	0.00100	AB103
2.06	Trapezoidal	0.00062	AB104
2.06	Natural	0.00062	AB105

**Table 5.4 Summary of Vicksburg experiments 2ft wide channel**

Test No.	Floodway Width (m)	Sinuosity	Meander Belt Width (m)	Radius of Curvature (m)	Assigned Test no
XII	4.877	1.570	4.420	1.829	201 202 203
XIII	4.877	1.400	3.761	1.865	204 205 206
XIV	4.877	1.200	2.822	2.137	207 208 209
XV	9.144	1.200	2.822	2.137	210
XVI	9.144	1.570	4.420	1.829	211

**Table 5.5 Geometric parameters lab studies meandering channels**

source	L Wave Length (m)	B Channel Width (m)	h Channel Depth (m)	rc Radius of Curvature (m)	s Sinuosity
SERC FCF	12.000	1.200	0.150	2.743	1.374
	10.310	0.174	0.150	2.743	2.043
Aberdeen	2.570	0.174	0.050	0.413	1.215
	1.909	0.174	0.050	0.413	1.406
	1.154	0.174	0.050	0.307	2.043
	7.315	0.762	0.152	1.829	1.571
Vicksburg	7.315	0.762	0.152	1.865	1.400
	7.315	0.762	0.152	2.136	1.200
	1.803	0.200	0.050	0.400	1.224
Kiely	1.803	0.200	0.050	0.400	1.224
Toebes and Sooky	1.280	0.209	0.038	1.392	1.090
Smith	3.352	0.274	0.076	1.097	1.172
James and Brown	9.144	0.279	0.051	1.143	1.068
Stein and Rouve	6.500	0.400	0.100	1.800	~1.200

**Table 5.6 Non-dimensional geometric parameters meandering channels**

source	L/B	B/h	$r_f/B$
Natural Rivers	~10.0	~10.0	2 - 3.0
SERC FCF	10.0	8.0	2.3
	8.6	8.0	2.3
Aberdeen	14.8	3.5	2.4
	11.0	3.5	2.4
	6.6	3.5	1.8
Vicksburg	9.6	5.0	2.4
	9.6	5.0	2.5
	9.6	5.0	2.8
Kiely	9.0	4.0	2.0
Toebes and Sooky	6.1	5.5	6.7
Smith	12.2	3.6	4.0
James and Brown	32.8	5.5	4.1
Stein and Rouve	16.2	4.0	4.5

**Table 5.7 Bend losses for 60° meander geometry, trapezoidal cross-section**

Depth (m)	Discharge (m <sup>3</sup> /s)	T (°C)	$S_o - S_f$ (x10 <sup>-3</sup> )	K	n/n
0.05932	0.01975	11.4	0.0634	0.0851	1.0477
0.06726	0.02512	11.0	0.0228	0.0312	1.0201
0.07198	0.02654	12.4	0.1039	0.1168	1.0805
0.07714	0.03056	10.8	0.0701	0.0690	1.0524
0.08263	0.03308	12.4	0.1176	0.1146	1.0920
0.08608	0.03630	11.6	0.0882	0.0780	1.0673
0.09170	0.04015	11.5	0.0947	0.0786	1.0279
0.09765	0.04425	11.6	0.1050	0.0824	1.0806
0.10192	0.04708	12.7	0.1203	0.0916	1.0943
0.10302	0.04782	11.5	0.1185	0.0894	1.0930
0.10593	0.05015	11.7	0.1188	0.0868	1.0931
0.10596	0.04974	10.9	0.1252	0.0930	1.0995
0.10680	0.04953	12.4	0.1489	0.1136	1.1219
0.11150	0.05467	13.7	0.1261	0.0869	1.0995
0.11394	0.05702	12.7	0.1163	0.0772	1.0916
0.11900	0.06035	13.6	0.1377	0.0899	1.1110
0.13150	0.07073	12.9	0.1457	0.0867	1.0576
Average :			0.1073	0.0809	1.0782
Standard Deviation :			0.0320	0.0262	0.0285

\* At cross-over section

**Table 5.8 Non-friction losses for 60° meander geometry, natural cross-section**

*Depth (m)	Discharge (m <sup>3</sup> /s)	T (°C)	S <sub>o</sub> - S <sub>f</sub> (x10 <sup>-3</sup> )	K	n/n
0.09957	0.01019	16.1	0.2569	0.6762	1.2329
0.10359	0.01207	16.1	0.2284	0.5202	1.2084
0.10860	0.01442	16.1	0.2130	0.4228	1.1900
0.11225	0.01612	16.0	0.2248	0.4209	1.2040
0.11648	0.01806	16.1	0.2351	0.4146	1.2166
0.12316	0.02150	16.0	0.2407	0.3807	1.2237
0.12566	0.02288	16.0	0.2417	0.3669	1.2249
0.12923	0.02498	16.2	0.2413	0.3445	1.2244
0.13165	0.02646	16.0	0.2398	0.3287	1.2225
0.14235	0.03341	17.1	0.2398	0.2789	1.2227
Average :			0.2362	0.4154	1.2170
Standard Deviation :			0.0118	0.1125	0.0127

\* At cross-over section

**Table 5.9 Non-friction losses for 110° meander geometry, natural cross-section**

*Depth (m)	Discharge (m <sup>3</sup> /s)	T (°C)	S <sub>o</sub> - S <sub>f</sub> (x10 <sup>-3</sup> )	K	n/n
0.11006	0.01135	10.4	0.1805	0.7819	1.2512
0.11516	0.01322	15.0	0.1920	0.7558	1.2743
0.12030	0.01533	10.5	0.1808	0.6419	1.2518
0.12073	0.01560	14.4	0.1857	0.6464	1.2615
0.12420	0.01699	14.1	0.1881	0.6228	1.2664
0.12791	0.01873	10.3	0.1774	0.5459	1.2452
0.13072	0.02006	15.9	0.1878	0.5502	1.2657
0.13566	0.02206	14.9	0.1950	0.5473	1.2806
0.13854	0.02342	10.3	0.1872	0.5057	1.2646
0.14027	0.02432	10.5	0.1868	0.4908	1.2638
0.14672	0.02778	10.4	0.1844	0.4397	1.2589
Average :			0.1860	0.5935	1.2622
Standard Deviation :			0.0051	0.1077	0.0103

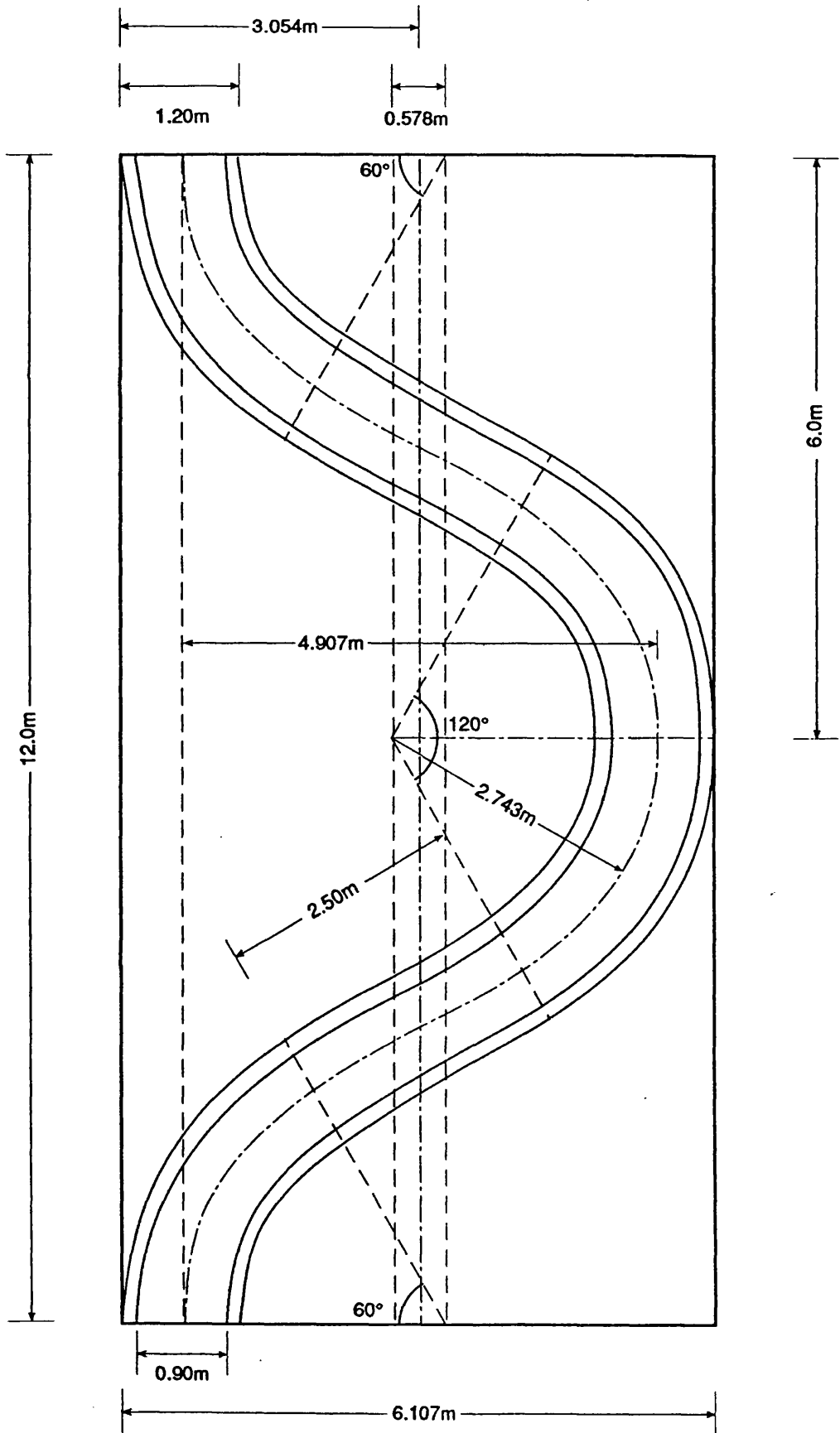
\* At cross-over section

**Table 5.10 Summary of mean errors in bend loss predictions**

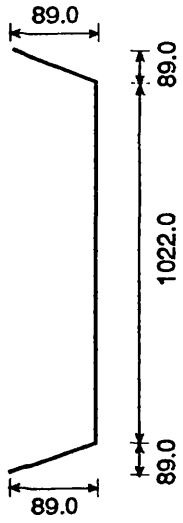
Data Set	Friction Only	SCS (1963)	Toebes & Sooky (1967)	Leopold et al (1960)	Agarwal et al (1984)	Mockmore	Chang Rect. (1944)	Modified Chang (1983)	SCSL
SERC s = 1.37	9.54 2.88	-6.38 2.51	-14.60 1.62	-13.15 1.42	-15.97 3.30	-33.69 4.36	-5.31 3.03	0.85 1.34	-7.36 2.49
Aberdeen s = 1.21	19.80 9.43	1.50 8.12	8.75 7.08	-6.74 6.22	-16.29 8.29	-51.73 3.65	-23.84 6.37	1.97 4.50	8.13 8.60
Aberdeen s = 1.4	11.90 3.59	-5.24 3.11	1.70 2.94	-12.84 2.48	-30.57 3.34	-46.12 6.73	-27.71 10.29	-8.66 4.32	-7.36 3.05
Aberdeen s = 2.06	28.66 3.26	-6.18 2.52	16.07 2.13	-12.68 1.63	-43.63 2.15	-37.42 3.95	-34.27 7.14	-10.78 2.78	-6.18 2.52
Vicksburg wide	37.30 6.01 20.21* 7.88*	14.53 2.72	3.56 4.53	11.70 2.98	-4.79 2.34	-30.13 4.35	-6.19 2.11	16.29 2.19	17.68 1.92
Vicksburg narrow	10.61 7.27 -4.89* 10.25*	-6.40 11.34	-13.09 5.72	10.32 5.54	-25.81 8.21	-20.59 5.43	-16.17 5.43	-2.00 5.46	0.37 11.44
All Data (62 points)	16.14 9.86 -2.76* 8.48*	-3.46 7.74	-1.02 12.06	-7.68 9.36	-22.80 11.48	-39.43 11.12	-19.03 12.33	-1.76 7.35	-1.45 9.84

**Notes**

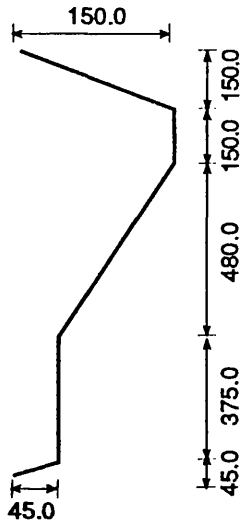
- 1 Upper value is average error in %; lower value is standard deviation
- 2 \* lower adjustment where there is an option, otherwise higher value



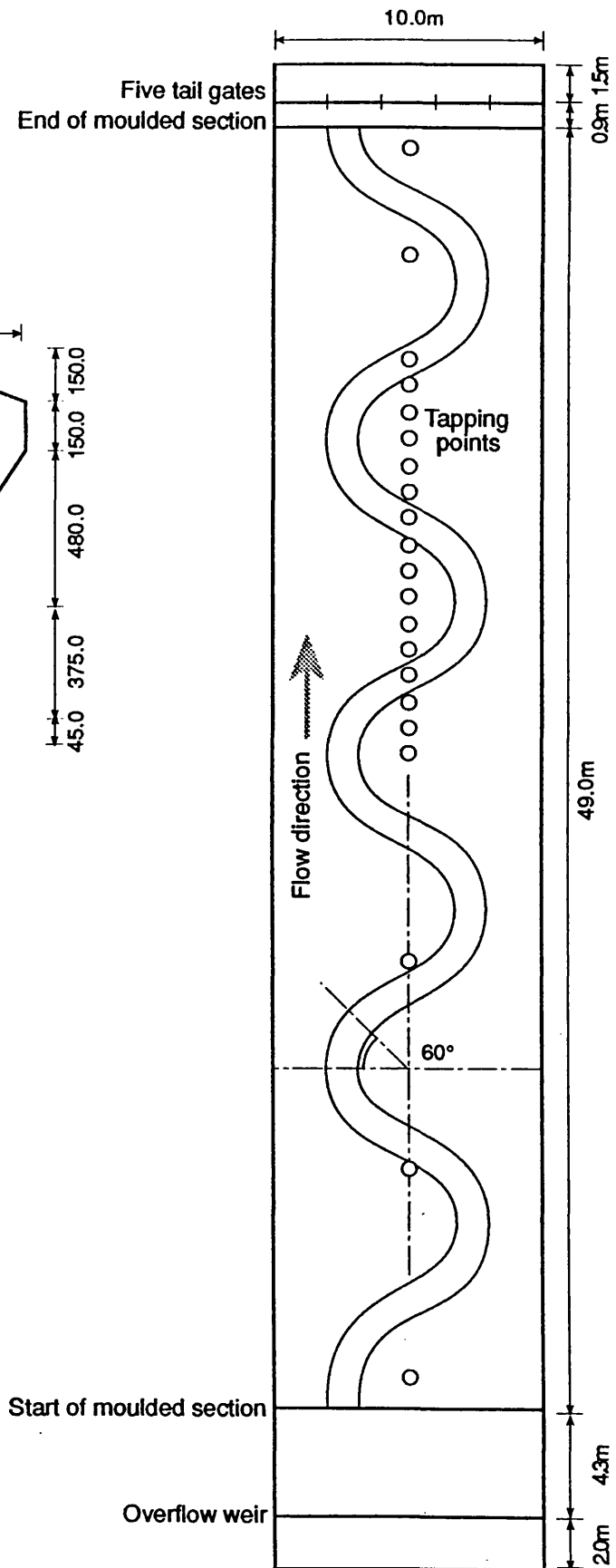
5.1 Detailed plan geometry of FCF 60° meander



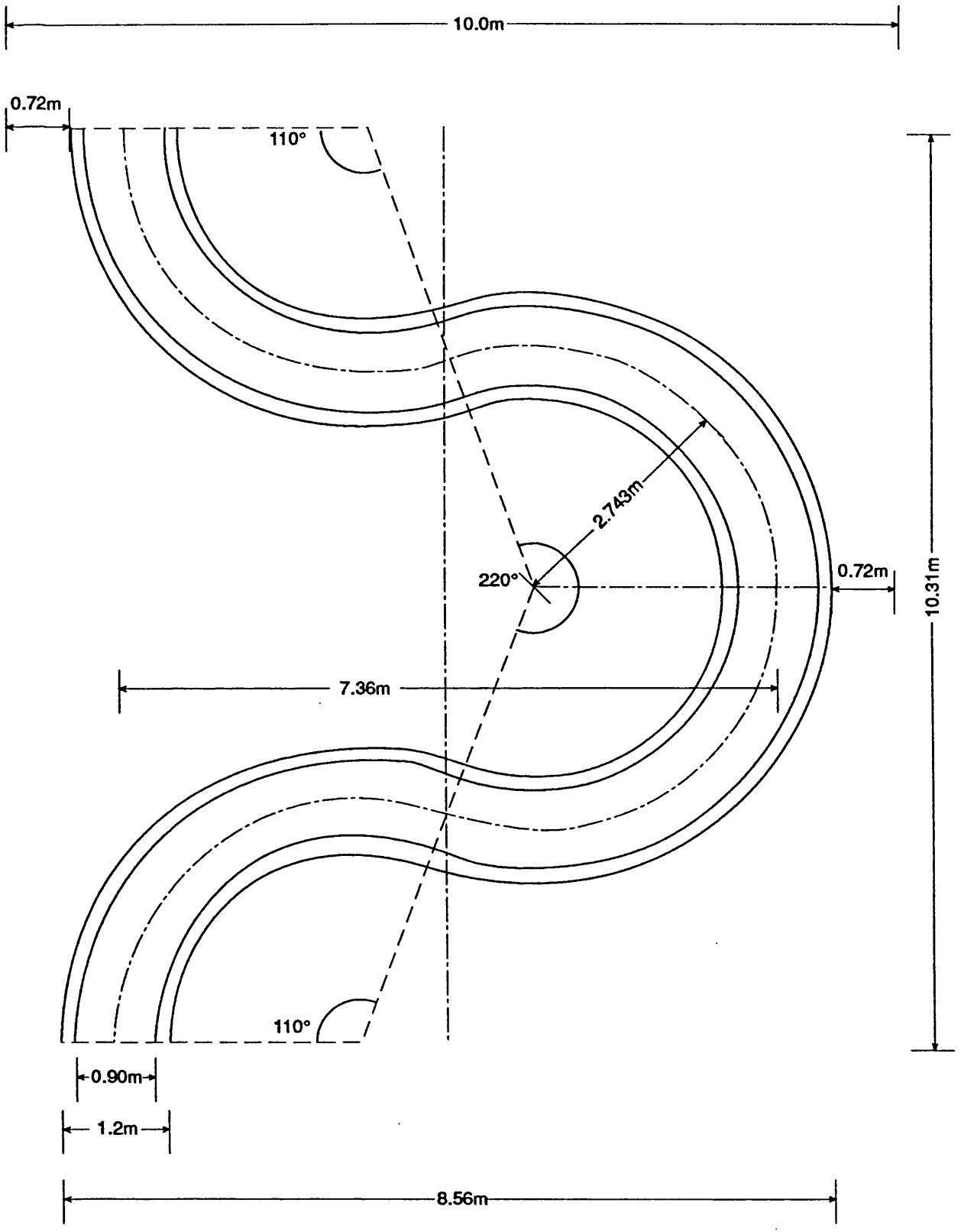
**Natural cross-section  
at cross-over between  
meander bends**



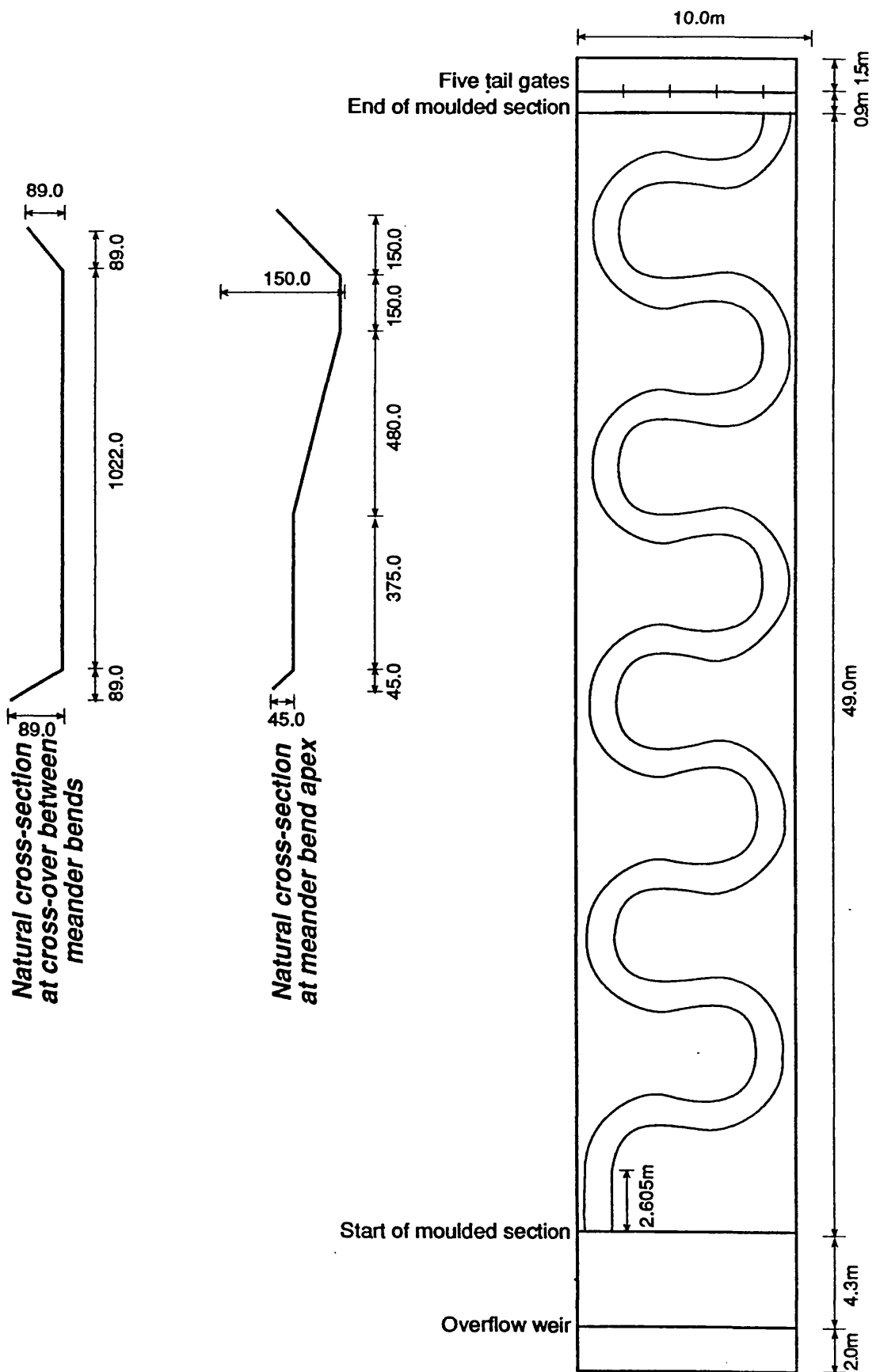
**Natural cross-section  
at meander bend apex**



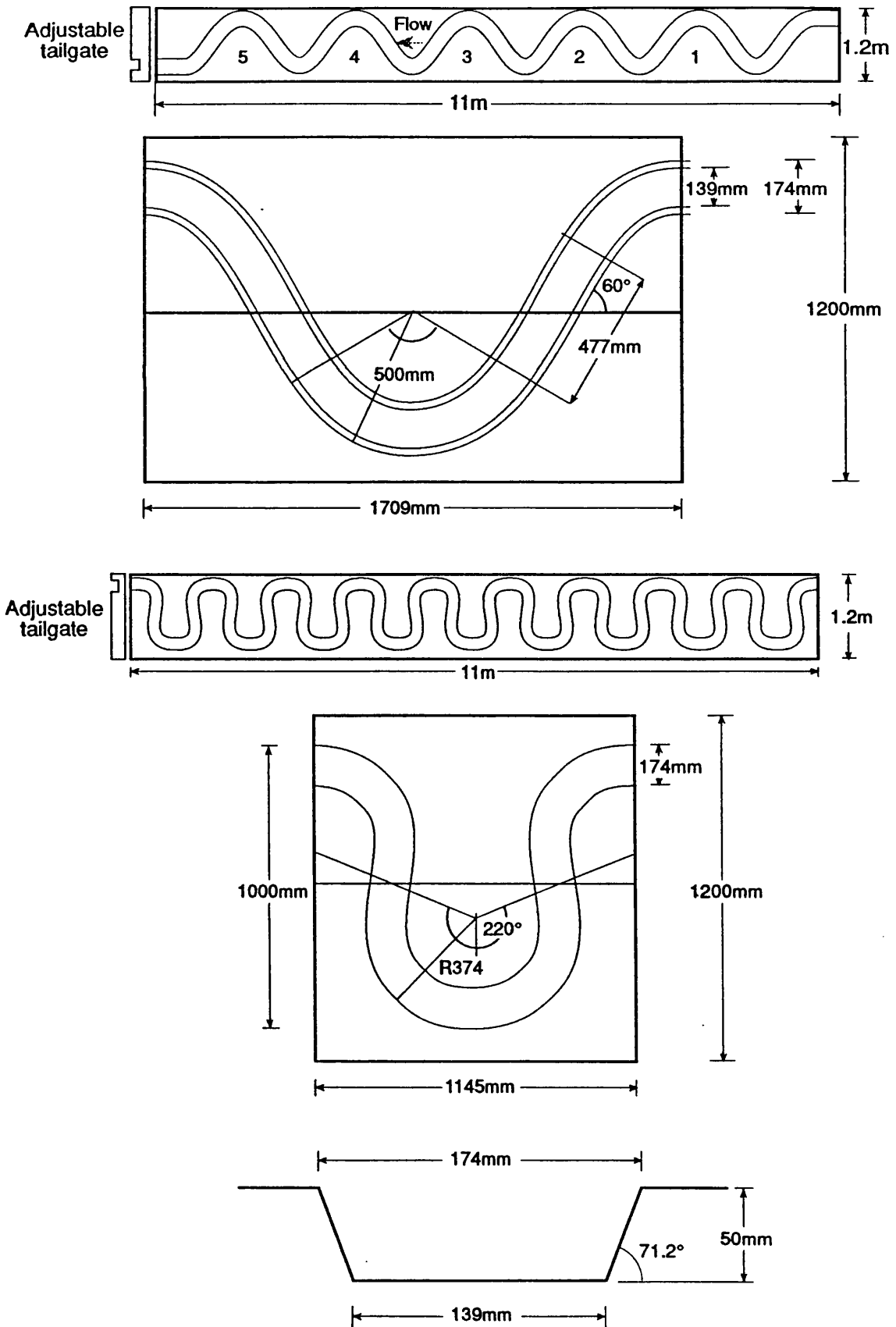
**5.2 Plan of flume and natural cross-section geometry for 60° meander**



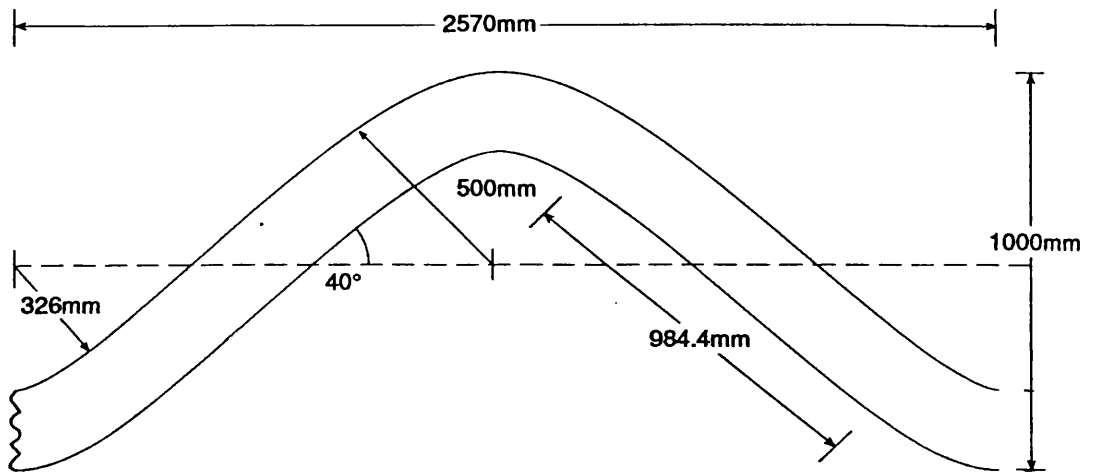
**5.3 Detailed plan geometry for FCF 110° meander**



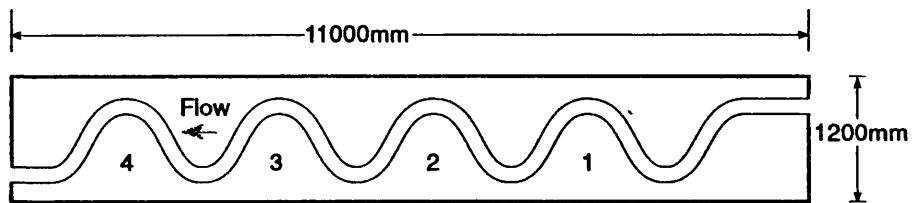
5.4 Plan of flume and natural cross-section geometry for 110° meander



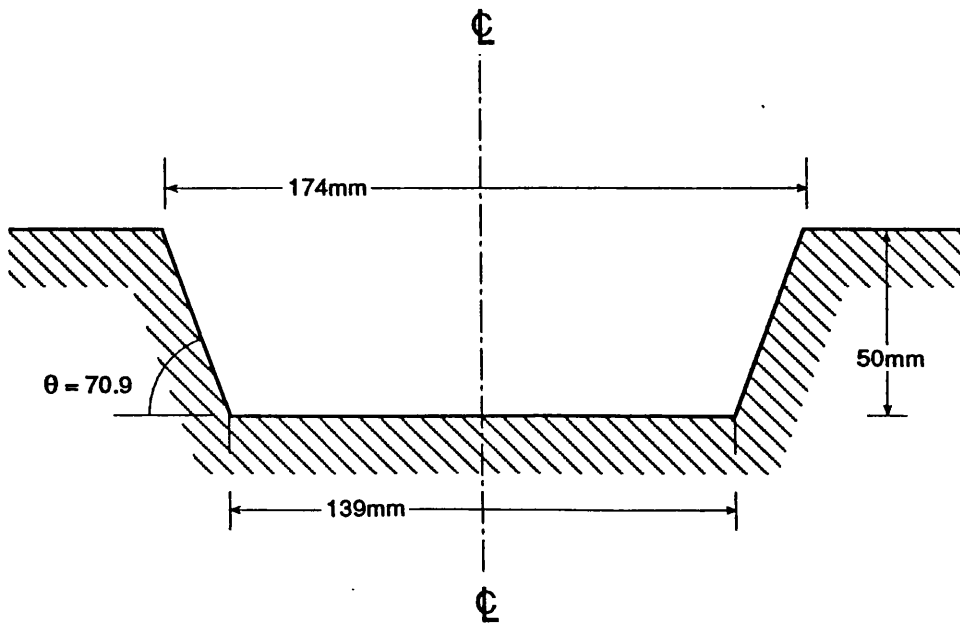
**5.5 Plan geometries of the Aberdeen flume with channel sinuosities of 1.40 and 2.04 (after Willetts 1992)**



**Enlarged view of one bend**

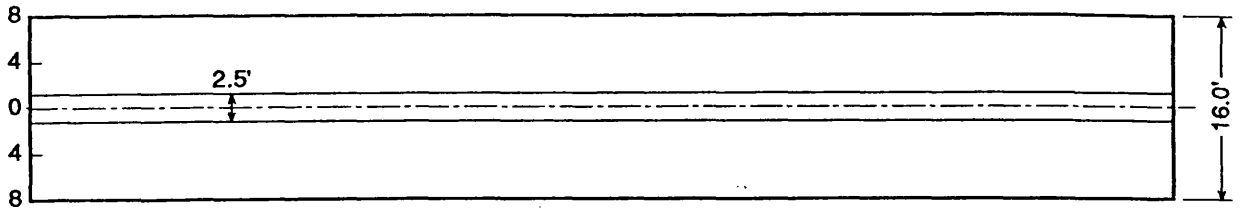


**Plan view of whole section**

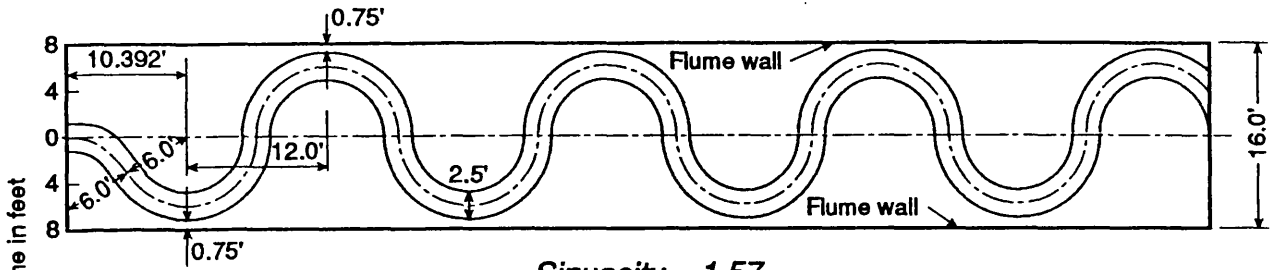


**Cross-section through channel**

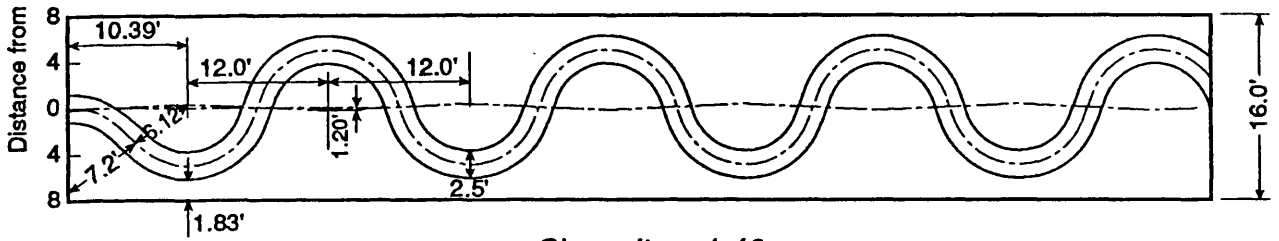
**5.6 Plan geometry of the Aberdeen flume with channel sinuosity of 1.21 (after Willetts 1992)**



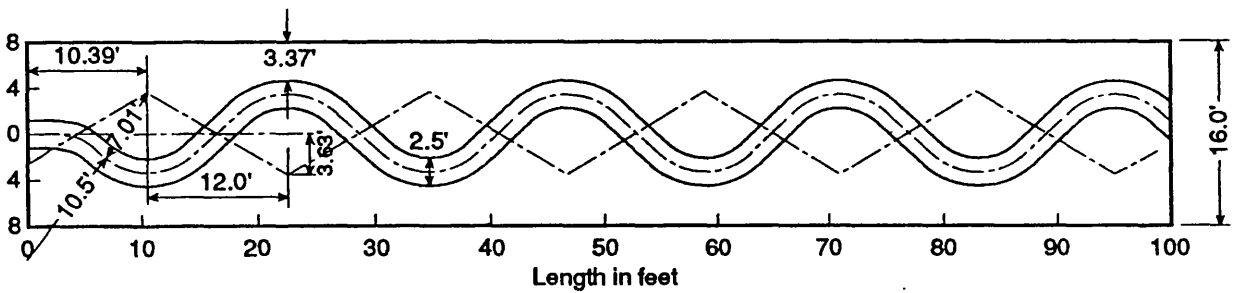
*Sinuosity = 1.00*



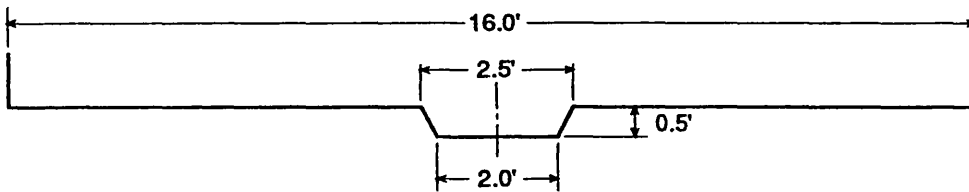
*Sinuosity = 1.57*



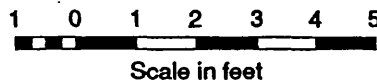
*Sinuosity = 1.40*



*Sinuosity = 1.20*

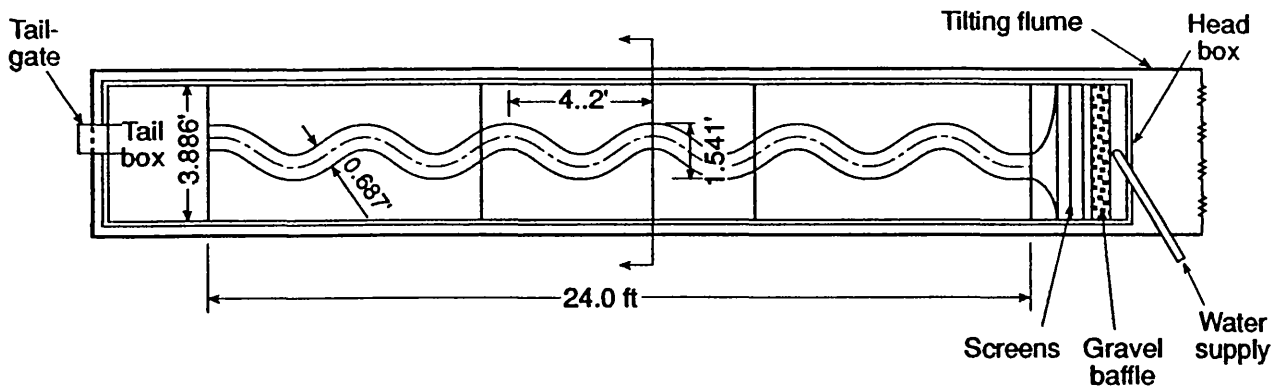


*End view*



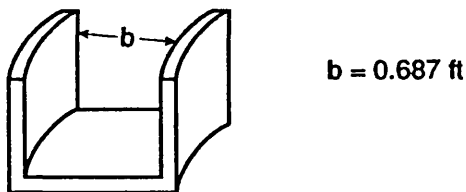
**5.7 Plan and cross-sections for Vicksburg flume (after US Army 1956)**

**Plan view**

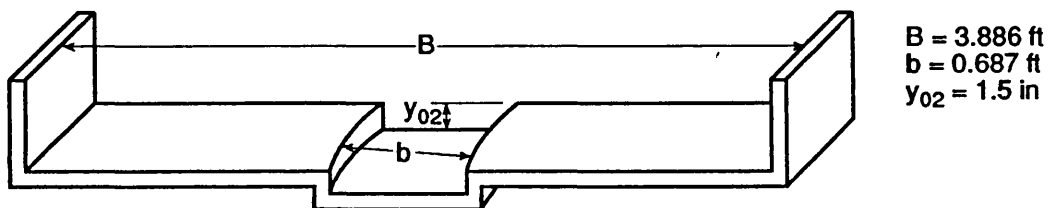


**Cross-sections**

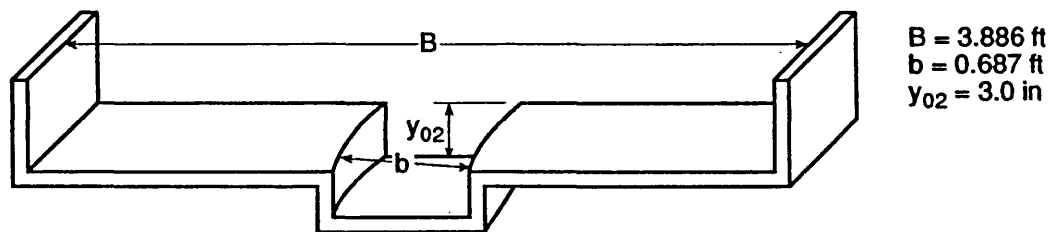
**Geometry 3: Meandering narrow channel**



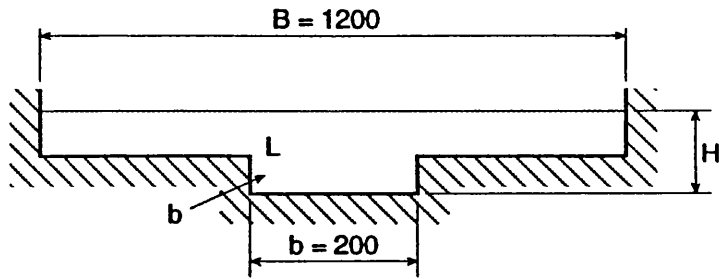
**Geometry 4: Composite channel**



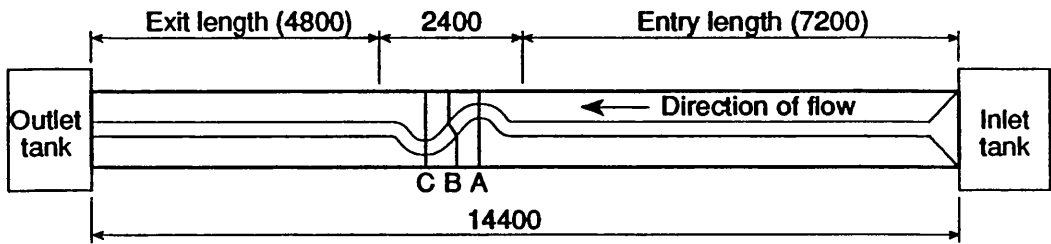
**Geometry 5: Composite channel**



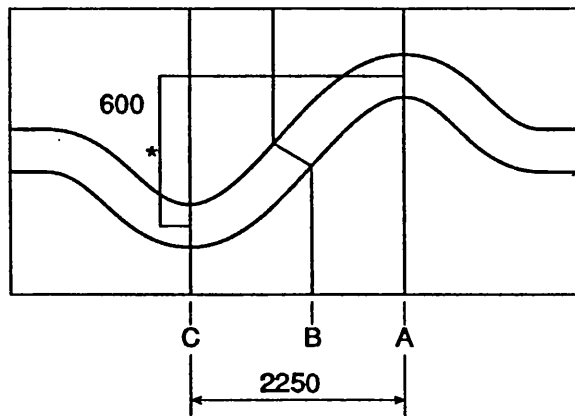
**5.8 Plan and cross-sections for Sooky's flume (after Sooky 1964)**



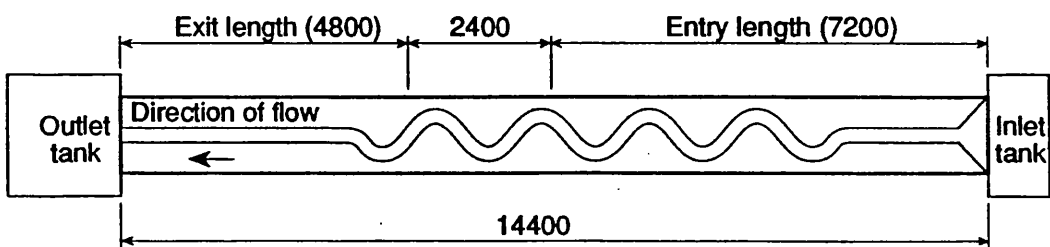
**Single meander compound channel**



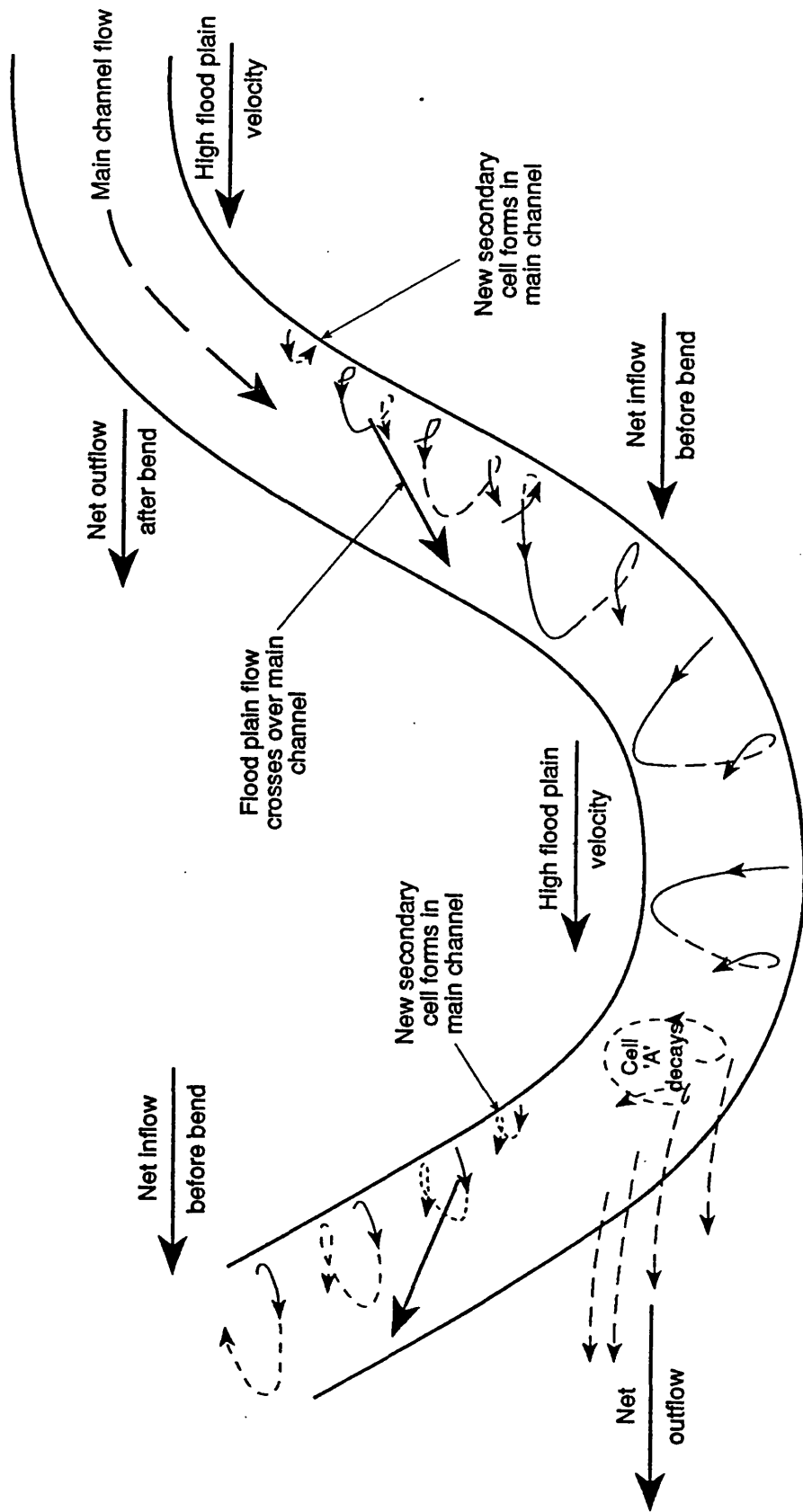
**Test section**



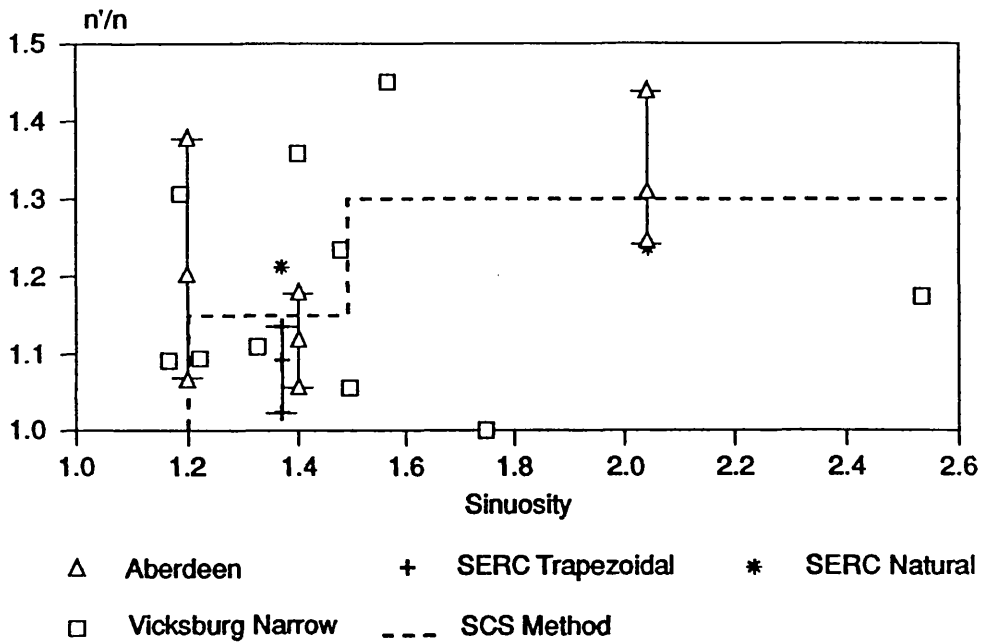
**Multiple meander compound channel**



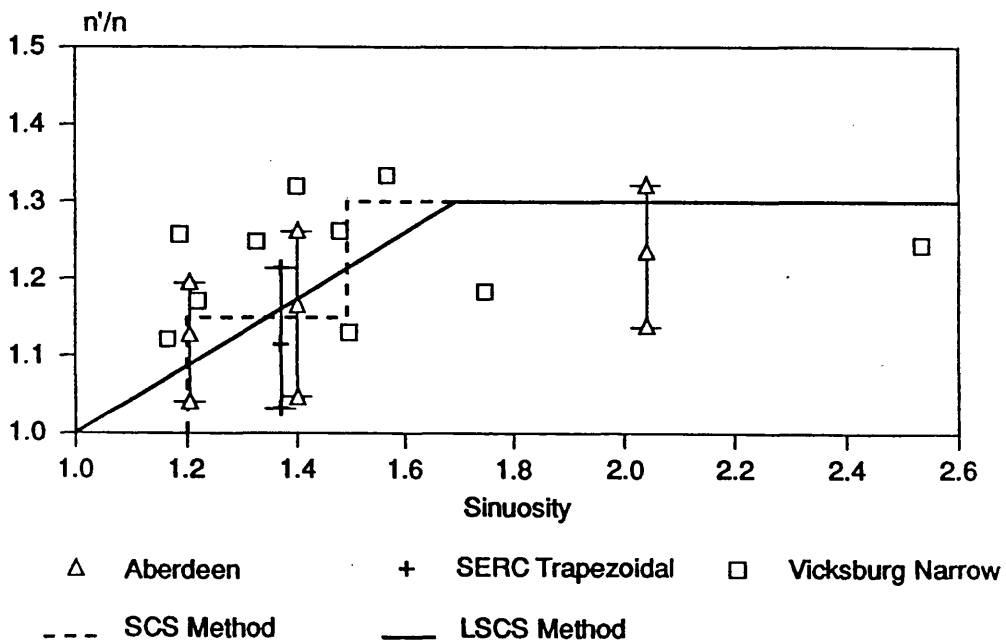
**5.9 Plan and cross-sections for Kiely's flume (after Kiely 1990)**



5.10 Flow processes in a meandering compound channel (after Ervine and Jasem)



**5.11 Adjustment to Manning's n for bend losses: measured and predicted**



**5.12 Predicted adjustments to n for bend losses: modified Chang method**

**Table 6.1 Mean errors straight methods meandering data**

Method	All Data		Smooth Data		Rough Data	
	Mean % Error	SD	Mean % Error	SD	Mean % Error	SD
DCM	38.5	17.8	44.8	16.2	24.4	12.5
SCM	37.6	56.7	7.7	10.0	104.6	61.0
SSGM	70.1	30.6	69.4	29.9	71.6	32.5
DCM2	41.6	16.8	47.0	15.9	29.3	11.7
ACKM	24.8	26.0	39.9	14.2	-9.1	8.2
HOR1	30.8	29.0	42.4	21.5	4.6	26.6
HOR2	13.8	23.5	25.5	16.8	-12.3	12.7
HOR3	20.6	23.3	32.9	14.2	-7.0	14.4
HOR4	7.3	23.2	19.5	16.6	-19.8	6.6

**Notes**

- 1 % Error =  $100 \cdot (Q_{calc} - Q_{meas}) / Q_{meas}$
- 2 SD = Standard Deviation in Mean % Error
- 3 All Data - B21 B26 B31 B34 B39 B43 B47
- 4 Smooth Data - B21 B26 B31 B39 B47
- 5 Rough Data - B34 B43

**Table 6.2 Contraction loss coefficients (Rouse, 1950)**

$y_2/(y_2+h)$	:	0.00	0.10	0.20	0.30	0.40	0.50	0.60	0.70	0.80	0.90	1.00
$K_c$	:	0.50	0.48	0.45	0.41	0.36	0.29	0.21	0.13	0.07	0.01	0.00

**Table 6.3 Main channel integrated discharges**

Run	Channel Type	Flow Depth on Flood Plain (mm)	Main Channel Discharge (m <sup>3</sup> /s)	Bankfull Discharge (m <sup>3</sup> /s)
B23	60° Trap	50.5	0.0580	0.0865
B24	smooth	100.9	0.0710	0.0865
B28	60° Nat	15.2	0.0270	0.0385
B29	smooth	50.0	0.0334	0.0385
B30		99.7	0.0437	0.0385
B35	60° Nat	15.3	0.0271	0.0385
B36	rough	50.1	0.0223	0.0385
B37		101.0	0.0243	0.0385
B41	110° Nat	15.0	0.0190	0.0297
B42	smooth	50.8	0.0204	0.0297
B44	110° Nat	15.6	0.0208	0.0297
B45	rough	50.3	0.0173	0.0297

**Table 6.4 Variables for defining main channel flow**

Run	$Q_1'$	$y'$	$B^2/A$	$s$	$f_2$	$f_1$	$f'$
B23	0.671	0.385	9.142	1.37	0.02221	0.01682	1.320
B24	0.821	0.769	9.142	1.37	0.01708	0.01664	1.026
B28	0.701	0.185	14.60	1.37	0.03691	0.01936	1.907
B29	0.868	0.607	14.60	1.37	0.02158	0.01900	1.136
B30	1.135	1.211	14.60	1.37	0.01670	0.01883	0.887
B35	0.704	0.186	14.60	1.37	0.05150	0.01956	2.633
B36	0.579	0.609	14.60	1.37	0.10850	0.01945	5.578
B37	0.631	1.227	14.60	1.37	0.18050	0.01938	9.314
B41	0.640	0.183	14.60	2.04	0.03776	0.02050	1.842
B42	0.687	0.620	14.60	2.04	0.02906	0.02066	1.407
B44	0.700	0.190	14.60	2.04	0.05200	0.01996	2.605
B45	0.583	0.614	14.60	2.04	0.10850	0.01993	5.444

**Table 6.5 Adjusted variables for defining main channel flow**

Test	$Q_1'$	$y'$	$B^2/A$	$s$	$f'$
B23'	0.690	0.385	9.142	1.37	1.026
B24'	0.802	0.769	9.142	1.37	1.320
B29'	0.884	0.607	14.60	1.37	0.887
B30'	1.113	1.211	14.60	1.37	1.136
B36'	0.336	0.609	14.60	1.37	9.314
B37'	0.963	1.227	14.60	1.37	5.578

**Table 6.6 Roughness and sinuosity adjustment to  $Q_1'$** 

Run	$Q_{1p}'$	$Q_1'$	$Q_1'/Q_{1p}'$
B23	0.691	0.671	0.971
B24	0.816	0.821	1.006
B29	0.885	0.868	0.981
B30	1.129	1.135	1.005
B36	0.972	0.579	0.596
B37	1.466	0.631	0.430
B42	0.693	0.687	0.991
B45	0.770	0.583	0.757

**Table 6.7 Roughness and sinuosity adjustment to  $c$** 

Run	$c_p$	$c$	$c/c_p$
B23	0.558	0.537	0.962
B24	0.558	0.562	1.007
B29	0.630	0.613	0.973
B30	0.630	0.636	1.010
B36	0.630	0.237	0.376
B37	0.630	-0.205	-0.325
B42	0.428	0.427	0.999
B45	0.428	0.240	0.561

**Table 6.8 Errors (%) in reproducing  $Q_1'$  for high values of  $y'$** 

Run No.	Method						
	1	2	3	4	5	6	7
B23	0.70	-0.40	-15.33	0.85	-2.47	-0.06	-2.57
B24	-0.71	-0.52	-6.55	0.49	1.87	-0.03	2.08
B29	1.00	0.90	3.47	-1.62	-7.91	-0.04	-0.09
B30	-3.03	-2.73	5.51	-0.22	-5.36	1.13	0.20
B36	14.30	0.62	5.78	2.59	-2.58	0.05	1.63
B37	-2.42	19.90	4.81	12.74	0.32	6.63	-0.71
B42	-0.53	-0.41	13.16	11.61	20.06	24.56	23.65
B45	-8.85	-11.94	-15.51	-12.91	1.17	1.29	2.72
Ave	5.75	0.68	-0.58	1.69	0.64	4.19	3.27
S D	6.13	8.25	9.92	7.51	7.97	7.98	7.88

**Table 6.9 Data sets for inner flood plain analysis**

Run	Channel Type	$B^2/A$	s
B21	SERC 60° trapezoidal	9.142	1.374
B26	SERC 60° natural, smooth	14.600	1.374
B34	SERC 60° natural, rough	14.600	1.374
B39	SERC 110° natural, smooth	14.600	2.041
B43	SERC 110° natural, rough	14.600	2.041
101	Aberdeen, trapezoidal	3.837	1.215
102	Aberdeen, trapezoidal	3.837	1.406
104	Aberdeen, trapezoidal	3.837	2.041

**Table 6.10 Equation parameters for  $y'$  greater than 0.2**

Run	a	b
B21	0.675	-0.2846
B26	0.792	-0.2051
B34	0.760	-0.2051
B39	0.660	-0.0356
B43	0.490	-0.2468
AB101	0.910	-0.3912
AB102	0.710	-0.3741
AB104	0.510	-0.4743

**Table 6.11 Geometric data overbank laboratory studies**

Test	$\theta$ (°)	$L_{co}$ (m)	$r_c$ (m)	B (m)	$S_o$ x10-3	L (m)	s	$W_2$ (m)	$W_T$ (m)	$S_{sf}$
<b>SERC FCF Phase B</b>										
21	60	2.500	2.743	1.200	0.996	12.000	1.374	6.107	10.000	0.00
26	60	2.500	2.743	1.200	0.996	12.000	1.374	6.107	10.000	0.00
31	60	2.500	2.743	1.200	0.996	12.000	1.374	6.107	6.107	1.00
33	60	2.500	2.743	1.200	0.996	12.000	1.374	6.107	10.000	0.00
34	60	2.500	2.743	1.200	0.996	12.000	1.374	6.107	10.000	0.00
39	110	0.000	2.743	1.200	1.021	10.310	2.043	8.560	10.000	0.00
43	110	0.000	2.743	1.200	1.021	10.310	2.043	8.560	10.000	0.00
47	110	0.000	2.743	1.200	1.021	10.310	2.043	8.560	8.560	1.00
<b>Aberdeen</b>										
101	40	0.984	0.413	0.174	1.000	2.570	1.215	1.000	1.200	0.00
102	60	0.477	0.413	0.174	1.000	1.909	1.406	1.000	1.200	0.00
104	110	0.000	0.307	0.174	0.621	1.154	2.043	1.000	1.200	0.00
<b>Vicksburg</b>										
201	90	0.000	1.829	0.762	1.000	7.315	1.571	4.420	4.877	0.00
204	78.7	0.000	1.865	0.762	1.000	7.315	1.400	3.761	4.877	0.00
207	58.8	0.000	2.136	0.762	1.000	7.315	1.200	2.822	4.877	0.00
<b>Kiely</b>										
301	45	0.475	0.4000	0.200	1.000	1.803	1.224	0.770	1.200	0.00

**Table 6.12 Geometric data Sooky's laboratory study**

Test	NOP	$r_c$	B (m)	$S_o$ (m)	L $\times 10^{-3}$	s (m)	$W_2$ (m)	$W_T$ (m)	$S_{sf}$
<b>Geometry 4</b>									
401	5	1.392	0.209	0.675	1.280	1.090	0.462	1.184	0.00
402	6	1.392	0.209	8.700	1.280	1.090	0.462	1.184	0.00
403	6	1.392	0.209	1.600	1.280	1.090	0.462	1.184	0.00
404	6	1.392	0.209	3.670	1.280	1.090	0.462	1.184	0.00
<b>Geometry 5</b>									
405	5	1.392	0.209	0.300	1.280	1.090	0.462	1.184	0.00
406	7	1.392	0.209	0.675	1.280	1.090	0.462	1.184	0.00
407	7	1.392	0.209	0.870	1.280	1.090	0.462	1.184	0.00
408	5	1.392	0.209	1.000	1.280	1.090	0.462	1.184	0.00
409	6	1.392	0.209	1.600	1.280	1.090	0.462	1.184	0.00
410	5	1.392	0.209	3.000	1.280	1.090	0.462	1.184	0.00
411	5	1.392	0.209	3.670	1.280	1.090	0.462	1.184	0.00

Note :

1 NOP = number of data points

**Table 6.13 Main channel geometric data**

Test	Type of xs	h (m)	A <sub>1</sub> (m <sup>2</sup> )	P <sub>1</sub> (m)	Q <sub>b</sub> (l/s)	S <sub>s</sub>	θ <sub>m</sub> (°)
21	Trapezoidal	0.150	0.1575	1.324	86.50	1.00	39.10
26	Natural	0.150	0.0988	1.288	38.50	1.00	39.10
31	Natural	0.150	0.0988	1.288	38.50	1.00	39.10
33	Natural	0.150	0.0988	1.288	38.50	1.00	39.10
34	Natural	0.150	0.0988	1.288	38.50	1.00	39.10
39	Natural	0.150	0.0983	1.281	29.70	1.00	55.00
43	Natural	0.150	0.0983	1.281	29.70	1.00	55.00
47	Natural	0.150	0.0983	1.281	29.70	1.00	55.00
101	Trapezoidal	0.050	0.0078	0.245	1.76	0.35	32.61
102	Trapezoidal	0.050	0.0078	0.245	1.72	0.35	40.66
104	Trapezoidal	0.050	0.0078	0.245	0.94	0.35	55.00
201	Trapezoidal	0.152	0.1045	0.950	34.60	2.00	45.00
204	Trapezoidal	0.152	0.1045	0.950	39.08	2.00	39.35
207	Trapezoidal	0.152	0.1045	0.950	43.90	2.00	29.41
301	Rectangular	0.050	0.0100	0.300	2.32	0.00	32.19
401	Rectangular	0.038	0.0080	0.286	1.30	0.00	11.73
402	Rectangular	0.038	0.0080	0.286	1.50	0.00	11.73
403	Rectangular	0.038	0.0080	0.286	2.18	0.00	11.73
404	Rectangular	0.038	0.0080	0.286	2.90	0.00	11.73
405	Rectangular	0.076	0.0160	0.362	3.55	0.00	11.73
406	Rectangular	0.076	0.0160	0.362	3.55	0.00	11.73
407	Rectangular	0.076	0.0160	0.362	4.20	0.00	11.73
408	Rectangular	0.076	0.0160	0.362	4.65	0.00	11.73
409	Rectangular	0.076	0.0160	0.362	5.98	0.00	11.73
410	Rectangular	0.076	0.0160	0.362	7.62	0.00	11.73
411	Rectangular	0.076	0.0160	0.362	7.99	0.00	11.73

**Table 6.14 Mean % errors in discharge FCF data**

TEST	NOP	BFO	JW	JW2	EE	GH4	GH5
21	16	38.7	3.9	7.1	12.2	16.3	15.4
		8.4	6.1	1.3	15.1	3.3	3.5
26	16	29.2	-2.7	-1.3	4.2	9.8	8.7
		5.4	2.9	2.6	14.1	6.0	5.5
31	14	37.0	-7.5	-5.5	0.8	10.0	9.6
		5.4	5.3	22.8	19.1	5.2	4.9
33	12	8.9	-6.4	-13.7	6.0	-3.2	-6.0
		12.5	4.9	3.9	11.0	5.1	5.9
34	18	9.3	-6.9	-20.2	5.8	-5.3	-7.8
		15.1	3.7	8.5	13.8	9.1	9.7
39	14	59.1	-3.8	-11.7	3.2	39.0	15.1
		6.9	12.5	8.6	24.3	6.4	9.8
43	15	18.5	-2.4	-33.3	12.8	8.3	-8.2
		24.6	8.1	17.1	23.1	21.6	23.7
47	14	63.0	-7.3	-16.7	3.0	40.2	14.9
		6.0	13.3	9.2	27.5	5.7	9.9
smooth	74	44.8	-3.3	-5.2	4.9	22.5	12.7
		14.7	9.6	10.1	20.2	14.6	7.5
rough	45	12.3	-5.3	-22.8	8.2	-0.2	-7.5
		18.4	6.0	13.7	16.9	15.0	15.0
All	119	32.5	-4.0	-11.8	6.1	13.9	5.1
		22.6	8.4	14.4	19.0	18.4	14.6

Note :

The lower values are standard deviations in the means

**Table 6.15 Mean % errors in discharge Aberdeen, Vicksburg and Kiely data**

TEST	NOP	BFO	JW	JW2	EE	GH4	GH5
<b>Aberdeen</b>							
101	33	28.2	-6.1	-3.4	-4.0	0.5	2.5
		11.8	5.5	7.4	16.7	7.4	7.6
102	30	41.6	1.5	3.4	-2.0	14.2	11.9
		7.9	4.5	4.7	14.4	6.5	5.2
104	20	77.0	10.4	3.6	0.1	47.8	30.8
		22.4	8.3	7.1	15.7	14.6	11.7
All	83	44.8	0.6	0.8	-2.3	16.9	12.7
		23.7	8.7	7.2	15.5	20.7	13.6
<b>Vicksburg</b>							
201	3	59.3	-2.5	6.0	1.1	34.6	26.0
		7.6	6.1	3.8	13.4	6.3	4.2
204	3	45.3	-5.3	5.3	6.8	21.1	19.2
		9.9	11.2	10.0	2.5	9.6	8.4
207	3	32.9	-8.0	1.3	1.8	8.1	12.6
		5.8	11.3	12.6	4.9	7.0	7.8
All	9	45.8	-5.3	4.2	3.2	21.3	19.3
		13.3	8.9	8.6	7.7	13.3	8.4
<b>Kiely</b>							
301	5	39.2	-0.8	6.3	-1.9	11.1	14.9
		8.0	3.1	8.2	11.1	5.6	6.0

Note :

The lower values are standard deviations in the means

**Table 6.16 Mean % errors in discharge Sooky data**

TEST	NOP	BFO	JW	JW2	EE	GH4	GH5
401	5	22.8	3.2	2.7	15.8	0.1	8.6
		5.0	4.3	4.7	4.8	4.2	4.7
402	6	23.5	3.7	3.8	16.6	0.8	9.4
		6.3	5.2	6.4	6.5	5.3	5.9
403	6	24.8	5.0	7.3	18.6	2.0	10.9
		7.7	6.1	7.5	8.1	6.2	6.8
404	6	40.2	12.8	17.9	34.4	14.4	24.2
		17.7	12.9	14.5	17.8	14.2	15.2
405	5	-13.9	-18.4	-14.9	-18.7	-29.8	-25.5
		4.9	7.9	6.0	6.0	4.0	3.7
406	7	7.5	-15.0	-7.9	1.1	-12.1	-6.5
		10.8	7.0	7.2	11.4	8.7	8.7
407	7	12.0	-10.8	-4.3	5.7	-8.5	-2.9
		11.4	8.5	6.3	12.1	9.1	8.9
408	5	17.9	-2.4	-0.7	12.4	-4.1	0.4
		9.2	11.0	5.1	10.2	6.9	5.7
409	6	20.7	-4.3	1.4	14.6	-1.3	4.4
		13.1	10.9	5.0	13.4	10.4	10.2
410	5	37.0	6.2	6.3	30.8	11.6	16.7
		8.1	9.6	3.7	8.8	6.0	4.6
411	5	39.7	3.0	1.7	33.4	13.9	19.4
		11.1	10.4	5.4	11.3	8.6	8.0
All	63	20.8	-1.9	1.2	14.6	-1.4	5.2
		17.5	12.4	10.6	17.6	14.2	15.1

Note :

The lower values are standard deviations in the means

**Table 6.17 Mean % errors in discharge all data**

TEST	NOP	BFO	JW	JW2	EE	GH4	GH5
1	74	44.8	-3.3	-5.2	4.9	22.5	12.7
		14.7	9.6	10.1	20.2	14.6	7.5
2	45	12.3	-5.3	-22.8	8.2	-0.2	-7.5
		18.4	6.0	13.7	16.9	15.0	15.0
3	119	32.5	-4.0	-11.8	6.1	13.9	5.1
		22.6	8.4	14.4	19.0	18.4	14.6
4	83	44.8	0.6	0.8	-2.3	16.9	12.7
		23.7	8.7	7.2	15.5	20.7	13.6
5	9	45.8	-5.3	4.2	3.2	21.3	19.3
		13.3	8.9	8.6	7.7	13.3	8.4
6	63	20.8	-1.9	1.2	14.6	-1.4	5.2
		17.5	12.4	10.6	17.6	14.2	15.1
7	279	34.1	-2.1	-4.3	5.3	11.5	8.0
		23.2	9.7	13.2	18.3	19.3	14.7
8	77	24.9	-2.6	1.8	11.9	2.0	7.4
		18.8	11.7	10.2	17.2	15.6	14.8

**Notes:**

The lower values are standard deviations in the means

- 1 - SERC PHASE B SMOOTH 21 26 31 39 47
- 2 - SERC PHASE B ROD ROUGHEND 33 34 43
- 3 - ALL SERC
- 4 - ALL ABERDEEN 101 102 104
- 5 - VICKSBURG 201 204 207
- 6 - ALL SOOKY 401 - 411
- 7 - ALL DATA
- 8 - VICKSBURG, KIELY AND SOOKY data only

**Table 6.18 Ranking of methods**

TEST	1st	2nd	3rd	4th	5th	6th
1	JW	EE	JW2	GH5	GH4	BFO
2	GH4	GH5	JW	EE	BFO	JW2
3	JW	GH5	EE	JW2	GH4	BFO
4	JW	JW2	EE	GH5	GH4	BFO
5	EE	JW2	JW	GH5	GH4	BFO
6	JW2	GH4	JW	GH5	EE	BFO
7	JW	JW2	EE	GH5	GH4	BFO
8	JW2	GH4	JW	GH5	GH4	BFO

**Table 6.19 Mean % errors in stage FCF data**

TEST	NOP	BFO	JW	JW2	EE	GH4	GH5
21	16	-5.3	-0.6	-1.2	-1.0	-2.5	-2.4
		1.6	0.9	0.4	2.3	1.2	1.1
26	16	-4.0	0.8	0.5	0.5	-1.7	-1.5
		2.0	1.3	1.1	2.4	1.5	1.3
31	14	-4.9	2.4	1.6	2.5	-1.7	-1.6
		2.2	3.4	2.7	5.9	1.5	1.4
33	12	-0.8	0.9	3.2	-0.4	1.3	2.1
		1.0	0.9	2.2	1.0	1.6	2.2
34	18	-0.6	2.2	8.5	0.2	3.1	4.1
		2.2	1.4	5.8	2.4	3.5	4.0
39	14	-7.2	2.3	3.8	1.9	-5.3	-2.1
		3.5	3.1	3.5	4.0	2.6	0.7
43	15	-1.3	1.5	19.7	-0.2	1.2	7.7
		2.9	2.1	15.5	3.2	4.4	9.3
47	14	-7.1	3.3	5.1	2.7	-5.1	-2.0
		3.5	4.3	4.9	5.5	2.5	0.7
smooth	74	-5.6	1.6	1.9	1.2	-3.2	-1.9
		2.9	3.1	3.6	4.3	2.4	1.1
rough	45	-0.9	1.6	10.8	-0.1	2.0	4.8
		2.2	1.6	11.6	2.4	3.5	6.3
All	119	-3.8	1.6	5.2	0.7	-1.2	0.6
		3.5	2.6	8.8	3.8	3.8	5.1

Note :

The lower values are standard deviations in the means

**Table 6.20 Mean % errors in stage Aberdeen, Vicksburg and Kiely data**

TEST	NOP	BFO	JW	JW2	EE	GH4	GH5
<b>Aberdeen</b>							
101	33	-4.8	1.4	0.9	2.6	0.0	-0.3
		2.2	1.2	1.5	4.7	1.3	1.3
102	30	-5.7	-0.4	-0.7	2.2	-2.5	-2.1
		3.0	0.8	0.7	4.2	2.1	1.7
104	20	-8.7	-1.8	-0.7	1.7	-6.5	-4.7
		5.3	1.6	1.1	3.5	4.1	2.7
All	83	-6.1	0.0	0.0	2.2	-2.5	-2.0
		3.7	1.7	1.4	4.2	3.5	2.5
<b>Vicksburg</b>							
201	3	-8.5	0.1	-1.5	4.9	-5.9	-4.8
		3.9	1.2	1.4	10.0	3.0	2.3
204	3	-7.3	0.5	-1.6	-1.5	-4.2	-4.0
		3.8	1.8	2.3	0.2	3.0	2.7
207	3	-5.9	1.0	-1.0	4.0	-1.9	-2.8
		2.9	1.7	2.4	7.5	2.0	2.4
All	9	-7.2	0.5	-1.3	2.4	-4.0	-3.9
		3.3	1.4	1.8	6.9	2.9	2.3
<b>Kiely</b>							
301	5	-6.6	2.3	-1.6	3.3	-2.3	-3.0
		1.8	5.0	1.7	7.3	1.1	1.3

Note:

The lower values are standard deviations in the means

**Table 6.21 Mean % errors in stage Sooky data**

TEST	NOP	BFO	JW	JW2	EE	GH4	GH5
401	5	-6.1	-0.2	0.0	-4.5	0.8	-2.6
		1.4	2.5	2.9	1.3	2.7	1.2
402	6	-5.9	-0.9	0.1	-4.4	0.9	-2.5
		1.1	1.4	3.5	1.2	3.3	1.4
403	6	-5.7	-1.1	-1.7	-4.5	0.5	-2.6
		0.8	1.3	1.5	1.1	2.8	1.1
404	6	-7.8	-2.5	-3.7	-7.0	-3.0	-4.9
		1.3	1.9	1.9	1.7	2.2	1.7
405	5	5.0	8.4	5.6	8.1	11.8	9.9
		5.0	6.7	5.8	6.7	7.4	6.6
406	7	-1.2	4.7	2.5	0.6	4.3	2.5
		2.8	3.5	3.1	3.8	4.1	3.5
407	7	-2.1	3.4	1.5	-0.5	3.1	1.4
		2.6	3.3	2.5	3.4	3.6	3.1
408	5	-3.6	1.2	0.9	-1.5	2.2	1.1
		1.6	5.3	3.3	4.2	4.3	3.7
409	6	-4.0	1.2	-0.1	-2.8	0.8	-0.6
		2.0	3.1	1.3	2.6	2.9	2.4
410	5	-7.0	-1.6	-1.6	-6.1	-2.5	-3.3
		0.8	3.3	1.2	1.0	1.1	0.6
411	5	-7.3	-0.5	-0.2	-6.5	-2.9	-3.7
		1.1	3.1	1.6	1.3	1.5	1.1
All	63	-4.1	1.2	0.3	-2.6	1.5	-0.5
		4.0	4.4	3.5	4.9	5.1	4.7

Note :

The lower values are standard deviations in the means

**Table 6.22 Mean % errors in stage all data**

TEST	NOP	BFO	JW	JW2	EE	GH4	GH5
1	74	-5.6	1.6	1.9	1.2	-3.2	-1.9
		2.9	3.1	3.6	4.3	2.4	1.1
2	45	-0.9	1.6	10.8	-0.1	2.0	4.8
		2.2	1.6	11.6	2.4	3.5	6.3
3	119	-3.8	1.6	5.2	0.7	-1.2	0.6
		3.5	2.6	8.8	3.8	3.8	5.1
4	83	-6.1	0.0	0.0	2.2	-2.5	-2.0
		3.7	1.7	1.4	4.2	3.5	2.5
5	9	-7.2	0.5	-1.3	2.4	-4.0	-3.9
		3.3	1.4	1.8	6.9	2.9	2.3
6	63	-4.1	1.2	0.3	-2.6	1.5	-0.5
		4.0	4.4	3.5	4.9	5.1	4.7
7	279	-4.7	1.0	2.2	0.5	-1.1	-0.6
		3.8	3.0	6.6	4.7	4.3	4.4
8	77	-4.6	1.8	0.0	-1.4	0.6	-1.0
		4.0	4.7	3.3	5.9	5.1	4.5

**Notes:**

The lower values are standard deviations in the means

1 - SERC PHASE B SMOOTH 21 26 31 39 47

2 - SERC PHASE B ROD ROUGHEND 33 34 43

3 - ALL SERC

4 - ALL ABERDEEN 101 102 104

5 - VICKSBURG 201 204 207

6 - ALL SOOKY 401 - 411

7 - ALL DATA

8 - VICKSBURG, KIELY AND SOOKY data only

**Table 6.23 Sensitivity tests : effect of errors in wave length**

Factor	% Error in L	mean % Error in discharge
0.50	-50.0	-10.3
0.75	-25.0	-5.5
1.00	0.0	-2.1
1.25	25.0	0.4
1.50	50.0	2.3

**Table 6.24 Sensitivity tests : effect of errors in channel side slope**

Factor	% Error in $S_s$	mean % Error in discharge
0.00	-100.0	-5.3
0.50	-50.0	-3.9
1.00	0.0	-2.1
1.50	50.0	-0.1
2.00	100.0	2.4

**Table 6.25 Measured zonal discharges, Sooky and Kiely data**

Test	source	Depth (mm)	Discharge (l/s)				
			Total	zone 1	zone 2	zone 3	zone 4
403	Sooky	61.3	7.89	2.09	2.58	1.54	1.68
409	Sooky	99.4	12.62	4.82	3.33	2.11	2.36
301	Kiely	60.0	3.10	1.49	1.11	0.40	0.40
301	Kiely	80.0	11.10	3.10	5.48	1.26	1.26

**Table 6.26 Errors (%) in calculated total flows, Sooky and Kiely data**

Test	Depth	BFO	JW	JW2	Method		
					EE	GH4	GH5
403	61.3	33.9	12.6	16.0	27.8	9.5	19.1
409	99.4	12.4	-10.3	2.2	5.8	-7.8	-1.8
301	60.0	52.9	3.8	6.8	14.8	20.6	24.6
301	80.0	36.0	-0.9	12.6	-9.0	10.5	15.3

**Table 6.27 Measured and calculated flow distributions**

Zone	Measured	% (Zonal flow / Total flow)					
		BFO	JW	JW2	EE	GH4	GH5
	Test 403	Sooky	depth = 61.3mm				
1	26.5	21.3	19.1	19.1	21.9	19.6	18.0
2	32.7	38.2	32.9	32.9	35.7	31.0	38.8
3	19.5	20.2	24.0	24.0	21.2	24.7	21.6
4	21.3	20.2	24.0	24.0	21.1	24.0	21.6
	Test 409	Sooky	depth = 99.4mm				
1	38.2	41.1	33.5	29.4	42.2	40.4	37.8
2	26.4	28.5	28.7	37.6	25.8	23.0	29.6
3	16.7	15.0	18.9	16.5	16.0	18.3	16.3
4	16.7	15.0	18.9	16.5	16.0	18.3	16.3
	Test 301	Kiely	depth = 60.0mm				
1	48.1	61.2	47.7	46.7	59.5	59.4	57.4
2	35.9	27.2	35.1	36.9	25.1	26.2	29.0
3	8.0	5.8	8.6	8.2	7.7	7.2	6.8
4	8.0	5.8	8.6	8.2	7.7	7.2	6.8
	Test 301	Kiely	depth = 80.0mm				
1	27.8	19.2	14.8	13.0	21.0	18.0	17.3
2	49.4	57.2	53.0	58.6	43.8	53.0	58.3
3	11.4	11.8	16.1	14.2	17.6	14.5	12.2
4	11.4	11.8	16.1	14.2	17.6	14.5	12.2

**Table 6.28 Reach averaged geometric parameters Roding study**

$y_2$ (m)	Area (m <sup>2</sup> )	Width (m)	Wetted perimeter (m)
Main channel at bankfull			
0.0	5.3	7.1	7.7
Zone 2			
0.1	2.1	20.5	10.8
0.2	4.4	25.3	15.7
0.3	7.1	27.9	18.4
0.4	10.0	29.0	19.5
0.5	12.9	29.9	20.4
0.6	15.9	30.4	20.9
0.7	19.0	30.9	21.4
0.8	22.1	31.3	21.9
0.9	25.3	31.8	22.5
1.0	28.5	32.4	23.1

**Table 6.29 Errors in predicting overbank discharges**

Case Method	P2	Standard Deviation	M2	Standard Deviation
	Mean %Error		Mean %Error	
Bed Friction Only	9.5	9.0	7.3	8.6
James and Wark	-2.0	1.7	-2.2	3.2
James and Wark 2	-27.1	10.0	-30.5	10.9

Note %Error =  $100 \cdot (Q_{\text{calc}} - Q_{\text{meas}}) / Q_{\text{meas}}$

**Table 6.30 Sensitivity tests on the effect of floodplain roughness**

Zone 2 Manning n	Mean %Errors		Difference in Means (BFO - JW)
	BFO	JW	
0.01	305	142	163
0.02	122	78	44
0.03	61	40	21
0.04	31	16	15
0.05	10	-2	12
0.06	1	-10	11
0.08	-14	-25	11
0.10	-24	-33	9
0.18	-40	-47	7
0.30	-48	-58	10

Note %Error =  $100 \cdot (Q_{\text{calc}} - Q_{\text{meas}}) / Q_{\text{meas}}$

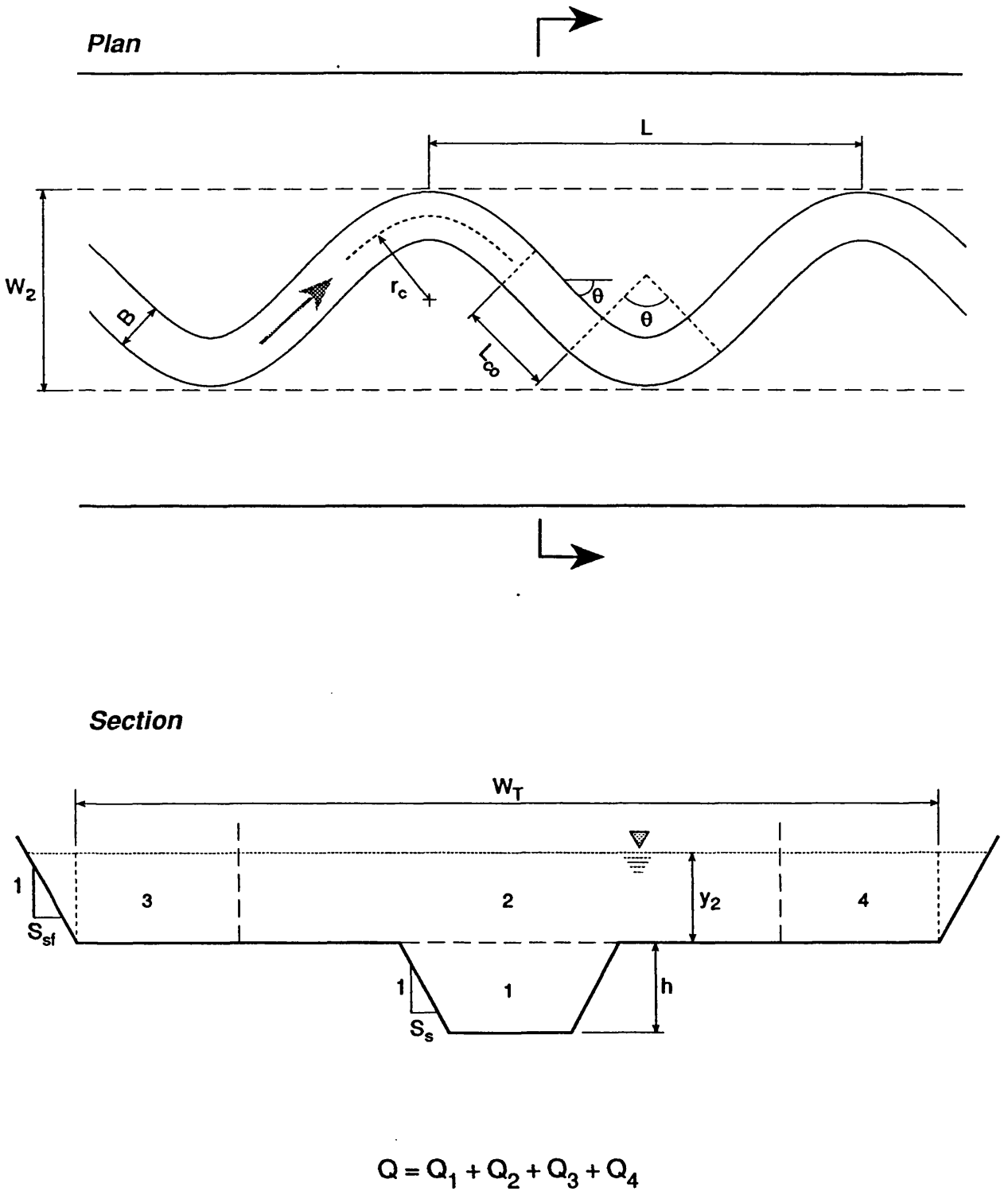
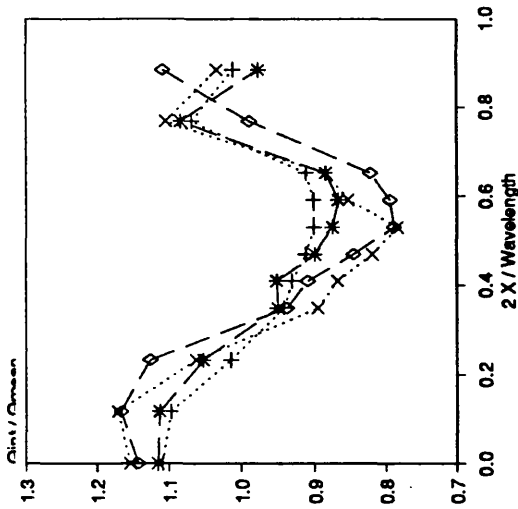


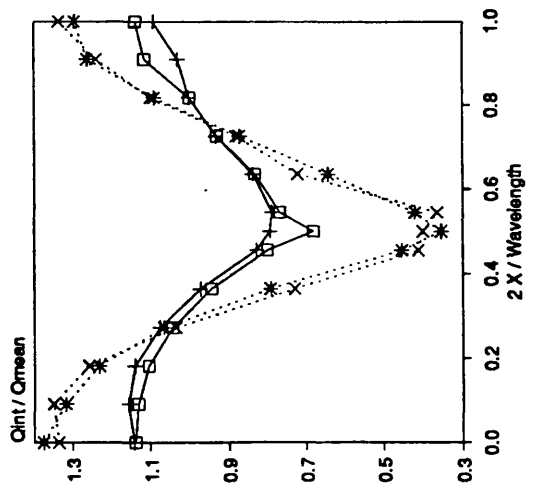
**Figure 6.1 Cross-section subdivision for overbank flows Ervine and Ellis method**

A) Sinuosity 1.374 effect of X-S shape



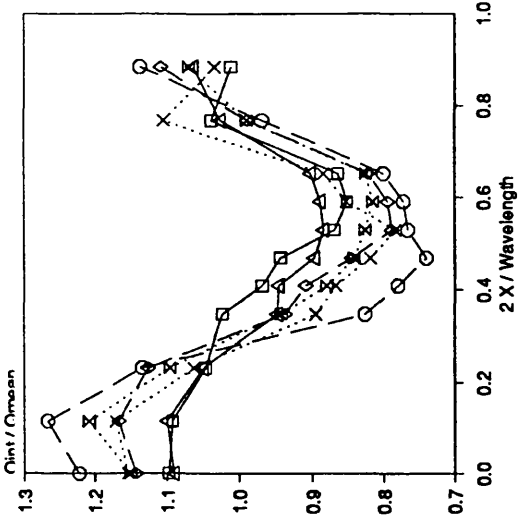
- + B23 60 T 200
- \* B24 60 T 250
- x· B29 60 N 200
- ◇ B30 60 N 250

C) Sinuosity 2.043 effect of roughness



- + B41 110 N 165
- \* B42 110 N 200
- B44 110 N 165 R
- x· B45 110 N 200 R

B) Sinuosity 1.374 effect of roughness



- B28 60 N 165
- x· B29 60 N 200
- ◇ B30 60 N 250
- △ B35 60 N 165 R
- x· B36 60 N 200 R
- B37 60 N 250 R

Figure 6.2 Variation of main channel discharge along a meander during overbank flow (FCF Phase B)

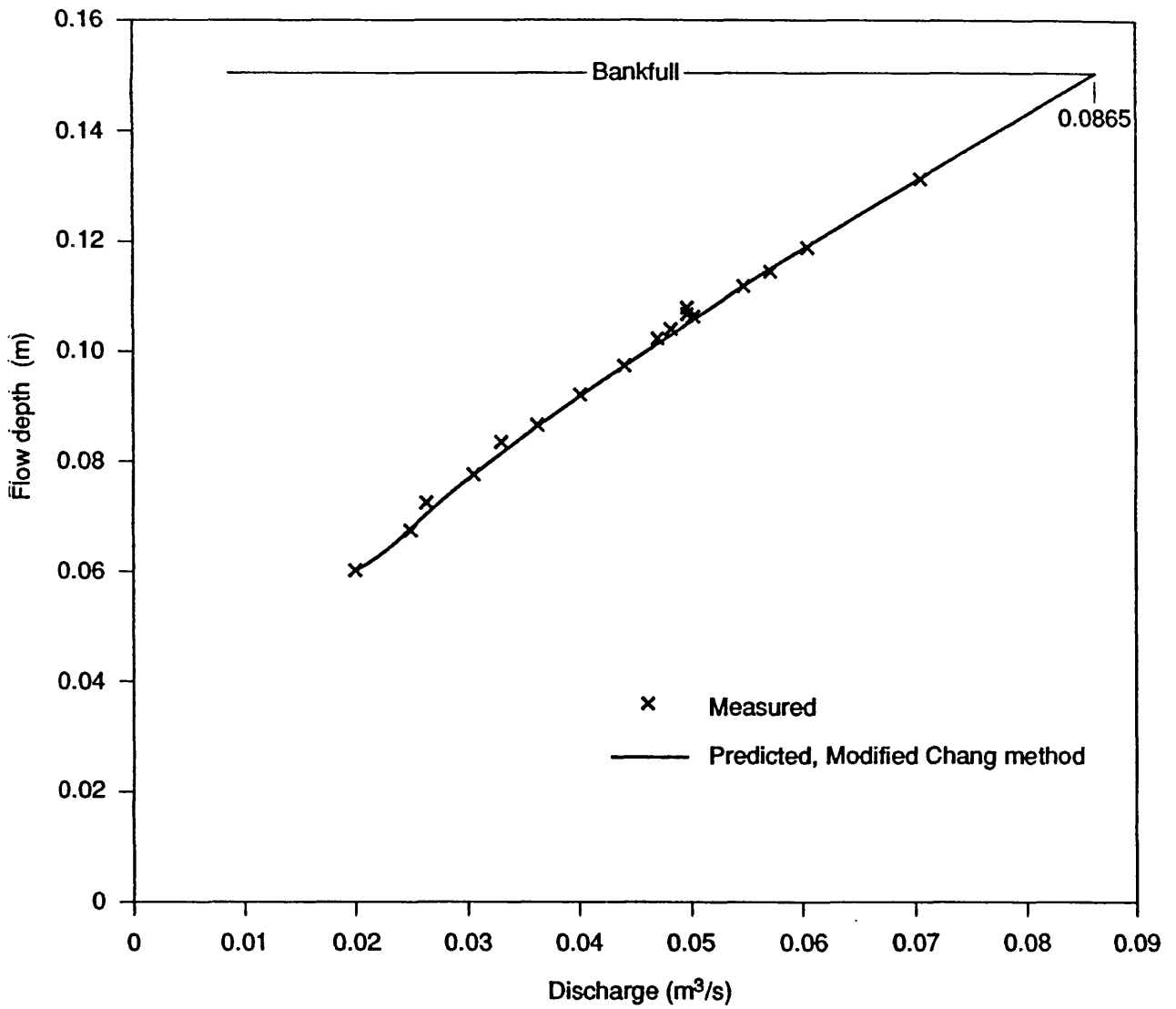
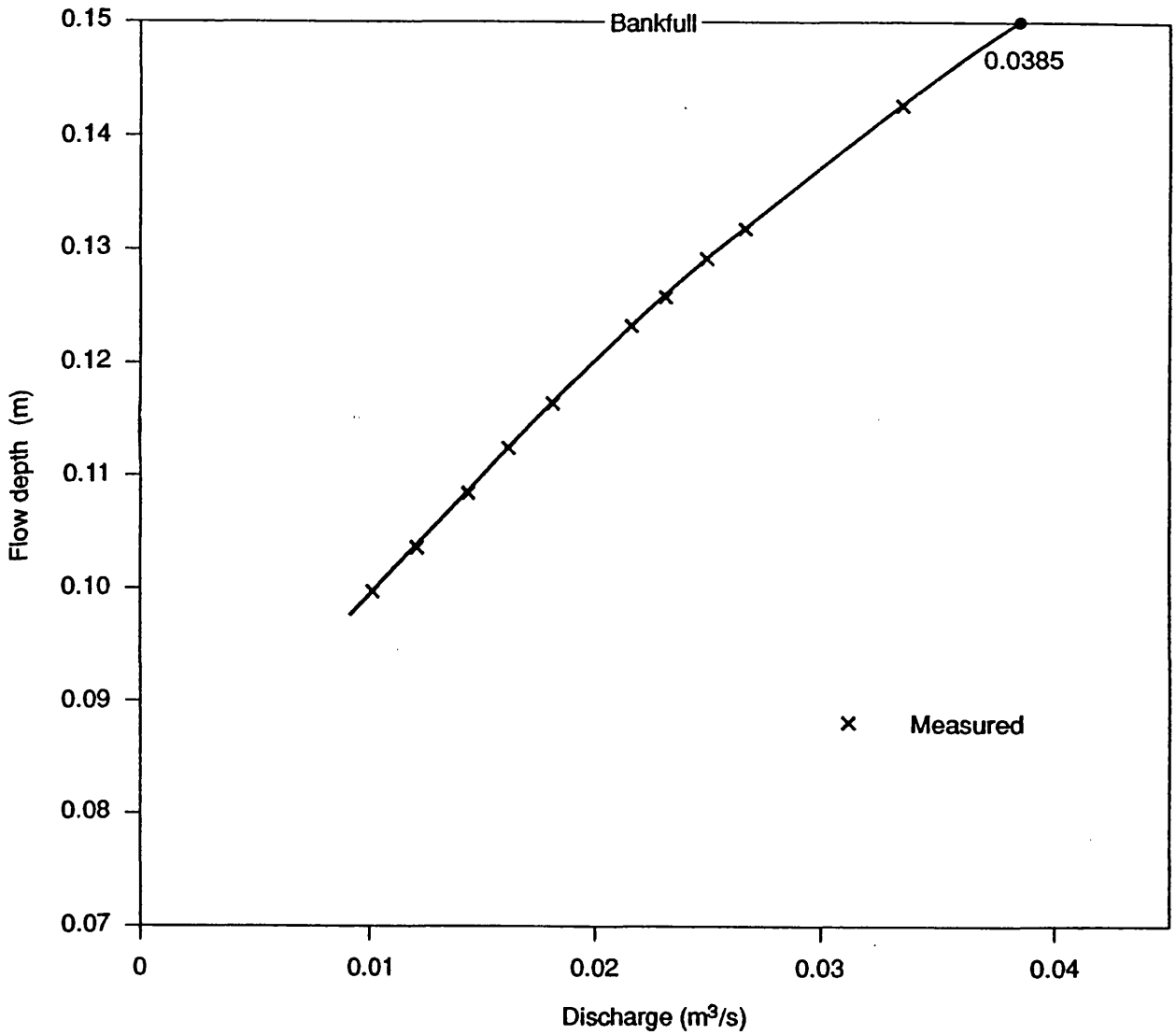
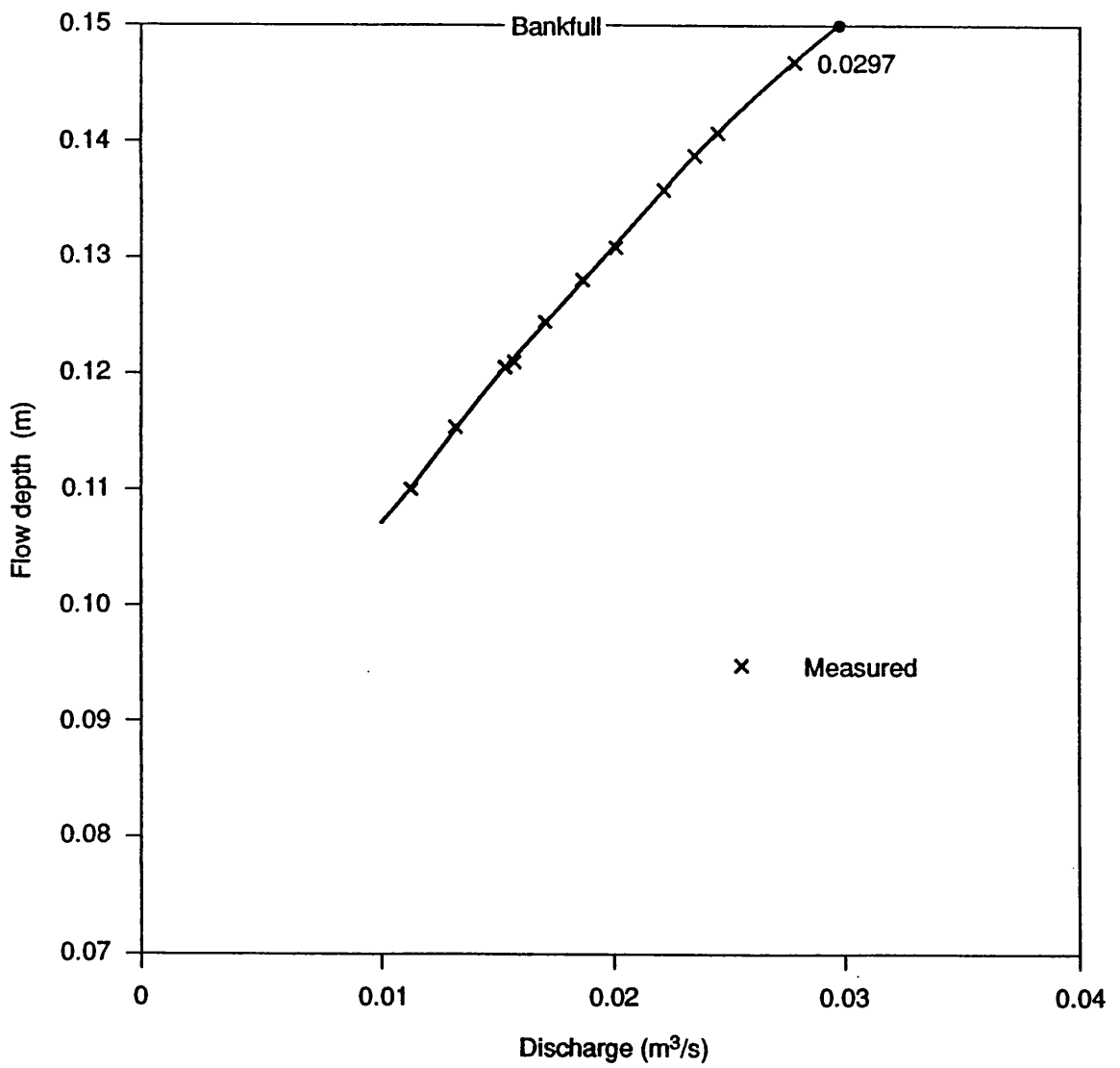


Figure 6.3 Inbank stage-discharge relationship for 60° trapezoidal channel



**Figure 6.4** Inbank stage-discharge relationship for 60° natural channel



**Figure 6.5 Inbank stage-discharge relationship for 110° natural channel**

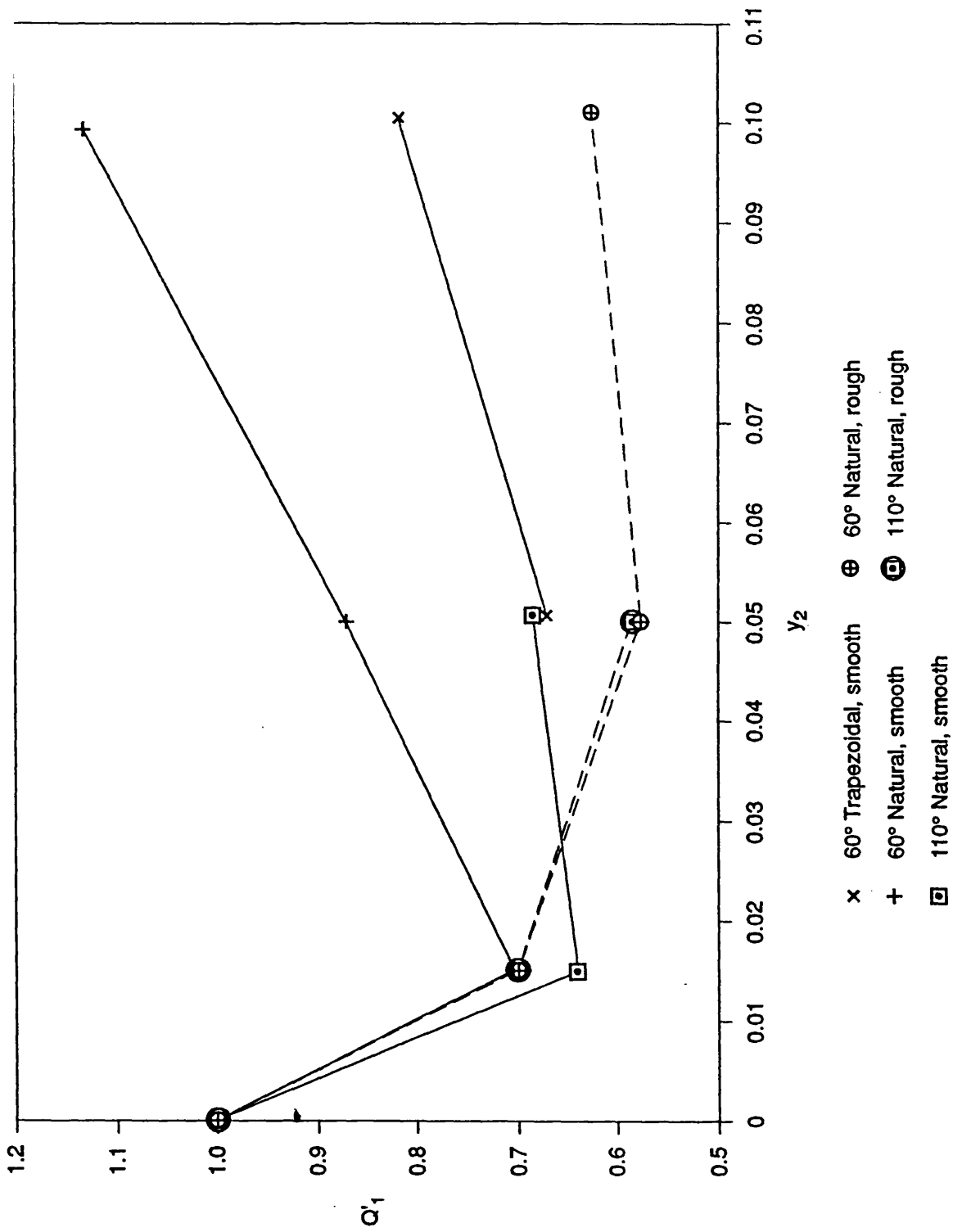
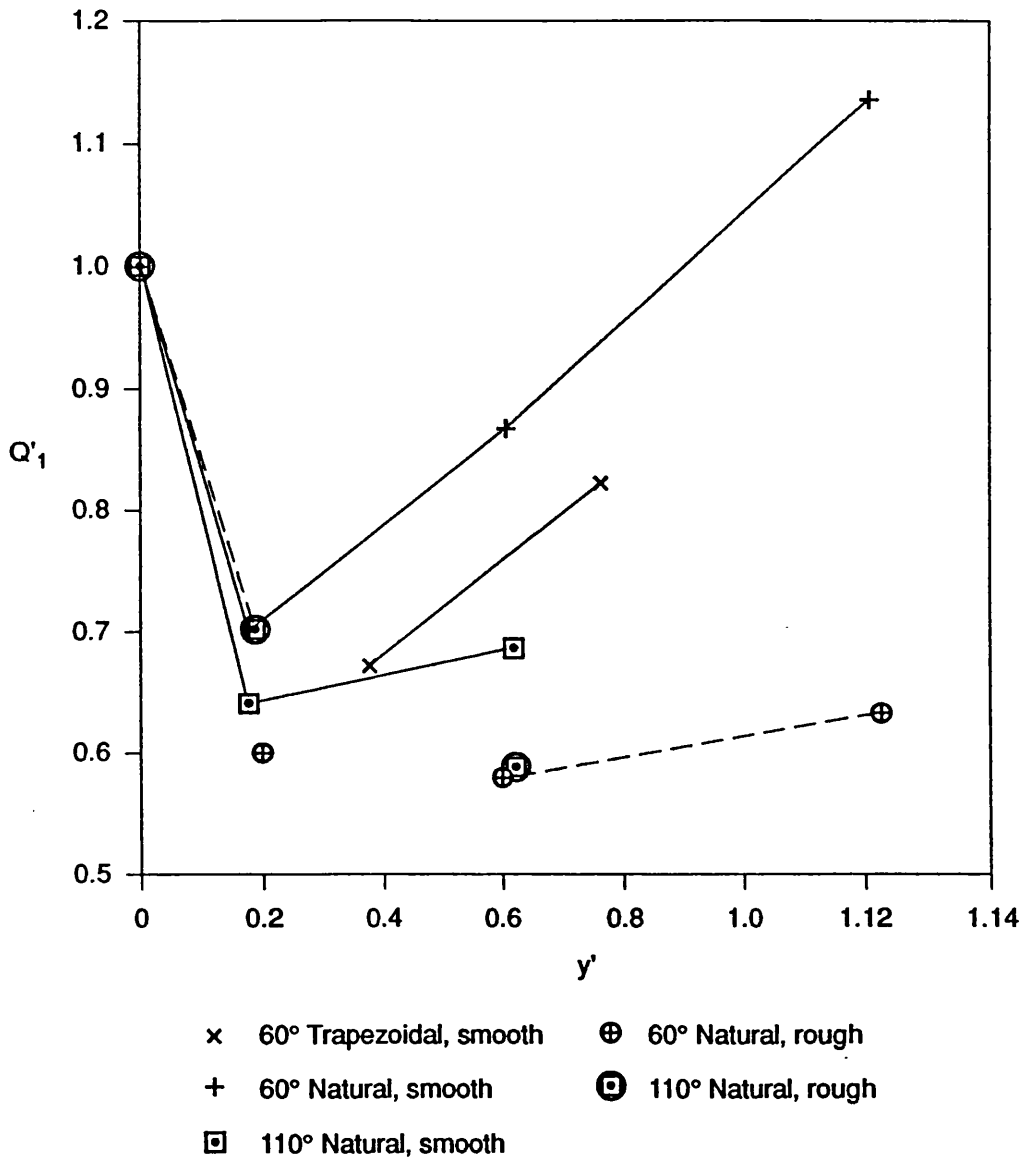


Figure 6.6 Variation of dimensionless main channel discharge with flow depth on floodplain



**Figure 6.7** Variation of dimensionless main channel discharge with dimensionless floodplain flow depth

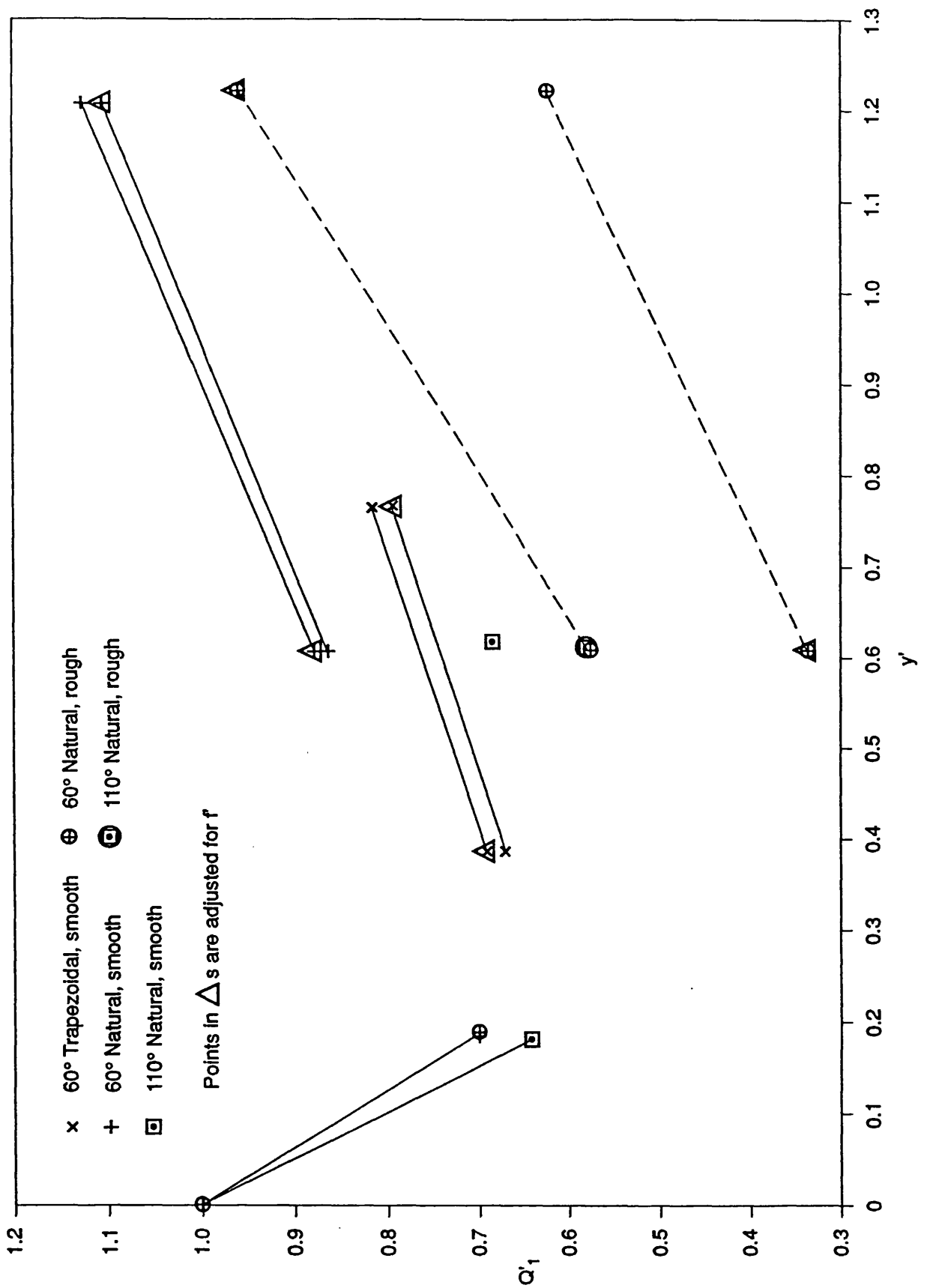


Figure 6.8 Variation of dimensionless main channel discharge with dimensionless flow depth with points adjusted for friction factor ratio

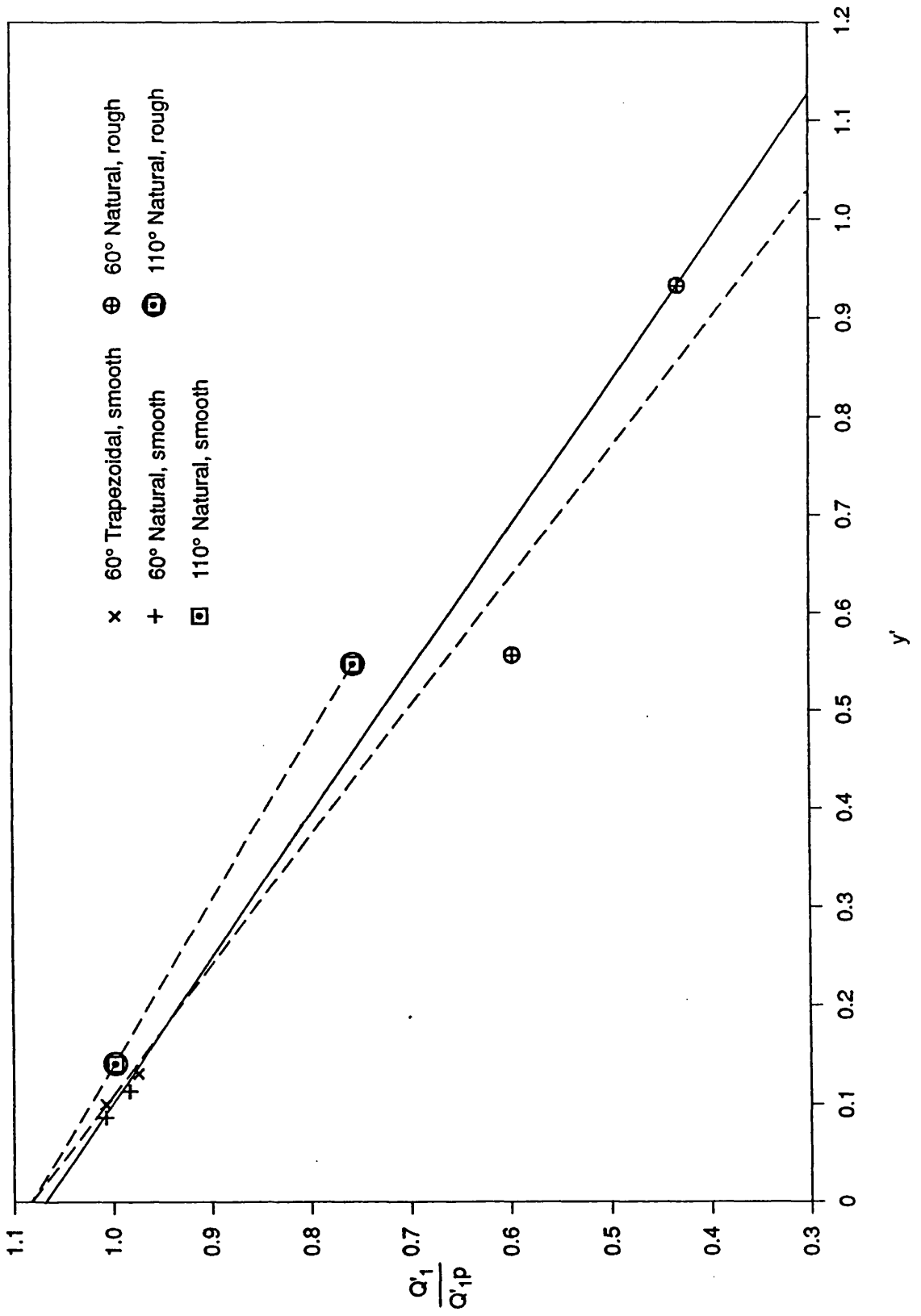
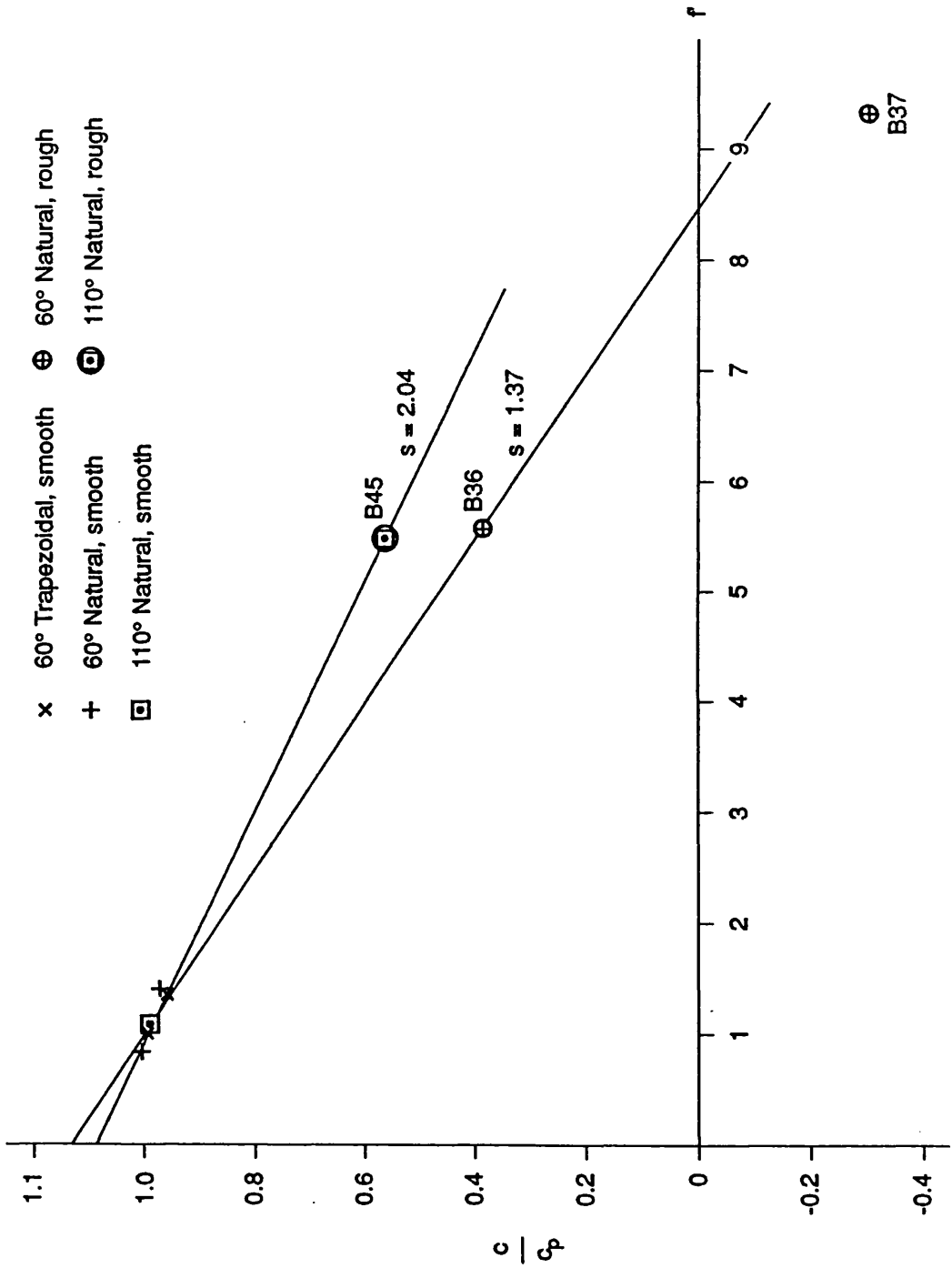
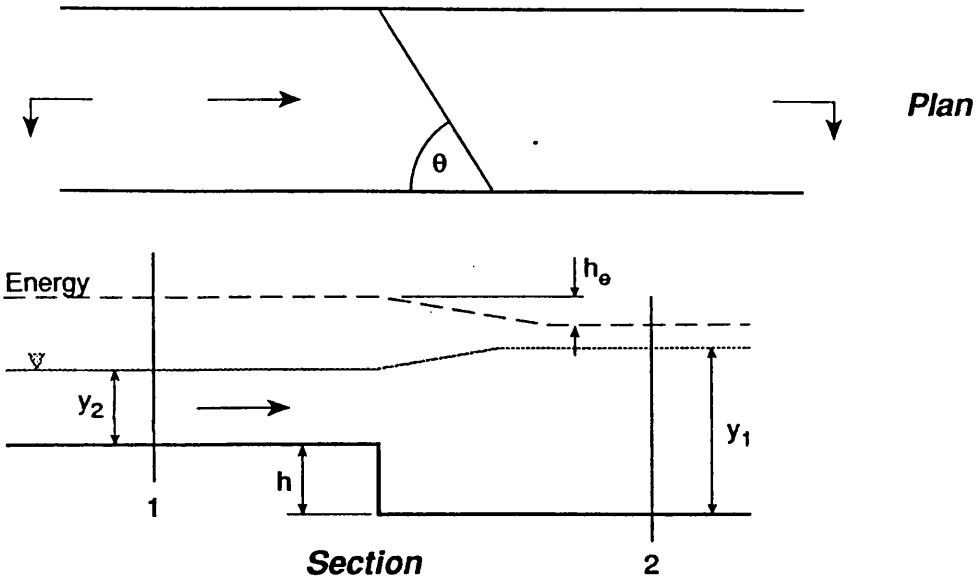


Figure 6.9 Additional adjustment to discharge for relative roughness



⊕ B37

Figure 6.10 Adjustment to c for relative roughness



**Figure 6.11 Flow expansion over a downward step**

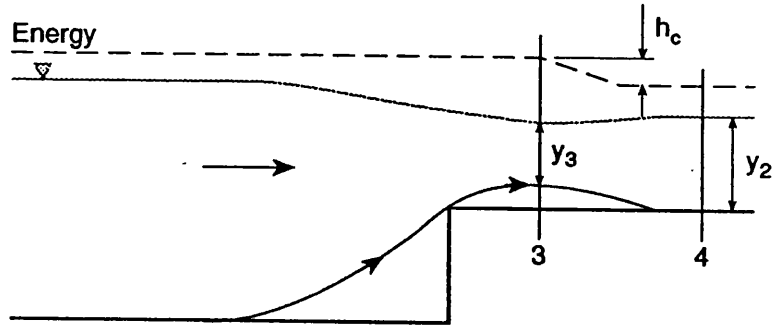


**Figure 6.12 Flow contraction over an upward step**

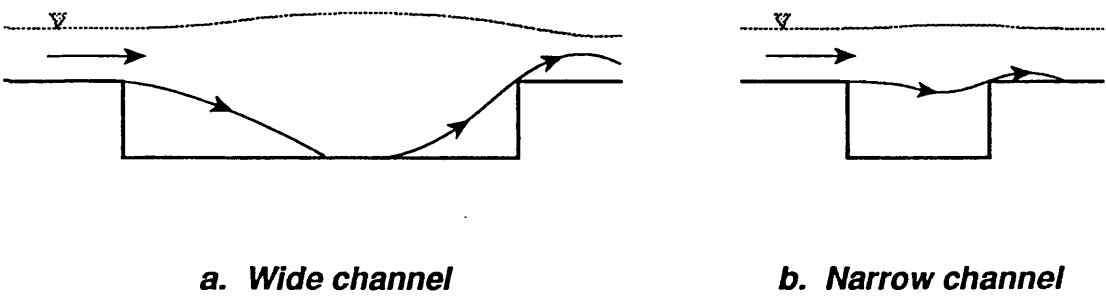


**Figure 6.13 Expansion and contraction flow patterns**

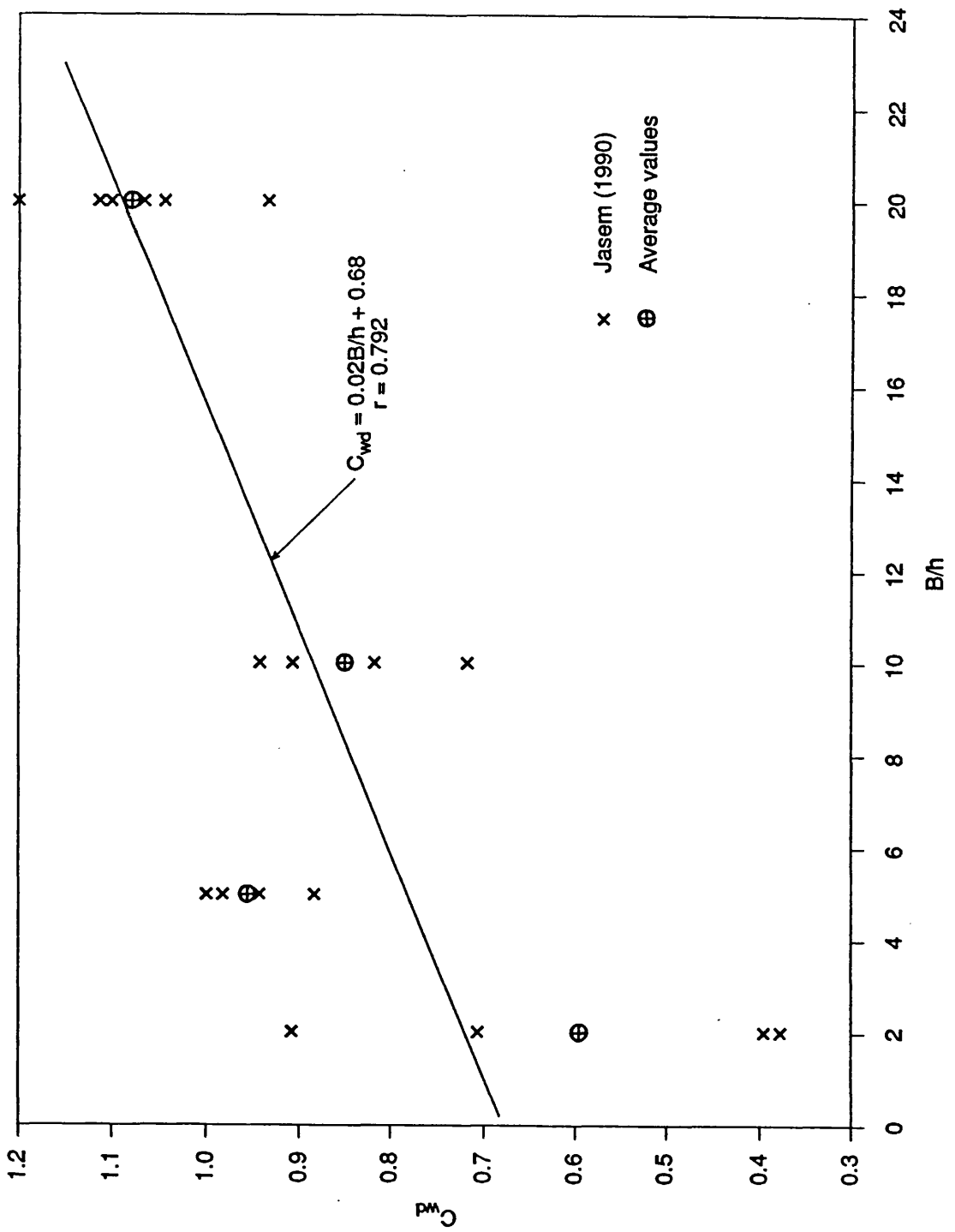


Figure 6.14 Width to depth ratio correction for expansion losses

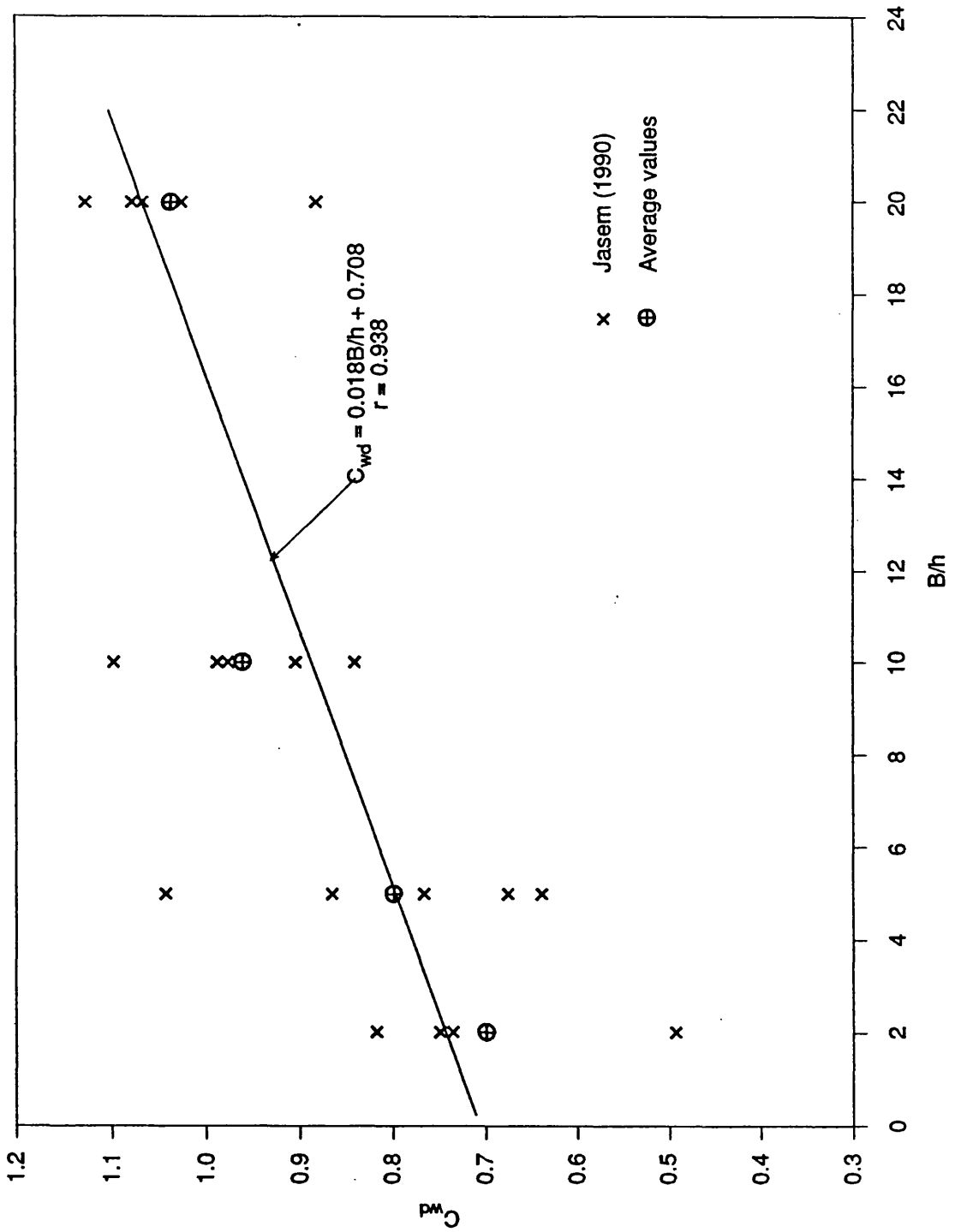


Figure 6.15 Width to depth ratio correction for contraction losses

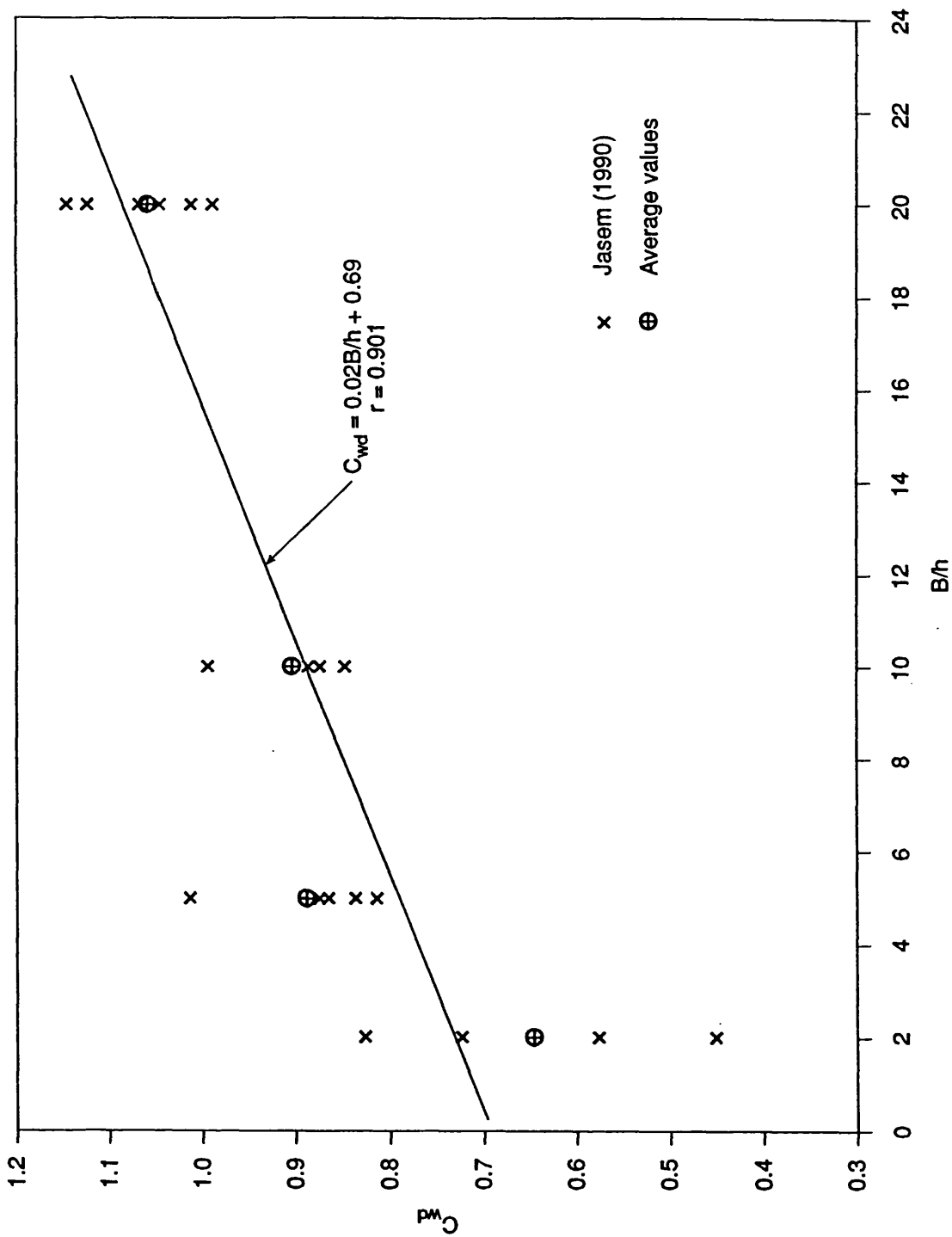


Figure 6.16 Width to depth ratio correction for combined expansion and contraction losses

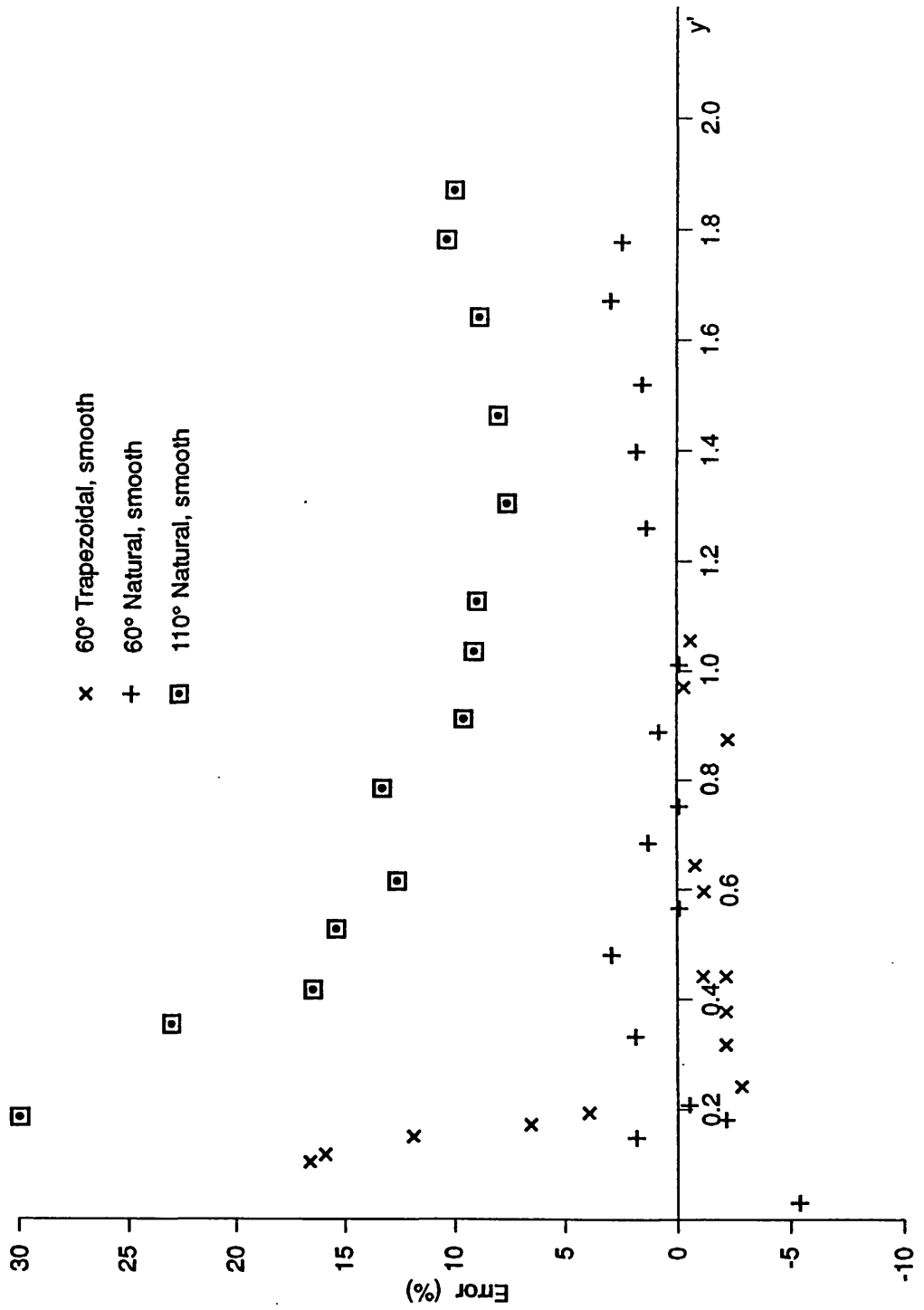


Figure 6.17 Errors for SERC FCF Phase B data predictions before sinuosity corrections

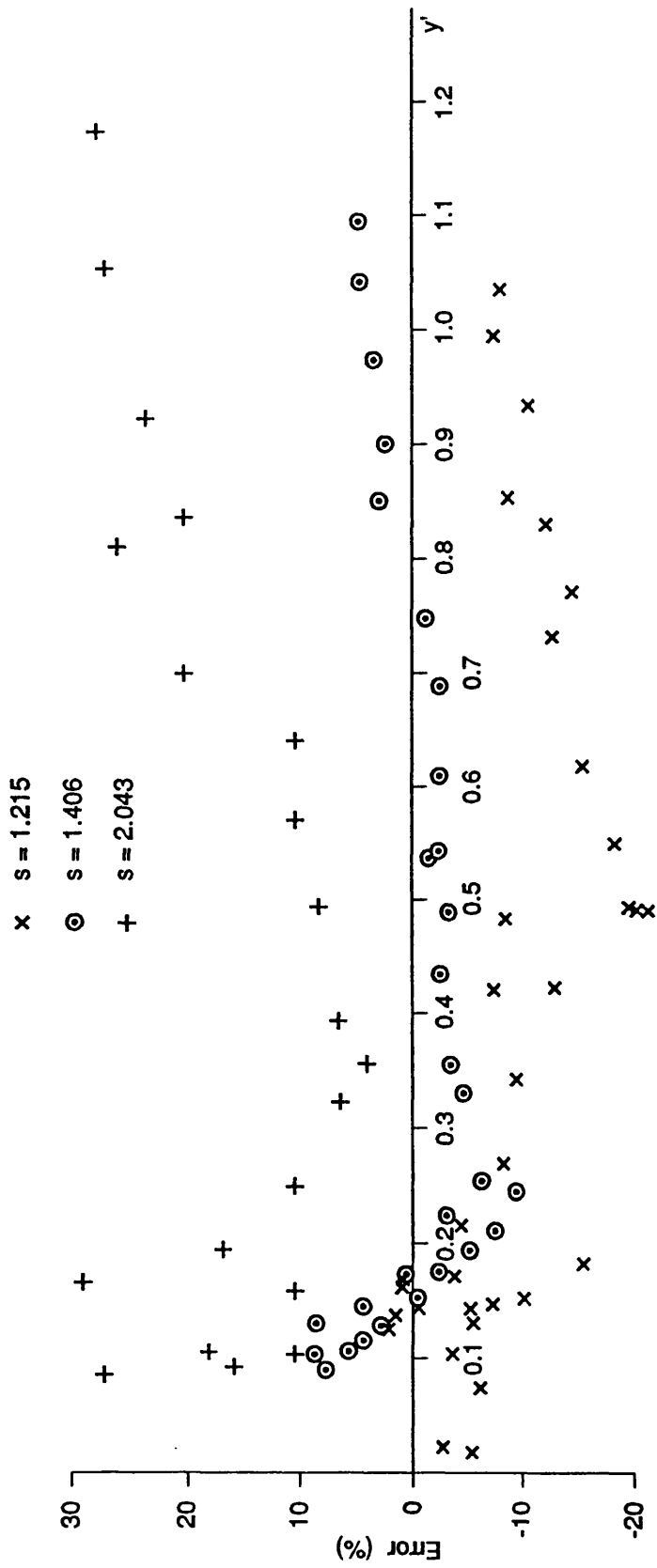
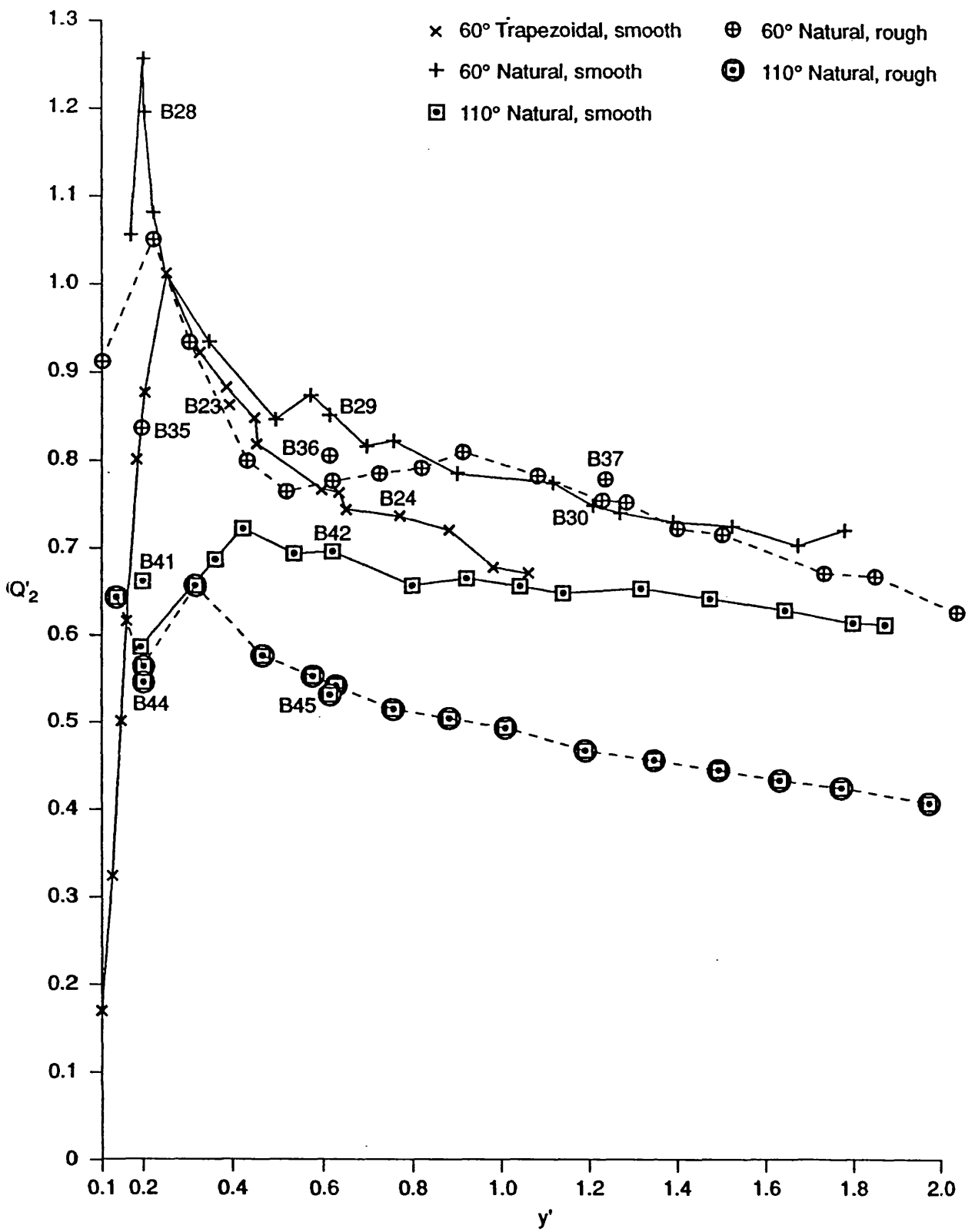


Figure 6.18 Errors for Aberdeen predictions before sinuosity corrections



**Figure 6.19 Adjustment factor for inner flood plain discharges for SERC FCF Phase B experiments**

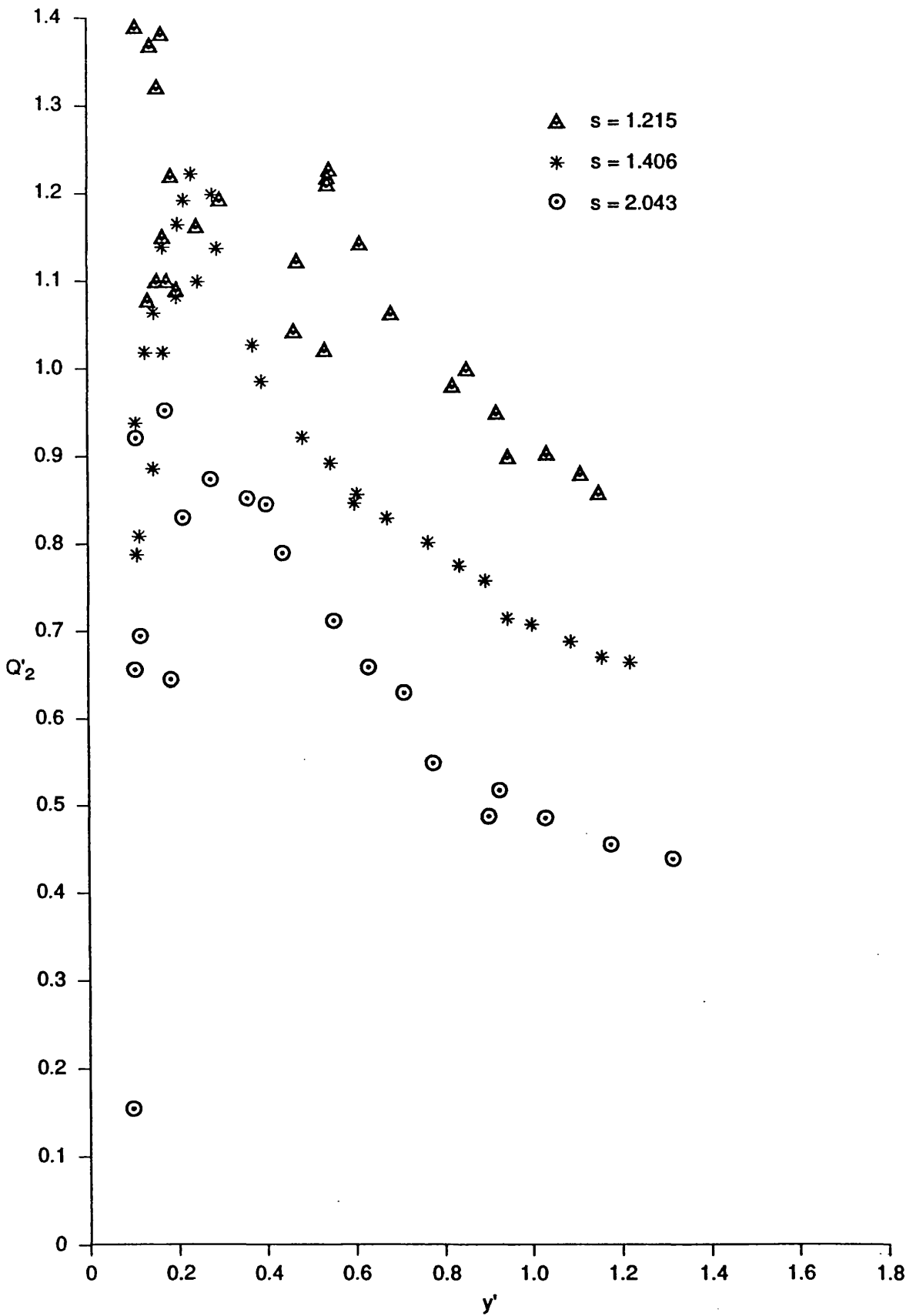


Figure 6.20 Adjustment factor for inner flood plain discharges for Aberdeen experiments

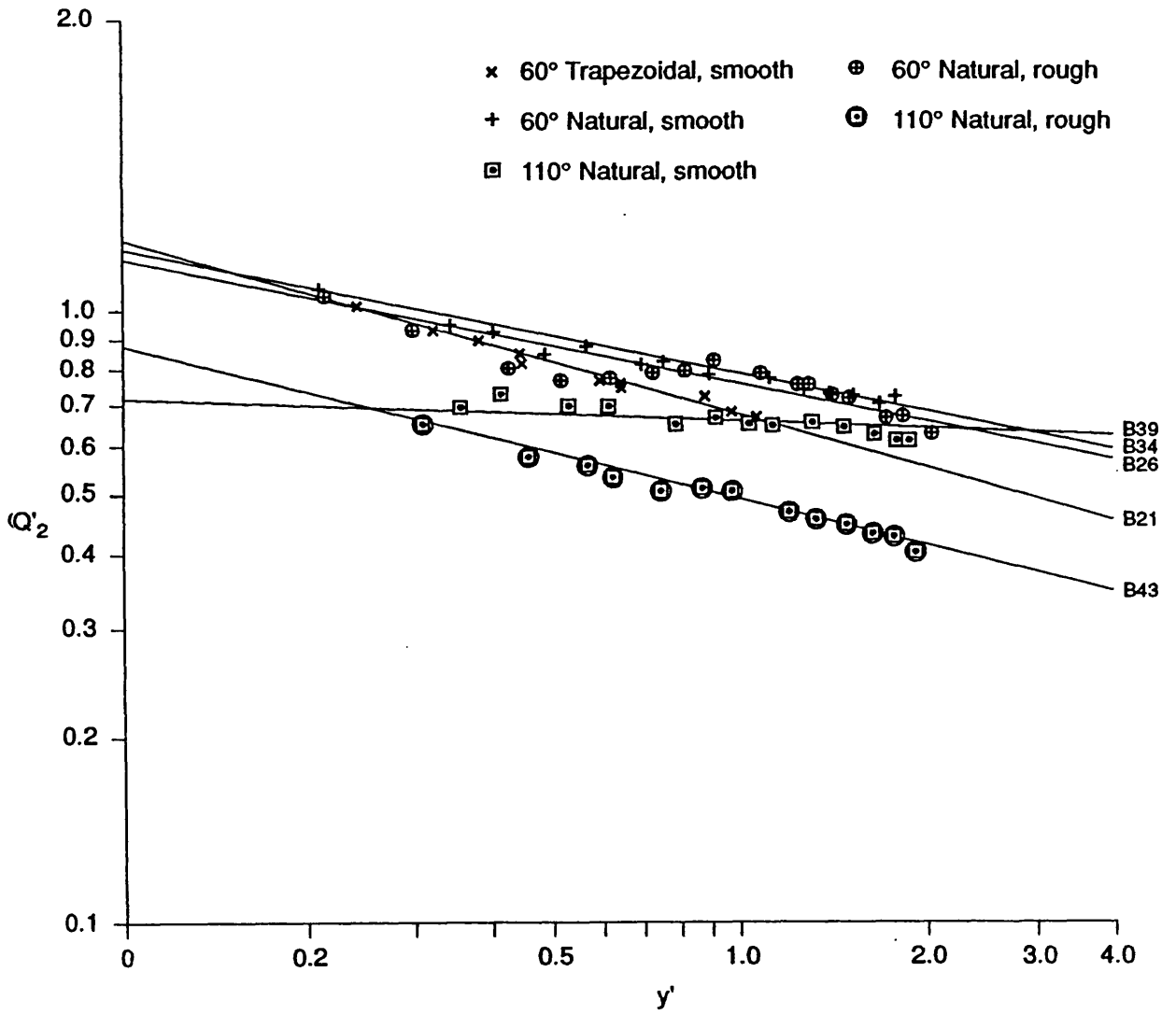


Figure 6.21 Adjustment factor for inner flood plain discharges for  $y' > 0.2$ , SERC FCF Phase B data

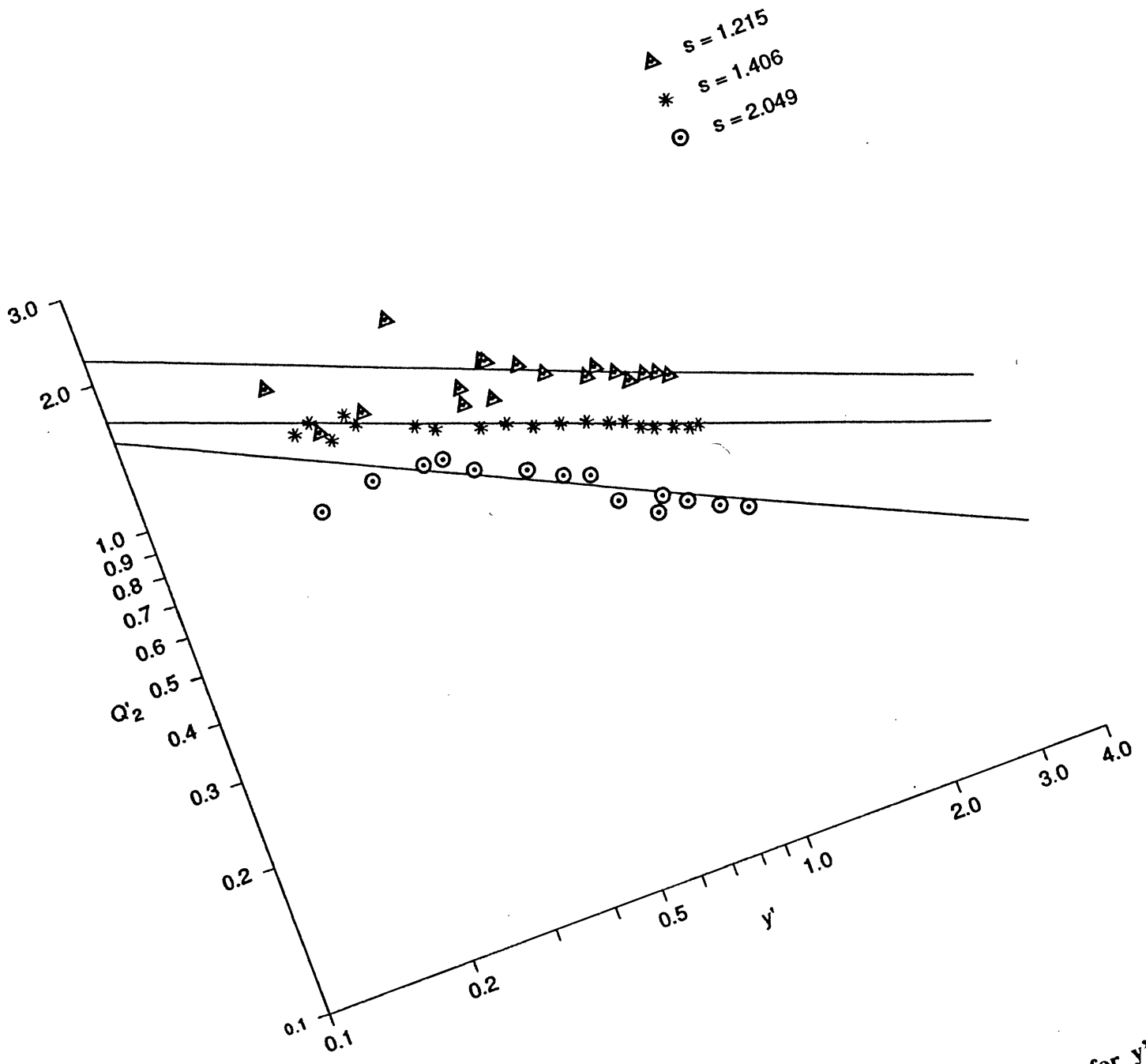


Figure 6.22 Adjustment factor for inner flood plain discharges for  $y' > 0.2$ , Aberdeen data

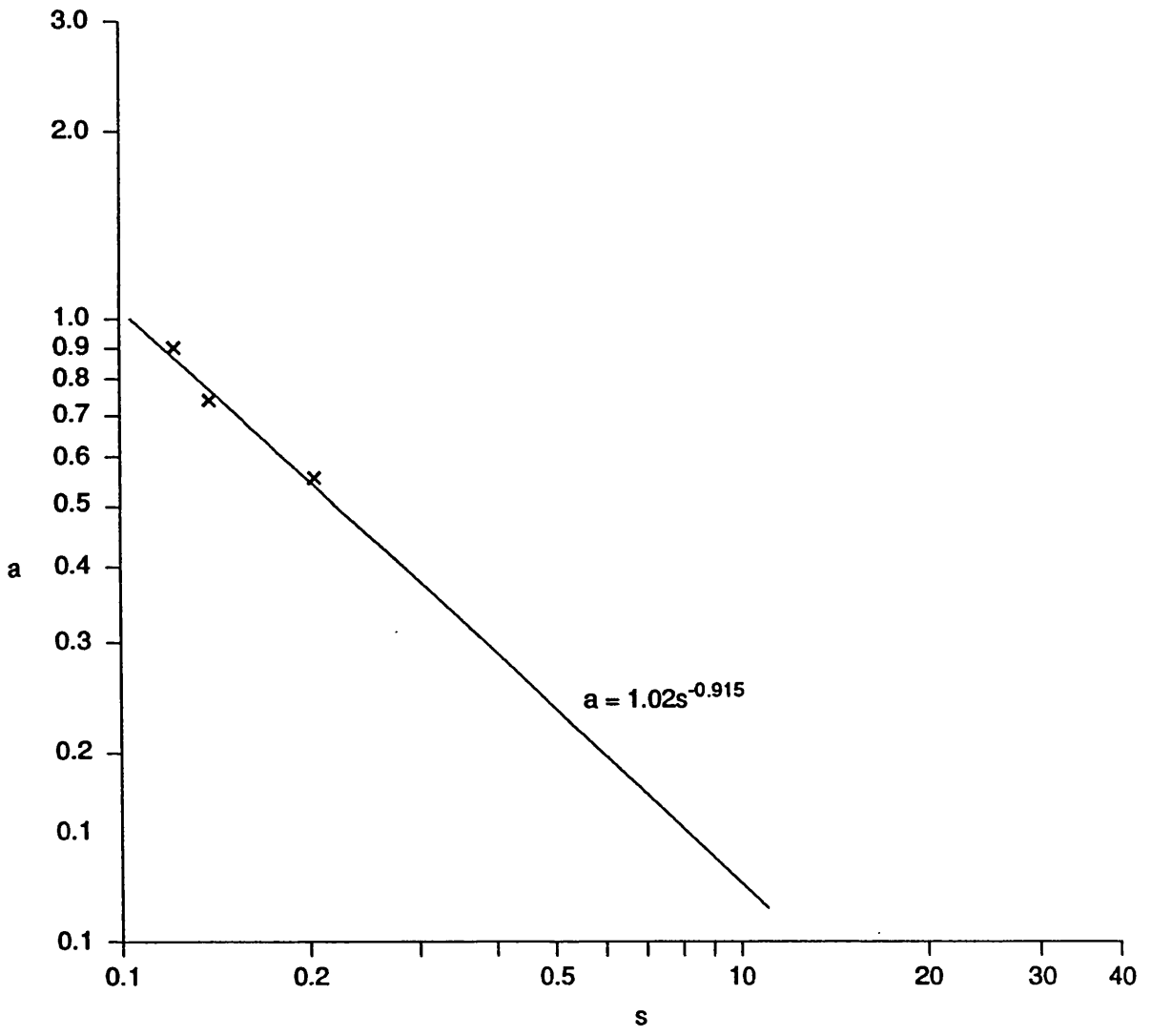


Figure 6.23 Variation of a with s

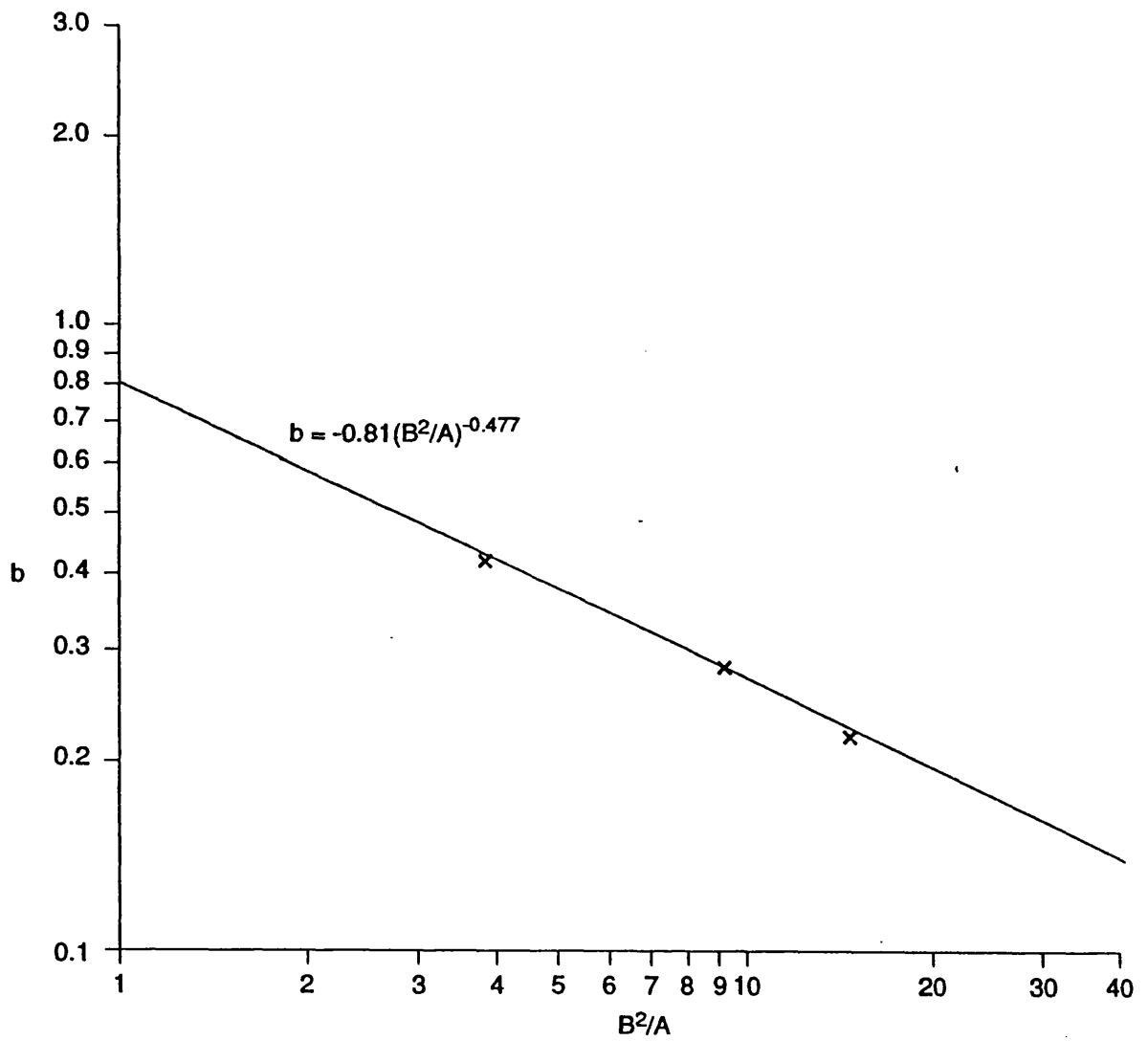


Figure 6.24 Variation of  $b$  with  $B^2/A$

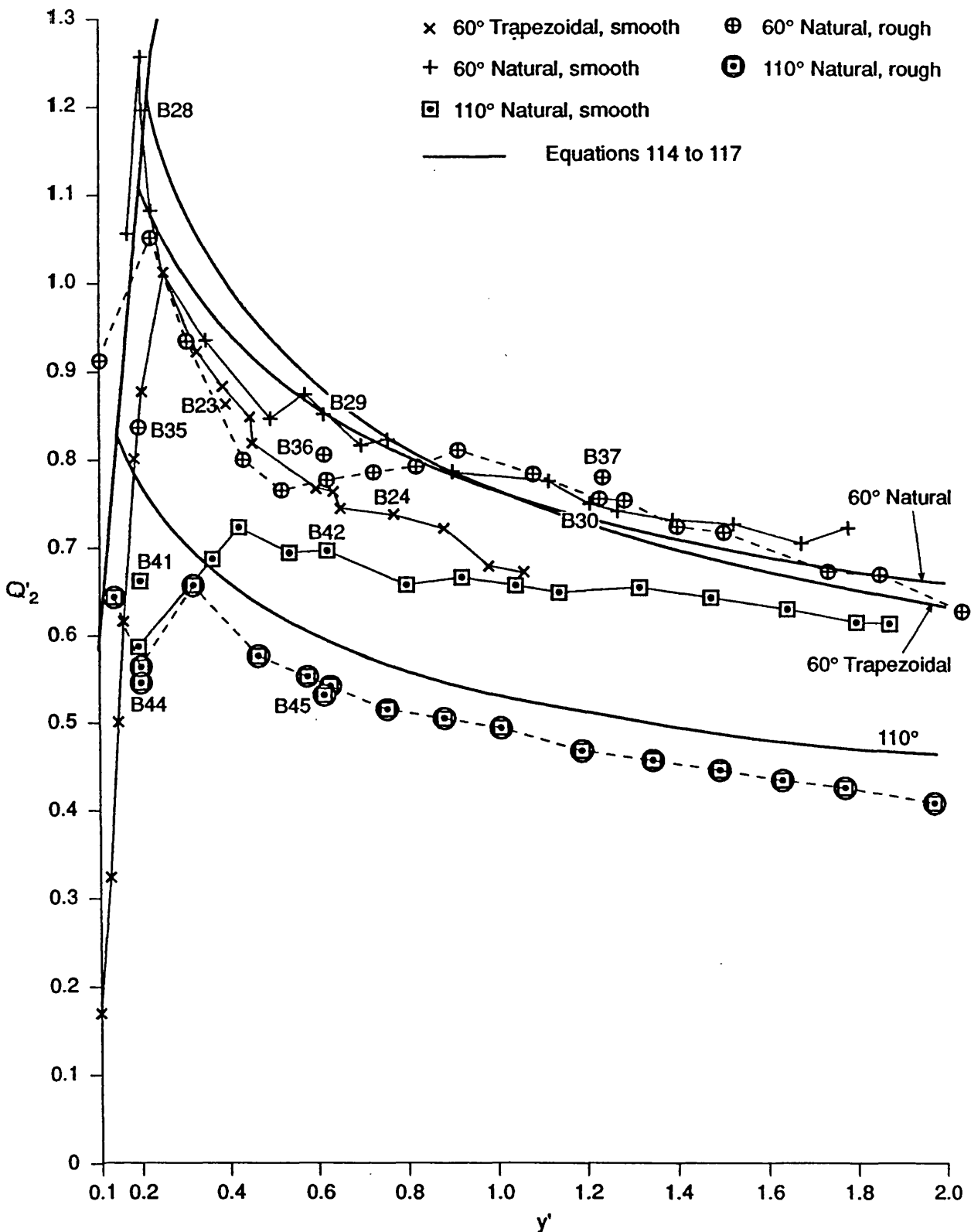


Figure 6.25 Comparison of predicted zone 2 adjustment factor with SERC FCF Phase B data

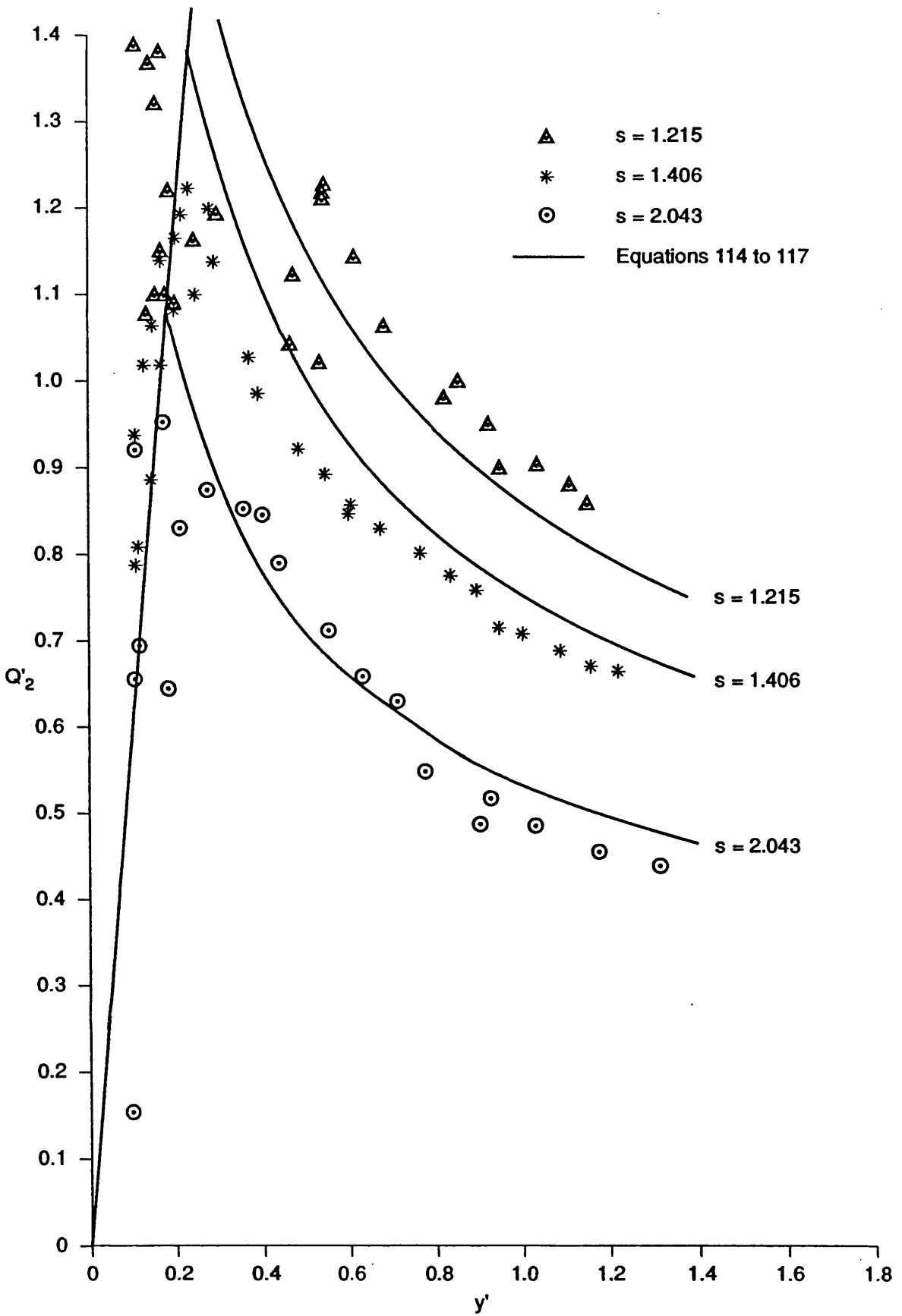


Figure 6.26 Comparison of predicted zone 2 adjustment factor with Aberdeen data

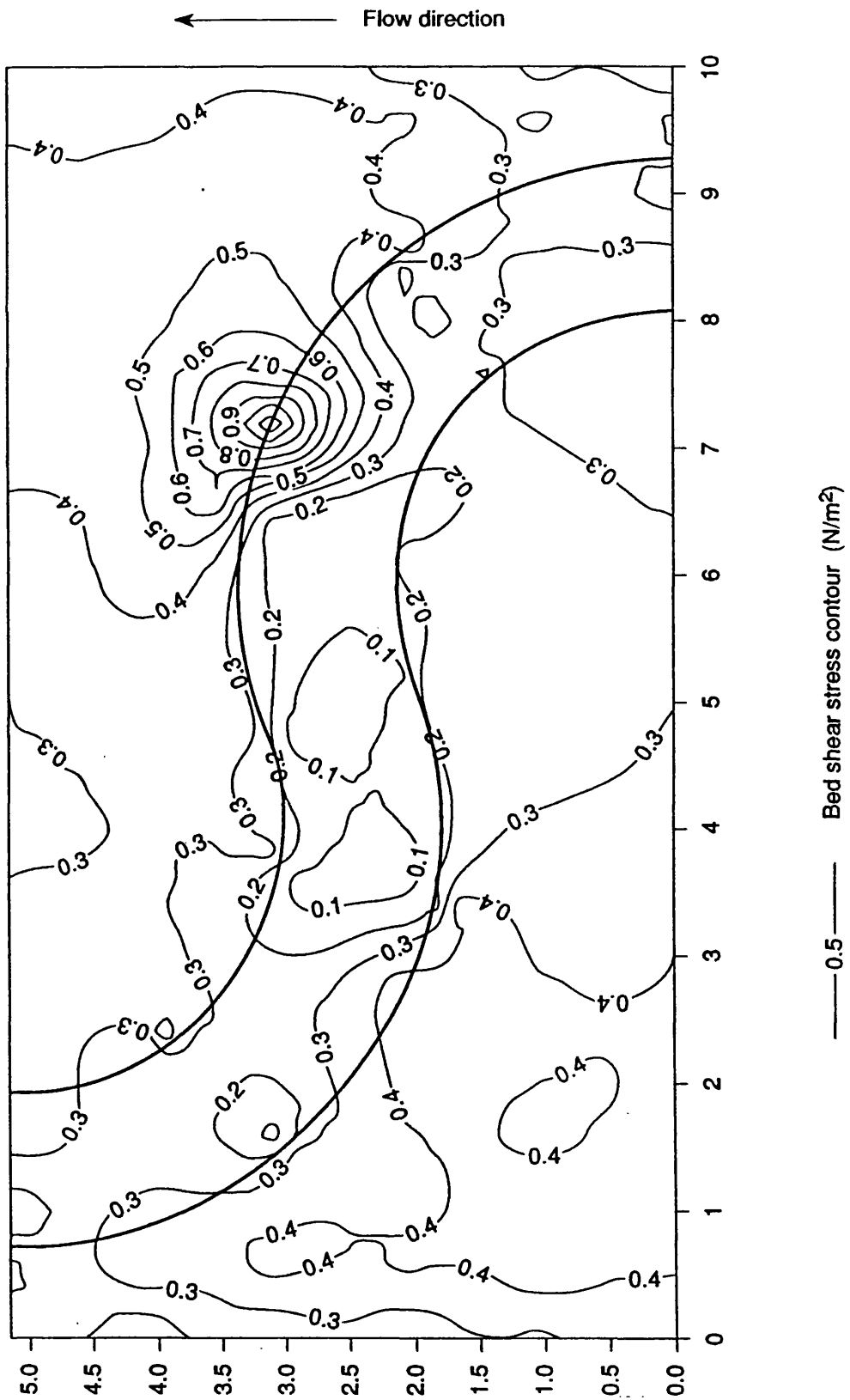
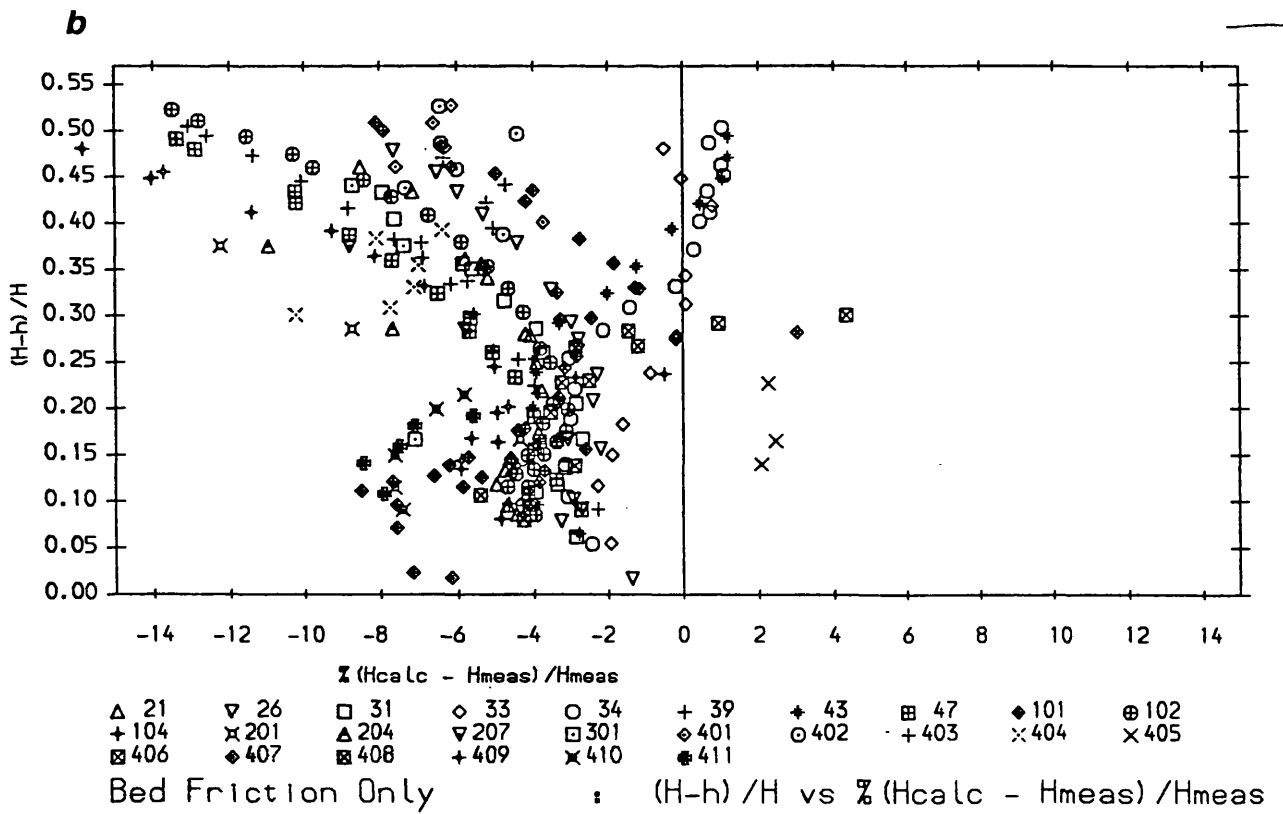
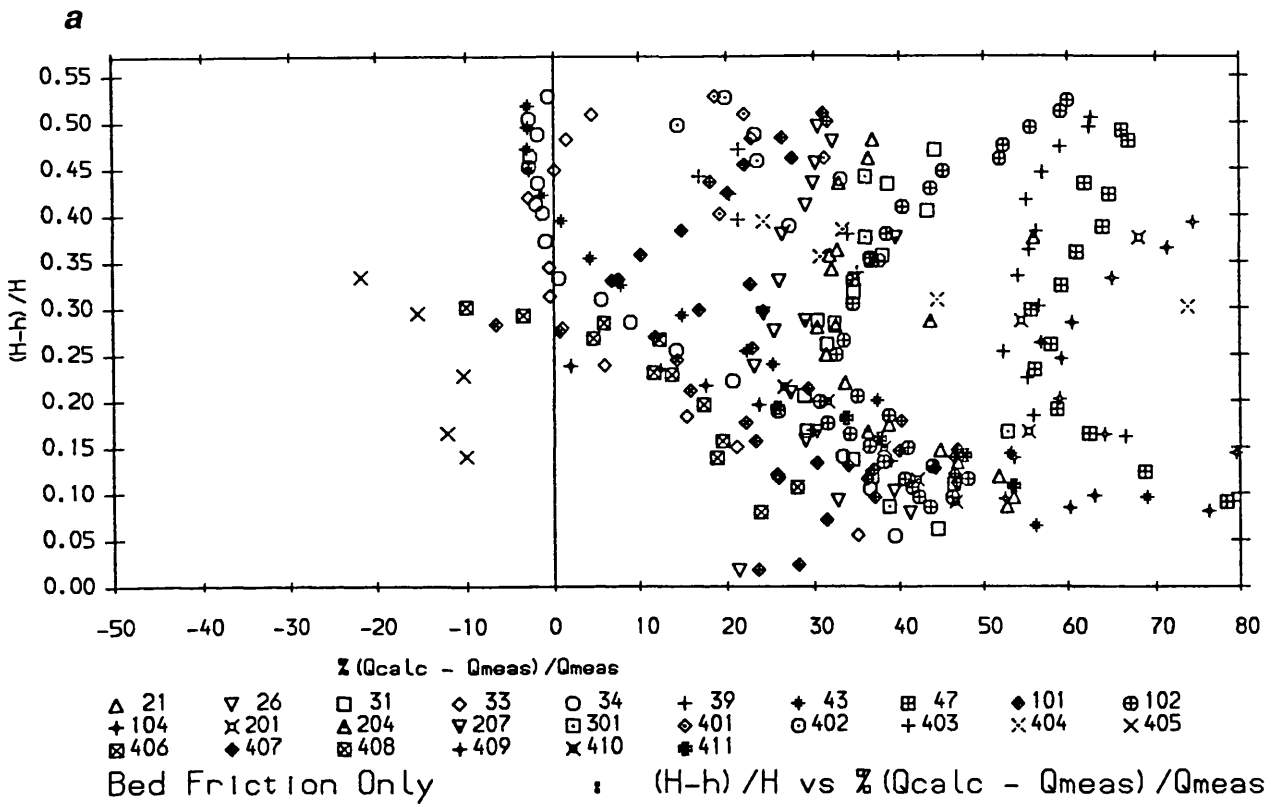


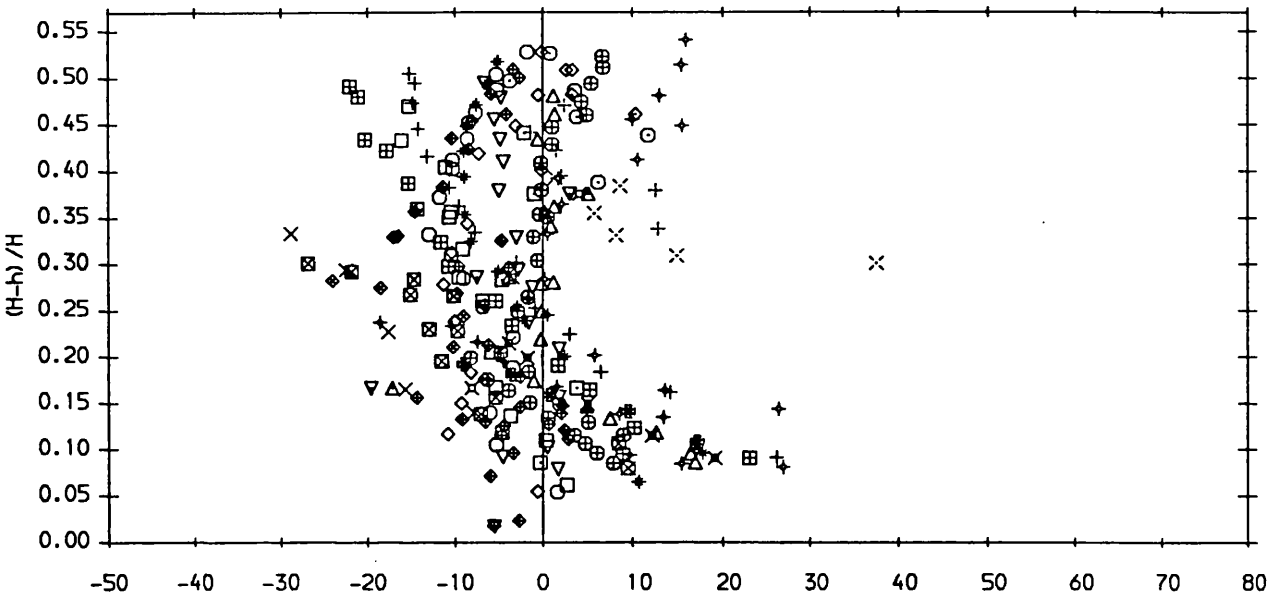
Figure 6.27 Example of boundary shear stress distribution in a meandering compound channel (after Lorena 1992)





**Figure 6.29 Errors in predicted discharge and depth BFO**

**a**

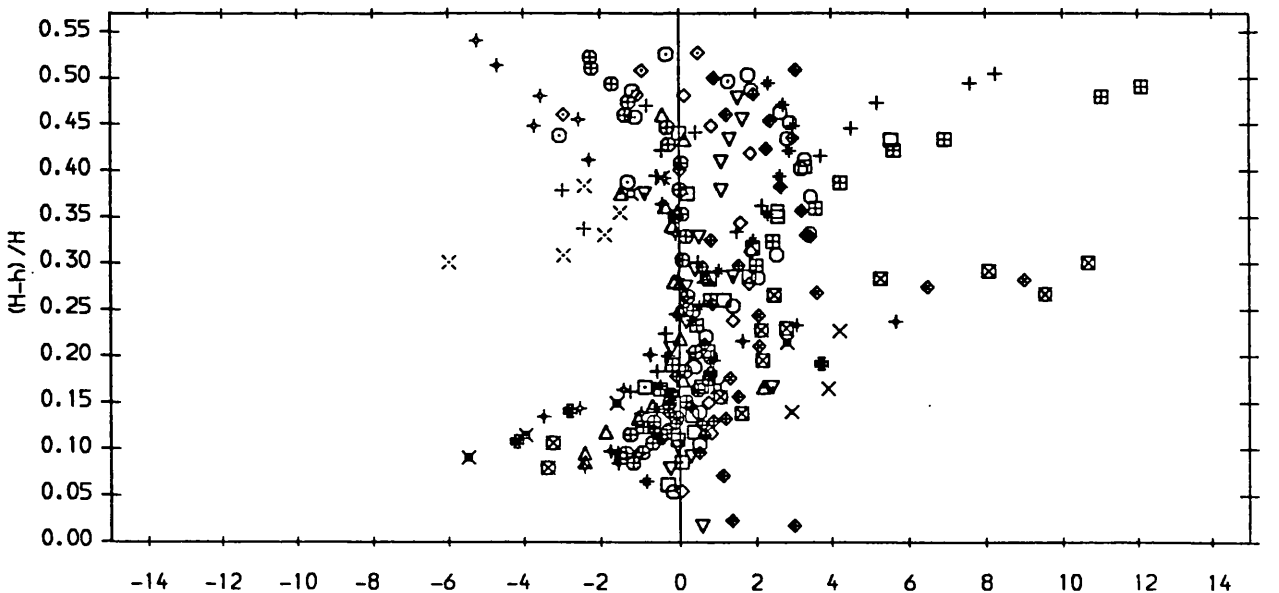


$\% (Q_{calc} - Q_{meas}) / Q_{meas}$

$\Delta$ 21	$\nabla$ 26	$\square$ 31	$\diamond$ 33	$\circ$ 34	+	+	$\boxplus$ 47	$\blacklozenge$ 101	$\oplus$ 102
+ 104	$\times$ 201	$\triangle$ 204	$\nabla$ 207	$\square$ 301	$\diamond$ 401	$\circ$ 402	+ 403	$\times$ 404	$\times$ 405
$\boxtimes$ 406	$\blacklozenge$ 407	$\boxtimes$ 408	+	$\times$ 410	$\bullet$ 411				

James and Wark Method :  $(H-h) / H$  vs  $\% (Q_{calc} - Q_{meas}) / Q_{meas}$

**b**



$\% (H_{calc} - H_{meas}) / H_{meas}$

$\Delta$ 21	$\nabla$ 26	$\square$ 31	$\diamond$ 33	$\circ$ 34	+	+	$\boxplus$ 47	$\blacklozenge$ 101	$\oplus$ 102
+ 104	$\times$ 201	$\triangle$ 204	$\nabla$ 207	$\square$ 301	$\diamond$ 401	$\circ$ 402	+ 403	$\times$ 404	$\times$ 405
$\boxtimes$ 406	$\blacklozenge$ 407	$\boxtimes$ 408	+	$\times$ 410	$\bullet$ 411				

James and Wark Method :  $(H-h) / H$  vs  $\% (H_{calc} - H_{meas}) / H_{meas}$

**Figure 6.30 Errors in predicted discharge and depth JW**

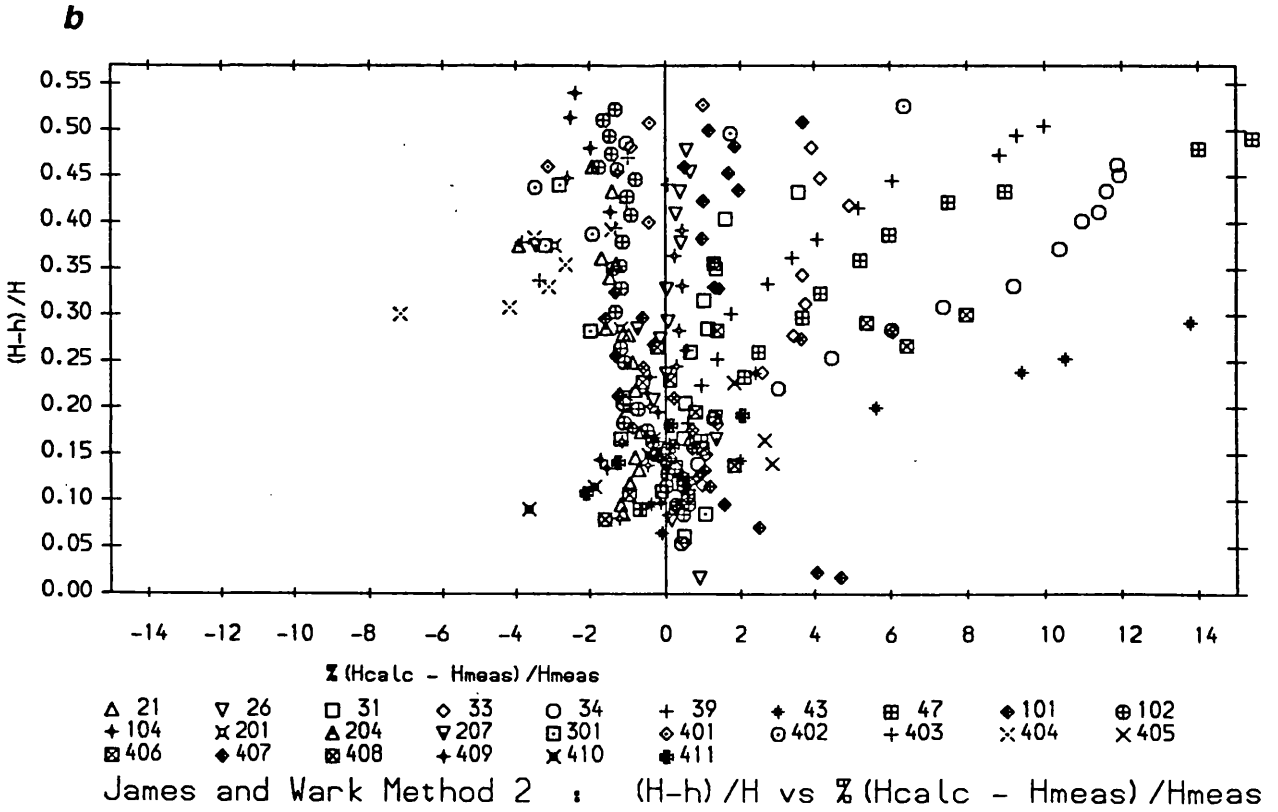
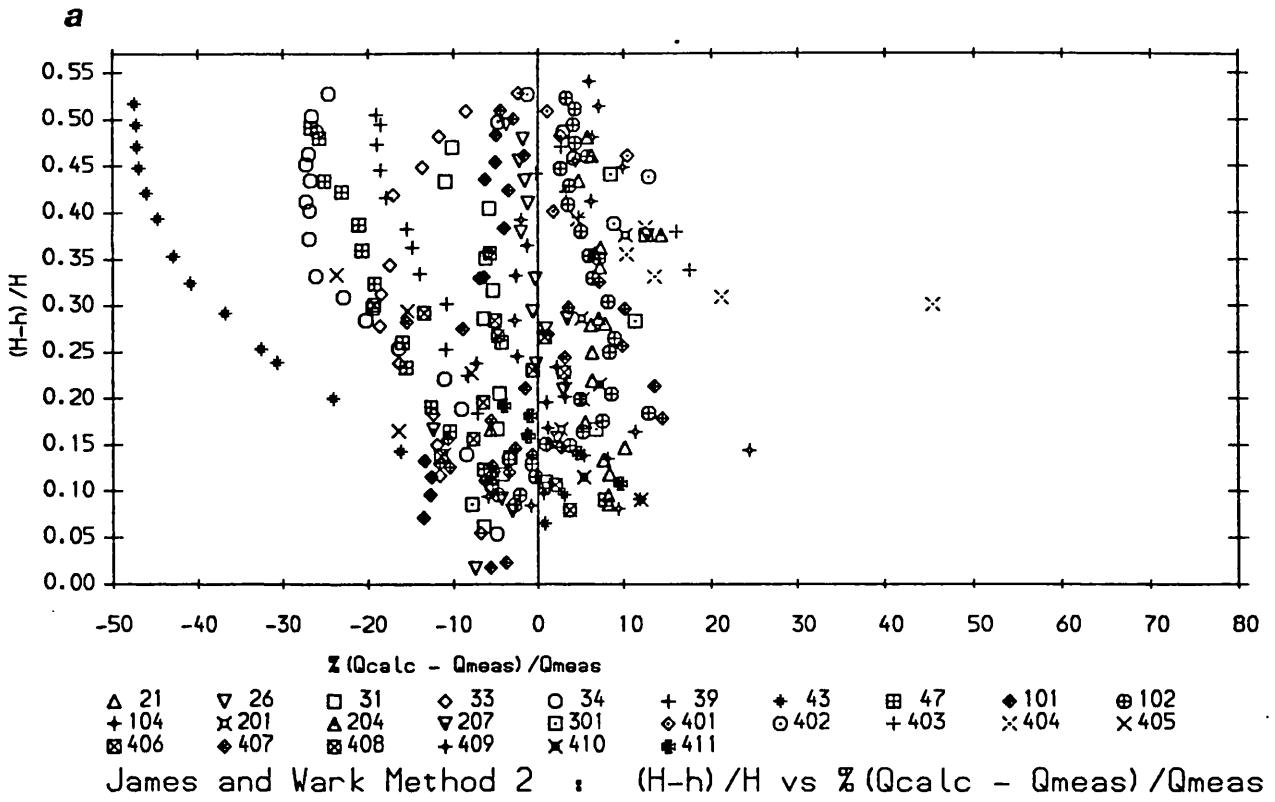
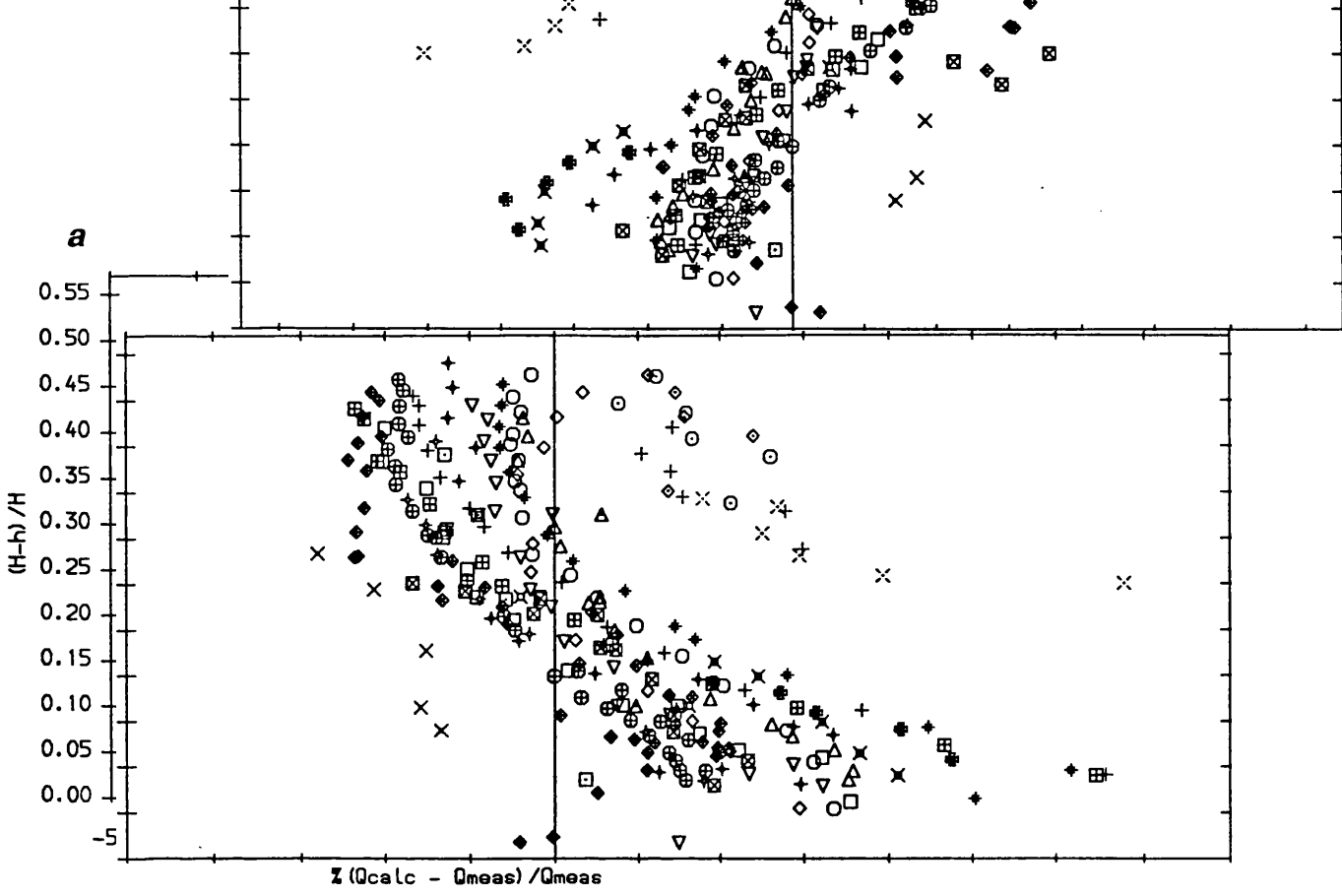
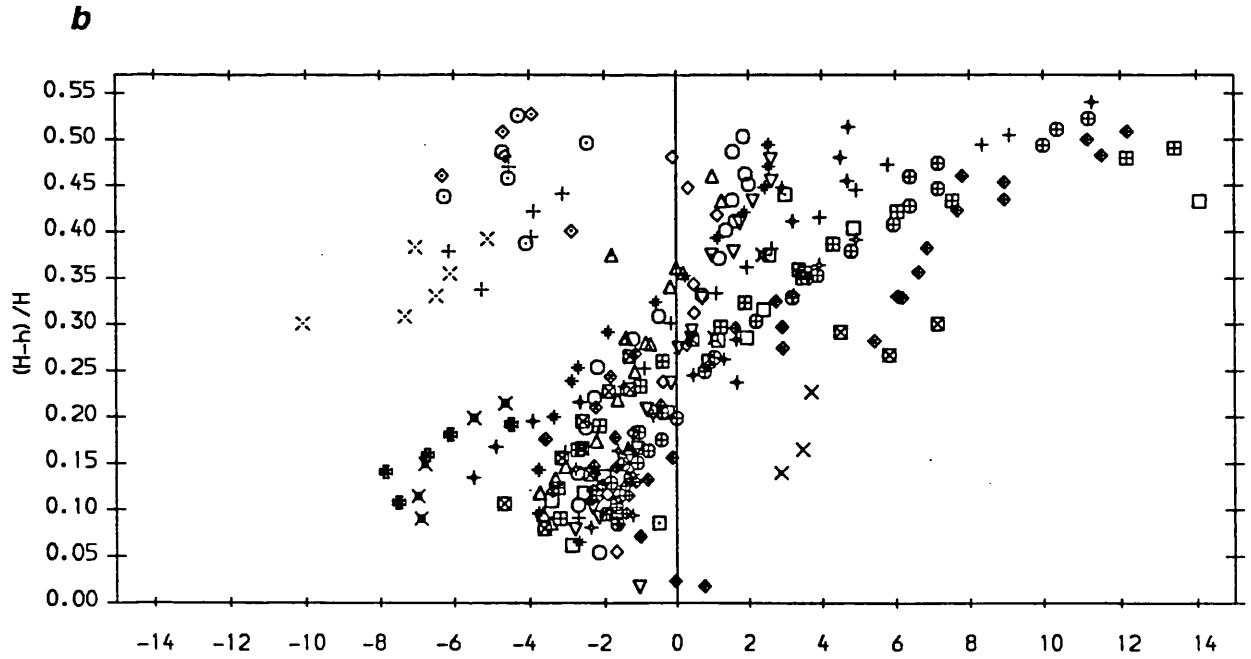


Figure 6.31 Errors in predicted discharge and depth JW2



Ervine and Ellis Method :  $(H-h) / H$  vs  $\% (Q_{calc} - Q_{meas}) / Q_{meas}$

- |       |       |       |       |       |       |       |       |       |       |
|-------|-------|-------|-------|-------|-------|-------|-------|-------|-------|
| △ 21  | ▽ 26  | □ 31  | ◇ 33  | ○ 34  | + 39  | + 43  | ⊞ 47  | ◆ 101 | ⊕ 102 |
| + 104 | × 201 | △ 204 | ▽ 207 | □ 301 | ◇ 401 | ○ 402 | + 403 | × 404 | × 405 |
| ⊞ 406 | ◆ 407 | ⊞ 408 | + 409 | × 410 | ◆ 411 |       |       |       |       |



Ervine and Ellis Method :  $(H-h) / H$  vs  $\% (H_{calc} - H_{meas}) / H_{meas}$

- |       |       |       |       |       |       |       |       |       |       |
|-------|-------|-------|-------|-------|-------|-------|-------|-------|-------|
| △ 21  | ▽ 26  | □ 31  | ◇ 33  | ○ 34  | + 39  | + 43  | ⊞ 47  | ◆ 101 | ⊕ 102 |
| + 104 | × 201 | △ 204 | ▽ 207 | □ 301 | ◇ 401 | ○ 402 | + 403 | × 404 | × 405 |
| ⊞ 406 | ◆ 407 | ⊞ 408 | + 409 | × 410 | ◆ 411 |       |       |       |       |

**Figure 6.32 Errors in predicted discharge and depth EE**

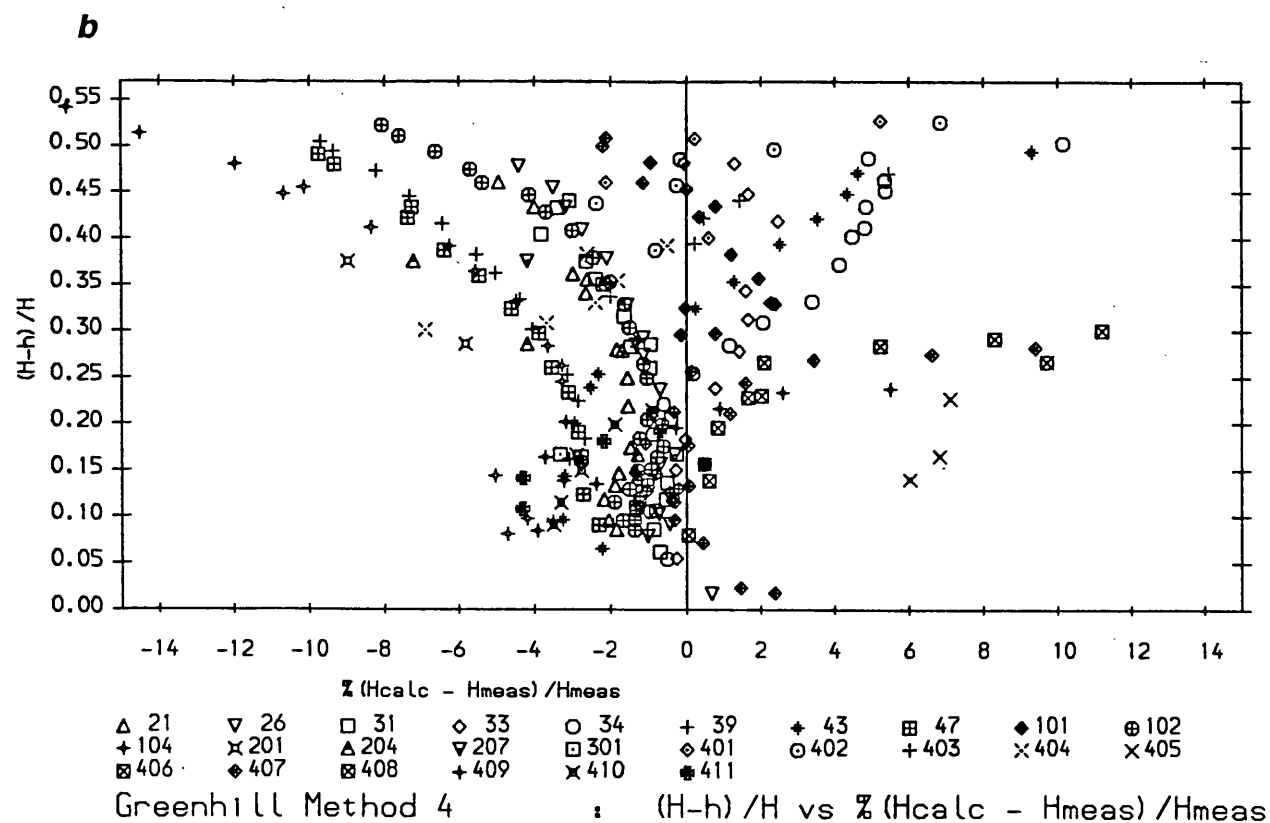
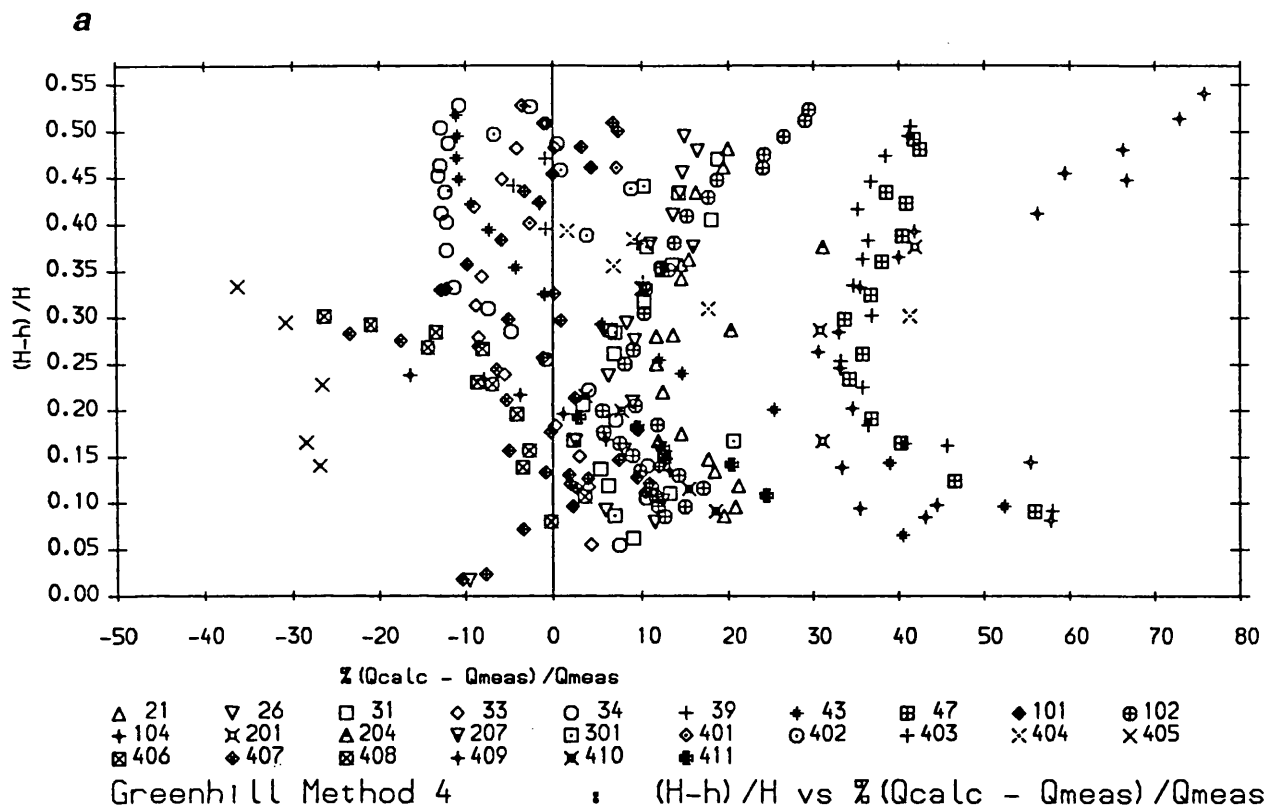


**Figure 6.33 Errors in predicted discharge and depth GH4**

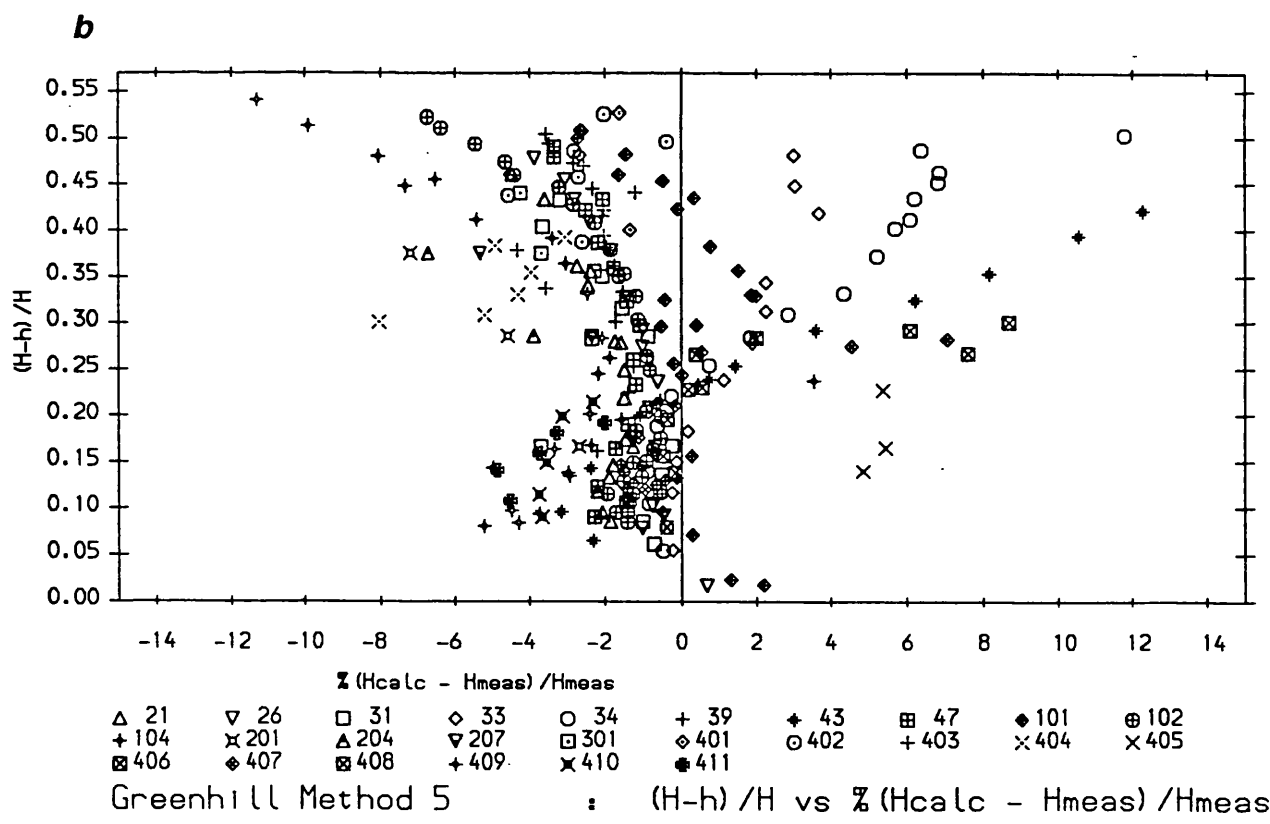
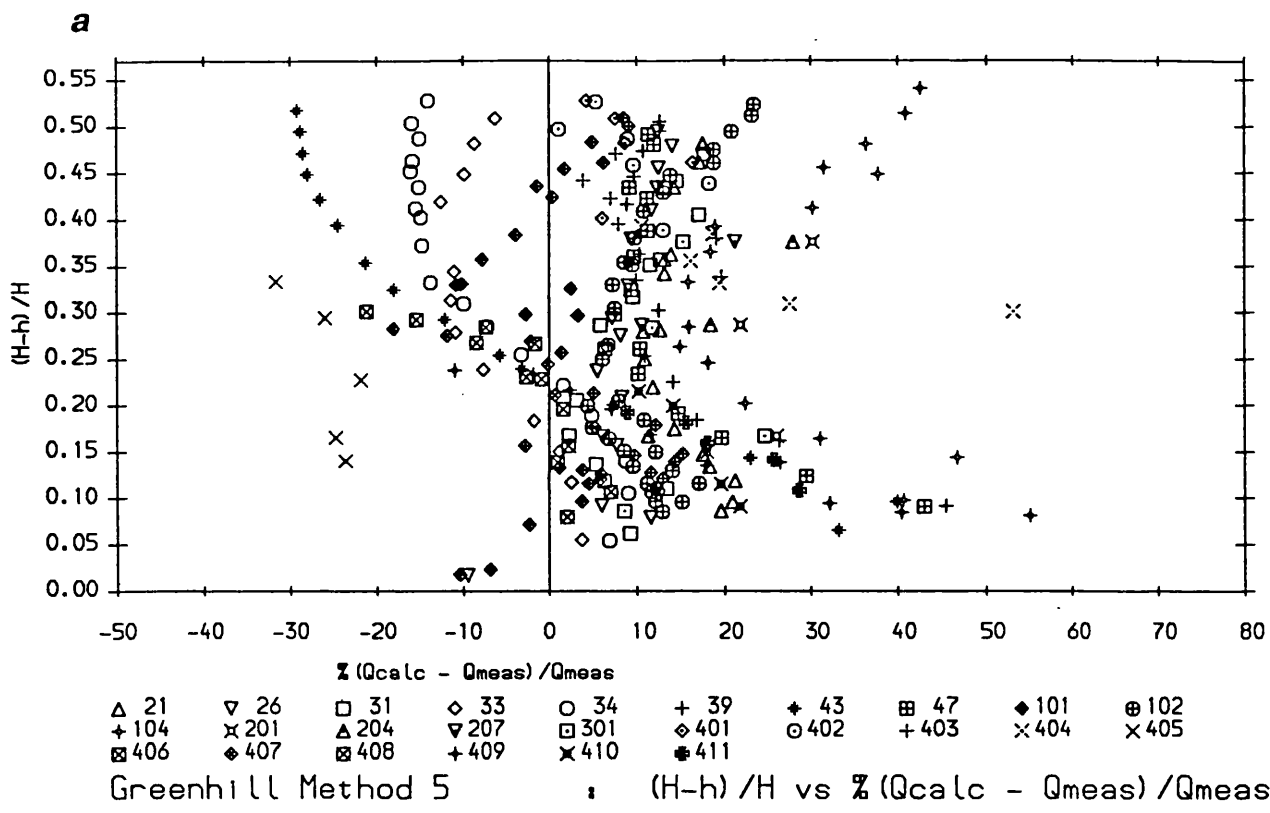
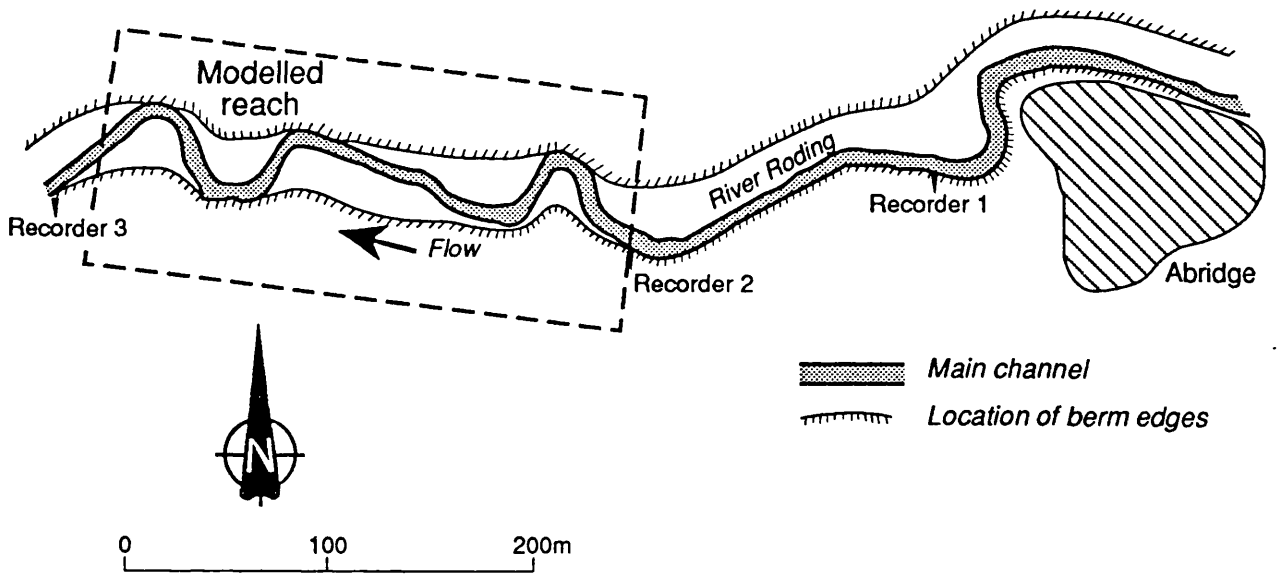
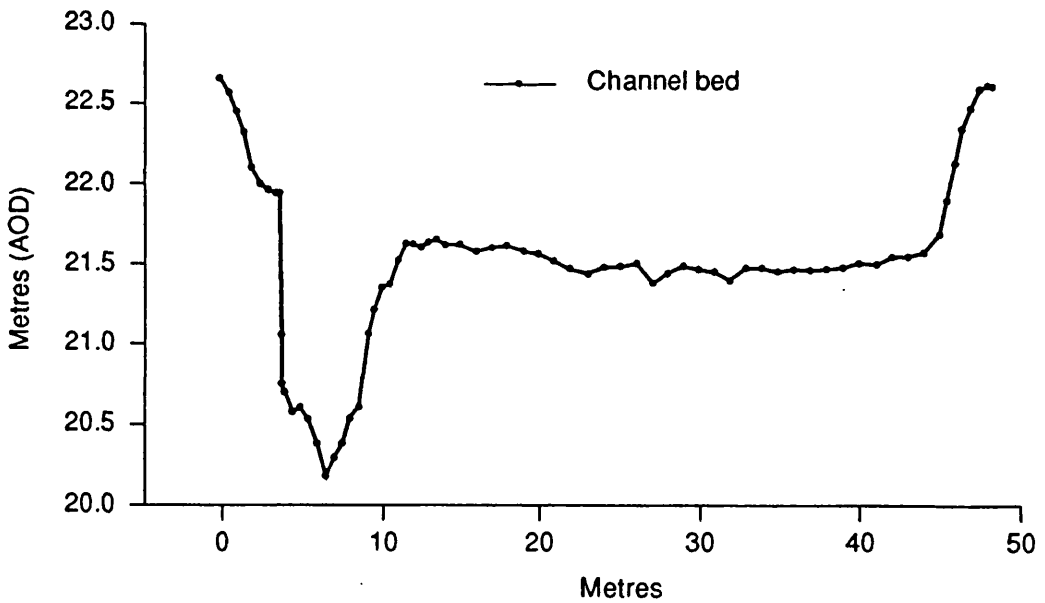


**Figure 6.34 Errors in predicted discharge and depth GH5**



6.35 Location plan of study area on River Roding at Abridge (after Sellin et al 1990)



6.36 Roding at Abridge sample cross-section

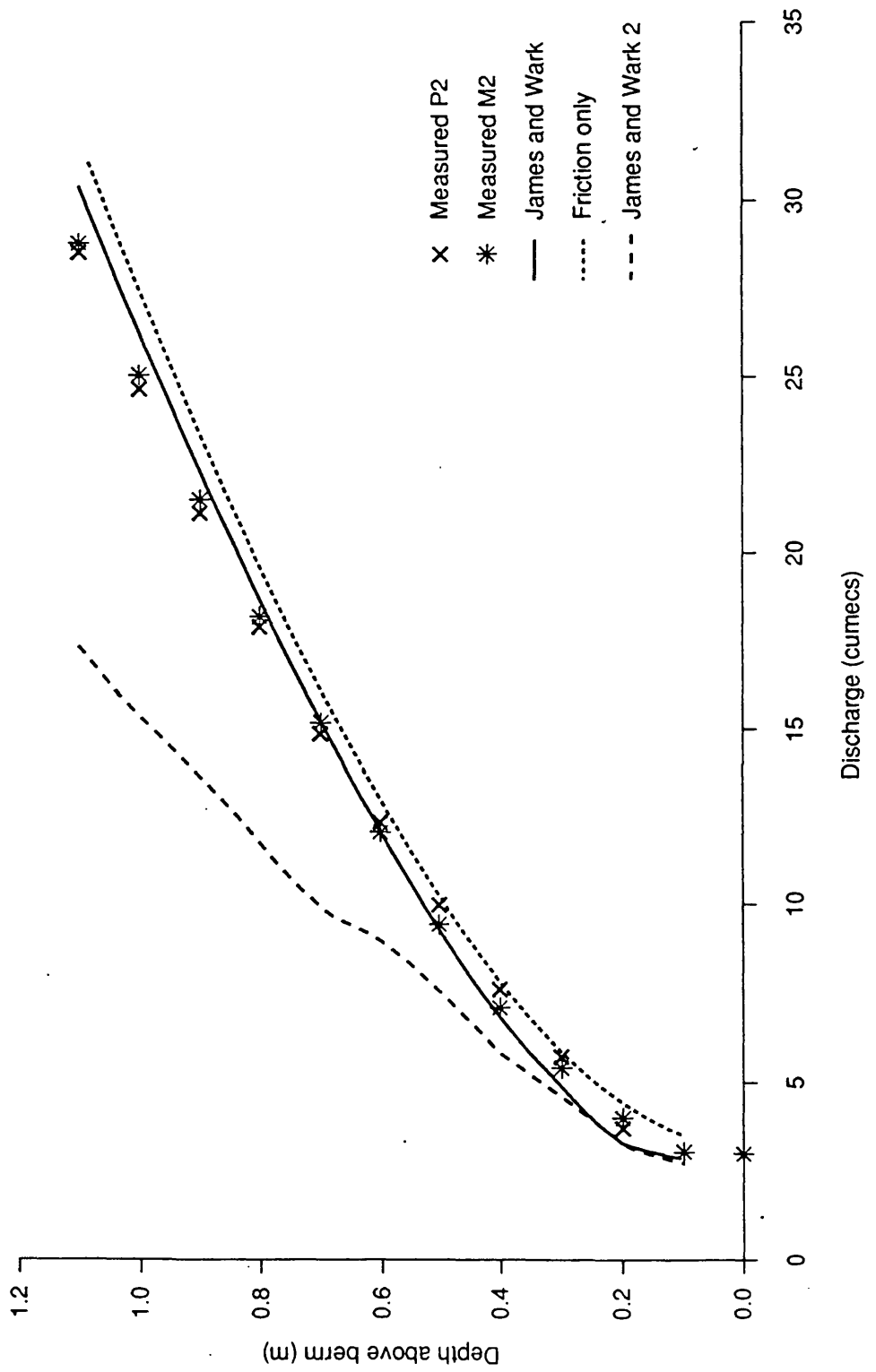


Figure 6.37 Roding at Abridge measured and calculated stage-discharges

## APPENDIX 1

### Summary of Tensor Mathematics

#### 1 Tensor Notation

Consider  $A_{ij}$  and  $B_{ij}$  etc. to be elements of general tensors. Where the subscripts may take the integer values 1, 2, 3, . . . ,n.

#### 2 The Summation Convention

Any expression involving a repeated index shall automatically stand for its sum over the values (1,2,3, . . . ,n) of the repeated index. Where n is the range of all summations.

The repeated index is referred to as the dummy index and any other index in the expression as a free index.

Any free index in an expression shall have the same range as the summation indices, unless stated otherwise.

No index may occur more than twice in any given expression.

#### 3 Coordinate Transformations

Tensor notation is particularly convenient when considering transformations from one coordinate system,  $x_i$ , to another,  $\tilde{x}_i$ . The following is restricted to transformations between sets of right handed cartesian coordinate systems, for a more general treatment see Kay (1988 chapters 1,2 and 3).

Consider a linear, orthogonal transformation, J, which takes the cartesian coordinate system,  $x_i$ , to another cartesian system with the same origin,  $\tilde{x}_i$ , (i=1,2,3). Such a transformation may be expressed as:

$$\tilde{x}_i = a_{ij} x_j \quad (\text{A1-1})$$

Where

$$a_{ij} = \frac{\partial \tilde{x}_i}{\partial x_j} \quad (\text{A1-2})$$

$a_{ij}$  are the components of the Jacobian matrix, [J], of the transformation.

For linear, orthogonal transformations the inverse transformation,  $J^{-1}$ , is given by:

$$x_i = b_{ij} \tilde{x}_j \quad (\text{A1-3})$$

Where  $b_{ij} = a_{ji}$  (A1-4)

Obviously by the definitions of the transformations J and J<sup>-1</sup>

$$a_{ij} b_{ij} = \delta_{ij} \quad (\text{A1-5})$$

#### 4 Tensor transformation Laws.

Under the transformations defined above by A1-1 and A1-3 first order tensors (vectors) transform according to :

$$\tilde{T}_i = a_{ij} T_j \quad (\text{A1-6})$$

and

$$T_i = a_{ji} \tilde{T}_j \quad (\text{A1-7})$$

And second order tensors according to :

$$\tilde{T}_{ij} = a_{ir} a_{js} T_{rs} \quad (\text{A1-8})$$

and

$$T_{ij} = a_{ri} a_{sj} \tilde{T}_{rs} \quad (\text{A1-9})$$

It is possible to define transformation laws for higher order tensors but A1-6 to A1-9 are sufficient for our purposes.

#### 5 The Jacobian Matrix

An important property of the Jacobian Matrix is that its elements, (a<sub>ij</sub>), are the cosines of the angles between the x<sub>i</sub> coordinate directions and the  $\tilde{x}_j$  coordinate directions. Consider the two cartesian coordinate systems related to each other by A1-1 and A1-3. Let  $\hat{i}_p$  and  $\tilde{\hat{i}}_l$  be the unit vectors along the x<sub>p</sub> and the  $\tilde{x}_l$  coordinate directions respectively, (p,l = 1,2,3). Then taking the scalar product of these unit vectors.

$$\begin{aligned} \hat{i}_p \cdot \tilde{\hat{i}}_l &= |\hat{i}_p| |\tilde{\hat{i}}_l| \cos \theta_{pl} \\ &= \cos \theta_{pl} \end{aligned} \quad (\text{A1-10})$$

Where  $\theta_{pl}$  is the angle between  $\hat{i}_p$  and  $\tilde{\hat{i}}_l$ . Replacing  $\hat{i}_p$  in A1-10 with A1-7 gives :

$$\hat{i}_p \cdot \tilde{\hat{i}}_l = a_{lp} \tilde{\hat{i}}_l \cdot \tilde{\hat{i}}_l = a_{lp} \quad (\text{A1-11})$$

Hence  $a_{lp} = a_{pl} = \cos \theta_{pl}$  (A1-12)

The elements of the Jacobian Matrix are often referred to as direction cosines and the determinant as the Jacobian.

## APPENDIX 2

### The Stress Vector on an Arbitrary Surface

Note : The material below is based on Hunter, section 4.4

Definition : Let the element  $\alpha_j$  of the stress tensor  $\underline{\sigma}$  be the component of stress acting in the  $i$  coordinate direction on a surface whose +ve normal lies in the  $j$  direction.

Consider the tetrahedron shown in Figure A2 and let the  $\tilde{x}_i$  coordinate system be such that  $\tilde{x}_3$  lies along the direction of the outward unit normal,  $\underline{n}$ , of the sloping area  $\Delta S$ . ie :

$$\underline{n} = \begin{cases} (n_1, n_2, n_3) & \text{in terms of } x_i \\ \tilde{i}_3 & \text{in terms of } \tilde{x}_i \end{cases} \quad (\text{A2-1})$$

If the element is small enough for the body forces to be considered negligible and the stresses on the boundaries to be constant. Then if the element is at rest the force balance is the vector sum of the stresses multiplied by the appropriate area :

$$\Delta S \tilde{\sigma}_{rs} \tilde{i}_r = \Delta S_m \alpha_{lm} \tilde{i}_l \quad (\text{A2-2})$$

Thus by considering the element to be infinitely small it is clear that the force vector,  $\underline{dF}$ , acting on an arbitrary area,  $ds$ , can be expressed in terms of either the locally defined coordinate system,  $\tilde{x}_i$ .

$$\underline{dF} = ds \tilde{\sigma}_{p3} \tilde{i}_p \quad (\text{A2-3})$$

or the global coordinate system,  $x_i$ .

$$\underline{dF} = ds_m \alpha_{lm} \tilde{i}_l \quad (\text{A2-4})$$

by definition  $\alpha_{3m}$  is the only non-zero element of the tensor  $\underline{\sigma}$  and corresponds to  $d\tilde{\sigma}_3$  so by application of A1-6 and A1-7 :

$$ds_m = a_{3m} ds \quad (\text{A2-5})$$

Defining the stress vector  $\underline{M}$  as the force vector,  $\underline{dF}$ , divided by the area over which it acts,  $ds$ , then in terms of the global coordinate system :

$$\begin{aligned}\underline{\mathbf{M}} &= \underline{\mathbf{dF}} / ds \\ &= a_{3m} \alpha_{lm} \underline{\mathbf{i}}_l\end{aligned}\quad (A2-6)$$

Considering the scalar products of the unit vectors,  $\underline{\mathbf{i}}_p$ , and the unit normal to the surface,  $\underline{\mathbf{n}}$ .

$$\begin{aligned}\underline{\mathbf{i}}_p \cdot \underline{\mathbf{n}} &= n_p = n_p \\ &= |\underline{\mathbf{i}}_p| |\underline{\mathbf{n}}| \cos\theta_{pn} \\ &= \cos\theta_{pn}\end{aligned}\quad (A2-7)$$

but by A2-1 it is obvious that

$$\underline{\mathbf{n}} = \tilde{\underline{\mathbf{i}}}_3 \quad (A2-8)$$

Thus by A1-12, A2-7 and A2-8

$$\begin{aligned}n_p &= \cos\theta_{p3} \\ &= a_{p3} = a_{3p}\end{aligned}\quad (A2-9)$$

Replacing  $a_{3m}$  in equation A2-6 with  $n_m$ , by virtue of A2-9, gives the result :

$$\underline{\mathbf{M}} = n_m \alpha_{lm} \underline{\mathbf{i}}_l \quad (A2-10)$$

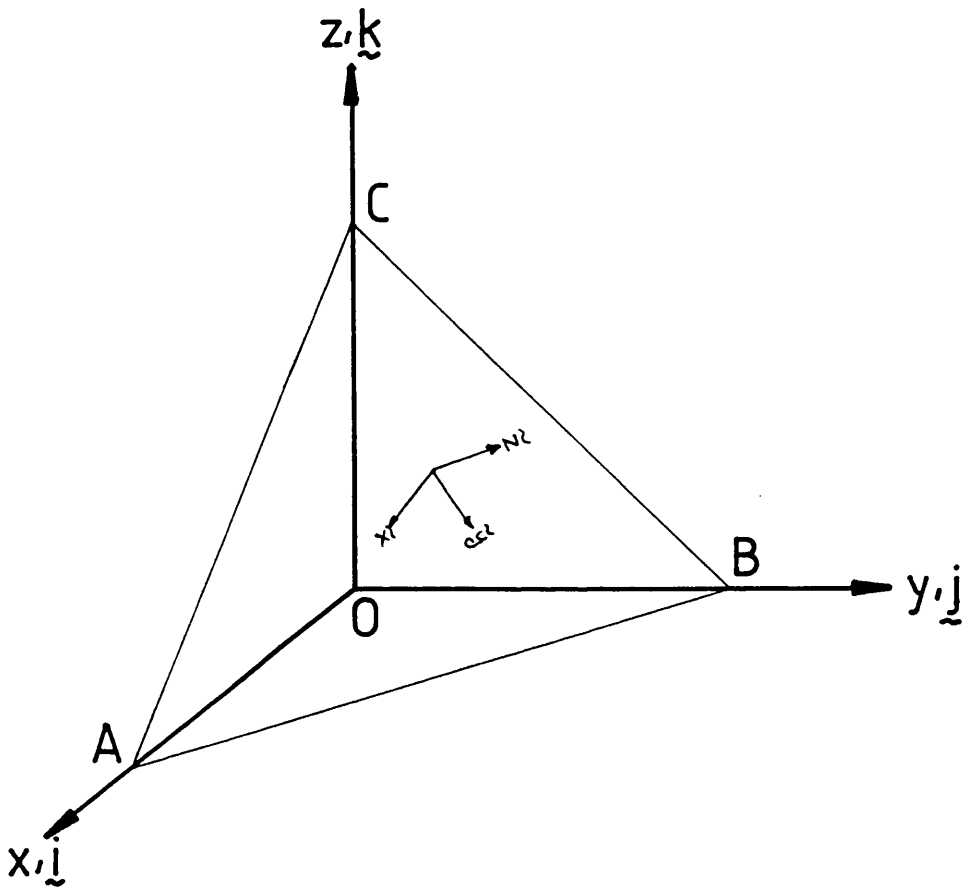
Hence  $\underline{\mathbf{M}}$  has components,  $M_l$ , in the global coordinate directions  $\underline{\mathbf{i}}_l$  given by :

$$M_l = n_m \alpha_{lm} \quad (A2-11)$$

## REFERENCE

HUNTER S C (1983) *Mechanics of Continuous Media*, 2<sup>nd</sup> edition, Ellis Horwood, Sussex, England.

Fig.A2      Stress on a Sloping Surface  
Definition Sketch



OBC	—	$\Delta S_x$
OAC	—	$\Delta S_y$
OAB	—	$\Delta S_z$
ABC	—	$\Delta S$

### APPENDIX 3 SERC PHASE A DATA

The stage-discharge data available from Phase A of the SERC Flood Channel Facility work into straight compound channels are listed below. The data includes series:

A1, A2, A3, A4, A5, A6, A7, A7B, A8, A9, A10, A11, A13

The file format is as follows:

The first three lines at the top of each file are comment lines. Information about the data is listed here.

The first two numbers after this are:

- 1 The test series number
- 2 The number of data points

The stage discharge data for each discharge point follows. An Example data line is shown below.

Date	discharge	depth	slope	temp
291189	0.01975	59.34	0.996	11.4

Date is given as a single integer: daymonthyear  
ie 291189 is 29/11/89

Discharge is given in cubic metres per second.

Depth is the depth in millimetres as recorded in the main channel.

Slope is the longitudinal valley slope of the water surface. These values should be multiplied by 1/1000. The Flume was constructed with a bed slope of  $1.021 \times 10^{-3}$ .

Temp is the temperature in degrees centigrade of the water in the flume as recorded by the investigators. Where the temperature was not recorded a default value of 15 °C has been assumed.

### Series 1

DATA IS FOR B/b = 6.667 OVER BANK ONLY  
DATES VARY BETWEEN 25/11/86 & 25/04/88  
STAGE DISCHARGE DATA FILE - ALL DATA

01 26

130587	0.15899	0.2082	1.013	13.0
080587	0.16519	0.2337	1.035	13.0
140487	0.16544	0.2335	1.027	11.5
251186	0.16725	0.2387	1.027	12.0
070587	0.17563	0.2852	1.046	13.0
090487	0.17590	0.2851	1.027	11.5
100487	0.17628	0.2851	1.005	11.5
281186	0.17770	0.2948	1.027	12.0
010487	0.18656	0.3535	1.029	11.5
261186	0.18830	0.3639	1.027	12.0
010587	0.19866	0.4514	1.032	12.5
130487	0.19871	0.4513	1.021	11.5
050587	0.19881	0.4511	1.030	13.0
261186	0.20479	0.5002	1.036	12.0
270488	0.21411	0.6001	0.999	12.5
250488	0.21443	0.6046	1.016	13.0
101286	0.21610	0.6236	1.027	12.0
101286	0.22550	0.7152	1.027	12.0
111286	0.23290	0.8082	1.027	12.0
111286	0.24040	0.9130	1.027	12.0
181286	0.24870	0.9906	1.027	12.0
260488	0.25012	1.0145	1.028	12.5
270488	0.25037	1.0166	1.019	12.5
060387	0.25072	1.0111	1.011	12.0
080487	0.25366	1.0365	1.027	11.5
121286	0.25770	1.1053	1.027	12.0

160187 0.15955 0.1898 1.027 12.0 \*

SUSPICIOUS DATA POINT HAS  
BEEN REMOVED

### Series 2

DATA BELOW IS FOR B/b = 4.2 OVER BANK ONLY  
DATES VARY BETWEEN 20/5/87 & 16/7/87  
STAGE DISCHARGE DATA FILE - ALL DATA

02 29

200587	0.15238	0.2168	1.027	14.0
150687	0.15604	0.2095	1.016	13.5
100787	0.15649	0.2123	1.003	15.5
120687	0.15965	0.2185	1.027	13.5
120687	0.16384	0.2299	1.034	13.5
160787	0.16873	0.2483	1.026	17.0
090687	0.16985	0.2498	1.027	13.5
110687	0.16992	0.2492	1.032	13.25
200587	0.17268	0.2702	1.027	14.0
040687	0.17784	0.2821	1.034	15.0

150787	0.18676	0.3237	1.028	16.5
010687	0.18695	0.3238	1.022	15.0
210587	0.18752	0.3239	1.027	14.0
210587	0.18800	0.3239	1.027	14.0
220587	0.19680	0.3723	1.027	14.0
010787	0.19796	0.3832	1.019	16.0
260587	0.20725	0.4299	1.027	14.0
180687	0.21346	0.4792	1.033	14.25
020787	0.21355	0.4800	1.013	16.0
260587	0.22392	0.5513	1.027	14.0
270587	0.23265	0.6326	1.026	14.0
270587	0.24290	0.7117	1.022	14.0
030787	0.24855	0.7630	1.023	16.0
190687	0.24908	0.7642	0.968	14.5
270587	0.25351	0.8003	1.027	14.0
280587	0.26779	0.9024	1.029	14.0
290587	0.28648	1.1170	1.027	14.5
070787	0.28688	1.1150	1.077	16.0
090787	0.28795	1.1142	1.078	16.0

### Series 3

DATA BELOW IS FOR B/b = 2.2 OVER BANK ONLY  
 DATES VARY BETWEEN 29/7/87 & 26/8/87  
 STAGE DISCHARGE DATA FILE - ALL DATA

3 22

140887	0.15800	0.2251	1.023	16.75
130887	0.16627	0.2412	1.016	16.5
120887	0.16675	0.2421	1.034	16.0
250887	0.17587	0.2668	1.029	16.0
110887	0.17712	0.2676	1.014	15.5
070887	0.18779	0.3031	1.036	16.0
240887	0.18786	0.3026	1.028	16.0
290787	0.18811	0.3027	1.027	16.0
060887	0.19804	0.3323	1.013	15.0
200887	0.19881	0.3325	1.030	16.5
040887	0.21454	0.3922	1.015	16.2
170887	0.21577	0.3913	0.956	16.5
290787	0.23905	0.5024	1.027	16.0
040887	0.24727	0.5552	1.027	16.2
260887	0.24774	0.5581	1.031	16.0
180887	0.24841	0.5579	1.025	16.5
310787	0.26391	0.6345	1.032	16.0
310787	0.28637	0.7603	1.027	16.0
190887	0.29874	0.8347	1.012	16.5
030887	0.29928	0.8360	1.027	15.8
260887	0.30014	0.8349	1.024	16.0
030887	0.30694	0.8851	1.027	15.8

#### Series 4

DATA BELOW IS FOR B/b = 1.2 OVER BANK ONLY (H > 0.15)  
DATES VARY BETWEEN 3/9/87 & 14/4/88  
STAGE DISCHARGE DATA FILE - ALL DATA

4 14

140987	0.15803	0.2237	1.019	15.0
140987	0.16509	0.2403	1.027	15.0
150987	0.16619	0.2414	1.032	15.0
160987	0.17533	0.2623	1.027	15.5
030987	0.18147	0.2717	1.027	15.5
170987	0.18687	0.2909	1.022	15.7
180987	0.19924	0.3240	1.028	15.8
230987	0.21347	0.3631	1.034	15.5
030987	0.21996	0.3764	1.027	15.5
240987	0.24738	0.4791	1.052	15.25
040987	0.27728	0.5660	1.027	15.5
250987	0.29587	0.6397	1.053	15.25
140488	0.30093	0.6536	1.039	13.0
070987	0.30735	0.6795	1.027	15.5

#### Series 5

DATA BELOW IS FOR B/b = 2.5 OVER BANK ONLY  
DATES VARY BETWEEN 21/07/87 & 24/07/87  
STAGE DISCHARGE DATA FILE - ALL DATA

05 8

240787	0.16115	0.2123	1.004	15.5	* query Q maybe 0.2295
210787	0.18640	0.3006	1.027	15.5	
240787	0.19979	0.3490	1.027	15.5	
230787	0.21466	0.4110	1.027	15.5	
210787	0.21903	0.4265	1.027	15.5	
210787	0.24256	0.5428	1.027	15.5	
220787	0.24858	0.5915	1.016	15.5	
220787	0.28432	0.8068	1.027	15.5	

## Series 6

DATA BELOW IS FOR B/b = 4.2 ASYMMETRIC OVER BANK ONLY  
DATES VARY BETWEEN 18/5/88 & 15/6/88  
STAGE DISCHARGE DATA FILE - ALL DATA

06 20

080688	0.15761	0.2235	1.040	14.0
010688	0.15781	0.2235	1.027	13.5
070688	0.15826	0.2235	1.039	13.75
100688	0.16505	0.2382	1.019	13.75
180588	0.17457	0.2534	1.029	13.0
080688	0.17607	0.2648	1.051	14.0
090688	0.17619	0.2648	1.037	14.25
140688	0.18596	0.2923	1.022	14.5
180588	0.18747	0.2933	1.048	13.0
190588	0.18836	0.2929	1.035	12.75
130688	0.19793	0.3426	1.045	14.5
060688	0.19981	0.3441	1.020	13.0
140688	0.21149	0.3917	1.008	14.5
150688	0.21235	0.3944	1.027	14.5
200588	0.21348	0.3952	1.019	12.75
240588	0.24755	0.5926	1.012	13.5
230588	0.24781	0.5929	1.018	13.25
230588	0.27348	0.7300	1.040	13.25
240588	0.30145	0.9292	1.021	13.5
250588	0.30185	0.9292	1.039	14.0

## Series 7

DATA BELOW IS FOR B/b = 4.2 OVER BANK ONLY ROUGHEND FPS  
DATES VARY BETWEEN 20/7/88 & 3/8/88  
STAGE DISCHARGE DATA FILE - ALL DATA

07 18

250788	0.15203	0.2084	1.027	18.0
250788	0.15586	0.2160	1.052	18.0
200788	0.16352	0.2296	1.027	14.8
030888	0.16551	0.2332	1.020	20.0
020888	0.17399	0.2482	1.014	20.5
220788	0.17494	0.2456	1.012	16.75
020888	0.17654	0.2540	1.035	20.5
010888	0.18594	0.2717	1.036	21.0
200788	0.19445	0.2856	1.027	14.8
290788	0.19950	0.2998	1.019	21.0
280788	0.21568	0.3383	1.022	20.5
280788	0.21661	0.3413	1.044	20.5
220788	0.21884	0.3429	1.036	16.75
220788	0.24666	0.4152	1.029	16.75
270788	0.24979	0.4238	1.026	21.0
210788	0.27574	0.4626	1.027	15.9
210788	0.28354	0.5006	1.027	15.9
260788	0.30251	0.5434	1.048	20.0

**Series 7B**

DATA FOR: STRAIGHT CHANNEL: OVERBANK FLOW :  
B/b = 4.2            SERIES =7B    ROUGHEND FP    SMALLER DENSITY  
RUN DATA BETWEEN: NO DATES

71            4  
000000 0.23710 0.42570 1.048 21.0  
000000 0.27182 0.52680 1.029 21.0  
000000 0.29056 0.57490 1.043 21.0  
000000 0.30402 0.57490 1.045 21.0

**Series 8**

DATA BELOW IS FOR B/b = 4.0 OVER BANK ONLY  
DATES VARY BETWEEN 17/10/88 & 2/11/88  
STAGE DISCHARGE DATA FILE - ALL DATA

08 25  
171088 0.15303 0.1802 1.027 15.0  
021188 0.15796 0.1858 1.044 12.0  
171088 0.16475 0.2024 1.027 15.0  
011188 0.16700 0.2064 1.021 12.0  
171088 0.17360 0.2306 1.027 15.0  
311088 0.17653 0.2382 1.034 12.5  
281088 0.18757 0.2841 1.045 14.5  
171088 0.19208 0.3065 1.027 15.0  
271088 0.20008 0.3440 1.036 15.0  
181088 0.20052 0.3471 1.027 15.0  
181088 0.21346 0.4244 1.027 15.0  
261088 0.21483 0.4273 1.020 15.0  
181088 0.21936 0.4618 1.028 15.0  
181088 0.22753 0.5133 1.027 15.0  
191088 0.23411 0.5747 1.026 15.0  
191088 0.24524 0.6552 1.027 15.0  
251088 0.25022 0.6902 1.017 15.0  
191088 0.25028 0.6911 1.026 15.0  
191088 0.25981 0.7655 1.027 15.0  
201088 0.26435 0.7986 1.027 15.0  
201088 0.27806 0.9153 1.027 15.0  
201088 0.28997 1.0260 1.026 15.0  
201088 0.29601 1.0780 1.027 15.0  
211088 0.29973 1.1034 1.017 15.0  
241088 0.29974 1.1034 0.999 15.0

**Series 9**

DATA BELOW IS FOR B/b = 4.0 OVER BANK ONLY ROUGH FP'S  
DATES VARY BETWEEN 14/11/88 & 17/11/88  
STAGE DISCHARGE DATA FILE - ALL DATA

09 10

141188	0.15244	0.1802	1.027	12.0
151188	0.16216	0.1928	1.027	11.25
151188	0.17050	0.2059	1.027	11.25
141188	0.18469	0.2315	1.027	12.0
161188	0.20686	0.2731	1.030	11.5
161188	0.22510	0.3072	1.031	11.5
161188	0.24544	0.3459	1.027	11.5
161188	0.25824	0.3739	1.027	11.5
171188	0.27627	0.4101	1.027	12.0
171188	0.30214	0.4639	1.027	12.0

**Series 10**

DATA BELOW IS FOR B/b = 4.4 OVER BANK ONLY  
DATES VARY BETWEEN 8/2/89 & 30/3/89  
STAGE DISCHARGE DATA FILE - ALL DATA

10 19

080289	0.15103	0.2207	1.027	14.2
300389	0.15803	0.2368	1.016	14.0
290389	0.16660	0.2627	1.042	14.0
160389	0.17645	0.3003	1.027	15.0
280389	0.17654	0.3006	1.017	14.0
090289	0.18657	0.3482	1.027	14.0
230389	0.18701	0.3514	1.033	15.1
090289	0.20032	0.4299	1.028	14.0
160389	0.20033	0.4290	1.026	15.0
090389	0.20051	0.4292	1.017	15.0
170389	0.21477	0.5220	1.033	15.0
090289	0.21479	0.5225	1.027	14.0
160389	0.21481	0.5220	1.028	14.9
130389	0.21800	0.5599	1.027	15.4
210389	0.23435	0.6876	1.033	15.0
200389	0.24930	0.8071	1.017	14.9
210389	0.26095	0.9175	1.027	14.9
210389	0.27970	1.0939	1.033	15.2
150389	0.27980	1.0915	1.024	14.5

### Series 11

DATA FOR: STRAIGHT CHANNEL: OVERBANK FLOW      total flows  
B/b = 4.4      SERIES =11 ROUGHEND FLOODPLAIN  
RUN DATA BETWEEN: 190589 & 250589

11	16			
240189	0.15663	0.23840	1.027	13.5
250589	0.16600	0.26010	1.019	16.8
250189	0.16796	0.26060	1.027	13.5
250589	0.17670	0.28110	1.011	16.5
260189	0.18536	0.29990	1.027	13.5
190589	0.18848	0.30740	1.008	14.9
200589	0.19824	0.33210	1.029	15.0
260189	0.20206	0.33870	1.027	14.0
260189	0.21115	0.35980	1.027	13.5
220589	0.21548	0.36860	1.025	15.4
250189	0.21822	0.37500	1.027	13.25
260189	0.22707	0.39960	1.027	13.0
260189	0.24368	0.44240	1.041	13.0
220589	0.25007	0.45920	1.033	15.9
250189	0.26001	0.48750	1.027	13.25
230589	0.30276	0.60660	1.025	17.0

### Series 13

DATA BELOW IS FOR IN BANK ROUGHNESS TESTS  
DATES VARY BETWEEN  
STAGE DISCHARGE DATA FILE - ALL DATA

13	7			
150889	0.04444	0.01380	1.027	13.50
150889	0.06439	0.02050	1.027	13.60
160889	0.06949	0.02250	1.027	13.70
160889	0.08200	0.02760	1.027	13.50
170889	0.08695	0.02970	1.027	13.50
170889	0.09856	0.03490	1.027	14.00
180889	0.11922	0.04530	1.027	13.60

## APPENDIX 4 RIVER GAUGING SITES AND LABORATORY DATA

This appendix lists the stage-discharge data obtained for seven river gauging sites and stage-discharges from two laboratory investigations in to straight compound channels.

The file format is given first, followed by the data files.

### Input file format

```
LINE
1      JBNAME
2      HEADNG
3      NUMNOD, NUMITR, IROUTP, NSTAGE, NEDYVS
4      LEDVDB, PIVAAR, PFVAAR, PCONVB, PINDAT
5      CGFVEL, CGFSD, CGFGEO, AMSCRS, CLCVF
6      S, SMC, NF
7      OLRDLS, LABLHS, LABRHS
8      NGP, YMIN, YMAX, ZMAX, ZBF, ZMINI, BMMC
9      (YGP (I), ZGP (I), I=1, NGP, 1)
10     EDGMC1, EDGMC2
11     CONVP (1), CONVP (2)
12     NBDRVS , (BEDRP (I), 1, NBDRVS)

EITHER  AMSCRS = 'YES'
13      (BEDRVS (I), I=1, NBDRVS)

OR      AMSCRS = 'NO'
13      (STAGE (J), (BEDRVS (I), I=1, NBDRVS), QMEAS (J), J=1, NSTAGE)

14     NTPVP, (TVPP (I), I=1, NTPVP)
15     (TVP (I), I=1, NTPVP)
```

### Input file description

```
1  JBNAME - ' ' - FOUR LETTER CHARACTER VARIABLE USED TO IDENTIFY JOB

2  HEADING - A80- EIGHTY LETTER LINE INPUT AS A WHOLE. USED FOR NOTES
    ETC ABOUT JOB.

3  NUMNOD - NUMBER OF NODES TO BE USED IN CALCULATIONS
    NUMITR - MAXIMUM NUMBER OF ITERATIONS TO BE CARRIED OUT FOR EACH STAGE
    IROUTP - INTEGER POINTER WHICH DEFINES THE FRICTION LAW TO BE USED :

    IROUTP = 1 COLEBROOK WHITE - COLWHT
              2 MANNINGS EQUATION
              3 CHEZY'S LAW
              4 ROUGH TURBULENT LAW
              5 SMOOTH TURBULENT LAW - SMTRB
              6 BARR'S APPROXIMATION TO COLEBROOK WHITE
              7 MODIFIED SMOOTH TURBULENT FOR SERC FLUME - SERCFL
              8 WIDE CHANNEL ROUGH TURBULENT
              9 WIDE CHANNEL SMOOTH TURBULENT - WCSMTB
             10 WIDE CHANNEL COLEBOOKE WHITE - WCCBWH
```

- NSTAGE - NUMBER OF WATER LEVELS (STAGES) FOR WHICH CALCULATIONS TO BE CARRIED OUT
- NEDYVS - NUMBER OF EDDY VISCOSITY COMBINATIONS FOR WHICH THE CALCULATIONS TO BE CARRIED OUT
- 4 LEDVDB - EDDY VISCOSITY TYPE POINTER :
- 'BGTSTO' BED GENERATED TURBULENT SHEAR STRESS ONLY  
 $\nu_t = NEV U^* D$   
 NEV = NON DIMENSIONAL EDDY VISCOSITY
  - 'CONEDY' CONSTANT EDDY VISCOSITY  
 $VT = NEV$
- PIVARR - PRINT INITIAL VALUES ALL ARRAYS - 'YES' OR 'NO'
- PFVAAR - PRINT FINAL VALUES ALL ARRAYS - 'YES' OR 'NO'
- PCONVB - PRINT CONVERGENCE BEHAVIOUR - 'YES' OR 'NO'
- PINDAT - PRINT INPUT DATA - 'YES' OR 'NO'
- 5 CGFVEL - CREATE GRAPH FILE VELOCITY - 'YES' OR 'NO'
- 'YES' - FILE JBNAME//VL CREATED
- CGFSD - CREATE GRAPH FILE FOR STAGE DISCHARGE
- 'YES' - FILE JBNAME//SD CREATED
- CGFGEO - CREATE GRAPH FILE FOR BED GEOMETRY
- 'YES' - FILE JBNAME/XS/ CREATED
- AMSCRS - AUTOMATIC STAGE CALCULATION AND ROUGHNESS SETTING
- 'YES' - THE VALUES OF STAGE FOR WHICH CALCULATION REQUIRED WILL BE SET AUTOMATICALLY BETWEEN THE MAXIMUM AND MINIMUM BED LEVELS INPUT. THE ROUGHNESS VALUES ARE ASSUMED TO BE CONSTANT WITH STAGE.
  - 'NO' - THE STAGE VALUES AND CORRESPONDING ROUGHNESS VALUES MUST BE INPUT EXPLICITLY.
- CLCFV - CALCULATE VARIOUS FACTORS - 'YES' OR 'NO'
- 'NO' - ONLY TABLE OF STAGE ,FLOW AREA, TOP WIDTH, CONVEYENCE AND QCRIT ARE OUTPUT
  - 'YES' - ANOTHER TABLE WITH STAGE, TOTAL FLOW , FLOWS IN LEFT FP , MAIN CHANNEL, RIGHT FP FLOW AREA AND ALPHA + BETA FACTORS ALSO OUTPUT
- 6 S - LONGITUDINAL SLOPE
- SMC - IDEALIZED MAIN CHANNEL SIDE SLOPES
- NF - NUMBER OF FLOODPLAINS
- 7 OLRlds - ORIGIN ON LEFT OR RIGHT LOOKING DOWNSTREAM
- 'LEFT' - THE CROSS SECTION DATA HAS BEEN GIVEN AS IT APPEARS LOOKING DOWNSTREAM. THE DATA WILL BE PROCESSED TO PRODUCE THE X-SECTION WITH THE ORIGIN ON THE FAR LEFT OF THE LEFT FLOODPLAIN.
  - 'RIGHT' - THE CROSS SECTION DATA HAS BEEN GIVEN AS IT APPEARS LOOKING UP STREAM. THE DATA WILL BE PROCESSED TO PRODUCE THE X-SECTION LOOKING DOWN STREAM AND THE ORIGIN WILL BE DISPLACED TO THE FAR LEFT HAND EDGE OF THE FLOODPLAIN
- LABLHS - LABEL LEFT HAND SIDE 'FIVE CHARACTER VARIABLE'
- LABRHS - LABEL RIGHT HAND SIDE 'FIVE CHARACTER VARIABLE'
- 8 NGP - NUMBER OF POINTS USED TO DEFINE X-SECTIONAL GEOMETRY
- YMIN - MINIMUM LATERAL COORDINATE USED
- YMAX - MAXIMUM LATERAL COORDINATE USED
- ZMAX - MAXIMUM BED LEVEL - LEVEL OF END POINTS SET TO THIS IF THEY ARE NOT IN INPUT DATA

- ZBF - BANKFUL STAGE
- ZMINI - IDEALIZED MAIN CHANNEL BED ELEVATION
- BWMC - IDEALIZED MAIN CHANNEL BOTTOM WIDTH
  
- 9 YGP,ZGP - PAIRS OF LATERAL AND VERTICAL COORDINATES OF THE POINTS  
DEFINING THE RIVER CROSS SECTION.
- 10 EDGMC1 - LATERAL COORDINATE OF THE LEFT HAND SIDE OF THE MAIN CHANNEL  
AS DATA INPUT
- EDGMC2 - LATERAL COORDINATE OF THE RIGHT HAND SIDE OF THE MAIN CHANNEL  
AS DATA INPUT (IE EDGMC2 > EDGMC1)
  
- 11 CONVP (1)
- CONVP (2) - LATERAL COORDINATES OF TWO 'CONVEYANCE POINTERS'  
NOT USED IN PRESENT VERSION
  
- 12 NBDRVS - NUMBER OF DIFERENT ROUGHNESS ZONES ACROSS CHANNEL
- BEDRP - POINTER ARRAY HOLDING THE COORDINATE OF THE RIGHT HAND  
EDGE OF EACH ZONE
  
- 13 STAGE - ARRAY HOLDING THE STAGE (WATER LEVELS) FOR WHICH  
CALCULATIONS TO BE CARRIED OUT
- BEDRVS - ARRAY HOLDING ROUGHNESS VALUES FOR EACH ZONE (MANNINGS N ONLY)
- QMEAS - ARRAY HOLDING VALUES OF MEASURED FLOWS
  
- 14 NTVPV - NUMBER OF DIFFERENT VISCOSITY ZONES ACROSS CHANNEL
- TVPP - POINTER ARRAY HOLDING THE COORDINATES OF THE RIGHT HAND  
EDGE OF EACH ZONE
  
- 15 TVP - TURBULENT VISCOSITY PARAMETERS - ARRAY HOLDING NON DIMESIONAL  
EDDY VISCOSITY VALUES FOR EACH ZONE

## DATA FILES FOR VARIOUS RIVER GAUGING SITES

'BLK2'

River Black water at Ower ACK actual measured data

1000 20 2 7 1

'BGTSTO' 'NO' 'NO' 'NO' 'NO'

'NO' 'YES' 'YES' 'NO' 'YES'

1.6E-3 0.00 2

'LEFT' 'LEFT' 'RIGHT'

28 -2.51 69.5 3.58 1.7 0.00

-2.51 3.58

-2.5 2.174 0.0 1.89 3.0 1.89 8.0 1.96 10.5 1.74

11.0 2.00 11.1 0.00 16.9 0.00 17.0 2.01 18.5 1.50

21.5 1.82 24.5 1.84 27.5 1.78 30.5 1.86 33.5 1.90

36.5 1.92 39.5 1.79 42.5 1.61 45.5 1.51 48.5 1.62

51.5 1.74 54.5 2.03 57.5 2.54 60.5 3.09 63.5 3.37

66.5 3.38 69.5 3.58

11.0 17.0

-2.51 69.5

3 11.0 17.0 69.5

1.760 0.094 0.046 0.099 9.241

1.774 0.094 0.046 0.099 11.120

1.786 0.094 0.046 0.099 9.476

1.810 0.094 0.046 0.099 9.816

1.847 0.094 0.046 0.099 10.193

1.885 0.094 0.046 0.099 10.997

1.987 0.094 0.046 0.099 12.008

1 69.5

0.16

'MAN6'

RIVER MAINE SECTION 6, NORTHERN IRELAND acker method VERSION

1000 20 2 14 1 actual measured data

'BGTSTO' 'NO' 'NO' 'NO' 'YES'

'NO' 'YES' 'YES' 'NO' 'YES'

1.906E-3 1.444444 2

'LEFT' 'LEFT' 'RIGHT'

8 0.00 27.50 2.20 0.9 0.000

0.00 2.20 0.10 1.30 6.60 0.90 7.90 0.00

19.00 0.00 20.30 0.90 27.40 1.30 27.50 2.20

6.6 20.3

0.00 27.50

3 6.6 20.3 27.5

0.950 0.040 0.032 0.040 14.82  
0.955 0.040 0.032 0.040 14.32  
0.960 0.040 0.032 0.040 15.40  
0.985 0.040 0.032 0.040 15.17  
1.010 0.040 0.032 0.040 18.46

1.075 0.040 0.032 0.040 17.10  
1.120 0.040 0.032 0.040 19.99  
1.130 0.040 0.032 0.040 18.19  
1.185 0.040 0.032 0.040 20.10  
1.290 0.040 0.032 0.040 27.24

1.440 0.040 0.032 0.040 29.91  
1.500 0.040 0.032 0.040 36.05  
1.850 0.040 0.032 0.040 44.38  
2.150 0.040 0.032 0.040 57.85

1 27.5  
0.16

'MN14'

RIVER MAINE SECTION 14, NORTHERN IRELAND ackermethod VERSION ! 1000 20 2 11

1 actual measured data

'BGTSTO' 'NO' 'NO' 'NO' 'YES' xs- corrected 4/4/92

'NO' 'YES' 'YES' 'NO' 'YES'

1.906E-3 0.996 2

'LEFT' 'LEFT' 'RIGHT'

9 0.0 40.80 4.89 0.92 0.00

0.00 4.81 0.001 4.54 5.30 1.41 13.50 0.92  
14.40 0.00 26.60 0.00 27.60 0.97 35.70 1.38  
40.80 4.89

13.50 27.60  
0.000 40.80

3 13.50 27.60 40.80

0.950 0.040 0.0276 0.040 18.46  
0.960 0.040 0.0276 0.040 17.1  
1.025 0.040 0.0276 0.040 18.19  
1.040 0.040 0.0276 0.040 19.99  
1.070 0.040 0.0276 0.040 20.10

1.200 0.040 0.0276 0.040 27.24  
1.270 0.040 0.0276 0.040 29.91  
1.385 0.040 0.0276 0.040 36.05  
1.500 0.040 0.0276 0.040 41.23  
1.580 0.040 0.0276 0.040 44.38

1.785 0.040 0.0276 0.040 57.85

1 40.8  
0.16

'OUSE'

River Ouse at Skelton acker method version using actual measured data

1000 20 2 13 1

'BGTSTO' 'NO' 'NO' 'NO' 'YES'

'NO' 'YES' 'YES' 'NO' 'YES'

1.46E-4 2.108 2

'LEFT' 'LEFT' 'RIGHT'

36 0.00 68.5 5.391 4.30 -4.548

0.00 5.391 2.50 4.591 4.00 4.291 5.50 4.191 7.00 4.341  
 8.50 3.891 10.00 3.531 11.50 2.521 13.00 1.410 14.50 0.271  
 16.00 0.131 17.50 -0.209 19.00 -1.400 20.50 -2.799 25.00 -3.609  
 28.00 -4.439 31.00 -4.958 34.00 -5.059 37.00 -4.889 40.00 -4.569  
 43.00 -4.319 44.50 -3.069 46.00 -2.229 47.50 -1.889 52.00 0.031  
 53.50 0.211 55.00 1.091 56.50 1.691 58.00 3.071 59.50 3.741  
 61.00 4.221 62.50 4.731 64.00 4.691 65.50 4.811 67.00 4.841  
 68.5 5.391

16.0 55.80

7.5 68.5

3 16.00 55.80 68.50

4.254 0.0448 0.0448 0.06 261.438  
 4.610 0.0448 0.0448 0.06 278.064  
 4.628 0.0448 0.0448 0.06 325.395  
 4.806 0.0448 0.0448 0.06 294.419  
 4.810 0.0448 0.0448 0.06 324.872

4.937 0.0448 0.0448 0.06 365.257  
 4.948 0.0448 0.0448 0.06 327.927  
 4.966 0.0448 0.0448 0.06 353.759  
 5.026 0.0448 0.0448 0.06 321.075  
 5.159 0.0448 0.0448 0.06 359.172

5.241 0.0448 0.0448 0.06 377.971  
 5.269 0.0448 0.0448 0.06 363.710  
 5.391 0.0448 0.0448 0.06 437.001

1 68.5

0.16

'SEV2'

RIVER SEVERN AT MONTFORD acker method VERSION data averaged in groups of 3

1000 20 2 36 1 using ackers final n values zmin and sc corrected

'BGTSTO' 'NO' 'NO' 'NO' 'NO'

'NO' 'YES' 'YES' 'NO' 'YES'

1.95E-4 1.425 2

'LEFT' 'LEFT' 'RIGHT'

8 0.00 125.20 6.087 4.087 -1.502

0.00 6.087 3.60 5.437 66.80 4.287 73.60 -1.663

90.80 -1.463 100.20 4.087 118.8 5.287 125.20 6.087  
66.5 101.0  
0.00 125.20

3 66.8 102.2 125.20

4.245333 0.0338 0.0307 0.0338 170.3667  
4.362667 0.0338 0.0307 0.0338 177.5  
4.491 0.0338 0.0307 0.0338 182.9333  
4.569333 0.0338 0.0307 0.0338 183.5667  
4.608 0.0338 0.0307 0.0338 183.8

4.625 0.0338 0.0307 0.0338 183.1667  
4.667333 0.0338 0.0307 0.0338 185.1  
4.702333 0.0338 0.0307 0.0338 187.7  
4.735 0.0338 0.0307 0.0338 189.1  
4.858 0.0338 0.0307 0.0338 196.3333

4.987333 0.0338 0.0307 0.0338 205.2333  
5.141 0.0338 0.0307 0.0338 215.9  
5.192333 0.0338 0.0307 0.0338 222.9333  
5.293 0.0338 0.0307 0.0338 233.1  
5.370333 0.0338 0.0307 0.0338 239.5667

5.434333 0.0338 0.0307 0.0338 245.3  
5.442333 0.0338 0.0307 0.0338 243.9  
5.461667 0.0338 0.0307 0.0338 252.5667  
5.503667 0.0338 0.0307 0.0338 257.3333  
5.553 0.0338 0.0307 0.0338 262.6667

5.593667 0.0338 0.0307 0.0338 267.3333  
5.607333 0.0338 0.0307 0.0338 276.6667  
5.617333 0.0338 0.0307 0.0338 285.5  
5.637 0.0338 0.0307 0.0338 282.7667  
5.662333 0.0338 0.0307 0.0338 278.1

5.687 0.0338 0.0307 0.0338 276.3667  
5.7 0.0338 0.0307 0.0338 282.5  
5.718333 0.0338 0.0307 0.0338 283.1667  
5.749333 0.0338 0.0307 0.0338 284.3333  
5.791 0.0338 0.0307 0.0338 282.3333

5.827667 0.0338 0.0307 0.0338 284  
5.848333 0.0338 0.0307 0.0338 285.0333  
5.858667 0.0338 0.0307 0.0338 283.5  
5.875 0.0338 0.0307 0.0338 282.8667  
5.935667 0.0338 0.0307 0.0338 296.2667

6.009333 0.0338 0.0307 0.0338 313.3333

1 125.20  
0.16

'SEV2'  
RIVER SEVERN AT MONTFORD acker method VERSION data averaged in groups of 3  
1000 20 2 36 1  
'BGTSTO' 'NO' 'NO' 'NO' 'NO'  
'NO' 'YES' 'YES' 'NO' 'YES'

1.95E-4 1.425 2

'LEFT' 'LEFT' 'RIGHT'

8 0.00 125.20 6.087 4.087 -1.520

0.00 6.087 3.60 5.437 66.80 4.287 73.60 -1.663  
90.80 -1.463 100.20 4.087 118.8 5.287 125.20 6.087  
66.5 101.0  
0.00 125.20 .

3 66.8 102.2 125.20

4.245333 0.025 0.031 0.045 170.3667  
4.362667 0.025 0.031 0.045 177.5  
4.491 0.025 0.031 0.045 182.9333  
4.569333 0.025 0.031 0.045 183.5667  
4.608 0.025 0.031 0.045 183.8  
  
4.625 0.025 0.031 0.045 183.1667  
4.667333 0.025 0.031 0.045 185.1  
4.702333 0.025 0.031 0.045 187.7  
4.735 0.025 0.031 0.045 189.1  
4.858 0.025 0.031 0.045 196.3333  
  
4.987333 0.025 0.031 0.045 205.2333  
5.141 0.025 0.031 0.045 215.9  
5.192333 0.025 0.031 0.045 222.9333  
5.293 0.025 0.031 0.045 233.1  
5.370333 0.025 0.031 0.045 239.5667  
  
5.434333 0.025 0.031 0.045 245.3  
5.442333 0.025 0.031 0.045 243.9  
5.461667 0.025 0.031 0.045 252.5667  
5.503667 0.025 0.031 0.045 257.3333  
5.553 0.025 0.031 0.045 262.6667  
  
5.593667 0.025 0.031 0.045 267.3333  
5.607333 0.025 0.031 0.045 276.6667  
5.617333 0.025 0.031 0.045 285.5  
5.637 0.025 0.031 0.045 282.7667  
5.662333 0.025 0.031 0.045 278.1  
  
5.687 0.025 0.031 0.045 276.3667  
5.7 0.025 0.031 0.045 282.5  
5.718333 0.025 0.031 0.045 283.1667  
5.749333 0.025 0.031 0.045 284.3333  
5.791 0.025 0.031 0.045 282.3333  
  
5.827667 0.025 0.031 0.045 284  
5.848333 0.025 0.031 0.045 285.0333  
5.858667 0.025 0.031 0.045 283.5  
5.875 0.025 0.031 0.045 282.8667

5.935667 0.025 0.031 0.045 296.2667

6.009333 0.025 0.031 0.045 313.3333

1 125.20  
0.16

'TEES'

River Tees at Lowmoor acker method version using actual measured data

1000 20 2 5 1

'BGTSTO' 'NO' 'NO' 'NO' 'YES'

'NO' 'YES' 'YES' 'NO' 'YES'

8.00E-4 1.412 2

'LEFT' 'LEFT' 'RIGHT'

27 0.00 186.00 10.808 8.50 4.32

0.000 10.808 6.696 10.375 12.192 9.949 18.288 9.644 24.384 9.530  
30.480 9.491 36.576 9.240 43.282 8.817 48.463 8.876 51.816 9.868  
53.340 10.113 57.912 9.299 59.436 9.189 61.569 9.068 67.056 4.260  
85.340 4.280 91.440 4.270 103.630 4.140 109.730 4.200 115.824 8.294  
120.396 9.040 128.016 9.409 137.160 9.637 149.352 10.230 161.540 10.440  
179.830 10.620 186.000 10.808

62.00 118.5  
0.00 186.00

3 62.00 118.5 186.00

8.828 0.100 0.056 0.100 277.89  
8.909 0.100 0.056 0.100 262.90  
9.205 0.100 0.056 0.100 346.89  
9.278 0.100 0.056 0.100 338.69  
9.947 0.100 0.056 0.100 400.70

1 186.0  
0.16

'TORR'

RIVER TORRIDGE AT TORRINGTON acker method VERSION observed flows conveyance  
limited by flood bank

1000 20 2 15 1

'BGTSTO' 'NO' 'NO' 'NO' 'NO'

'NO' 'NO' 'NO' 'NO' 'NO'

1.45E-3 0.787 1

'RIGHT' 'RIGHT' 'LEFT'

38 0.00 120 19.716 17.2 14.41

0.00 19.716 0.01 16.556 1.00 15.867 1.90 14.472 3.00 14.426  
26.40 14.521 27.50 16.409 28.40 17.197 32.00 17.460 35.00 17.472  
38.00 17.509 41.00 17.559 44.00 17.553 47.00 17.504 50.00 17.518  
52.00 17.962 55.00 18.254 56.50 18.348 57.50 18.348 60.00 17.953

63.00 17.522 66.00 17.321 69.00 17.218 71.50 17.136 73.50 17.518  
75.50 16.549 77.00 16.698 80.00 16.860 83.00 16.985 86.00 17.190  
90.00 17.333 95.00 17.451 100.00 17.640 105.00 17.885 110.00 18.425  
115.00 19.102 119.09 19.688 120.00 19.716

0.00 30.00  
0.00 57.50

3 0.0 30.00 120

17.205 99999 0.027 0.060 169.67  
17.213 99999 0.027 0.060 168.752  
17.225 99999 0.027 0.060 169.996  
17.275 99999 0.027 0.060 200.279  
17.278 99999 0.027 0.060 196.883

17.281 99999 0.027 0.060 189.61  
17.339 99999 0.027 0.060 180.333  
17.382 99999 0.027 0.060 203.824  
17.427 99999 0.027 0.060 196.362  
17.483 99999 0.027 0.060 208.074

17.692 99999 0.027 0.060 268.822  
17.695 99999 0.027 0.060 264.379  
17.834 99999 0.027 0.060 256.307  
18.004 99999 0.027 0.060 314.13  
18.008 99999 0.027 0.060 287.261

1 0.00 120.00  
0.16

'TORR'

RIVER TORRIDGE AT TORRINGTON acker method VERSION observed flows conveyance limited  
by flood bank using ackers definition of bankfull

1000 20 2 6 1

'BGTSTO' 'NO' 'NO' 'NO' 'NO'

'NO' 'NO' 'NO' 'NO' 'NO'

1.45E-3 0.787 1

'RIGHT' 'RIGHT' 'LEFT'

38 0.00 120 19.716 17.46 14.41

0.00 19.716 0.01 16.556 1.00 15.867 1.90 14.472 3.00 14.426  
26.40 14.521 27.50 16.409 28.40 17.197 32.00 17.460 35.00 17.472  
38.00 17.509 41.00 17.559 44.00 17.553 47.00 17.504 50.00 17.518  
52.00 17.962 55.00 18.254 56.50 18.348 57.50 18.348 60.00 17.953  
63.00 17.522 66.00 17.321 69.00 17.218 71.50 17.136 73.50 17.518  
75.50 16.549 77.00 16.698 80.00 16.860 83.00 16.985 86.00 17.190  
90.00 17.333 95.00 17.451 100.00 17.640 105.00 17.885 110.00 18.425  
115.00 19.102 119.09 19.688 120.00 19.716

0.00 30.00  
0.00 57.50

3 0.0 30.00 120

17.483 99999 0.027 0.060 208.074  
 17.692 99999 0.027 0.060 268.822  
 17.695 99999 0.027 0.060 264.379  
 17.834 99999 0.027 0.060 256.307  
 18.004 99999 0.027 0.060 314.13  
 18.008 99999 0.027 0.060 287.261

1 0.00 120.00  
 0.16

'TRT3'

RIVER TRENT AT NORTH MUSKHAM ameth ver actual data running averages

1000 15 2 26 1 of 3 conveyance at flood bank

'BGTSTO' 'NO' 'NO' 'NO' 'NO'

'NO' 'YES' 'NO' 'NO' 'YES'

3.2E-4 1.357 1

'LEFT' 'LEFT' 'RIGHT'

58 2.0 380.1 10.11 7.6 2.109

1.0 10.11

2.0 10.11 6.0 9.90 10.0 7.30 15.0 4.10 20.0 2.28  
 30.0 2.25 35.0 2.15 40.0 2.15 45.0 2.05 50.0 2.01  
 60.0 1.90 65.0 7.62  
 73.0 7.55 83.0 7.36 87.0 7.36 90.0 7.70 93.0 7.92  
 96.0 8.35 102.0 8.04 103.0 8.31 104.0 8.31 112.0 8.38  
 122.0 8.13 125.0 7.55 130.0 7.63 134.0 7.45 138.0 8.04  
 143.0 8.22 152.0 8.2 162.0 8.22 173.0 8.03 182.0 7.95  
 192.0 7.90 197.0 7.92 200.0 7.91 203.0 7.88 223.0 7.75  
 232.0 7.71 242.0 7.70 253.0 7.75 263.0 7.70 274.0 7.71  
 283.0 7.82 286.0 7.65 289.0 7.75 297.0 7.90 303.0 7.71  
 313.0 7.90 323.0 7.90 332.0 8.03 342.0 8.11 346.0 8.19  
 362.0 7.39 369.0 7.30 370.0 7.40 380.0 9.55 380.1 10.11

2.0 65.0  
 2.0 112.0

3 2.0 65.00 380.1

7.660667 9999 0.032 0.032 395.098  
 7.7 9999 0.032 0.032 399.3577  
 7.733333 9999 0.032 0.032 402.158  
 7.77 9999 0.032 0.032 404.378  
 7.786667 9999 0.032 0.032 401.679

7.803333 9999 0.032 0.032 402.9807  
 7.81 9999 0.032 0.032 407.4273  
 7.816667 9999 0.032 0.032 409.478  
 7.82 9999 0.032 0.032 404.91  
 7.82 9999 0.032 0.032 387.616

7.826667 9999 0.032 0.032 395.995  
 7.836667 9999 0.032 0.032 407.4637  
 7.853333 9999 0.032 0.032 434.091  
 7.866667 9999 0.032 0.032 433.922  
 7.880667 9999 0.032 0.032 435.9037

7.894	9999	0.032	0.032	429.9037
7.917333	9999	0.032	0.032	432.858
7.943333	9999	0.032	0.032	438.831
8.03	9999	0.032	0.032	459.7753
8.120333	9999	0.032	0.032	481.516
8.250333	9999	0.032	0.032	498.1583
8.327667	9999	0.032	0.032	523.0607
8.390667	9999	0.032	0.032	490.3747
8.417333	9999	0.032	0.032	518.2343
8.446667	9999	0.032	0.032	529.91
8.476333	9999	0.032	0.032	594.5023

1 380.1  
0.16

# DATA FILES FOR MYERS LABORATORY DATA

'MASD'

Myers DATA ackermethod VERSION symetric smooth series A

1000 20 2 12 1

'BGTSTO' 'NO' 'NO' 'NO' 'NO'

'NO' 'NO' 'NO' 'NO' 'NO'

1.906E-3 0.783974 2

'LEFT' 'LEFT' 'RIGHT'

8 0.00 1.630 0.130 0.049 0.002 0.6013

0.000 0.130 0.118 0.065 0.478 0.051 0.543 0.000

1.093 0.000 1.153 0.047 1.513 0.059 1.630 0.130

0.478 1.153

0.00 1.630

3 0.478 1.153 1.630

0.05265 0.010 0.010 0.010 19.37E-3

0.05310 0.010 0.010 0.010 18.98E-3

0.05332 0.010 0.010 0.010 18.79E-3

0.05759 0.010 0.010 0.010 20.66E-3

0.06138 0.010 0.010 0.010 22.75E-3

0.06595 0.010 0.010 0.010 28.03E-3

0.06832 0.010 0.010 0.010 28.20E-3

0.07233 0.010 0.010 0.010 32.05E-3

0.07641 0.010 0.010 0.010 34.10E-3

0.08395 0.010 0.010 0.010 44.31E-3

0.09131 0.010 0.010 0.010 57.13E-3

0.09793 0.010 0.010 0.010 74.46E-3

1 1.630

0.16

'MFSD'

Myers DATA LATERAL VERSION assymetric smooth series F

1000 20 2 8 1

'BGTSTO' 'NO' 'NO' 'NO' 'YES'

'NO' 'YES' 'YES' 'NO' 'YES'

1.906E-3 1.27572 1

'LEFT' 'LEFT' 'RIGHT'

6 0.00 1.259 0.130 0.047 0.001 0.5624

0.000 0.130 0.118 0.065 0.478 0.051 0.543 0.000

1.093 0.000 1.259 0.130

0.478 1.258

0.00 1.259

3 0.478 1.153 1.259

0.05998 0.010 0.010 0.010 23.30E-3

0.06258 0.010 0.010 0.010 26.80E-3

0.06797 0.010 0.010 0.010 27.70E-3

0.06816 0.010 0.010 0.010 29.01E-3

0.07074 0.010 0.010 0.010 32.99E-3

0.08177 0.010 0.010 0.010 45.81E-3

0.09115 0.010 0.010 0.010 54.52E-3

0.10100 0.010 0.010 0.010 66.90E-3

1 1.259

0.16

**DATA FILES FROM MARTIN LAMERT'S FLUME UNIVERSITY OF NEWCASTLE NSW**

All tests were conducted with rectangular main channel and flood plains

**Example file format**

1 Martin Lambert University of Newcastle NSW Australia  
2  
3 Test no - 01  
4 **First ten lines are info on test**  
5 Conditions  
6  
7 Mild Slope (9.4544e-4) - Centre strip smooth Outer Strips Rough  
8  
9 Depth Discharge Temperature  
10 (m) (m3/s) (C)

01 1 01 - series number of test, 1 - number of data points

0.05 0.012409 23

**0.05 depth in metres**  
**0.012409 discharge in ncubic metres**  
**23 water temperature in centigrade**

0.767 0.400 0.767 0.015 1.00

**0.767 width of left hand floodplain**  
**0.400 width of main channel**  
**0.767 width of right hand floodplain**  
**0.015 bank full depth (metres)**  
**1.00 maximum allowable depth**

9.4544e-4 - longitudinal bed slope

1 3 main channel and floodplain roughness pointers

Darcy f given by :

- 1  $1/f^{1/2} = 2.027 \log_{10} (Re f^{1/2}) - 1.898$
- 2  $1/f^{1/2} = 2.027 \log_{10} (Re f^{1/2}) - 1.567$
- 3  $1/f^{1/2} = -2.0 \log_{10} (0.01843 / 12.3 R) (k_s = 0.01843m)$
- 4  $1/f^{1/2} = -2.0 \log_{10} (0.01309 / 12.3 R) (k_s = 0.01309m)$

Re - Reynolds number

R - Hydraulic radius

1 Martin Lambert University of Newcastle NSW Australia  
 2  
 3 Test no - 01  
 4  
 5 Conditions  
 6  
 7 Mild Slope (9.4544e-4) - Centre strip smooth Outer Strips Rough  
 8  
 9 Depth Discharge Temperature  
 10 (m) (m3/s) (C)  
 01 14  
 0.05 0.012409 23  
 0.06 0.018112 24  
 0.07 0.025801 25  
 0.08 0.034240 23  
 0.09 0.043102 24  
 0.10 0.054599 25  
 0.11 0.063184 24  
 0.12 0.072272 26  
 0.13 0.081362 25  
 0.14 0.094517 25  
 0.15 0.098565 26  
 0.16 0.117330 27  
 0.17 0.128148 25  
 0.18 0.147743 23  
  
 0.767 0.400 0.767 0.015 1.00  
 9.4544e-4  
 1 3

1 Martin Lambert University of Newcastle NSW Australia  
 2  
 3 Test no - 02  
 4  
 5 Conditions  
 6  
 7 Steep Slope (0.012053) - Centre Strip smooth Outer Strips rough  
 8  
 9 Depth Discharge Temperature  
 10 (m) (m3/s) (C)  
 02 11  
 0.040 0.028729 23  
 0.045 0.037122 23  
 0.050 0.045733 23  
 0.050 0.045679 23  
 0.055 0.056675 23  
 0.060 0.068826 23  
 0.065 0.080001 24  
 0.070 0.094009 28  
 0.075 0.110203 24  
 0.080 0.126178 27  
 0.085 0.141083 29  
  
 0.767 0.400 0.767 0.015 1.00  
 0.012053  
 2 4

1 Martin Lambert University of Newcastle NSW Australia

2

3 Test no - 03

4

5 Conditions

6

7 Mild Slope (9.9276e-4) Smooth Channel Smooth Berm

8

9 Depth Discharge Temperature

10 (m) (m<sup>3</sup>/s) (C)

03 21

0.0877 0.013394 24

0.0877 0.014233 24

0.0927 0.015342 25

0.0977 0.018129 25

0.1027 0.021449 26

0.1077 0.027056 24

0.1127 0.031899 25

0.1177 0.038059 26

0.1227 0.043985 26

0.1277 0.049567 26

0.1327 0.057098 28

0.1377 0.065078 30

0.1427 0.071289 27

0.1477 0.079630 28

0.1527 0.085607 30

0.1577 0.092044 31

0.1627 0.110260 26

0.1677 0.118270 28

0.1727 0.124260 28

0.1777 0.134160 26

0.1827 0.148620 26

0.767 0.400 0.767 0.0827 1.00

9.9276e-4

1 1

1 Martin Lambert University of Newcastle NSW Australia

2

3 Test no - 04

4

5 Conditions

6

7 Steep Slope (0.012058) Smooth Channel Smooth Berms

8

9 Depth Discharge Temperature

10 (m) (m<sup>3</sup>/s) (C)

04 7

0.0877 0.047023 24

0.0927 0.056914 24

0.0977 0.071226 25

0.1027 0.085640 25

0.1077 0.101700 26

0.1127 0.120600 27

0.1177 0.139100 27

0.767 0.400 0.767 0.0827 1.00

0.012058

2 2

1 Martin Lambert University of Newcastle NSW Australia

2

3 Test no - 05

4

5 Conditions

6

7 Mild Slope (9.9276e-4) Smooth Channel Rough Berms

8

9 Depth Discharge Temperature

10 (m) (m3/s) (C)

05 22

0.1077 0.018541 24

0.1127 0.019383 24

0.1177 0.020562 25

0.1227 0.022590 25

0.1277 0.024194 25

0.1327 0.027387 26

0.1377 0.030564 24

0.1427 0.033137 25

0.1477 0.037572 25

0.1527 0.041147 26

0.1577 0.045585 25

0.1627 0.048402 27

0.1677 0.053738 23

0.1727 0.057950 26

0.1777 0.062468 26

0.1827 0.067052 28

0.1927 0.074715 26

0.2027 0.085199 26

0.2127 0.098842 26

0.2227 0.110990 28

0.2327 0.119210 28

0.2427 0.137510 30

0.767 0.400 0.767 0.0977 1.000

9.9276e-4

1 3

1 Martin Lambert University of Newcastle NSW Australia

2

3 Test no - 06

4

5 Conditions

6

7 Steep Slope (0.012058) Smooth Channel Rough Berms

8

9 Depth Discharge Temperature

10 (m) (m3/s) (C)

06 10

0.1062 0.047588 26

0.1112 0.052426 27

0.1162 0.060620 27

0.1212 0.068554 28

0.1262 0.076271 29

0.1312 0.087271 28

0.1362 0.096899 31

0.1412 0.113110 25

0.1462 0.125900 26

0.1512 0.139800 28

0.767 0.400 0.767 0.0977 1.00

0.012058

2 4

**APPENDIX 5**  
**DATA FROM LABORATORY STUDIES INTO MEANDERING FLOW**

The stage discharge data available from the various laboratory studies are listed below. The data includes:

SERC FCF B20, B21, B25, B26, B31, B32, B33, B34, B38, B39, B43, B46, B47, B48, B49, B50.

Aberdeen AB100, AB100A, AB101, AB102, AB103, AB104, AB105.

Vicksburg VB201, VB202, VB203, VB204, VB205, VB206, VB207, VB208, VB209, VB210, VB211.

Kiely KI301.

Sooky SK401, SK402, SK403, SK404, SK405, SK406, SK407, SK408, SK409, SK410, SK411.

**The file format is as follows:**

The first ten lines at the top of each file are comment lines. Information about the data is listed here.

The first two numbers after this are:

- 1 The test series number
- 2 The number of data points

The stage discharge data for each discharge point follows. An Example data line is shown below.

Date	discharge	depth1	depth2	slope	tailgate	temp
29 11 89	0.01975	59.34	59.32	0.996	667.84	11.4

Date is given as three integers: day, month and year.

Discharge is given in cubic metres per second.

Depth1 is the depth in millimetres as recorded in the original data files.

Depth2 is the depth in millimetres as corrected to the channel bed slope. This value of depth should be used in any analysis. It is worth noting that only the SERC FCF data was adjusted in this way. Depth1 and Depth2 for the other data sets are identical.

Slope is the longitudinal valley slope of the flume. These values should be multiplied by 1/1000.

Tailgate is the tailgate setting for the SERC FCF. This data was retained in the files but should not be used.

Temp is the temperature in degrees centigrade of the water in the flume as recorded by the investigators. Where the temperature was not recorded a default value of 15 °C has been assumed.

## SERC DATA

1 SERC FCF Stage Discharge Data Phase B Meandering case

2

3 File name (ASSIGNED FOR MEANDR) : SDB20

4 Plan geometry (angle of cross over) : 60

5 Main Channel X-sn : Trapezoidal

6 Floodplain width : Standard

7 Floodplain roughness : Smooth

8

9	DATE	DISCHARGE	DEPTH AS	DEPTH AS	SLOPE	TAILGATE	TEMP
10		m3 sec.	RECORDED mm	PLOTTED mm		c.	

20 17

29	11	89	0.01975	59.34	59.32	0.996	667.84	11.4
27	11	89	0.02512	67.16	67.26	0.996	663.84	11.0
17	11	89	0.02654	71.89	71.98	0.996	661.81	12.4
27	11	89	0.03056	77.56	77.14	0.996	658.72	10.8
17	11	89	0.03308	82.43	82.63	0.996	656.68	12.4
29	11	89	0.03630	86.06	86.08	0.996	653.81	11.6
30	11	89	0.04015	91.56	91.70	0.996	650.83	11.5
01	12	89	0.04425	97.79	97.65	0.996	648.15	11.6
07	12	89	0.04708	101.92	101.92	1.001	646.00	12.7
30	11	89	0.04782	102.99	103.02	0.996	644.92	11.5
29	11	89	0.05015	105.29	105.93	0.996	643.39	11.7
27	11	89	0.04974	105.68	105.96	0.996	643.49	10.9
20	11	89	0.04953	106.92	106.80	0.996	643.22	12.4
16	11	89	0.05467	111.57	111.50	0.996	641.12	13.7
16	11	89	0.05702	113.94	113.94	0.9969	640.00	12.7
15	11	89	0.06035	118.84	119.00	0.996	636.81	13.6
16	11	89	0.07073	131.24	131.50	0.996	629.67	12.9

1 SERC FCF Stage Discharge Data Phase B Meandering case

2

3 File name (ASSIGNED FOR MEANDR) : SDB21

4 Plan geometry (angle of cross over) : 60

5 Main Channel X-sn : Trapezoidal

6 Floodplain width : Standard

7 Floodplain roughness : Smooth

8

9	DATE	DISCHARGE	DEPTH AS	DEPTH AS	SLOPE	TAILGATE	TEMP
10		m3/sec.	RECORDED mm	PLOTTED mm		C	

21 16

28	11	89	0.08240	163.93	164.13	0.9960	562.37	11.5
28	11	89	0.08576	165.56	165.84	0.9960	561.56	11.5
28	11	89	0.09753	169.85	170.11	0.9660	560.13	11.4
24	11	89	0.10960	172.73	173.05	0.9660	559.72	11.6
24	11	89	0.11980	175.48	175.70	0.9660	559.42	11.6

02	11	89	0.14940	181.49	181.66	0.9660	559.00	14.6
01	11	89	0.20390	191.98	191.98	0.9986	557.00	14.0
06	11	89	0.24960	199.61	199.73	0.9960	556.00	12.8
23	11	89	0.30228	207.65	207.95	0.9960	556.90	12.2
01	11	89	0.30300	208.46	208.46	0.9903	555.00	14.5

16	11	89	0.44020	227.59	227.63	0.9960	552.00	13.2
16	11	89	0.48501	232.90	232.90	1.0069	551.41	14.4
28	11	89	0.49360	235.02	235.00	0.9960	551.74	11.0
10	02	90	0.76670	264.84	264.84	0.9978	546.00	12.3
10	02	90	0.87861	277.48	277.95	0.9960	543.40	12.3

10	02	90	0.98939	289.11	288.73	0.9960	541.40	12.3
----	----	----	---------	--------	--------	--------	--------	------

1 SERC FCF Stage Discharge Data Phase B Meandering case

2

3 File name (ASSIGNED FOR MEANDR) : SDB25

4 Plan geometry (angle of cross over) : 60

5 Main Channel X-sn : Natural inbank

6 Floodplain width : Standard

7 Floodplain roughness : Smooth

8

9	DATE	DISCHARGE	DEPTH AS	DEPTH AS	SLOPE	TAILGATE	TEMP
10		m3 sec.	RECORDED mm	PLOTTED mm		c.	

25 10

17	7	90	0.01019	99.57	99.57	0.9960	610.00	16.1
17	7	90	0.01207	103.59	103.59	0.9954	610.03	16.1
16	7	90	0.01442	108.40	108.60	0.9660	606.67	16.1
16	7	90	0.01612	112.36	112.25	0.9960	605.31	16.0
16	7	90	0.01806	116.50	116.48	0.9960	603.21	16.1
16	7	90	0.02150	123.20	123.16	0.9960	600.20	16.0
19	7	90	0.02288	125.73	125.66	0.9960	599.10	16.0
17	7	90	0.02498	129.09	129.23	0.9960	597.59	16.2
18	7	90	0.02646	131.04	131.65	0.9960	596.53	16.0
06	8	90	0.03341	142.34	132.34	0.9977	592.00	17.1

1 SERC FCF Stage Discharge Data Phase B Meandering case

2

3 File name (ASSIGNED FOR MEANDR) : SDB26

4 Plan geometry (angle of cross over) : 60

5 Main Channel X-sn : Natural Over bank

6 Floodplain width : Standard

7 Floodplain roughness : Smooth

8

9	DATE	DISCHARGE	DEPTH AS	DEPTH AS	SLOPE	TAILGATE	TEMP
10		m3 /sec.	RECORDED mm	PLOTTED mm		c.	

26 16

12	07	90	0.03993	152.75	152.64	0.9960	562.06	16.2
06	08	90	0.04965	162.89	162.89	0.9942	557.00	17.1
10	10	90	0.05791	165.23	165.23	1.0030	557.00	13.5
13	07	90	0.06051	166.93	167.11	0.9960	555.53	15.9
10	07	90	0.10310	177.91	177.89	0.9960	555.10	14.7
12	07	90	0.16018	189.58	189.58	0.9962	555.00	15.9
10	07	90	0.20447	196.64	196.53	0.9960	554.87	14.4
13	07	90	0.26744	206.84	206.84	0.9980	553.88	16.0
10	07	90	0.30725	212.06	212.26	0.9960	553.56	14.7
12	07	90	0.38733	222.92	223.35	0.9960	552.31	15.5
11	07	90	0.53963	241.21	241.38	0.9960	549.70	14.9
11	07	90	0.64651	253.42	253.94	0.9960	547.39	15.5
11	07	90	0.75203	264.59	264.96	0.9960	545.60	15.6
11	07	90	0.85873	274.82	275.23	0.9960	544.47	15.7
27	10	90	0.97758	287.76	287.69	0.9960	542.59	13.9
27	10	90	1.09296	296.46	296.46	1.0167	541.33	14.2

1 SERC FCF Stage Discharge Data Phase B Meandering case

2

3 File name (ASSIGNED FOR MEANDR) : SDB31

4 Plan geometry (angle of cross over) : 60

5 Main Channel X-sn : Natural

6 Floodplain width : Narrow

7 Floodplain roughness : Smooth

8

9	DATE	DISCHARGE	DEPTH AS	DEPTH AS	SLOPE	TAILGATE	TEMP
10		m3/sec.	RECORDED mm	PLOTTED mm		c.	

31 14

22	9	90	0.03871	159.80	159.83	0.9960	562.57	14.0
22	9	90	0.05079	168.51	168.51	0.9973	559.88	13.9
19	9	90	0.05766	170.21	170.15	0.9960	559.68	14.4
21	9	90	0.06616	173.64	173.64	0.9948	560.0	14.4
18	9	90	0.08538	180.03	180.05	0.9960	559.13	14.0
18	9	90	0.11231	188.91	188.75	0.9960	558.81	14.1
21	9	90	0.16120	202.76	202.76	0.9951	559.07	14.4
21	9	90	0.19296	209.76	209.94	0.9960	558.21	14.4
18	9	90	0.22834	218.89	219.18	0.9960	556.68	14.3
19	9	90	0.28208	230.53	230.85	0.9960	554.39	14.7
21	9	90	0.29029	232.86	232.86	0.9968	555.00	15.4
20	9	90	0.38009	251.55	251.58	0.9960	552.93	15.6
20	9	90	0.47314	264.45	264.68	0.9960	550.69	15.3
20	9	90	0.57135	282.52	282.78	0.9960	547.47	15.0

1 SERC FCF Stage Discharge Data Phase B Meandering case

2

3 File name (ASSIGNED FOR MEANDR) : SDB32

4 Plan geometry (angle of cross over) : 60

5 Main Channel X-sn : Natural

6 Floodplain width : Standard

7 Floodplain roughness : Breeze blocks simulating piers

8

9	DATE	DISCHARGE	DEPTH AS	DEPTH AS	SLOPE	TAILGATE	TEMP
10		m3/sec.	RECORDED mm	PLOTTED mm		c.	

32 13

10	01	91	0.04333	159.91	158.85	0.9960	558.62	12.3
10	01	91	0.05430	165.26	165.37	0.9960	556.60	12.2
10	01	91	0.09961	178.41	178.54	0.9960	554.55	13.4
10	01	91	0.13331	185.85	186.00	0.9960	553.62	13.3
11	01	91	0.19814	198.68	198.50	0.9960	533.37	13.4
10	01	91	0.26714	210.92	210.92	0.9973	550.00	13.3
11	01	91	0.33568	221.92	221.87	0.9960	547.56	13.0
11	01	91	0.39576	231.31	231.88	0.9960	545.49	13.4
26	10	90	0.45946	238.23	238.23	0.9959	543.00	15.2
26	10	90	0.57207	254.93	254.77	0.9960	539.20	15.0
26	10	90	0.68564	269.36	269.52	0.9960	535.29	14.5
26	10	90	0.80040	284.61	284.43	0.9960	531.22	14.2
26	10	90	0.91832	297.51	298.55	0.9960	527.53	13.9

1 SERC FCF Stage Discharge Data Phase B Meandering case

2

3 File name (ASSIGNED FOR MEANDR) : SDB33

4 Plan geometry (angle of cross over) : 60

5 Main Channel X-sn : Natural

6 Floodplain width : Standard

7 Floodplain roughness : Partially roughened dowel rods

8

9	DATE	DISCHARGE	DEPTH AS	DEPTH AS	SLOPE	TAILGATE	TEMP
10		m3/sec.	RECORDED mm	PLOTTED mm		c.	

33 12

05	11	90	0.04161	158.77	158.68	0.9960	558.15	12.2
05	11	90	0.06651	169.86	169.83	0.9960	553.06	12.2
01	11	90	0.08653	176.51	176.51	1.0012	551.72	12.8
01	11	90	0.11244	183.67	183.60	0.9960	550.17	13.0
01	11	90	0.16988	196.35	196.83	0.9960	546.61	13.0
05	11	90	0.22181	207.55	207.80	0.9660	543.63	12.1
05	11	90	0.27174	218.23	218.23	0.9966	540.00	11.8
05	11	90	0.32182	228.39	228.50	0.9960	535.81	11.6
31	10	90	0.49790	258.89	257.87	0.9960	524.22	13.4
31	10	90	0.56938	271.79	271.95	0.9960	517.76	13.0
31	10	90	0.67561	289.11	289.22	0.9960	509.89	13.3
31	10	90	0.76534	305.01	305.01	0.9975	503.00	13.3

1 SERC FCF Stage Discharge Data Phase B Meandering case

2

3 File name (ASSIGNED FOR MEANDR) : SDB34

4 Plan geometry (angle of cross over) : 60

5 Main Channel X-sn : Natural

6 Floodplain width : Standard

7 Floodplain roughness : Roughened with Dowel Rods

8

9	DATE	DISCHARGE	DEPTH AS	DEPTH AS	SLOPE	TAILGATE	TEMP
10		m3/sec.	RECORDED mm	PLOTTED mm		c.	

34 18

16	11	90	0.04015	158.61	158.58	0.9960	557.03	15.0
16	11	90	0.05445	167.64	167.64	0.9957	552.01	14.5
16	11	90	0.06742	174.00	174.32	0.9960	549.24	14.4
15	11	90	0.09209	184.90	184.80	0.9960	544.63	15.0
15	11	90	0.11197	192.13	192.50	0.9960	541.24	14.7
15	11	90	0.13203	200.79	201.01	0.9960	537.18	15.0
15	11	90	0.15440	209.36	209.60	0.9960	532.63	14.8
14	11	90	0.17485	217.21	217.17	0.9960	529.05	15.4
12	11	90	0.19857	224.48	224.45	0.9960	525.09	13.8
12	11	90	0.23395	238.71	238.65	0.9960	517.06	14.2
14	11	90	0.26401	250.38	250.83	0.9960	510.00	15.0
12	11	90	0.27588	255.26	254.83	0.9960	507.97	14.8
14	11	90	0.30182	265.00	265.35	0.9960	501.62	15.0
12	11	90	0.32655	272.95	273.40	0.9960	497.12	14.6
13	11	90	0.34158	278.44	279.08	0.9960	493.31	14.8
14	11	90	0.37602	292.09	292.25	0.9960	485.36	14.6
13	11	90	0.41000	301.68	301.96	0.9960	479.64	15.4
13	11	90	0.45527	317.31	317.55	0.9960	469.64	15.0

1 SERC FCF Stage Discharge Data Phase B Meandering case

2

3 File name (ASSIGNED FOR MEANDR) : SDB38

4 Plan geometry (angle of cross over) : 110

5 Main Channel X-sn : Natural Inbank

6 Floodplain width : Standard

7 Floodplain roughness : Smooth

8

9	DATE	DISCHARGE	DEPTH AS	DEPTH AS	SLOPE	TAILGATE	TEMP
10		m3/sec.	RECORDED mm	PLOTTED mm		c.	

38 11

23	4	91	0.01135	109.80	110.06	1.0210	604.17	10.4
31	7	91	0.01322	115.16	115.16	1.0144	601.00	15.0
24	4	91	0.01533	120.30	120.30	1.0218	598.95	10.5
31	7	91	0.01560	120.73	120.73	1.0217	597.92	14.4
01	8	91	0.01699	124.20	124.20	1.0161	596.00	14.1 *
23	4	91	0.01873	127.91	127.91	1.0205	595.00	10.3
30	7	91	0.02006	130.72	130.72	1.0161	594.22	15.9 *
01	8	91	0.02206	135.66	135.66	1.0262	590.50	14.9 *
23	4	91	0.02342	138.82	138.54	1.0210	588.59	10.3
24	4	91	0.02432	140.08	140.27	1.0210	587.69	10.5
23	4	91	0.02778	146.72	146.72	1.0210	584.46	10.4

\* DEPTHS SET FOR DR I GUYMER FOR DISPERSION TESTS

1 SERC FCF Stage Discharge Data Phase B Meandering case

2

3 File name (ASSIGNED FOR MEANDR) : SDB39

4 Plan geometry (angle of cross over) : 110

5 Main Channel X-sn : Natural

6 Floodplain width : Standard

7 Floodplain roughness : Smooth

8

9	DATE	DISCHARGE	DEPTH AS	DEPTH AS	SLOPE	TAILGATE	TEMP
10		m3/sec.	RECORDED mm	PLOTTED mm			c.

39 14

05	7	91	0.03815	165.14	165.14	1.0177	557.00	15.5
22	4	91	0.07693	178.92	178.92	1.0210	553.50	10.3
22	4	91	0.09972	183.58	183.76	1.0210	553.35	10.3
23	5	91	0.14208	193.65	193.43	1.0210	552.56	12.7
08	5	91	0.17925	200.61	200.61	1.0221	552.00	11.4
23	5	91	0.25282	214.07	214.75	1.0210	549.63	12.9
03	7	91	0.32467	225.21	225.20	1.0210	548.26	14.5
03	7	91	0.39138	235.01	235.13	1.0210	546.61	15.4
03	7	91	0.44517	242.66	242.77	1.0210	545.20	15.3
07	5	91	0.55351	256.86	256.86	1.0201	541.07	11.2
07	5	91	0.66137	270.05	270.33	1.0210	538.6	11.6
07	5	91	0.77988	284.50	284.48	1.0210	535.60	12.0
24	5	91	0.88127	296.88	296.71	1.0210	532.73	13.2
24	5	91	0.94356	302.82	302.88	1.0210	532.43	14.5

1 SERC FCF Stage Discharge Data Phase B Meandering case

2

3 File name (ASSIGNED FOR MEANDR) : SDB43

4 Plan geometry (angle of cross over) : 110

5 Main Channel X-sn : Natural

6 Floodplain width : Standard

7 Floodplain roughness : Roughened with dowel rods

8

9	DATE	DISCHARGE	DEPTH AS	DEPTH AS	SLOPE	TAILGATE	TEMP
10		m3/sec.	RECORDED mm	PLOTTED mm			c.

43 15

02	9	91	0.03252	160.54	160.47	1.0210	558.13	16.6
23	8	91	0.03688	165.98	165.98	1.0124	556.00	16.7
16	8	91	0.05451	175.02	175.06	1.0210	550.42	16.3
16	8	91	0.08361	187.39	187.60	1.0210	544.68	16.3
15	8	91	0.10803	197.19	197.08	1.0210	540.27	16.1
29	8	91	0.11685	200.85	200.85	1.0205	539.00	16.7
21	8	91	0.14392	211.73	211.75	1.0210	533.30	16.9
21	8	91	0.17375	221.75	221.93	1.0210	527.26	16.7
19	8	91	0.20112	231.55	231.93	1.0210	523.13	16.3
21	8	91	0.24342	247.40	247.35	1.0210	514.40	16.4
19	8	91	0.27848	259.26	259.27	1.0210	507.51	16.5
19	8	91	0.31616	272.21	271.89	1.0210	500.31	16.3
20	8	91	0.34940	283.40	283.42	1.0210	493.42	16.5
20	8	91	0.38851	296.31	296.60	1.0210	486.25	17.0
20	8	91	0.43331	311.19	310.53	1.0210	477.62	16.4

1 SERC FCF Stage Discharge Data Phase B Meandering case  
 2  
 3 File name (ASSIGNED FOR MEANDR) : SDB46  
 4 Plan geometry (angle of cross over) : 110  
 5 Main Channel X-sn : Natural  
 6 Floodplain width : Standard  
 7 Floodplain roughness : Roughened with breeze blocks

8  
 9 DATE DISCHARGE DEPTH AS DEPTH AS SLOPE TAILGATE TEMP  
 10 m3/sec. RECORDED mm PLOTTED mm c.

46 14

DATE	DISCHARGE m3/sec.	DEPTH AS RECORDED mm	DEPTH AS PLOTTED mm	SLOPE	TAILGATE	TEMP c.
17 9 91	0.03525	162.88	162.83	1.0210	559.07	15.7
17 9 91	0.05185	171.30	171.30	1.0224	555.00	15.7 *
16 9 91	0.10064	184.99	185.18	1.0210	552.82	15.7
19 9 91	0.12617	190.98	190.89	1.0209	552.00	15.4 *
19 9 91	0.15775	197.96	197.96	1.0203	555.00	15.3 *
17 9 91	0.16817	200.65	200.64	1.0210	549.54	15.8
19 9 91	0.21985	210.96	210.77	1.0210	547.34	15.4
19 9 91	0.25247	216.84	217.15	1.0210	545.67	15.7
17 9 91	0.31685	229.81	229.45	1.0210	542.83	16.0
20 9 91	0.36295	237.38	237.55	1.0210	539.78	14.7
20 9 91	0.46613	254.90	254.95	1.0210	533.93	15.0
18 9 91	0.53525	263.78	263.60	1.0210	531.27	15.8
18 9 91	0.64489	280.09	280.15	1.0210	526.63	16.6
18 9 91	0.75729	296.26	296.35	1.0210	520.87	16.3

1 SERC FCF Stage Discharge Data Phase B Meandering case  
 2  
 3 File name (ASSIGNED FOR MEANDR) : SDB47  
 4 Plan geometry (angle of cross over) : 110  
 5 Main Channel X-sn : Natural  
 6 Floodplain width : Narrow  
 7 Floodplain roughness : Smooth

8  
 9 DATE DISCHARGE DEPTH AS DEPTH AS SLOPE TAILGATE TEMP  
 10 m3/sec. RECORDED mm PLOTTED mm c.

47 14

DATE	DISCHARGE m3/sec.	DEPTH AS RECORDED mm	DEPTH AS PLOTTED mm	SLOPE	TAILGATE	TEMP c.
03 10 91	0.03559	164.84	164.94	1.0210	556.44	13.9
01 10 91	0.05023	171.12	171.12	1.0206	555.02	14.3
30 09 91	0.07456	179.60	179.50	1.0210	553.62	14.2
30 09 91	0.09496	185.23	185.30	1.0210	553.60	13.8
07 10 91	0.13586	195.66	195.63	1.0210	551.44	13.2
30 09 91	0.16491	202.48	202.65	1.0210	549.50	14.0
01 10 91	0.22050	213.55	213.54	1.0210	547.00	13.6
03 10 91	0.25933	221.65	221.65	1.0210	544.78	14.7
01 10 91	0.32792	234.20	234.12	1.0210	540.65	14.1
03 10 91	0.38649	244.55	244.52	1.0210	538.20	14.0
07 10 91	0.48556	259.96	259.63	1.0210	534.10	13.3
04 10 91	0.53429	264.95	264.93	1.0210	532.85	14.5
08 10 91	0.69847	288.42	288.46	1.0210	526.23	14.3
08 10 91	0.75055	294.75	294.60	1.0210	524.70	13.4

1 SERC FCF Stage Discharge Data Phase B Meandering case

2

3 File name (ASSIGNED FOR MEANDR) : SDB48

4 Plan geometry (angle of cross over) : 110

5 Main Channel X-sn : Natural

6 Floodplain width : Standard

7 Floodplain roughness : Smooth with walls

8

9	DATE	DISCHARGE	DEPTH AS	DEPTH AS	SLOPE	TAILGATE	TEMP
10		m3/sec.	RECORDED mm	PLOTTED mm		c.	

48 8

15	10 91	0.03353	170.30	169.85	1.0210	560.46	13.5
14	10 91	0.03499	174.95	175.05	1.0210	555.90	14.0
14	10 91	0.04065	189.95	189.95	1.0210	544.80	14.0
11	10 91	0.04540	202.60	202.60	1.0210	534.12	13.9
14	10 91	0.04945	212.68	212.68	1.0210	525.50	13.7
15	10 91	0.05538	232.44	232.44	1.0223	510.00	13.4
11	10 91	0.05659	233.15	233.25	1.0210	509.45	13.6
15	10 91	0.06312	242.35	242.05	1.0210	502.40	13.2

1 SERC FCF Stage Discharge Data Phase B Meandering case

2

3 File name : SDB49

4

5 Main Channel X-sn : trapezoidal

6

7 Floodplain roughness : rod roughness Phase A orientation

8

9	DATE	DISCHARGE	DEPTH AS	DEPTH AS	SLOPE	TAILGATE	TEMP
10		m3/sec.	RECORDED mm	PLOTTED mm		c.	

49 7

03	01 92	0.02252	29.586	29.64	1.0224	540.0	11.1
03	01 92	0.04432	50.644	50.57	1.0130	527.0	10.9
02	01 92	0.06183	65.082	65.08	1.0210	518.0	10.5
05	01 92	0.07971	84.130	83.78	1.0152	505.0	11.6
02	01 92	0.10305	110.895	109.25	0.9897	485.0	10.8
05	01 92	0.13002	134.722	135.52	1.0284	470.0	12.1
03	01 92	0.16352	162.180	163.43	1.0363	453.0	11.4

1 SERC FCF Stage Discharge Data Phase B Meandering case

2

3 File name : SDB50

4

5 Main Channel X-sn : trapezoidal

6

7 Floodplain roughness : rod roughness Phase B orientation

8

9	DATE	DISCHARGE	DEPTH AS	DEPTH AS	SLOPE	TAILGATE	TEMP
10		m3/sec.	RECORDED mm	PLOTTED mm			c.

50 7

10	01	92	0.02225	28.241	28.24	1.0210	542	12.3
09	01	92	0.04134	45.233	45.42	1.0277	533	13.1
08	01	92	0.06159	62.602	62.00	1.0038	522	12.9
08	01	92	0.07982	84.135	83.40	1.0060	505	13.1
08	01	92	0.10015	101.256	101.98	1.0439	495	13.3
09	01	92	0.13394	132.168	132.11	1.0190	475	13.3
09	01	92	0.16028	153.969	154.10	1.0238	460	13.1

### US ARMY VICKSBURG DATA

1 VICKSBURG DATA SET 2ft WIDE MAIN CHANNEL

2

3 File name (ASSIGNED FOR MEANDR) : SDVB201

4 Plan geometry (SINUOSITY) : 1.571

5 Main Channel X-sn : Trapezoidal

6 Floodplain width : 4.877

7 Floodplain roughness : 0.012

8

9	DATE	DISCHARGE	DEPTH AS	DEPTH AS	SLOPE	TAILGATE	TEMP
10		m3/sec.	RECORDED mm	PLOTTED mm			C

201 3

01	01	01	0.0702	182.88	182.88	1.0000	0.00	15.0
01	01	01	0.1424	213.36	213.36	1.0000	0.00	15.0
01	01	01	0.2231	243.84	243.84	1.0000	0.00	15.0

1 VICKSBURG DATA SET 2ft WIDE MAIN CHANNEL

2

3 File name (ASSIGNED FOR MEANDR) : SDVB202

4 Plan geometry (SINUOSITY) : 1.571

5 Main Channel X-sn : Trapezoidal

6 Floodplain width : 4.877

7 Floodplain roughness : 0.025

8

9	DATE	DISCHARGE	DEPTH AS	DEPTH AS	SLOPE	TAILGATE	TEMP
10		m3/sec.	RECORDED mm	PLOTTED mm			C

202 3

01	01	01	0.0430	182.88	182.88	1.0000	0.00	15.0
01	01	01	0.0875	213.36	213.36	1.0000	0.00	15.0
01	01	01	0.1546	243.84	243.84	1.0000	0.00	15.0

1 VICKSBURG DATA SET 2ft WIDE MAIN CHANNEL

2

3 File name (ASSIGNED FOR MEANDR) : SDVB203

4 Plan geometry (SINUOSITY) : 1.571

5 Main Channel X-sn : Trapezoidal

6 Floodplain width : 4.877

7 Floodplain roughness : 0.035

8

9	DATE	DISCHARGE	DEPTH AS	DEPTH AS	SLOPE	TAILGATE	TEMP
10		m3/sec.	RECORDED mm	PLOTTED mm		C	

203 3

01	01	01	0.0396	182.88	182.88	1.0000	0.00	15.0
----	----	----	--------	--------	--------	--------	------	------

01	01	01	0.0733	213.36	213.36	1.0000	0.00	15.0
----	----	----	--------	--------	--------	--------	------	------

01	01	01	0.1283	243.84	243.84	1.0000	0.00	15.0
----	----	----	--------	--------	--------	--------	------	------

1 VICKSBURG DATA SET 2ft WIDE MAIN CHANNEL

2

3 File name (ASSIGNED FOR MEANDR) : SDVB204

4 Plan geometry (SINUOSITY) : 1.400

5 Main Channel X-sn : Trapezoidal

6 Floodplain width : 4.877

7 Floodplain roughness : 0.012

8

9	DATE	DISCHARGE	DEPTH AS	DEPTH AS	SLOPE	TAILGATE	TEMP
10		m3/sec.	RECORDED mm	PLOTTED mm		C	

204 3

01	01	01	0.0830	182.88	182.88	1.0000	0.00	15.0
----	----	----	--------	--------	--------	--------	------	------

01	01	01	0.1560	213.36	213.36	1.0000	0.00	15.0
----	----	----	--------	--------	--------	--------	------	------

01	01	01	0.2430	243.84	243.84	1.0000	0.00	15.0
----	----	----	--------	--------	--------	--------	------	------

1 VICKSBURG DATA SET 2ft WIDE MAIN CHANNEL

2

3 File name (ASSIGNED FOR MEANDR) : SDVB205

4 Plan geometry (SINUOSITY) : 1.400

5 Main Channel X-sn : Trapezoidal

6 Floodplain width : 4.877

7 Floodplain roughness : 0.025

8

9	DATE	DISCHARGE	DEPTH AS	DEPTH AS	SLOPE	TAILGATE	TEMP
10		m3/sec.	RECORDED mm	PLOTTED mm		C	

205 3

01	01	01	0.0490	182.88	182.88	1.0000	0.00	15.0
----	----	----	--------	--------	--------	--------	------	------

01	01	01	0.0985	213.36	213.36	1.0000	0.00	15.0
----	----	----	--------	--------	--------	--------	------	------

01	01	01	0.1679	243.84	243.84	1.0000	0.00	15.0
----	----	----	--------	--------	--------	--------	------	------

1 VICKSBURG DATA SET 2ft WIDE MAIN CHANNEL

2

3 File name (ASSIGNED FOR MEANDR) : SDVB206

4 Plan geometry (SINUOSITY) : 1.400

5 Main Channel X-sn : Trapezoidal

6 Floodplain width : 4.877

7 Floodplain roughness : 0.035

8

9	DATE	DISCHARGE	DEPTH AS	DEPTH AS	SLOPE	TAILGATE	TEMP
10		m3/sec.	RECORDED mm	PLOTTED mm		C	

206 3

01 01 01	0.0439	182.88	182.88	1.0000	0.00	15.0
----------	--------	--------	--------	--------	------	------

01 01 01	0.0832	213.36	213.36	1.0000	0.00	15.0
----------	--------	--------	--------	--------	------	------

01 01 01	0.1373	243.84	243.84	1.0000	0.00	15.0
----------	--------	--------	--------	--------	------	------

1 VICKSBURG DATA SET 2ft WIDE MAIN CHANNEL

2

3 File name (ASSIGNED FOR MEANDR) : SDVB207

4 Plan geometry (SINUOSITY) : 1.200

5 Main Channel X-sn : Trapezoidal

6 Floodplain width : 4.877

7 Floodplain roughness : 0.012

8

9	DATE	DISCHARGE	DEPTH AS	DEPTH AS	SLOPE	TAILGATE	TEMP
10		m3/sec.	RECORDED mm	PLOTTED mm		C	

207 3

01 01 01	0.0915	182.88	182.88	1.0000	0.00	15.0
----------	--------	--------	--------	--------	------	------

01 01 01	0.1792	213.36	213.36	1.0000	0.00	15.0
----------	--------	--------	--------	--------	------	------

01 01 01	0.2772	243.84	243.84	1.0000	0.00	15.0
----------	--------	--------	--------	--------	------	------

1 VICKSBURG DATA SET 2ft WIDE MAIN CHANNEL

2

3 File name (ASSIGNED FOR MEANDR) : SDVB208

4 Plan geometry (SINUOSITY) : 1.200

5 Main Channel X-sn : Trapezoidal

6 Floodplain width : 4.877

7 Floodplain roughness : 0.025

8

9	DATE	DISCHARGE	DEPTH AS	DEPTH AS	SLOPE	TAILGATE	TEMP
10		m3/sec.	RECORDED mm	PLOTTED mm		C	

208 3

01 01 01	0.0550	182.88	182.88	1.0000	0.00	15.0
----------	--------	--------	--------	--------	------	------

01 01 01	0.1090	213.36	213.36	1.0000	0.00	15.0
----------	--------	--------	--------	--------	------	------

01 01 01	0.1798	243.84	243.84	1.0000	0.00	15.0
----------	--------	--------	--------	--------	------	------

1 VICKSBURG DATA SET 2ft WIDE MAIN CHANNEL

2  
 3 File name (ASSIGNED FOR MEANDR) : SDVB209  
 4 Plan geometry (SINUOSITY) : 1.200  
 5 Main Channel X-sn : Trapezoidal  
 6 Floodplain width : 4.877  
 7 Floodplain roughness : 0.035  
 8

9	DATE	DISCHARGE	DEPTH AS	DEPTH AS	SLOPE	TAILGATE	TEMP
10		m3/sec.	RECORDED mm	PLOTTED mm		C	

209	3						
01	01	01	0.0484	182.88	182.88	1.0000	0.00 15.0
01	01	01	0.0864	213.36	213.36	1.0000	0.00 15.0
01	01	01	0.1437	243.84	243.84	1.0000	0.00 15.0

1 VICKSBURG DATA SET 2ft WIDE MAIN CHANNEL

2  
 3 File name (ASSIGNED FOR MEANDR) : SDVB210  
 4 Plan geometry (SINUOSITY) : 1.200  
 5 Main Channel X-sn : Trapezoidal  
 6 Floodplain width : 9.144  
 7 Floodplain roughness : 0.035  
 8

9	DATE	DISCHARGE	DEPTH AS	DEPTH AS	SLOPE	TAILGATE	TEMP
10		m3/sec.	RECORDED mm	PLOTTED mm		C	

210	3						
01	01	01	0.0674	182.88	182.88	1.0000	0.00 15.0
01	01	01	0.1399	213.36	213.36	1.0000	0.00 15.0
01	01	01	0.2449	243.84	243.84	1.0000	0.00 15.0

1 VICKSBURG DATA SET 2ft WIDE MAIN CHANNEL

2  
 3 File name (ASSIGNED FOR MEANDR) : SDVB211  
 4 Plan geometry (SINUOSITY) : 1.571  
 5 Main Channel X-sn : Trapezoidal  
 6 Floodplain width : 9.144  
 7 Floodplain roughness : 0.035  
 8

9	DATE	DISCHARGE	DEPTH AS	DEPTH AS	SLOPE	TAILGATE	TEMP
10		m3/sec.	RECORDED mm	PLOTTED mm		C	

211	3						
01	01	01	0.0507	182.88	182.88	1.0000	0.00 15.0
01	01	01	0.1178	213.36	213.36	1.0000	0.00 15.0
01	01	01	0.2226	243.84	243.84	1.0000	0.00 15.0

**KIELY'S DATA**

1 KIELY (UNIV COLLEGE CORK) DATA SET  
 2  
 3 File name (ASSIGNED FOR MEANDR) : SDKI301  
 4 Plan geometry (SINUOSITY) : 1.224  
 5 Main Channel X-sn : RECTANGULAR  
 6 Floodplain width : 1.200  
 7 Floodplain roughness : Smooth  
 8  
 9 DATE DISCHARGE DEPTH AS DEPTH AS SLOPE TAILGATE TEMP  
 10 m3/sec. RECORDED mm PLOTTED mm C

301 5

DATE	DISCHARGE m3/sec.	DEPTH AS RECORDED mm	DEPTH AS PLOTTED mm	SLOPE	TAILGATE	TEMP C
01 01 01	2.43E-3	54.7	54.7	1.0000	0.00	15.0
01 01 01	3.10E-3	60.0	60.0	1.0000	0.00	15.0
01 01 01	6.70E-3	69.7	69.7	1.0000	0.00	15.0
01 01 01	11.1E-3	80.0	80.0	1.0000	0.00	15.0
01 01 01	16.3E-3	89.4	89.4	1.0000	0.00	15.0

POINTS BELOW ARE THREE INBANK RESULTS AND THE BANKFULL POINT FROM THE RATING CURVE

01 01 01	0.669E-3	20.0	20.0	1.0000	0.00	15.0
01 01 01	1.303E-3	28.4	28.4	1.0000	0.00	15.0
01 01 01	2.042E-3	40.0	40.0	1.0000	0.00	15.0
01 01 01	2.324E-3	50.0	50.0	1.0000	0.00	15.0

NOTE THESE DATA HAVE BEEN SCALED OFF OF A PLOT

SOOKY'S DATA

1 TOEBES+SOOKY (SOOKY'S THESIS) DATA SET

2

3 File name (ASSIGNED FOR MEANDR) : SDSK401

4 Plan geometry (SINUOSITY) : 1.1 (GIVEN BY SOOKY)

5 Main Channel X-sn : RECT 1.5" DEEP

6 Floodplain width : 3.886' 1.1845m SL = 0.675E-3

7 Floodplain roughness : Smooth

8

9	DATE	DISCHARGE	DEPTH AS	DEPTH AS	SLOPE	TAILGATE	TEMP
10		m3/sec.	RECORDED mm	PLOTTED mm		C	

401 5

01	01	01	6.309E-3	63.6	63.6	0.675	0.00	15.0
----	----	----	----------	------	------	-------	------	------

01	01	01	7.886E-3	70.6	70.6	0.675	0.00	15.0
----	----	----	----------	------	------	-------	------	------

01	01	01	9.463E-3	73.5	73.5	0.675	0.00	15.0
----	----	----	----------	------	------	-------	------	------

01	01	01	11.041E-3	77.5	77.5	0.675	0.00	15.0
----	----	----	-----------	------	------	-------	------	------

01	01	01	12.618E-3	80.6	80.6	0.675	0.00	15.0
----	----	----	-----------	------	------	-------	------	------

1 TOEBES+SOOKY (SOOKY'S THESIS) DATA SET

2

3 File name (ASSIGNED FOR MEANDR) : SDSK402

4 Plan geometry (SINUOSITY) : 1.1 (GIVEN BY SOOKY)

5 Main Channel X-sn : RECT 1.5" DEEP

6 Floodplain width : 3.886' 1.1845m SL = 0.87E-3

7 Floodplain roughness : Smooth

8

9	DATE	DISCHARGE	DEPTH AS	DEPTH AS	SLOPE	TAILGATE	TEMP
10		m3/sec.	RECORDED mm	PLOTTED mm		C	

402 6

01	01	01	6.309E-3	62.2	62.2	0.87	0.00	15.0
----	----	----	----------	------	------	------	------	------

01	01	01	7.886E-3	67.8	67.8	0.87	0.00	15.0
----	----	----	----------	------	------	------	------	------

01	01	01	9.463E-3	70.3	70.3	0.87	0.00	15.0
----	----	----	----------	------	------	------	------	------

01	01	01	11.041E-3	74.1	74.1	0.87	0.00	15.0
----	----	----	-----------	------	------	------	------	------

01	01	01	12.618E-3	75.7	75.7	0.87	0.00	15.0
----	----	----	-----------	------	------	------	------	------

01	01	01	14.195E-3	80.4	80.4	0.87	0.00	15.0
----	----	----	-----------	------	------	------	------	------

1 TOEBES+SOOKY (SOOKY'S THESIS) DATA SET

2  
 3 File name (ASSIGNED FOR MEANDR) : SDSK403  
 4 Plan geometry (SINUOSITY) : 1.1 (GIVEN BY SOOKY)  
 5 Main Channel X-sn : RECT 1.5" DEEP  
 6 Floodplain width : 3.886' 1.1845m SL = 1.6E-3  
 7 Floodplain roughness : Smooth

9	DATE	DISCHARGE	DEPTH AS	DEPTH AS	SLOPE	TAILGATE	TEMP
10		m3/sec.	RECORDED mm	PLOTTED mm		C	
403	6						
01	01 01	6.309E-3	57.5	57.5	1.60	0.00	15.0
01	01 01	7.886E-3	61.3	61.3	1.60	0.00	15.0
01	01 01	9.463E-3	62.9	62.9	1.60	0.00	15.0
01	01 01	11.041E-3	65.9	65.9	1.60	0.00	15.0
01	01 01	12.618E-3	68.2	68.2	1.60	0.00	15.0
01	01 01	14.195E-3	71.9	71.9	1.60	0.00	15.0

1 TOEBES+SOOKY (SOOKY'S THESIS) DATA SET

2  
 3 File name (ASSIGNED FOR MEANDR) : SDSK404  
 4 Plan geometry (SINUOSITY) : 1.1 (GIVEN BY SOOKY)  
 5 Main Channel X-sn : RECT 1.5" DEEP  
 6 Floodplain width : 3.886' 1.1845m SL = 3.67E-3  
 7 Floodplain roughness : Smooth

9	DATE	DISCHARGE	DEPTH AS	DEPTH AS	SLOPE	TAILGATE	TEMP
10		m3/sec.	RECORDED mm	PLOTTED mm		C	
404	6						
01	01 01	6.309E-3	54.5	54.5	3.67	0.00	15.0
01	01 01	7.886E-3	55.1	55.1	3.67	0.00	15.0
01	01 01	9.463E-3	56.9	56.9	3.67	0.00	15.0
01	01 01	11.041E-3	59.0	59.0	3.67	0.00	15.0
01	01 01	12.618E-3	61.8	61.8	3.67	0.00	15.0
01	01 01	14.195E-3	62.7	62.7	3.67	0.00	15.0

1 TOEBES+SOOKY (SOOKY'S THESIS) DATA SET

2  
 3 File name (ASSIGNED FOR MEANDR) : SDSK405  
 4 Plan geometry (SINUOSITY) : 1.1 (GIVEN BY SOOKY)  
 5 Main Channel X-sn : RECT 3.0" DEEP  
 6 Floodplain width : 3.886' 1.1845m SL = 0.3E-3  
 7 Floodplain roughness : Smooth

9	DATE	DISCHARGE	DEPTH AS	DEPTH AS	SLOPE	TAILGATE	TEMP
10		m3/sec.	RECORDED mm	PLOTTED mm		C	
405	5						
01	01 01	4.100E-3	88.6	88.6	0.30	0.00	15.0
01	01 01	4.732E-3	91.3	91.3	0.30	0.00	15.0
01	01 01	6.309E-3	98.6	98.6	0.30	0.00	15.0
01	01 01	9.463E-3	107.9	107.9	0.30	0.00	15.0
01	01 01	12.618E-3	114.3	114.3	0.30	0.00	15.0

1 TOEBES+SOOKY (SOOKY'S THESIS) DATA SET

2  
 3 File name (ASSIGNED FOR MEANDR) : SDSK406  
 4 Plan geometry (SINUOSITY) : 1.1 (GIVEN BY SOOKY)  
 5 Main Channel X-sn : RECT 3.0" DEEP  
 6 Floodplain width : 3.886' 1.1845m SL = 0.675E-3  
 7 Floodplain roughness : Smooth

8

9	DATE	DISCHARGE	DEPTH AS	DEPTH AS	SLOPE	TAILGATE	TEMP
10		m3/sec.	RECORDED mm	PLOTTED mm		C	
406	7						
01	01 01	4.732E-3	88.4	88.4	0.675	0.00	15.0
01	01 01	6.309E-3	94.7	94.7	0.675	0.00	15.0
01	01 01	7.886E-3	98.9	98.9	0.675	0.00	15.0
01	01 01	9.463E-3	103.8	103.8	0.675	0.00	15.0
01	01 01	11.041E-3	106.4	106.4	0.675	0.00	15.0
01	01 01	12.618E-3	107.6	107.6	0.675	0.00	15.0
01	01 01	14.195E-3	109.0	109.0	0.675	0.00	15.0

1 TOEBES+SOOKY (SOOKY'S THESIS) DATA SET

2  
 3 File name (ASSIGNED FOR MEANDR) : SDSK407  
 4 Plan geometry (SINUOSITY) : 1.1 (GIVEN BY SOOKY)  
 5 Main Channel X-sn : RECT 3.0" DEEP  
 6 Floodplain width : 3.886' 1.1845m SL = 0.87E-3  
 7 Floodplain roughness : Smooth

8

9	DATE	DISCHARGE	DEPTH AS	DEPTH AS	SLOPE	TAILGATE	TEMP
10		m3/sec.	RECORDED mm	PLOTTED mm		C	
407	7						
01	01 01	4.732E-3	86.6	86.6	0.87	0.00	15.0
01	01 01	6.309E-3	92.5	92.5	0.87	0.00	15.0
01	01 01	7.886E-3	96.5	96.5	0.87	0.00	15.0
01	01 01	9.463E-3	100.7	100.7	0.87	0.00	15.0
01	01 01	11.041E-3	104.2	104.2	0.87	0.00	15.0
01	01 01	12.618E-3	105.0	105.0	0.87	0.00	15.0
01	01 01	14.195E-3	106.2	106.2	0.87	0.00	15.0

1 TOEBES+SOOKY (SOOKY'S THESIS) DATA SET

2  
 3 File name (ASSIGNED FOR MEANDR) : SDSK408  
 4 Plan geometry (SINUOSITY) : 1.1 (GIVEN BY SOOKY)  
 5 Main Channel X-sn : RECT 3.0" DEEP  
 6 Floodplain width : 3.886' 1.1845m SL = 1.0E-3  
 7 Floodplain roughness : Smooth

8

9	DATE	DISCHARGE	DEPTH AS	DEPTH AS	SLOPE	TAILGATE	TEMP
10		m3/sec.	RECORDED mm	PLOTTED mm		C	
408	5						
01	01 01	4.416E-3	82.8	82.8	1.00	0.00	15.0
01	01 01	4.732E-3	85.3	85.3	1.00	0.00	15.0
01	01 01	6.309E-3	90.3	90.3	1.00	0.00	15.0
01	01 01	9.463E-3	98.7	98.7	1.00	0.00	15.0
01	01 01	12.618E-3	104.0	104.0	1.00	0.00	15.0

1 TOEBES+SOOKY (SOOKY'S THESIS) DATA SET

2  
 3 File name (ASSIGNED FOR MEANDR) : SDSK409  
 4 Plan geometry (SINUOSITY) : 1.1 (GIVEN BY SOOKY)  
 5 Main Channel X-sn : RECT 3.0" DEEP  
 6 Floodplain width : 3.886' 1.1845m SL = 1.6E-3  
 7 Floodplain roughness : Smooth

8	9 DATE	DISCHARGE	DEPTH AS	DEPTH AS	SLOPE	TAILGATE	TEMP
10		m3/sec.	RECORDED mm	PLOTTED mm		C	
409	6						
01	01 01	6.309E-3	88.1	88.1	1.60	0.00	15.0
01	01 01	7.886E-3	91.6	91.6	1.60	0.00	15.0
01	01 01	9.463E-3	94.7	94.7	1.60	0.00	15.0
01	01 01	11.041E-3	97.2	97.2	1.60	0.00	15.0
01	01 01	12.618E-3	99.4	99.4	1.60	0.00	15.0
01	01 01	14.195E-3	99.9	99.9	1.60	0.00	15.0

1 TOEBES+SOOKY (SOOKY'S THESIS) DATA SET

2  
 3 File name (ASSIGNED FOR MEANDR) : SDSK410  
 4 Plan geometry (SINUOSITY) : 1.1 (GIVEN BY SOOKY)  
 5 Main Channel X-sn : RECT 3.0" DEEP  
 6 Floodplain width : 3.886' 1.1845m SL = 3.0E-3  
 7 Floodplain roughness : Smooth

8	9 DATE	DISCHARGE	DEPTH AS	DEPTH AS	SLOPE	TAILGATE	TEMP
10		m3/sec.	RECORDED mm	PLOTTED mm		C	
410	5						
01	01 01	6.940E-3	83.8	83.8	3.00	0.00	15.0
01	01 01	7.886E-3	86.1	86.1	3.00	0.00	15.0
01	01 01	9.463E-3	89.6	89.6	3.00	0.00	15.0
01	01 01	12.618E-3	95.1	95.1	3.00	0.00	15.0
01	01 01	14.195E-3	97.0	97.0	3.00	0.00	15.0

1 TOEBES+SOOKY (SOOKY'S THESIS) DATA SET

2  
 3 File name (ASSIGNED FOR MEANDR) : SDSK411  
 4 Plan geometry (SINUOSITY) : 1.1 (GIVEN BY SOOKY)  
 5 Main Channel X-sn : RECT 3.0" DEEP  
 6 Floodplain width : 3.886' 1.1845m SL = 3.67E-3  
 7 Floodplain roughness : Smooth

8	9 DATE	DISCHARGE	DEPTH AS	DEPTH AS	SLOPE	TAILGATE	TEMP
10		m3/sec.	RECORDED mm	PLOTTED mm		C	
411	5						
01	01 01	7.886E-3	85.4	85.4	3.67	0.00	15.0
01	01 01	9.463E-3	88.7	88.7	3.67	0.00	15.0
01	01 01	11.041E-3	90.6	90.6	3.67	0.00	15.0
01	01 01	12.618E-3	93.0	93.0	3.67	0.00	15.0
01	01 01	14.195E-3	94.3	94.3	3.67	0.00	15.0

## APPENDIX 6

### ACKERS' DESIGN METHOD FOR STRAIGHT COMPOUND CHANNELS

#### 1. INTRODUCTION

A "compound" channel consists of a main channel, which accommodates normal flows, flanked on one or both sides by a flood plain which is inundated during high flows. Figure A6.1 illustrates a typical compound cross-section and defines the geometric variables used in the procedures to follow.

For water levels above the flood plain, the flow is strongly influenced by the interaction between the fast-flowing water in the main channel and the relatively slow-flowing water over the plains. This significantly complicates the estimation of stage-discharge relationships. The extra turbulence generated by the flow interaction introduces energy loss over and above that associated with boundary resistance. This is not accounted for by the conventional resistance equations (such as Chézy, Manning and Darcy-Weisbach), and their direct application may result in considerable error. If the channel cross-section is treated as a unit with one of these equations, the discharge for any given stage will invariably be underestimated.

The usual approach presented in hydraulics text books is to divide the cross-section into distinct subsections corresponding to the main channel and flood plain flows. The discharge for each subsection is then calculated separately using the Manning (or other similar) equation, and the total discharge obtained by adding these together. This approach invariably overestimates the discharge for any given stage.

Various attempts have been made to improve the latter approach, usually by including subdivision interfaces in the wetted perimeters to account for the apparent shear stresses induced by the interaction, or by locating the subdivisions on planes of zero shear. To date, all of these methods have been based on the results of small scale laboratory experiments and are unreliable on natural river scales.

The procedure presented here was developed by P Ackers (1991) and follows the channel subdivision approach. Subsection discharges are calculated and added to obtain a "basic" discharge, which is then adjusted to account for the effects of the

obtain a "basic" discharge, which is then adjusted to account for the effects of the interaction between the subsection flows. The adjustment required depends on the characteristics of the channel and also varies with stage. Four regions of flow behaviour are identified, as shown in Figure A6.2. This diagram presents some typical experimental results, showing the ratio of actual to basic discharge (on the horizontal axis) for a range of dimensionless flow depths (on the vertical axis). The effect of flow interaction is complex, alternately increasing and decreasing with flow depth through the different regions. Also shown on this diagram is the curve of channel coherence. This is the ratio of the conveyance calculated as a single cross-section to that calculated by summing the conveyances of the separate flow zones. A different adjustment function is defined for each region, but as the limits of the regions vary with channel characteristics it is not possible to identify the appropriate region for a particular water level beforehand. A logical procedure is given, however, for selecting the correct discharge value from those calculated assuming each adjustment function in turn. An additional correction is provided to account for the effect of deviations of up to  $10^0$  between the alignments of the main channel and the flood plains.

The adjustment functions were derived from experimental results from the large scale SERC Flood Channel Facility at HR Wallingford. They have been validated by comparison of predictions with measured results from smaller scale laboratory studies and some full scale river data. These data cover a range of discharges from 5 l/s to over 500 m<sup>3</sup>/s and a range of gradients from less than 0.0002 to more than 0.002. The comparisons suggest a computational accuracy for the method within two or three per cent, which is within the probable tolerances of the river data.

A procedure is also given for dividing the computed total discharge at any stage into main channel and flood plain components.

The interaction between main channel and flood plain flows also affects the magnitude and distribution of boundary shear stress, and will therefore influence scour patterns and requirements for scour protection. Local shear stresses on the flood plain close to the main channel may be five times greater than the value calculated from flow depth and channel gradient. The average boundary shear stress

within the main channel is reduced, and a relationship for estimating the reduced value is given.

The effects of the flow interaction also have significant implications for sediment transport. Calculations for a hypothetical case have suggested that total bed material discharge could be reduced by a factor of two or three. Detailed assessment of these effects will be the subject of future research. Until new results are available, the effects should be provisionally accounted for by using conventional methods with the relevant hydraulic parameters, such as flow velocity and boundary shear stress, determined according to the procedures presented here.

The procedures for applying the methods are outlined below. Full details of their background and development are presented in the comprehensive reports by Ackers (1991).

## **2. PROCEDURE FOR STAGE-DISCHARGE COMPUTATION**

The steps which follow outline the procedure for computing discharge values corresponding to specified water levels. Steps 1 to 3 define the physical characteristics of the channel reach and cross-section in terms of the variables required for the subsequent calculations. Steps 4 to 6 compute the basic discharges for the main channel, flood plains, and the whole cross-section for a specified water level. Steps 7, 8, 10 and 12 adjust the basic total discharge to account for flow interaction between the main channel and flood plains, assuming the flow to be in Regions 1, 2, 3 and 4 respectively. Steps 9, 11 and 13 apply the logical procedure for identifying the correct flow region and hence the correct adjusted discharge. The adjustment and selection steps are interspersed so that the correct region is identified at the earliest opportunity, to avoid unnecessary calculations. Step 14 applies the additional correction to account for deviation between the main channel and flood plain alignments.

Preliminary investigations suggest that most UK rivers with compound sections will flow in Regions 1 or 2 for floods with recurrence intervals up to about 20 years. Calculations should be carefully checked if higher regions are indicated. Artificial

or modified channels may operate over a wider range of regions than natural ones.

**Step 1. Determine the longitudinal gradient of the channel reach,  $S_o$ , from survey information.**

**Step 2. Determine the geometric variables required to define the adjustment functions.** The basic discharges for the main channel and flood plain zones can be computed using flow areas and wetted perimeters obtained directly from the appropriate surveyed cross-section. The discharge adjustment functions, however, include the geometric variables defined in Figure A6.1, and their estimation requires representation of the cross-section by a basic trapezoidal geometry. This is done using the following steps.

- 2.1 Plot the surveyed cross-section, as illustrated by Figure A6.3, for example.
- 2.2 Identify the points on the cross-section which most realistically mark the divisions between the main channel and the flood plains on both sides. Draw vertical lines through these points to define the bank lines separating the main channel and flood plain zones. The distance between the bank lines is  $2w_c$ . If there is a flood plain on one side of the main channel only, then just one bank line is defined and  $w_c$  is half the main channel width at the level of the division point.
- 2.3 Determine the river bank elevation. This is defined by the bank elevations at the locations of the bank lines - one value if there is only one flood plain, and the average of the two values for two flood plains.
- 2.4 By eye, fit a uniform slope to the main channel bank on each side. If the banks are irregular and the actual slopes vary, fit the straight lines to the upper two thirds of the bank profiles. The average of these slopes, expressed as ratios of horizontal to vertical distances, defines  $s_c$ .
- 2.5 Calculate the cross-sectional area of the main channel below the river bank elevation (as determined in step 2.3 above) and

- 2.6 Determine the depth of the main channel,  $h$ . This is the distance below the river bank elevation of a horizontal channel bed located so that the area of the trapezium defined by the bed, the top width ( $2w_c$ ) at the river bank elevation, and the side slopes ( $s_c$ ), is the same as  $A_{C_{\text{surv}}}$ . It can be calculated as
- $$h = \frac{2w_c + \{((2w_c)^2 - 4 s_c A_{C_{\text{surv}}})\}^{0.5}}{2s_c}$$

It will be obvious which of the two solutions of this equation is correct.

- 2.7 Determine the bottom width of the main channel,  
 $2b = 2w_c - 2 h s_c$
- 2.8 Identify the positions of the backs of the flood plains. The distance between these defines the maximum total compound channel width,  $2B$ , for two flood plains. For one flood plain the maximum value of  $B$  is the distance from the back of the flood plain to the bank line, plus  $w_c$ . Note that if the flood plains slope upwards and are not completely inundated, the total width ( $2B$ ) is less than the maximum, with the dry part ignored (see Figure A6.3). The limits of the water surface can be determined from the surveyed cross-section.

**Step 3. Estimate roughness coefficients for the main channel and flood plains.** The resistance equation used is a matter of personal choice. Manning's equation (with corresponding  $n$  values) is probably the most widely accepted and will be used for describing the procedure, although this does not necessarily imply recommendation for its general use. If measured stage-discharge data are available, they should be used to estimate roughness coefficients. For the main channel, the value ( $n_c$ ) adopted should correspond to near bank-full flows. It is not possible to infer the value for the flood plains ( $n_f$ ) directly from measured data; a value must be assumed, which can be checked subsequently and refined. The slope used for calculating the  $n$  values should be the hydraulic gradient, but if reliable measurements of this are not available the surveyed channel gradient ( $S_o$ ) can be

used. If no measured data are available,  $n_C$  and  $n_F$  should be estimated in the usual way.

**Step 4.** Specify a value for  $H$ , the flow depth measured above the idealized bed of the main channel. The steps that follow lead to an estimate of the discharge for this water level. These steps should be repeated for the required range of  $H$  values to define the stage-discharge relationship.

**Step 5.** Calculate the basic discharges in the main channel and flood plain zones for the specified flow depth, using Manning's equation. In these calculations the bank lines between the zones should be excluded from the wetted perimeters. Areas and wetted perimeters should be measured from the surveyed cross-section, not the idealized trapezoidal section.

**Step 6.** Add the zonal basic discharges together to obtain  $Q_{\text{basic}}$ , the basic discharge for the whole cross-section. This must now be adjusted to account for flow interaction effects. The adjustment must be made using the adjustment function applicable in each of four possible flow regions; the correct value will be selected from these as calculations proceed.

**Step 7.** Adjust  $Q_{\text{basic}}$  assuming flow is in Region 1.

7.1 Calculate  $H_*$ , the ratio of flow depths on the flood plains and in the main channel,

$$H_* = (H-h) / H$$

7.2 Calculate the Darcy-Weisbach friction factors for the main channel,  $f_C$ , and the flood plains,  $f_F$ , using the relationship

$$f = (8 g R S) / V^2$$

$g$  is the gravitational acceleration = 9.81 m/s<sup>2</sup>,

$R$  is the appropriate hydraulic radius (=  $A/P$ , excluding the bank lines from  $P$ ) (m),

$S$  is the hydraulic gradient, equal to the channel gradient ( $S_o$ ) for uniform flow, and

$V$  is the appropriate basic average flow velocity (m/s).

$V_C$  and  $V_F$  can be calculated by dividing the basic zonal

discharges (step 5) by the appropriate areas. If there are two flood plains a single value of  $f_F$  should be calculated by using the combined areas, wetted perimeters and basic discharges.

- 7.3 Calculate the dimensionless flood plain discharge deficit,

$$Q_{*2F} = - 1.0 H_c ( f_c / f_F )$$

- 7.4 Calculate the dimensionless main channel discharge deficit,

$$Q_{*2C} = - 1.240 + 0.395 ( B / w_c ) + G H_c$$

for one flood plain, or

$$Q_{*2C} = - 1.240 + 0.395 ( 2B / 2w_c ) + G H_c$$

for two flood plains.

In these equations

$$G = 10.42 + 0.17 ( f_F / f_c ) \quad \text{for } s_c \geq 1.0$$

$$G = 10.42 + 0.17 s_c ( f_F / f_c ) + 0.34 ( 1 - s_c ) \quad \text{for } s_c < 1.0$$

The value of  $Q_{*2C}$  should not be less than 0.5. If the calculated value is less than this, set it to 0.5 and set  $Q_{*2F}$  to zero.

- 7.5 Calculate the aspect ratio adjustment factor,

$$ARF = 2b / 10h$$

ARF should not exceed 2.0. If the calculated value is greater than this, set it to 2.0.

- 7.6 Calculate the total discharge deficit, the difference between  $Q_{basic}$  and the actual discharge,

$$DISDEF = ( Q_{*2C} + N_F Q_{*2F} ) ( V_c - V_F ) H_c h ARF$$

$N_F$  is the number of flood plains (1 or 2), and

$V_c, V_F$  are the zonal main channel and flood plain average flow velocities respectively.

- 7.7 Calculate the Region 1 adjusted discharge for the specified water level,

$$Q_{R1} = Q_{basic} - DISDEF$$

**Step 8. Adjust  $Q_{basic}$  assuming flow is in Region 2.** The adjustment is defined by the channel coherence at a flow depth greater than that specified. (Channel coherence is the ratio of the conveyance calculated as a single cross-section to that calculated by summing the conveyances of the separate flow zones).

- 8.1 Calculate the "shift" to be applied to the specified flow depth,  
 shift =  $0.05 + 0.05 N_F$  for  $s_C \geq 1.0$   
 shift =  $-0.01 + 0.05 N_F + 0.06 s_C$  for  $s_C < 1.0$

- 8.2 Calculate the shifted flow depth,

$$H' = H h / (h - \text{shift } H)$$

- 8.3 Calculate the channel coherence for the shifted flow depth,  $H'$ ,

$$\text{COH} = \frac{(1 + A_*) \{((1 + A_*) / (1 + f_* P_*))\}^{0.5}}{1 + A_* \{(A_* / (f_* P_*))\}^{0.5}}$$

Where

$$A_* = A_F / A_C,$$

$A_F$  is the total flood plain flow area (i.e. for both sides if there are two flood plains),

$A_C$  is the main channel flow area,

$$f_* = f_F / f_C,$$

$f_F$  is the Darcy-Weisbach friction factor for the flood plains,

$f_C$  is the Darcy-Weisbach friction factor for the main channel,

$$P_* = P_F / P_C,$$

$P_F$  is the total flood plain wetted perimeter (i.e. for both sides if there are two flood plains), excluding the bank lines,

$P_C$  is the main channel wetted perimeter, excluding the bank lines.

The areas and wetted perimeters should correspond to the required flow depth, i.e.  $H'$  for this calculation. The friction factors should also be recalculated, as in Step 7.2, using  $H'$ .

If the shifted flow depth is above the extreme lateral points of the surveyed cross-section, extend the cross-section vertically from these points to the required level to enable areas and wetted perimeters to be calculated.

- 8.4 Define the Region 2 discharge adjustment factor,

$$\text{DISADF}_2 = \text{COH}$$

8.5 Calculate the Region 2 adjusted discharge for the specified water level,

$$Q_{R2} = Q_{\text{basic}} \times \text{DISADF}_2$$

**Step 9. Determine if  $Q_{R1}$  is the actual discharge,  $Q$ .**

If  $Q_{R1} \geq Q_{R2}$  then  $Q = Q_{R1}$

If  $Q = Q_{R1}$  the calculations are complete for the specified water level, unless a skew correction (step 14) is required. If  $Q_{R1} < Q_{R2}$  the actual discharge is still unknown; in this case proceed with step 10.

**Step 10. Adjust  $Q_{\text{basic}}$  assuming flow is in Region 3.**

10.1 Calculate the channel coherence, COH, using the equation given for the  $Q_{R2}$  calculation, but for the specified flow depth,  $H$ , instead of  $H'$ .

10.2 Calculate the Region 3 discharge adjustment factor,

$$\text{DISADF}_3 = 1.567 - 0.667 \text{ COH}$$

10.3 Calculate the Region 3 adjusted discharge for the specified water level,

$$Q_{R3} = Q_{\text{basic}} \times \text{DISADF}_3$$

**Step 11. Determine if  $Q_{R2}$  is the actual discharge.**

If  $Q_{R2} \leq Q_{R3}$  then  $Q = Q_{R2}$

If  $Q = Q_{R2}$  the calculations are complete for the specified water level, unless a skew correction (step 14) is required. If  $Q_{R2} > Q_{R3}$  the actual discharge is still unknown; in this case proceed with step 12.

**Step 12. Adjust  $Q_{\text{basic}}$  assuming flow is in Region 4.**

12.1 Define the Region 4 discharge adjustment factor. This is equal to the channel coherence for the specified flow depth,  $H$ , as calculated above for Region 3, i.e.

$$\text{DISADF}_4 = \text{COH}$$

12.2 Calculate the Region 4 adjusted discharge for the specified water level,

$$Q_{R4} = Q_{\text{basic}} \times \text{DISADF}_4$$

**Step 13. Determine which of  $Q_{R3}$  and  $Q_{R4}$  is the actual discharge.**

If  $Q_{R3} > Q_{R4}$  then  $Q = Q_{R3}$

If  $Q_{R3} < Q_{R4}$  then  $Q = Q_{R4}$

Discharge calculations are now complete for the specified water level, unless a skew correction is required. If so, proceed with step 14.

**Step 14. Apply the skew correction if the main channel is not aligned with the flood plains.** This is done as follows and applies for angles of skew up to 10°.

14.1 Measure the angle of skew (in degrees) between the main channel and the flood plain ( $\Phi$ ) on a suitable map.

14.2 Calculate the discharge deficiency from the results already obtained,

$$\text{DISDEF} = Q_{\text{basic}} - Q$$

14.3 Correct the discharge deficiency to account for skewness,

$$\text{DISDEF}_{\text{skew}} = \text{DISDEF} \times (1.03 + 0.074 \Phi)$$

14.4 Recalculate the actual discharge,

$$Q = Q_{\text{basic}} - \text{DISDEF}_{\text{skew}}$$

Q is the actual discharge for the specified flow depth, H.

### **3. PROCEDURE FOR SEPARATION OF MAIN CHANNEL AND FLOOD PLAIN DISCHARGES**

If discharges for the main channel and flood plains are required separately, they can be estimated as follows. This will be necessary if  $f_F$  is to be estimated from measured data. The procedure has not been verified for skewed main channels and should be applied with caution for such cases.

**Step 1. Determine the actual, adjusted, total discharge for the required water level, as described in section 2.**

**Step 2. Identify the flow region and calculate the separate discharges.**

2.1 If the actual discharge is in Region 1, i.e.  $Q = Q_{R1}$ , determine the separate discharges using the results from the predictive method described in the section 2, i.e.

$$Q_C = Q_{C\text{basic}} - Q_{*2C} (V_C - V_F) H h \text{ ARF}$$

for the main channel, and

$$Q_F = Q_{F\text{basic}} - Q_{*2F} (V_C - V_F) H h \text{ ARF}$$

for each flood plain.

2.2 If the actual discharge is in one of Regions 2, 3 or 4, assume

that the flood plain discharges are unaffected by the interaction, and allocate all the adjustment to the main channel discharge, i.e.

$$Q_C = Q_{C_{\text{basic}}} - \text{DISDEF}$$

$$Q_F = Q_{F_{\text{basic}}}$$

#### 4. PROCEDURE FOR ESTIMATION OF BOUNDARY SHEAR STRESS

Boundary shear stresses are required for predicting locations of scour, designing scour protection, and estimating sediment transport rates. These issues will be addressed by future research. The following steps can be used for obtaining provisional estimates of the average shear stress on the main channel bed and the average and maximum shear stresses on the flood plains.

##### Step 1. Calculate the average shear stress on the bed in the main channel.

- 1.1 Calculate the average boundary shear stress, ignoring the interaction effects,

$$\tau_{oC} = \rho g R_C S$$

in which

$\rho$  is the density of water (1000 kg/m<sup>3</sup>), and

$R_C$  is the hydraulic radius of the main channel, excluding the bank lines from the wetted perimeter.

- 1.2 Calculate the discharge adjustment factor for the main channel,  
 $\text{DISADF}_C = Q_C / Q_{C_{\text{basic}}}$   
 in which  $Q_C$  is the actual main channel discharge, as calculated in section 3, and  $Q_{C_{\text{basic}}}$  is the basic main channel discharge, as calculate in section 2, step 5.

- 1.3 Calculate the corrected average boundary shear stress, accounting for the interaction effect,

$$\tau_{oC}' = \tau_{oC} (\text{DISADF}_C)^2$$

##### Step 2. Calculate the average shear stress on the surface of the flood plain, ignoring the interaction effects,

$$\tau_{oF} = \rho g (H - h) S$$

This will apply on the flood plain surface beyond the zone of interaction with the main channel flow. Allow for a maximum

local value of  $5 \tau_{oF}$  within a distance of 3 h from the bank line.

## 5. REFERENCE

Ackers, P. (1991) The hydraulic design of straight compound channels, Report SR 281, HR Wallingford, (in preparation).

## 6. NOTATION

A	cross-sectional area
$A_{C_{\text{surv}}}$	area of main channel below bank elevation, from surveyed cross-section
$A_*$	ratio $A_F/A_C$
B	half the total compound channel width. For sloping flood plains which are partially inundated this should be taken as half the water surface width
b	half the bottom width of the main channel
COH	channel coherence
DISADF	adjustment factor applied to basic discharge to account for interaction effects; subscript will indicate appropriate region
DISDEF	discharge deficit, i.e. difference between actual and basic discharges
DISDEF <sub>skew</sub>	discharge deficit, accounting for main channel skew
f	Darcy-Weisbach friction factor, $= 8gRS/V^2$
$f_*$	ratio $f_F/f_C$
G	parameter in Region 1 discharge deficit prediction
g	gravitational acceleration
H	depth of flow in main channel
$H_*$	ratio of flow depths on flood plain and main channel, i.e. $(H-h)/H$
$H'$	shifted flow depth in main channel (for Region 2 prediction)
h	depth of main channel bed below river bank elevation
$N_F$	number of flood plains, 1 or 2
n	Manning's roughness coefficient
P	wetted perimeter
$P_*$	ratio $P_F/P_C$
Q	actual discharge, unsubscripted for whole compound channel
$Q_{\text{basic}}$	zonal discharge ignoring bank lines from wetted perimeter, unsubscripted for sum of main channel and flood plain values
$Q_R$	discharge as adjusted to account for interaction effects in region indicated by numerical subscript
$Q_{*2}$	discharge deficit normalized by $(V_C - V_F)Hh$
R	hydraulic radius, $= A/P$
S	hydraulic gradient of channel
$S_o$	surveyed channel gradient
$s_c$	side slope of main channel bank, horizontal/vertical
shift	addition to main channel flow depth in Region 2 adjustment prediction
V	average flow velocity
$w_c$	half width of main channel between bank lines

$\rho$  density of water  
 $\tau_o$  average bed shear stress  
 $\tau_{oc}$  average main channel bed shear stress adjusted for interaction effect  
 $\Phi$  angle of skew between main channel and flood plains

subscripts :

C main channel  
F flood plain  
L left bank  
R right bank  
1,2,3,4 region of flow behaviour

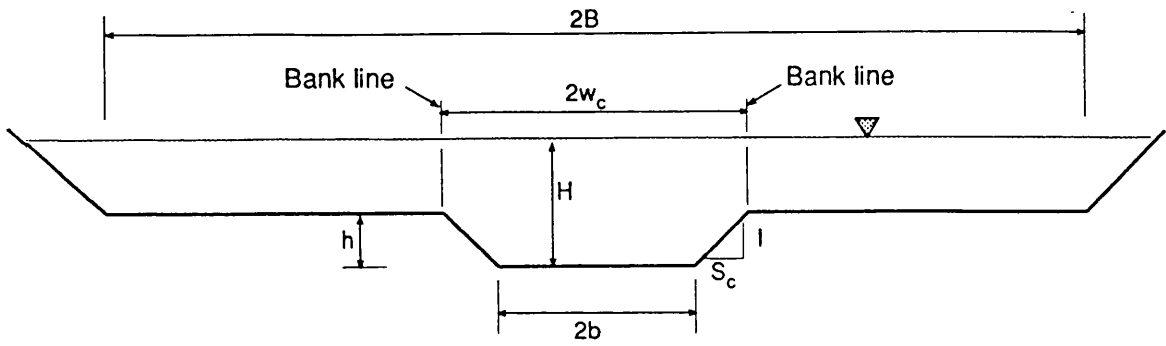


**Figure A6.1 Compound channel cross-section with definition of variables**

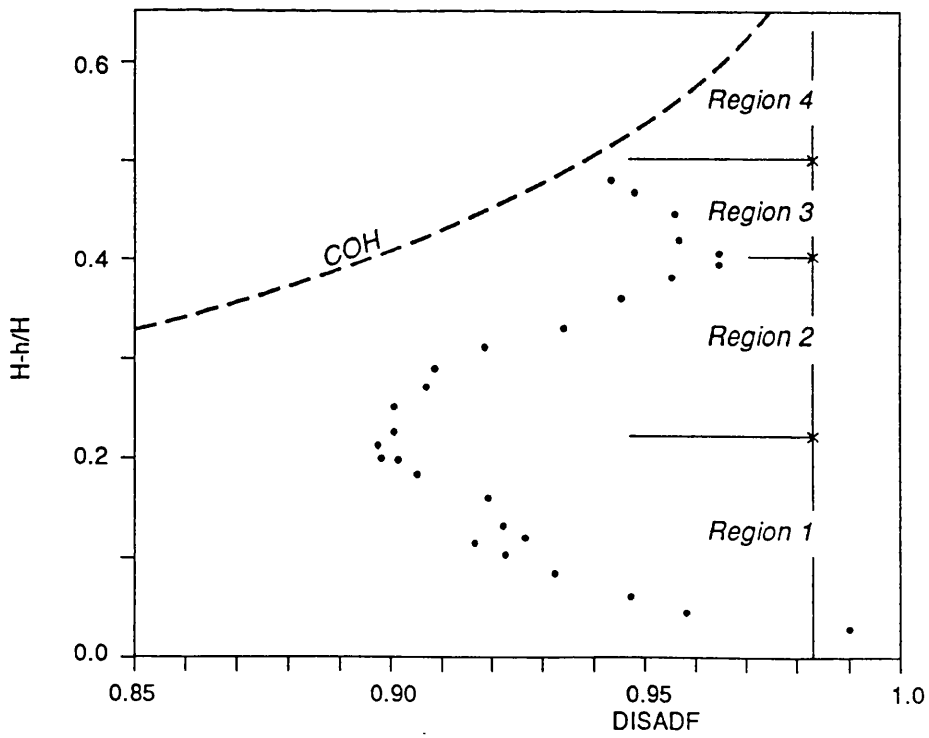


**Figure A6.2 Regions of flow behaviour**

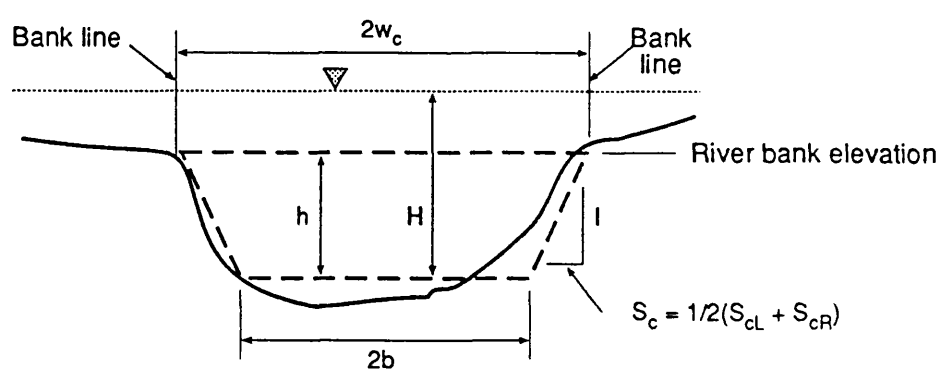
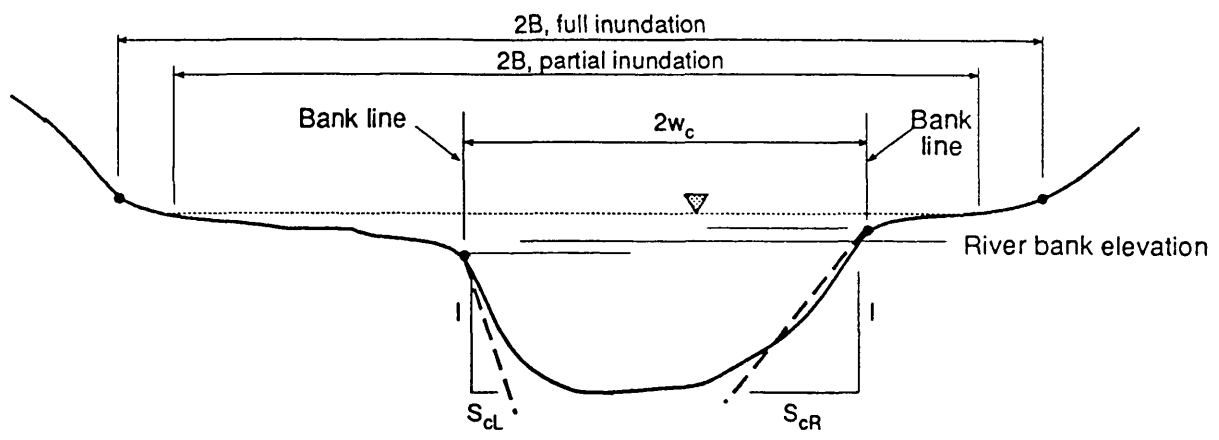


**Figure A6.3 Assessment of geometric variables for natural cross-sections**

## APPENDIX 7

### SUMMARY OF THE ACKERS ROD ROUGHNESS METHOD

Basic resistance calculations for rod roughness as used in the SERC FCF tests may be based on the following set of formulae, which allow for different numbers of rods in alternate rows:

$$B_1 = (1 - n_1 z d / A)^2$$

$$B_2 = (1 - n_2 z d / A)^2$$

for  $1.75 < Z_* < 6.6$ :

$$\alpha C_D = 1.184 - 0.277 Z_* + (0.529 Z_* - 0.843)^{0.5}$$

else

$$\alpha C_D = 0.95$$

$$f_s^{-0.5} = 2.02 \log_{10} (\text{Re } f_s^{0.5}) - 1.38$$

$$f_{\text{TOT}} = 8gRS/V^2$$

$$= 4\alpha C_D (B_1 N_1 + B_2 N_2) d z/P + (B_1 + B_2) f_s/2$$

Where:

Re Reynolds number of blocked channel =  $2 V R (B_1^{0.5} + B_2^{0.5})/ \nu$

$B_{1,2}$  blockage effect, ie square area of rows for alternate rows

$n_{1,2}$  number of rods of diameter  $d$  across rows 1 and 2

$N_{1,2}$  number of rods per unit length of zone, rows 1 and 2

$z$  depth of flow

$A$  cross sectional area of zone

$f_s$  Darcy friction factor due to smooth boundary

$f_{\text{TOT}}$  overall friction factor

$V$  nominal velocity = component discharge /  $A$

$\alpha C_D$  effective drag coefficient of rods

$Z_*$   $z/d$

$R$  hydraulic mean depth ( $A/P$ )

$S$  hydraulic gradient (water surface slope)

The vertical rods were mounted in wooden frames (2.46m by 2.33m) to allow them to be lifted in and out of the flume. During Phase A the frames were placed in the flume with their short dimension perpendicular to the flow and during phase B the frames were used with the long dimension perpendicular to the flow direction, Figure 1.

Thus the appropriate values of  $n$  and  $N$  etc is slightly different for Phase A and B.

#### Phase A

Zone width	= 2.33m
Length of frame	= 2.46m
lateral rod spacing	= 0.315m
longitudinal rod spacing	= 0.537m
$n_{1,2}$	= 8, 7
$N_{1,2}$	= $n_{1,2} / \text{longitudinal rod spacing}$
rod diameter	= 0.025m

#### Phase B

Zone width	= 2.46m
Length of frame	= 2.33m
lateral rod spacing	= 0.537m
longitudinal rod spacing	= 0.315m
$n_{1,2}$	= 5, 5
$N_{1,2}$	= $n_{1,2} / \text{longitudinal rod spacing}$
rod diameter	= 0.025m

Thus the Ackers procedure was applied to a single frame when computing rod roughness friction factors. The method was developed based on calibration data collected during phase A and it was considered necessary to carry out an independent check on the method for the phase B orientation of the frames.

In order to carry out an independent assessment of the Ackers rod roughness method two extra sets of stage discharge tests were carried out as part of HR's internal research programme. The FCF had already been infilled and effectively turned in to a rectangular channel with width 10m. The portable side walls were used to narrow the flume and the extra tests were carried out in a trapezoidal channel with bottom width 4.6078m and side slopes of 1:1. The longitudinal bed slope was assumed to be the Phase B 110 floodplain slope of  $1.021 \times 10^{-3}$ .

Two sets of stage discharge results were measured and the important aspects of each are listed below:

- B49 Stage Discharge results in trapezoidal channel with the roughness frames oriented as during Phase A.
- B50 Stage Discharge results in trapezoidal channel with the roughness frames oriented as during Phase B.

Seven individual values of stage and discharge were measured for each roughness configuration. These two sets of data are listed in Table A7.1. The stage discharge data were analyzed in two ways:

- 1 Values of friction factor were back calculated from the measured flows and the known channel geometry and compared with the values obtained from the Ackers rod roughness method. The results of this analysis are shown in Table A7.2
- 2 The Ackers rod roughness method was used to calculate the flow in the channel and this was compared with the measured flows. The results of this analysis are shown in Table A7.3.

The calculated D'arcy friction factors are in error by between -9.47% and 23.80%. The data point which gave this large error was judged to be suspect and the mean error was calculated for Phase B case both including this point and omitting it. The mean errors in the calculated friction factors were 2.9% for the phase A case and 4.5% for the phase B case. As can be seen the Ackers method gave mean errors in discharge of 0.7% and -2.0% for the Phase A and B roughness patterns respectively. The standard deviations for these results are 4.8% and 2.9%. The fairly wide range of errors is probably due to the fact that a wider tolerance was allowed on the measured water surface slopes in these measurements than during either Phase A or B.

The Ackers rod roughness method has been tested against two independent sets of stage discharge data and reproduced the measured discharges and total friction factors to an acceptable level of accuracy. Hence the Ackers rod roughness method may be used in all future analysis of rod roughened SERC FCF data.

**Table A7.1 Stage Discharge Measurements**

Date	Discharge cumecs	Depth mm	Temp °C
<b>B49 Phase A Roughness</b>			
030192	0.02252	29.64	11.1
030192	0.04432	50.57	10.9
020192	0.06183	65.08	10.5
050192	0.07971	83.78	11.6
020192	0.10315	109.25	10.8
050192	0.13002	135.52	12.1
030192	0.16352	163.43	11.4
<b>B50 Phase B Roughness</b>			
100192	0.02225	28.24	12.3
090192	0.04134	45.42	13.1
080192	0.06159	62.00	12.9
080192	0.07982	83.40	13.1
080192	0.10015	101.98	13.3
090192	0.13394	132.11	13.3
090192	0.16028	154.10	13.1

**Notes**

1 Depths are adjusted for floodplain slope  $1.021 \times 10^{-3}$

**Table A7.2 Friction Factor Analysis**

Discharge cumecs	Depth mm	Actual D'arcy f	Calculated D'arcy f	% Error in D'arcy f
Phase A Roughness				
0.02252	29.64	0.0874	0.0767	13.95
0.04432	50.57	0.1121	0.1105	-1.43
0.06183	65.08	0.1230	0.1400	13.82
0.07971	83.78	0.1579	0.1729	9.50
0.10315	109.25	0.2100	0.2101	0.05
0.13002	135.52	0.2523	0.2373	-5.95
0.16352	163.43	0.2798	0.2533	-9.47
MEAN % ERROR				2.92
Phase B Roughness				
0.02225	28.24	0.0774	0.0732	-5.43
0.04134	45.42	0.0934	0.0964	3.21
0.06159 <sup>2</sup>	62.00	0.1074	0.1326	23.80
0.07982	83.40	0.1554	0.1713	10.23
0.10015	101.98	0.1808	0.1996	10.40
0.13394	132.11	0.2200	0.2341	6.41
0.16028	154.10	0.2442	0.2494	2.13
MEAN % ERROR				7.25 <sup>3</sup>
MEAN % ERROR				4.49 <sup>4</sup>

**Notes**

- 1 % Error = 100\*(Calc - Meas)/Meas
- 2 This data point is out of sequence and is suspect
- 3 Mean Error including suspect point
- 4 Mean Error with suspect point omitted

**Table A7.3 Flow Analysis**

Discharge cumecs	Depth mm	Calculated flow	% Error in Calc Flow
Phase A Roughness			
0.02252	29.64	0.02405	6.78
0.04432	50.57	0.04467	0.80
0.06183	65.08	0.05795	-6.27
0.07971	83.78	0.07622	-4.38
0.10315	109.25	0.10304	-0.01
0.13002	135.52	0.13002	3.10
0.16352	163.43	0.16352	5.18
MEAN % ERROR			0.74
Phase B Roughness			
0.02225	28.24	0.02289	2.88
0.04134	45.42	0.04070	-1.55
0.07982	83.40	0.07604	-4.73
0.10015	101.98	0.09530	-4.84
0.13394	132.11	0.12989	-3.02
0.16028	154.10	0.15867	-1.00
MEAN % ERROR		-2.05 <sup>2</sup>	

**Notes**

- 1 % Error = 100\*(Calc - Meas)/Meas
- 2 Mean Error with suspect point omitted

- Flow direction Phase A
- ↑ Flow direction Phase B
- Dowel rod, 25mm diameter

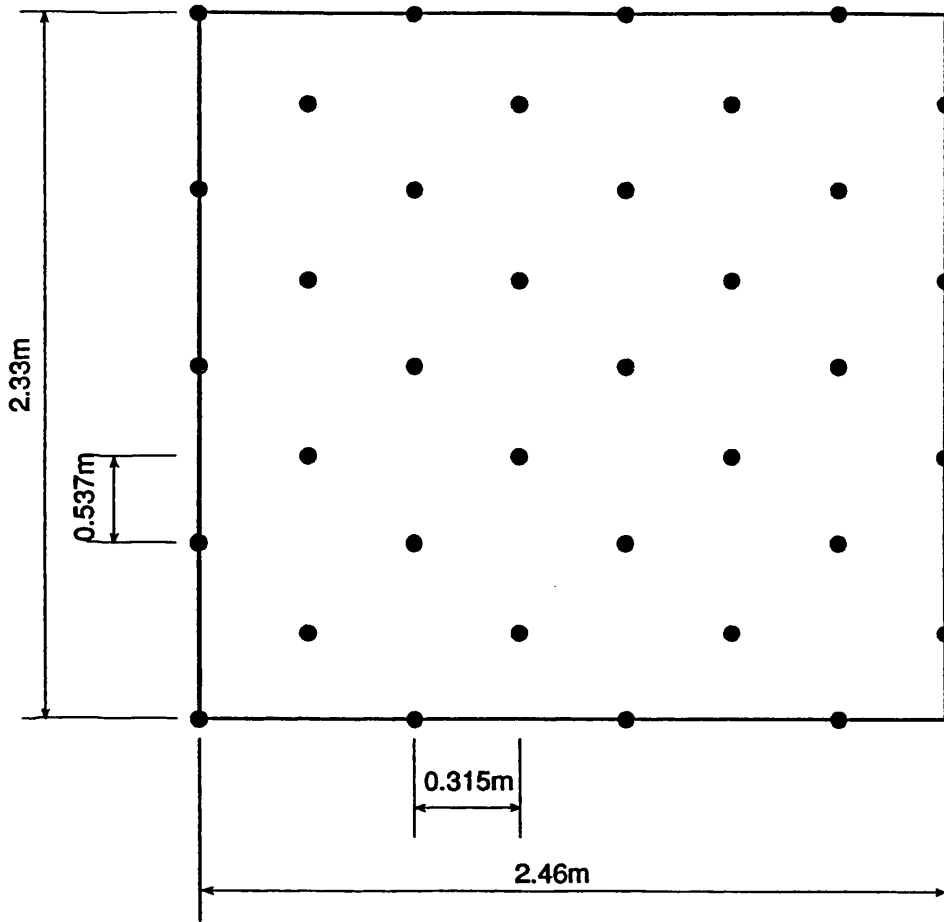


Figure A7.1 Schematic of rod roughness frame

**APPENDIX 8  
PUBLISHED PAPERS**

- 1      WARK J B, SAMUELS P G and ERVINE D A (1990) A Practical Method of Estimating Velocity and Discharge in Compound Channels, Intl. Confr. on River Flood Hydraulics, Wallingford, Oxfordshire, Sept.
  
- 2      WARK J B and SAMUELS P G (1992) Applying a Simple Turbulence Model to River Flows, Presented at IAHR seminar: Is Turbulence Modelling of Any Use?, Institution of Civil Engineers, Great George Street, London, 9th April.

International Conference on  
**RIVER FLOOD HYDRAULICS**

17-20 September, 1990

A PRACTICAL METHOD OF ESTIMATING VELOCITY AND  
DISCHARGE IN COMPOUND CHANNELS

J.B. Wark      Dept. of Civil Engineering, University of Glasgow.  
P.G. Samuels    Hydraulics Research Ltd., Wallingford.  
D.A. Ervine     Dept. of Civil Engineering, University of Glasgow.

ABSTRACT

A method of estimating velocity and discharge in compound channels is presented. This is based on solving the equation for the lateral distribution of flow in a channel. Results are given for laboratory and natural river channels.

1. INTRODUCTION

Two-stage or compound channels are of interest to the river engineer for several reasons. Many rivers have compound channels, possessing a main channel, which always carries flow, and one or two floodplains, which only carry flow at above bankfull stages, fig. 1. The use of artificial compound channels in flood relief schemes is achieved by cutting berms on either side of the existing channel. This increases the capacity of the channel and reduces downstream water levels, during extreme flood events. Sellin, 1989, describes an example of this type of scheme.

It is important that the engineer be able to estimate the stage-discharge relationship of compound channels. First to predict the effect of possible floods in natural channels and second to enable design of economic flood relief schemes using two-stage channel sections.

2. ESTIMATING FLOW IN COMPOUND CHANNELS

Traditionally flow in two-stage channels has been calculated using simple 1-D theory. The two most commonly applied approaches are:

Single Channel Method in which the complete channel is treated as a single unit. Usually no account is taken of roughness variation across the channel. In terms of Manning's equation this may be expressed :

$$Q_t = \frac{1}{n_t} A_t R_t^{2/3} S_{xf}^{1/2} \quad (1)$$

$$R_t = A_t / P_t \quad (2)$$

Where

$A_t$  - Total area of channel

$n_t$  - Manning's coefficient for whole channel

$P_t$  - Wetted perimeter of whole channel

$Q_t$  - Total flow  
 $R_t$  - Hydraulic radius of whole channel  
 $S_{xf}$  - A longitudinal slope, taken as the bed slope in uniform flow  
 and as the slope of the energy line in non-uniform flow.

This method underpredicts flows by up to 30% at low overbank stages.

Divided Channel Methods are based on splitting the main channel from the floodplains, fig. 2, and calculating the flow in each sub-area separately, using equations 3 and 4. Variations in roughness can be included and the total flow is obtained by summation.

$$Q_i = \frac{1}{n_t} A_i R_i^{2/3} S_{xf}^{1/2} \quad (3)$$

$$R_t = A_i / P_i \quad (4)$$

(Where  $Q_i$  is the flow in sub-area  $i$ , etc.)

There are many divided channel methods which differ in the position and direction of the dividing lines and whether or not these lines are included when calculating the wetted perimeters of the sub-areas. In general they all tend to overpredict the total flow by significant margins, Ramsbottom, 1989.

Other methods for calculating flow in compound channels have appeared in the literature, (eg. the effective stress method or the correction factor method). These procedures are largely empirical and require calibration, this is usually provided based on small scale laboratory tests. See Ervine and Baird, 1982, and James and Brown, 1977. Because of scale effects such methods are unlikely to be accurate in application to prototype channels.

The main reason that the above methods all fail to give accurate results, when applied to compound channels, is that the flow distribution is nonuniform. The simple 1-D theory is based on the underlying assumption of uniform flow and bed shear stress, which is untrue in two-stage channels. The above empirical approaches to taking this non-uniformity into account are based on simplistic analysis and inadequate understanding of the basic flow mechanisms occurring in compound channels. In recent years work has concentrated on gaining an accurate picture of the processes taking place and has stimulated interest in methods of discharge estimation based on 2-D, depth averaged, flow theory.

### 3. LATERAL DISTRIBUTION METHOD OF DISCHARGE ESTIMATION

This is based on calculating the distribution of flow within the channel. The governing equation, (either 5 or 6), is derived from the general 2-D, shallow water equations. There are many assumptions and approximations involved in the derivation of these equations including : Flow is steady and uniform (in the longitudinal direction) and the water surface is horizontal across the channel. Further discussion of these aspects is outwith the scope of this paper, see Samuels, 1985 or Wark, 1988. Most authors have solved for the depth averaged velocity,  $U$ , using equation 5. Samuels, 1988, shows that in certain cases the use of unit flow,  $q$ , and equation 6 may be theoretically more sound. It is unclear, as yet, which form of the equation is to be preferred in practice.

$$gDS_x f - \frac{Bf|U|U}{8} + \frac{\partial}{\partial y} \left[ \nu_t D \frac{\partial U}{\partial y} \right] - 0 \quad (5)$$

$$gDS_x f - \frac{Bf|q|q}{8 D^2} + \frac{\partial}{\partial y} \left[ \nu_t \frac{\partial q}{\partial y} \right] - 0 \quad (6)$$

Gravity                      Bed shear                      Lateral shear

Where

B =  $(1 + S_x^2 + S_y^2)^{1/2}$  : A factor relating stress on an inclined surface to stress in the horizontal plane, see Wark, 1988.

D - Flow depth

f - Darcy friction factor

g - Gravitational acceleration

$S_x$  - Longitudinal slope of channel bed

$S_y$  - Lateral slope of channel bed

x - Longitudinal coordinate direction

y - Lateral coordinate direction

q - Longitudinal unit flow (=UD)

U - Longitudinal depth averaged velocity

$\nu_t$  - Lateral eddy viscosity

Given estimates of the bed shear and lateral shear terms it is possible to solve equation 5 or 6 for the distribution of flow within the channel. This in turn may be integrated to provide the discharge or used to calculate the distribution of bed shear stress across the channel.

The bed shear term is calculated by local application of 1-D theory. For example Manning's equation :

$$f = 8gn^2 / D^{1/3} \quad (7)$$

n - Manning's n

The lateral shear term is more difficult to evaluate and various models for the lateral eddy viscosity have been proposed. An early example, Vreugdenhil and Wijbenga, 1982, used a constant value of  $\nu_t$  but did not compare the solution with measured data. More physically realistic models may be obtained by dimensional analysis. The lateral eddy viscosity relating to bed roughness generated turbulence is given by equation 8.

$$\nu_t = \lambda U_* D \quad (8)$$

Where

$U_*$  - The shear velocity =  $(\tau_b/\rho)^{1/2}$

$\lambda$  - The nondimensional eddy viscosity (NEV)

$\rho$  - Fluid density

$\tau_b$  - Bed shear stress

Values of  $\lambda$  are usually quoted as being approximately  $0.16 \pm 50\%$  in straight laboratory flumes increasing to between 0.6 and 2.0 in river channels, see Okoye, 1970. Some authors, eg. Wormleaton, 1988, suggest that shear layer driven turbulence may be an important source of lateral shear in compound channels. In this case it can be shown that the lateral eddy viscosity is given by an expression of the form :

$$\nu_t = C l_s \Delta U \quad (9)$$

Where

C - A constant

$l_s$  - A length scale related to the width of shear layer

$\Delta U$  - Velocity difference across the shear layer

More sophisticated attempts have been made using a depth averaged form of the  $k-\epsilon$  turbulence model, Keller and Rodi, 1989. However the cost of the additional computation is large and  $k-\epsilon$  models are unlikely to form the basis of practical design aids. Analytic solutions to equation 5 are available only for certain simplified cases, Samuels, 1988 and Shiono and Knight, 1988. In general a numerical solution must be sought and the following section describes the method developed by the authors.

#### 4. NUMERICAL SOLUTION METHOD

The authors have found that an appropriate finite difference scheme to use, when solving equation 6, is one in which the lateral shear term is computed at the mid-node positions, (Staggered grid). Equation 6 is nonlinear and the solution is obtained by iteration using Newton's method. The initial 'seed' solution is obtained from equation 6 by setting  $\nu_t = 0$ . The required boundary conditions are that  $q = 0$  at the solid channel boundaries. The numerical model has been developed to require the minimum amount of information : the channel geometry; the bed roughness and eddy viscosity parameters in each sub-area of the channel. Convergence is usually obtained within five or six iterations and the method is computationally efficient. It is simple to incorporate variations in roughness and eddy viscosity in the method.

#### 5. COMPARISONS BETWEEN THE COMPUTATIONAL MODEL AND PHYSICAL MEASUREMENTS

The above model has been applied to a wide range of data, varying from small scale laboratory flumes to large scale laboratory channels to real rivers. In all of the examples quoted below equation 8 was used to estimate the lateral eddy viscosity.

Small Scale Model Kiely, 1989, presents velocity distributions and stage-discharge data for a small flume. The cross-sectional geometry is shown in figure 3, with the main channel being 0.2 m wide and the bankfull depth 0.05 m. The Floodplains were each 0.5 m wide and the bed slope set to 0.001. Calculations were carried out with the Manning's n in the main channel, for bankfull stage and above, set to 0.0095. On the floodplains n was varied between 0.02 and 0.005, depending on stage. The nondimensional eddy viscosity (NEV),  $\lambda$ , was taken as zero on the floodplains. The calculations were carried out for a range of  $\lambda$  values in the main channel. Figure 4 shows measured and computed velocity

distributions for a stage of approximately 100 mm and figure 5 is a comparison between measured and computed stage-discharge relationships. As can be seen the computed velocity and discharge distributions follow the measured values closely, the best agreement being obtained with  $\lambda$  in the range 0.16 to 0.24.

Large Scale Model The SERC Flood Channel Facility, Wallingford is a large experimental flume, approximately 50 m long by 10 m wide. A long term research programme into the behaviour of two stage channels is being carried out using this facility. Series A of the the programme, now complete, dealt with straight channels. A number of different cross sectional shapes were investigated with stage-discharge, velocity and bed shear distributions all being measured.

Figure 8 shows one of the geometries, the main channel was 1.5 m wide and bankfull depth 0.15 m. The main channel and floodplains had laterally sloping sides of gradient 1.0 and the longitudinal slope was  $1.027 \times 10^{-3}$ . Several different floodplain widths were tested and comparisons between measured and computed stage-discharges are shown in figures 6 and 7, for narrow and wide floodplains respectively.

The friction factors were obtained from equation 10, as recommended by Ackers, 1989, and the  $\lambda$  factor was taken as constant across the channel.

$$\frac{1}{\sqrt{f}} = 2.02 \log_{10} (Re \sqrt{f}) - 1.38 \quad (10)$$

Again best agreement between computed and measured values was obtained with the  $\lambda$  factor between 0.16 and 0.24. In this case the computed stage-discharges are closer to the measurements than the computed velocity distributions.

River Measurements Stage-discharge and velocity data are available for the River Severn at Montford, Ramsbottom, 1989. The irregular cross-sectional geometry was approximated with straight lines, as shown in figure 9. The main channel is 34 m wide with Bankfull depth about 5.5 m. The floodplains extend 65 m to the left and about 25 m to the right. The longitudinal bed slope is  $1.94 \times 10^{-4}$ .

Calculations were carried out, see figure 10, with the bankfull Manning's  $n$  0.033. On the floodplain  $n$  was taken as 0.045, which is consistent with the vegetation being mainly short, cropped grass. The  $\lambda$  value appears to lie in the range 0.08 to 0.24. This is considerably lower than typical values normally associated with natural channels.

## 6. CONCLUSIONS

- (1) A 1-D numerical model of the lateral distribution of flow has been developed which requires the minimum of input information. This model has been shown to predict reliable stage-discharge and velocity distributions for compound channels. Although based on uniform, (in the longitudinal direction), flow theory the method can be applied to the non-uniform case.
- (2) The numerical model has been applied satisfactorily to small scale model data, large scale model results and field measurements in seven British rivers.
- (3) In applying the model values of roughness and lateral eddy viscosity are

required. The computed stage-discharges were found to be more sensitive to variations in roughness than to changes in the lateral eddy viscosity. Given an accurate value of bankfull roughness the method can produce discharge estimates to within  $\pm 5\%$  of measured values.

(4) The authors have found that the lateral eddy viscosity can be modelled with adequate precision using only the bed generated shear model, (equation 8). The  $\lambda$  factor was found to lie within the range  $0.16 \pm 0.08$ . In View of the uncertainty relating to lateral eddy viscosity the use of constant values of  $\lambda$  in each sub-area of the channel is recommended.

(5) The method is numerically efficient and is suitable for inclusion in general river modelling packages.

(6) The experimental channels and river gauging sites which have been simulated with the above 1-D model are not typical. They are straight and exhibit a greater degree of uniformity than is common. Care will be required when extending application of the model to more typical, sinuous, river channels.

## 7. ACKNOWLEDGEMENTS

The first author is grateful to The Science and Engineering Research Council and Hydraulics Research Ltd. for financial support, in the form of a CASE Studentship.

## 8. REFERENCES

Ackers P., (1989), Private Communication

Ervine D.A. and Baird J.I., (1982), Rating curves for rivers with overbank flow, Proc. Instn. Civ. Engrs., Part 2, 73.

James M. and Brown B.J., (1977), Geometric parameters which influence floodway flow, United States Waterways Experimental Station, Research Report H-77-1.

Keller R.J. and Rodi W., (1989), Prediction of flow characteristics in main channel/floodplain flows, Jrnl. of Hydr. Resch., Vol. 26, no. 4.

Kiely G.K., (1989), An experimental study of overbank flow in straight and meandering compound channels, Ph.D. Thesis, Dept. of Civil Engineering, University College, Cork.

Okoye J.K., (1970), Characteristics of transverse mixing in open channel flows, California Institute of Technology, Pasadena, California, Report No. KH-R-23.

Ramsbottom D.R., (1989), Flood discharge assessment, Interim Report, Hydraulics Research Ltd., Report SR195.

Samuels P.G., (1985), Modelling of river and floodplain flow using the finite element method, Hydraulics Research Ltd., Report SR61.

Samuels P.G., (1988), Lateral shear layers in compound channels, Proc. Intl. Confr. on fluvial hydraulics, Vitaki, Budapest.

Sellin R.H.J., (1989), Two stage channel flow, University of Bristol, Dept. of Civil Engineering, Final Report prepared for Thames Water Authority.

Shiono K. and Knight D.W., (1988), Two dimensional analytic solution for a compound channel, Third Intl. Symp. on refined flow modelling and turbulence measurements, Tokyo, Japan.

Wark J.B., (1988), The equations of river and floodplain flow, Research Report submitted to the Dept. of Civil Engineering, University of Glasgow.

Wormleaton D.R., (1988), Determination of discharge in compound channels using the dynamic equation for lateral velocity distribution., Proc. Intl. Confr. on fluvial hydraulics, Vitaki, Budapest.

2. FIGURES

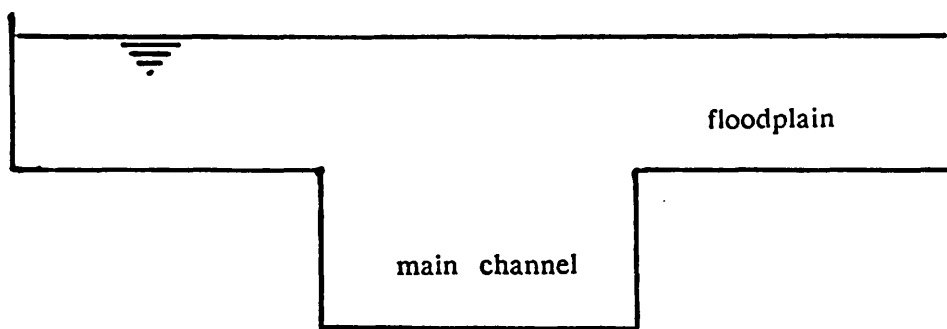


Figure 1. Compound Channel

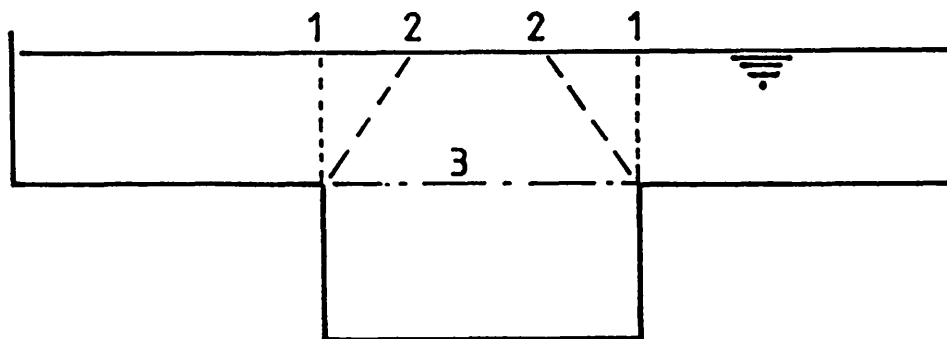


Figure 2. Divided Channel Methods

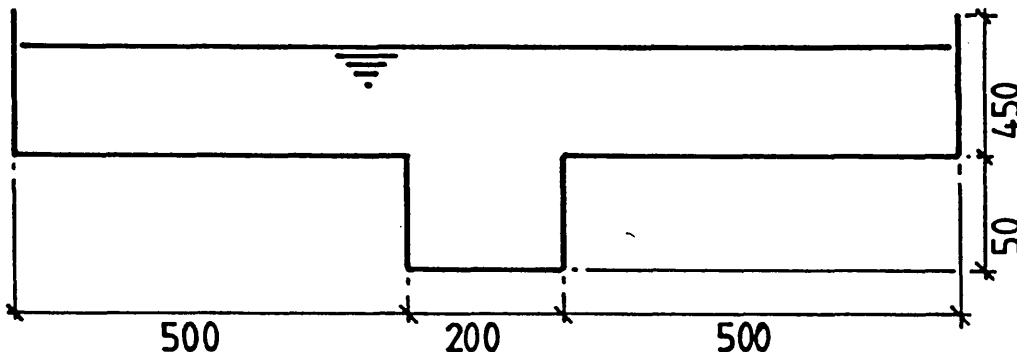


Figure 3. Cross-Section of Kiely's Channel

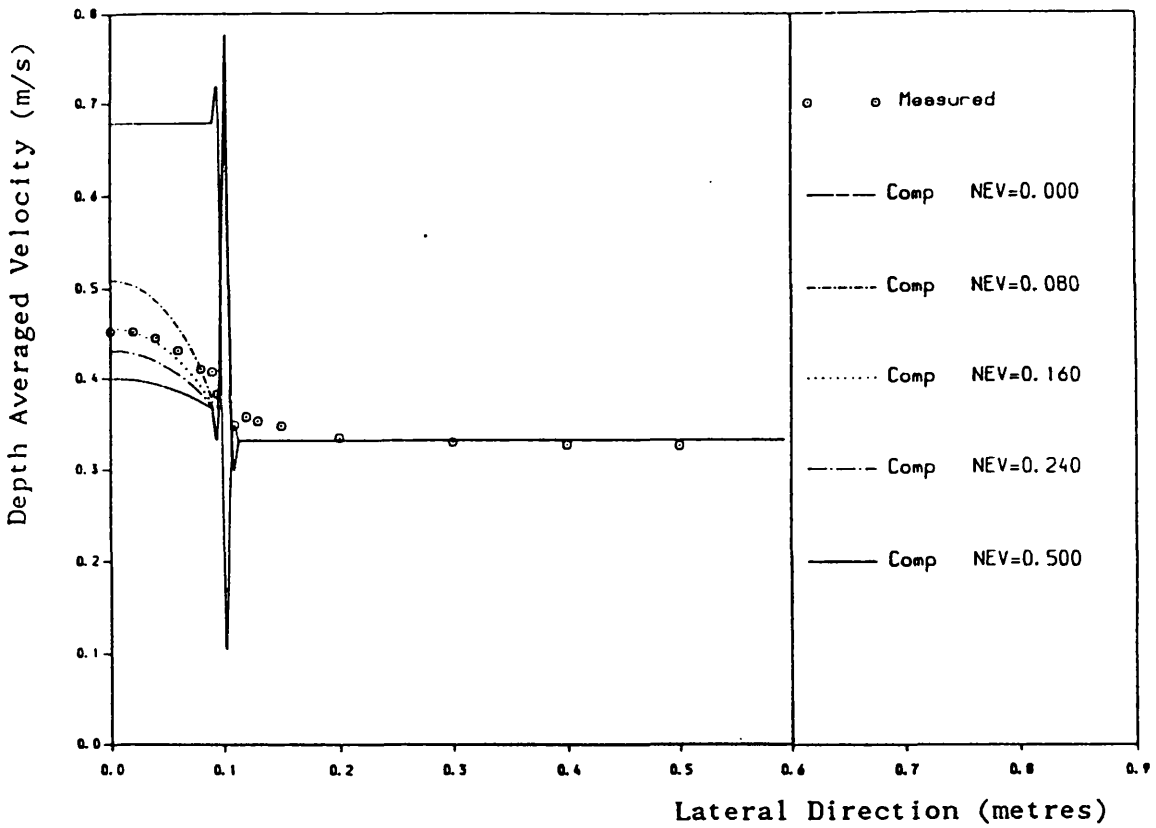


Figure 4. Velocity Distribution, Stage 100 mm, Kiely

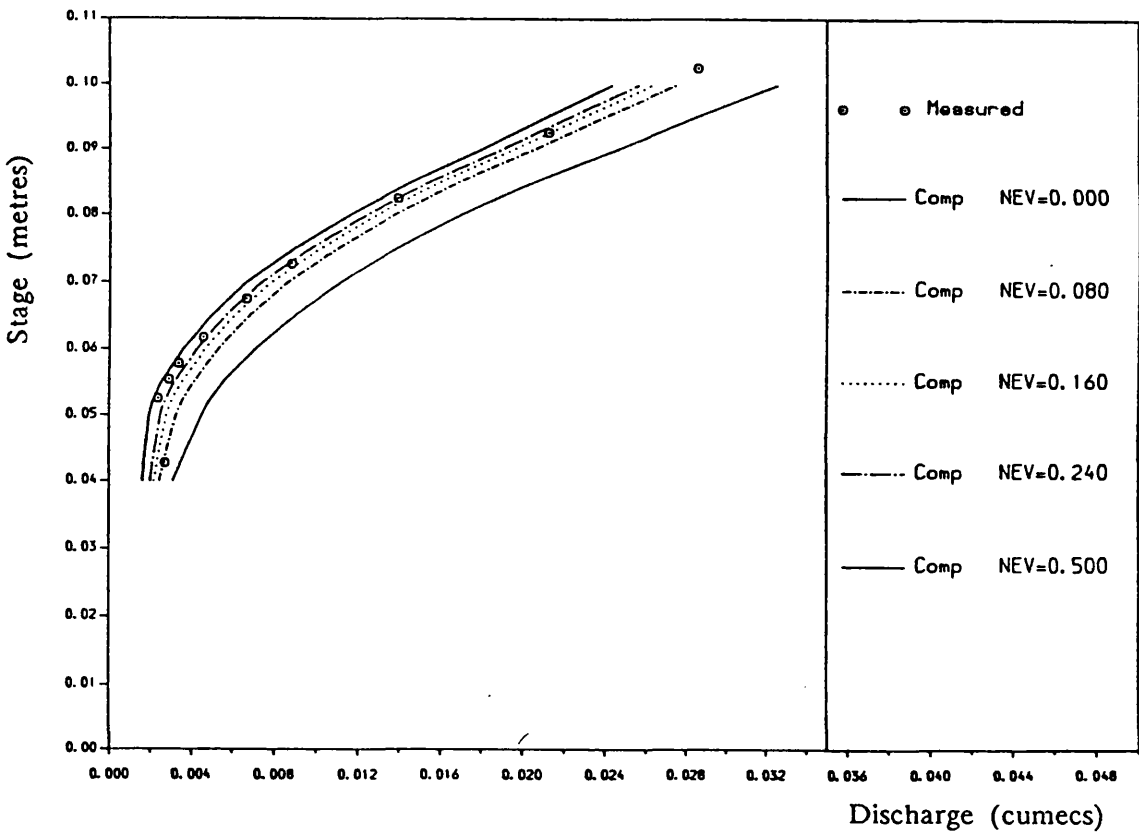


Figure 5. Stage-Discharge Relationship, Kiely

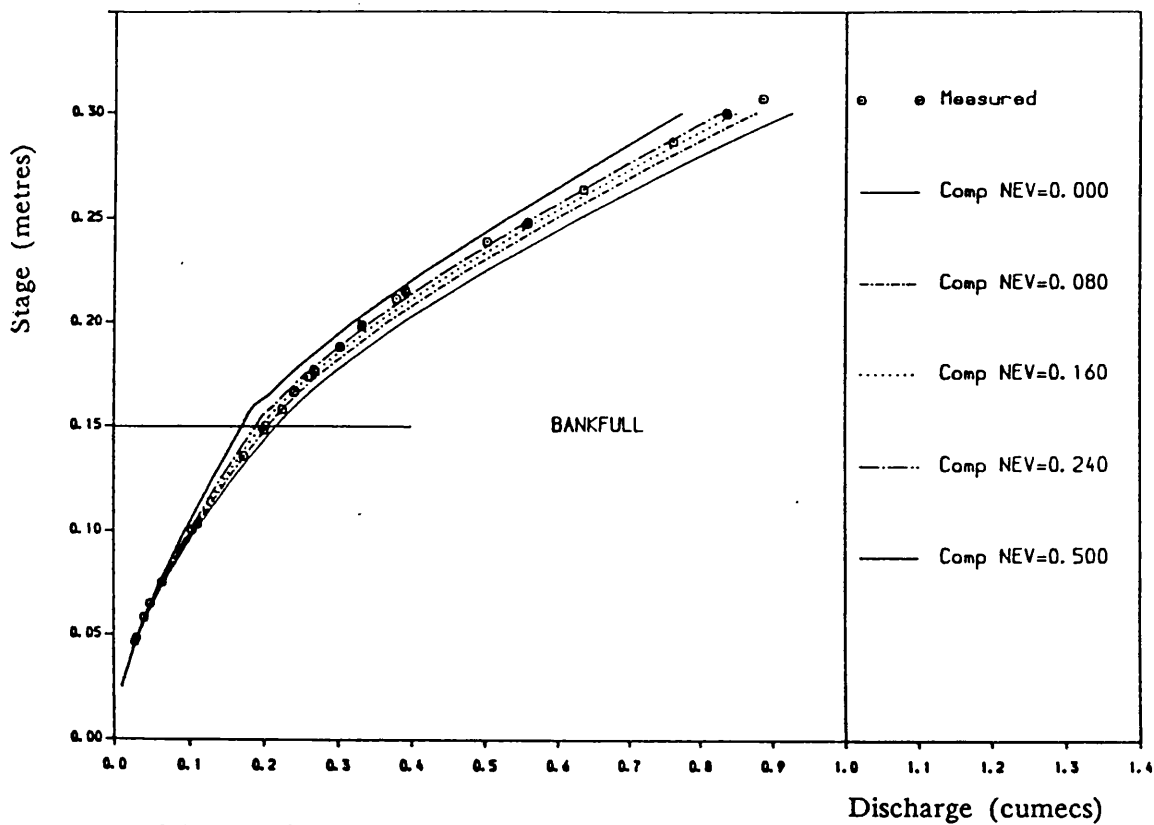


Figure 6. Stage-Discharge Relationship, FCF  
Narrow Floodplain, B/b = 2.2

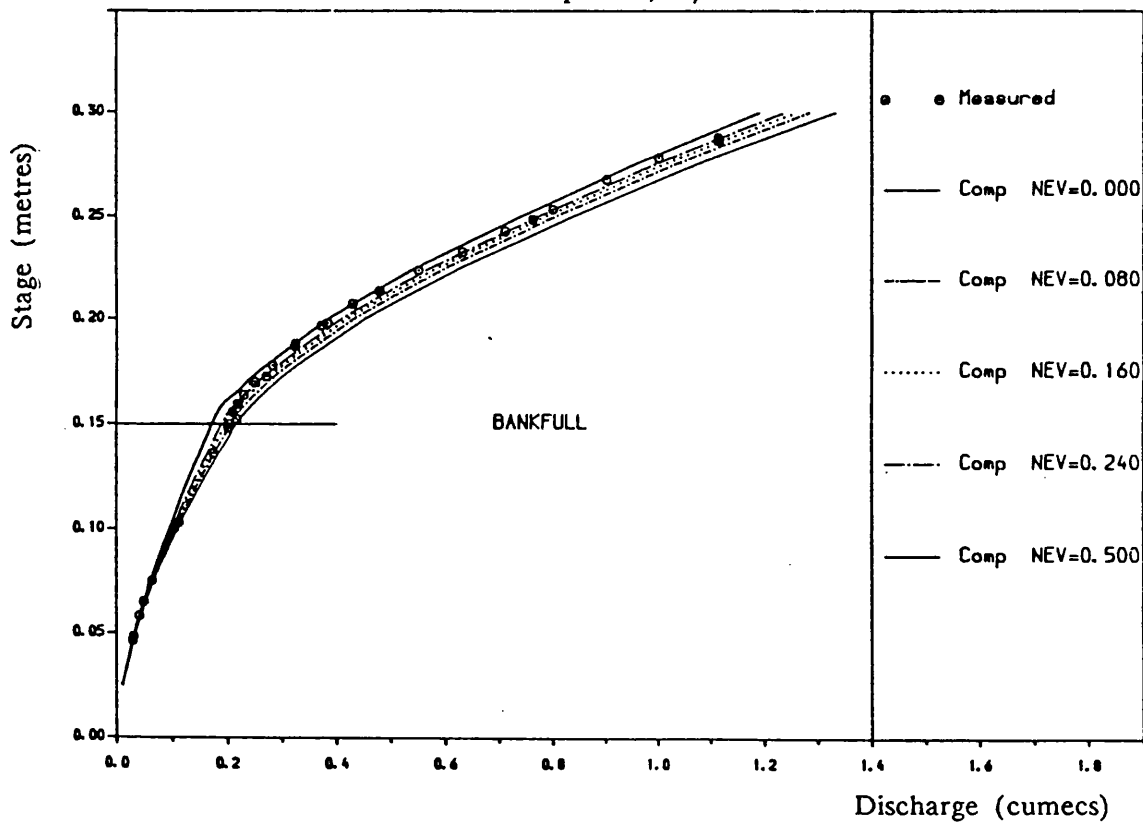


Figure 7. Stage-Discharge Relationship, FCF  
Wide Floodplain, B/b = 4.2

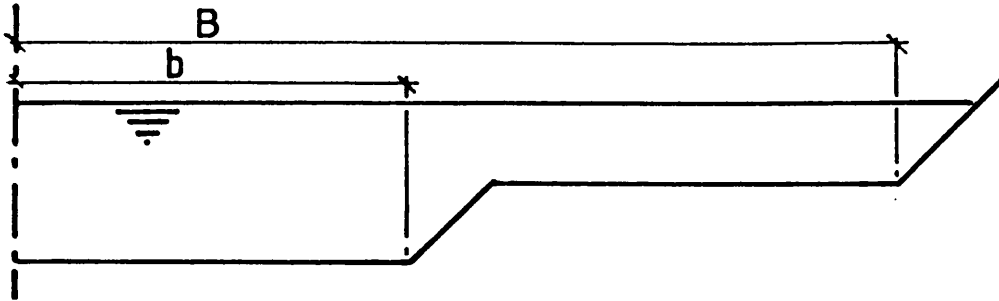


Figure 8. Cross-Section of Flood Channel Facility

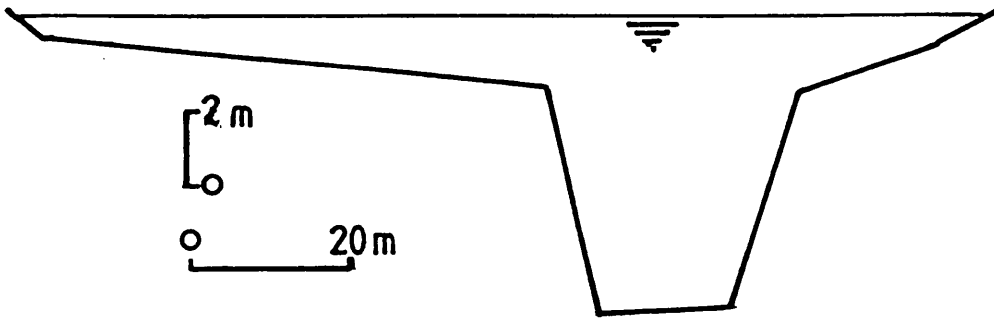


Figure 9. Cross-Section of River Severn at Montford

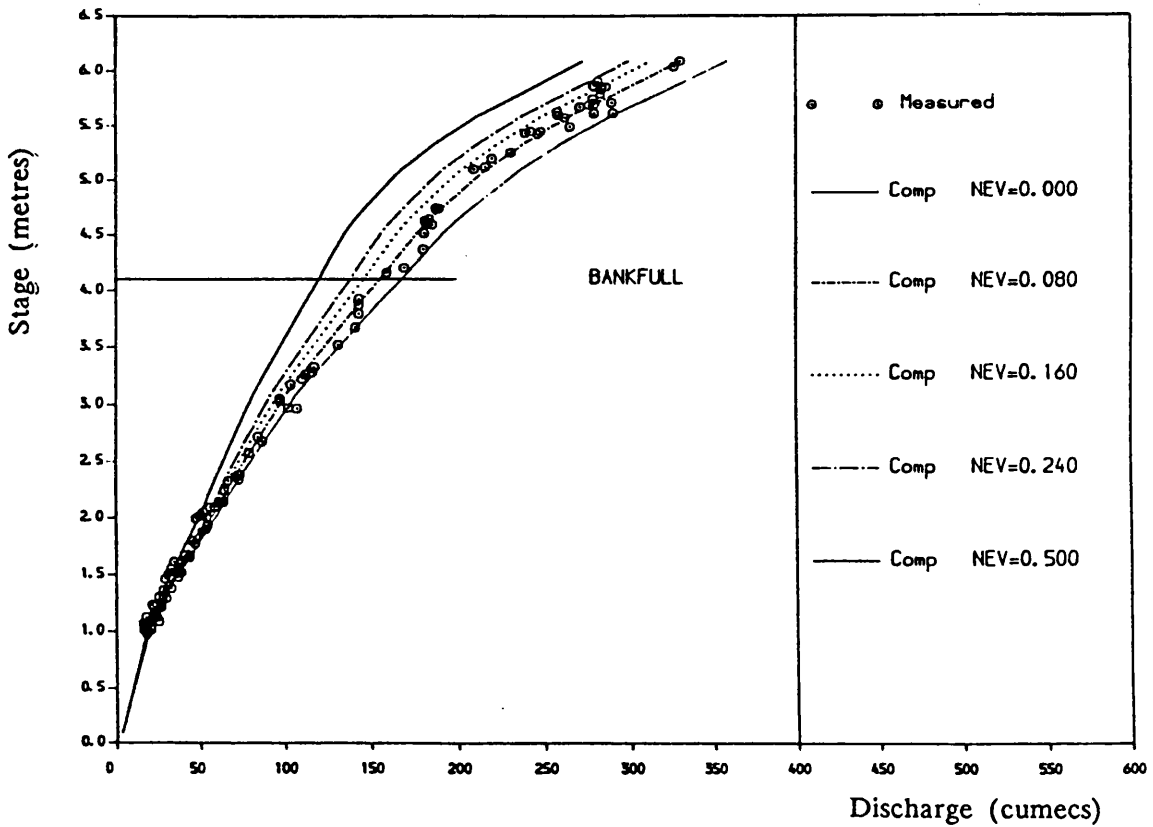


Figure 10. Stage-Discharge Relationship River Severn at Montford

# IS TURBULENCE MODELLING OF ANY USE?

IAHR Meeting Thursday 9th April  
ICE Great George Street

## APPLYING A SIMPLE TURBULENCE MODEL TO RIVER FLOWS

J B WARK and Dr P G SAMUELS  
Computational Methods Group, Research Department,  
HR Wallingford Ltd, Wallingford, OXON, OX10 8BA

### 1. INTRODUCTION

Engineers routinely model river flows. A typical exercise involves predicting water levels along a length of channel which is several kilometres long. These problems are usually tackled using one dimensional models based on the St Venant equations. Numerical solutions may be obtained using finite difference techniques, with the spacing between numerical grid points typically about ten times the channel width.

Considering a kilometre length of hypothetical channel which is ten metres wide and one metre deep then a numerical solution of the steady state St Venant equations solves for 1 unknown variable per grid point and so for a total of about 10 unknowns.

Turbulent flow structures within a river channel occur at scales ranging from about the order of the flow depth down to the molecular. There is a transfer of energy from the large turbulent structures to the smaller, until eventually energy is dissipated through viscous friction. In order to produce a numerical solution which describes these processes a computational grid with spacings of the order of a tenth of the channel depth (or smaller) is required. At each grid point variables related to the mean flow conditions and the turbulence must be computed. Hence depending on the turbulence model the number of unknowns per grid point is between 6 and 10. For the example above these rules of thumb give  $10^7$  grid points and between  $6 \times 10^7$  and  $10^8$  unknown variables.

The cost of collecting such detailed survey data and the computational effort required is not justified in typical engineering applications. However it is possible to introduce some simplifying assumptions and so account for the effects of the small scale turbulence on the overall flow pattern. This is the approach the authors have adopted and some results from a simplified, steady state, depth integrated model of the lateral distribution of flow across channels is presented.

### 2. THE MATHEMATICAL MODEL

Basic turbulence modelling : The eddy viscosity concept assumes that the Reynolds stresses which arise from the turbulent nature of the flow are linear functions of the appropriate velocity gradients.

In a simple unidirectional flow this may be expressed as equation 1. Where  $\tau$  is the shear stress,  $\rho$  is the fluid density,  $\nu_t$  is the eddy viscosity and  $U$  is the velocity.

$$\tau = \rho \nu_t \left[ \frac{\partial U}{\partial y} \right] \quad (1)$$

Depth integrated flow : If the general 3-D Reynolds equations are integrated through the water column and the flow is assumed to be steady then an equation which describes the lateral distribution of flow across a straight channel is derived. There are two possible versions of the equation which can be obtained depending whether the simple Boussinesq eddy viscosity concept is applied before or after the integration. If applied before then an equation in terms of the unit flow (2) is obtained otherwise the basic flow variable is depth averaged velocity (3).

$$gDS - \frac{Bf|q|q}{8D^2} + \frac{\partial}{\partial y} \left[ \nu_t \frac{\partial q}{\partial y} \right] = 0 \quad (2)$$

$$gDS - \frac{Bf|U|U}{8} + \frac{\partial}{\partial y} \left[ \nu_t D \frac{\partial U}{\partial y} \right] = 0 \quad (3)$$

Where  $B$  is a factor relating stress on an inclined surface to stress on a horizontal plane,  $D$  is the local flow depth,  $f$  is the Darcy friction factor,  $g$  is gravitational acceleration,  $q$  is the unit flow (ie the discharge per unit width =  $UD$ ),  $S$  is the surface slope and  $U$  is the depth averaged velocity (refs 1,2). It has been argued elsewhere (ref 3) that equation (2) is the preferred form since the variable  $q$  must be continuous even across a vertical step in depth where as the depth averaged velocity will display large discontinuities in these situations. It is obviously preferable to base calculations on a variable which is known to vary smoothly across the domain.

Turbulence model for depth integrated flow : At this point some model must be assumed for the lateral eddy viscosity  $\nu_t$ . It is possible to use a sophisticated turbulence model (ref 4) but again a price must be paid in terms of computational effort. The authors have found that the simple model (4) can give acceptable results in many situations.

$$\nu_t = \lambda U \cdot D \quad (4)$$

The problem in applying this model is in choosing appropriate values of  $\lambda$ , the Non-dimensional Eddy Viscosity (NEV) and  $U$  is the local shear velocity. Undoubtedly the choice of basic model affects the values of  $\lambda$  which are found to be appropriate. Knight et al (ref 7), using models based on equations 3 and 4, have reported derived values of  $\lambda$  which vary strongly across channel and floodplain both in laboratory and natural channels. While not disagreeing with this conclusion the authors experience in applying a model based on equations 2 and 4 indicates that

adequate precision can be achieved with a single value of  $\lambda$  applied to both channel and floodplain. However this is likely to be true only for the gross distribution of flow across the channel. The transport of pollutants or suspended sediments is far more sensitive to the local turbulent structure, secondary currents etc, which affects the value of  $\lambda$ . Hence if one is interested in the distribution of transported substances this simple one value model is inappropriate.

### 3. THE NUMERICAL METHOD

The sets of equations (2 and 4, LDM) or (3 and 4, LDM2) may be solved analytically only in certain simple situations and in general a numerical solution must be sought. The authors use a finite difference technique with a staggered grid and Newtons' method to linearize the coupled non-linear equations. Iteration is required and the initial guess is provided by setting  $v_i = 0$ . Convergence is usually attained within 5 iterations. Typically over 100 points are used for the numerical integration across a section.

### 4. MODELLING LABORATORY CHANNELS AND REAL RIVERS

THE SERC FCF This large scale physical modelling programme has yielded some of the best quality data available on flows in compound channels. Stage-discharges, point velocities and bed shear stresses were all measured. The flume and experimental programme are described in detail elsewhere. Both versions of the LDM have been applied to this data. Fig 1 shows typical depth averaged velocity distributions obtained from the LDM and Fig 2 shows similar results from the LDM2. The bed friction terms were computed using a modified smooth turbulent law (ref 9,1). The results produced with  $\lambda = 0$  show the initial guess that was used as the starting point of the iteration.

The predicted velocities are identical on the floodplains where the influence of the lateral shear stress is small. The shear layers within the main channel are more significant and the two versions give different results with the LDM values being lower than those from the LDM2. These differences arise from the third terms of equations 2 and 3. Expressing the equation in terms of unit flow appears to give larger lateral shear stresses than the equivalent model in terms of depth averaged velocity.

The calculated flow distributions can be integrated to provide the total discharge and the distribution of discharge within a channel. Fig 3 shows the stage discharges for one geometry of the SERC FCF. Three values of  $\lambda$  are shown and give very similar discharges. Fig 4 shows computed and measured flow distributions, expressed as the % of the total discharge within the main channel, for several of the cases tested on the FCF. In general the results are good with the LDM tending to overpredict slightly. The flow depths are increasing as the  $\%(Q_{mc}/Q_{tot})$  decrease and the LDM gives excellent results at the lower overbank depths.

Severn at Montford This gauging station has proved to be very suitable as a test case for various flow models (refs 1,7 and 9). Current metering has been carried

out across the whole channel and floodplain. Fig 5 shows the channel cross section. The main channel is about 35m wide and total channel and floodplain width 125m. Inbank gaugings were used to estimate the value of Manning's n at bankfull stage (0.031), this value was used for all overbank modelling. The floodplain roughnesses were assessed individually and values of 0.025 and 0.045 were found to be appropriate. Knight et al (ref 7) also used this site and found that in order to model the measured velocities  $\lambda$  values 0.2, 3.0 and 0.07 were required for intermediate side slopes, the floodplains and the main channel respectively. Fig 6 shows the computed stage discharges from the LDM using a fixed value of  $\lambda = 0.16$  and the values quoted above. The differences between using a single value and varying values of  $\lambda$  are negligible. This is confirmed by Table 1 which lists actual computed discharges for the two cases.

**Table 1 Comparison of discharges with  $\lambda$  constant and varying**

Stage m AOD	Discharges (cumecs)			% Difference
	$\lambda$ 0.16	$\lambda$ 0.2	$\lambda$ 3.0 0.07	
6.087	346.0	344.3		0.5
5.20	235.2	235.2		0.0
4.73	197.3	197.3		0.0

Figs 7 and 8 show computed velocity profiles (LDM), at one overbank stage, with constant and varying  $\lambda$  values. Again the influence of the lateral shear stress terms is most significant within the main channel. The constant value of  $\lambda$  gives slightly larger peaks in the depth averaged velocities at the channel floodplain interfaces than do the varying  $\lambda$ , however, the unit flow (UD) varies smoothly. Overall the values quoted by Knight et al do give a better prediction of the velocities.

Thames at Wallingford The LDM has been programmed into LORIS, one of the HR Wallingford river models. The LDM is applied to each section in turn to determine a table of conveyance against depth, this table is then used as the primary data in the hydraulic computations. An existing model of a reach of the Thames at Wallingford was chosen to carry out some comparisons between the existing LORIS model and LORIS combined with the LDM. The steady state backwaters which resulted are shown in figs 9 and 10. These results are for a high discharge and the floodplains along the reach were inundated. The large head loss in the middle of the reach is caused by the constricted arches of Wallingford bridge. The LDM does produce a significant difference compared to the original model. For the case shown it improves the overall agreement with observed water levels. For smaller discharges the differences were not so significant.

## 5. LIMITATIONS

These models are based on the assumption that the flow is relatively uniformly distributed with depth through the water column. Where strong secondary currents exist such as in tight bends then these simple models will not give good predictions. It is possible to modify the basic theory to account for mildly curved flow paths and differing slopes in the main channel and floodplains. These empirical adjustments are intended to widen application of a model which is theoretically only applicable to straight channels. The simple one parameter turbulence model (eqn 3) is attractive when considering river flows since it relates the turbulent shear stresses to the channel bed friction. In rivers bed friction is usually the dominant process but in situations where other effects become important this model is less appropriate. One difficulty in practice is that calibrated values of  $\lambda$  include the effects of secondary currents on the lateral transport of momentum and so it is difficult to give definitive guidance on appropriate values.

## 6. CONCLUSIONS

- 1 The model has been applied to a wide range of data from small scale laboratory channels to full scale river gauging data and has performed reasonably well.
- 2 The authors have found that for the cases investigated  $\lambda$  values in the range 0.08 to 0.24 gave reasonable results.
- 3 Further work is required to identify general values of  $\lambda$  which are appropriate to different conditions.
- 4 More basic research is required to quantify bed friction in natural channels. The biggest problem facing a river engineer is often how to assess accurate roughness values. The bed has a significant effect on the turbulent flow within the channel and so any sophisticated modelling exercise must be based on sound knowledge of the bed roughness characteristics.
- 5 More research is required to identify which version of the basic equation (2 or 3) which should be preferred in practice.
- 6 The use of a simple turbulence model combined with a depth integrated description of the lateral distribution of flow can give useful information to the river engineer.

## **7. ACKNOWLEDGEMENTS**

The LDM was programmed into the LORIS suite of river modelling programs by Mrs J E Slade in the Computational Methods Group of HR Wallingford. Some of the work presented in this paper was carried out by the first author under a Science and Engineering Research Council Case Award, this financial support is gratefully acknowledged. Both Authors would like to acknowledge support from the MAFF Strategic Research Commission 13 at HR Wallingford. The paper represents neither the opinions nor the policy of either organisation.

## **8. REFERENCES**

- 1 WARK J.B., SAMUELS P.G. and ERVINE D.A. (1990) - "A Practical Method of Estimating Velocity and Discharge in Compound Channels", Intl. Confr. on River Flood Hydraulics, Wallingford, Oxfordshire, Sept.
- 2 WARK J.B., RAMSBOTTOM D.M. AND SLADE J.E. (1991) - "Flood Discharge Assessment by the Lateral Distribution Method", HR Wallingford, Report SR 277, December.
- 3 SAMUELS P.G. (1989) - "Some Analytical Aspects of Depth Averaged Flow Models", Intl. Conf. Hydraulic and Environmental Modelling of Coastal, Estuarine and River Waters, Bradford, England, 19-21, Sept.
- 4 KELLER R.J. and RODI W. (1988) - "Prediction of Flow Characteristics in Main Channel/Flood Plain Flows, Jrnl. of Hydr. Resch., Vol.26, No.4.
- 5 SHIONO K. and KNIGHT D.W. (1988) - "Two Dimensional Analytical Solution for a Compound Channel", Third Int'l. Symp. Refined Flow Modelling and Turbulence Measurements. Tokyo, Japan, July.
- 6 SHIONO K. and KNIGHT D.W. (1990) - "Mathematical Models of Flow in Two or Multi Stage Straight Channels", Paper G1, Proc. Intl. Confr. on River Flood Hydraulics, Wallingford, England, 17,20th Sept.
- 7 KNIGHT D.W., SHIONO K. and PIRT J. (1989) - "Prediction of Depth Mean Velocity and Discharge in Natural Rivers with Overbank Flow", Int'l. Conf. of Coastal, Estuarine and River Waters, Bradford, England, 19-21 Sept.
- 8 SAMUELS P.G. (1988) - "Lateral Shear Layers in Compound Channels", Int's. Congr. on Fluvial Hydraulics, Budapest.
- 9 ACKERS P. (1991) - Private Communication

SERC FCF Phase A Series 02 stage 0.169m

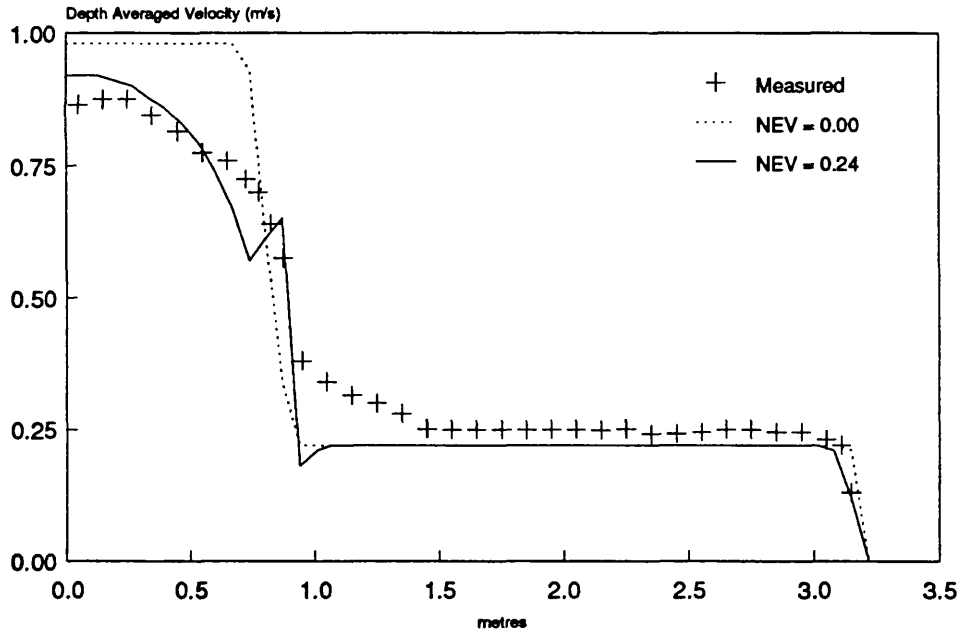


Fig 1 Calculated depth averaged velocity profiles LDM

SERC FCF Phase A Series 2 Stage = 0.169m

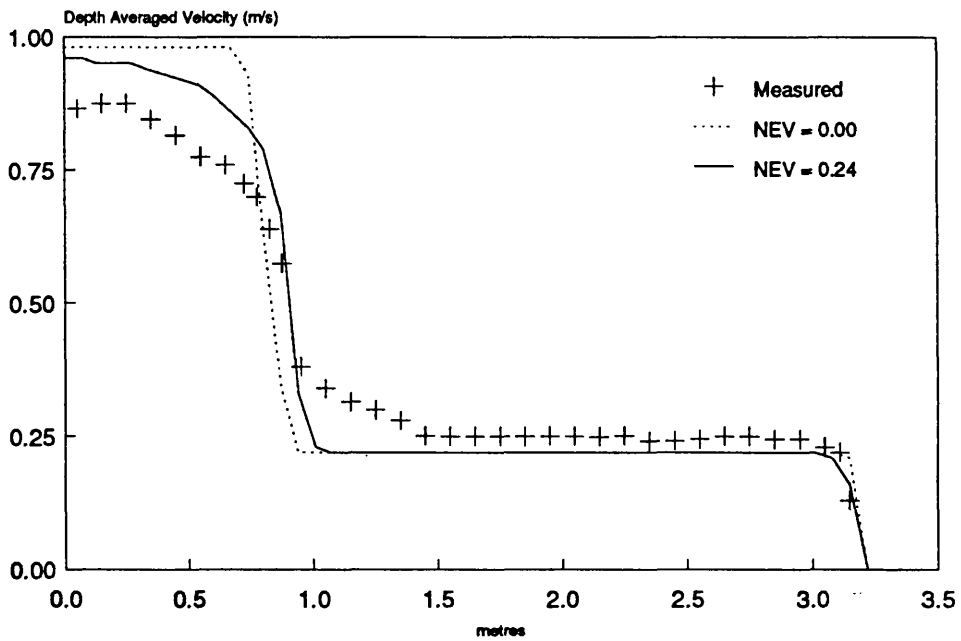


Fig 2 Calculated depth averaged velocity profiles LDM2

### SERC FCF Phase A Series 02

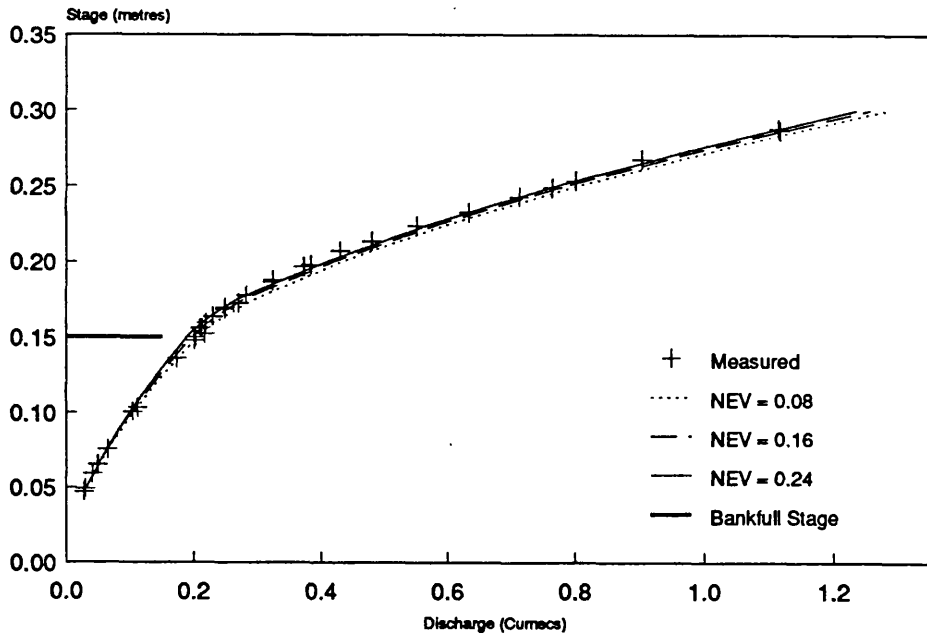


Fig 3 Calculated and measured stage-discharges LDM

### LDM NEV = 0.16 SERC FCF Smooth Case

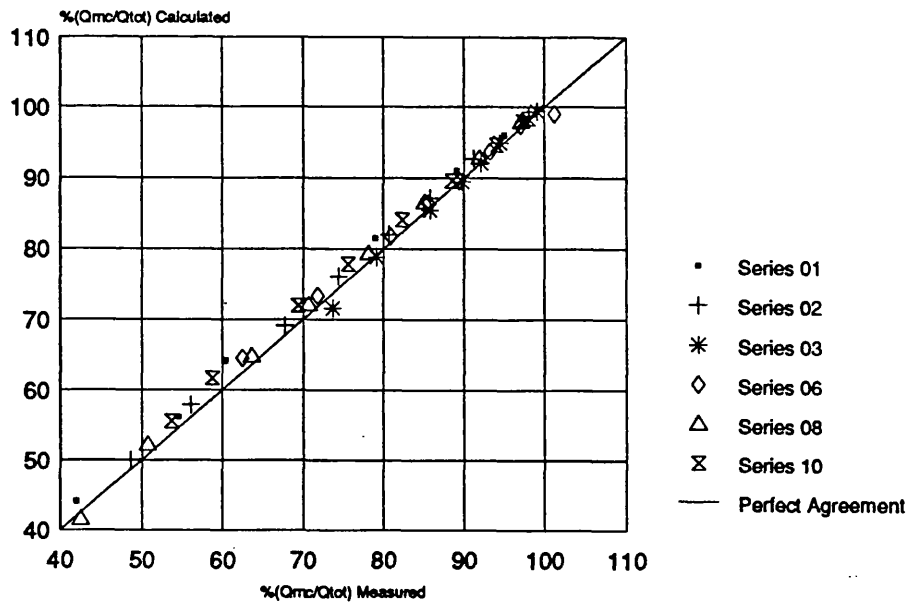


Fig 4 Calculated and measured flow distributions

Cross section geometry

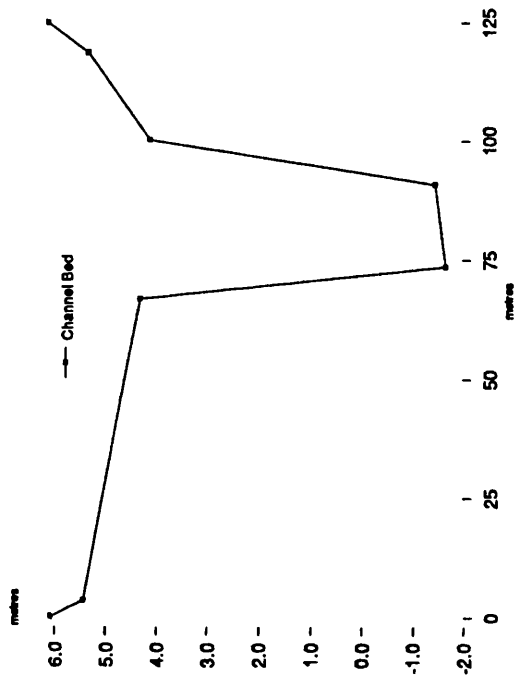


Fig 5 Severn at Montford

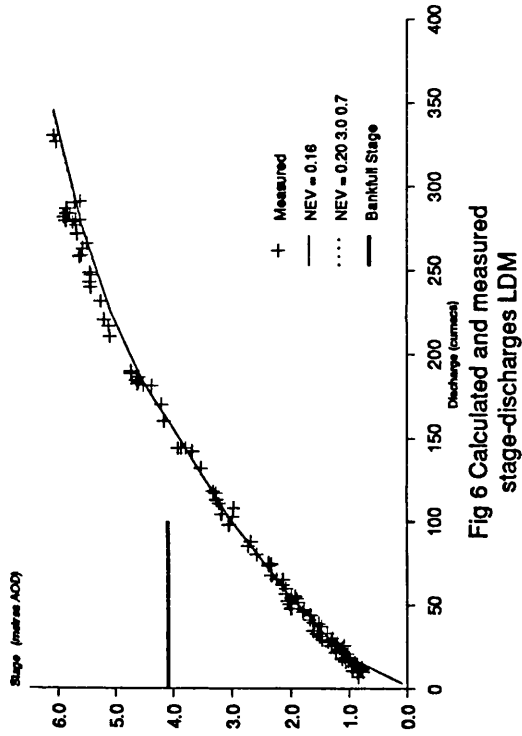


Fig 6 Calculated and measured stage-discharges LDM

River Severn at Montford  
nb = 0.031 nf = 0.025 0.045

River Severn at Montford  
nb = 0.031 nf = 0.025 0.045

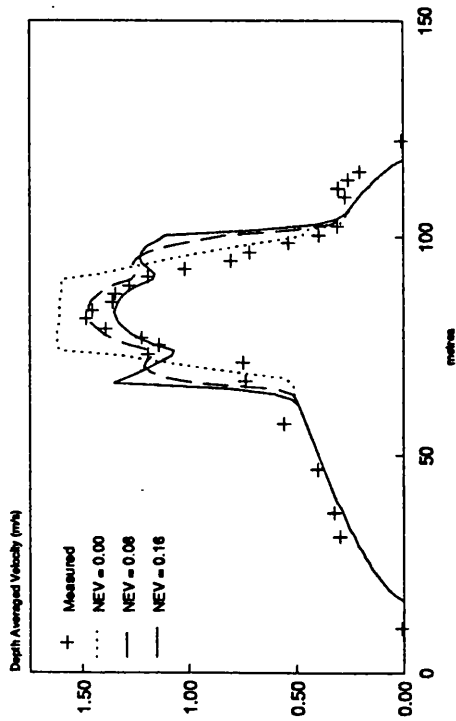


Fig 7 Calculated and measured velocities stage = 5.20 m AOD NEV constant

River Severn at Montford  
nb = 0.031 nf = 0.025 0.045

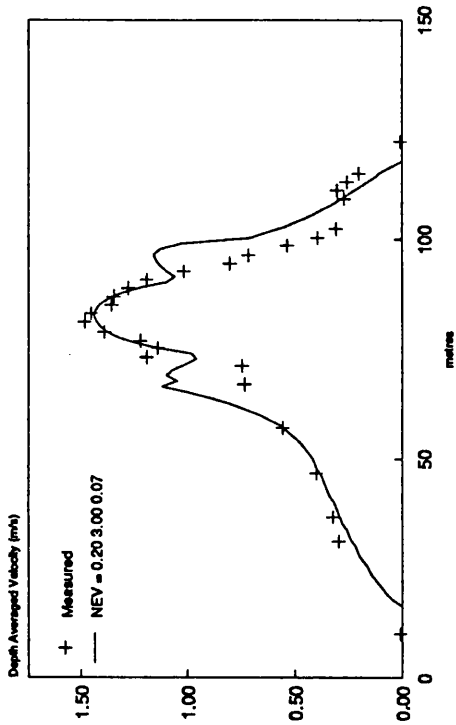


Fig 8 Calculated and measured velocities Stage = 5.20 m AOD NEV Varies

Thames at Wallingford  
Discharge = 500 cumecs

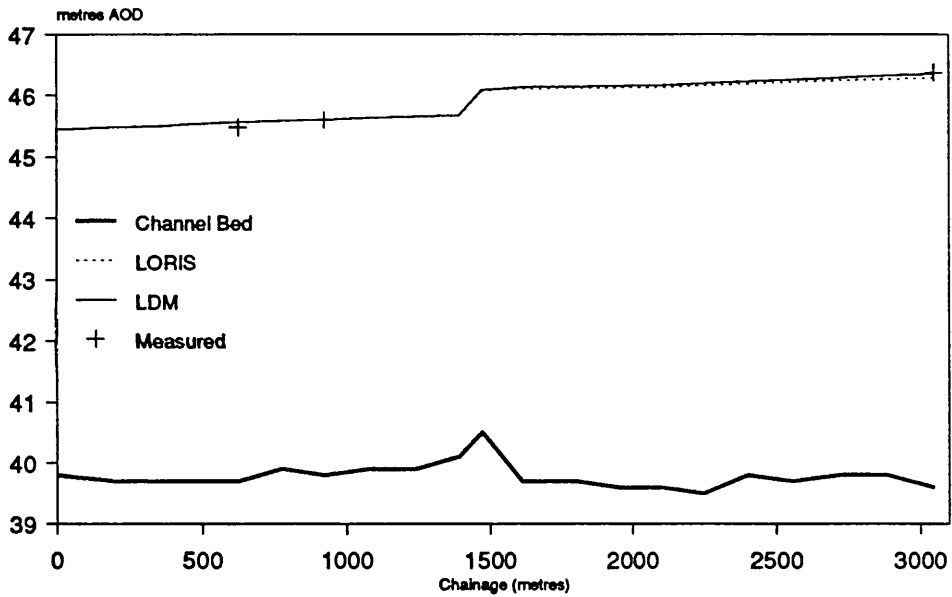


Fig 9 Comparison of LDM with existing LORIS model

Thames at Wallingford  
Discharge = 500 cumecs

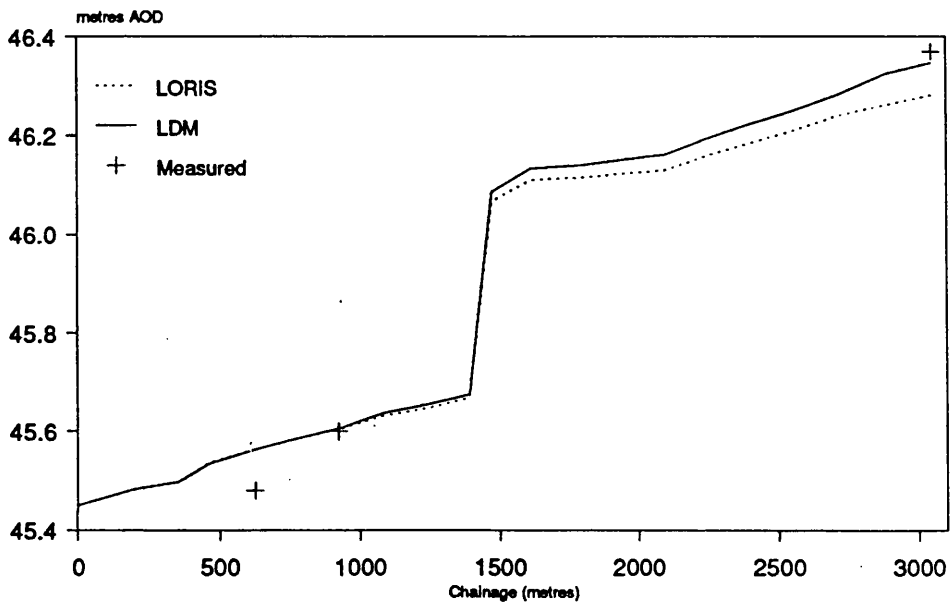


Fig 10 Comparison of LDM with existing LORIS Model (expanded scale)